EMERGING INFECTIOUS DISEASES®

CDC
SAFER • HEALTHIER • PEOPLE™

Emerging Viruses

April 2017

Joseph Stella (1877–1946) Spring (The Procession) c. 1914–1916. Oil on canvas, 75 5/16 in x 40 3/16 in / 191.3 x 102.1 cm. Gift of Collection Société Anonyme, Yale University Art Gallery, New Haven, Connecticut, USA.

EMERGING INFECTIOUS DISEASES®

Emerging Infectious Diseases is published monthly by the Centers for Disease Control and Prevention, 1600 Clifton Road, Mailstop D61, Atlanta, GA 30329-4027, USA. Telephone 404-639-1960, fax 404-639-1954, email eideditor@cdc.gov.

∞ Emerging Infectious Diseases is printed on acid-free paper that meets the requirements of ANSI/NISO 239.48-1992 (Permanence of Paper)

EMERGING INFECTIOUS DISEASES®

April 2017

On the Cover

Joseph Stella (1877–1946) Spring (The Procession)

c. 1914–1916 (detail).

Oil on canvas, 75 5/16 in x 40 3/16 in /191.3 x 102.1 cm. Gift of Collection Société Anonyme, Yale University Art Gallery, New Haven, Connecticut, USA.

About the Cover p. 725

Perspective

Synopses

Research

Dispatches

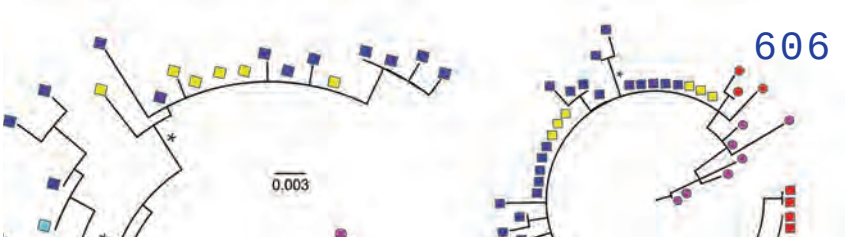

EMERGING INFECTIOUS DISEASES®
April 2017

Research Letters

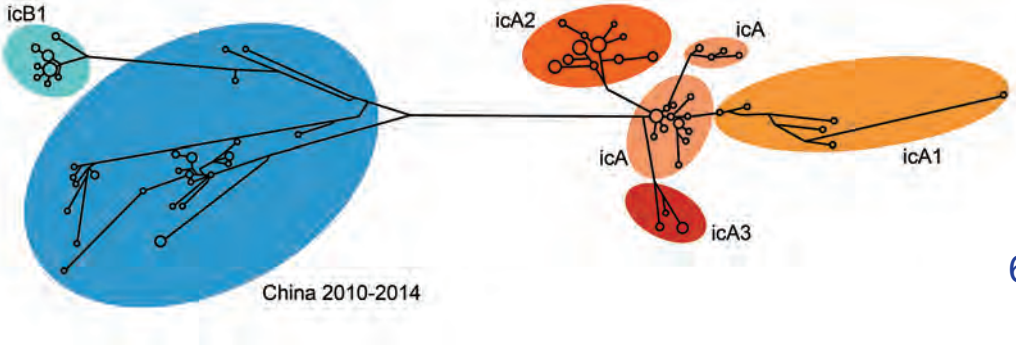

Letter

Books and Media

EMERGING INFECTIOUS DISEASES®
April 2017

About the Cover

Etymologia

Corrections

Vol. 22, No. 11

The name of author Massimo Ciccozzi was misspelled in **Mayaro Virus in Child with Acute Febrile Illness, Haiti, 2015** (J. Lednicky et al.). The article has been corrected online (https://wwwnc.cdc.gov/eid/article/22/11/16-1015_article).

Vol. 23, No. 1

The GenBank accession no. KX757840 was listed incorrectly in **Puumala Virus in Bank Voles, Lithuania** (P. Straková et al.). The article has been corrected online (https://wwwnc.cdc.gov/eid/article/23/1/16-1400_article).

Vol. 23, No. 3

The name of author Apurva Narechania was misspelled in ***Mycobacterium tuberculosis* Infection among Asian Elephants in Captivity** (G. Simpson et al.). The article has been corrected online (https://wwwnc.cdc.gov/eid/article/23/3/16-0726_article).

World Malaria Day, April 25, 2017

The massive scale-up of malaria efforts from 2000–2015 saved 6.2 million lives and decreased the number of malaria deaths by 60% worldwide and by 66% in Africa, according to the World Malaria Report 2015. However, malaria killed an estimated 438,000 in 2015, mainly children under five years of age in sub-Saharan Africa. The ever-evolving challenges of drug and insecticide resistance, changes in the malaria landscape, and aspirations for elimination will all require new interventions and new science.

EMERGING INFECTIOUS DISEASES®

https://wwwnc.cdc.gov/eid/page/world-malaria-day

EID *SPOTLIGHT*

These spotlights highlight the latest articles and information on emerging infectious disease topics in our global community.

Antimicrobial Resistance

Ebola

Food Safety

HIV/AIDS

Lyme Disease

Influenza

MERS

Pneumonia

Rabies

Tuberculosis

Ticks

Zika

EMERGING INFECTIOUS DISEASES®

http://wwwnc.cdc.gov/eid/page/spotlight-topics

Biologic Evidence Required for Zika Disease Enhancement by Dengue Antibodies

Scott B. Halstead

The sudden appearance of overt human Zika virus infections that cross the placenta to damage fetal tissues, target sexual organs, and are followed in some instances by Guillain-Barré syndrome raises questions regarding whether these outcomes are caused by genetic mutations or if prior infection by other flaviviruses affects disease outcome. Because dengue and Zika viruses co-circulate in the urban *Aedes aegypti* mosquito–human cycle, a logical question, as suggested by in vitro data, is whether dengue virus infections result in antibody-dependent enhancement of Zika virus infections. This review emphasizes the critical role for epidemiologic studies (retrospective and prospective) in combination with the studies to identify specific sites of Zika virus infection in humans that are needed to establish antibody-dependent enhancement as a possibility or a reality.

Recently, polyclonal and monoclonal dengue virus (DENV)–elicited antibodies have been shown to neutralize or enhance Zika virus infection in vitro (*1*,*2*). Three studies have shown that monoclonal antibodies to the DENV fusion loop epitope reliably enhanced Zika virus infection (i.e., antibody-dependent enhancement [ADE]) in Fc receptor–bearing K-562 human myelogenous leukemia cells or the U-937 human monocytic cell line (*1*–*3*). By contrast, broadly neutralizing DENV monoclonal antibodies directed at a conformational quaternary epitope on the virion formed at the interface of 2 envelope dimer epitopes (EDE1 and EDE2) potently neutralized Zika virus in a picomolar range similar to the neutralization of DENV (*2*). X-ray crystallographic structures of antigen binding fragments of EDE1 and EDE2 in complex with the Zika virus envelope protein have been obtained (*4*). These observations raise important questions about the past and future of human infections with Zika virus.

Outside Africa, Zika virus occupies the same epidemiologic niche as do the DENVs. During the ongoing pandemic in the Western Hemisphere, infections in the sequence of DENV followed by Zika virus must have occurred often and will continue to occur. Might placental transfer of Zika virus or Guillain-Barré syndrome (GBS), fueled by the ADE phenomenon, occur specifically in DENV-immune persons? If Zika virus infections are enhanced by DENV antibodies, might ADE also occur after administering a dengue vaccine? Indeed, if Zika virus infections can be enhanced by DENV antibodies, might that also be an outcome following administration of a poorly protective Zika virus vaccine? Correspondingly, might Zika virus antibodies enhance DENV infections? These crucial questions require biologically valid answers. What information do we need to answer them, and where shall we start looking?

Zika virus, a member of the *Flavivirus* genus, is maintained in complex African zoonotic cycles, spilling from time to time into the *Aedes aegypti* mosquito urban transmission cycle (*5*). This spillover might be a very old phenomenon. Because many flaviviruses infect humans in Africa, it was logical to ask if antibodies to these viruses enhanced Zika virus infections. The answer obtained in vitro was affirmative (*6*). After having been first isolated in Africa in 1947, human Zika virus disease remained sparse and mild, with no reports of diverse clinical syndromes associated with infection (*7*). Nor was Zika disease reported from India or Southeast Asia, where Zika virus and DENV co-circulated, evidenced by detection of neutralizing antibodies in humans as early as 1954 (*8*–*10*). Zika virus was isolated from *Ae. aegypti* mosquitoes collected in rural Malaysia in 1966 (*11*). No alarms were raised in Asia until 2007, on the Yap Islands in the Western Pacific, when it was estimated that ≈900 cases of a mild febrile exanthema caused by Zika virus infections had occurred among a total population of ≈7,000 (*12*). Then, during 2013–2014, on Tahiti, a Zika virus epidemic was followed in 4 weeks by an outbreak of GBS (*13*). Of the 42 case-patients with Zika virus infection and subsequent GBS, 95% had evidence of prior DENV infection, although this percentage did not differ from that of controls (*13*). This illness phenomenon spread to South America, where remarkably, GBS often followed acute Zika virus infections by only a few days (*14*–*17*). Then, abruptly, in Brazil, Zika virus was found to destroy fetal tissues (*18*). Next, it was learned that Zika virus infected the male reproductive tract and could be sexually transmitted (*19*).

Author affiliation: Uniformed Services University of the Health Sciences, Bethesda, Maryland, USA

DOI: http://dx.doi.org/10.3201/eid2304.161879

Is the expanded pathogenicity of Zika virus the result of viral mutations, or might DENV ADE play a role, or are both true? An opinion has emerged that Zika virus genomes in Asia have acquired 1 or more mutations, contributing to its newly emerged pathogenicity (*5*,*20*). A recent analysis of full-length RNA sequences of 84 Zika virus genomes in Africa, Asia, the Pacific region, and the Americas has noted a stable amino acid change in the matrix protein of Asian viruses that accompanied placental invasiveness and GBS in Tahiti and the Americas (*21*). It is not clear what specific biologic properties might have been acquired by Zika virus that contributed to the observed new behaviors. The original strain of Zika virus recovered in Uganda in 1947 was neurotropic for 6-week-old mice (*22*). A strain genetically similar to the prototype in Africa productively infected human neural progenitor cells in vitro, dysregulating cell growth (*23*). In type 1 interferon receptor knockout mice or mice inoculated with type 1 interferon receptor–blocking antibodies, subcutaneous inoculation of a strain of Zika virus from French Polynesia infected maternal trophoblasts and resulted in apoptosis. In infected pregnant female mice, Zika virus crossed into the fetal circulation, where it infected endothelial cells, resulting in apoptosis and greatly impaired fetal circulation leading to ischemia and fetal loss (*24*).

Knowledge that a microbial disease is worsened by ADE derives from 2 evidentiary pillars: 1) epidemiologic evidence demonstrating that a unique syndrome or severe disease is significantly associated with persons who circulate antibodies (presumably "enhancing") before infection, and 2) evidence of in situ replication by the causative organism in myeloid cells that serve as major targets of cellular infection. DENV disease enhancement was established by recording a strong association between severe disease in humans and a secondary-type DENV antibody response, by direct association of severe cases with sequential DENV infections in prospective cohort studies, and by the occurrence of severe disease during first DENV infections in infants born to dengue-immune mothers (*25*–*30*). This latter observation provides population-level evidence that DENV antibodies are the critical risk factor for the occurrence of severe DENV disease. However, severe disease in infants occurs only when infants acquire antibodies acquired by 2 or more lifetime DENV infections in the mother (*25*,*30*). Importantly, the same IgG antibodies that enhance DENV infections in infants are protective for the first several months after birth (*29*). Evidence that myeloid cells support intracellular DENV infection in vivo in humans derives from studies on tissues from virologically documented patients obtained during surgery, at autopsy, or by venesection (*31*–*34*). These studies, although few, are buttressed by the demonstration that DENV immune complex infection of Fc receptor–bearing cells leads directly to vascular permeability in mouse models (*32*,*35*–*40*).

To establish whether ADE caused by DENV antibodies modifies the course of Zika virus infections, evidence will be required from the same 2 pillars. The outcomes of DENV–Zika virus sequential infections might be diverse and complicated. First, antibodies derived from monotypic infections with each of the 4 DENV serotypes, if they enhance at all, might affect Zika virus infections differently. As an example, infections in the sequence DENV-1 followed by DENV-2 or DENV-3 then DENV-2 result in more severe clinical outcome than infections in any of the other 10 secondary infection sequences (*41*). Second, the interval between DENV followed by Zika virus infection might regulate disease severity. In dengue, the interval between initial and a heterotypic DENV infection exerts a remarkable bidirectional effect. Sequential DENV infections at a short interval (<2 years) blunt the clinical severity of responses to a second infection, whereas as the interval widens (2–20 years), the outcome becomes increasingly severe (*42*–*44*). Third, Zika virus infection enhancement could be critically dependent upon the parity of past DENV infections of the host. For example, as is true for dengue, a single prior DENV experience might enhance infection, whereas antibodies deriving from ≥2 past DENV infections might protect against further infection (*45*).

By using a simple protocol (Table), it should be possible to gather evidence using a case-control format comparing the frequency of a secondary flavivirus antibody response in convalescent-phase serum samples of persons experiencing any defined acute Zika virus disease syndromes, such as exanthematous fever, congenital Zika syndrome, or GBS (i.e., case-patients) with the prevalence of past DENV infection in Zika virus–infected age-, sex-, residence-, and ethnicity-matched persons from the same exposure group (i.e., controls). Such a comparison should be undertaken promptly in several different Zika virus–endemic locales. If these studies fail to provide evidence that prior flavivirus infection is a risk factor for any of the defined clinical outcomes of Zika virus infections, the search for Zika virus ADE can halt. However, if evidence compatible with ADE is obtained, it will be important to investigate the possibly complicated interactions between DENV and Zika virus infections alluded to here.

In the case of DENV, the ADE phenomenon requires infection of myeloid cells by infectious immune complexes; therefore, it will important to determine if myeloid cells are major targets of Zika virus syndromes in humans. DENV and Zika virus infections are each expressed clinically as febrile exanthema. In monkey and human DENV infections, infected peripheral blood leukocytes circulate transiently just before the appearance of virus in the skin (monkeys) or the appearance of a generalized body rash (humans) (*33*,*46*). In children in Nicaragua, DENV-infected

Table. Case–control epidemiologic research protocol for assessing DENV antibody enhancement of Zika virus syndromes*

Category	Description
Case-patients	Zika virus PCR positive or serologically positive symptomatic persons (i.e., with febrile illness, Guillain-Barré syndrome or congenital Zika syndrome) of any age who have convalescent-phase serum samples available to test for DENV IgG by ELISA.
Controls	Serum samples from age-, sex-, residence-, and ethnicity-matched controls with blood drawn at about the same time as each index case-patient. Ratio: 4 controls to 1 index case-patient.
Laboratory studies	1. Convalescent-phase serum samples from case-patients are tested by indirect pan-DENV IgG ELISA. (A positive result indicates that the Zika virus infection occurred in a DENV-immune person.) 2. Control serum samples are tested for Zika virus neutralizing antibodies. 3. Control serum samples are tested for past DENV infections by using indirect pan-DENV IgG ELISA. 4. DENV IgG ELISA–positive serum samples from case-patients and controls are tested for DENV serotypes 1–4 neutralizing antibodies. 5. Frequency of prior DENV infections in symptomatic Zika virus case-patients is compared with frequency of DENV antibodies in Zika virus–immune controls. A statistically significant increase in past DENV infection indicates enhancement; a statistically significant reduction indicates protection. 6. All comparisons should be made separately and combined for persons of white and black† race.

*DENV, dengue virus.
†The powerful DENV disease resistance gene(s) in black sub-Saharan Africans might also protect against Zika virus diseases.

peripheral blood leukocytes circulating late in the viremic period were definitively identified as monocytes (*33*). This finding might be a general phenomenon in viral exanthmata given that infected monocytes also circulate in blood during the rash stage in children with measles (*47*,*48*). A plausible hypothesis is that maculopapular rashes derive from DENV-infected monocytes originating in the bone marrow that are targeted to skin. By analogy, human Zika virus pathogenesis might involve myeloid cells and blood monocytes as infection targets. A search to prove or disprove this hypothesis should be undertaken promptly.

Should Zika virus infect circulating monocytes, this still leaves unanswered the question whether tissue macrophages are an important component of so-called "normal" Zika virus human infections. In A129 mice lacking type 1 interferon receptors, peripheral inoculation of Zika virus produced observable illness and high titers of virus in spleen, liver, and brain, but no attempt was made to identify target cells (*49*). As suggested by excretion of Zika virus in seminal fluid, urine, saliva, and tears, Zika virus might predominantly infect nonmyeloid tissues. As reviewed briefly here, there is ample evidence from studies on human uterine contents, plus validation in mouse models, that Zika virus infects neuronal tissues, a wide range of fetal organs, placental cells, endothelial cells, and reproductive organs. Clearly, we have much to learn about the pathogenesis and pathology of human Zika virus infections. The issue of ADE poses a unique challenge to researchers, the resolution of which rests in the first instance on epidemiologic evidence.

Dr. Halstead is an adjunct professor in the Department of Preventive Medicine and Biostatistics, Uniformed Services University of the Health Sciences. As a consultant to the Rockefeller Foundation, he founded the Pediatric Dengue Vaccine Initiative in 2003. His career interests have included arbovirology, epidemiology, vaccinology, and international health. He is a member of the Editorial Board of the Emerging Infectious Diseases journal.

References

1. Priyamvada L, Quicke KM, Hudson WH, Onlamoon N, Sewatanon J, Edupuganti S, et al. Human antibody responses after dengue virus infection are highly cross-reactive to Zika virus. Proc Natl Acad Sci U S A. 2016;113:7852–7. http://dx.doi.org/10.1073/pnas.1607931113
2. Dejnirattisai W, Supasa P, Wongwiwat W, Rouvinski A, Barba-Spaeth G, Duangchinda T, et al. Dengue virus sero-cross-reactivity drives antibody-dependent enhancement of infection with Zika virus. Nat Immunol. 2016;17:1102–8. http://dx.doi.org/10.1038/ni.3515
3. Paul LM, Carlin ER, Jenkins MM, Tan AL, Barcellona CM, Nicholson CO, et al. Dengue virus antibodies enhance Zika virus infection. Clin Transl Immunology. 2016;5:e117. http://dx.doi.org/10.1038/cti.2016.72
4. Barba-Spaeth G, Dejnirattisai W, Rouvinski A, Vaney MC, Medits I, Sharma A, et al. Structural basis of potent Zika-dengue virus antibody cross-neutralization. Nature. 2016;536:48–53. http://dx.doi.org/10.1038/nature18938
5. Musso D, Gubler DJ. Zika virus. Clin Microbiol Rev. 2016;29:487–524. http://dx.doi.org/10.1128/CMR.00072-15
6. Fagbami AH, Halstead SB, Marchette NJ, Larsen K. Cross-infection enhancement among African flaviviruses by immune mouse ascitic fluids. Cytobios. 1987;49:49–55.
7. Fagbami AH. Zika virus infections in Nigeria: virological and seroepidemiological investigations in Oyo State. J Hyg (Lond). 1979;83:213–9. http://dx.doi.org/10.1017/S0022172400025997
8. Smithburn KC, Kerr JA, Gatne PB. Neutralizing antibodies against certain viruses in the sera of residents of India. J Immunol. 1954;72:248–57.
9. Smithburn KC. Neutralizing antibodies against arthropod-borne viruses in the sera of long-time residents of Malaya and Borneo. Am J Hyg. 1954;59:157–63.
10. Hammon WM, Schrack WD Jr, Sather GE. Serological survey for arthropod-borne virus infections in the Philippines. Am J Trop Med Hyg. 1958;7:323–8.
11. Marchette NJ, Garcia R, Rudnick A. Isolation of Zika virus from *Aedes aegypti* mosquitoes in Malaysia. Am J Trop Med Hyg. 1969;18:411–5.
12. Duffy MR, Chen TH, Hancock WT, Powers AM, Kool JL, Lanciotti RS, et al. Zika virus outbreak on Yap Island,

Federated States of Micronesia. N Engl J Med. 2009;360:2536–43. http://dx.doi.org/10.1056/NEJMoa0805715
13. Cao-Lormeau VM, Blake A, Mons S, Lastère S, Roche C, Vanhomwegen J, et al. Guillain-Barré syndrome outbreak associated with Zika virus infection in French Polynesia: a case-control study. Lancet. 2016;387:1531–9. http://dx.doi.org/10.1016/S0140-6736(16)00562-6
14. Brasil P, Sequeira PC, Freitas AD, Zogbi HE, Calvet GA, de Souza RV, et al. Guillain-Barré syndrome associated with Zika virus infection. Lancet. 2016;387:1482. http://dx.doi.org/10.1016/S0140-6736(16)30058-7
15. do Rosário MS, de Jesus PA, Vasilakis N, Farias DS, Novaes MA, Rodrigues SG, et al. Guillain-Barré syndrome after Zika virus infection in Brazil. Am J Trop Med Hyg. 2016;95:1157–60. http://dx.doi.org/10.4269/ajtmh.16-0306
16. Parra B, Lizarazo J, Jiménez-Arango JA, Zea-Vera AF, González-Manrique G, Vargas J, et al. Guillain-Barré syndrome associated with Zika virus infection in Colombia. N Engl J Med. 2016;375:1513–23. http://dx.doi.org/10.1056/NEJMoa1605564
17. Dos Santos T, Rodriguez A, Almiron M, Sanhueza A, Ramon P, de Oliveira WK, et al. Zika Virus and the Guillain-Barré syndrome - case series from seven countries. N Engl J Med. 2016;375:1598–601. http://dx.doi.org/10.1056/NEJMc1609015
18. Teixeira MG, Costa MC, de Oliveira WK, Nunes ML, Rodrigues LC. The epidemic of Zika virus–related microcephaly in Brazil: detection, control, etiology, and future scenarios. Am J Public Health. 2016;106:601–5. http://dx.doi.org/10.2105/AJPH.2016.303113
19. Atkinson B, Hearn P, Afrough B, Lumley S, Carter D, Aarons EJ, et al. Detection of Zika virus in semen. Emerg Infect Dis. 2016;22:940. http://dx.doi.org/10.3201/eid2205.160107
20. Russell PK. The Zika pandemic—a perfect storm? PLoS Negl Trop Dis. 2016;10:e0004589. http://dx.doi.org/10.1371/journal.pntd.0004589
21. Pettersson JH, Eldholm V, Seligman SJ, Lundkvist Å, Falconar AK, Gaunt MW, et al. How did Zika virus emerge in the Pacific Islands and Latin America? MBio. 2016;7:e01239-16. http://dx.doi.org/10.1128/mBio.01239-16
22. Dick GW, Kitchen SF, Haddow AJ. Zika virus. I. Isolations and serological specificity. Trans R Soc Trop Med Hyg. 1952;46:509–20. http://dx.doi.org/10.1016/0035-9203(52)90042-4
23. Tang H, Hammack C, Ogden SC, Wen Z, Qian X, Li Y, et al. Zika virus infects human cortical neural progenitors and attenuates their growth. Cell Stem Cell. 2016;18:587–90. http://dx.doi.org/10.1016/j.stem.2016.02.016
24. Miner JJ, Cao B, Govero J, Smith AM, Fernandez E, Cabrera OH, et al. Zika virus infection during pregnancy in mice causes placental damage and fetal demise. Cell. 2016;165:1081–91. http://dx.doi.org/10.1016/j.cell.2016.05.008
25. Halstead SB, Nimmannitya S, Cohen SN. Observations related to pathogenesis of dengue hemorrhagic fever. IV. Relation of disease severity to antibody response and virus recovered. Yale J Biol Med. 1970;42:311–28.
26. Halstead SB. Neutralization and antibody-dependent enhancement of dengue viruses. Adv Virus Res. 2003;60:421–67. http://dx.doi.org/10.1016/S0065-3527(03)60011-4
27. Halstead SB, Cohen SN. Dengue hemorrhagic fever at 60 years: early evolution of concepts of causation and treatment. Microbiol Mol Biol Rev. 2015;79:281–91. http://dx.doi.org/10.1128/MMBR.00009-15
28. Kliks SC, Nimmanitya S, Nisalak A, Burke DS. Evidence that maternal dengue antibodies are important in the development of dengue hemorrhagic fever in infants. Am J Trop Med Hyg. 1988;38:411–9.
29. Halstead SB, Lan NT, Myint TT, Shwe TN, Nisalak A, Kalyanarooj S, et al. Dengue hemorrhagic fever in infants: research opportunities ignored. Emerg Infect Dis. 2002;8:1474–9. http://dx.doi.org/10.3201/eid0812.020170
30. Simmons CP, Chau TN, Thuy TT, Tuan NM, Hoang DM, Thien NT, et al. Maternal antibody and viral factors in the pathogenesis of dengue virus in infants. J Infect Dis. 2007;196:416–24. http://dx.doi.org/10.1086/519170
31. Jessie K, Fong MY, Devi S, Lam SK, Wong KT. Localization of dengue virus in naturally infected human tissues, by immunohistochemistry and in situ hybridization. J Infect Dis. 2004;189:1411–8. http://dx.doi.org/10.1086/383043
32. Balsitis SJ, Coloma J, Castro G, Alava A, Flores D, McKerrow JH, et al. Tropism of dengue virus in mice and humans defined by viral nonstructural protein 3-specific immunostaining. Am J Trop Med Hyg. 2009;80:416–24.
33. Durbin AP, Vargas MJ, Wanionek K, Hammond SN, Gordon A, Rocha C, et al. Phenotyping of peripheral blood mononuclear cells during acute dengue illness demonstrates infection and increased activation of monocytes in severe cases compared to classic dengue fever. Virology. 2008;376:429–35. http://dx.doi.org/10.1016/j.virol.2008.03.028
34. Aye KS, Charngkaew K, Win N, Wai KZ, Moe K, Punyadee N, et al. Pathologic highlights of dengue hemorrhagic fever in 13 autopsy cases from Myanmar. Hum Pathol. 2014;45:1221–33. http://dx.doi.org/10.1016/j.humpath.2014.01.022
35. Balsitis SJ, Williams KL, Lachica R, Flores D, Kyle JL, Mehlhop E, et al. Lethal antibody enhancement of dengue disease in mice is prevented by Fc modification. PLoS Pathog. 2010;6:e1000790. http://dx.doi.org/10.1371/journal.ppat.1000790
36. Kyle JL, Beatty PR, Harris E. Dengue virus infects macrophages and dendritic cells in a mouse model of infection. J Infect Dis. 2007;195:1808–17. http://dx.doi.org/10.1086/518007
37. Orozco S, Schmid MA, Parameswaran P, Lachica R, Henn MR, Beatty R, et al. Characterization of a model of lethal dengue virus 2 infection in C57BL/6 mice deficient in the alpha/beta interferon receptor. J Gen Virol. 2012;93:2152–7. http://dx.doi.org/10.1099/vir.0.045088-0
38. Shresta S, Sharar KL, Prigozhin DM, Beatty PR, Harris E. Murine model for dengue virus-induced lethal disease with increased vascular permeability. J Virol. 2006;80:10208–17. http://dx.doi.org/10.1128/JVI.00062-06
39. Zellweger RM, Prestwood TR, Shresta S. Enhanced infection of liver sinusoidal endothelial cells in a mouse model of antibody-induced severe dengue disease. Cell Host Microbe. 2010;7:128–39. http://dx.doi.org/10.1016/j.chom.2010.01.004
40. Martínez Gómez JM, Ong LC, Lam JH, Binte Aman SA, Libau EA, Lee PX, et al. Maternal antibody-mediated disease enhancement in type I interferon-deficient mice leads to lethal disease associated with liver damage. PLoS Negl Trop Dis. 2016;10:e0004536. http://dx.doi.org/10.1371/journal.pntd.0004536
41. Guzman MG, Alvarez M, Halstead SB. Secondary infection as a risk factor for dengue hemorrhagic fever/dengue shock syndrome: an historical perspective and role of antibody-dependent enhancement of infection. Arch Virol. 2013;158:1445–59. http://dx.doi.org/10.1007/s00705-013-1645-3
42. Anderson KB, Gibbons RV, Cummings DA, Nisalak A, Green S, Libraty DH, et al. A shorter time interval between first and second dengue infections is associated with protection from clinical illness in a school-based cohort in Thailand. J Infect Dis. 2014;209:360–8. http://dx.doi.org/10.1093/infdis/jit436
43. Grange L, Simon-Loriere E, Sakuntabhai A, Gresh L, Paul R, Harris E. Epidemiological risk factors associated with high global frequency of inapparent dengue virus infections. Front Immunol. 2014;5:280. http://dx.doi.org/10.3389/fimmu.2014.00280
44. Guzmán MG, Kourí G, Valdés L, Bravo J, Vázquez S, Halstead SB. Enhanced severity of secondary dengue-2 infections: death rates

in 1981 and 1997 Cuban outbreaks. Rev Panam Salud Publica. 2002;11:223–7.
45. Gibbons RV, Kalanarooj S, Jarman RG, Nisalak A, Vaughn DW, Endy TP, et al. Analysis of repeat hospital admissions for dengue to estimate the frequency of third or fourth dengue infections resulting in admissions and dengue hemorrhagic fever, and serotype sequences. Am J Trop Med Hyg. 2007;77:910–3.
46. Marchette NJ, Halstead SB, Falkler WA Jr, Stenhouse A, Nash D. Studies on the pathogenesis of dengue infection in monkeys. 3. Sequential distribution of virus in primary and heterologous infections. J Infect Dis. 1973;128:23–30. http://dx.doi.org/10.1093/infdis/128.1.23
47. Moench TR, Griffin DE, Obriecht CR, Vaisberg AJ, Johnson RT. Acute measles in patients with and without neurological involvement: distribution of measles virus antigen and RNA. J Infect Dis. 1988;158:433–42. http://dx.doi.org/10.1093/infdis/158.2.433
48. Esolen LM, Ward BJ, Moench TR, Griffin DE. Infection of monocytes during measles. J Infect Dis. 1993;168:47–52. http://dx.doi.org/10.1093/infdis/168.1.47
49. Dowall SD, Graham VA, Rayner E, Atkinson B, Hall G, Watson RJ, et al. A susceptible mouse model for Zika virus infection. PLoS Negl Trop Dis. 2016;10:e0004658. http://dx.doi.org/10.1371/journal.pntd.0004658

Address for correspondence: Scott B. Halstead, Uniformed Services University of the Health Sciences, Preventive Medicine, 5824 Edson Ln N, Bethesda, MD 20852, USA; email: halsteads@erols.com

SYNOPSIS

Neurologic Complications of Influenza B Virus Infection in Adults, Romania

Corneliu P. Popescu, Simin A. Florescu, Emilia Lupulescu, Mihaela Zaharia, Gratiela Tardei, Mihaela Lazar, Emanoil Ceausu, Simona M. Ruta

Medscape EDUCATION ACTIVITY

This activity has been planned and implemented through the joint providership of Medscape, LLC and *Emerging Infectious Diseases*. Medscape, LLC is accredited by the American Nurses Credentialing Center (ANCC), the Accreditation Council for Pharmacy Education (ACPE), and the Accreditation Council for Continuing Medical Education (ACCME), to provide continuing education for the healthcare team.

Medscape, LLC designates this Journal-based CME activity for a maximum of 1.00 ***AMA PRA Category 1 Credit(s)™***. Physicians should claim only the credit commensurate with the extent of their participation in the activity.

All other clinicians completing this activity will be issued a certificate of participation. To participate in this journal CME activity: (1) review the learning objectives and author disclosures; (2) study the education content; (3) take the post-test with a 75% minimum passing score and complete the evaluation at http://www.medscape.org/journal/eid; and (4) view/print certificate. For CME questions, see page 728.

Release date: March 16, 2017; Expiration date: March 16, 2018

Learning Objectives

Upon completion of this activity, participants will be able to:

- Recognize clinical and neurologic manifestations of influenza B virus infection in adults, based on a case series from a tertiary facility in Romania
- Determine the course and treatment of influenza B virus infection in adults with neurologic complications
- Identify laboratory and neuroimaging findings of influenza B virus infection in adults with neurologic complications.

CME Editor

Thomas J. Gryczan, MS, Technical Writer/Editor, Emerging Infectious Diseases. *Disclosure: Thomas J. Gryczan, MS, has disclosed no relevant financial relationships.*

CME Author

Laurie Barclay, MD, freelance writer and reviewer, Medscape, LLC. *Disclosure: Laurie Barclay, MD, has disclosed the following relevant financial relationships: owns stock, stock options, or bonds from Pfizer.*

Authors

Disclosures: ***Corneliu Petru Popescu, MD; Simin Aysel Florescu, MD, PhD; Emilia Lupulescu, MD, PhD; Mihaela Zaharia, MD; Gratiela Tardei, MD, PhD; Mihaela Lazar, MD, PhD;*** *and* ***Simona Maria Ruta, MD, PhD,*** *have disclosed no relevant financial relationships.* ***Emanoil Ceausu, MD, PhD,*** *has disclosed the following relevant financial relationships: received grants for clinical research from MSD, Gilead.*

Author affiliations: Carol Davila University of Medicine and Pharmacy, Bucharest, Romania (C.P. Popescu, S.A. Florescu, E. Ceausu, S.M. Ruta); Dr. Victor Babes Clinical Hospital of Infectious and Tropical Diseases, Bucharest (C.P. Popescu, S.A. Florescu, M. Zaharia, G. Tardei, E. Ceausu); European Society of Clinical Microbiology and Infection Study Group for Infectious Diseases of the Brain, Basel, Switzerland (C.P. Popescu, M. Zaharia); National Institute of Research Cantacuzino, Bucharest (E. Lupulescu, M. Lazar); Stefan S. Nicolau Institute of Virology, Bucharest (S.M. Ruta)

DOI: http://dx.doi.org/10.3201/eid2304.161317

We characterized influenza B virus–related neurologic manifestations in an unusually high number of hospitalized adults at a tertiary care facility in Romania during the 2014–15 influenza epidemic season. Of 32 patients with a confirmed laboratory diagnosis of influenza B virus infection, neurologic complications developed in 7 adults (median age 31 years). These complications were clinically diagnosed as confirmed encephalitis (4 patients), possible encephalitis (2 patients), and cerebellar ataxia (1 patient). Two of the patients died. Virus sequencing identified influenza virus B (Yam)-lineage clade 3, which is representative of the B/Phuket/3073/2013 strain, in 4 patients. None of the patients had been vaccinated against influenza. These results suggest that influenza B virus can cause a severe clinical course and should be considered as an etiologic factor for encephalitis.

Influenza viruses are negative single-stranded RNA viruses belonging to the family *Orthomyxoviridae* and cause worldwide epidemics of influenza with high rates of illness and death. Human influenza A and B viruses cause a self-limited acute respiratory infection. This infection has an abrupt onset and causes fever, chills, headache, cough, and myalgia. Every year, different strains of influenza viruses emerge because of continuous antigenic drift and interspecies gene reassortment, which cause antigenic shifts. Severe complications of influenza can involve the lower respiratory tract (pneumonia), heart (myocarditis), and central nervous system (encephalitis, myelitis, meningitis, febrile and afebrile seizures, Guillain-Barré syndrome, cerebellar ataxia) and can lead to death (*1–3*).

Although type A and B influenza viruses might induce neurologic complications, most published studies on virus neurotropism have focused on influenza A viruses, with an emphasis on the new A(H1N1)pdm09 virus strain after 2009 (*4–7*). Influenza B virus, which was isolated from a child in 1940, has steadily adapted to humans without a stable animal reservoir (*8–10*). The earliest report of a case of influenza B viral encephalitis was in London, UK, in 1946 (*11*), but only sporadic cases with neurologic manifestations have been reported, especially in children and adolescents. Influenza B is generally considered a mild disease with less frequent neurologic complications than influenza A (*4–7*).

There was major increased influenza activity in Romania during the 2014–15 influenza season: 3.5 times more cases of influenza-like illness (ILI) and acute respiratory infections than in the previous season. A total of 4,511 case-patients with ILI were reported, of which 1,709 (37.9%) were hospitalized; 3,297 (73.1%) were >14 years of age. Influenza B viruses prevailed (in 529 [56.4%] of the 938 laboratory-confirmed influenza cases), unlike the rest of Europe, where there was a predominance of type A influenza strains (*12*). We characterized influenza B virus–related neurologic manifestations diagnosed at a tertiary care facility in Romania during the 2014–15 influenza season.

Materials and Methods

Ethical Approval

This study was approved by the ethics committee of the Stefan S. Nicolau Institute of Virology (Bucharest, Romania). Although this was a retrospective study, informed consent was obtained from each patient included in the study, as part of routine hospital activity.

Patients

We conducted a retrospective study of 7 patients given a diagnosis of influenza in whom neurologic complications developed. These patients were hospitalized in a tertiary care facility (Dr. Victor Babes Clinical Hospital of Infectious and Tropical Diseases, Bucharest, Romania) during the 2014–15 influenza season.

We used the case definition for encephalitis from the 2013 Consensus Statement of the International Encephalitis Consortium. Major criterion was altered mental status (defined as decreased or altered level of consciousness, lethargy, or personality change) lasting ≥24 hours with no alternative cause identified. Minor criteria were fever (temperature ≥38°C), generalized or partial seizures, new onset of focal neurologic findings, CSF leukocyte count ≥5 cells/mm^3, and abnormality of brain parenchyma on neuroimaging suggestive of encephalitis (*13*).

We collected nasopharyngeal swab specimens from all patients with ILI and sent these specimens to the National Reference Center for Influenza (Cantacuzino Institute, Bucharest, Romania) for antigenic and genetic characterization. Specimens were examined by using real-time reverse transcription PCRs (RT-PCRs) with the Superscript III Platinum One-Step Quantitative RT-PCR System (Invitrogen, Carlsbad, CA, USA) for influenza type A and type B viruses. Samples positive for influenza A viruses were tested by using a second real-time RT-PCR that discriminated between influenza A(H1N1)pdm09 and A(H3N2) virus subtypes. For samples positive for influenza B viruses, we used a second real-time RT-PCR and specific minor-groove binder probes to determine lineage (*14*).

Positive specimens were inoculated into an MDCK line, and virus isolates were characterized antigenically by using a hemagglutination inhibition assay and turkey/guinea pig erythrocytes. We used the conventional Sanger sequencing technique to monitor influenza virus evolution for the complete hemagglutinin (HA) gene. The PRISM BigDye Terminator v3.1 Ready Reaction Cycle Sequencing Kit (Applied Biosystems, Foster City, CA, USA) was used to sequence DNA templates on a PRISM 3100-Avant Genetic Analyzer (Applied Biosystems). We determined

genotypes of all virus sequences from patients by alignment with sequences found in Romania with World Health Organization reference viruses. We performed phylogenic analysis by using maximum-likelihood inference and a generalized time-reversible model of nucleotide substitution and a Γ model of rate heterogeneity with RAxML version 8.00 software (*15*).

Results

Patients

Patient 1 was a 28-year-old woman who had uncontrolled hyperthyroidism, a 3-day history of high fever (temperature >39°C), headache, sleepiness, left upper limb motor deficit, and a Glasgow Coma Scale (GCS) score of 3–4/15. Results of cerebrospinal fluid (CSF) testing were unremarkable. The patient was intubated and mechanically ventilated after 4 hours of hospitalization.

Magnetic resonance imaging (MRI) of the brain (Figure 1) showed multiple areas of T2-associated hyperintensities associated with restricted diffusion with involvement of the genu corpus callosum bilateral internal capsule and several areas of white matter in the right frontal lobe. Hyperintensities were visible at the limit between the right parietal and occipital lobe (axial T2-associated and diffusion-weighted imaging), and multiple high-signal lesions associated with restricted diffusion were present in the right caudate nucleus head and the subcortical and deep white matter of the frontal lobes (coronal fluid–attenuated inversion recovery and diffusion-weighted imaging). Despite intensive antimicrobial drug treatment with oseltamivir, acyclovir, meropenem, mannitol, corticosteroids, and thyrozol, the patient died 7 days after admission.

Patient 2 was a previously healthy 37-year-old woman who was hospitalized after 2 days of fever, rhinorrhea, myalgia that progressed to a headache, sleepiness, photophobia, vertigo, stiff neck, and a positive Romberg sign. Results of computed tomography (CT) and analysis of CSF were unremarkable. Complete resolution occurred after 9 days of treatment with oseltamivir and mannitol.

Patient 3 was a previously healthy 55-year-old woman with a history of influenza A(H3N2) virus encephalitis (in

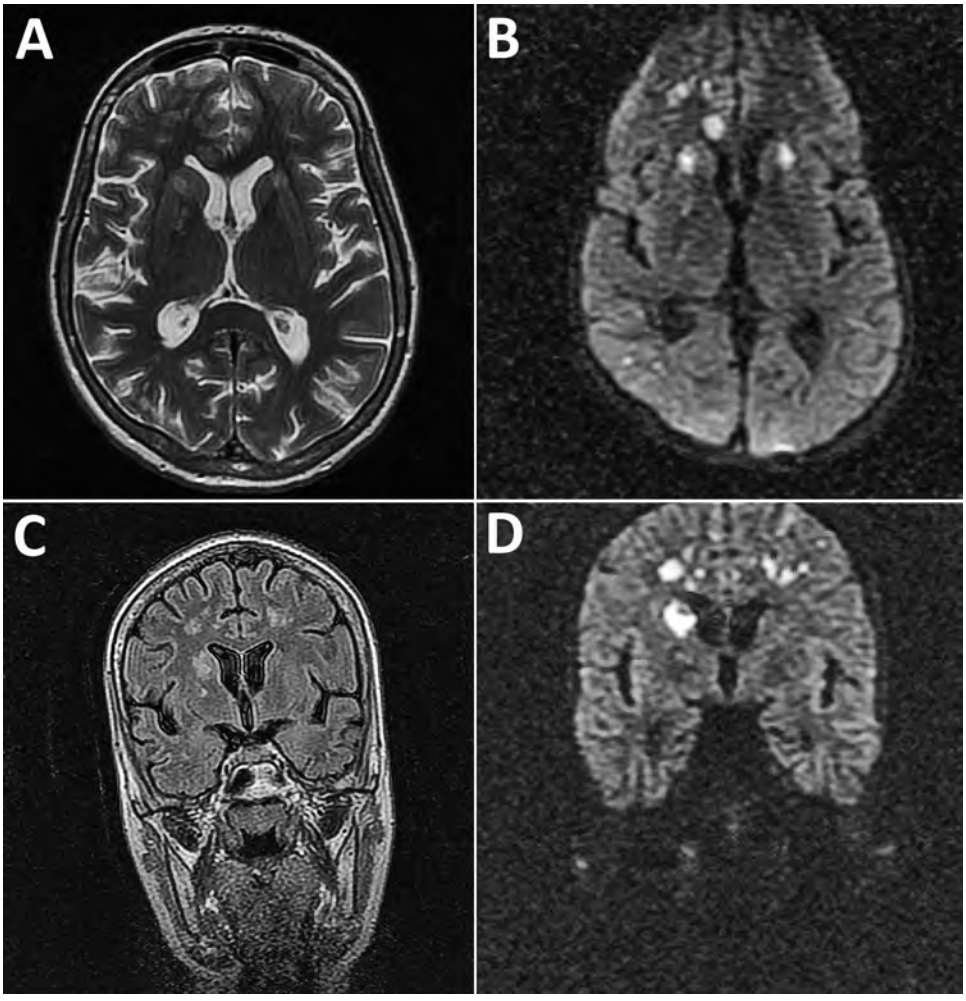

Figure 1. Magnetic resonance imaging of the brain of a 28-year-old woman (patient 1) who had neurologic complications of influenza B virus infection, Romania. A) Axial T2 image showing multiple areas of T2-associated hyperintense lesions with involvement of the genu corpus callosum, bilateral internal capsule, and several areas of white matter in the right frontal lobe, and more discreetly at the limit between the right parietal and occipital lobe. B) Axial diffusion-weighted image showing restricted diffusion associated with lesions. C) Coronal fluid–attenuated inversion recovery image showing multiple hyperintense lesions in the right caudate head and the cortical and deep white matter of the frontal lobes. D) Coronal diffusion-weighted image showing restricted diffusion associated with lesions.

2012). The patient was hospitalized after transfer from another clinic 10 days after onset of illness with signs and symptoms that included fever, confusion, photophobia, dizziness, right facial paralysis, aphasia, stiff neck, and coma (GCS score 8). Onset of neurologic signs occurred on day 5. Results of CT on day 7 were unremarkable. We found increased levels of proteins and cells in the CSF. Brain MRI showed symmetric diffusion restriction in the bilateral anterior frontal cortex (Figure 2). The patient was intubated and mechanically ventilated for 24 hours. She showed good progression after being given mannitol, dexamethasone, oseltamivir, and acyclovir. The patient was discharged with complete resolution after 18 days of hospitalization.

Patient 4 was a 20-year-old woman who had Russell–Silver syndrome and was being given prednisone and levothyroxine. She was admitted to an intensive care unit (ICU) already mechanically ventilated. Onset of illness was 5 days before admission and included fever, cough, and agitation. After 3 days in the hospital, nystagmus, stiff neck, and a GCS score of 9–10 were observed. Results of CSF testing and cerebral CT and MRI were unremarkable. She was given mannitol, methylprednisolone, and oseltamivir. Her condition improved after 17 days of hospitalization and was followed by complete recovery.

Patient 5 was a 57-year-old man who came to our clinic after 3 days of fever, chills, and cough. In the preceding 24 hours, headache, dysarthria, right side motor deficit, and vomiting developed. Results of CSF testing and cranial CT and MRI were unremarkable. The patient was given oseltamivir and mannitol. After 10 days, the patient was discharged, and he showed complete resolution.

Patient 6 was a 31-year-old woman who had recent breast implants. The patient was hospitalized after 4 days of fever, headache, vomiting, vertigo, photophobia, and movement and balance disorders. Results of CSF testing were unremarkable. She was given oseltamivir and mannitol, and her condition improved after 5 days.

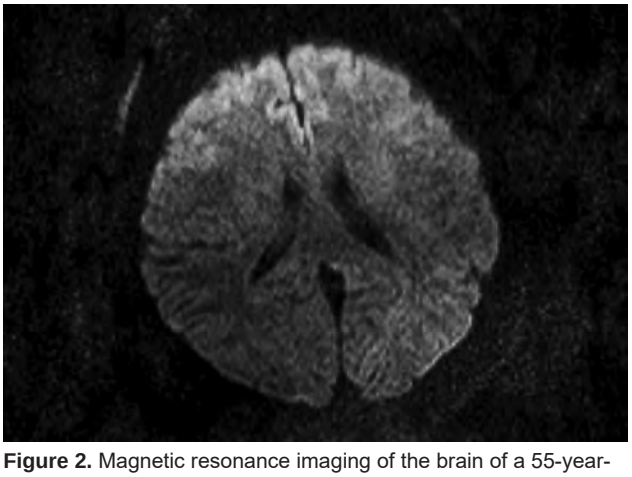

Figure 2. Magnetic resonance imaging of the brain of a 55-year-old woman (patient 3) who had neurologic complications of influenza B virus infection, Romania. Axial diffusion-weighted image showing restricted diffusion in the bilateral frontal cortex.

Patient 7 was a 27-year-old woman who had influenza, fever, myalgia, headache, and vomiting 3 days before hospitalization. After 2 days, she became lethargic, had aphasia and seizures, and entered a coma; GCS score decreased to 3. Results of initial CSF testing were unremarkable. She was intubated, mechanically ventilated, and transferred to our clinic. Results of CT were unremarkable. However, MRI showed an abnormal result (multiple areas of hyperintensities).

At admission, patient 7 was comatose and intubated. She had unreactive fixed mydriasis, upward deviation of the eyes, and no corneal reflex and plantar cutaneous reflexes. Results of additional CSF testing showed pleocytosis and a high level of albumin (3.906 g/L). Renal failure and ventricular tachyarrhythmia developed. Despite treatment with oseltamivir, acyclovir, mannitol, methylprednisolone, and meropenem, the patient continued to show signs of brain death and died 3 days after admission.

Observations

The peak of the influenza season in Romania was during February–March 2015. A total of 110 patients with ILI (90 female patients and 20 male patients) were hospitalized at the tertiary care facility during January–April 2015. The median age of patients was 43 years (range 4–93 years); only 3 patients were <18 years of age. None of the patients had been vaccinated against influenza for the current season. There were 57 patients with ILI laboratory-confirmed influenza infection: 32 patients (56.2%) were infected with an influenza B strain, 14 (24.5%) with an influenza A/H3 strain, and 11 (19.3%) with the A(H1N1)pdm09 strain. These 3 strains were present in Romania at similar prevalences throughout the influenza season.

A complicated form of influenza was diagnosed for 28 (49.1%) patients, of whom 19 (33.3%) had respiratory complications (8 infected with the A(H1N1)pdm09 strain, 6 with the A/H3 strain, and 5 with the B strain), and 9 (15.7%) had neurologic complications (8 with the B strain and 1 with the (A/H1N1)pdm09 strain). Two patients who had febrile seizures as the only neurologic manifestation were excluded from analysis (1 child with a history of febrile seizures and 1 adult with epilepsy). Eight of the 9 patients with neurologic complications were female patients. Of those infected with an influenza B strain, 7 were adults (median age 31 years, range 20–57 years), and 1 was a 4-year-old girl. Six of the 7 adult patients infected with an influenza B strain in whom neurologic manifestations developed were women.

Antiviral treatment with a neuraminidase inhibitor (oseltamivir, 75 mg 2×/d for adults and 37.5 mg 2×/d for the child) was administered to all patients upon presentation.

However, most patients presented late after onset of disease, and only 1 received oseltamivir within the first 48 hours of disease onset; the other patients received antiviral treatment 72 hours after disease onset.

Demographic, clinical, imaging and laboratory data for the 7 adult patients with neurologic manifestations and laboratory-confirmed influenza B virus infection are shown in the Table. None of the patients had preexisting neurologic diseases, and the average time from disease onset to hospitalization was 4.28 days. On the basis of the case definition, 4 patients were given a diagnosis of confirmed encephalitis (major criteria and ≥3 minor criteria and laboratory-confirmed influenza), 2 were given a diagnosis of possible encephalitis (major criteria and 2 minor criteria), and 1 was given a diagnosis of cerebellar ataxia (no major criteria but with neurologic manifestations).

Cerebral MRI was performed for 6 patients and CT was performed for 2 patients. Abnormal brain imaging results were observed for 3 patients: changes consistent with multiple areas of hyperintensities visible in T2-associated with restricted diffusion for patients 1 and 7 (patient 1; Figure 1) and cerebral edema and diffusion restriction for patient 3 (Figure 2). Six patients were admitted to the ICU; 4 of these patients required intubation and mechanical ventilation because of neurologic complications. Two patients died, 3 and 7 days after admission. The other 5 patients showed a good outcome with complete resolution. At a follow-up 1 month after discharge, results of neurologic examinations for the 5 patients were unremarkable without any signs or symptoms during this period.

Lumbar puncture was performed for all 7 patients. Results of CSF analysis were abnormal for 3 patients (pleocytosis [>5 cells/mm^3] and increased protein levels). All CSF samples were negative for influenza virus nucleic acids, enteroviruses, and herpes viruses.

Genetic analysis of the HA sequences of influenza B viruses isolated from nasopharyngeal swab specimens was successful for 4 patients (patients 1, 2, 5, and 7) (Table).

Table. Characteristics of 7 patients with neurologic complications of influenza B virus infection, Romania*

Characteristic	Patient 1	2	3	4	5	6	7
Age, y/sex	28/F	37/F	55/F	20/F	57/M	31/F	27/F
Days from illness onset	3	2	10	5	3	4	3
Medical history	Uncontrolled hyperthyroidism	Unremarkable	Influenza A(H3N2) virus encephalitis in 2012	Treated for Russell–Silver syndrome	Unremarkable	Recent breast implants	Unremarkable
Leukocyte count, cells/mm^3	2	2	10	5	2	3	13
CSF							
Protein, g/L	0.143	0.270	2.305	0.251	0.313	0.162	7.156
Glucose, g/L	0.61	0.50	0.74	1.07	0.55	0.71	1.22
Chloride, g/L	ND	ND	7.60	6.78	7.10	6.80	7.02
Virus type	B seq EPI_ISL_ 179707	B seq EPI_ISL_ 179711	B	B	B seq EPI_ISL_ 182519	B	B seq EPI_ISL_ 182518
Cerebral imaging result	MRI, abnormal†	CT, normal	MRI, abnormal‡	MRI, normal	MRI, normal	NA	MRI, abnormal§
Diagnosis	Confirmed encephalitis	Possible encephalitis	Confirmed encephalitis	Confirmed encephalitis	Possible encephalitis	Cerebellar ataxia	Confirmed encephalitis
Length of hospitalization, d	7	9	18	17	10	5	3
Outcome	Died	Complete resolution	Complete resolution	Complete resolution	Complete resolution	Complete resolution	Died
Clinical findings	Fever, headache, sleepiness, left upper limb motor deficit, coma, GCS score 3–4	Fever, headache, sleepiness, photophobia, vertigo, stiff neck, positive Romberg sign	Fever, confusion, photophobia, dizziness, right facial paralysis, aphasia, stiff neck, coma, GCS score 8	Fever, agitation, nystagmus, stiff neck, coma, GCS score 9–10	Fever, headache, dysarthria, right side motor deficit, vomiting	Fever, headache, vomiting, vertigo, photophobia, ataxia, positive Romberg sign, movement and balance disorder	Fever, headache, vomiting, lethargy, aphasia, upward deviation of eyes, seizures, coma, GCS score 3

*All patients showed negative RT-PCR results for influenza B virus in CSF. CSF, cerebrospinal fluid; CT, computed tomography; GCS, Glasgow coma scale; MRI, magnetic resonance imaging; NA, not available; ND, not determined.
†MRI on day 3. See Figure 1 for a detailed description.
‡MRI on day 8. See Figure 2 for a detailed description.
§MRI on day 2 showed multiple areas of hyperintensities.

HA phylogenetic analysis showed that all strains belonged to Yamagata-lineage clade 3, representative strain B/Phuket/3073/2013, which is distinct from the World Health Organization recommended strain included in the 2014–2015 vaccine (B/Massachusetts/2/2012–like virus).

Discussion

We report an unusually high number of adults infected with influenza B virus who had neurologic complications at a tertiary care facility in Romania. Influenza B neurologic manifestations have been reported mainly in children. In Japan in 1998–1999, an outbreak of influenza-associated encephalitis/encephalopathy (148 cases, mostly linked with influenza A/H3N2 infection, only 17 with influenza B viruses) was observed primarily in children <5 years of age (*16*). In a 2-year National British Surveillance study, 25 cases (21 in children) of neurologic disorders were identified in patients with influenza in the United Kingdom, but only 4 of these patients (all children) were infected with influenza B virus (*17*). Eleven cases of neurologic complications in children with influenza B virus infection were reported in Taiwan in 2006 (*18*). Other cases were also reported: 1 case of influenza B virus–associated optic neuritis after meningoencephalitis in a 10-year-old boy in Italy (*19*), and 1 case of influenza B virus–associated acute necrotizing encephalopathy in a 3-year-old boy in North America (*20*).

Sporadic cases of influenza B virus with neurologic manifestations in adults have also been reported: 2 adults with influenza B virus–associated encephalopathy (*21*), 1 person with nonconvulsive epilepticus after influenza virus B infection (*22*), and 6 of 15 patients with influenza B virus–associated encephalitis (*7*). In our study, we report 7 case-patients with influenza B virus–associated neurologic complications; 2 of these case-patients died. In Romania during the 2014–15 influenza season, the mortality rate for patients with confirmed influenza B virus infections was 1.7% (*12*). In the tertiary care facility we studied, the overall mortality rate for patients infected with influenza B virus was 9.3% (3/32 confirmed case-patients), and the mortality rate for patients with influenza B virus–related neurologic complications was 28.5% (2/7 adult case-patients). All patients with neurologic complications admitted to the ICU who required intubation and mechanical ventilation did not have respiratory complications, the 2 deaths were caused by neurologic manifestations, not respiratory failure.

Although the 2014–15 influenza season in Romania was severe, older persons were less frequently infected (12.8% of ILI cases recorded were in patients >65 years of age), but hospitalization rates increased with age (from 23.7% in persons <0–1 year of age to 36.7% in persons 15–49 years of age, and 61.5% in persons >65 years of age) (*12*). The high mortality rate is not necessarily representative of the severity of influenza B virus infection because persons with severe cases are generally referred to the tertiary care facility. However, these data highlight the potentially severe progression of influenza B virus infection in adults. This severe evolution has been reported in children. In the United States in 2010–11, influenza B viruses were involved in 38% of deaths in children caused by influenza (*23*). In Japan, a 6-year national surveillance identified 50 patients (median age 4.5 years) with of influenza B virus–associated encephalopathy/encephalitis, of whom 7 (14%) died (*24*).

Most patients in our study had no previous concurrent conditions. One patient (patient 3) had a prior episode of influenza-related encephalitis with the same clinical pattern as the present infection (the previous infection was diagnosed at the same hospital in 2012). At that time, the isolated virus was identified as influenza A(H3N2) virus. This isolate was not tested for genetic mutations that might predispose a person to recurrent encephalitis. However, such infections have been reported in a family infected with a virus containing a Ran binding protein 2 mutation, which is autosomal dominantly transmitted (*17*,*25*).

In our study we isolated virus from nasopharyngeal samples; none of the CSF samples were positive for virus nucleic acids. However, influenza viruses are rarely identified in the CSF (*2*,*26*). Abnormal findings for CSF were observed in 3 patients with encephalitis who required hospitalization in the ICU (1 patient died). Two patients, both admitted to the ICU, showed major increases in protein levels in CSF, a profile usually seen in patients with severe cases (*2*,*26*,*27*). Although influenza virus nucleic acids have been detected in brain tissue, ependymal, and Purkinje cells (*28*), several studies have emphasized the role of neuroinflammation in the pathogenesis of neurologic complications mediated by high levels of proinflammatory cytokines in the CSF (cytokine storm), increased systemic inflammatory responses, or blood–brain barrier dysfunction (*29*–*34*). However, neurotropism has been investigated mainly for influenza A viruses; information on neurovirulence caused by influenza B viruses is lacking.

All isolated virus strains belonged to B(Yam)-lineage clade 3, representative strain B/Phuket/3073/2013, which belongs to a distinct antigenic cluster different from that recommended by the World Health Organization for vaccination in the Northern Hemisphere during the 2014–15 influenza season. This strain and the vaccine strain (B/Massachusetts/02/2012–like from the B/Yamagata/16/88 lineage) were cocirculating in Romania during the 2014–15 influenza season (*35*). Antigenic mismatch between a vaccine strain and a strain that prevails in a specific influenza season is common for influenza B viruses because of cocirculation of the Victoria and Yamagata lineages (*36*), and additional challenges are increased by antigenic drift of the B/Yamagata strain.

None of the patients in our study in whom neurologic complications developed were vaccinated against influenza. Vaccination coverage in Romania was extremely low; only 2.5% of the general population were vaccinated (*12*). The efficacy of the 2014–15 vaccine against influenza B virus was modest, ranging from 41% in persons 15–59 years of age to 62% in persons <14 years of age, as reported by a multicenter case–control study in the population in Europe (*37*). Some studies support the inclusion of both lineages of influenza B virus in the vaccine to reduce illness (*38*), although others suggest a more cautious approach, arguing that addition of a second influenza B virus lineage leads to a modest reduction in influenza-associated outcomes (*39*). Recently, a hedging strategy for selection of the influenza B virus lineage included in the standard trivalent vaccine has been suggested as the most effective in terms of long-term protection rates (*40*).

This study had several limitations. A cluster of severe cases is not uncommon in a tertiary care facility with an ICU, which might lead to overestimation of the neurologic complication rate. Nevertheless, the hospital admissions we analyzed are representative for Romania (18,710 admissions in 2015 for a 500-bed hospital that covers the capital city of Bucharest and 8 adjacent counties in Romania; ≈3 million inhabitants). Oseltamivir was given to all patients, often with a delay after infection onset because of late presentation. Although neuraminidase inhibitors are considered more effective against influenza A viruses than influenza B viruses, the mechanisms of influenza B virus drug resistance are not well understood (*41*). Sequencing the isolated strains was successful for isolates from 4 of the patients. Lack of amplification for the other 3 isolates could be partially associated with low levels of nucleic acids in the clinical specimens and lower sensitivity of the amplification procedures used for sequencing than the techniques used for initial virus detection.

In conclusion, we report that influenza B virus infection can cause a severe clinical course in adults, with neurologic complications in a large number of patients. Continuous evolution of influenza viruses can give rise to virulent strains that escape the immune response, particularly when a large part of the population remains unvaccinated.

Acknowledgment

We thank Vasile Theodor for interpreting MRIs.

Dr. Popescu is an assistant professor in the Virology Department, Carol Davila University of Medicine and Pharmacy, Bucharest; head of the Intensive Care Unit and Infectious and Tropical Diseases Department, Dr. Victor Babes Clinical Hospital of Infectious and Tropical Diseases, Bucharest; a member of the European Society of Clinical Microbiology and Infection Study Group for Infectious Diseases of the Brain, Basel, Switzerland; and a doctoral candidate at the School of Advanced Studies of the Romanian Academy, Bucharest. Her primary research interest is virus infections of the central nervous system.

References

1. Studahl M. Influenza virus and CNS manifestations. J Clin Virol. 2003;28:225–32. http://dx.doi.org/10.1016/S1386-6532(03)00119-7
2. Ekstrand JJ. Neurologic complications of influenza. Semin Pediatr Neurol. 2012;19:96–100. http://dx.doi.org/10.1016/j.spen.2012.02.004
3. Ravenholt RT, Foege WH. 1918 influenza, encephalitis lethargica, parkinsonism. Lancet. 1982;2:860–4. http://dx.doi.org/10.1016/S0140-6736(82)90820-0
4. McCullers JA, Facchini S, Chesney PJ, Webster RG. Influenza B virus encephalitis. Clin Infect Dis. 1999;28:898–900. http://dx.doi.org/10.1086/515214
5. Newland JG, Laurich VM, Rosenquist AW, Heydon K, Licht DJ, Keren R, et al. Neurologic complications in children hospitalized with influenza: characteristics, incidence, and risk factors. J Pediatr. 2007;150:306–10. http://dx.doi.org/10.1016/j.jpeds.2006.11.054
6. Sazgar M, Robinson JL, Chan AK, Sinclair DB. Influenza B acute necrotizing encephalopathy: a case report and literature review. Pediatr Neurol. 2003;28:396–9. http://dx.doi.org/10.1016/S0887-8994(03)00008-0
7. Newland JG, Romero JR, Varman M, Drake C, Holst A, Safranek T, et al. Encephalitis associated with influenza B virus infection in 2 children and a review of the literature. Clin Infect Dis. 2003;36:e87–95. http://dx.doi.org/10.1086/368184
8. Francis T Jr. A new type of virus from epidemic influenza. Science. 1940;92:405–8. http://dx.doi.org/10.1126/science.92.2392.405
9. Chen R, Holmes EC. The evolutionary dynamics of human influenza B virus. J Mol Evol. 2008;66:655–63. http://dx.doi.org/10.1007/s00239-008-9119-z
10. McCullers JA, Hayden FG, Fatal Influenza B. Fatal influenza B infections: time to reexamine influenza research priorities. J Infect Dis. 2012;205:870–2. http://dx.doi.org/10.1093/infdis/jir865
11. Leigh AD. Infections of the nervous system occurring during an epidemic of influenza B. BMJ. 1946;2:936–8. http://dx.doi.org/10.1136/bmj.2.4485.936
12. National Center for Infectious Diseases Control. Analyses of trends of communicable diseases under surveillance, 2014 [in Romanian] [cited 2016 Sep 9]. http://www.cnscbt.ro/index.php/rapoarte-anuale/548-analiza-evolutiei-bolilor-transmisibile-aflate-in-supraveghere-raport-pentru-anul-2014 /file
13. Tunkel AR, Glaser CA, Bloch KC, Sejvar JJ, Marra CM, Roos KL, et al.; Infectious Diseases Society of America. The management of encephalitis: clinical practice guidelines by the Infectious Diseases Society of America. Clin Infect Dis. 2008;47:303–27. http://dx.doi.org/10.1086/589747
14. Cherciu CM, Necula G, Mihai ME, Ivanciuc AE, Lazăr M, Ţecu C, et al. Differentiation of influenza B lineages from clinical samples by one-step real-time RT-PCR. Roum Arch Microbiol Immunol. 2014;73:25–9.
15. Stamatakis A. RAxML version 8: a tool for phylogenetic analysis and post-analysis of large phylogenies. Bioinformatics. 2014;30:1312–3. http://dx.doi.org/10.1093/bioinformatics/btu033
16. Morishima T, Togashi T, Yokota S, Okuno Y, Miyazaki C, Tashiro M, et al.; Collaborative Study Group on Influenza-Associated Encephalopathy in Japan. Encephalitis and encephalopathy associated with an influenza epidemic in Japan. Clin Infect Dis. 2002;35:512–7. http://dx.doi.org/10.1086/341407

17. Goenka A, Michael BD, Ledger E, Hart IJ, Absoud M, Chow G, et al. Neurological manifestations of influenza infection in children and adults: results of a National British Surveillance Study. Clin Infect Dis. 2014;58:775–84. http://dx.doi.org/10.1093/cid/cit922
18. Lin CH, Huang YC, Chiu CH, Huang CG, Tsao KC, Lin TY. Neurologic manifestations in children with influenza B virus infection. Pediatr Infect Dis J. 2006;25:1081–3. http://dx.doi.org/10.1097/01.inf.0000243194.80616.a9
19. Vianello FA, Osnaghi S, Laicini EA, Milani GP, Tardini G, Cappellari AM, et al. Optic neuritis associated with influenza B virus meningoencephalitis. J Clin Virol. 2014;61:463–5. http://dx.doi.org/10.1016/j.jcv.2014.09.010
20. Samanta D. Influenza B-associated acute necrotizing encephalopathy of childhood: a report from North America. Acta Neurol Belg. 2016;116:383–5. http://dx.doi.org/10.1007/s13760-015-0573-2
21. Ak Ö, Biteker F, Cag Y, Öcal G, Benzonana N, Ciblak MA, et al. Influenza B-associated encephalopathy in two adults. J Infect Chemother. 2012;18:961–4. http://dx.doi.org/10.1007/s10156-012-0413-8
22. Une H, Uehara T, Tateishi T, Shigetou H, Oyagi Y, Kira J. Case of non-convulsive status epilepticus after influenza virus B infection [in Japanese]. Rinsho Shinkeigaku. 2014;54:227–30. http://dx.doi.org/10.5692/clinicalneurol.54.227
23. Centers for Disease Control and Prevention. Influenza-associated pediatric deaths—United States, September 2010–August 2011. MMWR Morb Mortal Wkly Rep. 2011;60:1233–8.
24. Gu Y, Shimada T, Yasui Y, Tada Y, Kaku M, Okabe N. National surveillance of influenza-associated encephalopathy in Japan over six years, before and during the 2009–2010 influenza pandemic. PLoS One. 2013;8:e54786. http://dx.doi.org/10.1371/journal.pone.0054786
25. Wang GF, Li W, Li K. Acute encephalopathy and encephalitis caused by influenza virus infection. Curr Opin Neurol. 2010;23:305–11. http://dx.doi.org/10.1097/WCO.0b013e328338f6c9
26. Maricich SM, Neul JL, Lotze TE, Cazacu AC, Uyeki TM, Demmler GJ, et al. Neurologic complications associated with influenza A in children during the 2003-2004 influenza season in Houston, Texas. Pediatrics. 2004;114:e626–33. http://dx.doi.org/10.1542/peds.2004-0143
27. Kawashima H, Morichi S, Okumara A, Nakagawa S, Morishima T; Collaborating Study Group on Influenza-Associated Encephalopathy in Japan. National survey of pandemic influenza A (H1N1) 2009-associated encephalopathy in Japanese children. J Med Virol. 2012;84:1151–6. http://dx.doi.org/10.1002/jmv.23317
28. Takahashi M, Yamada T, Nakashita Y, Saikusa H, Deguchi M, Kida H, et al. Influenza virus-induced encephalopathy: clinico-pathologic study of an autopsied case. Pediatr Int. 2000;42:204–14. http://dx.doi.org/10.1046/j.1442-200x.2000.01203.x
29. Ichiyama T, Morishima T, Kajimoto M, Matsushige T, Matsubara T, Furukawa S. Matrix metalloproteinase-9 and tissue inhibitors of metalloproteinases 1 in influenza-associated encephalopathy. Pediatr Infect Dis J. 2007;26:542–4. http://dx.doi.org/10.1097/INF.0b013e31803994a0
30. To KK, Hung IF, Li IW, Lee KL, Koo CK, Yan WW, et al. Delayed clearance of viral load and marked cytokine activation in severe cases of pandemic H1N1 2009 influenza virus infection. Clin Infect Dis. 2010;50:850–9. http://dx.doi.org/10.1086/650581
31. Christian LM, Franco A, Iams JD, Sheridan J, Glaser R. Depressive symptoms predict exaggerated inflammatory responses to an in vivo immune challenge among pregnant women. Brain Behav Immun. 2010;24:49–53. http://dx.doi.org/10.1016/j.bbi.2009.05.055
32. Cárdenas G, Soto-Hernández JL, Díaz-Alba A, Ugalde Y, Mérida-Puga J, Rosetti M, et al. Neurological events related to influenza A (H1N1) pdm09. Influenza Other Respi Viruses. 2014;8:339–46. http://dx.doi.org/10.1111/irv.12241
33. Henry CJ, Huang Y, Wynne AM, Godbout JP. Peripheral lipopolysaccharide (LPS) challenge promotes microglial hyperactivity in aged mice that is associated with exaggerated induction of both pro-inflammatory IL-1beta and anti-inflammatory IL-10 cytokines. Brain Behav Immun. 2009;23:309–17. http://dx.doi.org/10.1016/j.bbi.2008.09.002
34. Davis LE, Koster F, Cawthon A. Neurologic aspects of influenza viruses. Handb Clin Neurol. 2014;123:619–45. http://dx.doi.org/10.1016/B978-0-444-53488-0.00030-4
35. World Health Organization. Recommended composition of influenza virus vaccines for use in the 2014–2015 northern hemisphere influenza season [cited 2016 Sep 5]. http://www.who.int/influenza/vaccines/virus/recommendations/2014_15_north/en/
36. Ambrose CS, Levin MJ. The rationale for quadrivalent influenza vaccines. Hum Vaccin Immunother. 2012;8:81–8. http://dx.doi.org/10.4161/hv.8.1.17623
37. Valenciano M, Kissling E, Reuss A, Rizzo C, Gherasim A, Horváth JK, et al. I-MOVE multicentre case-control team. Vaccine effectiveness in preventing laboratory-confirmed influenza in primary care patients in a season of co-circulation of influenza A(H1N1)pdm09, B and drifted A(H3N2), I-MOVE Multicentre Case-Control Study, Europe 2014/15. Euro Surveill. 2016;21:30139. http://dx.doi.org/10.2807/1560-7917.ES.2016.21.7.30139
38. Belshe RB. The need for quadrivalent vaccine against seasonal influenza. Vaccine. 2010;28(Suppl 4):D45–53. http://dx.doi.org/10.1016/j.vaccine.2010.08.028
39. Reed C, Meltzer MI, Finelli L, Fiore A. Public health impact of including two lineages of influenza B in a quadrivalent seasonal influenza vaccine. Vaccine. 2012;30:1993–8. http://dx.doi.org/10.1016/j.vaccine.2011.12.098
40. Mosterín Höpping A, Fonville JM, Russell CA, James S, Smith DJ. Influenza B vaccine lineage selection: an optimized trivalent vaccine. Vaccine. 2016;34:1617–22. http://dx.doi.org/10.1016/j.vaccine.2016.01.042
41. Burnham AJ, Baranovich T, Govorkova EA. Neuraminidase inhibitors for influenza B virus infection: efficacy and resistance. Antiviral Res. 2013;100:520–34. http://dx.doi.org/10.1016/j.antiviral.2013.08.023

Address for correspondence: Corneliu P. Popescu, Carol Davila University of Medicine and Pharmacy, Dr Victor Babes Clinical Hospital of Infectious and Tropical Diseases, Sos Mihai Bravu 281, Sector 3, Bucharest, Romania; email: cornel160@yahoo.com

Implementation and Initial Analysis of a Laboratory-Based Weekly Biosurveillance System, Provence-Alpes-Côte d'Azur, France

Michael Huart, Gabriel Bedubourg, Cédric Abat, Philippe Colson, Jean Marc Rolain, Hervé Chaudet, Pierre Edouard Fournier, Didier Raoult, Xavier Deparis

We describe the implementation of an automated infectious disease surveillance system that uses data collected from 210 microbiologic laboratories throughout the Provence-Alpes-Côte d'Azur region in France. Each week, these facilities report bacterial species that have been isolated from patients in their area. An alarm is triggered whenever the case count for a bacterial species infection exceeds 2 SDs of the historical mean for that species at the participating laboratory. At its inception in July 2013, the system monitored 611 bacterial species. During July 1, 2013–March 20, 2016, weekly analyses of incoming surveillance data generated 34 alarms signaling possible infectious disease outbreaks; after investigation, 14 (41%) of these alarms resulted in health alerts declared by the regional health authority. We are currently improving the system by developing an Internet-based surveillance platform and extending our surveillance to include more laboratories in the region.

During the second half of the 20th century, infectious diseases were considered a public health concern belonging to the past (*1*). However, despite some decrease in epidemiologic importance (*2*), infectious diseases remain a major cause of illness and lead to >25% of annual deaths (*3*–*5*). To ensure the timely detection of infectious diseases, health authorities have proposed the implementation of health surveillance systems. Historically, surveillance started with the use of mortality and morbidity data for public health purposes, which was first proposed by John Graunt in 1657 (*6*). The concept of surveillance has evolved over the centuries, and surveillance is now conducted mainly through the monitoring of symptoms and syndromes. During the 20th century, an expansion of the surveillance concept occurred with the emergence of numerous surveillance systems (*4*,*7*). Epidemiologic surveillance came to be known for 3 basic characteristics: systematic collection of data, consolidation and analysis of the collected data, and dissemination of information through narrative epidemiologic reports (*3*). Since 2001, because of the threat of bioterrorist attacks and the emergence and reemergence of infectious diseases, such as the recent Ebola outbreak in West Africa, interest in the methods for detection of infectious diseases has increased (*4*,*8*).

In the Assistance Publique-Hôpitaux de Marseille (AP-HM) public hospital network in Marseille, France, weekly automated epidemiologic surveillance systems have been implemented since 2002 (*9*,*10*). The objectives of these systems are to analyze clinical data produced by the microbiologic laboratories of 4 public hospitals in Marseille. The first program implemented, the Epidemiologic Surveillance and Alert Based on Microbiological Data, has monitored more than 293 infectious disease–related items on a weekly basis since November 2002 (*9*), including 38 clinical samples, 86 pathogens, 79 diagnosis tests, and 39 antimicrobial-resistance patterns. After the introduction of this system, several other systems based on a previously described historical database (*11*) were set up, such as the Bacterial Real-Time Laboratory-Based Surveillance System (BALYSES) and the Marseille Antibiotic Resistance Surveillance System (MARSS) (*10*). The latter 2 systems have routinely operated in the AP-HM network since 2013. During May 21, 2013–June 4, 2014, BALYSES detected

Author affiliations: Centre d'Epidémiologie et de Santé Publique des Armées, Marseille, France (M. Huart, G. Bedubourg, X. Deparis); Unité de Recherche sur les Maladies Infectieuses et Tropicales Emergentes, Aix-Marseille Université, Marseille (M. Huart, C. Abat, P. Colson, J.M. Rolain, H. Chaudet, P.E. Fournier, D. Raoult); Fondation Institut Hospitalo-Universitaire Méditerranée Infection–Assistance Publique-Hôpitaux de Marseille, Marseille (M. Huart, C. Abat, P. Colson, J.M. Rolain, P.E. Fournier, D. Raoult); Sciences Economiques et Sociales de la Santé et Traitement de l'Information Médicale, Aix Marseille Université, Marseille (M. Huart, C. Abat, P. Colson, J.M. Rolain, P.E. Fournier, D. Raoult)

DOI: http://dx.doi.org/10.3201/eid2304.161399

21 alarms (triggered when the number of cases of an infectious disease exceeds the statistic threshold), and MARSS detected 31. For BALYSES, 5 alarms either were escalated into alerts after further investigation or led to official reports to the Regional Health Agency (Agence Régionale de Santé [ARS]) of PACA, and for MARSS, 16 alarms led to official reports (*10*).

In July 2013, we aimed to expand the epidemiologic surveillance implemented in the AP-HM network to the entire PACA region by developing a new specific surveillance tool. This tool was developed in collaboration with the Armed Forces Center for Epidemiology and Public Health in France (CESPA). Until that time, no laboratory network in France had been implemented to monitor so many infectious disease–related events (*12*). Several other epidemiologic surveillance networks of microbiologic laboratories exist worldwide, such as the system set up by C. Paddy Farrington et al. in England and Wales (*13*) or the "Vigie" network in Belgium (*14*).

The PACA region is a population hub with many airports and ports with large flows of migrants and travelers. These population flows could bring infectious disease into the PACA region. Therefore, implementation of such a biosurveillance system based on previously unused data from microbiologic laboratories in the PACA region was expected to improve infectious diseases surveillance. Here we describe the procedure for implementing this biosurveillance system in and the initial results obtained from July 2013 through the end of March 2016.

Implementing a Biosurveillance System

Study Setting

The PACA region is located in southeastern France and is the third most populated region in the country, with ≈4.9 million inhabitants (≈7.5% of the total French population) (*15*). Several major cities are located in the region, such as Marseille, Toulon, and Nice, with 850,636, 163,974, and 343,064 inhabitants, respectively, in 2014 (*15*). The PACA region, which borders on Italy, is an important hub, with large population flows from North Africa across the Mediterranean Sea. In 2015, the PACA region had ≈611 private or public microbiologic laboratories according to ARS (ARS, unpub. data). Some of these laboratories have formed groups or networks, which can consist of up to 70 laboratories (Table 1). The geographic coverage of the laboratories included in our biosurveillance network is homogeneous over the region (Figure 1).

Biosurveillance System

We created a biosurveillance system, the PACA Surveillance Epidemiologic System (PACASurvE), capable of collecting, standardizing, and computing the laboratory results produced by public (i.e., hospital-affiliated) and private-sector microbiology laboratories located in the PACA region every week. The system's objectives are to provide early detection capability and an initial description of possible infectious disease threats (*10*,*16*); accordingly, the system is designed to issue alarms if an outbreak is detected or if a single case of a rare but severe infectious disease or an unknown infectious agent is discovered.

PACASurvE is Internet-based and uses Excel software (Microsoft, Redmond, WA, USA) for data collection and management and R version 3.0.1 software (*17*) for analysis. The system was implemented and has been routinely used since July 2013. Public hospital and private sector laboratories of the PACA region were invited to participate in the surveillance network. Fifteen institutions

Table 1. Selected characteristics of facilities participating in the Provence Alpes Côte d'Azur Surveillance Epidemiologic System, France, July 1, 2013–March 20, 2016*

Facility	Status	Geographic area	No. laboratories, N = 210	Wks since launch	Continuous or discontinuous	Start date of surveillance
LABM Labazur Provence	Private	Bouches-du-Rhône, Var, Vaucluse	26	142	Continuous	2013 Jul 1
LABM Alphabio	Private	Marseille	17	142	Continuous	2013 Jul 1
Clinique La Casamance	Public	Marseille	1	139	Continuous	2013 Jul 22
LABM Analys	Private	Boûches-du-Rhône	19	127	Discontinuous	2013 Oct 14
CH Aix-en-Provence	Public	Aix-en-Provence	1	122	Discontinuous	2013 Nov 18
CHU Nice	Public	Nice	1	118	Continuous	2013 Dec 16
CH Martigues	Public	Martigues	1	114	Continuous	2014 Jan 13
CH Salon-de-Provence	Public	Salon-de-Provence	1	109	Discontinuous	2014 Feb 14
Hôpital Inter-Armées, Laveran	Public	Marseille	1	100	Discontinuous	2014 Apr 21
LABM Cerba	Private	PACA	70	63	Continuous	2015 Jan 5
Hôpital Saint-Joseph	Public	Marseille	1	59	Discontinuous	2015 Feb 3
LABM BioAlliance	Private	Marseille	21	42	Continuous	2015 Jun 1
LABM Labazur Nice	Private	Alpes Maritimes	28	23	Continuous	2015 Oct 12
CH Dignes	Public	Dignes	1	11	Discontinuous	2016 Jan 1
LABM Barla	Private	Nice	21	7	Continuous	2016 Feb 3

*CH, Centre Hospitalier (Central Hospital); CHU, Centre Hospitalier Universitaire (Central University Hospital); LABM, Laboratoire de Biologie Médicale (Medical Laboratory); PACA, Provence Alpes Côte d'Azur.

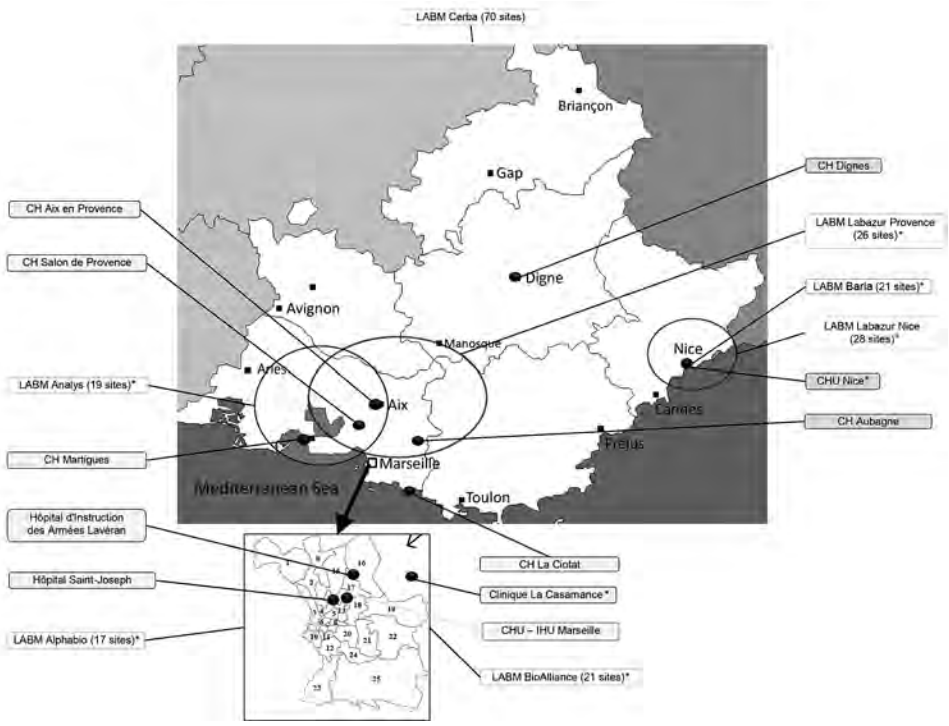

Figure 1. Laboratories participating in the Provence Alpes Côte d'Azur Surveillance Epidemiologic System, France, July 1, 2013–March 20, 2016. Black dots indicate participating laboratories; black boxes indicate public laboratories; text labels indicate private laboratories and areas of activity. Asterisks (*) denote laboratories using matrix-assisted laser desorption/ionization time-of-flight mass spectrometry for identification of species; all other laboratories shown use biochemical bacterial identification. CH, Centre Hospitalier (Central Hospital); CHU, Centre Hospitalier Universitaire (Central University Hospital); IHU, Institut Hospitalo-Universitaire (Hospital–University Institute); LABM, Laboratoire de Biologie Médicale (Medical Laboratory).

were first selected among the leading laboratories in terms of volume of activity to rapidly achieve a better geographic representation of PACA (Figure 1). Their participation was based on several criteria proposed in the literature and relevant to the implementation of our network, including those described by Walckiers et al. (*14*): participation of laboratories on an unpaid and voluntary basis, participation of microbiologic laboratories, anonymity of data, and a standard, predefined frequency for data collection (*14*).

After identifying the participating institutions, the second task was to define which events should be monitored and their respective definitions, which were transmitted to all laboratories. Data collected included information on bacterial identification and virologic, bacteriologic, mycologic, and parasitologic laboratory results. Currently, PACASurvE is particularly geared toward the monitoring of bacterial species.

We defined a case as illness in a patient from whom ≥1 bacterial species was isolated and confirmed. Two different bacterial species isolated from samples collected from the same patient resulted in 2 reported cases. The samples without bacterial identification were considered to be negative. Laboratories were free to use the microbiologic methods of their choice to identify bacterial species, including PCR, matrix-assisted laser desorption/ionization time-of-flight mass spectrometry, or conventional phenotypic methods (e.g., Gram coloration and API galleries).

A weekly coordination meeting, which included members from AP-HM and CESPA, was defined to optimize data collection and organize analyses and feedback. Currently, PACASurvE is included in a comprehensive biosurveillance system at the AP-HM network with the other epidemiologic surveillance systems previously described (Figure 2).

Data Flow, Analyses, and Feedback

All the steps of data flow, analyses, and feedback were mapped (Figure 2). Every week, biologists at participating institutions sent a report of new cases, in the form of anonymized data contained in Excel spreadsheets or encrypted PDFs, to the system coordinator.

The first step before analysis was validating and standardizing the reported data, which were checked, cleaned, and deduplicated. The search for duplicates was performed weekly according to the unique patient identifier and the isolated microorganism, and data were then automatically compared with a thesaurus of all identified bacterial species (*10*). All analysis steps (e.g., deduplication, merging of data from different laboratories, statistical analysis, and visualization tools production) were performed automatically by using a specific algorithm written in a Visual Basic (Microsoft) script for Excel.

To detect outbreaks as early as possible, an alarm was triggered when the weekly count of cases for a bacterial species was higher than 2 SDs of the mean of historical data since the beginning of surveillance for each laboratory (*10*).

After 6 months, once the collection procedures were stabilized, the C1-mild epidemics detection method used by the Early Aberration Reporting System (*18*,*19*) was performed. This method enables the detection of outbreaks on a dataset with limited historical data (≥7 weeks). Both of these statistical methods operate in parallel at the Institut Hospitalo-Universitaire Méditérannée Infection and CESPA.

A statistical alarm is triggered if the observed value is significantly different from the expected value (*16*). After checking biologic criteria, alarms were assessed as confirmed or unconfirmed by senior biologists during the weekly AP-HM epidemiologic surveillance meeting. Alarms that were escalated into an alert (after further investigations that included diagnosis confirmation and descriptive analysis of cases in terms of time, place, and population) led to further epidemiologic investigation, which then had to be declared to ARS if a real outbreak was confirmed. Specific countermeasures also had to be implemented, such as patient isolation, implementation of specific care protocols, or a large scale information campaign (Figure 2). For feedback, a weekly epidemiologic report was addressed to all participating laboratories, AP-HM department officials, CESPA, ARS, and the Interregional Epidemiology Unit (otherwise known as CIRE).

Results

Scalability of the System

In July 2013, when PACASurvE started, 3 main structures that collected data from 44 laboratories sent their anonymized data to the network coordinator every Monday. In March 2016, a total of 15 participating institutions were included in the biosurveillance system (Table 1). Several participated irregularly; 2 (Centre Hospitalier Dignes and Centre Hospitalier Aix en Provence) transmitted a common declaration file. Currently, PACASurvE includes 8 public and 7 private sector participating institutions (Figure 1), representing a total of 210 laboratories (34.4% of all laboratories in the PACA region).

Description of Collected Cases

An average of 14,000 cases (positive and negative) were reported every week. Since the beginning of the biosurveillance system, 217,621 bacterial infections have been reported by participating structures (i.e., ≈1,532 confirmed cases per week). These identifications resulted from the analysis of an estimated 315,000 urine samples, 140,000 blood cultures, 6,700 respiratory specimens, 32,000 stool samples, 4,400 cerebrospinal fluid samples, and 176,000 serologic examinations.

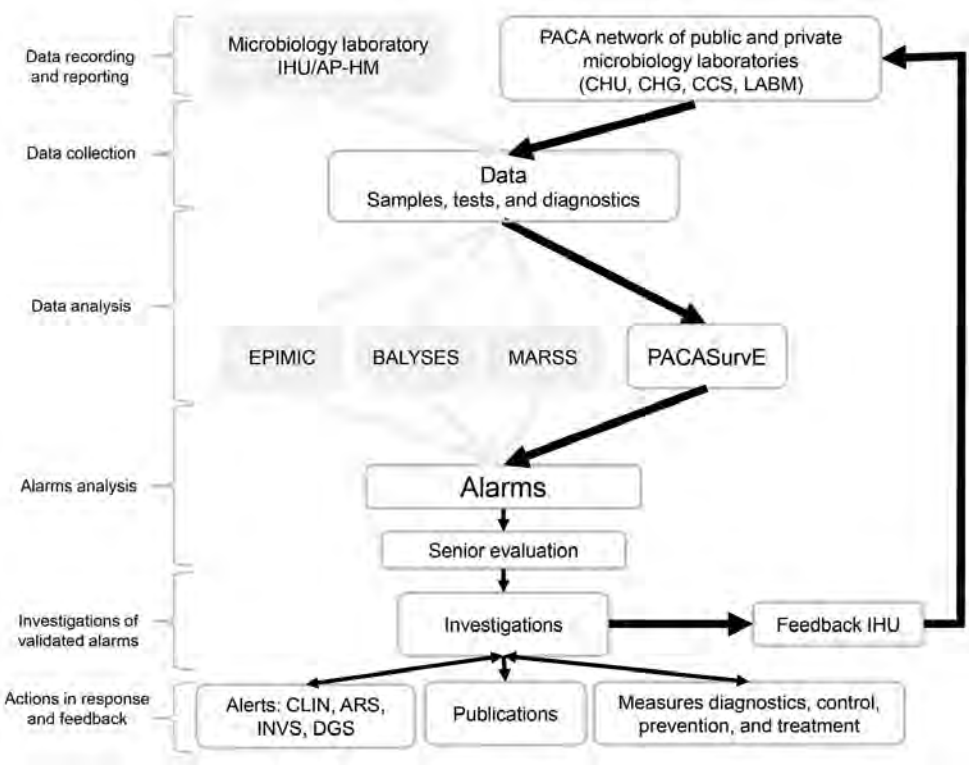

Figure 2. Flow diagram of all epidemiologic surveillance systems implemented by the Institut Hospitalo-Universitaire Méditérannée Infection, Assistance Publique-Hôpitaux de Marseille, France. ARS, Agence Régionale de Santé (Regional Health Agency); BALYSES, Bacterial Real-Time Laboratory-Based Surveillance System; CDS, Centre de Santé (Health Center); CHG, Centre Hospitalier Général (General Hospital Center); CHU, Centre Hospitalier Universitaire (Central University Hospital); CLIN, Comité de Lutte contre les Infections Nosocomiales (Committee for the Fight Against Nosocomial Infections); DGS, Direction Générale de la Santé (Directorate General for Health); EPIMIC, Epidemiologic Surveillance and Alert Based on Microbiological Data; IHU/AP-HM, Institut Hospitalo-Universitaire/Assistance Publique-Hôpitaux de Marseille; INVS, Institut Nationale de Veille Sanitaire (National Institute for Public Health Surveillance); LABM, Laboratoire de Biologie Médicale (Medical Laboratory); MARSS, Marseille Antibiotic Resistance Surveillance System; PACASurvE, Provence Alpes Côte d'Azur Surveillance Epidemiologic System. Diagram is based on the workflow described by Abat et Al. 2013 (*10*).

Table 2. Ten bacterial species with the most alarms triggered by the Provence Alpes Côte d'Azur Surveillance Epidemiologic System, France, July 1, 2013–March 20, 2016*

Bacterial species	No. alarms total	Average weekly no. alarms
Pseudomonas putida	87	0.6
Stenotrophomonas maltophilia	82	0.6
Neisseria gonorrhoeae	78	0.6
Hafnia alvei	74	0.5
Enterobacter aerogenes	72	0.5
Staphylococcus capitis	72	0.5
Staphylococcus lugdunensis	70	0.5
Streptococcus constellatus	68	0.5
Staphylococcus haemolyticus	66	0.5
Haemophilus parainfluenzae	65	0.5

*Total no. alarms for the entire system during this period was 5,915 (averaging 42 alarms weekly).

Thesaurus

Data were compared automatically to a thesaurus that included 611 bacterial species at the time of the system's inception in 2013 (*10*). Currently, the number of bacterial species is 673.

Top 10 Identified Bacteria in PACASurvE and Biodiversity

We ranked the overall top 10 bacterial species isolated since the beginning of the biosurveillance system and the top 10 per laboratory. The 10 most frequently reported bacterial species in PACASurvE represented 181,241 identifications (83.1% of total cases) (online Technical Appendix, https://wwwnc.cdc.gov/EID/article/23/4/16-1399-Techapp1.xlsx). *Escherichia coli* infections were the most frequently reported cases in all the laboratories. For others species, diversity increased when frequency decreased (online Technical Appendix).

Bacterial Species Specifically Isolated by PACASurvE

PACASurvE has also made it possible to identify bacterial species that were unknown in the initial thesaurus of AP-HM (*10*). A total of 12 bacterial species have been isolated and added to this thesaurus: *Citrobacter werkmanii, Kluyvera cryocrescens, Lactobacillus brevis, Streptococcus pluranimalium, Paenibacillus peoriae, Rhodotorula minuta, Cronobacter malonaticus, Paenibacillus durus, Rhodotorula mucilaginosa, Rhizobium radiobacter, Buttiauxella agrestis,* and *Plesiomonas shigelloides*.

Alarms and Alerts

The biosurveillance system issued alarms every week after analysis. These alarms were triggered by an increasing number of reported cases for some bacterial species. The system has issued 5,915 alarms since July 2013, averaging 2,160 alarms per year and 41 alarms per week. Since July 2013, after analysis at the weekly coordination meetings, 34 alarms required further investigations after validation by a senior epidemiologist or a biologist, and 14 (41%) of those were escalated to an alert. We ranked the 10 bacterial species that have triggered the largest number of alarms since the beginning of the surveillance network (Table 2).

Fourteen notifications have been reported to ARS as outbreaks, which were caused by the following bacterial species: *Enterococcus faecalis*, *Clostridium difficile* (serotype O27 and non-O27), *Escherichia coli, Acinetobacter radioresistens, Serratia marcescens, Enterobacter aerogenes, Proteus penneri, Streptococcus pyogenes*, and *Streptococcus aerogenes.* All these epidemiologic events were identified by PACASurvE and confirmed after further detection by other surveillance systems. Other alarms were declared for laboratories or hospitals involved in investigations. These investigations did not necessarily lead to an alert but more often to an internal investigation.

Alarms regarding an *E. faecalis* outbreak were issued by PACASurvE in March 2015 (*20*), largely because of an increase in the number of declared cases of *E. faecalis* isolated in urine samples in Marseille and surroundings areas. That outbreak was reported to ARS, and investigations are still ongoing to find out if a single or multiple clones were responsible.

Alarms regarding *C. difficile* were issued in the hospital monitoring system BALYSES and among private-sector laboratories in the PACASurvE system. These alarms led to a further investigation into *C. difficile*–related illness and death in patients. We found the presence of a hypervirulent strain (O27) (*21*). However, this strain does not account for all the deaths attributable to *C. difficile* (*22*) because other strains of this bacterial species exist. Therefore, an alert was issued to ARS, which led to specific countermeasures (e.g., systematic screening, isolation of patients, transport to the infectious diseases unit at Hôpital Nord in Marseille, and establishment of a specific treatment protocol with early fecal transplant) (*23*).

Feedback and Network Management

The feedback bulletin was set up to keep all participants in the surveillance network informed. It consisted of a presentation with 2–3 slides per participating laboratory, with a summary of their declared activity during the previous week. It was accompanied by an email newsletter with information on the main alarms that led to further investigations and interpretation by a college of experts. The weekly epidemiologic bulletin was also available on the website of the Institut Hospitalo-Universitaire Méditérannée Infection (http://www.mediterranee-infection.com/article.php?larub=23&titre=surveillance-epidemiologique).

Discussion

Since July 2013, we have been operating a biosurveillance system based on a network of clinical microbiology laboratories in the PACA region to monitor infectious diseases, especially those attributable to bacterial species.

To date, to our knowledge, the PACASurvE network is unique in France. It is a collaborative system (one relying on the participation of private and hospital laboratories) which is different from BALYSES (a hospital system) (*10*). Similar biosurveillance networks were developed in Belgium (*14*,*24*), the United Kingdom (*13*), and the United States, where the Laboratory Response Network was implemented by the Centers for Disease Control and Prevention in 1999 (*25*). In Belgium, a sentinel network using microbiology laboratory data was created for the weekly monitoring of selected pathogens (*24*,*26*). In contrast, PACASurvE focuses on the monitoring of 673 bacterial species.

In the United States, the Laboratory Response Network was implemented to build a network of laboratories that can respond to biologic and chemical emergencies. Our surveillance system only focused on biologic threats and was intended for the early detection of infectious disease outbreaks on a weekly basis.

After initial difficulties in enrolling laboratories, the biosurveillance system now functions regularly. The system has generated 14 alarms that have been investigated and reported to ARS. These alarms made it possible to detect actual outbreaks and helped to develop effective countermeasures, as in the case of the *C. difficile* (*23*) and *E. faecalis* (*20*) outbreaks.

This system has several strengths and some limitations. The first and main strength of the system is that it can easily be replicated, thanks to its low implementation cost and its use of Excel software. The use of this software allowed the system to be set up rapidly, and any necessary modifications can be made easily, compared with the software used by other surveillance systems, such as Real Time Outbreak and Disease Surveillance (*27*). This simplicity could allow it to be implemented in developing countries.

Continuous improvement also is a major strength of PACASurvE. The number of laboratories increases regularly, which improves the representativeness of the PACA region. Improving geographic representativeness is important for the purposes of extrapolating our results or extending the system to other regions. Currently, the coverage of the system includes 214 laboratories in the PACA region, representing 81% of major urban areas of the PACA region (e.g., Marseille, Nice, and Toulon). Only 1 department of the region, the Hautes Alpes, is not properly covered.

The third strength is the diversity of bacterial species identified and transmitted by the network of laboratories in the PACA region. The number of samples tested and their diversity are greater in the PACASurvE than in other surveillance systems currently active in France (*10*). This difference could be explained by the higher number of participating laboratories, which increases continually. This high diversity underlines the relevance of a private-sector laboratory surveillance system operating in parallel with a hospital epidemiologic surveillance system. Currently, PACASurvE monitors only bacterial species, but it would be interesting to extend this surveillance to other subjects, such as antibiograms or viruses.

Our biosurveillance system has some limitations. The first relates to the statistical analyses used at the beginning for the detection of abnormal events. The use of a threshold of 2 SDs higher than the historical weekly mean is not necessarily appropriate, although it is easy to set up rapidly and enabled detection of an abnormal event. At the beginning of the surveillance system data collection, in the absence of strong historical data, this basic algorithm seemed to be the most appropriate and easy to use given the circumstances. After studying the methods used to address seasonal variations and sporadic emergence of rare bacterial species as described by Enki et al. (*13*) in 2013, Farrington et al. (*28*) in 1996, Buckeridge et al. (*29*) in 2004, and Frickers et al. (*30*) in 2008, we decided to implement another method and this introduced the C1-mild epidemics detection method (*18*) with R software into the surveillance package. This method is now used routinely in CESPA.

The second limitation concerns the laboratories' willingness to participate, which could lead to problems in reporting. For example, we have to encourage laboratories to report their data automatically by using the Internet platform.

After only 2 years in operation, the results achieved by our network are already promising. The economic cost of this system will be calculated, being a major criteria for the first planned evaluation of the system. In the future, we will improve the completeness of transmitted data and will try to extend our network to other regions in France. This type of regional biosurveillance network could be linked to data from existing networks implemented by the National Institute for Public Health Surveillance (Santé Publique France) to enable comprehensive surveillance of all French territory. An equivalent of the Epidemiologic Surveillance and Alert Based on Microbiological Data system has been set up in Senegal with the participation of several health centers. In conclusion, the recent development of a surveillance network based on data from microbiologic laboratories in the PACA region has demonstrated its value for early identification of regional epidemics.

Acknowledgments

We would like to thank Gaetan Texier for his help with the organization of his paper. We would also like to thank the additional members of PACASurvE who contributed data: Jean Paul Casalta, Pierre Yves Levy, Jean Pierre Arzouni, Philippe Halfon, Alexandre Toro, Patricia Roussellier, Raymond Ruimy, Philippe Seyral, Jean Dominique Poveda, Éric Garnotel, Patrick Brunet, Pierre Hance, Nathalie Brieu, Christophe Maruejouls, Olivier Ridoux, Evelyne Jean.

This work was supported by the University Hospital Institute Méditerranée Infection and the Armed Forces Center for Epidemiology and Public Health.

Authors' contributions: M.H. wrote the manuscript. G.B. participated in the development of the technical analysis in R and corrected the manuscript. C.A., X.D., D.R. provided comments on the manuscript and final approval.

Dr. Huart was a PhD student at the Institut Hospitalo-Universitaire Méditerranée Infection, Aix-Marseille Université, and at the Centre d'Epidémiologie et de Santé Publique des Armées. His research interest is the development of a system for epidemiologic surveillance of infectious diseases that uses data from microbiologic laboratories in the Provence-Alpes-Côte d'Azur region.

References

1. Raoult D. The causes underlying the emergence of disease agents [in French]. Annales des Mines—Responsabilité et Environnement. 2008;3:21–4. https://dx.doi.org/10.3917/re.051.0021
2. GBD 2013 Mortality and Causes of Death Collaborators. Global, regional, and national age-sex specific all-cause and cause-specific mortality for 240 causes of death, 1990–2013: a systematic analysis for the Global Burden of Disease Study 2013. Lancet. 2015;385:117–71. http://dx.doi.org/10.1016/S0140-6736(14)61682-2
3. Declich S, Carter AO. Public health surveillance: historical origins, methods and evaluation. Bull World Health Organ. 1994;72:285–304.
4. M'ikanatha N, de Valk H, Lynfield R, Van Benden C. Infectious disease surveillance: a cornerstone for prevention and control. In: M'ikanatha N, de Valk H, Lynfield R, Van Benden C, editors. Introduction to infectious disease surveillance. 2nd ed. Oxford: John Wiley & Sons; 2013. p. 1–20.
5. Morens DM, Folkers GK, Fauci AS. The challenge of emerging and re-emerging infectious diseases. Nature. 2004;430:242–9. http://dx.doi.org/10.1038/nature02759
6. De Cos H. Treatise on the airs, waters, and places. In: É Littré. Complete works of Hippocrates [in French]. Vol. 2. Paris: J.B. Baillière; 1840. p. 1–93.
7. Abat C, Chaudet H, Rolain J-M, Colson P, Raoult D. Traditional and syndromic surveillance of infectious diseases and pathogens. Int J Infect Dis. 2016;48:22–8. http://dx.doi.org/10.1016/j.ijid.2016.04.021
8. Buckeridge D. Detection of outbreaks using laboratory data: an epidemiological perspective [cited 2016 Dec 22]. https://www.inspq.qc.ca/sites/default/files/jasp/archives/2006/jasp2006-laboratoire-lbuckeridge1.pdf
9. Colson P, Rolain J-M, Abat C, Charrel R, Fournier P-E, Raoult D. EPIMIC: a simple homemade computer program for real-time epidemiological surveillance and alert based on microbiological data. PLoS One. 2015;10:e0144178. http://dx.doi.org/10.1371/journal.pone.0144178
10. Abat C, Chaudet H, Colson P, Rolain J-M, Raoult D. Real-time microbiology laboratory surveillance system to detect abnormal events and emerging infections, Marseille, France. Emerg Infect Dis. 2015;21:1302–10.http://dx.doi.org/10.3201/eid2108.141419
11. Seng P, Abat C, Rolain JM, Colson P, Lagier J-C, Gouriet F, et al. Identification of rare pathogenic bacteria in a clinical microbiology laboratory: impact of matrix-assisted laser desorption ionization-time of flight mass spectrometry. J Clin Microbiol. 2013;51:2182–94.http://dx.doi.org/10.1128/JCM.00492-13
12. Plouin-Gaudon I, Vanhems P, Allard R, Sahajian F, Fabry J. Surveillance of laboratory based infections by biological and medical analyses: review of the literature [in French]. Sante Publique. 2000;12:149–59.
13. Enki DG, Noufaily A, Garthwaite PH, Andrews NJ, Charlett A, Lane C, et al. Automated biosurveillance data from England and Wales, 1991–2011. Emerg Infect Dis. 2013;19:35–42. http://dx.doi.org/10.3201/eid1901.120493
14. Walckiers D, Vandepitte J, Stroobant A, Cornelis R, Van Casteren VD, Walckiers JV. A new method of surveillance of infectious diseases in Belgium: the "Vigie" network of microbiology laboratories [in French]. Med Mal Infect. 1986;16:147–50. http://dx.doi.org/10.1016/S0399-077X(86)80217-7
15. French National Institute of Statistics and Economic Studies. Legal population in force as of January 1, 2014: census of population [in French] [cited 2016 Apr 1]. https://www.insee.fr/fr/statistiques/fichier/2119747/dep91.pdf
16. Hulth A, Andrews N, Ethelberg S, Dreesman J, Faensen D, van Pelt W, et al. Practical usage of computer-supported outbreak detection in five European countries. Euro Surveill. 2010;15:19658.
17. R Core Team. R: a language and environment for statistical computing [cited 2016 Dec 22]. http://www.R-project.org
18. Hutwagner L, Thompson W, Seeman GM, Treadwell T. The bioterrorism preparedness and response Early Aberration Reporting System (EARS). J Urban Health. 2003;80(Suppl 1):i89–96.
19. Wang X, Zeng D, Seale H, Li S, Cheng H, Luan R, et al. Comparing early outbreak detection algorithms based on their optimized parameter values. J Biomed Inform. 2010;43:97–103. http://dx.doi.org/10.1016/j.jbi.2009.08.003
20. Abat C, Huart M, Garcia V, Dubourg G, Raoult D. *Enterococcus faecalis* urinary-tract infections: do they have a zoonotic origin? J Infect. 2016;2016:305–13. https://dx.doi.org/10.1016/j.jinf.2016.07.012
21. Lagier J-C, Dubourg G, Cassir N, Fournier P-E, Colson P, Richet H, et al. *Clostridium difficile* 027 emerging outbreak in Marseille, France. Infect Control Hosp Epidemiol. 2013;34:1339–41.http://dx.doi.org/10.1086/673995
22. Huart M, Abat C, Jimeno MT, Deparis X, Raoult D, Fournier P-E. Compared lethality rates of *Clostridium difficile* infections at the local, regional and national levels in France. New Microbes New Infect. 2016;14:6–7. http://dx.doi.org/10.1016/j.nmni.2016.07.006
23. Lagier J-C, Delord M, Million M, Parola P, Stein A, Brouqui P, et al. Dramatic reduction in *Clostridium difficile* ribotype 027-associated mortality with early fecal transplantation by the nasogastric route: a preliminary report. Eur J Clin Microbiol Infect Dis. 2015;34:1597–601. https://dx.doi.org/10.1007/s10096-015-2394-x
24. Walckiers D, Stroobant A, Yourassowsky E, Lion J, Cornelis R. A sentinel network of microbiological laboratories as a tool for surveillance of infectious diseases in Belgium. Epidemiol Infect. 1991;106:297–303.http://dx.doi.org/10.1017/S0950268800048445
25. Kalish BT, Gaydos CA, Hsieh Y-H, Christensen BE, Carroll KC, Cannons A, et al. National survey of Laboratory Response Network sentinel laboratory preparedness. Disaster Med Public Health Prep. 2009;3(Suppl):S17–23. http://dx.doi.org/10.1097/DMP.0b013e31819e09b4
26. Walckiers D, Van Ros G, Stroobant A. Monitoring of malaria in Belgium through a network of microbiology laboratories [in French]. Ann Soc Belg Med Trop. 1986;66:15–21.

27. Silva JC, Shah SC, Rumoro DP, Bayram JD, Hallock MM, Gibbs GS, et al. Comparing the accuracy of syndrome surveillance systems in detecting influenza-like illness: GUARDIAN vs. RODS vs. electronic medical record reports. Artif Intell Med. 2013;59:169–74.http://dx.doi.org/10.1016/j.artmed.2013.09.001
28. Farrington CP, Andrews NJ, Beale AD, Catchpole MA. A statistical algorithm for the early detection of outbreaks of infectious disease. J R Stat Soc Ser A Stat Soc. 1996;159:547–63. http://dx.doi.org/10.2307/2983331
29. Buckeridge DL, Burkom H, Campbell M, Hogan WR, Moore AW. Algorithms for rapid outbreak detection: a research synthesis. J Biomed Inform. 2005;38:99–113. http://dx.doi.org/10.1016/j.jbi.2004.11.007
30. Fricker RD Jr, Hegler BL, Dunfee DA. Comparing syndromic surveillance detection methods: EARS' versus a CUSUM-based methodology. Stat Med. 2008;27:3407–29. http://dx.doi.org/10.1002/sim.3197

Address for correspondence: Michael Huart, Centre d'Epidémiologie et de Santé Publique des Armées (CESPA), Camp de Sainte Marthe, 408 Rue Jean Queillau, 13014 Marseille, France; email: mikoli@hotmail.fr

Transmission of Hepatitis A Virus through Combined Liver–Small Intestine–Pancreas Transplantation

Monique A. Foster, Lauren M. Weil, Sherry Jin, Thomas Johnson, Tonya R. Hayden-Mixson, Yury Khudyakov, Pallavi D. Annambhotla, Sridhar V. Basavaraju, Saleem Kamili, Jana M. Ritter, Noele Nelson, George Mazariegos, Michael Green, Ryan W. Himes, David T. Kuhar, Matthew J. Kuehnert, Jeffrey A. Miller, Rachel Wiseman, Anne C. Moorman

Medscape EDUCATION ACTIVITY

This activity has been planned and implemented through the joint providership of Medscape, LLC and *Emerging Infectious Diseases*. Medscape, LLC is accredited by the American Nurses Credentialing Center (ANCC), the Accreditation Council for Pharmacy Education (ACPE), and the Accreditation Council for Continuing Medical Education (ACCME), to provide continuing education for the healthcare team.

Medscape, LLC designates this Journal-based CME activity for a maximum of 1.00 ***AMA PRA Category 1 Credit(s)™***. Physicians should claim only the credit commensurate with the extent of their participation in the activity.

All other clinicians completing this activity will be issued a certificate of participation. To participate in this journal CME activity: (1) review the learning objectives and author disclosures; (2) study the education content; (3) take the post-test with a 75% minimum passing score and complete the evaluation at http://www.medscape.org/journal/eid; and (4) view/print certificate. For CME questions, see page 729.

Release date: March 15, 2017; Expiration date: March 15, 2018

Learning Objectives

Upon completion of this activity, participants will be able to:

- Analyze the epidemiology of hepatitis A virus (HAV) infection
- Evaluate how organ donors are assessed for HAV infection
- Evaluate laboratory results of the organ recipient and caregivers exposed to HAV infection in the current study.

CME Editor

Karen L. Foster, Technical Writer/Editor, Emerging Infectious Diseases. *Disclosure: Karen L. Foster has disclosed no relevant financial relationships.*

CME Author

Charles P. Vega, MD, Clinical Professor of Family Medicine, University of California, Irvine. *Disclosure: Charles P. Vega, MD, has disclosed the following financial relationships: served as an advisor or consultant for Allergan, Inc.; McNeil Consumer Healthcare; served as a speaker or a member of a speakers bureau for Shire Pharmaceuticals.*

Authors

Disclosures: ***Monique A. Foster, MD, MPH; Lauren M. Weil, PhD, MPH; Sherry Jin, MD, MPH; Thomas Johnson, BS; Tonya Mixson-Hayden, PhD; Yury Khudyakov, PhD; Pallavi D. Annambhotla, DrPH; Sridhar V. Basavaraju, MD; Saleem Kamili, PhD; Jana M. Ritter, DVM; Noele P. Nelson, MD, PhD; George Mazariegos, MD; David T. Kuhar, MD; Matthew J. Kuehnert, MD; Jeffrey A. Miller, MD, MPH; Rachel Wiseman, MPH;*** *and* ***Anne C. Moorman, RN, MPH,*** *have disclosed no relevant financial relationships.* ***Michael Green, MD,*** *has disclosed the following relevant financial relationships: served as an advisor or consultant for Chimerix, Bristol-Myers Squibb.* ***Ryan W. Himes, MD,*** *has disclosed the following relevant financial relationships: served as an advisor or consultant for Alexion; served as a speaker or a member of a speakers bureau for Alexion; received grants for clinical research from Alexion.*

Author affiliations: Centers for Disease Control and Prevention, Atlanta, Georgia, USA (M.A. Foster, T.R. Hayden-Mixson, Y. Khudyakov, P.D. Annambhotla, S.V. Basavaraju, S. Kamili, J.M. Ritter, N. Nelson, D.T. Kuhar, M.J. Kuehnert, J.A. Miller, A.C. Moorman); Texas Department of State Health Services, Austin, Texas, USA (L.M. Weil); Harris County Public Health and Environmental Services, Houston, Texas, USA (S. Jin); Houston Health Department, Houston (T. Johnson); Children's Hospital of Pittsburgh of University of Pittsburgh Medical Center, Pittsburgh, Pennsylvania, USA (G. Mazariegos, M. Green); Texas Children's Hospital, Houston, (R.W. Himes); Pennsylvania Department of Health, Harrisburg, Pennsylvania, USA (J.A. Miller); Texas Department of State Health Services, Austin (R. Wiseman)

DOI: http://dx.doi.org/10.3201/eid2304.161532

Although transmission of hepatitis A virus (HAV) through blood transfusion has been documented, transmission through organ transplantation has not been reported. In August 2015, state health officials in Texas, USA, were notified of 2 home health nurses with HAV infection whose only common exposure was a child who had undergone multi–visceral organ transplantation 9 months earlier. Specimens from the nurses, organ donor, and all organ recipients were tested and medical records reviewed to determine a possible infection source. Identical HAV RNA sequences were detected from the serum of both nurses and the organ donor, as well as from the multi–visceral organ recipient's serum and feces; this recipient's posttransplant liver and intestine biopsy specimens also had detectable virus. The other organ recipients tested negative for HAV RNA. Vaccination of the donor might have prevented infection in the recipient and subsequent transmission to the healthcare workers.

Hepatitis A virus (HAV), the most common cause of viral hepatitis, is a nonenveloped RNA virus belonging to the family *Picornaviridae* (*1*,*2*). Approximately 1.5 million clinical cases of HAV occur worldwide annually; the virus is commonly spread person to person through the fecal–oral route (*2*). Although rates of HAV infection have declined by 95% in the United States since a vaccine became available, infections continue to result from close personal contact with an infected household member or common-source outbreaks from contaminated food or water (*3*). HAV can cause relapsing and fulminant hepatitis, but fatal infection is rare.

Parenteral transmission of HAV through contaminated blood products or needles is also rare, despite the presence of viremia up to 30 days before symptom onset (*4*). No screening tests for HAV infection are required for blood, organ, or tissue donation in the United States (*5*). HAV transmission through solid-organ transplantation has not been reported in the literature.

In August 2015, genetically identical HAV was recovered from 2 healthcare workers (HCWs) participating in the care of a child recipient of multiple visceral organs. To prevent infection in other organ recipients and contacts, the Centers for Disease Control and Prevention (CDC), along with state and local health departments, conducted an investigation to determine the source of the HCW infection and whether HAV was transmitted through the solid-organ transplantation.

Case Report

In August 2015, the Texas Department of State Health Services received requests from 2 separate local health departments for postexposure prophylaxis recommendations for contacts of 2 nurses with confirmed HAV infection. In both nurses, symptomatic infections developed within days of each other; both nurses worked for the same pediatric home healthcare agency. The nurses did not have shared exposures other than 1 patient and had not been vaccinated for hepatitis A.

The shared patient was a 7-year-old who underwent multiorgan (liver, small bowel, and pancreas) transplantation because of megacystis microcolon intestinal hypoperistalsis syndrome, a rare congenital condition characterized by a largely dilated nonobstructed urinary bladder (megacystis), very small colon (microcolon), and decreased or absent intestinal movements (intestinal peristalsis). The transplantation occurred in December 2014.

This patient's posttransplant course was complicated by intraabdominal abscesses, acute liver rejection, Epstein-Barr virus enteritis, cytomegalovirus infection, and lymphoproliferative disorder. The patient was discharged to home in March 2015 with an alanine aminotransferase (ALT) level of 49 IU/L (reference 0–50 IU/L). By the following month, ALT had increased to 324 IU/L, and by June 2015, to 515 IU/L. During the time of ALT increase, the patient, who had a colostomy and ileostomy, also had increased stoma output. Because of worsening clinical symptoms, a liver biopsy was conducted on June 19, 2015; results showed features of moderate acute cellular rejection, as well as diffuse, lobular acute and chronic inflammation. On June 30, a repeat liver biopsy was performed because of persistent ALT elevation despite increased treatment for rejection.

The multi–visceral organ recipient had received 2 doses of hepatitis A vaccine, as part of routine childhood vaccinations, and was IgG HAV positive in 2013, indicating prior immunity against HAV, although the patient was immune suppressed after transplantation. Because of the other clinical conditions that could have explained the ALT elevation and gastrointestinal symptoms, HAV infection was initially not considered. When subsequent testing prompted by the infections in the recipient's caregivers revealed the multi–visceral organ recipient was positive for HAV RNA, a laboratory and epidemiologic investigation focused on whether infection was due to recent fecal–oral transmission or from solid-organ transplantation. Available transplant-related specimens were tested to rule out transmission through transplantation.

Methods

Clinical and Epidemiologic Review

The case was reported to the Organ Procurement and Transplantation Network and reviewed by the Network's ad hoc Disease Transmission Advisory Committee as a suspected donor-derived disease event. Through representation on advisory committee, CDC, with support from state and local health departments, investigates potential transmission to other organ recipients. To determine whether the multi–visceral organ recipient acquired HAV

infection through transplantation and to identify other potentially infected HCWs, public health investigators reviewed medical records, interviewed household contacts, and conducted additional case finding among healthcare providers and other transplant recipients. This investigation included review of records from the home health agency that employed both home health nurses; consultation with occupational health staff from the treating facilities; and review of surveillance data from the jurisdictions in which the patient received care.

Laboratory Specimen Collection and Testing

Laboratory testing was conducted at the laboratory of CDC's Division of Viral Hepatitis, National Center for HIV, Viral Hepatitis, STD, and TB Prevention (Atlanta, GA, USA). IgG HAV, IgM HAV, and HAV RNA extraction of serum was conducted on both HCWs; the organ donor; and recipients of the visceral organs, heart, and kidneys. When HAV RNA was detected from serum samples, PCR and phylogenetic analysis was conducted to determine relatedness. Similar testing was conducted on frozen and paraffin-embedded liver and small bowel tissue biopsy specimens from the multi–visceral organ recipient. Methods of viral extraction from paraffin-embedded tissue have been described previously (*6*). All HAV RNA–positive samples were used to sequence the HAV VP1/P2B (viral protein 1/amino terminus of 2B) genomic region, and phylogenetic analysis was performed by comparing these sequences with archived HAV sequences contained within the CDC HAV sequence database (*7*).

Results

Results of Epidemiologic Investigation

Case investigations revealed that, during their incubation and infectious periods, the home health nurses cared for a total of 12 children. However, they had only 1 patient in common: the multi–visceral organ recipient (*8*).

An additional HCW with HAV infection was identified during a case-contact interview with the mother of the multi–visceral organ recipient. This nurse also provided care to the multi–visceral organ recipient, and jaundice, diarrhea, and arthralgia later developed that required inpatient admission. HAV infection was diagnosed by serologic testing during that hospitalization; this nurse also had not received a hepatitis A vaccination. Care for the multi–visceral organ recipient provided by all 3 nurses included managing watery feces (e.g., changing diapers and ostomy bags). Epidemiologic investigation and the resulting timeline (Figure 1) provide evidence that all 3 nurses most likely were infected by exposure to the multi–visceral organ recipient.

The organ donor, an 8-year-old who died in a motor vehicle collision, traveled to Guatemala, a country to which HAV is endemic, 6 months before death. In addition to the visceral organs, which were transplanted into the index patient, the heart and both kidneys were transplanted into 3 other recipients. The organ donor's name was found in a vaccination registry maintained by 1 of the states of residence, which indicated that the hepatitis A vaccination was not given. Serum banked from donation was negative for evidence of antibody to hepatitis B surface antigen, further indicating that the donor might not have completed recommended childhood vaccinations against any viral hepatitis.

Results of Laboratory Investigation

PCR results for HAV RNA of serum specimens from the 2 home health nurses and the multi–visceral organ recipient are shown in Table 1. The third HCW had recovered by the time the outbreak was identified and had no available specimen from when she was symptomatic. The specimens from the 2 nurses and the organ recipient had detectable HAV RNA with sequences genetically identical to those of other isolates in the CDC HAV isolate database, thus confirming the multi–visceral organ recipient as the source of the HCW infections (Figure 2).

Retrospective testing of banked liver biopsy tissue from the multi–visceral organ recipient showed no detectable HAV RNA in native liver but detectable HAV RNA in all subsequent samples, as early as 5 days after transplantation. Sequential serum and fecal specimens from the multi–visceral organ recipient were positive for HAV RNA through January 2016; follow-up serum specimens drawn monthly during March–May 2016 and a fecal specimen from May 2016 showed clearance of HAV in serum but persistent low-level viremia in feces (Table 2). Frozen serum specimens from the 8-year-old organ donor also were positive for HAV RNA (Table 1). Serum specimens collected from the heart and kidney recipients ≈10 months after transplant tested negative for HAV RNA at CDC and negative for HAV IgM at their sites of clinical care (Table 1). These recipients also had no clinical signs or symptoms consistent with HAV infection.

Discussion

The isolation of genetically identical HAV RNA sequences from the multi–visceral organ recipient and the organ donor indicates HAV infection was transmitted through organ transplantation, even though the index patient had earlier evidence of immunity. The 3 HCWs associated with this investigation most likely were infected by the traditional fecal–oral route. The infectious period of the multi–visceral organ recipient is also among the longest documented in a person infected with HAV, typically an acute disease (*9*).

Figure 1. Polygenetic analysis of HAV isolates within the Centers for Disease Control and Prevention's US HAV database. The genomic regions are the 315-bp long HAV VP1/P2B (viral protein 1/amino terminus of 2B). Black squares indicate isolates from the outbreak of HAV transmitted through a combined liver–small intestine–pancreas transplantation, Texas, USA, 2014–2015. Scale bar indicates nucleotide variation. HAV, hepatitis A virus.

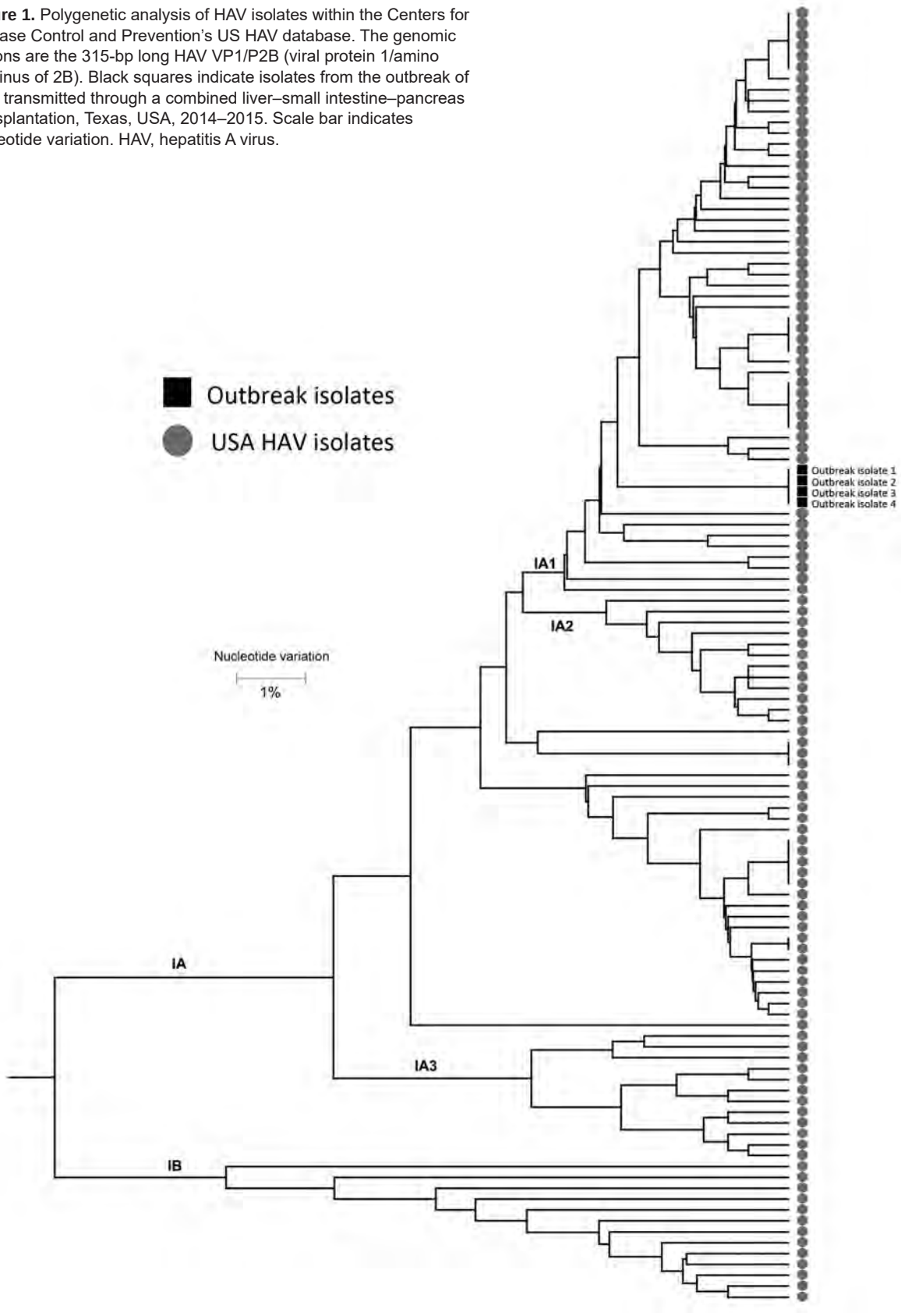

Table 1. Laboratory results for case-patients and contacts related to HAV outbreak, Texas, 2015*

Patient or source of specimen	Outcome or status	HAV rRT -PCR	Serologic testing		Vaccination status
			IgM	IgG	
Donor	Deceased	Detected	Detected	Not detected	Unvaccinated
Multi–visceral organ recipient	Persistent infection	Detected	Detected	Detected	Vaccinated
Heart recipient	Immune	Not detected	Not detected	Detected	Vaccinated
Left kidney recipient	Immune	Not detected	Not detected	Detected	Vaccinated
Right kidney recipient	Immune	Not detected	Not detected	Detected	Vaccinated
Home health nurse A	Recovered	Detected	Detected	Not detected	Unvaccinated
Home health nurse B	Recovered	Detected	Detected	Not detected	Unvaccinated
Inpatient nurse	Recovered	No sample	Detected	Not detected	Unvaccinated

*HAV, hepatitis A virus; rRT-PCR, real-time reverse transcription PCR.

Diagnosis in the multi–visceral organ recipient probably was delayed due to deferred testing because of concurrent conditions that provided alternative explanations for the recipient's clinical presentation and history of prior HAV immunity. The patient had history of vaccination but immune suppression probably blunted antibody response. Symptomatic persons typically show elevated ALT levels that coincide with onset of clinical illness. The infected organ recipient had elevated ALT shortly after liver transplantation, but it coincided with other viral infections (Epstein-Barr virus and cytomegalovirus) and was later assumed to be related to possible acute liver rejection.

The process that results in prolonged courses of HAV infection is unknown (*10*). In contrast to hepatitis B and C viruses, HAV is not typically associated with a prolonged infectious carrier state (*11*). Nonetheless, this case report, and scant longitudinal studies in the literature, demonstrate the potential for ongoing transmission. In published longitudinal studies, HAV viremia persisted for median periods of 22–42 days in immunocompetent persons and 256–490 days in immunocompromised persons (*11*,*12*). Similar findings have been published of persistent viral shedding in feces with median days of detection after symptom onset of 81–127 days (*11*). The level and length of HAV infection and fecal shedding make the carrier a potential continuing infectious source of the virus, which occurred in this case.

Because the primary transmission of HAV is fecal–oral, it is not surprising that diarrhea or fecal incontinence leads to the spread of infection (*13*). Nosocomial outbreaks are uncommon because hygienic practices are generally adhered to more consistently when the patient is symptomatic enough to be hospitalized (*14*). The use of contact precautions is recommended for HCWs caring for patients with HAV who are diapered or incontinent (*15*). Because HCWs do not have increased prevalence of HAV infection and because nosocomial outbreaks of HAV are rare, hepatitis A vaccination is not mandatory for HCWs in the United States (*16*,*17*). In this case, the multi–visceral organ recipient's ileostomy and colostomy output had increased, but it was difficult to determine whether these increases represented symptoms of HAV infection because

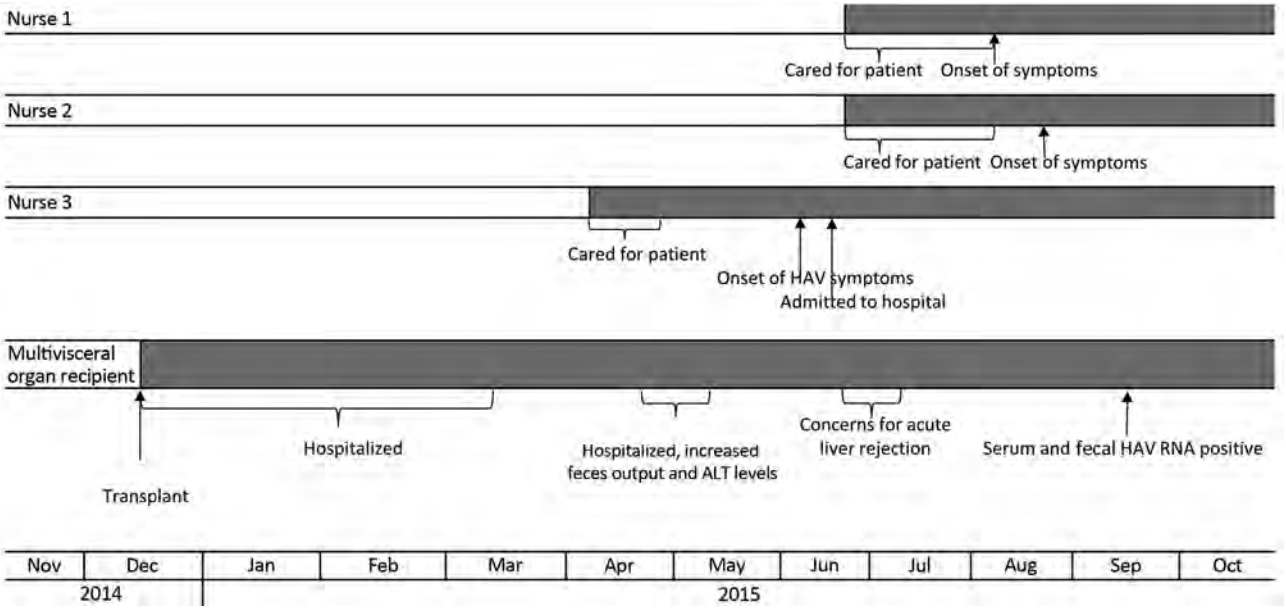

Figure 2. Clinical timeline of HAV infection among a multi–visceral organ transplantation recipient and infected healthcare workers, Texas, 2014–2015. ALT, alanine aminotransferase; HAV, hepatitis A virus.

Table 2. Pathologic, serum, and fecal HAV RNA quantification test results of multi–visceral organ recipient, Texas, 2014–2015*

Date collected	Liver HAV RNA, IU/mL	Small bowel HAV RNA, IU/mL	Serum HAV RNA, IU/mL	Fecal HAV RNA, IU/mL
2014 Dec 18	Native liver, none detected			
2014 Dec 23	34,000			
2015 Jan 23	1,500,00			
2015 Feb 10		7,000		
2015 Mar 10		5,400		
2015 Apr 16	>90,000,000			
2015 Sep 21			>90,000,000	>90,000,000
2015 Sep 29			746,000,000	>90,000,000
2015 Oct 15			1,400,000	372,000
2015 Nov 9			27,900	
2015 Nov 16			17,300	
2015 Nov 23			13,000	1,500,000
2015 Dec 3			38,900	51,900
2016 Jan 11			68,000	22,600
2016 Mar 9				320
2016 Apr 6			Not detected	270
2016 May 4			Not detected	Not detected

*Blank cells indicate that no specimen was available for testing. HAV, hepatitis A virus.

her stoma output was typically described as a continuous liquid, even before hepatitis developed. Also, the home health nurses were spending 12 hours per shift inside the patient's home, where they ate meals and shared space with the patient's family, and thus were considered household contacts, which increased their risk for infection. Previous studies have shown that length of contact with an infected patient increases the attack rate of HCWs, and postexposure prophylaxis is recommended for household contacts of infected patients (*14*,*16*). The parents of the organ recipient were tested for HAV infection before the patient was determined to be the source. The mother's test results indicated immunity to HAV, and the father was not HAV immune but received hepatitis vaccination at testing. Once the infection was detected, contact precautions were instituted during subsequent hospitalizations, the local health department recommended the patient's home health nurses be fully vaccinated against HAV, and no further transmissions to HCWs were detected during the subsequent 8 months of continued viral shedding in the patient's feces.

Transmission of HAV after blood transfusion has been established previously but has not been reported through organ transplantation (*5*). Organ procurement organizations typically complete a medical history questionnaire focusing on prior vaccinations, infections, and exposures to screen donors and recipients for multiple types of infection (*18*). Because of the acute nature of HAV infection, pretransplant testing is not routinely done, although hepatitis A vaccination of transplantation candidates is recommended (*16*). The multi–visceral organ recipient was vaccinated, but studies have shown loss of immunity to HAV after transplantation because of immunosuppression (*19*,*20*). The heart and kidney transplant recipients had evidence of immunity and probably were protected through previous vaccination. It is unknown whether the differences in immunosuppression and types of organs transplanted in the heart and kidney recipients were also factors in preventing HAV infection after transplantation in these persons.

In 2006, the Advisory Committee on Immunization Practices recommended routine hepatitis A vaccination for all children beginning at 12–23 months of age (*16*). Both inactivated whole-virus vaccines available in the United States are well tolerated and effective, showing serologic levels of protection for at least 17 years (*21*,*22*). In 2014, however, 2-dose vaccination coverage among children 19–35 months of age in the United States was only 57.5%, the lowest vaccine coverage for a complete vaccine series among the routine childhood vaccines (*23*). The 8-year-old organ donor in this report most likely was not vaccinated against HAV, and transmission to the recipient and HCWs could have been prevented had vaccination occurred.

Rapid communication between public health officials, physicians, transplant centers, and organ procurement organizations made locating and testing the other organ recipients in this investigation possible. Because of the low US incidence of HAV infection and typically brief self-limiting course of disease, an HAV-unvaccinated organ donor is unlikely to be acutely infected at death and transmit HAV to a patient. The acute nature of HAV infection, low population HAV infection rate, and low rate of HAV infection–associated hospitalization make universal vaccination of HCWs and pretransplant testing for patients impractical. Vaccination against hepatitis A of the organ donor at 12–23 months of age, as recommended by the Advisory Committee on Immunization Practices, most likely would have prevented infection of the multi–visceral organ recipient and exposed HCWs.

This work was supported by the Division of Viral Hepatitis, National Center for HIV, Viral Hepatitis, STD, and TB Prevention, CDC.

Dr. Foster is a medical epidemiologist in the Division of Viral Hepatitis, National Center for HIV, Viral Hepatitis, STD, and TB Prevention, CDC. Her research interests include HAV foodborne outbreaks, hepatitis B and C virus healthcare-associated infections, and perinatal hepatitis C virus transmission and prevention.

References

1. Ciocca M. Clinical course and consequences of hepatitis A infection. Vaccine. 2000;18(Suppl 1):S71–4. http://dx.doi.org/10.1016/S0264-410X(99)00470-3
2. Franco E, Meleleo C, Serino L, Sorbara D, Zaratti L. Hepatitis A: epidemiology and prevention in developing countries. World J Hepatol. 2012;4:68–73. http://dx.doi.org/10.4254/wjh.v4.i3.68
3. Centers for Disease Control and Prevention. Hepatitis A questions and answers for health professionals [cited 2016 Mar 14]. http://www.cdc.gov/hepatitis/hav/havfaq.htm#general
4. Bower WA, Nainan OV, Han X, Margolis HS. Duration of viremia in hepatitis A virus infection. J Infect Dis. 2000;182:12–7. http://dx.doi.org/10.1086/315701
5. Hughes JA, Fontaine MJ, Gonzalez CL, Layon AG, Goodnough LT, Galel SA. Case report of a transfusion-associated hepatitis A infection. Transfusion. 2014;54:2202–6. http://dx.doi.org/10.1111/trf.12648
6. Bhatnagar J, Blau DM, Shieh WJ, Paddock CD, Drew C, Liu L, et al. Molecular detection and typing of dengue viruses from archived tissues of fatal cases by RT-PCR and sequencing: diagnostic and epidemiologic implications. Am J Trop Med Hyg. 2012;86:335–40. http://dx.doi.org/10.4269/ajtmh.2012.11-0346
7. Amon JJ, Devasia R, Xia G, Nainan OV, Hall S, Lawson B, et al. Molecular epidemiology of foodborne hepatitis a outbreaks in the United States, 2003. J Infect Dis. 2005;192:1323–30. http://dx.doi.org/10.1086/462425
8. Wiseman R, Weil LM, Lozano C, Johnson TJ Jr, Jin S, Moorman AC, et al. Notes from the field: health care–associated hepatitis A outbreak—Texas, 2015. MMWR Morb Mortal Wkly Rep. 2016;65:425–6. http://dx.doi.org/10.15585/mmwr.mm6516a5
9. Normann A, Jung C, Vallbracht A, Flehmig B. Time course of hepatitis A viremia and viral load in the blood of human hepatitis A patients. J Med Virol. 2004;72:10–6. http://dx.doi.org/10.1002/jmv.10532
10. Dotzauer A, Heitmann A, Laue T, Kraemer L, Schwabe K, Paulmann D, et al. The role of immunoglobulin A in prolonged and relapsing hepatitis A virus infections. J Gen Virol. 2012;93:754–60. http://dx.doi.org/10.1099/vir.0.038406-0
11. Tjon GM, Coutinho RA, van den Hoek A, Esman S, Wijkmans CJ, Hoebe CJ, et al. High and persistent excretion of hepatitis A virus in immunocompetent patients. J Med Virol. 2006;78:1398–405. http://dx.doi.org/10.1002/jmv.20711
12. Costa-Mattioli M, Allavena C, Poirier AS, Billaudel S, Raffi F, Ferré V. Prolonged hepatitis A infection in an HIV-1 seropositive patient. J Med Virol. 2002;68:7–11. http://dx.doi.org/10.1002/jmv.10163
13. Krober MS, Bass JW, Brown JD, Lemon SM, Rupert KJ. Hospital outbreak of hepatitis A: risk factors for spread. Pediatr Infect Dis. 1984;3:296–9. http://dx.doi.org/10.1097/00006454-198407000-00003
14. Azimi PH, Roberto RR, Guralnik J, Livermore T, Hoag S, Hagens S, et al. Transfusion-acquired hepatitis A in a premature infant with secondary nosocomial spread in an intensive care nursery. Am J Dis Child. 1986;140:23–7.
15. Centers for Disease Control and Prevention. Healthcare Infection Control Practices Advisory Committee (HICPAC). 2007 Guideline for isolation precautions: preventing transmission of infectious agents in healthcare settings, Table 2. Clinical syndromes or conditions warranting empiric transmission-based precautions in addition to standard precautions pending confirmation of diagnosis [cited 2016 Jun 6]. http://www.cdc.gov/hicpac/2007IP/2007ip_table2.html
16. Fiore AE, Wasley A, Bell BP. Prevention of hepatitis A through active or passive immunization: recommendations of the Advisory Committee on Immunization Practices (ACIP). MMWR Recomm Rep. 2006;55(RR-7):1–23.
17. Guturu P, Cicalese L, Duchini A. Hepatitis A vaccination in healthcare personnel. Ann Hepatol. 2012;11:326–9.
18. Schaffner A. Pretransplant evaluation for infections in donors and recipients of solid organs. Clin Infect Dis. 2001;33(Suppl 1):S9–14. http://dx.doi.org/10.1086/320898
19. Arslan M, Wiesner RH, Poterucha JJ, Gross JB Jr, Zein NN. Hepatitis A antibodies in liver transplant recipients: evidence for loss of immunity posttransplantation. Liver Transpl. 2000;6:191–5. http://dx.doi.org/10.1002/lt.500060216
20. Günther M, Stark K, Neuhaus R, Reinke P, Schröder K, Bienzle U. Rapid decline of antibodies after hepatitis A immunization in liver and renal transplant recipients. Transplantation. 2001;71:477–9. http://dx.doi.org/10.1097/00007890-200102150-00023
21. Centers for Disease Control and Prevention. Hepatitis A. In: Hamborsky J, Kroger A, Wolfe C, editors. Epidemiology and prevention of vaccine-preventable diseases (the pink book). 13th ed. Atlanta: Centers for Disease Control and Prevention; 2008. p 135–48.
22. Nolan T, Bernstein H, Blatter MM, Bromberg K, Guerra F, Kennedy W, et al. Immunogenicity and safety of an inactivated hepatitis A vaccine administered concomitantly with diphtheria-tetanus-acellular pertussis and *Haemophilus influenzae* type B vaccines to children less than 2 years of age. Pediatrics. 2006;118:e602–9. http://dx.doi.org/10.1542/peds.2005-2755
23. Hill HA, Elam-Evans LD, Yankey D, Singleton JA, Kolasa M. National, state, and selected local area vaccination coverage among children aged 19–35 months—United States, 2014. MMWR Morb Mortal Wkly Rep. 2015;64:889–96. http://dx.doi.org/10.15585/mmwr.mm6433a1

Address for correspondence: Monique A. Foster, Centers for Disease Control and Prevention, 1600 Clifton Rd NE, Mailstop G37, Atlanta, GA 30329-4027, USA; email: ydg9@cdc.gov

Influence of Referral Pathway on Ebola Virus Disease Case-Fatality Rate and Effect of Survival Selection Bias

Frauke Rudolf, Mads Damkjær, Suzanne Lunding, Kenn Dornonville de la Cour, Alyssa Young, Tim Brooks, Tom Sesay, Alex P. Salam, Sharmistha Mishra, Merete Storgaard

Case-fatality rates in Ebola treatment centers (ETCs) varied widely during the Ebola virus disease (EVD) outbreak in West Africa. We assessed the influence of referral pathway on ETC case-fatality rates with a retrospective cohort of 126 patients treated at the Mathaska ETC in Port Loko, Sierra Leone. The patients consisted of persons who had confirmed EVD when transferred to the ETC or who had been diagnosed onsite. The case-fatality rate for transferred patients was 46% versus 67% for patients diagnosed onsite (p = 0.02). The difference was mediated by Ebola viral load at diagnosis, suggesting a survival selection bias. Comparisons of case-fatality rates across ETCs and clinical management strategies should account for potential survival selection bias.

As of February 14, 2016, the 2014–2016 outbreak of Ebola virus in West Africa had resulted in >14,000 cases of Ebola virus disease (EVD) and ≈4,000 deaths in Sierra Leone (*1*). The country's strategy for managing the outbreak and isolating patients included decentralized Ebola treatment centers (ETCs) and Ebola isolation centers (EICs), which were also known as community care centers and holding centers (*2*,*3*). EICs were transitional facilities meant for admission and isolation of patients who were awaiting results of Ebola diagnostic testing (real-time PCR) and provision of basic care (e.g., administration of oral rehydration solution) (*2*). EIC patients with Ebola virus–negative test results were discharged, and those with positive results were transferred to an ETC. In contrast to EICs, ETCs could care for patients suspected of having and those confirmed to have EVD without transfer of patients between facilities. EICs were initially designed to address a shortfall in ETC bed capacity, although their use continued even as ETC bed capacity increased during the outbreak (*1*).

Recent studies on EVD clinical outcomes (*2*,*4*–*7*) demonstrate considerable variability in case-fatality rates (37%–74%) and call for further analyses to understand the reason(s) for this variability. Predictors of higher case-fatality rate after ETC admission are age (*4*–*6*,*8*) and higher viremia at diagnosis (*9*,*10*) and, less consistently, longer symptom duration before admission (*4*–*6*,*8*,*9*); clinical presentation with confusion, diarrhea, and conjunctivitis (*4*–*6*,*8*); and biochemical evidence of kidney injury, hepatitis, or both (*5*). One study reported early EVD-associated deaths (i.e., in the community) with a case-fatality rate of 24% before ETC transfer (*9*). None of these studies examined the care pathway of EVD patients or the extent to which direct admission to an ETC versus transfer from an EIC influenced case-fatality rates measured in ETCs.

We sought to investigate whether referral pathway had any influence on case-fatality rate. We specifically sought to determine whether there was a statistically significant difference in case-fatality rate between EVD patients admitted directly to the ETC compared with patients first admitted to an EIC and subsequently transferred to the ETC after confirmation of EVD status.

Methods

Study Setting

We conducted a retrospective cohort study on all patients with EVD admitted to the Mathaska ETC in Port Loko

Author affiliations: Aarhus University Hospital, Skejby, Denmark (F. Rudolf, M. Storgaard); GOAL Global, Port Loko, Sierra Leone (F. Rudolf, M. Damkjær, S. Lunding, K.D. de la Cour, A. Young, A.P. Salam, M. Storgaard); Danish Armed Forces Health Services, Brabrand, Denmark (M. Damkjær, S. Lunding, K.D. de la Cour, M. Storgaard); Hans Christian Andersen Children's Hospital, Odense, Denmark (M. Damkjær); Copenhagen University Hospital, Hillerod, Denmark (S. Lunding); Odense University Hospital, Odense (K.D. de la Cour); GOAL Global, Freetown, Sierra Leone (A. Young); Public Health England, Salisbury, UK (T. Brooks); Sierra Leone Ministry of Health and Sanitation, Freetown (T. Sesay); Wohl King's College Clinical Neuroscience Institute, London, UK (A.P. Salam); University of Toronto St. Michael's Hospital, Toronto, Ontario, Canada (S. Mishra);

DOI: http://dx.doi.org/10.3201/eid2304.160485

district, Sierra Leone, during December 12, 2014–March 14, 2015 (i.e., from the time the ETC opened until the first author of this article left Sierra Leone). GOAL Global (https://www.goalglobal.org/) ran the ETC with national and international staff, and the ETC received patients from Port Loko and the neighboring district, Kambia. The ETC received patients via 2 referral paths: 1) patients transferred from an EICs after testing positive for Ebola virus (cohort 1, confirmed cases); and 2) patients admitted after meeting the Sierra Leone Ministry of Health and Sanitation (MoHS) case definition of presumed EVD detected through active monitoring of contacts in quarantine or through passive surveillance in communities and non-EVD healthcare facilities (cohort 2, suspected or probable cases). We included cohort 2 patients in the study only if they were confirmed to have EVD (i.e., Ebola-positive real-time PCR results) after admission to the ETC.

All cases of EVD during the study period in Port Loko and Kambia were confirmed by PCR testing of blood; testing was performed at the Public Health England reference laboratory in Port Loko. Patients received symptomatic treatment according to World Health Organization and MoHS guidelines (*11*). The Sierra Leone Ethics and Scientific Review Committee approved the study.

Data and Analyses

We used EpiData version 3.1 software (EpiData Association, Odense, Denmark) to extract and compare the following data for directly admitted and transferred patients: demographic data (age, sex); clinical data (time from symptom onset to EVD test, death vs. survival in ETC); laboratory data (PCR results, cycle threshold [C_t]); and referral and admission data from clinical charts. For all patients, we used the C_t from the initial positive blood sample (i.e., for cohort 1, the blood sample was from the EIC). The C_t is inversely proportional to the level of virus in the blood sample (*12*). We verified clinical documentation of referral source and cohort 1 classification from MoHS surveillance data and by checking the EVD test date against the ETC admission date. While waiting for PCR results, 6 EIC patients were admitted to the ETC's ward for patients with suspected or probable EVD. To be consistent in our analysis, we considered those patients directly admitted patients (cohort 1).

We calculated the time from symptom onset to EVD test by subtracting the self-reported symptoms-onset date from the first EVD test (which occurred on the date of admission to an EIC or ETC). We assessed the number of symptoms at admission as well as the stage of disease (i.e., the presence of mild influenza-like symptoms, wet symptoms [i.e., diarrhea or vomiting, or both], or hemorrhagic symptoms). Case-fatality was recorded as a death in the ETC. Survival among patients with confirmed EVD was defined as a resolution of viremia, as confirmed by an Ebola virus–negative PCR result. We assessed for differences in proportions by using the χ^2 test for categorical variables with >5 observations/cell in a frequency table (death by cohort, admission stage by cohort, case-fatality rate by cohort). We used the *t*-test to compare continuous variables if normally distributed (age distribution between cohorts); we applied the Wilcoxon–Mann–Whitney rank test if nonnormal distribution was found (interval from symptom onset to EVD testing between cohorts, interval from symptom onset to ETC admission between cohorts, C_t between cohorts, association between low C_t and increased case-fatality rate). To graphically represent the time to death, we used Kaplan-Meier survival curves. To assess difference in fatality rates between transferred and directly admitted patients, we used Cox proportional hazards analysis adjusted for C_t value; no significant deviations from the proportional hazards assumption were found. We used Stata 12 (StataCorp LLC, College Station, TX, USA) to analyze data.

Results

During the study period, 227 patients were transferred and admitted to the ETC; 128 of these patients had EVD. Of those 128 patients, 126 were included in the study. The 2 excluded EVD patients were transferred to another ETC, and their outcomes were unknown. Female patients comprised 53% of the patients. The median age of patients was 30 years (interquartile range [IQR] 18–42); 27 patients were <15 years of age.

The overall EVD case-fatality rate at Mathaska ETC was 59% (74/126 patients). The case-fatality rate was highest among children ≤2 years of age (67%) and persons >35 years of age (78%). Of the 74 patients who died, 72 (97%) died within 9 days of ETC admission (Figure).

Cohort 1 comprised 48 patients who were transferred to Mathaska ETC from EICs (n = 45) or other local ETCs (n = 3) with a confirmed EVD diagnosis. Cohort 2 comprised 78 patients: 16 from quarantine, 1 from a non-EVD hospital, 6 from EICs in Kambia district, 1 from another ETC, and 53 who were referred through community surveillance. The referral pathway was missing for 1 patient. The age distribution was similar between cohorts ($p = 0.2$) (Table). The time from symptom onset to admission at the ETC was shorter for cohort 2 patients than cohort 1 patients (4 vs. 6 days; $p<0.001$), and the C_t at diagnosis was higher among cohort 1 patients than cohort 2 patients (23 vs. 20; $p<0.001$).

The median duration of symptoms before EVD testing was similar between cohorts 1 and 2 (median 4 [IQR 2–5] days vs. 4 [IQR 3–6] days; $p = 0.7$) (Table). A lower C_t was associated with an increased case-fatality rate ($p<0.001$). Neither the quantity of symptoms (mean 6.5 [cohort 1] vs. 6.2 [cohort 2]; $p = 0.3$) nor the distribution of

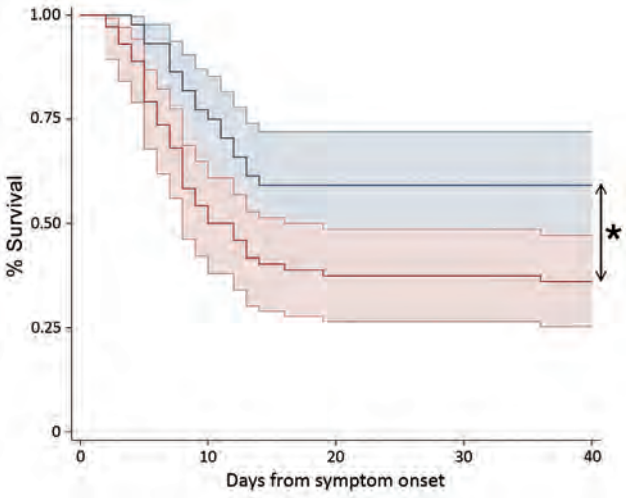

Figure. Kaplan-Meier survival plot stratified by referral pathway for patients admitted directly to an Ebola treatment center (ETC) with confirmed Ebola virus disease (cohort 1, blue line) and for patients diagnosed at the ETC (cohort 2, red line). Plots show the percentage of patients surviving as a function of time (days) from reported symptom onset. Shaded areas indicate 95% CIs. *p<0.05.

patients according to severity stages differed significantly between cohorts 1 and 2 (p = 0.8).

The case-fatality rate was lower for cohort 1 (EVD confirmed before transfer) than cohort 2 (46% vs. 67%; p = 0.02) (Table). After we adjusted for C_t at diagnosis, the case-fatality rate was no longer significantly different between cohorts 1 and 2 (p = 0.2).

Discussion

Understanding sources of variability in observed case-fatality rates during the 2014–2016 Ebola virus outbreak in West Africa is essential for interpreting case-fatality rate as part of routine monitoring of a clinical program (*1*) and for evaluating the effect of clinical interventions. We investigated whether patients transferred to Mathaska ETC had a lower case-fatality rate than patients directly admitted to the ETC, and our results show that referral pathway does influence the case-fatality rate. This finding confirms the observations from previous studies showing that virus load and patient age are associated with EVD case fatality (*4*).

In Sierra Leone, 5 ETCs with different referral pathways reported different case-fatality rates. Among EVD patients admitted and diagnosed onsite at Kenema Government Hospital early in the outbreak, the case-fatality rate was 74% (64 deaths/87 patients) (*6*). The Médecins Sans Frontières ETC in Kailahun admitted and diagnosed patients on-site and reported a case-fatality rate of 51% (270 deaths/525 patients) (*4*). In Bo, the case-fatality rate was 66% (142/216) among all confirmed EVD patients detected in the community during the study period, but it was 40% (49/123) among the detected EVD patients who survived until admittance to an ETC (*9*). In contrast, the Save the Children ETC in Kerry Town, Sierra Leone, had a case-fatality rate of 37% (55 deaths/150 patients) and was equipped to provide a higher level of care (additional diagnostics) but received only confirmed patients from EICs (*5*). Among the 85 EVD patients admitted to the EIC in the Jui Government Hospital in Sierra Leone, the case-fatality rate was 60%, although it was unclear whether the deaths occurred in the EIC or in the ETC to which confirmed patients were transferred (*7*).

We found that the influence of referral pathways on the estimated case-fatality rate at Mathaska ETC was probably mediated by differences in virus load at diagnosis. This finding supports the hypothesis that differences in observed case-fatality rates by referral pathway are probably due to survival selection bias rather than differences in patient care at individual ETCs. We did not measure case-fatality rates in the EICs. Thus, we cannot infer the role of EIC versus ETC on case-fatality rate before EVD confirmation and transfer to EVD-confirmed wards. Furthermore, although the difference in virus load among the 2 cohorts suggests that the transferred patients were in recovery, there was no difference in the number of symptoms nor in the severity of disease when patients were admitted to the ETC. We did not, however, assess the degree of the individual symptoms, and that information might have added clarity.

Our data, along with the case-fatality rates reported for other ETCs in Sierra Leone (*4*,*5*), suggest that if the referral pathway (i.e., time spent in EICs) is long, patients may die before getting tested for EVD disease. Thus, EVD patients transferred to the ETC represent a different patient population than those diagnosed on-site. Our findings of possible

Table. Demographic and epidemiologic differences between 2 patient cohorts in a study of the sources of variability in case-fatality rates in Ebola treatment centers, Sierra Leone, 2014–2016*

Variable	Cohort 1, n = 48	Cohort 2, n = 78	p value
Case-fatality rate, %	46	67	0.02
Age, median, IQR	29 (14–40)	34 (20–45)	0.2
Children <15 years of age, no. (%)	12 (44)	15 (56)	0.4
Days from symptom onset to EVD testing (IQR)	4 (2–5)	4 (3–6)	0.7
Days from symptom onset to admission at ETC, median (IQR)	6 (4–7)	4 (2–5)	<0.001
C_t, median (IQR)†	23 (21–26)	20 (18–23)	<0.001

*Cohort 1 consisted of patients admitted directly to the ETC (Ebola treatment center) with confirmed EVD (Ebola virus disease); cohort 2 consisted of patients admitted directly to the ETC, where they were subsequently diagnosed with EVD. C_t, cycle threshold; IQR, interquartile range.
†Obtained from first blood sample drawn.

survivor selection bias are consistent with findings in previous reports showing a higher case-fatality rate among patients who were admitted early after symptom onset (*4*,*5*), an initially counter-intuitive finding, given the provision early supportive management. In Kailahun, patients who traveled long distances to reach the ETC had a lower case-fatality rate than those who traveled shorter distances (*4*). Although, as pointed out by Hunt et al. (*5*), reported symptom onset date is subject to recall bias. Thus studies of clinical predictors and comparisons of case-fatality rates across ETCs must account for potential survivor selection bias. Symptom-onset date is prone to recall and social desirability bias, but referral pathways are an objective indicator of potential differences in patient populations admitted to ETCs. From a clinical perspective in the ETC, measuring and making decisions based on anticipated efficacy of supportive management or experimental drugs must account for these differences in patients. A key social mobilization message during the West Africa outbreak was the importance of early diagnosis and treatment to save lives (not just prevent transmission), drawing on experience and evidence from other infectious diseases with similar end-organ effects. Invasive monitoring and careful fluid management probably contributed to the low case-fatality rates observed in the study in Kerry Town, but as the authors noted, the study population was subject to selection bias (*5*), which limits the generalizability of care-associated predictors of outcome. Rigorous study of all patients with confirmed EVD and estimates of case-fatality rate at each point in the referral pathway (community, EIC, ETC) are needed to disentangle survival selection bias from the effect of early care and care-associated predictors of case-fatality rate.

In conclusion, case-fatality rates across ETCs may depend on which patients are referred to the facilities and, thus, the distribution of known predictors, such as age and virus load. Referral pathways and the potential for survival selection bias should be accounted for when comparing case-fatality rates between studies, ETCs, and interventions and when planning and evaluating future clinical trials.

Acknowledgment

We thank the personnel working at the Mathaska ETC for their dedicated and consistent work.

Dr. Rudolf is a registrar at the Department of Infectious Medicine, Aarhus University Hospital, and a postdoctoral researcher at the Center of Global Health, Department of Public Health, Aarhus University, Denmark. She has done research in the field of infectious medicine, with a primary interest in tuberculosis.

References

1. World Health Organization. Ebola situation report. February 17, 2016. 2016 [cited 2016 Feb 17]. http://apps.who.int/iris/bitstream/10665/204418/1/ebolasitrep_17Feb2016_eng.pdf?ua=1&ua=1
2. Lado M, Walker NF, Baker P, Haroon S, Brown CS, Youkee D, et al. Clinical features of patients isolated for suspected Ebola virus disease at Connaught Hospital, Freetown, Sierra Leone: a retrospective cohort study. Lancet Infect Dis. 2015;15:1024–33. http://dx.doi.org/10.1016/S1473-3099(15)00137-1
3. Michaels-Strasser S, Rabkin M, Lahuerta M, Harripersaud K, Sutton R, Ahoua LN, et al. Innovation to confront Ebola in Sierra Leone: the community-care-centre model. Lancet Glob Health. 2015;3:e361–2. http://dx.doi.org/10.1016/S2214-109X(15)00045-5
4. Fitzpatrick G, Vogt F, Moi Gbabai OB, Decroo T, Keane M, De Clerck H, et al. The Contribution of Ebola viral load at admission and other patient characteristics to mortality in a Médecins Sans Frontières Ebola case management centre, Kailahun, Sierra Leone, June–October 2014. J Infect Dis. 2015;212:1752–8. http://dx.doi.org/10.1093/infdis/jiv304
5. Hunt L, Gupta-Wright A, Simms V, Tamba F, Knott V, Tamba K, et al. Clinical presentation, biochemical, and haematological parameters and their association with outcome in patients with Ebola virus disease: an observational cohort study. Lancet Infect Dis. 2015;15:1292–9. http://dx.doi.org/10.1016/S1473-3099(15)00144-9
6. Schieffelin JS, Shaffer JG, Goba A, Gbakie M, Gire SK, Colubri A, et al.; KGH Lassa Fever Program; Viral Hemorrhagic Fever Consortium; WHO Clinical Response Team. Clinical illness and outcomes in patients with Ebola in Sierra Leone. N Engl J Med. 2014;371:2092–100. http://dx.doi.org/10.1056/NEJMoa1411680
7. Yan T, Mu J, Qin E, Wang Y, Liu L, Wu D, et al. Clinical characteristics of 154 patients suspected of having Ebola virus disease in the Ebola holding center of Jui Government Hospital in Sierra Leone during the 2014 Ebola outbreak. Eur J Clin Microbiol Infect Dis. 2015;34:2089–95. http://dx.doi.org/10.1007/s10096-015-2457-z
8. Bah EI, Lamah MC, Fletcher T, Jacob ST, Brett-Major DM, Sall AA, et al. Clinical presentation of patients with Ebola virus disease in Conakry, Guinea. N Engl J Med. 2015;372:40–7. http://dx.doi.org/10.1056/NEJMoa1411249
9. Crowe SJ, Maenner MJ, Kuah S, Erickson BR, Coffee M, Knust B, et al. Prognostic indicators for Ebola patient survival. Emerg Infect Dis. 2016;22:217–23. http://dx.doi.org/10.3201/eid2202.151250
10. Fasina FO, Adenubi OT, Ogundare ST, Shittu A, Bwala DG, Fasina MM. Descriptive analyses and risk of death due to Ebola virus disease, West Africa, 2014. J Infect Dev Ctries. 2015;9:1298–307. http://dx.doi.org/10.3855/jidc.6484
11. World Health Organization. Clinical management of patients with viral hemorrhagic fever. A pocket guide for the frontline health worker. 2014 [cited 2016 Feb 17]. http://www.who.int/csr/resources/publications/clinical-management-patients/en/
12. Spengler JR, McElroy AK, Harmon JR, Ströher U, Nichol ST, Spiropoulou CF. Relationship between Ebola virus real-time quantitative polymerase chain reaction-based threshold cycle value and virus isolation from human plasma. J Infect Dis. 2015;212(Suppl 2):S346–9. http://dx.doi.org/10.1093/infdis/jiv187

Address for correspondence: Frauke Rudolf, Department of Infectious Diseases, Hvidovre Hospital, Hvidovre, Denmark, Folehaven 133 2. Tv, 2500 Valby, Denmark; email: frudolf@dadlnet.dk

Plasmodium malariae Prevalence and *csp* Gene Diversity, Kenya, 2014 and 2015

Eugenia Lo, Kristie Nguyen, Jennifer Nguyen, Elizabeth Hemming-Schroeder, Jiaobao Xu, Harrisone Etemesi, Andrew Githeko, Guiyun Yan

In Africa, control programs that target primarily *Plasmodium falciparum* are inadequate for eliminating malaria. To learn more about prevalence and genetic variability of *P. malariae* in Africa, we examined blood samples from 663 asymptomatic and 245 symptomatic persons from western Kenya during June–August of 2014 and 2015. *P. malariae* accounted for 5.3% (35/663) of asymptomatic infections and 3.3% (8/245) of clinical cases. Among asymptomatic persons, 71% (32/45) of *P. malariae* infections detected by PCR were undetected by microscopy. The low sensitivity of microscopy probably results from the significantly lower parasitemia of *P. malariae.* Analyses of *P. malariae* circumsporozoite protein gene sequences revealed high genetic diversity among *P. malariae* in Africa, but no clear differentiation among geographic populations was observed. Our findings suggest that *P. malariae* should be included in the malaria elimination strategy in Africa and highlight the need for sensitive and field-applicable methods to identify *P. malariae* in malaria-endemic areas.

Over the past decade, malaria control strategies in Africa have reduced the number of malaria cases and deaths. Nevertheless, non–*Plasmodium falciparum* malaria still presents a major challenge for malaria elimination (*1*,*2*). Global malaria elimination programs focus primarily on *P. falciparum*. Recent research efforts and control programs have drawn resources to *P. vivax* malaria. By contrast, *P. malariae* and *P. ovale* receive little attention, and malaria caused by these organisms is among the most neglected tropical diseases (*3*). In those rural areas of Africa where malaria is most common, affordable diagnostic tools are rapid diagnostic tests and microscopy, but they are not effective for detecting these 2 species, mainly because parasitemia with these species is low (*4*–*6*). As a result, *P. malariae* and *P. ovale* infections are often underestimated, and epidemiologic information, such as distribution and prevalence of these species in malaria-endemic areas, is lacking. This knowledge is essential for implementation of specific strategies for monitoring and eliminating all types of malaria where it is endemic to Africa.

Although *P. malariae* infection is often asymptomatic and rarely leads to severe clinical illness or death, this species causes a low-grade chronic infection that persists for decades and is associated with nephropathy and anemia (*7*–*9*). The persistence, as well as submicroscopic features of *P. malariae*, have contributed to intermittent outbreaks of malaria in the Colombian Amazon region (*10*). In addition, *P. malariae* can cause irreversible stage 5 kidney failure (*11*). The prevalence of this species may increase the risk for kidney injuries and impair renal function, particularly in children with no immunity against *P. malariae*. Ample evidence shows peak prevalence for severe and uncomplicated clinical *P. falciparum* malaria among infants and children in sub-Saharan Africa (*12*–*14*). Contrary to this age pattern, patients with *P. malariae* infections in Papua, Indonesia, were older (median 22 years of age) than those with non–*P. malariae* infections (e.g., *P. vivax;* median 10 years of age) (*9*). Knowledge of the age patterns of patients with *P. malariae* infection is critical for understanding its epidemiology and developing effective preventative strategies.

Compared with the distribution of *P. falciparum* and *P. vivax,* the distribution of *P. malariae* is relatively sparse and variable. *P. malariae* is endemic to West Africa (*3*), South America (*15*), Asia (*16*,*17*), and the western Pacific region (*18*,*19*). Knowledge of genetic variation among isolates from these geographic areas is still lacking. One study indicated a remarkably low level of sequence diversity at the *msp*1 locus in *P. malariae* from Brazil (*20*). Similarly, the lack of variation at the *dhfr* and *dhps* loci has been shown for *P. malariae* from Asia and the western Pacific region (*21*,*22*). These findings suggested that antimalarial drugs might be imposing selective pressure on the genetic diversity of *P. malariae*. The circumsporozoite protein (*csp*) gene, which is known to be critical for plasmodia sporozoite motility and hepatocyte invasion (*23*), has been shown to be variable in length and is a sequence of the tandemly

Author affiliations: University of California Irvine, Irvine, California, USA (E. Lo, K. Nguyen, J. Nguyen, E. Hemming-Schroeder, G. Yan); Southern Medical University, Guangzhou, China (J. Xu); Kenya Medical Research Institute, Kisumu, Kenya (H. Etemesi, A. Githeko)

DOI: http://dx.doi.org/10.3201/eid2304.161245

repeated peptide units in *P. falciparum* (*24*,*25*), *P. vivax* (*26*,*27*), and *P. malariae* isolates from Central Africa (*28*). The vast antigenic variation observed in *P. falciparum* as a result of immune selection pressure can influence the capacity of mosquito transmission and the effectiveness of malaria vaccine (*29*). In this study, we sought to determine the prevalence of infection and age distribution of persons with asymptomatic and symptomatic *P. malariae* infection in western Kenya, the genetic affinity between *P. malariae* isolates from East Africa and other regions, and the level of *csp* gene diversity among *P. malariae* and the significance of this diversity.

Scientific and ethical clearance was given by the institutional scientific and ethical review boards of the Kenya Medical Research Institute and the University of California Irvine. Written informed consent/assent for study participation was obtained from all consenting heads of households, parents/guardians (for minors <18 years of age), and each person who was willing to participate in the study.

Materials and Methods

Study Areas and Participants

During June–August of 2014 and 2015, blood samples were collected from persons in 4 villages at the Lake Victoria basin (elevation ≈1,000 m) of western Kenya (Figure 1). These villages represent parts of the Lake Victoria area previously shown by nested and quantitative PCR (qPCR) methods to have high, stable rates of malaria transmission and prevalence (10%–40%) among children 5–14 years of age (*30*,*31*).

Community samples were collected from nonfebrile schoolchildren in 7 public primary schools (70–100 children/school, 2 schools/village except Kombewa). An equal number of boys and girls 6–15 years of age were randomly selected from each school. To determine *P. malariae* prevalence in the adult population, we randomly selected 63 persons (32 male and 31 female) >15 years of age from 18 households in Kombewa. We examined a total of 663 samples from the communities, which provided an estimation of 4% margin of error in parasite prevalence with 0.05 type I error. At the time of sampling, none of these persons exhibited fever or malaria-related symptoms.

Clinical samples were collected from 113 male and 132 female patients, <1 to 76 years of age, in 3 district hospitals. This sample size provided an estimation of 6% margin of error in parasite prevalence with 0.05 type I error. These patients had fever or malaria-related signs or symptoms and were determined to be positive for *Plasmodium* spp. by microscopy at the time of sampling. Thick and thin blood smears were prepared for microscopic examination to determine the *Plasmodium* species, and ≈50 μL blood was blotted onto Whatman 3MM filter (Sigma Aldrich, St. Louis, MO, USA) papers. Filter papers were air dried and stored in zip-sealed plastic bags with silica gel absorbent at room temperature until DNA extraction.

Microscopy and PCR of *Plasmodium* spp.

We examined slides under microscopes at 100× magnification and counted the number of parasites per 200 leukocytes. A slide was considered negative when no parasites were observed after counting >100 microscopic fields. At the time of sample collection, all slides were read by 2 microscopists. If counts were discordant, the slides were examined by a third microscopist. The density of parasitemia was expressed as the number of asexual parasites per microliter of blood, assuming a leukocyte count of 8,000 cells/μL, according to World Health Organization guidelines.

We extracted parasite DNA from half of a dried blood spot by using the Saponin/Chelex method (*32*). The final extracted volume was 200 μL. For all samples, nested amplification of the 18S rRNA gene region of plasmodia (*P. falciparum*, *P. vivax*, *P. malariae*, and *P. ovale*) was used for parasite detection and species identification. As positive controls for all amplifications, we used DNA from *P. falciparum* isolates 7G8 (MR4-MRA-926) and HB3 (MR4-MRA-155), *P. vivax* Pakchong (MR4-MRA-342G) and Nicaragua (MR4-MRA-340G), *P. malariae* (MR4-MRA-179), and *P. ovale* (MR4-MRA-180). As negative controls, we used water and noninfected samples to ensure lack of contamination. Reaction was performed in a Bio-Rad MyCycler thermal cycler according to the published protocol (*33*) (details in online Technical Appendix 1, https://wwwnc.cdc.gov/EID/article/23/4/16-1245-Techapp1.pdf).

In addition, the amount of parasite DNA was estimated by using the SYBR Green (Thermo Scientific, Foster City, CA, USA) qPCR detection method with *Plasmodium* species–specific primers that targeted the 18S rRNA genes (*34*,*35*). Reactions were performed in a CFX96 Touch Real-Time PCR Detection System (Bio-Rad, Foster City, CA, USA). To confirm specific amplifications of the target sequence, we performed melting curve analyses for each amplified sample. To measure reproducibility of the cycle threshold (C_t), we calculated the mean value and standard deviations from triplicates in 2 independent assays. The parasite gene copy number in a sample was quantified according to C_t by using the equation (*30*) $GCN_{sample} = e^{(E \times \Delta Ctsample)}$, where GCN stands for gene copy number; ΔCt, the difference in C_t between the negative control and the sample; e, exponential function; and E, amplification efficiency (online Technical Appendix 1).

CSP Sequencing and Phylogenetic Analyses

Four internal primers were designed specifically on the *P. malariae csp* gene region and used together with the

published primers (*28*; online Technical Appendix 1 Table) to unambiguously amplify the 3 segments, the N terminal, the central repeat, and the C-terminal regions of the *csp* gene. A total of 37 *P. malariae* isolates were amplified and sequenced. All resulted sequences were verified by comparing them with those in the GenBank database by using BLAST (https://blast.ncbi.nlm.nih.gov/Blast.cgi). Sequences were translated into protein sequences and analyzed together with all *csp* protein sequences available in GenBank of *P. malariae* from East Africa (Kenya and Uganda), West Africa (Cameroon), Central Africa (Côte d'Ivoire), and South America (Venezuela) and of *P. brasilianum* from South America (Brazil and Venezuela). It is noteworthy that although *P. malariae* and *P. brasilianum* coexist in Brazil, no *csp* sequence for *P. malariae* is available. Because of the potential for alignment errors associated with gaps in the nucleotide sequences, we used translated amino acid sequences with unambiguous indels in phylogenetic analyses. Sequence diversity, including measures of evolutionary distances and average pairwise divergence, were estimated and compared among geographic regions (online Technical Appendix 1).

Statistical Analyses

A 1-tailed *t*-test was used to test for the significance of differences in parasite gene copy number between *P. malariae* from symptomatic and asymptomatic patients and between *P. malariae* and *P. falciparum* in co-infected samples. In addition, we calculated the Pearson correlation coefficient (r^2) for parasite gene copy number and age by using R (https://www.r-project.org/).

Results

P. malariae Prevalence and Patient Age Distribution

Among the 663 samples from asymptomatic persons, *P. malariae* was detected by PCR in 35 (5.3% prevalence). Among these, 29 were mixed infections (with *P. falciparum*) and 6 were *P. malariae* monoinfections (Figure 1; Table 1). *P. malariae* was found to be most prevalent in Kombewa (14.3%, 19/133 cases), followed by Kendu Bay (5.3%, 8/150 cases). Prevalence of *P. falciparum* prevalence was relatively high at these 2 sites (44% and 59%, respectively; Table 1). In Kombewa, 13 of 19 *P. malariae* cases were detected in younger persons (<15 years of age), which was significantly higher than the number of cases detected in older persons (6 cases, p = 0.04; Table 1). Although such a comparison between age groups cannot be made for the other sites, a similar pattern was observed for symptomatic patients.

Among the 245 samples from symptomatic patients, 8 (3.3%) *P. malariae* cases were detected; 6 were mixed

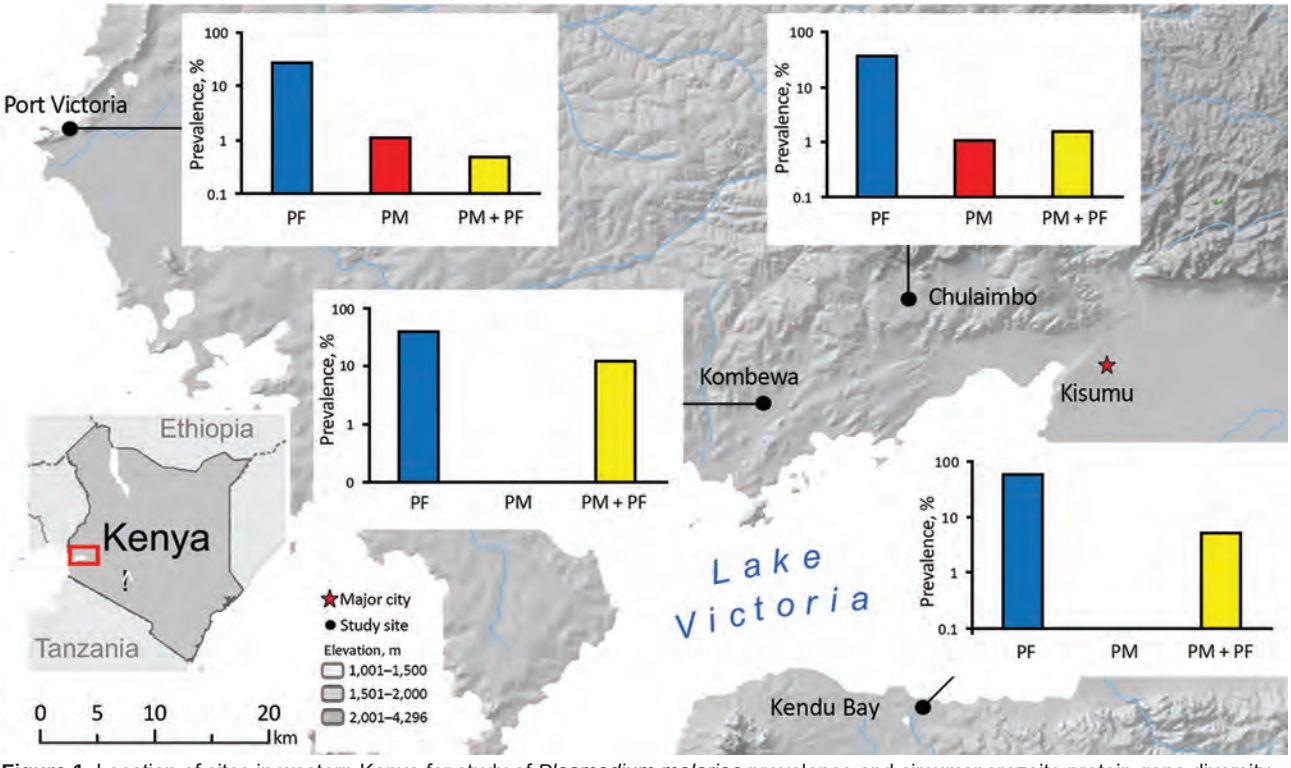

Figure 1. Location of sites in western Kenya for study of *Plasmodium malariae* prevalence and circumsporozoite protein gene diversity, Kenya, 2014 and 2015. Prevalence (logarithmic vertical scales) of *P. falciparum* monoinfections (PF), *P. malariae* monoinfections (PM), and *P. falciparum* and *P. malariae* co-infections (PF+PM) are shown for each study site.

Table 1. Prevalence of *Plasmodium malariae* and *P. falciparum* among asymptomatic persons in the community, Kenya, June–August 2014 and 2015*

Site, patient age, y	No. tested	No. (%) infections			
		Total	*P. malariae*	*P. falciparum*	Mixed†
Kombewa					
≤15	63	41 (65.1)	0	28 (44.4)	13 (20.6)
>15	70	35 (50)	2 (2.9)	29 (41.4)	4 (5.7)
Chulaimbo					
≤15	190	76 (40)	2 (1.1)	71 (37.4)	3 (1.6)
Kendu Bay					
≤15	150	97 (64.7)	0	89 (59.3)	8 (6)
Port Victoria					
≤15	190	57 (30)	2 (1.1)	54 (28.4)	1 (0.5)
Total	663	306 (46.2)	6 (0.9)	271 (40.9)	29 (4.4)

*According to nested PCR of the 18S rRNA gene.
†*P. malariae* and *P. falciparum*.

infections with *P. falciparum* and 2 were *P. malariae* monoinfections (Table 2). When the samples were stratified by patient age, all *P. malariae* infections in symptomatic persons were in infants or very young children of <5 years of age (8/135, 5.9% infection rate). Although *P. falciparum* infection was highest among patients >5 to ≤15 years of age, no *P. malariae* was detected in persons in this and older age groups despite smaller samples in these groups. No significant difference was detected between male and female patients.

Comparisons of Diagnostic Approaches and Parasitemia

Compared with microscopy, nested PCR revealed a significantly higher number of *P. malariae* infections in the community (Table 3). All samples that were *P. malariae* positive by microscopy were identified as positive by PCR and qPCR. Across the study sites, nested PCR–based prevalence ranged from 0 to 12.2% (average 4.8%), >2-fold higher than by microscopy (0 to 3.8%, average 1.9%; Table 3). The discrepancy between the 2 methods was also reflected by the difference in *P. falciparum* prevalence; 10% more positive infections were detected by nested PCR than by microscopy. Nevertheless, such a discrepancy was not as substantial as that for *P. malariae*.

Although the number of *P. malariae*–positive clinical samples detected in this study was low, these samples indicated an overlapping range of parasite gene copy number (geometric mean 6.4×10^1/μL, range 4.3×10^1 to 1.2×10^3/μL; Figure 2) with that of the samples from asymptomatic persons (geometric mean 4.8×10^1/μL, range 0.5×10^1 to 9.4×10^2/μL) without differing significantly ($p>0.05$). Similar results were observed in the level of *P. malariae* parasitemia, for which samples from symptomatic and asymptomatic persons did not differ significantly (Figure 2). Parasite gene copy number and *P. malariae* parasitemia were significantly positively correlated with each other ($r^2 = 0.77$, $p<0.01$; online Technical Appendix 1 Figure 1).

Parasite gene copy number and parasitemia for *P. falciparum* were generally higher than those for *P. malariae* (Figure 3, panel A). Among the 35 mixed infections, 28 (80%) gene copy numbers were higher for *P. falciparum* than for *P. malariae* (online Technical Appendix 1 Figure 2). Among these samples overall, the amount of *P. falciparum*

Table 2. Prevalence of *Plasmodium malariae* and *P. falciparum* among symptomatic persons, Kenya, June–August 2014 and 2015*

Site, patient age, y	No. tested	No. (%) infections			
		Total	*P. malariae*	*P. falciparum*	Mixed†
Chulaimbo					
≤5	27	18 (66.7)	2 (7.4)	15 (55.6)	0
>5 to ≤15	4	3 (75)	0	3 (75)	0
>15	13	3 (23.1)	0	3 (23.1)	0
Kendu Bay					
≤5	44	38 (86.4)	0	35 (79.5)	3 (6.8)
>5 to ≤15	34	31 (91.2)	0	31 (91.2)	0
>15	24	23 (95.8)	0	23 (95.8)	0
Port Victoria					
≤5	64	54 (84.4)	0	51 (79.7)	3 (4.7)
>5 to ≤15	22	20 (90.9)	0	20 (90.9)	0
>15	13	9 (69.2)	0	9 (69.2)	0
Total					
≤5	135	110 (81.5)	2 (1.5)	101 (74.8)	6 (4.4)
>5 to ≤15	60	54 (90)	0	54 (90)	0
>15	50	35 (70)	0	35 (70)	0

*According to nested PCR of the 18S rRNA gene.
†*P. malariae* and *P. falciparum*.

Table 3. Methods used to diagnose *Plasmodium* infections in asymptomatic populations, Kenya, June–August 2014 and 2015*

Site, method	No. tested	No. (%) infections					
		Total	*P. falciparum*	*P. vivax*	*P. malariae*	*P. ovale*	*P. falciparum/malariae*
Kombewa							
Microscopy	133	54 (41.2)	49 (37.4)	0	0	0	5 (3.8)
PCR	133	70 (53.4)	54 (41.2)	0	0	0	16 (12.2)
Chulaimbo							
Microscopy	190	46 (24.2)	42 (22.1)	0	1 (0.5)	0	3 (1.6)
PCR	190	76 (40.1)	71 (37.4)	0	2 (1.1)	0	3 (1.6)
Kendu Bay							
Microscopy	150	78 (52)	75 (50)	0	0	0	3 (2)
PCR	150	97 (64.6)	89 (59.3)	0	0	0	8 (5.3)
Port Victoria							
Microscopy	190	36 (18.5)	35 (18.5)	0	0	0	1 (0.5)
PCR	190	57 (30)	54 (28.4)	0	2 (1.1)	0	1 (0.5)
All sites							
Microscopy	663	214 (32.4)	201 (30.4)	0	1 (0.2)	0	12 (1.8)
PCR	663	300 (45.4)	268 (40.5)	0	4 (0.6)	0	28 (4.2)

DNA (geometric mean 1.6×10^2/μL, range 1×10^1 to 5.5×10^3/μL) was significantly higher than the amount of *P. malariae* DNA (geometric mean 4.7×10^1/μL, range 0.4×10^1 to 1.1×10^3/μL; p = 0.003), consistent with the difference in parasitemia according to microscopy (*P. malariae* geometric mean 3.2×10^2 parasites/μL vs. *P. falciparum* geometric mean 1.1×10^3 parasites/μL; online Technical Appendix 1 Figure 2).

When all *P. malariae* samples were pooled, the parasite gene copy number did not correlate significantly with patient age ($r^2 = 0.07$; online Technical Appendix 1 Figure 3). Neither *P. malariae* prevalence rate nor parasite gene copy number differed significantly according to patient sex.

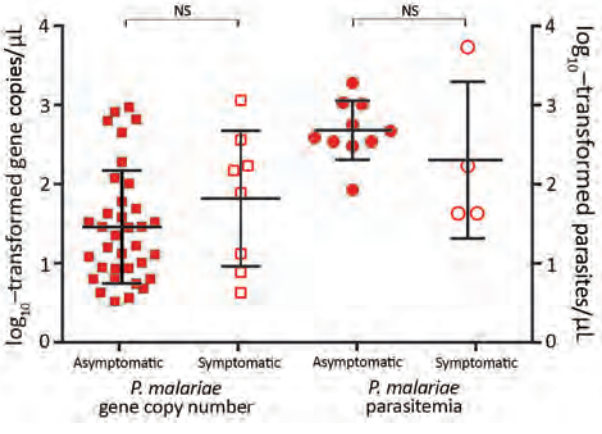

Figure 2. Parasite gene copy numbers (per microliter) detected by SYBR Green (Thermo Scientific, Foster City, CA, USA) quantitative PCR and parasitemia (parasites per microliter) determined by microscopy of *Plasmodium malariae* samples from asymptomatic and symptomatic persons. Median, first quartile, and fourth quartile of the data are shown for each sample category (horizontal lines). No significant difference was observed between asymptomatic and symptomatic persons in terms of *P. malariae* parasite gene copy number and parasitemia. Squares represent samples with gene copy number measured by quantitative PCR; circles, samples with parasitemia estimated by microscopy; closed squares and circles, *P. malariae* samples from asymptomatic persons; open squares and circles, *P. malariae* samples from symptomatic patients. NS, not significant.

Genetic Relatedness and *csp* Divergence of *P. malariae*

The *csp* alignment comprised 530 aa, of which 34 (6.4%) were polymorphic among the studied parasites of different taxa (online Technical Appendix 2, https://wwwnc.cdc.gov/EID/article/23/4/16-1245-Techapp2.pdf). To avoid polymorphism caused by PCR error, we sequenced each isolate at least twice in both directions. Substantial length variation was observed in the central repeat region, where the number of $NAAG_n$ (the repeat codon unit in which n denotes the number of repeats) in *P. malariae* ranged from 49 to 85 units. These tandem repeats could be rapidly evolving

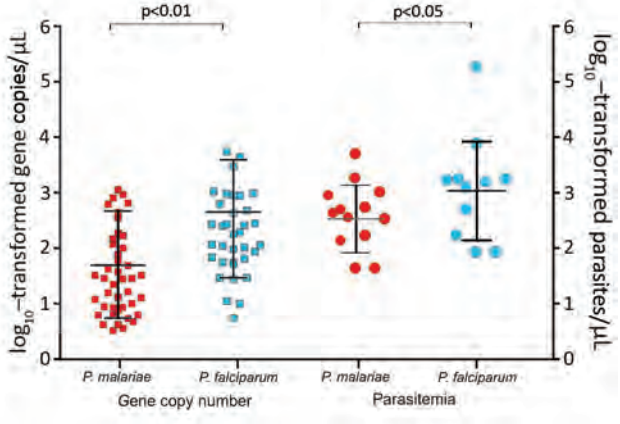

Figure 3. *Plasmodium malariae* and *P. falciparum* parasite gene copy numbers (per microliter) and parasitemia (parasites per microliter) in co-infected samples. Median, first quartile, and fourth quartile of the data are shown for each sample category (horizontal lines). Parasite gene copy number and parasitemia were lower in *P. malariae*–positive than in *P. falciparum*–positive samples. Squares represent samples with gene copy number measured by quantitative PCR; circles, samples with parasitemia estimated by microscopy; red, *P. malariae* samples; blue, *P. falciparum* samples.

through a different mechanism and may influence genetic relationships among the samples. To examine such effect, we constructed phylogenetic trees with 2 sets of data: the entire sequence (530 aa) and partial sequences without the central repeat region (225 aa).

Maximum-likelihood analyses of the entire *csp* gene showed a clear distinction between isolates from South America and those from the other geographic regions (Figure 4, panel A). *P. brasilianum* and *P. malariae* from Venezuela formed a monophyletic group (bootstrap >95%) closely associated with *P. brasilianum* from Brazil. Sequences of *P. malariae* from Venezuela were almost identical to those of *P. brasilianum* from the same area. Closely related to the clade from South America was a large monophyletic group that contained *P. malariae* from East, Central, and West Africa and from China (bootstrap >90%). The isolates from these regions were divided into 2 subclades: I and II (Figure 4, panel A). Subclade I comprised a mix of *P. malariae* isolates from Kenya, Cameroon, and Côte d'Ivoire. Subclade II comprised a mix of *P. malariae* isolates from Kenya, Cameroon, Uganda, and China. Sequences without the central repeat region indicated consistently the distinctiveness between *P. brasilianum* from Brazil and *P. malariae*, but the *P. malariae* samples from different geographic regions were poorly resolved (Figure 4, panel B). The *P. malariae* isolate from China was nested within the African subclade, suggestive of an African origin (Figure 4, panel C). No clear microgeographic structure was detected, although sample size at the population level was small.

Among the 3 geographic regions, the level of *csp* sequence divergence in *P. malariae* was higher in isolates from East Africa than from West Africa, as reflected by a higher number of polymorphic sites and a greater extent of *csp* length variation despite difference in sample size (Figure 5, panels A and B). These variations were located at the 3′ N terminal through the central repeat region, where the largest degree of mismatch was observed (Figure 5, panel B). To the contrary, the level of sequence polymorphism was lowest in isolates from South America (Figure 5, panel A), but the greatest range of difference in tandem repeat units where remarkable mismatch was observed was toward the end of the central region. Despite the small sample size, the number of tandem repeats was generally lower in *P. brasilianum* than *P. malariae* (Figure 5, panel C).

Discussion

In Kenya, areas along the shoreline of Lake Victoria and coastal regions are malaria hot spots, where intense and stable

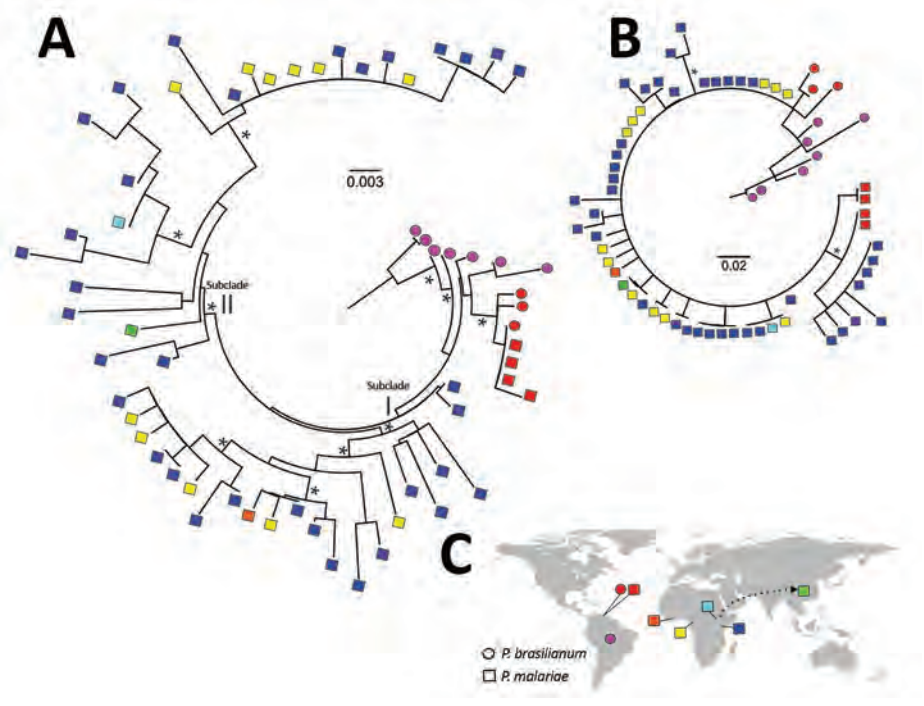

Figure 4. Maximum-likelihood analyses of circumsporozoite protein gene (*csp*) sequences of *Plasmodium malariae* and distribution of the samples. A) Phylogenetic tree based on maximum-likelihood analyses of the entire *csp* amino acid sequences of *P. malariae* isolates from different geographic regions, shown by different colors. Asterisks denote clade with >90% bootstrap support. Sequences of *P. malariae* from Venezuela (red squares) were almost identical to those of *P. brasilianum* (red circles) from the same area. These samples were genetically closely related with *P. brasilianum* from Brazil (violet circles) but distant from *P. malariae* from East and West Africa. The samples from Africa were subdivided into 2 subclades, I and II. Subclade I comprised a mix of *P. malariae* isolates from Kenya (dark blue squares), Cameroon (yellow squares), and Côte d' Ivoire (orange squares). Subclade II comprised a mix of *P. malariae* isolates from Kenya, Cameroon, Uganda (light blue squares), and China (green squares). B) Maximum-likelihood analyses of partial *csp* amino acid sequences without the central repeat region. *P. brasilianum* from Brazil was distant from *P. malariae*, but relationships among the *P. malariae* samples from different geographic areas were not well resolved. C) Locations of samples included in the analyses. Arrow indicates the possible African origin of *P. malariae* from China. Scale bars indicate length of phylogenetic tree. *Bootstrap value >90%.

plasmodia transmission occurs throughout the year (*31*). For achieving the ultimate goal of eliminating malaria in Kenya, existing control programs that primarily target *P. falciparum* are inadequate. The use of rapid diagnostic tests or microscopy as first-line diagnostic methods can lead to gross underestimation of the actual prevalence of *P. malariae* (*4*–*6*). Our findings indicated that *P. malariae* accounted for ≈3% of clinical cases and ≈5% of asymptomatic infections in this malaria-endemic region. The prevalence of asymptomatic *P. malariae* infections was comparable to that recently reported for nearby islands of Lake Victoria (1.7%–3.96%) on the basis of PCR (*36*,*37*). These asymptomatic *P. malariae* infections are concerning because they are parasite reservoirs that can sustain long-term transmission. For instance, in the Colombian Amazon region, *P. malariae* was thought to account for ≤1% of all malaria infections (*38*,*39*); however, a recent study revealed that 43.6% (294/675) of clinical cases were caused by *P. malariae* (*10*) and suggested that these parasites have been circulating in the community undetected. Underestimation or lack of awareness of its occurrence could thus lead to increased transmission. The infectiousness of *P. malariae* for *Anopheles* mosquitoes in malaria-endemic areas remains unclear and merits further investigation.

We found that *P. malariae* infections were more common among infants and children than adults. A similar pattern has been found for Senegal, West Africa, where 91% (265/290 cases) of clinical *P. malariae* cases occurred in children <15 years of age and the mean incidence density was highest for those 5–9 years of age (*3*). These findings indicate that children are vulnerable to *P. malariae* infection and contrast with those reported for Papua, Indonesia, where *P. malariae* infection was higher among older (median 21 years of age) than younger persons (*9*). It is possible that our study sites in western Kenya, as well as in West Africa, are high-transmission areas where *P. falciparum* malaria prevalence can be ≈60% during the rainy season (*30*,*40*). Cumulative exposure to the parasites over time may enable gradual acquisition of immunity in adults. Nevertheless, our community samples were mostly obtained from schoolchildren 6–15 years of age. Underrepresentation of adult populations may underestimate the overall malaria prevalence in the study area. Although young children are more vulnerable to *P. malariae* infections, the level of *P. malariae* parasitemia does not seem to be associated with age. Chronic nephrotic syndromes attributed to *P. malariae* have been reported (*41*,*42*) and shown to be associated with significant illness from anemia in young children (*8*,*9*). However, the lack of hematologic data from our study participants limits further investigation.

Our data indicate that ≈50% of *P. malariae*–positive samples detected by PCR were undetected by microscopy. Such a low sensitivity of microscopy could be attributed to a significantly lower *P. malariae* than *P. falciparum* parasitemia, according to qPCRs. Because most *P. malariae*–positive samples had mixed infections, microscopists could have recorded only the dominant *P. falciparum* and overlooked the sparse *P. malariae* trophozoites. Also, the ring forms of *P. falciparum* and *P. malariae* are morphologically more similar to each other than to *P. vivax* and *P. ovale* (*43*). Misdiagnosis of parasite species by microscopy is possible (*8*).

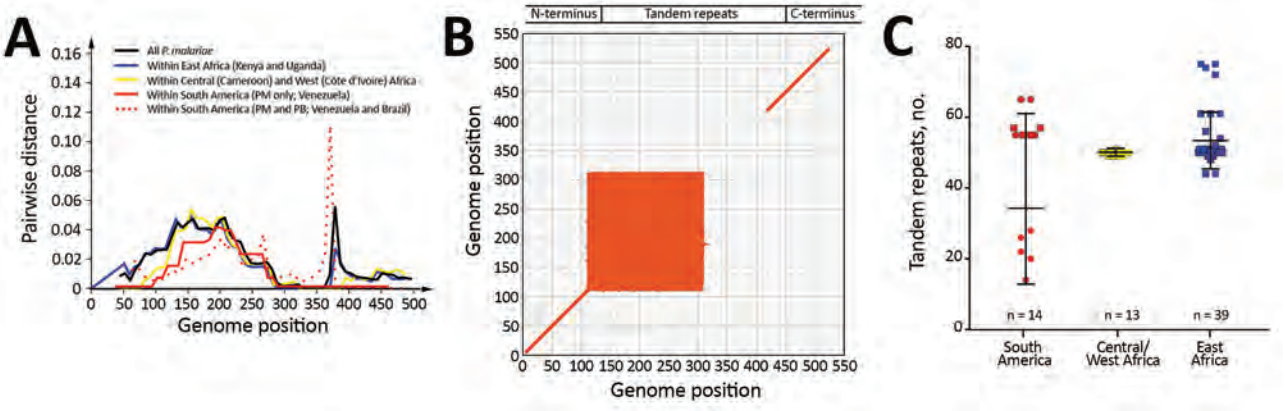

Figure 5. Comparison of circumsporozoite protein (*csp*) gene sequence divergence among *Plasmodium* isolates from different geographic regions. A) Pairwise genetic distance plot of all amino acid positions of the *csp* gene. The matrix-normalized distances based on the standard point accepted mutation (Dayhoff–PAM) model that account for the probability of change from 1 amino acid to another were calculated. Samples were analyzed as a whole and partitioned by geographic regions as indicated by colors. B) Dot plot showing matching scores, a proxy of sequence similarity, between pairwise samples calculated based on the standard Dayhoff–PAM matrix. The greatest mismatch was detected at amino acid positions 110–310, representing the 3′ N terminal through the central repeat regions. C) Variation in the number of tandem repeats in the central region of the *csp* gene. The greatest length variation was observed in the isolates from South America despite the fact that both *P. malariae* (PM) and *P. brasilianum* (PB) were included. *P. malariae* from East Africa was more variable in the number of repeats than isolates from Central/West Africa, despite difference in sample size. Median, first quartile, and fourth quartile of the data are shown for each sample category (horizontal lines). Red represents samples from South America; yellow, Central/West Africa; blue, East Africa. Circles represent *P. brasilianum*; squares, *P. malariae.*

In Africa, the standard treatment for *P. malariae* monoinfection is chloroquine, and for *P. falciparum* and mixed plasmodial infections it is artemisinin combination therapy (*31*). The combination treatment regime should cure *P. malariae* infections even in cases of misdiagnosis. However, *P. malariae* increases production of *P. falciparum* gametocytes in mixed infections, and these gametocytes can persist without proper antimalarial treatment or monitoring (*44*). Therefore, we highlight the need for sensitive methods to improve *P. malariae* diagnosis and provide accurate epidemiologic data for specific and effective management guidelines. Although PCR is a better diagnostic method, it uses a relatively small amount of blood from filter papers and could still underestimate *P. malariae* infections in samples with exceptionally low levels of parasitemia. More accurate prevalence data may be obtained from ultrasensitive PCR that targets multicopy regions of the parasite genome (*45*) or reverse transcription PCR of parasite RNA extracted from whole blood (*46*).

Sequences of the *csp* gene were shown to be highly polymorphic among *P. malariae* isolates from western Kenya. The most polymorphic region was in the central repeat region, where mutations and length differences were detected (*24*,*28*). Among the isolates from different geographic areas, *P. malariae* from East and Central/West Africa were genetically closely related and exhibited a comparable level of sequence variation. This variation could be attributed to positive selection, frequent recombination, and gene flow among the parasites, as follows. First, compared with *msp*1, *dhfr*, and *dhps* of *P. malariae* (*20*–*22*), the *csp* gene revealed a remarkably higher level of sequence diversity. It is possible that selection of *csp* genetic variants may confer immunogenic advantages to the pathogen during host invasion (*28*,*47*). Second, intense transmission and large vector populations in our study area might enhance frequent heterologous recombination of the parasite genome during reproduction in the mosquitoes and increase genetic diversity within populations (*24*,*25*). Third, recurrent gene flow between the parasite populations across countries, via human migration or dispersal of vector mosquitoes, promotes the spread of these genetic variants, leading to a lack of differentiation according to geographic region. Future study using other variable markers, such as microsatellites, on expanded population samples could validate our findings.

In summary, underestimation of the actual prevalence of asymptomatic infections hinders progress toward malaria elimination in Africa. The low parasitemia of *P. malariae* infections influences diagnostic sensitivity by microscopy. A more sensitive tool is needed to identify asymptomatic *P. malariae* and to improve control strategies, particularly among infants and children who are vulnerable to *P. malariae* infection.

Acknowledgments

We are greatly indebted to technicians and staff from the Kenya Medical Research Institute for sample collection, undergraduate students for assisting with data collection, and Ming-Chieh Lee for producing the map of the study area.

This research was supported by US National Institutes of Health grants R01 AI050243 and D43 TW001505 to G.Y.

Dr. Lo is a researcher focused on molecular epidemiology and evolution of pathogens. She is interested in exploring the effects of host–parasite interactions on parasite genomic and genetic structure.

References

1. Alonso PL, Tanner M. Public health challenges and prospects for malaria control and elimination. Nat Med. 2013;19:150–5. http://dx.doi.org/10.1038/nm.3077
2. Tanner M, Greenwood B, Whitty CJM, Ansah EK, Price RN, Dondorp AM, et al. Malaria eradication and elimination: views on how to translate a vision into reality. BMC Med. 2015;13:167. http://dx.doi.org/10.1186/s12916-015-0384-6
3. Roucher C, Rogier C, Sokhna C, Tall A, Trape JF. A 20-year longitudinal study of *Plasmodium ovale* and *Plasmodium malariae* prevalence and morbidity in a West African population. PLoS One. 2014;9:e87169. http://dx.doi.org/10.1371/journal.pone.0087169
4. Farcas GA, Zhong KJY, Lovegrove FE, Graham CM, Kain KC. Evaluation of the Binax NOW ICT test versus polymerase chain reaction and microscopy for the detection of malaria in returned travelers. Am J Trop Med Hyg. 2003;69:589–92.
5. Nkrumah B, Acquah SE, Ibrahim L, May J, Brattig N, Tannich E, et al. Comparative evaluation of two rapid field tests for malaria diagnosis: Partec Rapid Malaria Test® and Binax Now® Malaria Rapid Diagnostic Test. BMC Infect Dis. 2011;11:143. http://dx.doi.org/10.1186/1471-2334-11-143
6. Niño CH, Cubides JR, Camargo-Ayala PA, Rodríguez-Celis CA, Quiñones T, Cortés-Castillo MT, et al. *Plasmodium malariae* in the Colombian Amazon region: you don't diagnose what you don't suspect. Malar J. 2016;15:576. http://dx.doi.org/10.1186/s12936-016-1629-3
7. Vinetz JM, Li J, McCutchan TF, Kaslow DC. *Plasmodium malariae* infection in an asymptomatic 74-year-old Greek woman with splenomegaly. N Engl J Med. 1998;338:367–71. http://dx.doi.org/10.1056/NEJM199802053380605
8. Douglas NM, Lampah DA, Kenangalem E, Simpson JA, Poespoprodjo JR, Sugiarto P, et al. Major burden of severe anemia from non-*falciparum* malaria species in southern Papua: a hospital-based surveillance study. PLoS Med. 2013;10:e1001575, discussion e1001575. http://dx.doi.org/10.1371/journal.pmed.1001575
9. Langford S, Douglas NM, Lampah DA, Simpson JA, Kenangalem E, Sugiarto P, et al. *Plasmodium malariae* infection associated with a high burden of anemia: a hospital-based surveillance study. PLoS Negl Trop Dis. 2015;9:e0004195. http://dx.doi.org/10.1371/journal.pntd.0004195
10. Camargo-Ayala PA, Cubides JR, Niño CH, Camargo M, Rodríguez-Celis CA, Quiñones T, et al. High *Plasmodium malariae* prevalence in an endemic area of the Colombian Amazon Region. PLoS One. 2016;11:e0159968. http://dx.doi.org/10.1371/journal.pone.0159968
11. Naqvi R, Ahmad E, Akhtar F, Naqvi A, Rizvi A. Outcome in severe acute renal failure associated with malaria. Nephrol Dial Transplant. 2003;18:1820–3. http://dx.doi.org/10.1093/ndt/gfg260

12. Okiro EA, Al-Taiar A, Reyburn H, Idro R, Berkley JA, Snow RW. Age patterns of severe paediatric malaria and their relationship to *Plasmodium falciparum* transmission intensity. Malar J. 2009;8:4. http://dx.doi.org/10.1186/1475-2875-8-4
13. Carneiro I, Roca-Feltrer A, Griffin JT, Smith L, Tanner M, Schellenberg JA, et al. Age-patterns of malaria vary with severity, transmission intensity and seasonality in sub-Saharan Africa: a systematic review and pooled analysis. PLoS One. 2010;5:e8988. http://dx.doi.org/10.1371/journal.pone.0008988
14. Roca-Feltrer A, Carneiro I, Smith L, Schellenberg JRMA, Greenwood B, Schellenberg D. The age patterns of severe malaria syndromes in sub-Saharan Africa across a range of transmission intensities and seasonality settings. Malar J. 2010;9:282. http://dx.doi.org/10.1186/1475-2875-9-282
15. Scopel KKG, Fontes CJF, Nunes ÁC, Horta MF, Braga ÉM. High prevalence of *Plamodium malariae* infections in a Brazilian Amazon endemic area (Apiacás-Mato Grosso State) as detected by polymerase chain reaction. Acta Trop. 2004;90:61–4. http://dx.doi.org/10.1016/j.actatropica.2003.11.002
16. Zhou M, Liu Q, Wongsrichanalai C, Suwonkerd W, Panart K, Prajakwong S, et al. High prevalence of *Plasmodium malariae* and *Plasmodium ovale* in malaria patients along the Thai–Myanmar border, as revealed by acridine orange staining and PCR-based diagnoses. Trop Med Int Health. 1998;3:304–12. http://dx.doi.org/10.1046/j.1365-3156.1998.00223.x
17. Mohapatra PK, Prakash A, Bhattacharyya DR, Goswami BK, Ahmed A, Sarmah B, et al. Detection & molecular confirmation of a focus of *Plasmodium malariae* in Arunachal Pradesh, India. Indian J Med Res. 2008;128:52–6.
18. Kaneko A, Taleo G, Kalkoa M, Yaviong J, Reeve PA, Ganczakowski M, et al. Malaria epidemiology, glucose 6-phosphate dehydrogenase deficiency and human settlement in the Vanuatu Archipelago. Acta Trop. 1998;70:285–302. http://dx.doi.org/10.1016/S0001-706X(98)00035-7
19. Mueller I, Tulloch J, Marfurt J, Hide R, Reeder JC. Malaria control in Papua New Guinea results in complex epidemiological changes. P N G Med J. 2005;48:151–7.
20. Guimarães LO, Wunderlich G, Alves JMP, Bueno MG, Röhe F, Catão-Dias JL, et al. Merozoite surface protein-1 genetic diversity in *Plasmodium malariae* and *Plasmodium brasilianum* from Brazil. BMC Infect Dis. 2015;15:529. http://dx.doi.org/10.1186/s12879-015-1238-8
21. Tanomsing N, Imwong M, Pukrittayakamee S, Chotivanich K, Looareesuwan S, Mayxay M, et al. Genetic analysis of the dihydrofolate reductase-thymidylate synthase gene from geographically diverse isolates of *Plasmodium malariae*. Antimicrob Agents Chemother. 2007;51:3523–30. http://dx.doi.org/10.1128/AAC.00234-07
22. Tanomsing N, Mayxay M, Newton PN, Nosten F, Dolecek C, Hien TT, et al. Genetic variability of *Plasmodium malariae dihydropteroate synthase* (*dhps*) in four Asian countries. PLoS One. 2014;9:e93942. http://dx.doi.org/10.1371/journal.pone.0093942
23. Sultan AA. Molecular mechanisms of malaria sporozoite motility and invasion of host cells. Int Microbiol. 1999;2:155–60.
24. McCutchan TF, Lal AA, do Rosario V, Waters AP. Two types of sequence polymorphism in the circumsporozoite gene of *Plasmodium falciparum.* Mol Biochem Parasitol. 1992;50:37–45. http://dx.doi.org/10.1016/0166-6851(92)90242-C
25. Escalante AA, Grebert HM, Isea R, Goldman IF, Basco L, Magris M, et al. A study of genetic diversity in the gene encoding the circumsporozoite protein (CSP) of *Plasmodium falciparum* from different transmission areas—XVI. Asembo Bay Cohort Project. Mol Biochem Parasitol. 2002;125:83–90. http://dx.doi.org/10.1016/S0166-6851(02)00216-5
26. Zakeri S, Abouie Mehrizi A, Djadid ND, Snounou G. Circumsporozoite protein gene diversity among temperate and tropical *Plasmodium vivax* isolates from Iran. Trop Med Int Health. 2006;11:729–37. http://dx.doi.org/10.1111/j.1365-3156.2006.01613.x
27. Parobek CM, Bailey JA, Hathaway NJ, Socheat D, Rogers WO, Juliano JJ. Differing patterns of selection and geospatial genetic diversity within two leading *Plasmodium vivax* candidate vaccine antigens. PLoS Negl Trop Dis. 2014;8:e2796. http://dx.doi.org/10.1371/journal.pntd.0002796
28. Tahar R, Ringwald P, Basco LK. Heterogeneity in the circumsporozoite protein gene of *Plasmodium malariae* isolates from sub-Saharan Africa. Mol Biochem Parasitol. 1998;92:71–8. http://dx.doi.org/10.1016/S0166-6851(97)00226-0
29. Zeeshan M, Alam MT, Vinayak S, Bora H, Tyagi RK, Alam MS, et al. Genetic variation in the *Plasmodium falciparum* circumsporozoite protein in India and its relevance to RTS,S malaria vaccine. PLoS One. 2012;7:e43430. http://dx.doi.org/10.1371/journal.pone.0043430
30. Lo E, Zhou G, Oo W, Afrane Y, Githeko A, Yan G. Low parasitemia in submicroscopic infections significantly impacts malaria diagnostic sensitivity in the highlands of western Kenya. PLoS One. 2015;10:e0121763. http://dx.doi.org/10.1371/journal.pone.0121763
31. National Malaria Control Programme, Kenya National Bureau of Statistics, Ministry of Health, Kenya. Malaria indicator survey 2015. Nairobi (Kenya): The Ministry; 2015.
32. Wooden J, Kyes S, Sibley CH. PCR and strain identification in *Plasmodium falciparum.* Parasitol Today. 1993;9:303–5. http://dx.doi.org/10.1016/0169-4758(93)90131-X
33. Kimura K, Kaneko O, Liu Q, Zhou M, Kawamoto F, Wataya Y, et al. Identification of the four species of human malaria parasites by nested PCR that targets variant sequences in the small subunit rRNA gene. Parasitol Int. 1997;46:91–5. http://dx.doi.org/10.1016/S1383-5769(97)00013-5
34. Lo E, Nguyen J, Oo W, Hemming-Schroeder E, Zhou G, Yang Z, et al. Examining *Plasmodium falciparum* and *P. vivax* clearance subsequent to antimalarial drug treatment in the Myanmar–China border area based on quantitative real-time polymerase chain reaction. BMC Infect Dis. 2016;16:154–66. http://dx.doi.org/10.1186/s12879-016-1482-6
35. Phuong M, Lau R, Ralevski F, Boggild AK. Sequence-based optimization of a quantitative real-time PCR assay for detection of *Plasmodium ovale* and *Plasmodium malariae*. J Clin Microbiol. 2014;52:1068–73. http://dx.doi.org/10.1128/JCM.03477-13
36. Olanga EA, Okombo L, Irungu LW, Mukabana WR. Parasites and vectors of malaria on Rusinga Island, western Kenya. Parasit Vectors. 2015;8:250. http://dx.doi.org/10.1186/s13071-015-0860-z
37. Idris ZM, Chan CW, Kongere J, Gitaka J, Logedi J, Omar A, et al. High and heterogeneous prevalence of asymptomatic and sub-microscopic malaria infections on islands in Lake Victoria, Kenya. Sci Rep. 2016;6:36958. http://dx.doi.org/10.1038/srep36958
38. Suh KN, Kain KC, Keystone JS. Malaria. CMAJ. 2004;170:1693–702. http://dx.doi.org/10.1503/cmaj.1030418
39. Rodríguez JC, Uribe GA, Araújo RM, Narváez PC, Valencia SH. Epidemiology and control of malaria in Colombia. Mem Inst Oswaldo Cruz. 2011;106(Suppl 1):114–22. http://dx.doi.org/10.1590/S0074-02762011000900015
40. Githeko AK, Ayisi JM, Odada PK, Atieli FK, Ndenga BA, Githure JI, et al. Topography and malaria transmission heterogeneity in western Kenya highlands: prospects for focal vector control. Malar J. 2006;5:107. http://dx.doi.org/10.1186/1475-2875-5-107
41. Ehrich JHH, Eke FU. Malaria-induced renal damage: facts and myths. Pediatr Nephrol. 2007;22:626–37. http://dx.doi.org/10.1007/s00467-006-0332-y
42. Hedelius R, Fletcher JJ, Glass WF II, Susanti AI, Maguire JD. Nephrotic syndrome and unrecognized *Plasmodium malariae*

infection in a US Navy sailor 14 years after departing Nigeria. J Travel Med. 2011;18:288–91. http://dx.doi.org/10.1111/j.1708-8305.2011.00526.x
43. Collins WE, Jeffery GM. *Plasmodium malariae*: parasite and disease. Clin Microbiol Rev. 2007;20:579–92. http://dx.doi.org/10.1128/CMR.00027-07
44. Bousema JT, Drakeley CJ, Mens PF, Arens T, Houben R, Omar SA, et al. Increased *Plasmodium falciparum* gametocyte production in mixed infections with *P. malariae*. Am J Trop Med Hyg. 2008;78:442–8.
45. Hofmann N, Mwingira F, Shekalaghe S, Robinson LJ, Mueller I, Felger I. Ultra-sensitive detection of *Plasmodium falciparum* by amplification of multi-copy subtelomeric targets. PLoS Med. 2015;12:e1001788. http://dx.doi.org/10.1371/journal.pmed.1001788
46. Adams M, Joshi SN, Mbambo G, Mu AZ, Roemmich SM, Shrestha B, et al. An ultrasensitive reverse transcription polymerase chain reaction assay to detect asymptomatic low-density *Plasmodium falciparum* and *Plasmodium vivax* infections in small volume blood samples. Malar J. 2015;14:520. http://dx.doi.org/10.1186/s12936-015-1038-z
47. Casares S, Brumeanu TD, Richie TL. The RTS,S malaria vaccine. Vaccine. 2010;28:4880–94. http://dx.doi.org/10.1016/j.vaccine.2010.05.033

Address for correspondence: Eugenia Lo and Guiyun Yan, Program in Public Health, Rm 3501B, Hewitt Hall, Health Science Dr, University of California Irvine, Irvine, CA 92617, USA; email: eugenia.lo@uci.edu and guiyuny@uci.edu

Presence and Persistence of Zika Virus RNA in Semen, United Kingdom, 2016

Barry Atkinson, Fiona Thorburn, Christina Petridou, Daniel Bailey, Roger Hewson, Andrew J.H. Simpson, Timothy J.G. Brooks, Emma J. Aarons

Zika virus RNA has been detected in semen collected several months after onset of symptoms of infection. Given the potential for sexual transmission of Zika virus and for serious fetal abnormalities resulting from infection during pregnancy, information regarding the persistence of Zika virus in semen is critical for advancing our understanding of potential risks. We tested serial semen samples from symptomatic male patients in the United Kingdom who had a diagnosis of imported Zika virus infection. Among the initial semen samples from 23 patients, Zika virus RNA was detected at high levels in 13 (56.5%) and was not detected in 9 (39.1%); detection was indeterminate in 1 sample (4.4%). After symptomatic infection, a substantial proportion of men have detectable Zika virus RNA at high copy numbers in semen during early convalescence, suggesting high risk for sexual transmission. Viral RNA clearance times are not consistent and can be prolonged.

Zika virus is an emerging flavivirus currently causing a major outbreak of human disease in the Americas, the Caribbean, and Western Pacific regions; 71 countries and territories have reported mosquitoborne transmission since 2015 (*1*). Human infection can be subclinical (*2*). Symptomatic infection usually causes a mild, self-limiting illness accompanied by rash, fever, arthralgia, and myalgia (*2–5*). However, international scientific consensus holds that Zika virus infection is a cause of 2 severe clinical sequelae recognized recently: Guillain-Barré syndrome and congenital neurologic abnormalities, including microcephaly (*6*). The risk for adverse obstetric outcome after maternal infection during pregnancy is currently unknown, but the risk for microcephaly attributable to Zika virus infection in the first trimester has been estimated to be 0.88%–13.2% (*7*).

Zika virus is primarily mosquitoborne, but sexual transmission has also been described (*8–14*). To date, 12 countries have reported nonvectorborne transmission (*1*), usually sexual transmission from men after symptomatic infection, although transmission after asymptomatic infection also has been described (*15*,*16*). Sexual transmission is a major concern for pregnant women and couples considering pregnancy because of the risk for adverse fetal sequelae. Information on Zika virus persistence in semen is required to inform public health guidance for the prevention of sexual transmission. With few exceptions (*17*,*18*), published data are mostly limited to individual case reports, and few publications report isolation of infectious Zika virus from semen. However, Zika virus RNA has been detected in semen up to 6 months after onset of symptoms (*19*,*20*). This potential for prolonged onward transmission warrants further investigation. We describe the analysis of serial semen samples from 23 symptomatic Zika virus–infected male travelers to determine the presence and persistence of Zika virus RNA.

Author affiliations: Public Health England, Porton Down, UK (B. Atkinson, F. Thorburn, C. Petridou, D. Bailey, R. Hewson, A.J.H. Simpson, T.J.G. Brooks, E.J. Aarons); West of Scotland Specialist Virology Centre, Glasgow, Scotland, UK (F. Thorburn); Hampshire Hospitals National Health Service Foundation Trust, Basingstoke and Winchester, UK (C. Petridou).

DOI: http://dx.doi.org/10.3201/eid2304.161692

Methods

Testing of Diagnostic Samples

We diagnosed possible imported Zika virus infection in patients by using a real-time reverse transcription PCR (rRT-PCR) assay based on a published method targeting the nonstructural protein 1 (NS1) gene (*21*) and a commercial serologic assay (EUROIMMUN AG, Lübeck, Germany). (We diagnosed infection in patient 1 by using a different rRT-PCR assay [*22*]). We performed viral RNA extraction on the EZ1 platform by using the EZ1 Virus Mini Kit with Buffer AVL (QIAGEN, Valencia, CA, USA) inactivated samples. We also tested all patients for other pathogens, such as chikungunya and dengue viruses, by using published molecular and commercial serologic assays. The preferred sample type was serum or plasma, but published testing guidance specifically called for urine samples from pregnant women and male partners of pregnant women.

Testing of Semen Samples

We offered a Zika virus RNA semen testing service to adult male patients with diagnosed Zika virus infection. If Zika virus RNA was detected, we offered testing of serial

samples. We advised that samples be collected in sterile pots and transported at ambient temperature. We analyzed the samples by using the RNA extraction and rRT-PCR testing procedures described here, without modification.

Results

Since December 2013, nearly 2,500 Zika virus diagnostic molecular detection tests have been performed on travelers returning to the United Kingdom with possible Zika virus infection. As of October 5, 2016, a total of 116 persons, 55 of whom were males, had detectable Zika virus RNA in serum, plasma, or urine (*23*). Sixteen male patients (29.1%) submitted ≥1 semen sample (patients 1–16). In addition, 7 patients (patients 17–23) submitted semen samples after serologic diagnoses (i.e., detection of Zika virus IgM and IgG in serum but without detection of Zika virus RNA).

All patients had recently traveled from the Americas or Caribbean, except patient 1, who acquired Zika virus infection in the South Pacific in 2014. All patients reported a self-limiting, mild illness with fever and/or rash consistent with Zika virus infection (online Technical Appendix Tables 1 and 2, https://wwwnc.cdc.gov/EID/article/23/4/16-1692-Techapp1.pdf). None reported hematospermia.

We detected Zika virus RNA in ≥1 semen sample from 10 (62.5%) of the 16 patients with rRT-PCR–diagnosed infection and from 2 (28.6%) of the 7 patients with serologically diagnosed infection. For the 10 patients who had a positive initial blood or urine sample and a subsequent positive semen sample, the median cycle threshold (C_t) value was significantly lower for semen samples (C_t 27.3) than for acute-phase diagnostic serum, plasma, or urine samples (C_t 34.1; p = 0.01 by sign test).

Further semen samples were provided by 8 of the 12 Zika virus–positive patients (Figure). A series of samples sufficient to demonstrate seminal clearance of Zika virus RNA was available for 4 patients (*2*,*5*,*9*,*10*). Patient 5 demonstrated the longest time to clearance (from day 92 to day 131). For other patients from whom additional positive semen samples were received, C_t values increased consistently over time (i.e., genome copy number fell). The day 167 semen sample of patient 8 repeatedly demonstrated a subthreshold curve in the rRT-PCR test, suggesting evidence of Zika virus RNA at the assay detection limit. This patient was taking immunosuppressive drug therapy when infected (disease-modifying antirheumatic drugs [discontinued after his diagnoses with Zika virus infection] and oral steroids). No other patients were known to have immunosuppression.

Zika virus RNA was undetectable in semen samples from 5 of the 16 patients with rRT-PCR–diagnosed infection (31.3%); results were indeterminate (subthreshold) for 1 patient (6.3%). All 6 patients subsequently seroconverted for Zika virus IgG (data not shown). The indeterminate result occurred in the only patient who had undergone a vasectomy (day 16 sample). Zika virus RNA was also undetectable in the semen of 5 (71.4%) of the 7 patients with serologically diagnosed infection. Although Zika virus infection was not definitively confirmed by molecular testing in any of these 5 patients, laboratory tests excluded recent chikungunya or dengue infection (online Technical Appendix Table 2).

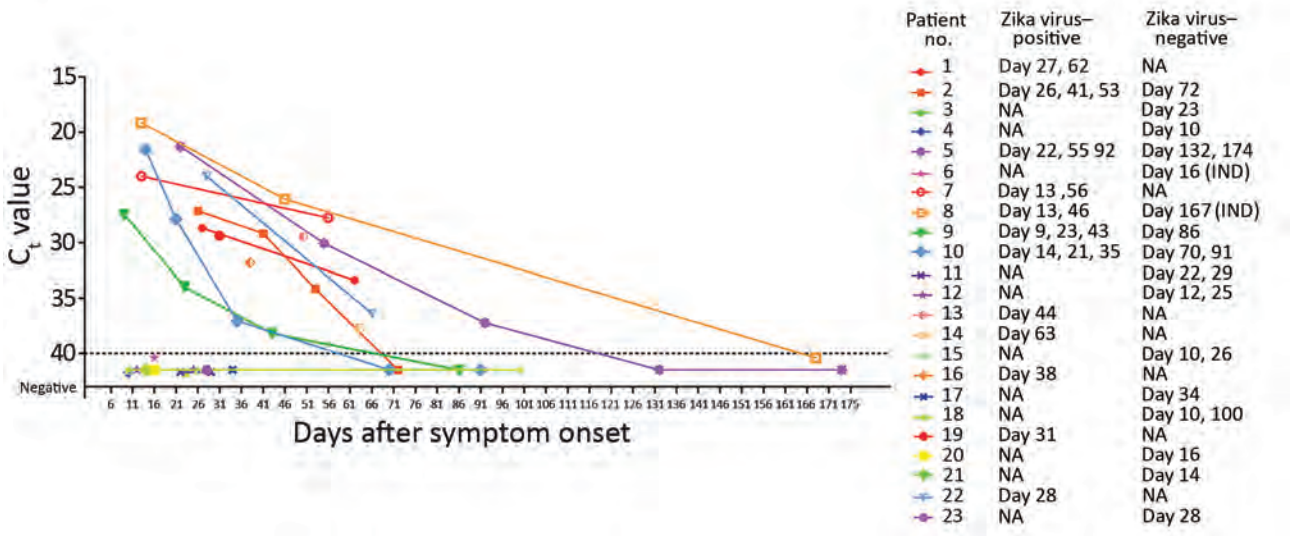

Figure. Cycle threshold (C_t) values of semen samples analyzed to determine presence and persistence of Zika virus RNA in semen, United Kingdom, 2016. All references to days indicate days after onset of symptoms. The dotted line represents the limit of detection for the assay. The lines represent implied decay rates based on longitudinal data; however, they should not be used to infer exact data between analyzed samples. In particular, the point at which viral RNA became undetected cannot be accurately inferred from the curves for patients 5, 8, 9, and 10. Patient 6 had a previous vasectomy, and patient 8 was receiving immunosuppressive drug therapy at the time of sampling. IND, indeterminate; NA, not available.

Of the 15 patients with rRT-PCR–confirmed infection in whom previous dengue serostatus could be assessed at the time of their initial Zika virus diagnosis (because no potentially cross-reactive Zika virus IgG was detectable at that time), only 3 had serologic evidence of previous dengue virus infection. Two of these patients (patients 3 and 6) did not have Zika virus RNA in subsequent semen samples (online Technical Appendix Table 1).

We attempted isolation of viable virus from all initial positive semen samples, with 1 successful isolation (day 13 sample from patient 7, C_t 24). We attempted virus isolation in Vero and C6/36 cells; we observed propagation only in C6/36 cells for the original sample, although C6/36 infected supernatant was capable of infecting Vero cells and produced a cytopathic effect. We deposited the complete genome for this isolate in GenBank (accession no. KX673530) (*24*).

Discussion

Although persistence of Zika virus in serum and plasma appears to be transient, our data show that Zika virus RNA is frequently detectable in semen for several weeks to months after recovery from symptomatic infection. Zika virus RNA persistence in semen is not consistent; 10 (43.5%) of the 23 patients we tested lacked detectable Zika virus RNA in semen on the first sample (all but 1 tested within 28 days after symptom onset). Our detection of Zika virus RNA in early semen samples from 12 (52.2%) of 23 infected patients is similar to the detection of viral RNA in 50% of case-patients in small-number Belgian (*17*) and French (*18*) series.

We observed no obvious differences in terms of age, travel history, or symptoms between the patients with and without Zika virus RNA in our series, although detailed clinical information about ethnic origin, symptom severity or duration, and laboratory parameters, such as platelet count or C-reactive protein, were not collected. Sample degradation probably could not explain the negative results because the time from sample collection to testing was shorter on average for negative samples than for samples yielding positive results (data not shown).

One patient with an indeterminate rRT-PCR result for his initial (day 16) semen sample was reported to have had a vasectomy; ongoing viral replication might have been occurring in the urogenital tract. A recent publication reported Zika virus RNA in the ejaculate of a vasectomized man 96 days after onset of symptoms in addition to infectious virus cultured at 69 days (*25*), suggesting that previous vasectomy does not necessarily preclude the possibility of viral RNA or infectious virions in the semen.

It has been hypothesized that previous dengue infection might drive greater Zika virus replication through the mechanism of antibody-dependent enhancement; this process has been observed in vitro (*26*,*27*). However, our data indicate that this process cannot be invoked as a potential sole explanation for seeding of infection in the urogenital tract; among the 9 patients with Zika virus RNA in their semen for whom dengue serostatus at the time of Zika virus infection could be determined, only 1 (patient 10) had serologic evidence of previous dengue virus infection. Our data are insufficient to allow speculation as to whether an altered immune response associated with previous dengue infection might protect against viral replication in the male urogenital tract.

Among the 12 patients in whom Zika virus RNA was detected in semen, all samples obtained within 28 days of symptom onset had C_t values <30, indicative of high genome copy number. This observation is concordant with other reports (*9*,*12*,*17*,*19*,*28–31*) and suggests that the risk for sexual transmission is particularly high in the first few weeks after infection.

The specimens analyzed in this report were provided at the discretion of the patients, and the data are subject to limitations. Monitoring was inconsistent, and patients were lost to follow-up. Clearance of Zika virus RNA from semen was demonstrated for only 4 patients. In all other patients from whom serial Zika virus RNA–positive semen samples were received, the C_t value increased over time, consistent with a fall in genome copy number, as has been observed previously (*12*,*17*,*30*,*32*). The patient with an indeterminate (subthreshold) result at 167 days (patient 8) was receiving immunosuppressive therapy. Because Zika virus is the only known arbovirus with evidence for human sexual transmission, we cannot compare the persistence of Zika virus RNA or infectious virions in semen to similar viruses. Although the presence of Zika virus in semen is presumed to be attributable to viral replication at an immunoprivileged site within the urogenital tract, the cell type in which replication occurs is not currently known. In a mouse model, viral RNA was detected in the testes, in spermatogonia, primary spermatocytes, and Sertoli cells (*33*)

Detection of Zika virus RNA in semen samples does not necessarily indicate the presence of infectious virus. We attempted in vitro isolation from all positive samples; only 1 sample (day 13 sample from patient 7, C_t 24) yielded replicating virus. Isolation from samples with similar C_t values was unsuccessful, highlighting the inconsistency for this technique at present. The inability to isolate virus cannot be taken to indicate the absence of infectious virus until more is known about the intricacies of virus isolation from semen. Although we have been unable to isolate virus in tissue culture consistently from semen samples, it is striking that all recognized transmission events to date have occurred relatively soon after infection in the male index patient (*8–13*,*34*). The longest published interval for sexual transmission after symptom onset is 32–41 days (*14*). Even if methodology for reliably isolating Zika virus

from semen samples is established, it will be difficult to determine whether semen samples with Zika virus RNA detected at lower copy numbers contain infectious virions.

The current World Health Organization (WHO) guidelines advise that male and female travelers should adopt safer sex practices or consider abstinence to reduce the risk for sexual transmission for 6 months after leaving a country with ongoing Zika virus transmission (*35*). This recommendation was a conservative estimate for symptomatic men given the maximum reported persistence of Zika virus RNA in semen (62 days) at the time the WHO guidelines were issued (May 2016). Our data, together with other recent case reports (*12*,*18*–*20*,*25*,*32*,*36*), show that Zika virus RNA is sometimes detectable beyond 62 days, with the maximum period of RNA detection observed to date being approximately 6 months (*20*). However, our understanding of the dynamics for virus or viral RNA clearance are still nascent, and further data are required to assess the validity of current recommendations.

Currently, we lack knowledge of viral persistence in semen. More data, especially from larger systematic studies, are urgently needed to support evidence-based policies to prevent sexual transmission of Zika virus. In the meantime, testing of semen from symptomatic men ≥8 weeks after leaving a Zika-affected area, as suggested by WHO (*35*), might be valuable for assessing individual risk and for contributing to global data.

Acknowledgments

We thank the staff of the Rare and Imported Pathogens Laboratory for processing routine clinical samples. We also thank the staff of the Diagnostic Support Group at Public Health England–Porton for assistance in processing semen samples. The authors also gratefully acknowledge the patients who volunteered semen samples and their clinicians. In addition, the authors acknowledge the work of Lisa Ottowell and Victoria Graham in performing in vitro isolation work.

This work was funded by Public Health England.

Dr. Atkinson is a molecular virologist at Public Health England, United Kingdom. His research interests focus on the design and development of molecular detection assays for rare and emerging high-consequence human pathogens.

References

1. World Health Organization. Zika situation report, 29 September 2016 [cited 2016 Oct 9]. http://www.who.int/emergencies/zika-virus/situation-report/29-september-2016/en
2. Duffy MR, Chen T-H, Hancock WT, Powers AM, Kool JL, Lanciotti RS, et al. Zika virus outbreak on Yap Island, Federated States of Micronesia. N Engl J Med. 2009;360:2536–43. http://dx.doi.org/10.1056/NEJMoa0805715
3. Brasil P, Calvet GA, Siqueira AM, Wakimoto M, de Sequeira PC, Nobre A, et al. Zika virus outbreak in Rio de Janeiro, Brazil: clinical characterization, epidemiological and virological aspects. PLoS Negl Trop Dis. 2016;10:e0004636. http://dx.doi.org/10.1371/journal.pntd.0004636
4. Cerbino-Neto J, Mesquita EC, Souza TML, Parreira V, Wittlin BB, Durovni B, et al. Clinical manifestations of Zika virus infection, Rio de Janeiro, Brazil, 2015. Emerg Infect Dis. 2016;22:1318–20. http://dx.doi.org/10.3201/eid2207.160375
5. Thomas DL, Sharp TM, Torres J, Armstrong PA, Munoz-Jordan J, Ryff KR, et al. Local transmission of Zika virus—Puerto Rico, November 23, 2015–January 28, 2016. MMWR Morb Mortal Wkly Rep. 2016;65:154–8. http://dx.doi.org/10.15585/mmwr.mm6506e2
6. World Health Organization. Zika causality statement [cited 2016 Oct 9]. http://www.who.int/emergencies/zika-virus/causality/en
7. Johansson MA, Mier-y-Teran-Romero L, Reefhuis J, Gilboa SM, Hills SL. Zika and the risk of microcephaly. N Engl J Med. 2016;375:1–4. http://dx.doi.org/10.1056/NEJMp1605367
8. Deckard DT, Chung WM, Brooks JT, Smith JC, Woldai S, Hennessey M, et al. Male-to-male sexual transmission of Zika virus—Texas, January 2016. MMWR Morb Mortal Wkly Rep. 2016;65:372–4. http://dx.doi.org/10.15585/mmwr.mm6514a3
9. D'Ortenzio E, Matheron S, Yazdanpanah Y, de Lamballerie X, Hubert B, Piorkowski G, et al. Evidence of sexual transmission of Zika virus. N Engl J Med. 2016;374:2195–8. http://dx.doi.org/10.1056/NEJMc1604449
10. Foy BD, Kobylinski KC, Chilson Foy JL, Blitvich BJ, Travassos da Rosa A, Haddow AD, et al. Probable non-vector-borne transmission of Zika virus, Colorado, USA. Emerg Infect Dis. 2011;17:880–2. http://dx.doi.org/10.3201/eid1705.101939
11. Frank C, Cadar D, Schlaphof A, Neddersen N, Günther S, Schmidt-Chanasit J, et al. Sexual transmission of Zika virus in Germany, April 2016. Euro Surveill. 2016;21:30252. http://dx.doi.org/10.2807/1560-7917.ES.2016.21.23.30252
12. Harrower J, Kiedrzynski T, Baker S, Upton A, Rahnama F, Sherwood J, et al. Sexual transmission of Zika virus and persistence in semen, New Zealand, 2016. Emerg Infect Dis. 2016;22:1855–7. PubMed https://dx.doi.org/10.3201/eid2210.160951
13. Hills SL, Russell K, Hennessey M, Williams C, Oster AM, Fischer M, et al. Transmission of Zika virus through sexual contact with travelers to areas of ongoing transmission—continental United States, 2016. MMWR Morb Mortal Wkly Rep. 2016;65:215–6. http://dx.doi.org/10.15585/mmwr.mm6508e2
14. Turmel JM, Abgueguen P, Hubert B, Vandamme YM, Maquart M, Le Guillou-Guillemette H, et al. Late sexual transmission of Zika virus related to persistence in the semen. Lancet. 2016;387:2501. http://dx.doi.org/10.1016/S0140-6736(16)30775-9
15. Brooks RB, Carlos MP, Myers RA, White MG, Bobo-Lenoci T, Aplan D, et al. Likely sexual transmission of Zika virus from a man with no symptoms of infection—Maryland, 2016. MMWR Morb Mortal Wkly Rep. 2016;65:915–6. http://dx.doi.org/10.15585/mmwr.mm6534e2
16. Fréour T, Mirallié S, Hubert B, Splingart C, Barrière P, Maquart M, et al. Sexual transmission of Zika virus in an entirely asymptomatic couple returning from a Zika epidemic area, France, April 2016. Euro Surveill. 2016;21:30254. http://dx.doi.org/10.2807/1560-7917.ES.2016.21.23.30254
17. Huits R, De Smet B, Ariën K, Van Esbroeck M, de Jong B, Bottieau E, et al. Kinetics of Zika virus persistence in semen. Bull World Health Organ Zika Open. 2016 Jul 6. http://dx.doi.org/10.2471/BLT.16.181370
18. Mansuy JM, Suberbielle E, Chapuy-Regaud S, Mengelle C, Bujan L, Marchou B, et al. Zika virus in semen and spermatozoa. Lancet Infect Dis. 2016;16:1106–7. http://dx.doi.org/10.1016/S1473-3099(16)30336-X
19. Barzon L, Pacenti M, Berto A, Sinigaglia A, Franchin E, Lavezzo E, et al. Isolation of infectious Zika virus from saliva and prolonged viral RNA shedding in a traveller returning from the

Dominican Republic to Italy, January 2016. Euro Surveill. 2016;21. https://dx.doi.org/10.2807/1560-7917.ES.2016.21.10.30159
20. Nicastri E, Castilletti C, Liuzzi G, Iannetta M, Capobianchi MR, Ippolito G. Persistent detection of Zika virus RNA in semen for six months after symptom onset in a traveller returning from Haiti to Italy, February 2016. Euro Surveill. 2016;21:30314. http://dx.doi.org/10.2807/1560-7917.ES.2016.21.32.30314
21. Pyke AT, Daly MT, Cameron JN, Moore PR, Taylor CT, Hewitson GR, et al. Imported Zika virus infection from the Cook Islands into Australia, 2014. PLoS Curr 2014;6: pii: ecurrents.outbreaks.4635a54dbffba2156fb2fd76dc49f65e. https://dx.doi.org/10.1371%2Fcurrents.outbreaks.4635a54dbffba2156fb2fd76dc49f65e
22. Lanciotti RS, Kosoy OL, Laven JJ, Velez JO, Lambert AJ, Johnson AJ, et al. Genetic and serologic properties of Zika virus associated with an epidemic, Yap State, Micronesia, 2007. Emerg Infect Dis. 2008;14:1232–9. http://dx.doi.org/10.3201/eid1408.080287
23. Public Health England. Zika virus: epidemiology and cases diagnosed in the UK [cited 2016 Oct 9]. https://www.gov.uk/government/publications/zika-virus-epidemiology-and-cases-diagnosed-in-the-uk/zika-virus-epidemiology-and-cases-diagnosed-in-the-uk
24. Atkinson B, Graham V, Miles RW, Lewandowski K, Dowall SD, Pullan ST, et al. Complete genome sequence of Zika virus isolated from semen. Genome Announc. 2016;4:e01116-16. http://dx.doi.org/10.1128/genomeA.01116-16
25. Arsuaga M, Bujalance SG, Díaz-Menéndez M, Vázquez A, Arribas JR. Probable sexual transmission of Zika virus from a vasectomised man. Lancet Infect Dis. 2016;16:1107. http://dx.doi.org/10.1016/S1473-3099(16)30320-6
26. Dejnirattisai W, Supasa P, Wongwiwat W, Rouvinski A, Barba-Spaeth G, Duangchinda T, et al. Dengue virus sero-cross-reactivity drives antibody-dependent enhancement of infection with Zika virus. Nat Immunol. 2016;17:1102–8. http://dx.doi.org/10.1038/ni.3515
27. Stettler K, Beltramello M, Espinosa DA, Graham V, Cassotta A, Bianchi S, et al. Specificity, cross-reactivity, and function of antibodies elicited by Zika virus infection. Science. 2016;353:823–6. http://dx.doi.org/10.1126/science.aaf8505
28. Mansuy JM, Dutertre M, Mengelle C, Fourcade C, Marchou B, Delobel P, et al. Zika virus: high infectious viral load in semen, a new sexually transmitted pathogen? Lancet Infect Dis. 2016;16:405. http://dx.doi.org/10.1016/S1473-3099(16)00138-9
29. Musso D, Roche C, Robin E, Nhan T, Teissier A, Cao-Lormeau V-M. Potential sexual transmission of Zika virus. Emerg Infect Dis. 2015;21:359–61. http://dx.doi.org/10.3201/eid2102.141363
30. Reusken C, Pas S. GeurtsvanKessel C, Mögling R, van Kampen J, Langerak T, et al. Longitudinal follow-up of Zika virus RNA in semen of a traveller returning from Barbados to the Netherlands with Zika virus disease, March 2016. Euro Surveill. 2016;21:30251. https://dx.doi.org/10.2807/1560-7917.ES.2016.21.23.30251
31. Jang H-C, Park WB, Kim UJ, Chun JY, Choi S-J, Choe PG, et al. First imported case of Zika virus infection into Korea. J Korean Med Sci. 2016;31:1173–7. http://dx.doi.org/10.3346/jkms.2016.31.7.1173
32. Matheron S, d'Ortenzio E, Leparc-Goffart I, Hubert B, de Lamballerie X, Yazdanpanah Y. Long-lasting persistence of Zika virus in semen. Clin Infect Dis. 2016;63:1264. https://dx.doi.org/10.1093/cid/ciw509
33. Govero J, Esakky P, Scheaffer SM, Fernandez E, Drury A, Platt DJ, et al. Zika virus infection damages the testes in mice. Nature. 2016. http://dx.doi.org/10.1038/nature20556
34. Venturi G, Zammarchi L, Fortuna C, Remoli ME, Benedetti E, Fiorentini C, et al. An autochthonous case of Zika due to possible sexual transmission, Florence, Italy, 2014. Euro Surveill. 2016;21:30148. http://dx.doi.org/10.2807/1560-7917.ES.2016.21.8.30148
35. World Health Organization. Prevention of sexual transmission of Zika virus. Interim guidance [cited 2016 Oct 9]. http://www.who.int/csr/resources/publications/zika/sexual-transmission-prevention/en
36. Mansuy JM, Pasquier C, Daudin M, Chapuy-Regaud S, Moinard N, Chevreau C, et al. Zika virus in semen of a patient returning from a non-epidemic area. Lancet Infect Dis. 2016;16:894–5. http://dx.doi.org/10.1016/S1473-3099(16)30153-0

Address for correspondence: Emma J. Aarons, Rare and Imported Pathogens Laboratory, Public Health England – Porton, Salisbury, Wiltshire SP4 0JG, United Kingdom; email: emma.aarons@phe.gov.uk

Three Divergent Subpopulations of the Malaria Parasite *Plasmodium knowlesi*

Paul C.S. Divis, Lee C. Lin, Jeffrine J. Rovie-Ryan, Khamisah A. Kadir, Fread Anderios, Shamilah Hisam, Reuben S.K. Sharma, Balbir Singh, David J. Conway

Multilocus microsatellite genotyping of *Plasmodium knowlesi* isolates previously indicated 2 divergent parasite subpopulations in humans on the island of Borneo, each associated with a different macaque reservoir host species. Geographic divergence was also apparent, and independent sequence data have indicated particularly deep divergence between parasites from mainland Southeast Asia and Borneo. To resolve the overall population structure, multilocus microsatellite genotyping was conducted on a new sample of 182 *P. knowlesi* infections (obtained from 134 humans and 48 wild macaques) from diverse areas of Malaysia, first analyzed separately and then in combination with previous data. All analyses confirmed 2 divergent clusters of human cases in Malaysian Borneo, associated with long-tailed macaques and pig-tailed macaques, and a third cluster in humans and most macaques in peninsular Malaysia. High levels of pairwise divergence between each of these sympatric and allopatric subpopulations have implications for the epidemiology and control of this zoonotic species.

Plasmodium knowlesi is a zoonotic malaria parasite that has only recently been recognized as a notable cause of malaria (*1*). Although cases have now been seen in most countries in Southeast Asia, the largest numbers have been reported in Malaysia (*1–4*). The extent to which this is a result of varying efforts in diagnosis is unclear, as specific molecular identification is required to discriminate *P. knowlesi* from other malaria parasite species. Moreover, although most reports are of cases presenting with clinical symptoms, asymptomatic infections may also occur (5).

Author affiliations: Malaria Research Centre, Universiti Malaysia Sarawak, Kota Samarahan, Sarawak, Malaysia (P.C.S. Divis, K.A. Kadir, B. Singh, D.J. Conway); London School of Hygiene and Tropical Medicine, London, United Kingdom (P.C.S. Divis, D.J. Conway); Universiti Putra Malaysia, Serdang, Malaysia (L.C. Lin, R.S.K. Sharma); Department of Wildlife and National Parks Peninsular Malaysia, Kuala Lumpur, Malaysia (J.J. Rovie-Ryan); Sabah State Public Health Laboratory, Kota Kinabalu, Malaysia (F. Anderios); Institute for Medical Research, Kuala Lumpur (S. Hisam)

DOI: http://dx.doi.org/10.3201/eid2304.161738

The *Plasmodium knowlesi* parasite is transmitted by mosquitoes to humans from monkey reservoir hosts, with different *Anopheles* species of the Leucosphyrus group having been incriminated as potential vectors in different areas (*1*,*6*). Two macaque species, the long-tailed macaque (*Macaca fascicularis*) and the pig-tailed macaque (*M. nemestrina*), are the major reservoirs of infection (*7*,*8*). Human infections in Malaysian Borneo, the portion of Malaysia on the island of Borneo, have divergent genetic subpopulations that are seen in the different macaque species locally, indicating that 2 independent zoonoses may be occurring sympatrically (*9*). Noticeable geographic differentiation of parasites between Malaysian Borneo and peninsular Malaysia was also evident in microsatellite analysis; separate studies have revealed divergence between the 2 regions at unlinked genes encoding the normocyte binding protein (*10–12*) and the Duffy binding protein (*13*,*14*), as well as the 18S rRNA and mitochondrial cytochrome oxidase subunit 1 (*15*). Whole-genome sequencing has confirmed the presence of 2 divergent subpopulations of *P. knowlesi* in Malaysian Borneo and revealed a third divergent cluster of laboratory isolates maintained in laboratories since the 1960s; most of these were recorded to have originated from peninsular Malaysia (*16*).

To resolve the population structure in relation to host species and geography, a new collection of 182 *P. knowlesi* infection samples from humans and wild macaques living in diverse areas of Malaysia was genotyped at 10 microsatellite loci. We first analyzed the new dataset separately and then analyzed a combined dataset incorporating previous multilocus microsatellite data, using several independent and complementary statistical approaches to identify genetic substructure. All analyses revealed that 2 divergent genetic subpopulations of human cases occur sympatrically in Malaysian Borneo, detected separately in long-tailed macaques and pig-tailed macaques in the same region, whereas a third divergent genetic subpopulation occurs in humans and most macaques in peninsular Malaysia. This parasite species has undergone different sympatric and allopatric processes of divergence, which will affect its future adaptation to a changing environmental landscape. Current

differences between the subpopulations need to be recognized in clinical and epidemiologic studies.

Materials and Methods

Study Sites and DNA Samples

We obtained blood samples infected with *P. knowlesi* from human clinical cases at 7 sites and from macaque hosts at 8 sites across Malaysia (Figure 1). We extracted DNA from anticoagulated venous blood samples or dried blood spots, and tested the DNA for the presence of different malaria parasite species by species-specific PCR using methods described previously (*7*). Samples from 134 *P. knowlesi*–positive human cases collected during 2012–2014 that had sufficient DNA for multilocus genotyping originated from Kapit (n = 35), Betong (n = 4), and Lawas (n = 15) in Sarawak state, Malaysian Borneo; from Kudat (n = 20), Ranau (n = 25), and Tenom (n = 22) in Sabah state, Malaysian Borneo; and from Kelantan (n = 13) in peninsular Malaysia.

Samples that were collected during 2007–2014 from 48 *P. knowlesi*–positive macaques had sufficient DNA for multilocus genotyping. Most were from long-tailed macaques, sampled from Selangor (n = 17), Perak (n = 6), and Negeri Sembilan (n = 15) in peninsular Malaysia and from Balingian (n = 1), Limbang (n = 2), Miri (n = 2), and Sarikei (n = 2) in Sarawak; pig-tailed macaque samples were from Limbang (n = 1) and Kapit (n = 2) in Sarawak. We performed the sampling according to the protocols of the Department of Wildlife and National Parks in Malaysia. We included DNA of *P. knowlesi* strain Nuri (kindly provided by Clemens Kocken at the Biomedical Primate Research Centre, the Netherlands) in the genotyping as a control (*17*).

Microsatellite Genotyping of New Samples

We genotyped each of the *P. knowlesi*–positive DNA samples at 10 microsatellite loci (NC03_2, CD05_06, CD08_61, NC0AU: 9_1, NC10_1, CD11_157, NC12_2, NC12_4, CD13_61, CD13_107) using hemi-nested PCR assays specific for *P. knowlesi*, as described previously (*9*). We analyzed fluorescent dye-labeled PCR products by using capillary electrophoresis on the Genetic Analyzer 3730 (Applied Biosystems, Cheshire, UK), with GeneScan 500 LIZ internal size standards, following which we scored alleles and peak heights with GeneMapper version 4.0 software (Applied Biosystems).

The genotypic multiplicity of infection (MOI) was defined as the maximum number of alleles detected at any individual locus. Electrophoretic peak heights above 200 fluorescent units of the expected molecular sizes were scored as alleles, and secondary peaks within an infection sample were scored if they had a height of at least 25% relative to the predominant allele. We determined the multilocus genotype profile of each infection, and allele frequency counts for population samples, by counting the predominant allele at each locus within each infection.

Analysis of Microsatellite Genotypes from Previous Data

We retrieved whole genome sequence data of *P. knowlesi* samples from the European Nucleotide Archive (http://www.ebi.ac.uk/ena), and we obtained the reference genome sequence of strain H from GeneDB (http://www.genedb.org/Homepage/Pknowlesi). Most of the parasite genome short-read Illumina sequences available are from patients sampled in Malaysian Borneo (*12*,*16*), but a few are from older laboratory lines that originated from peninsular Malaysia, as well as 1 supposedly from the Philippines (*16*). Although genome sequences indicate some historical mislabeling or contamination of the laboratory lines, meaning that individual identities are in question, it is clear that most are from peninsular Malaysia (*16*). We aligned the raw short reads to *P. knowlesi* genome strain H by using the

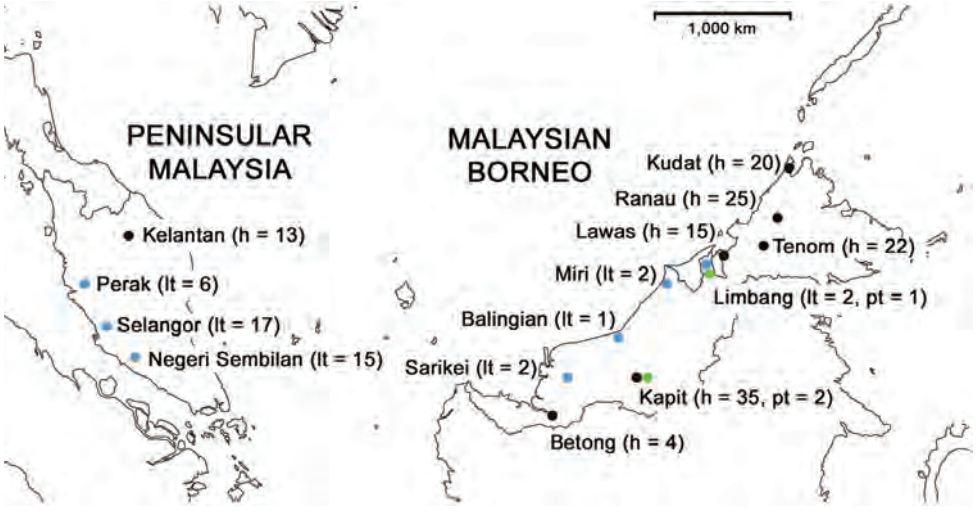

Figure 1. Geographic distribution of DNA samples of *Plasmodium knowlesi* infections derived from 134 humans and 48 macaques across Malaysia. h, human samples; lt, long-tailed macaque samples; pt, pig-tailed macaque samples.

BWA-MEM alignment tool with default parameters (https://arxiv.org/pdf/1303.3997.pdf). We identified lists of indels using the SAMTools and VCFtools software (*18*,*19*) with the following parameters, described elsewhere (*16*): *mpileup –B –Q 23 –d 2000 –C 50 -ugf; varFilter –d 10 –D 2000*. Using ARTEMIS software (*20*), we determined the putative microsatellite allele size by inspecting the indels within the location of the PCR primers used for the second amplification PCR. We assessed the quality of the mapping within the microsatellite allele regions with the minimum depth of short-read coverage at 30-fold.

Analyses of *P. knowlesi* Population Genetic Substructure

We evaluated population genetic structure by Bayesian clustering inference using STRUCTURE version 2.3.4 software (*21*), on samples for which there were no missing data at any locus. First, to allocate the probable ancestral assignment of a genotype into 1 or more *K* clusters, we set the parameters for the admixture model on the basis of correlated allele frequency, without providing the sample source information. However, the sensitivity for population structure analysis can be improved by providing population information, in which an algorithm assumes that the probability of an individual being part of a population varies among locations or sources of origins (*22*). For the second test, we set the parameter to LOCPRIOR. This parameter is informative when population structure signals are weak because of a close relationship between populations. We performed both LOCPRIOR and non-LOCPRIOR parameters in STRUCTURE runs separately with a burn-in period of 50,000 followed by 100,000 Markov chains (MCMC iterations). The simulations were replicated 20 times for *K* values ranging from 1 to 10. The optimal *K* value was calculated based on Evanno's method of ΔK statistics implemented in the STRUCTURE HARVESTER webpage interface (*23*,*24*). For the optimum *K*, we aligned the 20-replicate runs at 10,000 permutations to determine the consensus of cluster scores using CLUMPP version 1.1.2 (*25*).

To evaluate population structure independently, we performed principal coordinate analysis (PCoA) using the GenAlEx package version 6 implemented in Microsoft Excel (*26*). We first generated a genetic distance matrix using the multilocus microsatellite dataset, and we plotted a 2-dimensional PCoA based on the first 2 highest eigenvalues. We calculated the *K*-means clusters using the first and second eigenvectors generated from the PCoA, and subsequently used them to assign each individual infection to the most probable cluster. In addition, we applied the discriminant analysis of principal component from the *adegenet* 2.0.0 packages in R to assess the population structure (*27*). In this procedure, we first transformed genotype data into 40 uncorrelated principal components, and then, using the discriminant function, we partitioned the variances into within-group and among-group components, while optimizing separations between groups.

We calculated pairwise differentiation (F_{ST}) between different subpopulations of *P. knowlesi* by using FSTAT software version 2.9.3.2 (*28*). We estimated the mean allelic diversity across loci, measured as expected heterozygosity (H_E), using FSTAT software. We assessed multilocus linkage disequilibrium with the standardized index of association (I_A^S), calculated by LIAN version 3.7 (*29*), with Monte Carlo simulation of 10,000 data permutations.

Results

Genotypic Diversity within *P. knowlesi* Infections

Of 182 *P. knowlesi* infections genotyped for this study (134 from humans, 45 from long-tailed macaques, and 3 from pig-tailed macaques), 166 (91.2%) yielded complete genotype data for the panel of 10 microsatellite loci, whereas the remainder were each genotyped for at least 7 of the loci (Table; online Technical Appendix 1, http://wwwnc.cdc.gov/EID/article/23/4/16-1738-Techapp1.xlsx).

Among the human cases, single genotype infections were common, and the average number of genotypes per infection (MOI) was less than 2 at all sites sampled. This was expected when these samples were collectively reanalyzed with *P. knowlesi* infections of humans and macaques across Malaysia from previous studies (online Technical Appendix 2 Table 1, http://wwwnc.cdc.gov/EID/article/23/4/16-1738-Techapp2.pdf). We found no notable difference in numbers of genotypes per infection in Malaysian Borneo and peninsular Malaysia (mean MOI values of 1.50 and 1.77, respectively; $p = 0.14$ by Fisher exact test). In contrast, multiple genotype infections were more common in macaques both in Malaysian Borneo (mean MOI = 2.10, $p = 6.7 \times 10^{-3}$) and peninsular Malaysia (mean MOI = 2.39, $p = 9.8 \times 10^{-4}$) (Table; Figure 2). We counted the predominant allele at each locus per infection for subsequent statistical analyses on population structure.

Analysis of *P. knowlesi* Population Genetic Structure with New Samples

Bayesian clustering analyses using 2 admixture models on the new sample of 166 infections with complete genotype data for the full panel of 10 microsatellite loci identified 3 subpopulation clusters ($K = 3$; Figure 3; online Technical Appendix 2 Figures 1 and 2, panel A), hereafter referred to as clusters 1–3. Human infections in Malaysian Borneo were assigned to clusters 1 and 2, whereas long-tailed macaque infections were all in cluster 1 and pig-tailed macaque infections were mostly in cluster 2 (1 pig-tailed macaque infection was assigned as intermediate between clusters 2 and 3), confirming the existence of 2 major

Table. Summary of *Plasmodium knowlesi* mixed-genotype infections in 134 human and 48 macaque hosts across Malaysia obtained using 10 microsatellite loci*

Host and site	Region	No. samples	No. isolates by no. genotypes detected				Average		
			1	2	3	4	% Poly	MOI	MS_{10}
Human									
Kapit	Sarawak	35	27	5	2	1	23	1.34	35
Betong	Sarawak	4	4	0	0	0	0	1.00	3
Lawas	Sarawak	15	7	7	0	1	53	1.67	14
Kudat	Sabah	20	13	6	1	0	35	1.40	20
Ranau	Sabah	25	13	10	2	0	48	1.56	25
Tenom	Sabah	22	11	7	3	1	50	1.73	22
Kelantan	Peninsular Malaysia	13	5	6	2	0	62	1.77	13
Total		134							132
Long-tailed macaque									
Balingian	Sarawak	1	0	1	0	0	100	2.00	1
Limbang	Sarawak	2	0	1	1	0	100	2.50	1
Miri	Sarawak	2	1	1	0	0	50	1.50	1
Sarikei	Sarawak	2	1	0	1	0	50	2.00	2
Selangor	Peninsular Malaysia	17	8	6	2	1	53	1.76	15
Perak	Peninsular Malaysia	6	1	3	2	0	83	2.17	5
Negeri Sembilan	Peninsular Malaysia	15	0	3	6	6	100	3.20	6
Total		45							31
Pig-tailed macaque									
Limbang	Sarawak	1	0	0	1	0	100	3.00	1
Kapit	Sarawak	2	1	0	1	0	50	2.00	2
Total		3							3
All		182							166

*All samples were successfully genotyped at ≥7 loci, and 166 samples had complete genotypes for all 10 microsatellite loci (MS_{10}). MOI, multiplicity of infection; poly, polyclonal infections.

sympatric subpopulations in Malaysian Borneo, as reported previously (*9*,*12*,*16*).

Among the samples from peninsular Malaysia, those from human cases were all assigned to cluster 3, along with most of the infections from wild long-tailed macaques sampled in Kelantan, although long-tailed macaque infections from the other 2 sites had more intermediate cluster assignments, suggesting some ancestral affinity with cluster 2. All the laboratory isolates, originating many years ago mainly from peninsular Malaysia, were clearly assigned to cluster 3, consistent with results of a recent whole genome sequence analysis (*16*).

Analysis of Population Genetic Structure Incorporating New and Previously Acquired Microsatellite Data

To further evaluate the population structure of *P. knowlesi*, we collated the dataset in this study with data from samples analyzed previously (*9*). This yielded a total of 758 *P. knowlesi* infections with the complete panel of 10 microsatellite loci genotyped. This total comprises 166 samples from the present study (Table), 556 previously genotyped samples, 29 samples that had undergone repeat genotyping for all 10 loci completed here (online Technical Appendix 1 Figure 3), and 7 derived from Illumina short-read sequence data.

The admixture STRUCTURE analysis without the LOCPRIOR model identified 2 subpopulation clusters (K = 2; online Technical Appendix 2 Figure 2, panel B, and 4). This was consistent with a previous analysis showing that human cases in the Malaysian Borneo group fell into 2 different genotype clusters, which are also respectively seen in long-tailed and pig-tailed macaque infections, although the current analysis assigned samples from peninsular Malaysia to cluster 2 (previously, they had been grouped into cluster 1). However, incorporation of the LOCPRIOR model showed 3

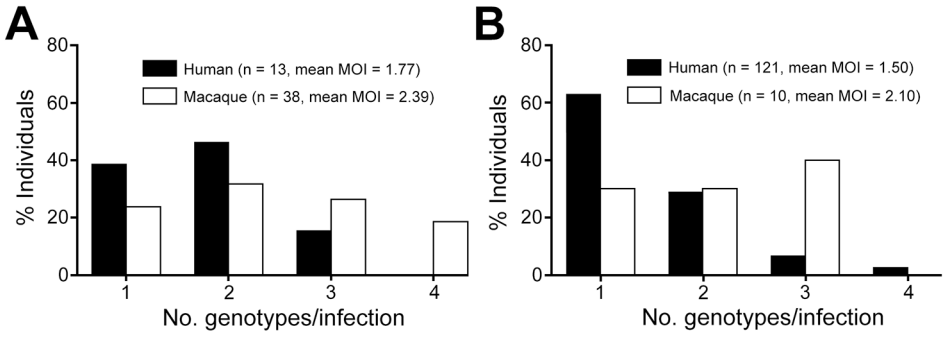

Figure 2. Multiplicity of infection (MOI) for *Plasmodium knowlesi* genotypes in 134 human and 48 macaque hosts across Malaysia. Means of MOI were higher in macaque hosts than in human hosts for both regions, but the values were not statistically significant for A) peninsular Malaysia (p = 0.25 by Fisher exact test) compared with B) Malaysian Borneo (p = 0.01).

subpopulation clusters (K = 3; Figure 4, panel A; online Technical Appendix 2 Figure 4), with most of the isolates from peninsular Malaysia belonging to cluster 3, as also seen with the analysis based solely on the new samples. Overall, this confirms that human *P. knowlesi* infections in Malaysian Borneo are divided into 2 different genetic subpopulations that are associated with different macaque reservoir host species, whereas human infections in peninsular Malaysia belong to a third subpopulation that is also seen in long-tailed macaques at 1 of the sites in peninsular Malaysia.

Robustness and Divergence of Subpopulation Clusters

Using an a priori designation of 3 subpopulation clusters (K = 3), we independently assigned all 758 infections into clusters using PCoA (Figure 4, panel B) and discriminant analysis (Figure 4, panel C), and compared the results with those derived from the STRUCTURE analysis (Figure 4, panel A). These showed highly concordant results (online Technical Appendix 1). PCoA indicated that infections in humans were strongly associated with infections in local macaque reservoir hosts for both Malaysian Borneo and peninsular Malaysia (online Technical Appendix 2 Figure 5). Discriminant analysis also showed clear clustering, with only minimal overlap among the inertia ellipses for the 3 major clusters.

To test the consistency and robustness of cluster assignment for all 758 infections, across the different methods used (Bayesian analysis using STRUCTURE, principal coordinates analysis, and discriminant analysis), we assessed a consensus for each individual (online Technical Appendix 1; online Technical Appendix 2 Table 2). A large majority (86.4%) of infections were assigned into the same cluster by all 3 methods (cluster 1, n = 384; cluster 2, n = 175; cluster 3, n = 96). Most of the remainder (12.9% of the total) had an agreed assignment for 2 of the methods (cluster 1, n = 65; cluster 2, n = 16; cluster 3, n = 17), whereas only 5 (0.7%) showed no agreement across the methods. Omitting the few infections that did not show agreement for 2 or more methods yielded a dataset of 753 *P. knowlesi* infections that grouped into 3 major subpopulation clusters (cluster 1, n = 449; cluster 2, n = 191; cluster 3, n = 113; online Technical Appendix 2 Table 3). We estimated values of allelic diversity (H_E) between 0.51 and 0.83 among different sites at each of the subpopulation clusters (online Technical Appendix 2 Table 4), and we observed similar patterns even without separating the infections by subpopulation cluster assignments (online Technical Appendix 2 Table 5). The index of multilocus linkage disequilibrium yielded various degrees (I_A^S range from -0.007 to 0.305), with loss of significance at majority of the sites among the 3-subpopulation clusters (online Technical Appendix 2 Table 4). However, the degree of significance increased when all infections were not assigned into subpopulation clusters (I_A^S range from -0.002 to 0.242 with p<0.01 at most sites; online Technical Appendix 2 Table 5). Analyses of allele frequencies across all 10 microsatellite loci confirmed strong genetic differentiation among these clusters (F_{ST} = 0.184 between clusters 1 and 2; F_{ST} = 0.152 between clusters 1 and 3;

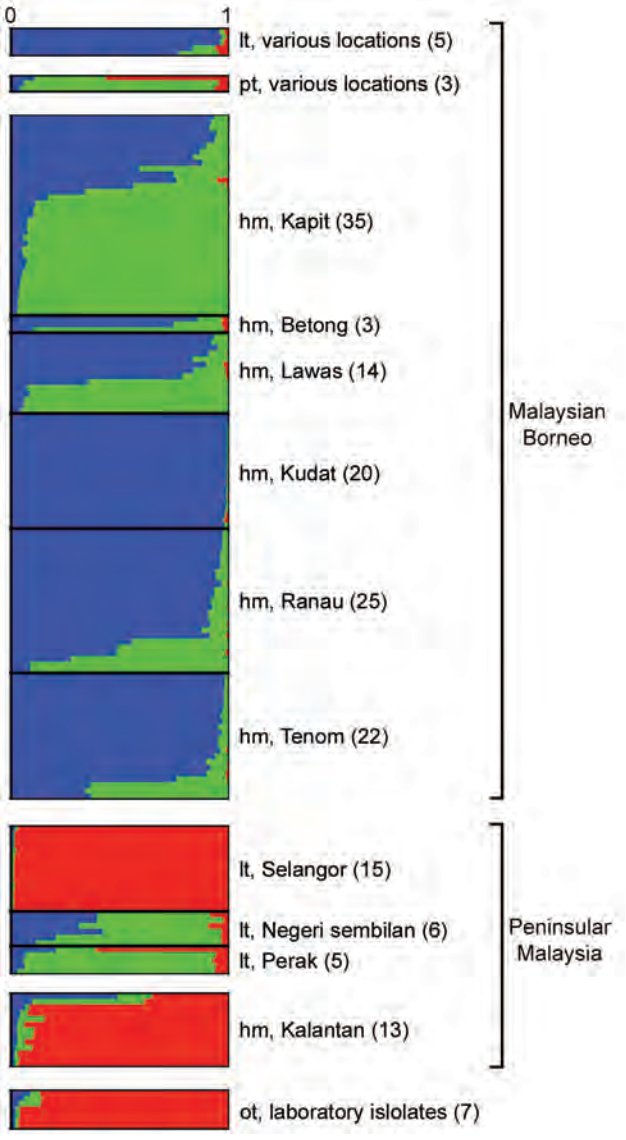

Figure 3. Subpopulation cluster assignments of individual *Plasmodium knowlesi* infections in human and macaque hosts across Malaysia and 7 laboratory isolates. The Bayesian-based STRUCTURE analysis with LOCPRIOR model (*22*) was applied on complete 10-microsatellite loci of 166 *P. knowlesi* infections and 7 laboratory isolates showing 3 subpopulation clusters (K = 3; ΔK = 37.72). Ancestral population clusters are referred to as cluster 1 (blue), cluster 2 (green), and cluster 3 (red). Numbers in parentheses indicate number of isolates. hm, human; lt, long-tailed macaque; pt, pig-tailed macaque; ot, various other sources.

F_{ST} = 0.201 between clusters 2 and 3; p<3.3 × 10^{-4} for each comparison using 3,000 randomized permutations). This indicates deep divergence among the 3 major parasite subpopulations that infect humans, 2 of which are sympatric and predominantly associated with different reservoir hosts (long-tailed and pig-tailed macaques in Malaysian Borneo), and 1 of which is allopatric in a different geographic region (peninsular Malaysia).

Discussion

Three major subpopulations of *P. knowlesi* have been demonstrated in natural human infections in Malaysia. These subpopulations show profound divergence, with pairwise F_{ST} values of ≈0.2, suggesting minimal or no current gene flow between parasites in Malaysian Borneo and peninsular Malaysia, nor between parasites in long-tailed and pig-tailed macaque hosts within Malaysian Borneo.

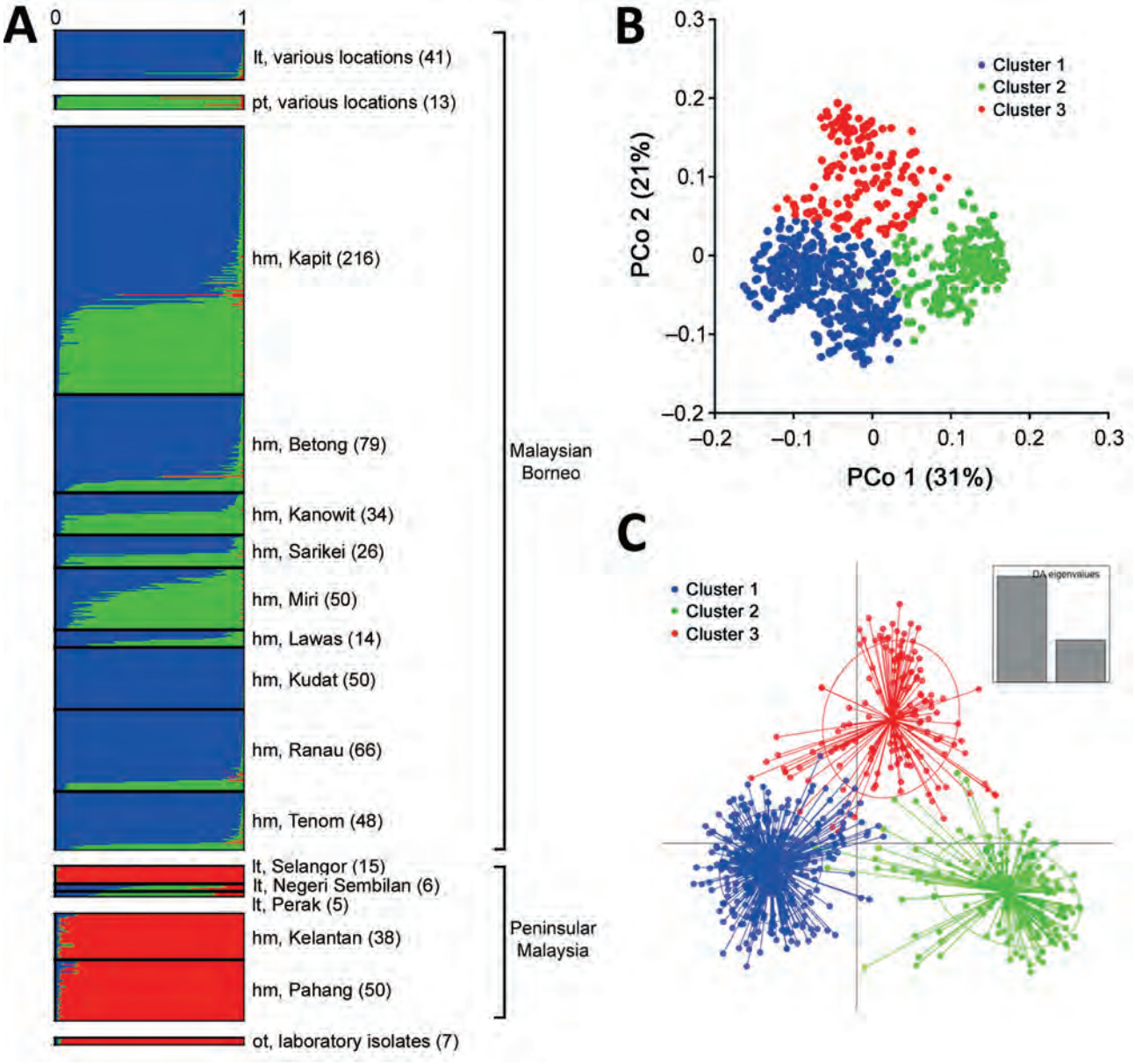

Figure 4. Population genetic structure of combined 751 P. knowlesi infections across Malaysia and 7 laboratory isolates. A) The inference of genetic clusters on complete 10-locus genotype dataset using the STRUCTURE analysis with LOCPRIOR model (*22*) showed 3 major subpopulation structures (K = 3, ΔK = 98.73), corresponding to those shown in Figure 3. Numbers in parentheses indicate number of isolates. B, C) Using a priori K = 3, individual genotypes were assigned to the most probable subpopulation clusters using independent genetic distance matrix inferred by the principal coordinate analysis (B) and discriminant analysis of principal component (DAPC) (C). In DAPC, clusters depicted as ellipses indicated the variance within the clusters and centered by K-means. hm, human; lt, long-tailed macaque; PCo, principal coordinate; pt, pig-tailed macaque.

The existence of 3 divergent clusters was initially indicated from whole genome sequence-based single nucleotide polymorphism analysis of *P. knowlesi* clinical isolates and laboratory lines (*16*). Whereas 2 of the clusters of genome sequences (clusters 1 and 2) had been seen in clinical infections in Malaysian Borneo, the third (cluster 3) was seen only in old laboratory lines that were originally isolated mostly from peninsular Malaysia. Using microsatellite scoring obtained from genome sequences and combined with genotyping of infections from humans and macaques in the current study, we confirmed that the cluster 3 subpopulation is widespread in peninsular Malaysia. Furthermore, it is divergent from clusters 1 and 2, which account for all infections in Malaysian Borneo and apparently a minority of wild macaque infections in peninsular Malaysia. With smaller numbers of samples, recent studies on sequence diversity in genes encoding the normocyte binding protein (*Pknbpxa*) (*10*) and the Duffy binding protein (*PkDBP*) (*30*), as well as the 18S rRNA gene and the mitochondrial *Cox1* gene, have suggested that parasites in peninsular Malaysia had probably diverged from those in Malaysian Borneo.

It is likely that allopatric divergence occurred as a result of the ocean barrier between Borneo and mainland Southeast Asia, established at the end of the last ice age ≈13,000 years ago, which prevents the movement of wild macaque reservoir hosts (*31*). However, one of the old laboratory lines that was recently sequenced is labeled as having originally been isolated from a long-tailed macaque in "Philippines," and this sequence is clearly assigned to cluster 3 along with the parasites from peninsular Malaysia (*16*), although the islands of the Philippines have never been connected to peninsular Malaysia or any other part of mainland Southeast Asia (*32*). Unless there was a historical mislabeling or previous mixup of parasite material, this finding suggests that wider sampling of *P. knowlesi* in wild macaques will give a more complete understanding of divergence within this zoonotic parasite species (*31*,*33*–*35*). Similarly, the observation that a minority of *P. knowlesi* parasites in long-tailed macaques from peninsular Malaysia are assigned to cluster 2, which has otherwise been seen only in samples from Malaysian Borneo, indicates that additional sampling of macaques from different areas may uncover more features of the parasite population structure.

The sympatric differentiation between cluster 1 and cluster 2 parasites in Malaysian Borneo supports the idea that parasite subpopulations are transmitted independently in long-tailed and pig-tailed macaque populations (*36*,*37*). Although pig-tailed macaques occur mostly in forested areas, long-tailed macaques have a broader habitat range in both forested and nonforested areas (*38*). Because of the absence of parasite samples from pig-tailed macaques in peninsular Malaysia, it is unknown whether there is divergence in *P. knowlesi* between the different macaque host species in this region.

Analysis of genome sequences to derive the frequency distribution of single-nucleotide polymorphism alleles indicates that the cluster 1 subpopulation of *P. knowlesi* has undergone long-term population growth (*16*). It is unknown whether parasites of cluster 2 and cluster 3 subpopulations have a similar demographic history, but genome sequencing of more samples within these subpopulations should be able to address this in the future.

The observation that most infections in all macaque populations are polyclonal, whereas most human cases contain single parasite genotypes, probably reflects a higher intensity of transmission among macaques than from macaques to humans (*9*). It is not yet known whether there are any substantial differences in the clinical course of infections caused by the 3 major subpopulations of *P. knowlesi*; this question should be investigated in a manner that accounts for any confounding variables between different study sites. In any case, recognition of these divergent subpopulations provides a more accurate basis on which to understand and potentially control the transmission of this zoonosis. Furthermore, obtaining whole-genome sequence data from more clinical samples belonging to each of the 3 major types should enable a more thorough investigation of the genomic divergence, and identify loci at which there are signals of recent adaptation that may relate to differences in virulence or transmission.

Acknowledgments

We thank colleagues in Malaria Research Centre, Universiti Malaysia Sarawak, and the London School of Hygiene and Tropical Medicine for laboratory assistance and the Director General of Health in Malaysia for permission to publish this article. We also thank Sarawak Forestry Department, Sarawak Biodiversity Centre, and Department of Wildlife and National Parks Peninsular Malaysia for the permission to collect samples from macaques. We are also grateful to Clemens Kocken for providing *P. knowlesi* DNA control samples.

This study is supported by postgraduate scholarship from the Ministry of Higher Education in Malaysia and grants from UNIMAS (grant nos. 01/(TD03)/1003/2012(01) and F05/SpTDG/1447/2016/4), and from the European Research Council (AdG-2011-294428).

Mr. Divis is a lecturer at the Malaria Research Centre in Universiti Malaysia Sarawak, Malaysia, and a PhD student at the London School of Hygiene and Tropical Medicine, United Kingdom. His research interests include molecular epidemiology, population genetics, and genomics of *Plasmodium knowlesi*.

References

1. Singh B, Daneshvar C. Human infections and detection of *Plasmodium knowlesi.* Clin Microbiol Rev. 2013;26:165–84. http://dx.doi.org/10.1128/CMR.00079-12
2. Setiadi W, Sudoyo H, Trimarsanto H, Sihite BA, Saragih RJ, Juliawaty R, et al. A zoonotic human infection with simian malaria, *Plasmodium knowlesi*, in Central Kalimantan, Indonesia. Malar J. 2016;15:218. http://dx.doi.org/10.1186/s12936-016-1272-z
3. Yusof R, Lau YL, Mahmud R, Fong MY, Jelip J, Ngian HU, et al. High proportion of knowlesi malaria in recent malaria cases in Malaysia. Malar J. 2014;13:168. http://dx.doi.org/10.1186/1475-2875-13-168
4. William T, Rahman HA, Jelip J, Ibrahim MY, Menon J, Grigg MJ, et al. Increasing incidence of *Plasmodium knowlesi* malaria following control of *P. falciparum* and *P. vivax* Malaria in Sabah, Malaysia. PLoS Negl Trop Dis. 2013;7:e2026. http://dx.doi.org/10.1371/journal.pntd.0002026
5. Fornace KM, Nuin NA, Betson M, Grigg MJ, William T, Anstey NM, et al. Asymptomatic and submicroscopic carriage of *Plasmodium knowlesi* malaria in household and community members of clinical cases in Sabah, Malaysia. J Infect Dis. 2016;213:784–7. http://dx.doi.org/10.1093/infdis/jiv475
6. Vythilingam I, Wong ML, Wan-Yussof WS. Current status of *Plasmodium knowlesi* vectors: a public health concern? Parasitology. 2016:1–9. http://dx.doi.org/10.1017/S0031182016000901
7. Lee KS, Divis PC, Zakaria SK, Matusop A, Julin RA, Conway DJ, et al. *Plasmodium knowlesi:* reservoir hosts and tracking the emergence in humans and macaques. PLoS Pathog. 2011;7:e1002015. http://dx.doi.org/10.1371/journal.ppat.1002015
8. Vythilingam I, Noorazian YM, Huat TC, Jiram AI, Yusri YM, Azahari AH, et al. *Plasmodium knowlesi* in humans, macaques and mosquitoes in peninsular Malaysia. Parasit Vectors. 2008;1:26. http://dx.doi.org/10.1186/1756-3305-1-26
9. Divis PC, Singh B, Anderios F, Hisam S, Matusop A, Kocken CH, et al. Admixture in humans of two divergent *Plasmodium knowlesi* populations associated with different macaque host species. PLoS Pathog. 2015;11:e1004888. http://dx.doi.org/10.1371/journal.ppat.1004888
10. Ahmed MA, Fong MY, Lau YL, Yusof R. Clustering and genetic differentiation of the normocyte binding protein (nbpxa) of *Plasmodium knowlesi* clinical isolates from peninsular Malaysia and Malaysia Borneo. Malar J. 2016;15:241. http://dx.doi.org/10.1186/s12936-016-1294-6
11. Ahmed AM, Pinheiro MM, Divis PC, Siner A, Zainudin R, Wong IT, et al. Disease progression in *Plasmodium knowlesi* malaria is linked to variation in invasion gene family members. PLoS Negl Trop Dis. 2014;8:e3086. http://dx.doi.org/10.1371/journal.pntd.0003086
12. Pinheiro MM, Ahmed MA, Millar SB, Sanderson T, Otto TD, Lu WC, et al. *Plasmodium knowlesi* genome sequences from clinical isolates reveal extensive genomic dimorphism. PLoS One. 2015;10:e0121303. http://dx.doi.org/10.1371/journal.pone.0121303
13. Fong MY, Lau YL, Chang PY, Anthony CN. Genetic diversity, haplotypes and allele groups of Duffy binding protein (PkDBPαII) of *Plasmodium knowlesi* clinical isolates from peninsular Malaysia. Parasit Vectors. 2014;7:161. http://dx.doi.org/10.1186/1756-3305-7-161
14. Fong MY, Rashdi SA, Yusof R, Lau YL. Distinct genetic difference between the Duffy binding protein (PkDBPαII) of *Plasmodium knowlesi* clinical isolates from North Borneo and peninsular Malaysia. Malar J. 2015;14:91. http://dx.doi.org/10.1186/s12936-015-0610-x
15. Yusof R, Ahmed MA, Jelip J, Ngian HU, Mustakim S, Hussin HM, et al. Phylogeographic evidence for 2 genetically distinct zoonotic *Plasmodium knowlesi* parasites, Malaysia. Emerg Infect Dis. 2016;22:1371–80. http://dx.doi.org/10.3201/eid2208.151885
16. Assefa S, Lim C, Preston MD, Duffy CW, Nair MB, Adroub SA, et al. Population genomic structure and adaptation in the zoonotic malaria parasite *Plasmodium knowlesi*. Proc Natl Acad Sci U S A. 2015;112:13027–32.
17. Kocken CH, Ozwara H, van der Wel A, Beetsma AL, Mwenda JM, Thomas AW. *Plasmodium knowlesi* provides a rapid in vitro and in vivo transfection system that enables double-crossover gene knockout studies. Infect Immun. 2002;70:655–60. http://dx.doi.org/10.1128/IAI.70.2.655-660.2002
18. Li H, Handsaker B, Wysoker A, Fennell T, Ruan J, Homer N, et al.; 1000 Genome Project Data Processing Subgroup. The Sequence Alignment/Map format and SAMtools. Bioinformatics. 2009;25:2078–9. http://dx.doi.org/10.1093/bioinformatics/btp352
19. Danecek P, Auton A, Abecasis G, Albers CA, Banks E, DePristo MA, et al.; 1000 Genomes Project Analysis Group. The variant call format and VCFtools. Bioinformatics. 2011;27:2156–8. http://dx.doi.org/10.1093/bioinformatics/btr330
20. Rutherford K, Parkhill J, Crook J, Horsnell T, Rice P, Rajandream MA, et al. Artemis: sequence visualization and annotation. Bioinformatics. 2000;16:944–5. http://dx.doi.org/10.1093/bioinformatics/16.10.944
21. Pritchard JK, Stephens M, Donnelly P. Inference of population structure using multilocus genotype data. Genetics. 2000; 155:945–59.
22. Hubisz MJ, Falush D, Stephens M, Pritchard JK. Inferring weak population structure with the assistance of sample group information. Mol Ecol Resour. 2009;9:1322–32. http://dx.doi.org/10.1111/j.1755-0998.2009.02591.x
23. Earl DA, vonHoldt BM. STRUCTURE HARVESTER: a website and program for visualizing STRUCTURE output and implementing the Evanno method. Conserv Genet Resour. 2012;4:359–61. http://dx.doi.org/10.1007/s12686-011-9548-7
24. Evanno G, Regnaut S, Goudet J. Detecting the number of clusters of individuals using the software STRUCTURE: a simulation study. Mol Ecol. 2005;14:2611–20. http://dx.doi.org/10.1111/j.1365-294X.2005.02553.x
25. Jakobsson M, Rosenberg NA. CLUMPP: a cluster matching and permutation program for dealing with label switching and multimodality in analysis of population structure. Bioinformatics. 2007;23:1801–6. http://dx.doi.org/10.1093/bioinformatics/btm233
26. Peakall R, Smouse PE. GENALEX 6: genetic analysis in Excel. Population genetic software for teaching and research. Mol Ecol Res. 2006;6:288–95. http://dx.doi.org/10.1111/j.1471-8286.2005.01155.x
27. Jombart T, Devillard S, Balloux F. Discriminant analysis of principal components: a new method for the analysis of genetically structured populations. BMC Genet. 2010;11:94. http://dx.doi.org/10.1186/1471-2156-11-94
28. Goudet J. FSTAT (Version 1.2): A computer program to calculate F-statistics. J Hered. 1995;86:485–6.
29. Haubold B, Hudson RR. LIAN 3.0: detecting linkage disequilibrium in multilocus data. Bioinformatics. 2000;16:847–9. http://dx.doi.org/10.1093/bioinformatics/16.9.847
30. Putaporntip C, Kuamsab N, Jongwutiwes S. Sequence diversity and positive selection at the Duffy-binding protein genes of *Plasmodium knowlesi* and *P. cynomolgi*: analysis of the complete coding sequences of Thai isolates. Infect Genet Evol. 2016;44:367–75. http://dx.doi.org/10.1016/j.meegid.2016.07.040
31. Liedigk R, Kolleck J, Böker KO, Meijaard E, Md-Zain BM, Abdul-Latiff MA, et al. Mitogenomic phylogeny of the common long-tailed macaque (*Macaca fascicularis fascicularis*). BMC Genomics. 2015;16:222. http://dx.doi.org/10.1186/s12864-015-1437-0
32. Voris HK. Maps of Pleistocene sea levels in Southeast Asia: shorelines, river systems and time durations. J Biogeogr. 2000; 27;1153–67. http://dx.doi.org/10.1046/j.1365-2699. 2000.00489.x

33. Esselstyn JA, Widmann P, Heaney LR. The mammals of Palawan Island, Philippines. Proc Biol Soc Wash. 2004; 117:271–302.
34. Meijaard E. Mammals of south-east Asian islands and their Late Pleistocene environments. J Biogeogr. 2003;30:1245–57. http://dx.doi.org/10.1046/j.1365-2699.2003.00890.x
35. Smith DG, Ng J, George D, Trask JS, Houghton P, Singh B, et al. A genetic comparison of two alleged subspecies of Philippine cynomolgus macaques. Am J Phys Anthropol. 2014;155:136–48. http://dx.doi.org/10.1002/ajpa.22564
36. Muehlenbein MP, Pacheco MA, Taylor JE, Prall SP, Ambu L, Nathan S, et al. Accelerated diversification of nonhuman primate malarias in Southeast Asia: adaptive radiation or geographic speciation? Mol Biol Evol. 2015;32:422–39. http://dx.doi.org/10.1093/molbev/msu310
37. Ziegler T, Abegg C, Meijaard E, Perwitasari-Farajallah D, Walter L, Hodges JK, et al. Molecular phylogeny and evolutionary history of Southeast Asian macaques forming the *M. silenus* group. Mol Phylogenet Evol. 2007;42:807–16. http://dx.doi.org/10.1016/j.ympev.2006.11.015
38. Moyes CL, Shearer FM, Huang Z, Wiebe A, Gibson HS, Nijman V, et al. Predicting the geographical distributions of the macaque hosts and mosquito vectors of *Plasmodium knowlesi* malaria in forested and non-forested areas. Parasit Vectors. 2016;9:242. http://dx.doi.org/10.1186/s13071-016-1527-0

Address for correspondence: Paul C.S. Divis, Malaria Research Centre, Universiti Malaysia Sarawak, 94300 Kota Samarahan, Sarawak, Malaysia; email: pcsimon@unimas.my

Variation in *Aedes aegypti* Mosquito Competence for Zika Virus Transmission

Christopher M. Roundy,[1] Sasha R. Azar,[1] Shannan L. Rossi, Jing H. Huang, Grace Leal, Ruimei Yun, Ildefonso Fernandez-Salas, Christopher J. Vitek, Igor A.D. Paploski, Uriel Kitron, Guilherme S. Ribeiro, Kathryn A. Hanley, Scott C. Weaver, Nikos Vasilakis

To test whether Zika virus has adapted for more efficient transmission by *Aedes aegypti* mosquitoes, leading to recent urban outbreaks, we fed mosquitoes from Brazil, the Dominican Republic, and the United States artificial blood meals containing 1 of 3 Zika virus strains (Senegal, Cambodia, Mexico) and monitored infection, dissemination, and virus in saliva. Contrary to our hypothesis, Cambodia and Mexica strains were less infectious than the Senegal strain. Only mosquitoes from the Dominican Republic transmitted the Cambodia and Mexica strains. However, blood meals from viremic mice were more infectious than artificial blood meals of comparable doses; the Cambodia strain was not transmitted by mosquitoes from Brazil after artificial blood meals, whereas 61% transmission occurred after a murine blood meal (saliva titers up to 4 $\log_{10}$ infectious units/collection). Although regional origins of vector populations and virus strain influence transmission efficiency, *Ae. aegypti* mosquitoes appear to be competent vectors of Zika virus in several regions of the Americas.

Zika virus is an emerging arthropodborne virus (arbovirus) of the family *Flaviviridae*. Discovered in 1947 (*1*), Zika virus remained obscure and its detection largely limited to sylvatic transmission cycles between arboreal mosquitoes (*Aedes* [*Stegomyia*] *africanus*, *Ae.* [*Diceromyia*] *furcifer*) and primates (*1*). Before the recent outbreaks in Micronesia (*1*) and French Polynesia (*2*), only 14 human cases had been reported. In early 2015, autochthonous Zika virus transmission was detected for the first time in the Americas, in Brazil (*3*). After explosive spread in the Americas, transmission has been documented in 48 countries and territories, including the United States (*4*). Most Zika virus infections result in inapparent or mild illness; symptoms include fever, rash, malaise, and conjunctivitis. However, during the outbreak in Brazil, Zika virus was associated with serious congenital outcomes, including microcephaly (*5*), ocular abnormalities (*6*), meningoencephalitis (*7*), and myelitis (*8*), and Guillain-Barré syndrome in many age groups (*2*). These complications and the rapid spread of the virus prompted the World Health Organization to declare Zika virus a public health emergency of international concern (*5*).

There are 2 primary Zika virus lineages: Asian and African (*9*). The Zika virus strain currently circulating in the Americas (American lineage) is derived from the Asian lineage (*10*). Because no vaccines or antiviral drugs are available (*11*), efforts to prevent Zika virus infection focus on controlling mosquito vectors. Historically, Zika virus has been isolated from several *Aedes* spp. mosquitoes, including multiple sylvatic species in Africa (*1*,*12*,*13*) and the domestic species *Ae. aegypti* in Malaysia (*1*) and Mexico (*14*). *Ae. aegypti* mosquitoes are the main urban vector of other medically important urban arboviruses with similar origins, such as dengue virus (DENV), chikungunya virus (CHIKV), and yellow fever virus. However, studies of *Ae. aegypti* mosquito susceptibility for Zika virus have yielded varied results; some have suggested relative refractoriness (*15*). This finding has led to speculation that other vectors common in tropical cities, such as *Ae. albopictus* mosquitoes (*16*), implicated in a Gabon epidemic (*17*), and *Culex quinquefasciatus* mosquitoes, common in tropical cities, could be Zika virus vectors (*13*).

One hypothesis for the sudden emergence of Zika virus epidemics since 2007 is viral adaptation for more efficient transmission by *Ae. aegypti* mosquitoes (*18*). A precedent for this mechanism is the adaptation of CHIKV for infecting *Ae. albopictus* mosquitoes, mediated through a series

Author affiliations: University of Texas Medical Branch, Galveston, Texas, USA (C.M. Roundy, S.R. Azar, S.L. Rossi, J.H. Huang, G. Leal, R. Yun, S.C. Weaver, N. Vasilakis); Centro Regional de Salud Pública, Tapachula, México (I. Fernandez-Salas); University of Texas Rio Grande Valley, Brownsville, Texas, USA (C.J. Vitek); Ministério da Saúde, Candeal, Salvador, Brazil (I.A.D. Paploski, G.S. Ribeiro); Universidade Federal da Bahia, Salvador (I.A.D. Paploski, G.S. Ribeiro); Emory University, Atlanta, Georgia, USA (U. Kitron); New Mexico State University, Las Cruces, New Mexico, USA (K.A. Hanley)

DOI: http://dx.doi.org/10.3201/eid2304.161484

[1]These authors contributed equally to this article.

of envelope glycoprotein substitutions. This adaptation enabled the dramatic spread of CHIKV in the Indian Ocean Basin, Asia, and Europe since 2005 (*19*). Similar adaptive evolution of the Asian and/or American lineages of Zika virus for transmission by *Ae. aegypti* mosquitoes could explain the lack of past major urban outbreaks.

During 2016, we tested this hypothesis by examining the ability of 3 Zika virus strains representing African, Asian, and American lineages to be transmitted by *Ae. aegypti* mosquitoes. Because geographically disparate populations of this species can vary in their susceptibility to flaviviruses (*20*), including Zika virus (*15*), we tested populations from 3 at-risk sites in the Americas—Brazil (Salvador), the Caribbean (Dominican Republic [DR]), and the United States (Rio Grande Valley [RGV], Texas)—with Zika virus strains from Senegal (DAK AR 41525), Cambodia (FSS 13025), and a 2015 Mexico outbreak (MEX1–7) (*14*). We also estimated the extrinsic incubation period (EIP) and viral titers in mosquito saliva and characterized differences in infection and dissemination between artificial and viremic blood meals (*21*).

Materials and Methods

Cells

Vero cells were purchased from ATCC (Bethesda, MD, USA). Cells were maintained in Dulbecco's modification of Eagle's medium (DMEM) (Invitrogen, Carlsbad, CA, USA) supplemented with 5% fetal bovine serum (FBS) (Atlanta Biologicals, Flowery Branch, GA, USA) and penicillin/streptomycin (100 U/mL and 100 μg/mL respectively) (Invitrogen) in a humidified incubator at 37°C with 5% CO_2.

Viruses

We used the following Zika virus strains in these studies: FSS 130125 (GenBank accession no. KU955593.1), a human isolate from Cambodia isolated in Vero cells, passaged once in C6/36 before lyophilization; DAK AR 41525 (KU955591.1), an *Ae. africanus* isolate from Senegal isolated in AP61 cells and passaged once in C6/36; and MEX 1–7 (KX247632.1), isolated from *Ae. aegypti* mosquito on Vero cells with 3 additional passages. All viruses were acquired as lyophilized stocks from the World Reference Center for Emerging Viruses and Arboviruses at the University of Texas Medical Branch (Galveston, TX, USA). Viruses were cultured once in C6/36 *Ae. albopictus* cells, followed by 3 passages in Vero cells to generate stocks for mosquito feeding. All stocks were titered by focus-forming assay (FFA) and frozen at –80°C in 30% FBS before use in artificial blood meals or mouse infections.

Mosquitoes

Colonized *Ae. aegypti* mosquitoes from Salvador (generation F2), the DR (F6), and the RGV (F4) were housed in a 27° ± 1°C incubator (a typical temperature in tropical climates) with 80% ± 10% relative humidity in cardboard cups with mesh lids, fed 10% sucrose ad libitum, and maintained at 16:8 light:dark cycle. Mosquitoes were sex-sorted 3 days posteclosion. Twenty-four hours before experiments, sucrose was replaced with water, which was withdrawn 6 h before feeding.

Murine Infections

Four-week-old interferon type I receptor-knockout (A129) mice were infected intraperitoneally with 1×10^5 focus-forming units (FFU) of Zika virus FSS 13025 diluted in phosphate-buffered saline. This model generates viremias of 10^4–10^7 during 1–3 days post infection (dpi) (*22*). One animal per day was randomly selected, anesthetized with 100 mg/kg of ketamine, and placed on the screened lid of cups containing sucrose-starved *Ae. aegypti* mosquitoes (Salvador). Mosquitoes were allowed to feed for 30 min, then cold-anesthetized, and fully engorged specimens were incubated. After blood feeding, mice were euthanized and exsanguinated for viremia quantification by FFA.

Preparation of Infectious Blood Meals and Oral infection

Artificial blood meals containing Zika virus were prepared at ≈4×10^4, 4×10^5, or 4×10^6 FFU/mL. Blood meals comprised 1% (wt/vol) sucrose, 7.5% fetal bovine serum (FBS), 12.5% washed human erythrocytes (University of Texas Medical Branch blood bank), 900 μM adenosine triphosphate, and viral dilutions in DMEM containing 2% FBS and 100 U/mL penicillin and 100 μg/mL streptomycin. After 1 h of feeding, mosquitoes were cold-anesthetized, and engorged females were extrinsically incubated. Infections were conducted in 4 separated experiments, with 1 of the 3 mosquito strains studied at a time, followed by the murine blood meal experiments.

Mosquito Dissemination and Transmission Potential

On days 2, 4, 7, 10, and 14 after feeding, ≈9 mosquitoes per group (fewer in some groups because of feeding efficiency and survival) were cold-anesthetized, and legs were removed and placed into Eppendorf tubes containing a steel ball bearing and 500 μL of DMEM, supplemented with 2% FBS, 1% penicillin/streptomycin, and 2.5 μg/mL amphotericin B (GIBCO, Waltham MA, USA). On days 4, 7, 10, and 14, after removal of legs, mosquitoes were immobilized and their proboscis inserted for 30 min of salivation into a sterile 10-μL micropipette tip containing 8 μL of FBS, after which the expectorated saliva/FBS was added to 100 μL of DMEM. Mosquito bodies were then triturated for 5 min at 26 Hz in a Tissue Lyser II (QIAGEN, Venlo,

the Netherlands) in microfuge tubes containing a steel ball bearing and 500 μL of mosquito media. On day 2 after infection, only bodies and legs were collected. For mosquitoes fed on viremic mice, samples were collected 3, 7, and 14 days after feeding. Homogenized mosquito samples were clarified by centrifugation at 200 × *g* for 5 min.

FFA

FFAs were conducted as described previously (*23*) for viral stocks, blood meals, and all mosquito samples by inoculating 96-well plates of nearly confluent Vero cells with 50 μL of sample supplemented with 50 μL of mosquito media. After a 3-day incubation, plates were fixed, washed, and blocked before overnight incubation with mouse anti– Zika virus (strain MR-766). Plates were washed and incubated with goat anti-mouse secondary antibody conjugated to horseradish peroxidase (KPL, Gaithersburg, MD, USA). Plates were washed and developed with aminoethylcarbazole solution (Enzo Diagnostics, Farmingdale, NY, USA) prepared according to the manufacturer's protocol for detection.

Saliva Titration

Positive saliva samples were titrated by FFA on 24-well plates of Vero cells. Means and SDs were calculated for all positive samples. Samples that were positive during initial screening but below the limit of detection (10 FFU) for the titration assay were given a value of limit of detection–1 for calculations.

Statistical Analysis

For mosquitoes fed on artificial blood meals, the effect of mosquito strain, virus strain, and dpi, as well as interactions among these, on percentage of bodies infected was analyzed by using a nominal logistic regression, with separate analyses for each blood meal titer (≈4, 5, or 6 $\log_{10}$ FFU/mL). Because of the large number of comparisons, the threshold for significance (α) was set to an arbitrary but conservative threshold of 0.005. Next, the effects of mosquito strain, virus strain, and dpi on dissemination, measured as the percentage of infected bodies that produced infected legs, were analyzed by using a nominal logistic regression, with separate analyses for each blood meal titer. Similarly, the effects of mosquito strain, virus strain, and dpi on transmission, measured as the percentage of mosquitoes with disseminated infection that secreted virus in the saliva, were analyzed by using a nominal logistic regression, with separate analyses for each blood meal titer. For both dissemination and saliva infection, interactions among each of the 3 independent variables were not fully explored, because some combinations were not included (i.e., some mosquito strain × virus strain × dpi combinations did not yield infected bodies). Virus titer in the saliva was not subject to statistical analysis because of small sample sizes. The effects of feeding mode (mouse versus artificial blood meal), virus titer, and dpi on the percentage of infections, dissemination, and transmission in Salvador *Ae. aegypti* mosquitoes fed on Zika virus strain FSS were analyzed by nominal logistic regression.

Results

We detected no statistically significant interactions among mosquito strain, virus strain, and dpi in any analysis of infection, dissemination, or transmission after mosquitoes fed on an artificial blood meal (Table 1). Frequently, dpi significantly affected infection, dissemination, and transmission as expected based on the need for replication and dissemination in the mosquito, so these data are not presented in detail here.

When *Ae. aegypti* mosquitoes were fed on artificial blood meals at doses of 5 or 6 $\log_{10}$ FFU/mL of Zika virus, DAK AR 41525 (Figure 1, panels B, C; Figure 2, panels B, C; Figure 3, panels B, C) produced a significantly higher percentage of infection than did the same titers of strain FSS and MEX1–7 (Figure 1, panels B, C; Figure 2, panels B, C; Figure 3, panels B, C) across all 3 strains of *Ae. aegypti* ($p<0.001$ at 5 $\log_{10}$ FFU/mL, $p<0.002$ at 6 $\log_{10}$ FFU/mL). In addition, at the 2 higher doses, disseminated DAK AR 41525 infections produced a higher percentage of infectious saliva ($p<0.004$ at 5 $\log_{10}$ FFU/mL, $p<0.0001$ at 6 $\log_{10}$ FFU/mL). DAK AR 41525, however, did not result in a higher percentage of infections resulting in dissemination to the legs (a proxy for the hemocoel). At an artificial blood meal concentration of ≈4 $\log_{10}$ FFU/mL, we found no significant difference among the 3 Zika virus strains in infection, dissemination, or transmission. For all artificial blood meal concentrations, FSS 13025 and MEX 1–7 produced similar infection, dissemination, and transmission percentages in each mosquito population.

When *Ae. aegypti* mosquitoes were fed on artificial blood meals at doses of ≈4, 5, or 6 $\log_{10}$ FFU/mL of Zika virus, a significantly greater percentage of mosquitoes from the DR (Figure 2) became infected than from the RGV (Figure 3) and Salvador populations (Figure 1) ($p<0.001$ at 4 and 5 $\log_{10}$ FFU/mL, $p<0.002$ at 6 $\log_{10}$ FFU/mL). At doses of 5 and 6 $\log_{10}$ FFU/mL, a greater percentage of *Ae. aegypti* mosquitoes from the DR with disseminated infections had infectious saliva ($p<0.004$ at 5 $\log_{10}$ FFU/mL, $p<0.0001$ at 6 $\log_{10}$ FFU/mL). *Ae. aegypti* mosquitoes from the DR, however, did not have significantly higher percentages of infections that disseminated. For all artificial blood meal doses and Zika virus strains, *Ae. aegypti* from Salvador and the RGV had similar infection, dissemination, and transmission percentages.

Because virus titers and sampling days for mosquitoes fed on mice (4, 6, and 7 $\log_{10}$ FFU/mL sampled 7 and 14 days postfeeding) and artificial blood meals (4, 5, and 6

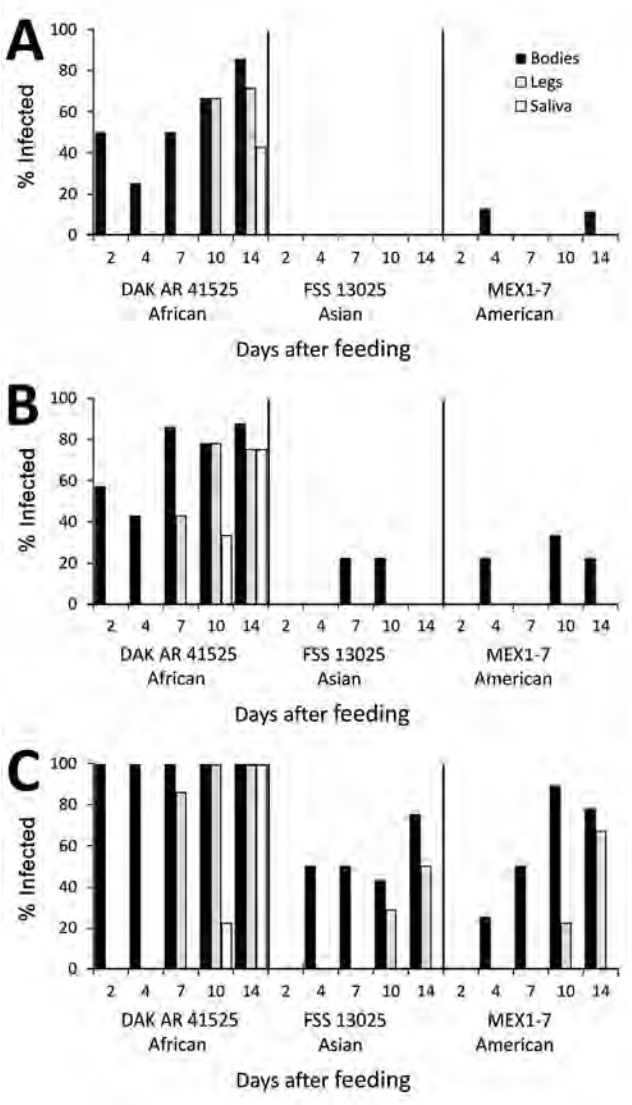

Figure 1. Infection, dissemination, and transmission of 3 Zika virus strains by *Aedes aegypti* mosquitoes from Salvador, Brazil, after artificial blood meals with a concentration of 4 $\log_{10}$ (A), 5 $\log_{10}$ (B), or 6 $\log_{10}$ (C) focus-forming units/mL.

$\log_{10}$ FFU/mL sampled 2, 4, 7, 10, and 14 dpi) did not completely overlap, we first compared mosquito infection only for blood meal titers (≈4 and 6 $\log_{10}$ FFU/mL) and dpi (7, 14 dpi) that coincided between the 2 feeding methods (Figure 1, panels A [middle panel], C [middle panel]; Figure 4). A nominal logistic regression using these data (N = 81) showed no significant interactions among the independent variables; virus titer (χ^2 24.3, df = 1, $p<0.0001$) and feeding method (χ^2 9.7, df = 1, $p<0.0019$) significantly affected the likelihood of infection, whereas dpi did not (χ^2 0.33, df = 1, $p = 0.56$). Using this same dataset, we found that virus titer, feeding method, and dpi all significantly affected dissemination from infected bodies to legs (N = 50, $p\leq0.0001$ for all 3 variables). Because only 8 mosquitoes in this group produced infected saliva, we did not attempt analysis on this small sample. However, it was striking that only mosquitoes fed on mice produced infected saliva. An analysis using all data from Salvador mosquitoes fed on Zika virus strain FSS 13025 in artificial blood meals and mice revealed a significant effect of all 3 independent variables on infection ($p<0.0001$ for all comparisons), with infection being greater at higher blood meal titers and later time points after infection and from blood meals acquired from mice.

Ae. aegypti mosquitoes from Salvador exhibited a minimum EIP of 10 days after artificial infection with Zika virus strain DAK AR 41525 at 5 and 6 $\log_{10}$ FFU/mL and 14 days after infection with FSS 13025 or MEX1–7 strains at 6 $\log_{10}$ FFU/mL and DAK AR 41525 at 4 $\log_{10}$ FFU/mL. *Ae. aegypti* mosquitoes from the DR exhibited an EIP of 10 days after artificial infection with Zika virus strain DAK AR 41525 at 5 and 6 $\log_{10}$ FFU/mL and 14 days after infection with FSS 13025 at 5 or 6 $\log_{10}$ FFU/mL, MEX1–7 strains at all 3 doses, and DAK AR 41525 at 4 $\log_{10}$ FFU/mL. *Ae. aegypti* mosquitoes from the RGV did not effectively transmit FSS 13025 or MEX1–7 at any titer (only 1 positive MEX1–7 saliva sample on 10 dpi) but showed an EIP of 7 days with strain DAK AR 41525 at 6 $\log_{10}$ FFU/mL, 10 days at 5 $\log_{10}$ FFU/mL, and 14 days at 4 $\log_{10}$ FFU/mL. Mosquitoes infected through murine blood meals showed an EIP of 7 days after a 6 or 7 $\log_{10}$ FFU/mL blood meal, and 14 days after a 4 $\log_{10}$ blood meal.

Discussion

Because no vaccine or therapeutic drugs are available, Zika virus prevention depends on controlling the mosquito vector. Although some previous studies (*15*) showed relatively low Zika virus competence in *Ae. aegypti* mosquitoes, raising questions about the role of other potential vectors, others have shown this species to be highly competent (*24*,*25*). We demonstrated that *Ae. aegypti* mosquito competency as a vector for Zika virus in the Americas varies greatly and depends on mosquito origin, Zika virus strain, and type of blood meal used. Recent studies demonstrated that preexisting DENV antibodies in Zika virus–endemic areas might enhance Zika virus infection in vitro (*26*); other studies have conversely demonstrated that monoclonal antibodies to DENV envelope neutralize Zika virus in vitro and protect immunocompromised mice from lethal infection (*27*). The role of preexisting immunity to heterologous viruses remains unclear; thus, even a moderately competent vector, such as *Ae. aegypti* mosquitoes, might be able transmit efficiently because of its highly anthropophilic behavior and ready access to homes without screening or air conditioning in much of Latin America and the Caribbean.

In agreement with previous studies (*15*), we demonstrated significant variation in competency for Zika virus

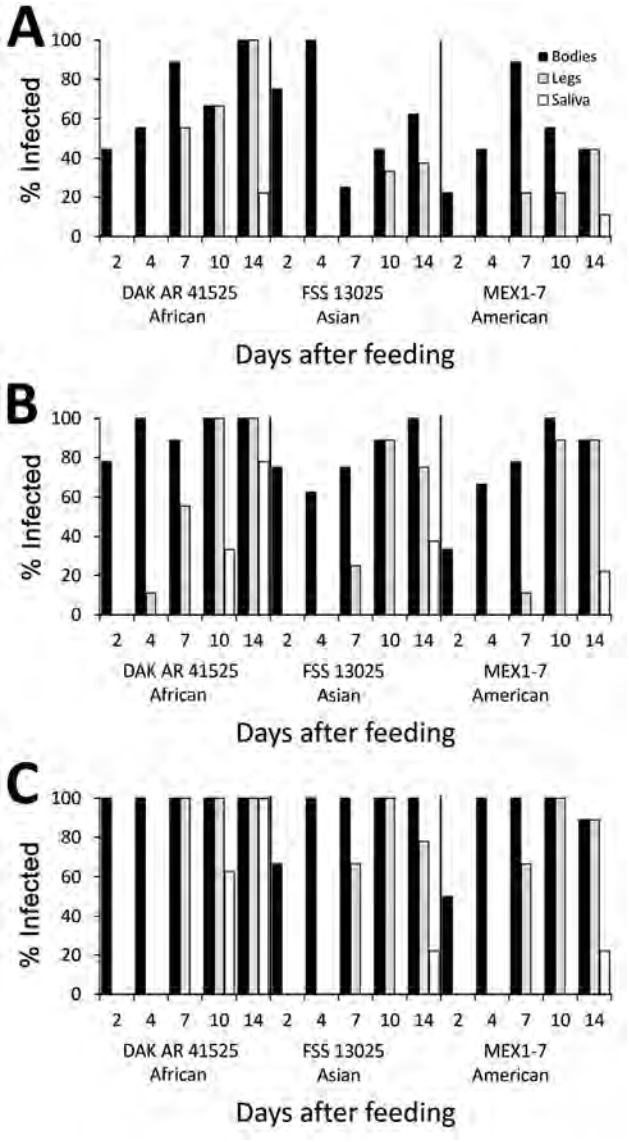

Figure 2. Infection, dissemination, and transmission of 3 Zika virus strains by *Aedes aegypti* mosquitoes from the Dominican Republic after artificial blood meals with a concentration of 4 $\log_{10}$ (A), 5 $\log_{10}$ (B), or 6 $\log_{10}$ (C) focus-forming units/mL.

transmission among *Ae. aegypti* mosquito populations from 3 different parts of the Americas. After artificial blood meals, strains FSS 13025 and MEX1–7 were refractory to transmission in all populations; we detected only 1 positive saliva sample after large oral doses. In contrast, mosquitoes from the DR were susceptible to and able to transmit all 3 Zika virus strains. A similar difference in DENV competency has been noted in comparisons of *Ae. aegypti* mosquito populations from different geographic locations (*20*). This variation could be due to genetic differences among mosquitoes or differences in microbiome, virome, or immune activation. Understanding differences in competency and underlying mechanisms could help guide new strategies to control this vector.

In addition to differences in competency among *Ae. aegypti* mosquito populations, we showed a significant difference in infectivity among Zika virus strains. DAK AR 41525 was the only strain capable of disseminating and being transmitted by all mosquito strains. Furthermore, in mosquitoes from the DR, which were susceptible to all 3 Zika virus strains, DAK AR 41525 disseminated the most rapidly and resulted in the greatest proportion of infectious saliva. This finding is surprising given that African Zika virus strains have never been associated with outbreaks involving *Ae. aegypti* mosquitoes.

Another contribution of our findings is the higher infectivity from murine blood meals than from artificial meals. Artificial blood meals are known to be less infectious than natural meals, at least in part because of the lack of coagulation and concentration of the virus adjacent to the mid-gut epithelium (*28*,*29*). Also, in the case of DENV and St. Louis encephalitis virus, frozen stocks are less infectious for *Ae. aegypti* mosquitoes than freshly harvested, cell culture–derived virus (*30*). The FSS 13025 strain of Zika virus infected only 75% of Salvador *Ae. aegypti* mosquitoes at 6 $\log_{10}$ FFU/mL by 14 dpi from an artificial blood meal, with 67% of these infections disseminating, and 0% involving the saliva. In contrast, 14 dpi after feeding on an infected mouse with a 6 $\log_{10}$ FFU/mL viremia, 100% infection occurred; 92% of these were disseminated, and 61% of disseminated infections reached the saliva. With titers as low as 4 $\log_{10}$ FFU/mL in murine blood meals, 40% of mosquitoes became infected, of which 100% were disseminated and had Zika virus detected in saliva. This dramatic difference in competency after artificial versus viremic blood meals undoubtedly contributed to the underestimation of *Ae. aegypti* mosquitoes as a Zika virus vector in previous studies (*15*,*25*).

An important determinant of vector capacity is the EIP, that is, the time before a virus can be found in the saliva of a mosquito after an infectious blood meal. The EIP for DENV varies depending on temperature and other factors, with an average of 6.5 days at 30°C and 15 days at 25°C (*31*). The EIP for CHIKV is as short as 2 days (*32*). A short EIP facilitates rapid spread, whereas a long EIP gives a larger window for mosquito death, including by human intervention. The 7-day minimum EIP we estimated after a murine blood meal, and 7–10 days after an artificial blood meal, are comparable to those of other flaviviruses in mosquitoes incubated at similar temperatures.

Another major factor in vector transmission is the amount of virus inoculated in the saliva, which can affect pathogenesis (*21*); this value is critical for determining realistic animal model doses. We found saliva titers of up to 4 $\log_{10}$ FFU per collection, with the following mean ±SD $\log_{10}$

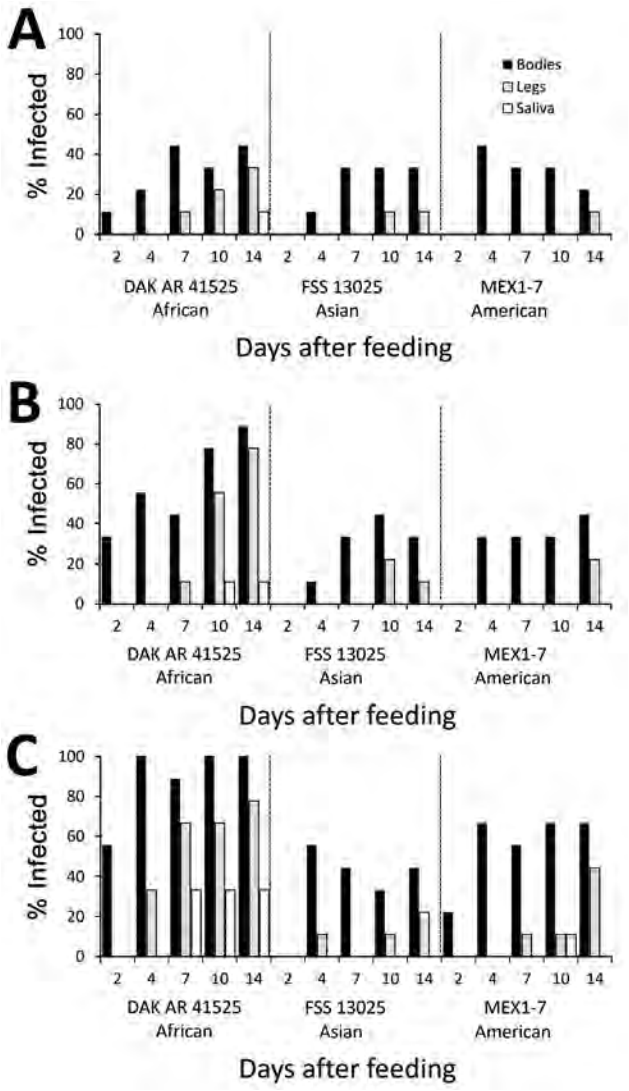

Figure 3. Infection, dissemination, and transmission of 3 Zika virus strains by *Aedes aegypti* mosquitoes from the Rio Grande Valley, Texas, USA, after artificial blood meals with a concentration of 4 $\log_{10}$ (A), 5 $\log_{10}$ (B), or 6 $\log_{10}$ (C) focus-forming units/mL.

FFU/collection for each mosquito–virus strain combination: Salvador mosquitoes, DAK AR 41525: 2.49 ±2.93; DR mosquitoes, DAK AR 41525: 2.72 ±3.26; DR mosquitoes, MEX1–7: 2.30 ±2.35; RGV mosquitoes, DAK AR: 2.20 ±1.96; Salvador mosquitoes, FSS 13025 infected through a murine blood meal: 2.77 ±3.00. Because of the dearth of positive saliva samples, no statistically significant differences were found for these means. These infectious saliva titers are based only on a small number of positive samples after artificial blood meals. Some studies have found that in vitro salivation overestimates the amount of an arbovirus inoculated in vivo (*33*); others have found the inverse (*34*). Additional studies are needed to precisely determine the amount of virus transmitted by a Zika virus–infected *Ae. aegypti* mosquito.

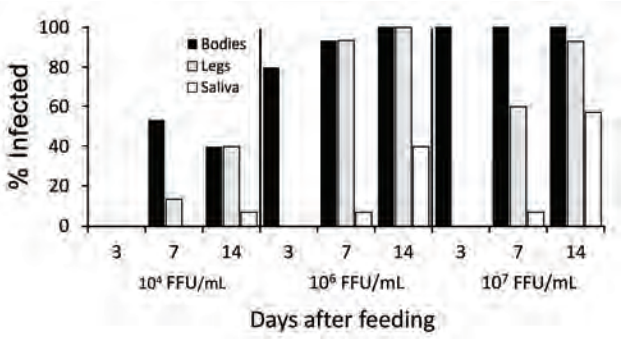

Figure 4. Infection, dissemination, and transmission of the Zika virus strain FSS 13025 by *Aedes aegypti* mosquitoes from Salvador, Brazil, after blood meals from infected A129 mice with viremic titers of 4 $\log_{10}$, 6 $\log_{10}$, or 7 $\log_{10}$ focus-forming units/mL.

Ideally, in investigations of viral adaption to vectors, virus and mosquito origins should be matched. The mosquitoes to match the locations of the Zika virus strains reported here were unavailable. However, vector-adaptive mutations in arboviruses are unlikely to remain geographically isolated because they spread more efficiently (*35*,*36*). Therefore, adaptive evolution was investigated on the basis of available mosquitoes with minimal colonization histories, from sites at risk for Zika virus transmission or with reported autochthonous transmission. Surprisingly, despite the use of minimally colonized mosquitoes, most susceptible population of *Ae. aegypti* from the DR had the longest history of 6 generations. Previous studies demonstrated altered DENV-2 susceptibility for *Ae. aegypti* colonized for ≥4 generations (*37*).

Although human Zika virus viremia is not well characterized, a Micronesia study found viral RNA concentrations of 900–729,000 RNA copies/mL (*38*). Recent case studies have estimated ranges of 1.47–2 $\log_{10}$ PFU/mL (*39*), 0.49–3.39 $\log_{10}$ FFU/mL (*14*), 2.20–2.75 $\log_{10}$ PFU/mL, and 1.88–2.80 $\log_{10}$ PFU/mL (*40*). This wide range might reflect the sampling of most patients after peak viremia has passed, which complicates selecting realistic doses for mosquito competency studies.

Acknowledgment

We thank L. Philip Lounibos for help with *Ae. aegypti* collections in the DR.

This work was supported by a pilot grant from the Institute for Human Infections and Immunity, grants R24AI120942 and 1U01AI115577 from the National Institutes of Health, as well as by National Institutes of Health grant 1R15AI113628-01 (to K.A.H.), Brazilian national Council of Technological and Scientific Development grants 440891/2016-7 and 370 400830/2013-2 (GSR), and Brazilian Coordination for the Improvement of Higher Education grant 440891/2016-7 (GSR). The funders had no role in study design, data collection and

analysis, decision to publish, or preparation of the manuscript. The authors have no conflicting financial interests.

Mr. Roundy is a PhD student at the University of Texas Medical Branch at Galveston. His research focuses on emerging arboviruses and the species that transmit them, including factors that affect their spread.

References

1. Hayes EB. Zika virus outside Africa. Emerg Infect Dis. 2009;15:1347–50. http://dx.doi.org/10.3201/eid1509.090442
2. Cao-Lormeau V-M, Blake A, Mons S, Lastère S, Roche C, Vanhomwegen J, et al. Guillain-Barré syndrome outbreak associated with Zika virus infection in French Polynesia: a case–control study. Lancet. 2016;387:1531–9. http://dx.doi.org/10.1016/S0140-6736(16)00562-6
3. Zanluca C, Melo VC, Mosimann ALP, Santos GI, Santos CN, Luz K. First report of autochthonous transmission of Zika virus in Brazil. Mem Inst Oswaldo Cruz. 2015;110:569–72. http://dx.doi.org/10.1590/0074-02760150192
4. Centers for Disease Control and Prevention. All countries & territories with active Zika virus transmission [cited 2016 Aug 11]. http://www.cdc.gov/zika/geo/active-countries.html
5. World Health Organization. WHO statement on the first meeting of the International Health Regulations (2005) (IHR 2005) Emergency Committee on Zika virus and observed increase in neurological disorders and neonatal malformations [cited 2016 Aug 11]. http://www.who.int/mediacentre/news/statements/2016/1st-emergency-committee-zika/en/
6. de Paula Freitas B, de Oliveira Dias JR, Prazeres J, Sacramento GA, Ko AI, Maia M, et al. Ocular findings in infants with microcephaly associated with presumed Zika virus congenital infection in Salvador, Brazil. JAMA Ophthalmol. 2016;134:529–35. http://dx.doi.org/10.1001/jamaophthalmol.2016.0267
7. Carteaux G, Maquart M, Bedet A, Contou D, Brugières P, Fourati S, et al. Zika virus associated with meningoencephalitis. N Engl J Med. 2016;374:1595–6. http://dx.doi.org/10.1056/NEJMc1602964
8. Mécharles S, Herrmann C, Poullain P, Tran T-H, Deschamps N, Mathon G, et al. Acute myelitis due to Zika virus infection. Lancet. 2016;387:1481. http://dx.doi.org/10.1016/S0140-6736(16)00644-9
9. Haddow AD, Schuh AJ, Yasuda CY, Kasper MR, Heang V, Huy R, et al. Genetic characterization of Zika virus strains: geographic expansion of the Asian lineage. PLoS Negl Trop Dis. 2012;6:e1477. http://dx.doi.org/10.1371/journal.pntd.0001477
10. Faria NR, da Silva Azevedo RdS, Kraemer MUG, Souza R, Cunha MS, Hill SC, et al. Zika virus in the Americas: early epidemiological and genetic findings. Science. 2016;352:345–9. http://dx.doi.org/10.1126/science.aaf5036
11. Barrows NJ, Campos RK, Soto-Acosta R, Lerner G, Prasanth KR, Powell S, et al. Repurposed drug candidates to treat ZIKV infection in pregnancy. Cell Host Microbe. 2016;20:1–12.
12. Berthet N, Nakouné E, Kamgang B, Selekon B, Descorps-Declère S, Gessain A, et al. Molecular characterization of three Zika flaviviruses obtained from sylvatic mosquitoes in the Central African Republic. Vector Borne Zoonotic Dis. 2014;14:862–5. http://dx.doi.org/10.1089/vbz.2014.1607
13. Ayres CFJ. Identification of Zika virus vectors and implications for control. Lancet Infect Dis. 2016;16:278–9. http://dx.doi.org/10.1016/S1473-3099(16)00073-6
14. Guerbois M, Fernandez-Salas I, Azar SR, Danis-Lozano R, Alpuche-Aranda CM, Leal G, et al. Outbreak of Zika virus infection, Chiapas state, Mexico, 2015, and first confirmed transmission by *Aedes aegypti* mosquitoes in the Americas. J Infect Dis. 2016;214:1349–56. http://dx.doi.org/10.1093/infdis/jiw302
15. Chouin-Carneiro T, Vega-Rua A, Vazeille M, Yebakima A, Girod R, Goindin D, et al. Differential susceptibilities of *Aedes aegypti* and *Aedes albopictus* from the Americas to Zika virus. PLoS Negl Trop Dis. 2016;10:e0004543.
16. Wong PS, Li MZ, Chong CS, Ng LC, Tan CH. *Aedes* (*Stegomyia*) *albopictus* (*Skuse*): a potential vector of Zika virus in Singapore. PLoS Negl Trop Dis. 2013;7:e2348. http://dx.doi.org/10.1371/journal.pntd.0002348
17. Grard G, Caron M, Mombo IM, Nkoghe D, Mboui Ondo S, Jiolle D, et al. Zika virus in Gabon (Central Africa)—2007: a new threat from *Aedes albopictus*? PLoS Negl Trop Dis. 2014;8:e2681.
18. Weaver SC, Costa F, Garcia-Blanco MA, Ko AI, Ribeiro GS, Saade G, et al. Zika virus: history, emergence, biology, and prospects for control. Antiviral Res. 2016;130:69–80. http://dx.doi.org/10.1016/j.antiviral.2016.03.010
19. Tsetsarkin KA, Chen R, Yun R, Rossi SL, Plante KS, Guerbois M, et al. Multi-peaked adaptive landscape for chikungunya virus evolution predicts continued fitness optimization in *Aedes albopictus* mosquitoes. Nat Commun. 2014;5:4084. http://dx.doi.org/10.1038/ncomms5084
20. Gonçalves CM, Melo FF, Bezerra JM, Chaves BA, Silva BM, Silva LD, et al. Distinct variation in vector competence among nine field populations of *Aedes aegypti* from a Brazilian dengue-endemic risk city. Parasit Vectors. 2014;7:320. http://dx.doi.org/10.1186/1756-3305-7-320
21. Althouse BM, Hanley KA. The tortoise or the hare? Impacts of within-host dynamics on transmission success of arthropod-borne viruses. Philos Trans R Soc Lond B Biol Sci. 2015;370:pii:20140299.
22. Rossi SL, Tesh RB, Azar SR, Muruato AE, Hanley KA, Auguste AJ, et al. Characterization of a novel murine model to study Zika virus. Am J Trop Med Hyg. 2016;94:1362–9. http://dx.doi.org/10.4269/ajtmh.16-0111
23. Williams M, Mayer SV, Johnson WL, Chen R, Volkova E, Vilcarromero S, et al. Lineage II of Southeast Asian/American DENV-2 is associated with a severe dengue outbreak in the Peruvian Amazon. Am J Trop Med Hyg. 2014;91:611–20. http://dx.doi.org/10.4269/ajtmh.13-0600
24. Aliota MT, Walker EC, Uribe Yepes A, Velez ID, Christensen BM, Osorio JE. The wMel strain of *Wolbachia* reduces transmission of chikungunya virus in *Aedes aegypti*. PLoS Negl Trop Dis. 2016;10:e0004677. http://dx.doi.org/10.1371/journal.pntd.0004677
25. Li MI, Wong PSJ, Ng LC, Tan CH. Oral susceptibility of Singapore *Aedes* (*Stegomyia*) *aegypti* (*Linnaeus*) to Zika virus. PLoS Negl Trop Dis. 2012;6:e1792. http://dx.doi.org/10.1371/journal.pntd.0001792
26. Dejnirattisai W, Supasa P, Wongwiwat W, Rouvinski A, Barba-Spaeth G, Duangchinda T, et al. Dengue virus sero-cross-reactivity drives antibody-dependent enhancement of infection with Zika virus. Nat Immunol. 2016;17:1102–8. http://dx.doi.org/10.1038/ni.3515
27. Swanstrom JA, Plante JA, Plante KS, Young EF, McGowan E, Gallichotte EN, et al. Dengue virus envelope dimer epitope monoclonal antibodies isolated from dengue patients are protective against Zika virus. MBio. 2016;7:e01123–16. http://dx.doi.org/10.1128/mBio.01123-16
28. Kramer LD, Hardy JL, Houk EJ, Presser SB. Characterization of the mesenteronal infection with western equine encephalomyelitis virus in an incompetent strain of *Culex tarsalis*. Am J Trop Med Hyg. 1989;41:241–50.
29. Weaver SC, Lorenz LH, Scott TW. Distribution of western equine encephalomyelitis virus in the alimentary tract of *Culex tarsalis* (Diptera: Culicidae) following natural and artificial blood meals. J Med Entomol. 1993;30:391–7. http://dx.doi.org/10.1093/jmedent/30.2.391

30. Richards SL, Pesko K, Alto BW, Mores CN. Reduced infection in mosquitoes exposed to blood meals containing previously frozen flaviviruses. Virus Res. 2007;129:224–7. http://dx.doi.org/10.1016/j.virusres.2007.06.019
31. Rohani A, Wong YC, Zamre I, Lee HL, Zurainee MN. The effect of extrinsic incubation temperature on development of dengue serotype 2 and 4 viruses in *Aedes aegypti* (L.). Southeast Asian J Trop Med Public Health. 2009;40:942–50.
32. Dubrulle M, Mousson L, Moutailler S, Vazeille M, Failloux AB. Chikungunya virus and *Aedes* mosquitoes: saliva is infectious as soon as two days after oral infection. PLoS One. 2009;4:e5895. http://dx.doi.org/10.1371/journal.pone.0005895
33. Smith DR, Aguilar PV, Coffey LL, Gromowski GD, Wang E, Weaver SC. Venezuelan equine encephalitis virus transmission and effect on pathogenesis. Emerg Infect Dis. 2006;12:1190–6. http://dx.doi.org/10.3201/eid1708.050841
34. Styer LM, Kent KA, Albright RG, Bennett CJ, Kramer LD, Bernard KA. Mosquitoes inoculate high doses of West Nile virus as they probe and feed on live hosts. PLoS Pathog. 2007;3:1262–70.
35. Ciota AT, Lovelace AO, Jia Y, Davis LJ, Young DS, Kramer LD. Characterization of mosquito-adapted West Nile virus. J Gen Virol. 2008;89:1633–42. http://dx.doi.org/10.1099/vir.0.2008/000893-0
36. Tsetsarkin KA, Weaver SC. Sequential adaptive mutations enhance efficient vector switching by chikungunya virus and its epidemic emergence. PLoS Pathog. 2011;7:e1002412. http://dx.doi.org/10.1371/journal.ppat.1002412
37. Armstrong PM, Rico-Hesse R. Differential susceptibility of *Aedes aegypti* to infection by the American and Southeast Asian genotypes of dengue type 2 virus. Vector Borne Zoonotic Dis. 2001;1:159–68. http://dx.doi.org/10.1089/153036601316977769
38. Lanciotti RS, Kosoy OL, Laven JJ, Velez JO, Lambert AJ, Johnson AJ, et al. Genetic and serologic properties of Zika virus associated with an epidemic, Yap State, Micronesia, 2007. Emerg Infect Dis. 2008;14:1232–9.
39. Barzon L, Pacenti M, Berto A, Sinigaglia A, Franchin E, Lavezzo E, et al. Isolation of infectious Zika virus from saliva and prolonged viral RNA shedding in a traveller returning from the Dominican Republic to Italy, January 2016. Euro Surveill. 2016;21:1–5.
40. Fourcade C, Mansuy JM, Dutertre M, Delpech M, Marchou B, Delobel P, et al. Viral load kinetics of Zika virus in plasma, urine and saliva in a couple returning from Martinique, French West Indies. J Clin Virol. 2016;82:1–4. http://dx.doi.org/10.1016/j.jcv.2016.06.011

Address for correspondence: Scott C. Weaver or Nikos Vasilakis, University of Texas Medical Branch—Pathology, 301 University Blvd, Galveston, TX 77555-0609, USA; email: sweaver@utmb.edu or nivasila@utmb.edu

Outbreaks among Wild Birds and Domestic Poultry Caused by Reassorted Influenza A(H5N8) Clade 2.3.4.4 Viruses, Germany, 2016

Anne Pohlmann, Elke Starick, Timm Harder, Christian Grund, Dirk Höper, Anja Globig, Christoph Staubach, Klaas Dietze, Günter Strebelow, Reiner G. Ulrich, Jan Schinköthe, Jens P. Teifke, Franz J. Conraths, Thomas C. Mettenleiter, Martin Beer

In November 2016, an influenza A(H5N8) outbreak caused deaths of wild birds and domestic poultry in Germany. Clade 2.3.4.4 virus was closely related to viruses detected at the Russia–Mongolia border in 2016 but had new polymerase acidic and nucleoprotein segments. These new strains may be more efficiently transmitted to and shed by birds.

During 2014–2015, after massive outbreaks of highly pathogenic avian influenza (HPAI) on the Korean Peninsula, subtype H5N8 viruses (group A clade 2.3.4.4) caused outbreaks among wild birds and domestic poultry in central Asia, Russia, and central Europe (*1*,*2*). Strains of this clade, and novel reassortants thereof, were transferred to North America (*3*). Transcontinental spread of these strains and an earlier HPAI virus (HPAIV) of the goose/Guangdong lineage of subtype H5N1 has been linked to dissemination by migratory wild birds (*4*). We describe a novel reassortant of HPAIV A(H5N8) within group B clade 2.3.4.4, which causes lethal infections in hundreds of wild birds and domestic poultry in Germany and elsewhere in Europe.

The Study

In late May 2016, a group B clade 2.3.4.4 H5N8 virus was detected in dead and hunted wild birds at Lake Uvs-Nuur, at the Russia–Mongolia border (*5*). On November 7, 2016, many dead tufted ducks (*Aythya fuligula*) were found at Lake Plön in Schleswig-Holstein, northern Germany, and at Lake Constance in Baden-Württemberg, southern Germany (Figure 1); most were positive for H5N8. The epidemic among wild birds continued and spread toward the center of the country (Figure 1). As of December 2016, several backyard holdings, 4 zoos, and a few large commercial operations were also affected. Direct or indirect contact with wild birds was the most likely route of virus introduction into the backyard holdings and zoos. Despite the generally high standards of commercial operations, possible biosecurity gaps were identified.

Most affected birds were found dead or exhibited severe clinical signs such as apathy or sudden deaths (in some parts of the affected chicken breeder farms, up to 90% died before culling). Macroscopic changes commonly observed in tufted ducks and poultry included severe diffuse hepatic necrosis, multifocal petechiae, and variably hyperemic and edematous lungs. Light microscopy confirmed influenza A virus nucleoprotein (NP) antigen and variably distinct necrotizing lesions in liver, heart, lungs, brain, pancreas, spleen, and thymus (online Technical Appendix Figure 1, https://wwwnc.cdc.gov/EID/article/23/4/16-1949-Techapp1.pdf). Some chickens also displayed severe diffuse catarrhal enterocolitis; influenza A virus NP antigen was present in the intestinal epithelium.

The spectrum of affected species of wild birds is broad and includes mainly diving ducks but also swans, grebes, gulls, buzzards, crows, and a white-tailed eagle (Table 1). As of November 30, 2016, ≈400 infected wild birds were detected in 13 federal states of Germany. H5N8 infections were also reported from Austria, Croatia, Denmark, Finland, France, Hungary, Poland, Romania, Sweden, Switzerland, and the Netherlands, indicating that the same subtype caused the recent outbreaks throughout Europe.

The high pathogenicity for gallinaceous poultry was confirmed; intravenous pathogenicity index for 1 isolate (A/tufted duck/Germany-SH/AR8444/2016) was 2.93, comparable to the 2.81 index for H5N8 circulating in 2014 (A/turkey/Germany-MV/AR2472/2014). However, deaths of wild birds of a variety of species, in particular diving ducks, and extended pathologic changes in dead wild birds suggested a marked shift of pathogenicity from the viruses in Germany in 2014 (*1*).

For genetic characterization, we analyzed virus sequences from several swab samples and the first 2 virus isolates from dead tufted ducks from Lake Plön and Lake Constance and compared them with sequences from H5N8-positive turkeys and chickens. We found few genetic differences between the analyzed strains from northern and southern Germany and only slight differences between sequences generated from wild bird or poultry samples. This finding clearly contrasts with those of the H5N1 clade

Author affiliation: Friedrich-Loeffler-Institut, Greifswald-Insel Riems, Germany

DOI: http://dx.doi.org/10.3201/eid2304.161949

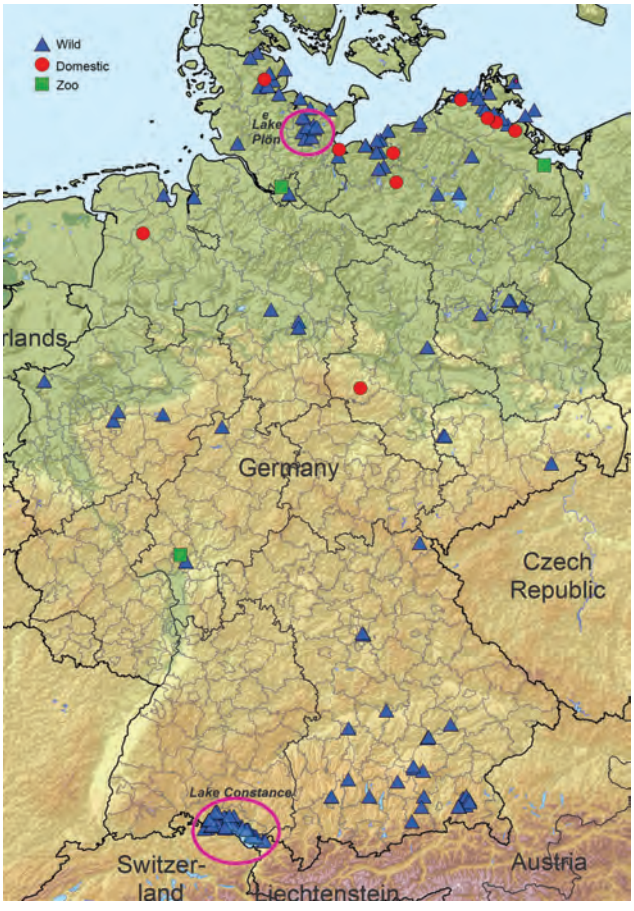

Figure 1. Highly pathogenic avian influenza A(H5N8) cases in wild birds and outbreaks in poultry holdings (10 backyard holdings, 4 zoos or pet farms, and a few commercial operations) in Germany, November 2016. Circles indicate original locations of outbreaks and isolates.

Table 1. Species of birds affected by highly pathogenic avian influenza virus A(H5N8), Germany, 2016

Group	Common name (taxonomic name)
Diving ducks	Tufted duck (*Aythya fuligula*)
	Common pochard (*Aythya ferina*)
	Common goldeneye (*Bucephala clangula*)
	Red-crested pochard (*Netta Rufina*)
	Greater scaup (*Aythya marila*)
	Common eider (*Somateria mollissima*)
	Common scoter (*Melanitta nigra*)
Dabbling ducks	Mallard (*Anas platyrhynchos*)
	Northern pintail (*Anas acuta*)
Diving birds	Great crested grebe (*Podiceps cristatus*)
	Little grebe (*Tachybaptus ruficollis*)
Mergansers	Common merganser (*Mergus merganserI*)
Geese	Greylag goose (*Anser anser*)
	Bean goose (*Anser fabalisI)*
	Canada goose (*Branta Canadensis*)
	White-fronted goose (*Anser albifrons*)
	Pink-footed goose (*Anser brachyrhynchus*)
Swans	Mute swan (*Cygnus olorI*)
	Black swan (*Cygnus atratus*)
	Whooper swan (*Cygnus cygnus*)
Gulls	Black-headed gull (*Chroicocephalus ridibundus*)
	European herring gull (*Larus argentatus*)
	Great black-backed gull (*Larus marinus*)
	Mew gull (*Larus canus*)
Rails	Common coot (*Fulica atra*)
Herons	Gray heron (*Ardea cinerea*)
Birds of prey	Common buzzard (*Buteo buteo*)
	Rough-legged buzzard (*Buteo lagopus*)
	White-tailed eagle (*Haliaeetus albicilla*)
Cormorants	Great cormorant (*Phalacrocorax carbo*)
Crows	Carrion crow (*Corvus corone*)
Domestic birds	Domestic duck (*Anas platyrhynchos domesticus*)
	Domestic chicken (*Gallus gallus domesticus*)
	Turkey (*Meleagris gallopavo*)
Zoo birds	Emu (*Dromaius novaehollandiae*)
	Great white pelican (*Pelecanus onocrotalus*)

2.2 outbreaks in Germany in 2006, which showed similar distribution (*6*) but 2 distinct H5N1 northern and southern subclusters and a difference in timing during the first transcontinental wave; virus was found in Europe in October 2005 but not in Germany until early 2006.

All genome segments of the novel H5N8 clade 2.3.4.4 group B strains from Germany in 2016 differed significantly from the H5N8 clade 2.3.4.4 group A strains detected in 2014–2015 in Germany and other European countries (*1*). This finding is in accord with results of studies suggesting that there was no continued circulation of group A–like viruses among wild birds in the Netherlands from mid-November 2014 to January 2016 (*7*). Database searches identified H5N8 clade 2.3.4.4 viruses (first detected in wild birds at the Russia–Mongolia border at the end of May 2016) as closest relatives. Extended searches confirmed that the isolates from Germany in 2016 described in this study are novel reassortants, which can be clearly distinguished from the isolates from Russia–Mongolia in 2016 (e.g., A/great crested grebe/Uvs-Nuur Lake/341/2016) by 2 segments (Table 2; online Technical Appendix Figure 2). Six segments (polymerase basic [PB] 2, PB1, hemagglutinin, neuraminidase, matrix protein, nonstructural protein [NS]) were highly similar to those of clade 2.3.4.4 viruses from Russia in 2016 (99% for each surface protein; Table 2). The NS1 protein of the new 2016 isolate from Germany is truncated (217 aa) compared with the Russia–Mongolia viruses (230 aa), a truncation also found in other influenza virus strains. However, the nuclear export protein is not affected. Of note, the Russia–Mongolia virus proved to be a novel reassortant from earlier H5N8 clade 2.3.4.4 viruses within group B (Table 2; Figure 2) (*5*). These new H5N8 viruses are central Asia reassortants, which originated from strains circulating in eastern Asia. Genes of 3 segments (hemagglutinin, neuraminidase, and NS protein) cluster with segments of H5N8 clade 2.3.4.4 group B viruses identified in eastern China; the other 5 genes (PB1, PB2, polymerase acidic [PA], nucleoprotein [NP], and matrix protein) cluster with avian

Table 2. Genetic composition of influenza virus A/tufted duck/SH-Germany/R8444/2016 isolated in Germany, 2016*

Genome segment, virus strain	Identity, %	Group
PB2		
A/wild duck/Poland/82A/2016 (H5N8)	99	Russia–Mongolia 2.3.4.4
A/duck/Mongolia/30/2015 (H3N8)	97	2016 reassortant
A/duck/Mongolia/118/2015 (H4N6)	97	
A/great crested grebe/Uvs-Nuur Lake/341/2016 (H5N8)	97	
PB1		
A/wild duck/Poland/82A/2016 (H5N8)	99	Russia–Mongolia 2.3.4.4
A/great crested grebe/Uvs-Nuur Lake/341/2016 (H5N8)	99	2016 reassortant
A/duck/Mongolia/179/2015 (H3N8)	97	
A/duck/Mongolia/518/2015 (H10N3)	97	
PA		
A/wild duck/Poland/82A/2016 (H5N8)	100	Central Europe 2.3.4.4
A/mallard/Republic of Georgia/13/2011 (H6N2)	97	2016 reassortant
A/duck/Mongolia/179/2015 (H3N8)	97	
A/duck/Hokkaido/W9/2015 (H1N1)	97	
A/greylag goose/Iceland/0921/2011 (H6N8)	97	
HA		
A/wild duck/Poland/82A/2016 (H5N8)	99	Russia–Mongolia 2.3.4.4
A/tufted duck/Denmark/17740–1/2016 (H5N8)	99	2016 reassortant
A/mute swan/Croatia/70/2016 (H5N8)	99	
A/great crested grebe/Uvs-Nuur Lake/341/2016 (H5N8)	99	
A/duck/Eastern China/S1109/2014 (H5N8)	98	
NP		
A/wild duck/Poland/82A/2016	99	Central Europe 2.3.4.4
A/mallard/Republic of Georgia/13/2011 (H6N2)	98	2016 reassortant
A/chicken/Netherlands/16007311–037041/2016 (H7N9)	97	
A/chicken/France/150169a/2015 (H5N1)	97	
A/greylag goose/Iceland/0921/2011 (H6N8)	97	
NA		
A/wild duck/Poland/82A/2016 (H5N8)	99	Russia–Mongolia 2.3.4.4
A/great crested grebe/Uvs-Nuur Lake/341/2016 (H5N8)	99	2016 reassortant
A/mute swan/Croatia/70/2016 (H5N8)	99	
A/duck/Eastern China/S1109/2014 (H5N8)	98	
MP		
A/wild duck/Poland/82A/2016 (H5N8)	99	Russia–Mongolia 2.3.4.4
A/great crested grebe/Uvs-Nuur Lake/341/2016 (H5N8)	99	2016 reassortant
A/mute swan/Croatia/70/2016 (H5N8)	99	
A/duck/Mongolia/179/2015 (H3N8)	98	
NS		
A/wild duck/Poland/82A/2016 (H5N8)	99	Russia–Mongolia 2.3.4.4
A/great crested grebe/Uvs-Nuur Lake/341/2016 (H5N8)	99	2016 reassortant
A/mute swan/Croatia/70/2016 (H5N8)	99	
A/duck/Eastern China/S1109/2014 (H5N8)	99	

* Sequences were compared with entries in the GISAID (http://platform.gisaid.org) database. Details and acknowledgments in online Technical Appendix (https://wwwnc.cdc.gov/EID/article/23/4/16-1949-Techapp1.pdf). HA, hemagglutinin; MP, matrix protein; NA, neuraminidase; NS, nonstructural protein; NP, nucleoprotein; PA, polymerase acidic protein; PB, polymerase basic protein.

influenza viruses of low pathogenicity, which were identified in Mongolia, China, and Vietnam (5).

The viruses from Germany (2016) further evolved from the strains from Russia and harbor 2 new segments (PA, NP). The virus sequences are essentially identical to sequences from an H5N8 virus isolate found November 2016 in a dead wild duck in Poland near the Germany border (Table 2) but differ significantly from sequences of other currently circulating isolates (online Technical Appendix Figure 2). The new PA sequences cluster with sequences of viruses detected in eastern and central Asia. The NP segment sequences are similar to those of viruses frequently found in central and northwestern Europe. The PA and NP segments in question occurred concurrently in different avian influenza viruses before; namely, in H6N8 strains from Iceland in 2011 (e.g., A/greylag goose/Iceland/0921/2011) and in an H6N2 isolate from Georgia in 2011 (A/mallard/Republic of Georgia/13/2011) (Table 2; online Technical Appendix Figure 2). It is reasonable to suggest that the novel reassortant strain from Germany was generated by ≥1 reassortment event that occurred during June–November 2016 between central Asia (Mongolia) and central Europe (Poland/Germany).

Conclusions

A new reassortant influenza A(H5N8) virus is responsible for the recent HPAIV outbreak in Germany. The observed differences in pathogenicity for a broad spectrum of waterfowl compared with that of H5N8 viruses from 2014–2015

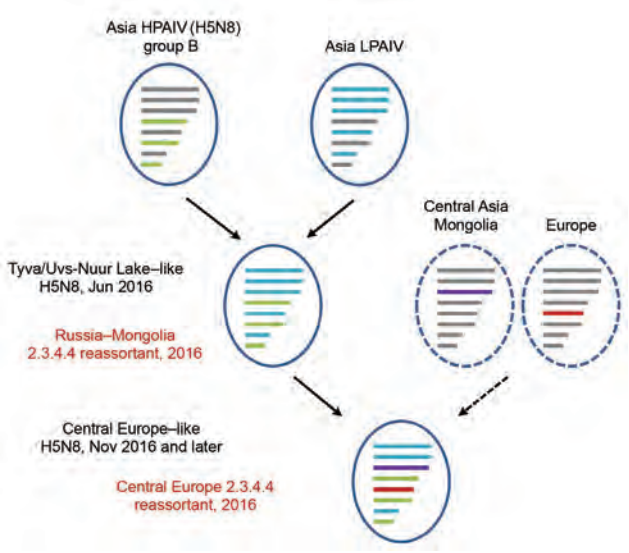

Figure 2. Proposed reassortment events leading to the novel central Europe HPAIV A(H5N8) clade 2.3.4.4 virus. The Russia–Mongolia reassortant clade 2.3.4.4 H5N8 virus acquired 2 new segments (polymerase acidic protein and nucleoprotein), leading to the novel central Europe clade 2.3.4.4 H5N8 in 2016. Similar segment origins are marked by similar colors. Dashed lines indicate putative precursors. HPAIV, highly pathogenic avian influenza virus; LPAIV, low pathogenicity avian influenza virus.

correlate with a new genome composition of these viruses. The novel NP and PA segments in the 2016 H5N8 viruses from Germany are candidates for future studies of the molecular basis of the biological differences. These new strains may be more efficiently transmitted by and shed to other wild and domestic birds, a hypothesis in line with the large number of cases among wild birds in November 2016. There is yet no indication that mammals (including humans) are infected by these novel strains. Future studies in mammalian models (e.g., ferrets, mice) will provide experimental data on the virulence for mammals.

Acknowledgments

We gratefully acknowledge professional support from local veterinarians, diagnosticians in regional laboratories in Neumünster (Schleswig-Holstein), Rostock (Mecklenburg-Western Pomerania), Aulendorf and Freiburg (Baden-Wuerttemberg), and technical assistance by Diana Wessler, Aline Maksimov, Nicole Reimer, Kathrin Steffen, Patrick Zitzow, Bianka Hillmann, Jörn Gethmann, the Tierseuchennachrichtensystem (national animal disease notification system) team, and Cornelia Illing.

This work was financed in part by COMPARE, under the European Union Horizon 2020 program (grant agreement no. 643476.)

Dr. Pohlmann is a microbiologist and senior scientist working at the Institute of Diagnostic Virology, Friedrich-Loeffler-Institut, Insel Riems, Germany. Her research interests are focused on influenza viruses, sequence analysis, phylogeny, and next-generation sequencing.

References

1. Harder T, Maurer-Stroh S, Pohlmann A, Starick E, Höreth-Böntgen D, Albrecht K, et al. Influenza A(H5N8) virus similar to strain in Korea causing highly pathogenic avian influenza in Germany. Emerg Infect Dis. 2015;21:860–3. http://dx.doi.org/10.3201/eid2105.141897
2. Verhagen JH, van der Jeugd HP, Nolet BA, Slaterus R, Kharitonov SP, de Vries PP, et al. Wild bird surveillance around outbreaks of highly pathogenic avian influenza A(H5N8) virus in the Netherlands, 2014, within the context of global flyways. Euro Surveill. 2015;20:21069. http://dx.doi.org/10.2807/1560-7917.ES2015.20.12.21069
3. Lee DH, Torchetti MK, Winker K, Ip HS, Song CS, Swayne DE. Intercontinental spread of Asian-origin H5N8 to North America through Beringia by migratory birds. J Virol. 2015;89:6521–4. http://dx.doi.org/10.1128/JVI.00728-15
4. Global Consortium for H5N8 and Related Influenza Viruses. Role for migratory wild birds in the global spread of avian influenza H5N8. Science. 2016;354:213–7. http://dx.doi.org/10.1126/science.aaf8852
5. Lee DH, Sharshov K, Swayne DE, Kurskaya O, Sobolev I, Kabilov M, et al. Novel reassortant clade 2.3.4.4 avian influenza A(H5N8) virus in wild aquatic birds, Russia, 2016. Emerg Infect Dis. 2017;23. http://dx.doi.org/10.3201/eid2302.161252
6. Starick E, Beer M, Hoffmann B, Staubach C, Werner O, Globig A, et al. Phylogenetic analyses of highly pathogenic avian influenza virus isolates from Germany in 2006 and 2007 suggest at least three separate introductions of H5N1 virus. Vet Microbiol. 2008;128:243–52. http://dx.doi.org/10.1016/j.vetmic.2007.10.012
7. Poen MJ, Verhagen JH, Manvell RJ, Brown I, Bestebroer TM, van der Vliet S, et al. Lack of virological and serological evidence for continued circulation of highly pathogenic avian influenza H5N8 virus in wild birds in the Netherlands, 14 November 2014 to 31 January 2016. Euro Surveill. 2016;21:30349. http://dx.doi.org/10.2807/1560-7917.ES.2016.21.38.30349

Address for correspondence: Martin Beer, Institute of Diagnostic Virology, Friedrich-Loeffler-Institut, Südufer 10, D-17493 Greifswald-Insel Riems, Germany; email: martin.beer@fli.de

Highly Pathogenic Avian Influenza A(H5N8) Virus in Wild Migratory Birds, Qinghai Lake, China

Mingxin Li, [1] Haizhou Liu,[1] Yuhai Bi,[1] Jianqing Sun,[1] Gary Wong, Di Liu, Laixing Li, Juxiang Liu, Quanjiao Chen, Hanzhong Wang, Yubang He, Weifeng Shi, George F. Gao, Jianjun Chen

In May 2016, a highly pathogenic avian influenza A(H5N8) virus strain caused deaths among 3 species of wild migratory birds in Qinghai Lake, China. Genetic analysis showed that the novel reassortant virus belongs to group B H5N8 viruses and that the reassortment events likely occurred in early 2016.

Since 2003, the A/Goose/Guangdong/1/96 lineage (Gs/Gd-lineage) of highly pathogenic avian influenza (HPAI) A(H5N1) viruses has been evolving into diverse clades and subclades (*1*). A novel subclade of HPAI A(H5N8), 2.3.4.4, which evolved from a clade 2.3.4 H5N1 variant, was initially isolated from domestic ducks in eastern China in 2010 (*2*) and caused outbreaks in domestic ducks and migratory birds in South Korea in early 2014 (*3*,*4*). In late 2014, several countries in Europe and East Asia experienced an invasion of HPAI H5N8 virus (*5*). This HPAI H5Nx (H5N8, H5N2, and H5N1) lineage subsequently emerged in North America, causing fatalities among wild birds and outbreaks in domestic poultry (*5*).

Available evidence strongly suggests that the HPAI H5N8 subclade 2.3.4.4 viruses were introduced and spread across the globe by migratory birds (*6*–*8*). Currently, 2 distinct H5N8 virus groups have been identified: group A (Buan2-like) and group B (Gochang1-like) (*3*). Group A H5N8 viruses predominate and have further evolved into 3 distinct subgroups: icA1, icA2, and icA3 (*6*). We report the emergence of a group B H5N8 virus in Qinghai Lake, China, a key breeding and stopover site for waterfowl along the Central Asian Flyway.

Author affiliations: CAS Key Laboratory of Special Pathogens and Biosafety, Chinese Academy of Sciences, Hubei, China (M. Li, H. Liu, J. Liu, Q. Chen, H. Wang, J. Chen); Center for Influenza Research and Early-warning (CASCIRE), Chinese Academy of Sciences, Beijing (Y. Bi, G. Wong, D. Liu, Q. Chen, G.F. Gao, J. Chen); Key Laboratory of Pathogenic Microbiology and Immunology, Chinese Academy of Sciences, Beijing, China (Y. Bi, G. Wong, D. Liu, G.F. Gao); Shenzhen Third People's Hospital, Shenzhen, China (Y. Bi, G.F. Gao); Qinghai Lake National Nature Reserve, Qinghai, China (J. Sun, Y. He); Northwest Institute of Plateau Biology of Chinese Academy of Sciences, Xining, China (L. Li); Institute of Pathogen Biology, Taishan Medical College, Shandong, China (W. Shi)

DOI: http://dx.doi.org/10.3201/eid2304.161866

The Study

On May 1, 2016, the carcass of a brown-headed gull (*Larus brunnicephalus*) was found on Egg Islet, a major breeding site of bar-headed geese, in Qinghai Lake. Carcasses of wild birds were recovered for 15 consecutive days, starting on May 8: 124 bar-headed geese (*Anserindicus*), 17 brown-headed gulls (*Larus brunnicephalus*), and 14 great black-headed gulls (*L. ichthyaetus*). As of June 4, a total of 158 birds, most of which were bar-headed geese, were found dead in Qinghai Lake, predominantly on Egg Islet (Figure 1; online Technical Appendix, https://wwwnc.cdc.gov/EID/article/23/4/16-1866-Techapp1.pdf)

In the first 9 days of the outbreak, multiple organs (brain, intestine, liver, lung, pancreas and kidney) were collected aseptically from 18 bar-headed geese, 6 brown-headed gulls, and 1 great black-headed gull. We inoculated 10-day-old chicken embryos with the homogenates of these organs for virus isolation. Almost all organs analyzed were positive for influenza virus, and we detected only H5- and N8- subtype-specific strains.

We sequenced full-length genomes and found the polybasic amino acid sequence, REKRRKR*GL in the hemagglutinin (HA) cleavage site, confirming the virus can be classified as highly pathogenic. Sequences of 48 Qinghai Lake H5N8 influenza isolates (QH-H5N8) were deposited into the GISAID database (http://www.gisaid.org) under accession nos. EPI774110–EPI774510.

Sequence comparisons showed high nucleotide identity among all 8 gene segments of the QH-H5N8 isolates (>99.2%; data not shown), indicating that the isolated strains are descendants of a common ancestral virus. A BLAST search (https://blast.ncbi.nlm.nih.gov/) suggested that QH-H5N8 is a reassortant virus (online Technical Appendix Table 1) and that the HA, neuraminidase (NA), and nonstructural protein (NS) genes of QH-H5N8 share high nucleotide identity (>99.1%) with those of the H5N8 virus that circulated among poultry in eastern China in 2014 (A/duck/Eastern China/S1109/2014[H5N8]). The remaining

[1]These authors contributed equally to this article.

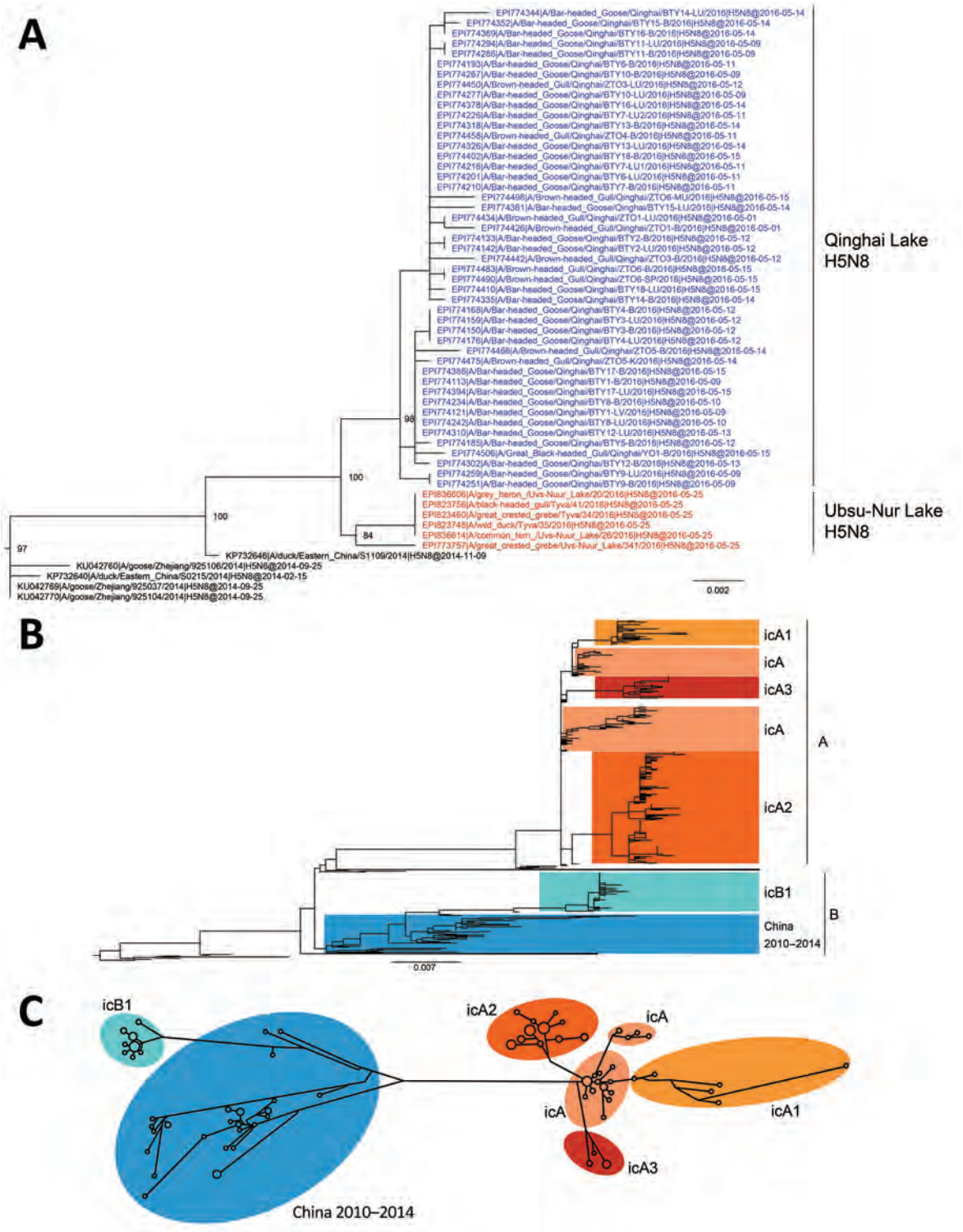

Figure 1. Phylogenetic analyses of 594 hemagglutinin (HA) sequences (1,704 nt) from clade 2.3.4.4 H5 influenza viruses. A) HA-coding sequence subtree from maximum-likelihood phylogenetic analysis of the clade 2.3.4.4 H5 viruses. Colored nodes: blue, Qinghai Lake H5N8 strains (this study); red, Ubsu-Nur Lake H5N8 strains. B) Maximum-likelihood phylogenetic tree of the clade 2.3.4.4 HA-coding sequences, rooted with A/Goose/Guangdong/1/96(H5N1). Scale bars indicate nucleotide substitutions per site. C) Median-joining phylogenetic network of the HA-coding gene sequences, including the most parsimonious trees linking the sequences. To simplify the network, nodes with only one sequence are not shown. Network branch lengths are proportional to the numbers of mutations. icA, intercontinental group A; icA1, intercontinental subgroup A1; icA2, intercontinental subgroup A2; icA3, intercontinental subgroup A3; icB1, intracontinental subgroup B1.

internal genes share high nucleotide identity with those of the low pathogenicity avian influenza (LPAI) viral pool in waterfowl from Mongolia and other regions (online Technical Appendix Table 1).

Phylogenetic analysis confirmed that the 8 segments had different origins. In the HA, NA, and NS phylogenetic trees, the QH-H5N8 virus clustered with H5N8 viruses isolated in late May 2016 from wild waterfowl at Ubsu-Nur Lake (UN-H5N8), forming a monophyletic cluster (Figure 1, panel A; online Technical Appendix Figure 2, panels D, F, H). Unlike the H5N8 strains previously described in South Korea in 2014–2015 (Buan2-like, group A), this cluster fell within group B (Gochang1-like) H5N8 viruses, forming a novel subgroup, intracontinental group B (icB1) (Figure 1, panel B; online Technical Appendix Figure 2, panel D). Neighbor-joining phylogenetic network analysis of the HA segment of the clade 2.3.4.4 H5 viruses also supported the finding that the QH-H5N8 and UN-H5N8 strains form a monophyletic cluster and appear to have evolved independently from group A H5N8 viruses (Figure 1, panel C).

Phylogenetic trees constructed by using sequences from the internal genes (all but polymerase basic 1 [PB1]) show that QH-H5N8 and UN-H5N8 viruses are closely related to various LPAI viruses circulating in aquatic birds in Mongolia in 2015. The PB1 gene, however, originated from various LPAI viruses dispersed across a relatively large geographic region (East and South Asia) over a long period (2010–2015) (online Technical Appendix Figure 2).

We used molecular dating to estimate the timing of the reassortment events that led to the emergence of QH-H5N8 (online Technical Appendix Figure 3). The HA, NA, and NS genes were transferred from domestic waterfowl in eastern China to wild migratory birds in approximately October 2015, January 2016, and December 2015, respectively (Figure 2; online Technical Appendix Table 2). Other internal gene segments (except PB1) originated from Mongolian waterfowl during July 2014–January 2016 (Figure 2; online Technical Appendix Table 2, Figure 3). The PB1 segment differs from the other segments, and was transferred from a LPAI virus circulating among waterfowl in Asia in February 2014 (Figure 2; online Technical Appendix Table 2, Figure 3). Thus, the generation of QH-H5N8 in wild migratory birds appears to have been a complex process and was likely completed in early 2016 (Figure 2).

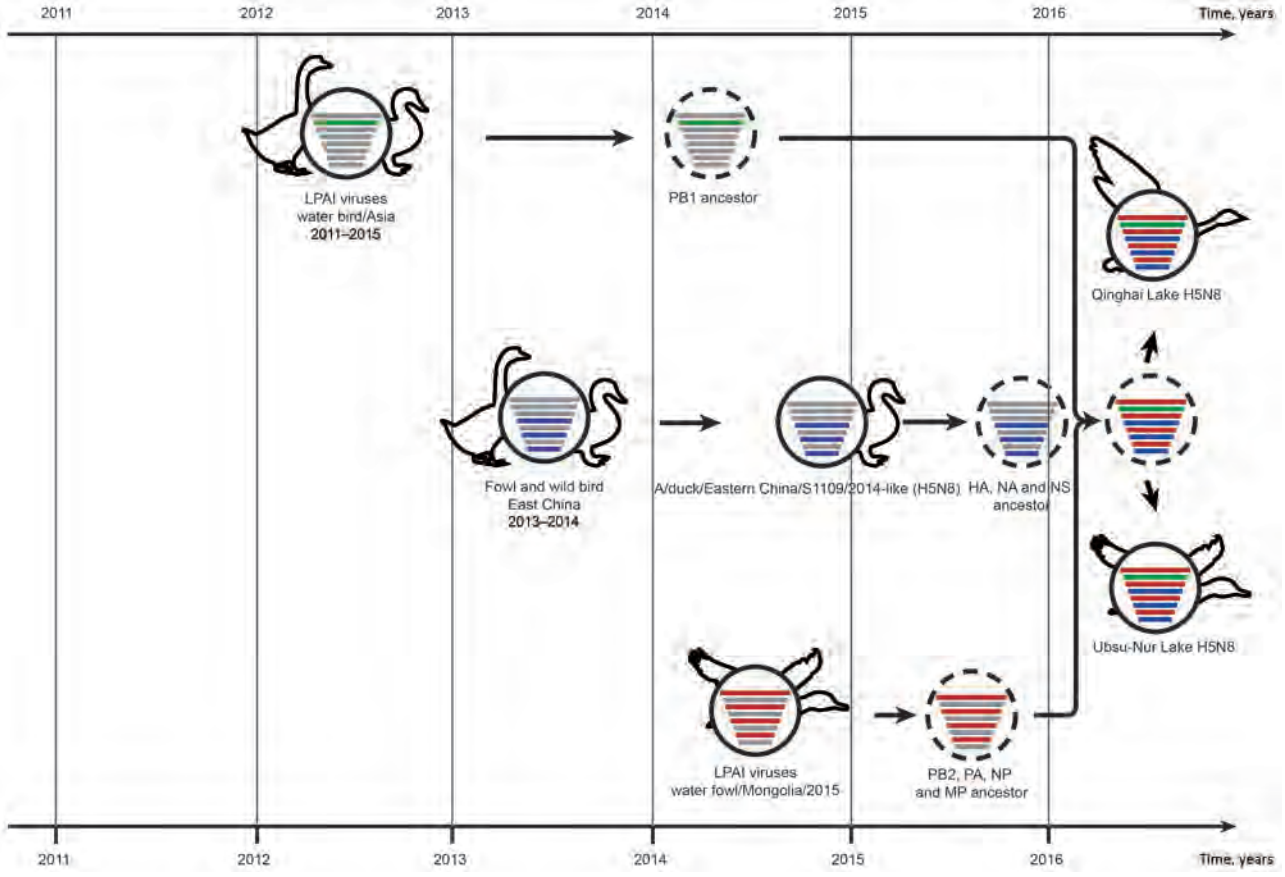

Figure 2. Hypothetical evolutionary pathway of influenza (H5N8) viruses from Qinghai Lake, China. Gene segments are colored according to their origins. Dashed virions indicate unidentified viruses. HA, hemagglutinin; LPAI, low pathogenicity avian influenza; MP, matrix protein; NA, neuraminidase; NP, nucleoprotein; NS, nonstructural protein; PA, acidic polymerase; PB, polymerase basic.

Conclusions

We show that a group B H5N8 virus emerged in Qinghai Lake, China, causing deaths in wild migratory birds. Phylogenetic analysis indicates that the QH-H5N8 virus is the descendant of an unidentified triple-reassortant strain (Figure 2). The reassortment event may have occurred in waterfowl, and can be traced back to early 2016. However, we cannot infer the geographic region where the reassortant virus was generated, because the gene constellation of the virus originated from different locations.

The absence of domestic poultry in the vicinity of Qinghai Lake strongly suggests that the virus was introduced to the area by wild birds. The deaths in Qinghai Lake occurred during May–June 2016, which corresponds with the breeding season for the affected species. In late May 2016, similar H5N8 strains were detected in wild migratory birds at Ubsu-Nur Lake, 1,600 km north of Qinghai Lake (*9*,*10*). This finding suggests that the early summer movement of wild migratory birds from unknown southern sites to northern breeding grounds resulted in the introduction of H5N8 to Qinghai Lake and to Ubsu-Nur Lake, infecting a diverse population of breeding waterbirds.

Currently, we know of 3 HPAI H5N1 virus clades that have been introduced to wild migratory birds in Qinghai Lake, which is located near multiple migratory flyways: clade 2.2 in 2005 (*11*,*12*), clade 2.3.2 in 2009 (*13*,*14*), and clade 2.3.2.1c in 2015 (*15*). On all 3 occasions, similar viruses were subsequently detected in other regions. Therefore, when wild birds left the breeding location for their wintering sites in the autumn of 2016, H5N8 virus could potentially have spread to other regions along the flyway. HPAI H5N8 viruses have already caused fatalities among wild birds or poultry in South Asia, Europe, the Middle East, and Africa (http://www.oie.int/) since late October 2016. Available genetic information shows that H5N8 strains isolated in other countries are highly similar to the QH-H5N8-like virus, suggesting that the QH-H5N8-like viruses may have already disseminated to other areas along the migratory flyways.

Acknowledgment

We thank the data submitters from the GISAID for their H5N8 sequences.

This study was supported by grants from the Special Project of Ministry of Science and Technology (2013FY113500), National Natural Science Foundation of China (31570026), intramural special grant for influenza virus research from the Chinese Academy of Sciences (KJZD-EW-L09 and KJZD-EW-L15), the Ministry of Science and Technology of China 973 Project (2015CB910501), and the Sanming Project of Medicine in Shenzhen (ZDSYS201504301534057). G.F.G. is a principal investigator in the National Natural Science Foundation of China Innovative Research Group (81321063). W.S. was supported by the "Taishan Scholar" project of Shandong Province. Y.B. is supported by the Youth Innovation Promotion Association of Chinese Academy of Sciences. G.W. is the recipient of a Banting Postdoctoral Fellowship from the Canadian Institutes of Health Research and the President's International Fellowship Initiative from the Chinese Academy of Sciences.

Mr. Li is a postgraduate student at CAS Key Laboratory of Special Pathogens and Biosafety of Chinese Academy of Sciences. His primary research interest is the epidemiology of influenza viruses.

References

1. World Health Organization/World Organisation for Animal Health/Food and Agriculture Organization (WHO/OIE/FAO) H5N1 Evolution Working Group. Revised and updated nomenclature for highly pathogenic avian influenza A (H5N1) viruses. Influenza Other Respi Viruses. 2014;8:384–8. http://dx.doi.org/10.1111/irv.12230
2. Zhao K, Gu M, Zhong L, Duan Z, Zhang Y, Zhu Y, et al. Characterization of three H5N5 and one H5N8 highly pathogenic avian influenza viruses in China. Vet Microbiol. 2013;163:351–7. http://dx.doi.org/10.1016/j.vetmic.2012.12.025
3. Lee YJ, Kang HM, Lee EK, Song BM, Jeong J, Kwon YK, et al. Novel reassortant influenza A(H5N8) viruses, South Korea, 2014. Emerg Infect Dis. 2014;20:1087–9. http://dx.doi.org/10.3201/eid2006.140233
4. Wu H, Peng X, Xu L, Jin C, Cheng L, Lu X, et al. Novel reassortant influenza A(H5N8) viruses in domestic ducks, eastern China. Emerg Infect Dis. 2014;20:1315–8. http://dx.doi.org/10.3201/eid2008.140339
5. World Organisation For Animal Health. Updated on highly pathogenic avian influenza in animals (type H5 and H7), 2014–2015. Paris: The Organisation; 2015.
6. Lee DH, Torchetti MK, Winker K, Ip HS, Song CS, Swayne DE. Intercontinental spread of Asian-origin H5N8 to North America through Beringia by migratory birds. J Virol. 2015;89:6521–4. http://dx.doi.org/10.1128/JVI.00728-15
7. Verhagen JH, Herfst S, Fouchier RAM. How a virus travels the world. Science. 2015;347:616–7. http://dx.doi.org/10.1126/science.aaa6724
8. Global Consortium for H5N8 and Related Influenza Viruses. Role for migratory wild birds in the global spread of avian influenza H5N8. Science. 2016;354:213–7. http://dx.doi.org/10.1126/science.aaf8852
9. Sims L, Khomenko S, Kamata A, Belot G, Bastard J, Palamara E, et al. H5N8 highly pathogenic avian influenza (HPAI) of clade 2.3.4.4 detected through surveillance of wild migratory birds in the Tyva Republic, the Russian Federation—potential for international spread. Food and Agriculture Organization. 2016;35 [cited 2016 Dec 7]. http://www.fao.org/3/a-i6113e.pdf
10. Lee DH, Sharshov K, Swayne DE, Kurskaya O, Sobolev I, Kabilov M, et al. Novel reassortant clade 2.3.4.4 avian influenza A(H5N8) virus in wild aquatic birds, Russia, 2016. Emerg Infect Dis. 2017 Feb [Epub ahead of print]. http://dx.doi.org/10.3201/eid2302.161252
11. Liu J, Xiao H, Lei F, Zhu Q, Qin K, Zhang XW, et al. Highly pathogenic H5N1 influenza virus infection in migratory birds. Science. 2005;309:1206. http://dx.doi.org/10.1126/science.1115273
12. Wang G, Zhan D, Li L, Lei F, Liu B, Liu D, et al. H5N1 avian influenza re-emergence of Lake Qinghai: phylogenetic and

antigenic analyses of the newly isolated viruses and roles of migratory birds in virus circulation. J Gen Virol. 2008;89:697–702. http://dx.doi.org/10.1099/vir.0.83419-0

13. Li Y, Liu L, Zhang Y, Duan Z, Tian G, Zeng X, et al. New avian influenza virus (H5N1) in wild birds, Qinghai, China. Emerg Infect Dis. 2011;17:265–7. http://dx.doi.org/10.3201/eid1702.100732
14. Hu X, Liu D, Wang M, Yang L, Wang M, Zhu Q, et al. Clade 2.3.2 avian influenza virus (H5N1), Qinghai Lake region, China, 2009-2010. Emerg Infect Dis. 2011;17:560–2. http://dx.doi.org/10.3201/eid1703.100948
15. Bi Y, Chen J, Zhang Z, Li M, Cai T, Sharshov K, et al. Highly pathogenic avian influenza H5N1 Clade 2.3.2.1c virus in migratory birds, 2014-2015. Virol Sin. 2016;31:300–5. http://dx.doi.org/10.1007/s12250-016-3750-4

Address for correspondence: Jianjun Chen, CAS Key Laboratory of Special Pathogens and Biosafety, Wuhan Institute of Virology, Chinese Academy of Sciences, Xiaohongshan 44# Wuhan 430071, China; email: chenjj@wh.iov.cn

Design Strategies for Efficient Arbovirus Surveillance

Samuel V. Scarpino, Lauren Ancel Meyers, Michael A. Johansson

As public health agencies struggle to track and contain emerging arbovirus threats, timely and efficient surveillance is more critical than ever. Using historical dengue data from Puerto Rico, we developed methods for streamlining and designing novel arbovirus surveillance systems with or without historical disease data.

Mosquitoborne viruses in the families *Flaviviridae* and *Togaviridae* cause substantial illness and death worldwide (*1*,*2*). Dengue is the most widespread arboviral disease, with an estimated 70–140 million cases occurring annually (*3*). Despite the large public health and economic costs of arboviruses, effective medical countermeasures are limited (*1*). Globally, primary arbovirus prevention and control efforts include personal protection, mosquito control, and clinical treatment. The success of these efforts depends on timely and accurate situational awareness: knowing spatiotemporal patterns of exposure, infection, and severity.

Puerto Rico has an islandwide passive dengue surveillance system similar to those found in other regions with endemic dengue (*4*). Healthcare providers (clinics or hospitals) report suspected dengue cases and submit blood samples for laboratory diagnosis. This comprehensive system captures spatiotemporal variation in incidence and enables characterization of circulating viruses, but it requires substantial resources and may lack efficiency.

Here, we extend a previous approach (*5*) to designing dengue surveillance systems with 4 sets of specific public health objectives: real-time estimation of island-wide dengue cases, regional dengue cases, island-wide cases of each dengue virus serotype, and all three preceding quantities combined. Using dengue case data from 1991 through 2005, we identified a surveillance system including a subset of Puerto Rican providers that was expected to achieve these objectives efficiently and demonstrated the robustness of that system with data for 2006–2012.

Author affiliations: University of Vermont, Burlington, Vermont, USA (S.V. Scarpino); Santa Fe Institute, Santa Fe, New Mexico, USA (S.V. Scarpino, L.A. Meyers); University of Texas at Austin, Austin, Texas, USA (L.A. Meyers); Centers for Disease Control and Prevention, San Juan, Puerto Rico, USA (M.A. Johansson); Harvard T.H. Chan School of Public Health, Boston, Massachusetts, USA (M.A. Johansson)

DOI: http://dx.doi.org/10.3201/eid2304.160944

The Study

Across Puerto Rico, we analyzed the weekly number of suspect cases, laboratory-positive cases, and cases of each serotype reported during 1991–2012. For each case, we considered the patient's municipality of residence and the identity of the reporting provider.

In designing a multipurpose dengue surveillance system, we sought to identify a small subset of providers that can provide accurate situational awareness. However, it is computationally unfeasible to evaluate all possible combinations of providers. Our procedure for solving this computational issue is described in the following sections, with a detailed description in the online Technical Appendix (https://wwwnc.cdc.gov/EID/article/23/4/16-0944-Techapp1.pdf).

Building from previous research (*6*), we design surveillance systems by sequentially adding providers that most improve system performance. To evaluate the performance of a system with respect to an objective, we repeatedly perform the following: fit multilinear models to historical reported dengue cases, use the fitted models to estimate dengue cases in another historical time period (one not used in model fitting), and quantify accuracy by using the coefficient of determination (R^2) resulting from a linear regression of the estimated on the actual time series. In each repetition, we used a different combination of training data and testing data, and average all the scores across repetitions (denoted as $\hat{R}^2$). That is, we chose the set of providers that achieved the highest average out-of-sample performance (see, e.g., online Technical Appendix Figure 1).

We compared our results to 3 systems in which providers were selected without historical disease data. Specifically, we selected providers on the basis of the population within 20 miles of a provider (proposed by Polgreen et al. [*7*]), the total number of patients seen (proposed by Mandl et al. [*8*]), and the diversity of the municipality of residence for patients, which does not require that each provider see an even distribution of patients; rather, providers are incorporated sequentially to achieve geographic complementarity.

We constructed surveillance systems ranging from 1 through 75 providers by using the selection algorithm for 4 objectives: island-wide cases (*Island*), island-wide cases for each of the 4 dengue virus serotypes (*Serotype*), health region-specific cases for all 8 health service regions (*Regional*), and all objectives combined (*Multi-objective*). We assessed 3 alternative systems: population coverage (*Population*), patient volume (*Volume*), and patient geographic diversity (*Diversity*). The Multi-objective system reached 99% of maximum accuracy with just 22 providers (online

Technical Appendix Figure 2) and performed almost as well as the systems designed specifically to achieve each objective individually (Figure 1). The Diversity system achieved 99%, 92%, and 90% of the performance of the systems specifically engineered for estimating island-wide, serotype, and regional cases, respectively, and showed similar geographic patterns to the Multi-objective system (online Technical Appendix Figure 3). For individual serotypes and regions, performance was best for objectives with less sparse data (online Technical Appendix Figure 4).

Finally, we assessed the robustness of the Multi-objective system, which offered the strongest combination of efficiency and performance. We tested it against 7 additional years' worth of data that were withheld from the analysis. The system performed well for each of the objectives (Figure 2), achieving average values of 0.86 and 0.78 for surveillance of individual serotypes and regions, respectively, and 0.97 for surveillance of island-wide cases. Among individual serotypes and regions, all had values greater than 0.75, except for the Fajardo region, where cases were particularly sparse.

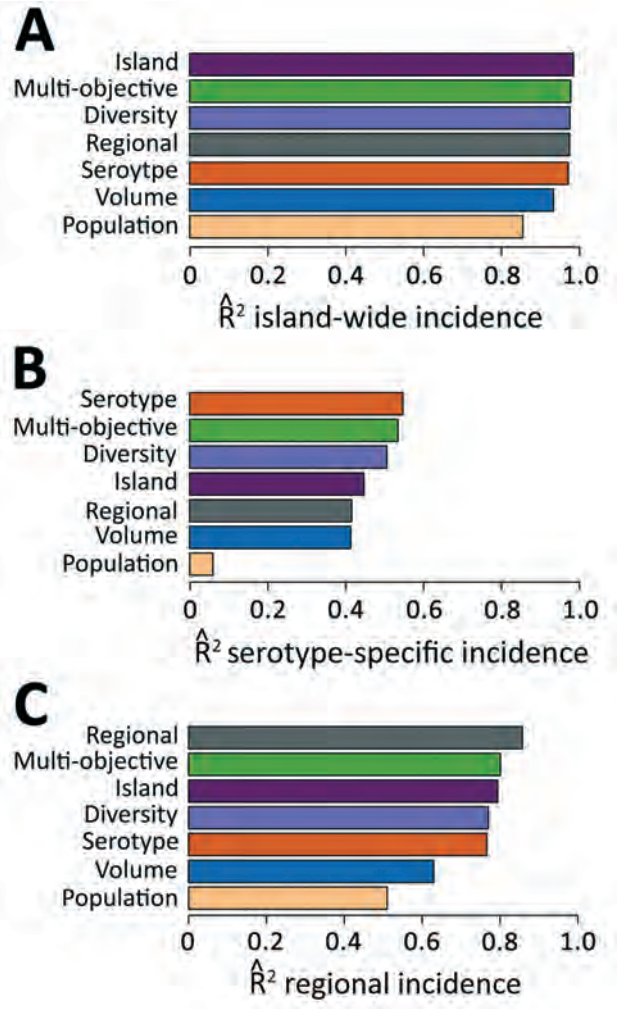

Figure 1. Relative surveillance system performance. The performance of the 4 optimized surveillance systems (Island, Regional, Serotype, and Multi-objective) compared with 3 alternative designs (Population, Volume, and Diversity), with respect to estimating A) island-wide cases, B) serotype-specific cases, and C) regional cases. Each system contains 22 providers. Systems are ordered from highest to lowest performance in each graph. Performance is measured by average out-of-sample across 100 different 3-year periods, resulting from linear regression of target time series (e.g., island-wide cases) on time series of cases occurring within the specified surveillance system.

Conclusions

Surveillance systems are widely used to support public health efforts, but they are rarely designed systematically to achieve clear, quantifiable objectives or surveillance goals, and to do so efficiently. Articulating such public health objectives is a critical first step toward evaluating, improving, and streamlining surveillance. Here, we applied a rigorous, quantitative approach to design a dengue surveillance system that efficiently achieves several distinct public health objectives. The method flexibly and robustly maximizes information collected while minimizing the effort required. In this application, we built a multi-objective system that efficiently tracks the spatiotemporal patterns of dengue in Puerto Rico. This system is almost as informative as the systems we optimized to achieve individual objectives, and it maintained its expected performance on recent data that were withheld during the design stage.

Although surveillance goals and resources may be highly specific to the disease threat and region of concern, the proposed optimization method can be applied broadly to enhance the detection of infectious disease threats, as we have shown now for both dengue and influenza (*5*). We hypothesize that the systems we designed for dengue in Puerto Rico may also serve well for other arboviruses transmitted by *Aedes* spp. mosquitoes, given their similar transmission mechanisms and the strong out-of-sample performance of the system. In some cases, additional data (e.g., mosquito or nonhuman host surveillance) and public health goals (e.g., vector density) could be integrated into the systems. Such data were not available for this study. For newly emerging arboviruses, when historical data are not available, systems optimized for similar pathogens may provide reasonable coverage. Nonetheless, emergence dynamics may have more sporadic and explosive characteristics that may not be captured by a system designed to track spatiotemporal patterns of an endemic disease.

Public health authorities seek situational awareness at multiple geopolitical scales as well as early warning of anomalous events across a wide spectrum of biologic threats beyond arboviruses. The method we present can also be used to redesign existing surveillance systems by manually including or excluding providers during optimization. Additionally, the method is well suited to integrating diverse data streams, such as climatic, mosquito vector, pharmacy, or digital data (*9*).

In an era of "right-sizing," quantitative development and evaluation are critical to the design, redesign, justification, and benchmarking of surveillance efforts. Given limited public health budgets on all scales, methods such as the one we present are critical to the future reliability and sustainability of infectious disease surveillance.

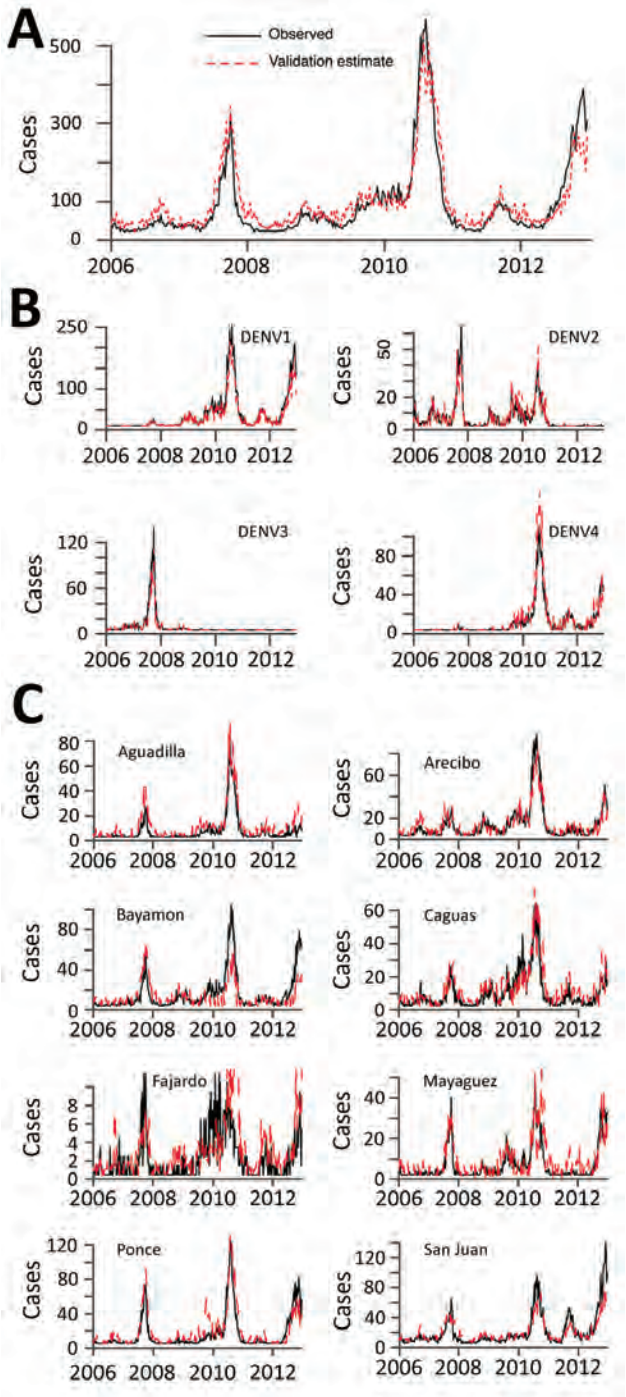

Figure 2. Independent evaluation of performance**.** The 22-provider Multi-objective surveillance system was designed using data before 2006 and then evaluated on data for 2006–2012 with respect to surveillance of A) island-wide, B) serotype-specific, and C) regional cases. Surveillance estimates from the 22-provider system (red) are compared with raw data from the complete passive surveillance system of 105 providers (black).

Acknowledgment

We thank Ned Dimitrov and Ben Althouse for productive discussions on surveillance and dengue.

S.V.S. acknowledges funding from the Omidyar Group and the Santa Fe Institute. M.A.J. acknowledges partial support from the Models of Infectious Disease Agent Study program (Cooperative Agreement no. 1U54GM088558).

Dr. Scarpino is an assistant professor in the department of mathematics and statistics and is a core faculty member in the Complex Systems Center at the University of Vermont. He investigates questions at the intersection of biology, behavior, and disease and works collaboratively with clinical and public health decision makers to improve disease surveillance.

References

1. World Health Organization and the Special Programme for Research and Training in Tropical Diseases. Dengue: guidelines for diagnosis, treatment, prevention and control. Geneva: The Organization; 2009.
2. LaBeaud AD, Bashir F, King CH. Measuring the burden of arboviral diseases: the spectrum of morbidity and mortality from four prevalent infections. Popul Health Metr. 2011;9:1. http://dx.doi.org/10.1186/1478-7954-9-1
3. Bhatt S, Gething PW, Brady OJ, Messina JP, Farlow AW, Moyes CL, et al. The global distribution and burden of dengue. Nature. 2013;496:504–7. http://dx.doi.org/10.1038/nature12060
4. Beatty ME, Stone A, Fitzsimons DW, Hanna JN, Lam SK, Vong S, et al.; Asia-Pacific and Americas Dengue Prevention Boards Surveillance Working Group. Best practices in dengue surveillance: a report from the Asia-Pacific and Americas Dengue Prevention Boards. PLoS Negl Trop Dis. 2010;4:e890. http://dx.doi.org/10.1371/journal.pntd.0000890
5. Scarpino SV, Dimitrov NB, Meyers LA. Optimizing provider recruitment for influenza surveillance networks. PLOS Comput Biol. 2012;8:e1002472. http://dx.doi.org/10.1371/journal.pcbi.1002472
6. Waterman SH, Novak RJ, Sather GE, Bailey RE, Rios I, Gubler DJ. Dengue transmission in two Puerto Rican communities in 1982. Am J Trop Med Hyg. 1985;34:625–32.
7. Polgreen PM, Chen Z, Segre AM, Harris ML, Pentella MA, Rushton G. Optimizing influenza sentinel surveillance at the state level. Am J Epidemiol. 2009;170:1300–6. http://dx.doi.org/10.1093/aje/kwp270
8. Mandl KD, Overhage JM, Wagner MM, Lober WB, Sebastiani P, Mostashari F, et al. Implementing syndromic surveillance: a practical guide informed by the early experience. J Am Med Inform Assoc. 2003;11:141–50. http://dx.doi.org/ 10.1197/jamia.M1356
9. Althouse BM, Scarpino SV, Meyers LA, Ayers JW, Bargsten M, Baumbach J, et al. Enhancing disease surveillance with novel data streams: challenges and opportunities. EPJ Data Science. 2015;4:17. http://dx.doi.org/10.1140/epjds/s13688-015-0054-0

Address for correspondence: Michael A. Johansson, Centers for Disease Control and Prevention, 1324 Calle Cañada, Mailstop P01, San Juan, PR 00920, USA; email: eyq9@cdc.gov

Typhus Group Rickettsiosis, Texas, USA, 2003–2013

Kristy O. Murray, Nicole Evert, Bonny Mayes, Eric Fonken, Timothy Erickson, Melissa N. Garcia, Tom Sidwa

We characterized the epidemiology of typhus group rickettsiosis in Texas, USA. During 2003–2013, a total of 1,762 cases were reported to the state health department. The number of diagnosed cases and geographic expansion increased over time. Physician awareness is critical to diagnose and effectively treat rickettsial infections.

Typhus group rickettsiosis (TGR) is a fleaborne disease. In Texas, USA, most infections are attributed to *Rickettsia typhi*, the causative agent of murine typhus (*1*). Rare cases of another TGR, *R. prowazekii*, have been reported in south Texas (*2*).

The established reservoirs of murine typhus are *Rattus* spp. rodents; however, opossums are thought to be an important reservoir in peridomestic settings, with the cat flea, *Ctenocephalides felis*, as the vector (*3*–*5*). Clinical disease in humans often is characterized by the classical triad of fever, headache, and rash, although 1 study found that rash was present in only 54% of cases and only 12.5% had the classical triad (*6*). Infections can be severe and potentially fatal if not treated appropriately (*7*).

In the United States, Texas reports the most TGR cases annually, and TGR is considered endemic to the southernmost part of the state (*8*). Since the mid-2000s, public health authorities have observed an increase in the number of reported cases and geographic expansion into areas of the state to which TGR is not considered endemic. Our objective with this study was to characterize the epidemiology of TGR in Texas and identify high-risk geographic and demographic populations.

The Study

The state of Texas mandates reporting of rickettsial diseases to the Texas Department of State Health Services (TxDSHS). TxDSHS maintains demographic, clinical, and environmental data on each case in a database for surveillance purposes. Confirmed cases of TGR were defined as clinically compatible illness with 1 of the following: 1) ≥4-fold rise in antibody titer by immunofluorescent antibody, complement fixation, latex agglutination, microagglutination, or indirect hemagglutination antibody between acute and convalescent specimens; 2) a positive PCR result; 3) bacterial isolation from a clinical specimen; 4) positive immunofluorescence from tissue; or 5) a single IgM or IgG titer of ≥1,024 in the TGR-endemic area of south Texas or Travis County, beginning in 2007 and 2012, respectively. Probable cases were defined as clinically compatible illness and a single serologic titer of ≥128 by immunofluorescent antibody, latex agglutination, microagglutination or indirect hemagglutination antibody or a single titer of ≥16 by complement fixation.

We analyzed surveillance data on all confirmed and probable cases reported to TxDSHS during 2003–2013. Census data from the 2010 national census (*9*) were used to derive attack rates for sex, age, and race/ethnicity, as well as cumulative incidence by county. Statistical estimates were calculated by using Epi Info version 7.2 (Centers for Disease Control and Prevention [CDC], Atlanta, GA, USA). Incidence by county was graphed using MapInfo version 10.2.5 (Pitney Bowes Software, Troy, NY, USA).

During 2003–2013, a total of 1,762 TGR cases (770 confirmed and 992 probable) were reported. We observed evidence of increased numbers of cases over time and expanded geographic locations. We know of no specific reason that would have prompted physicians to increase diagnosing or reporting cases. During the study period, case numbers reported ranged from 27 in 2003 to 222 in 2013 (Figure 1). An average of 102 cases were reported yearly during 2003–2007, which is less than half (209) of the average number reported during 2008–2013. As expected, illness onset peaked in June and July; however, in south Texas (≤28°N), 2 peaks occurred: the first in summer (June and July) and the other in winter (December and January). The reason for this bimodal distribution of cases in south Texas is unknown and requires further investigation.

TGR cases expanded geographically during the study period. In 2003, cases were reported from 9 counties in south Texas. By 2013, cases had been reported from 41 counties (Figure 2). Cumulative incidence was highest in south Texas; an average of 59.5 cases per 100,000 population were reported during the study period (Figure 2). Nueces County in south Texas had the highest cumulative incidence (139.9 cases/100,000 population). One county (Kenedy) in south

Author affiliations: Baylor College of Medicine and Texas Children's Hospital, Houston, Texas, USA (K.O. Murray, T. Erickson, M.N. Garcia); Texas Department of State Health Services, Austin, Texas, USA (N. Evert, B. Mayes, E. Fonken, T. Sidwa)

DOI: http://dx.doi.org/10.3201/eid2304.160958

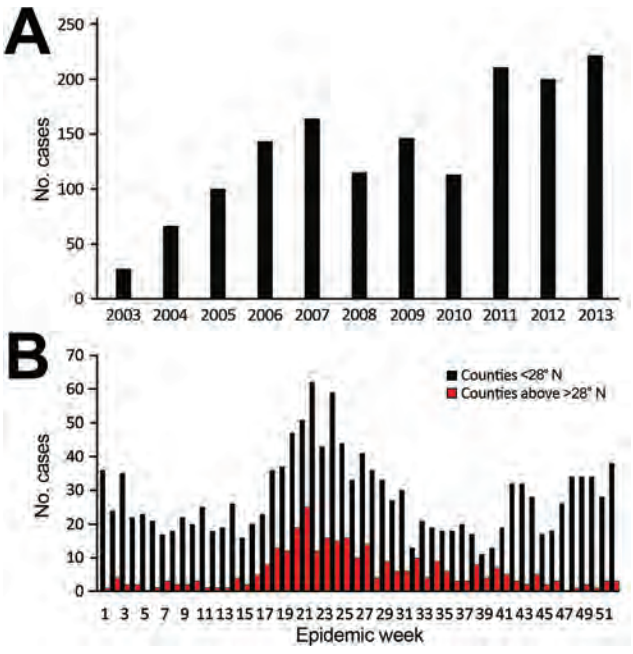

Figure 1. Typhus group rickettsiosis, Texas, 2003–2013. A) Number of reported cases by year. B) Illness onset by epidemic week during the study period, by location; ≤28°N represents south Texas.

Texas reported no cases; this is most likely due to this county's low population count (416 persons) (*10*).

The attack rate was slightly higher for female than for male residents (7.3 vs. 6.7/100,000 population) (Table 1). Median age of case-patients was 33 years, and the highest attack rate was for 5–19-year-olds (10.4 cases/100,000 population). These findings contrast with a 1980s study of 345 murine typhus case-patients in south Texas for whom median age was 48 years, and only 5 (1.4%) case-patients were <11 years of age (*6*).

Fifty-four percent of case-patients reported fleas in the home, and 34.0% reported a flea bite before illness onset (Table 2). The most common animals in the home environment were dogs (67.0%), cats (46.2%), wildlife (42.4%), and rodents (28.9%); 57.7% of homes had ≥1 animal.

A total of 1,047 (59.6%) case-patients were hospitalized (Table 2). The most commonly reported signs and symptoms were fever (99.7%), headache (77.2%), chills (70.1%), malaise (64.1%), anorexia (52.8%), nausea/vomiting (51.4%), and myalgias (50.8%). Rash was reported in 42.5% of cases; children were more likely than adults to have a rash (54.5% vs. 35.7%; odds ratio 2.2, p<0.001). One third (33.7%) of case-patients had the classical triad of fever, headache, and rash, which was higher than the previously reported 12.5% by Dumler et al. (*6*). Children were more likely than adults to have all 3 symptoms (41.1% vs. 29.3%; p<0.001). Four deaths were reported (0.2% case-fatality rate). The median age of persons who died was 51.5 years (range 36–55 years).

Identification and reporting of *Rickettsia*-positive persons is critical to identifying disease outbreaks. Although TGR is reportable in Texas, our study probably underrepresents the true number of cases because the illness was mild or not recognized as TGR, the clinical provider did not realize the disease is reportable, or the disease was misclassified (false negative) because specimens were collected too early after symptom onset (*11*).

Another potential limitation is the propensity of cross-reactions with other rickettsial pathogens. We would expect some degree of serologic cross-reaction

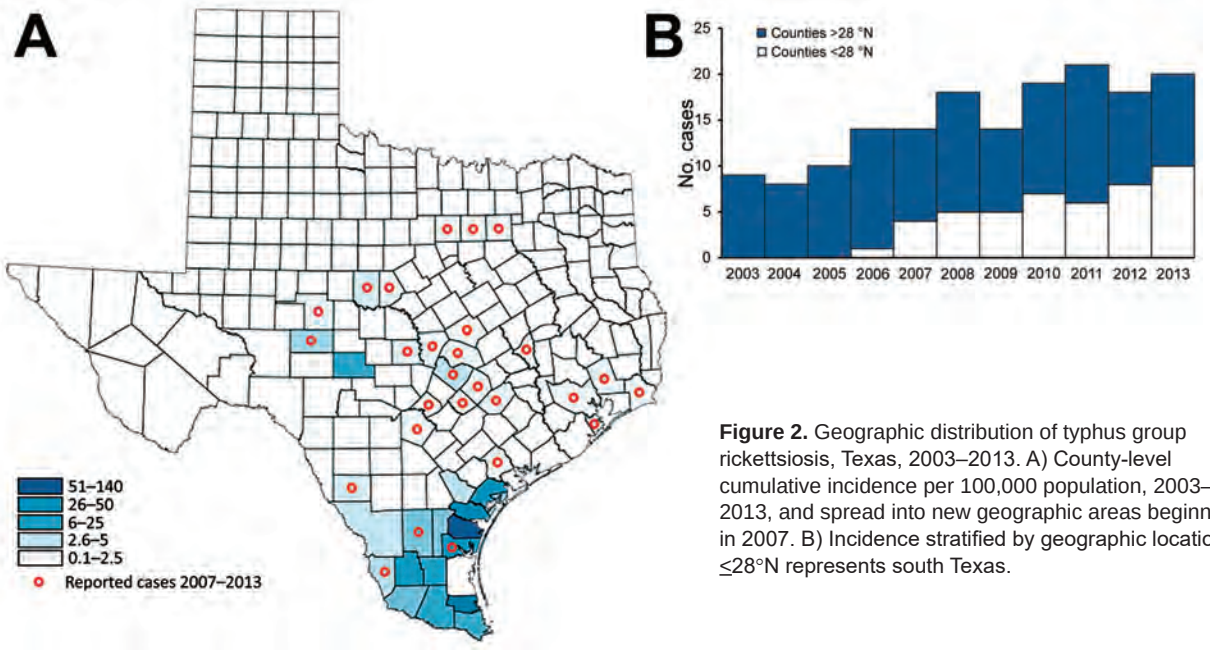

Figure 2. Geographic distribution of typhus group rickettsiosis, Texas, 2003–2013. A) County-level cumulative incidence per 100,000 population, 2003–2013, and spread into new geographic areas beginning in 2007. B) Incidence stratified by geographic location; ≤28°N represents south Texas.

Table 1. Demographic characteristics and attack rates for typhus group rickettsiosis, Texas, 2003–2013

Characteristic	Cases, no. (%), n = 1,762	Census population*	Attack rate†
Sex			
F	921 (52)	12,673,281	7.3
M	841 (48)	12,472,280	6.7
Race/ethnicity			
White, non-Hispanic	429 (24)	11,397,345	3.8
White, Hispanic	1,133 (64)	9,460,921	12.0
Black	23 (1)	2,886,825	0.8
Unknown or other	177 (10)	1,400,470	12.6
Age group, y			
<5	40 (2)	1,928,473	2.1
5–19	591 (34)	5,693,241	10.4
20–39	398 (23)	7,194,139	5.5
40–64	575 (33)	7,727,822	7.4
≥65	158 (9)	2,601,886	6.1

*Based on 2010 Population Census for Texas.
†Per 100,000 population.

between the 2 pathogens within the TGR group, *R. typhi* and *R. prowazekii*; hence, we collectively call these diagnoses TGR, even though we presume most cases were attributed to *R. typhi* infections. Serum reactive to typhus group antigen might cross-react, albeit infrequently and at a lower titer, to spotted fever group antigen (*12*). Finally, until 2015, TxDSHS included in the case definition for a confirmed case a single IgM titer ≥1,024 in TGR-endemic areas. This decision was based on CDC's criteria for diagnosing spotted fever rickettsiosis (*13*). As mentioned by CDC, a single IgM result is not ideal for diagnosing acute infections due to reduced specificity. Further research is needed to understand the true incidence of TGR in Texas.

Conclusions

We observed increased cases and geographic spread of TGR in Texas. Our results highlight the importance of educating the public about flea-bite prevention and raising physician awareness to identify cases, particularly in children. Further research is needed to better understand the transmission dynamics between rodents, fleas, and other potential new reservoir/vector systems and determine risk factors for infection.

Acknowledgments

We thank the local and regional TxDSHS offices for their time and assistance in completing the case investigation forms.

This study was reviewed and approved by the TxDSHS Institutional Review Board and was considered exempt by the Baylor College of Medicine Institutional Review Board.

Dr. Murray is the Associate Vice-Chair for Research and associate professor of Pediatric Tropical Medicine in the Department of Pediatrics at Baylor College of Medicine and Texas Children's Hospital and serves as Assistant Dean of the National School of Tropical Medicine. Her research focuses on vectorborne and zoonotic diseases.

Table 2. Clinical and environmental characteristics of reported TGR cases, Texas, 2003–2013*

Characteristic	Total, no. (%)	Confirmed case,† no. (%)	Probable case,‡ no. (%)
Clinical features			
Hospitalized	1,047/1,758 (59.6)	473/767 (61.7)	574/991 (57.9)
Fever	1,747/1,752 (99.7)	759/764 (99.3)	988/988 (100)
Headache	1,353/1,753 (77.2)	569/765 (74.4)	784/988 (79.4)
Chills	1,228/1,753 (70.1)	511/765 (66.8)	717/988 (72.6)
Malaise	1,123/1,753 (64.1)	471/765 (61.6)	652/988 (66.0)
Anorexia	925/1,753 (52.8)	399/765 (52.2)	526/988 (53.2)
Nausea/vomiting	901/1,753 (51.4)	381/765 (49.8)	520/988 (52.6)
Myalgia	890/1,753 (50.8)	388/765 (50.7)	502/988 (50.8)
Rash	722/1,700 (42.5)	325/747 (43.5)	397/953 (41.7)
Diarrhea	394/1,753 (22.5)	184/765 (24.1)	210/988 (21.3)
Photophobia	381/1,752 (21.7)	160/765 (20.9)	221/987 (22.4)
Retroorbital pain	266/1,753 (15.2)	121/765 (15.8)	145/988 (14.7)
Classical triad (fever, headache, rash)	572/1,697 (33.7)	240/745 (32.2)	332/952 (34.9)
Abnormal laboratory findings			
Elevated liver function	478/1,751 (27.3)	192/765 (25.1)	286/986 (29.0)
Thrombocytopenia	290/1,752 (16.6)	123/765 (16.1)	167/987 (16.9)
Environmental findings			
Fleas present in home	707/1,310 (54.0)	313/580 (54.0)	394/730 (54.0)
History of flea bite	418/1,231 (34.0)	187/538 (34.8)	231/693 (33.3)
Rodents present	379/1,312 (28.9)	192/584 (32.9)	187/728 (25.7)
Wildlife present	587/1,383 (42.4)	273/617 (44.2)	314/764 (41.1)
Dogs present	973/1,452 (67.0)	411/640 (64.2)	562/809 (69.5)
Cats present	659/1,427 (46.2)	298/633 (47.1)	361/792 (45.6)
>1 species present	844/1,463 (57.7)	371/644 (57.6)	472/816 (57.8)

*Denominators are the number of case-patients for whom the information was available. CF, complement fixation; IFA, immunofluorescent antibody; IHA, indirect hemagglutination antibody; LA, latex agglutination; MA, microagglutination; TGR, typhus group rickettsiosis.
†A confirmed case was defined as clinically compatible illness with 1) a >4-fold rise in antibody titer by IFA, CF, LA, MA, or IHA between acute and convalescent specimens; 2) a positive PCR result; 3) bacterial isolation from a clinical specimen; 4) positive immunofluorescence from tissue; or 5) a single IgM or IgG titer of >1,024 in a TGR-endemic region of south Texas (beginning in 2007) or Travis County (beginning in 2012).
‡A probable case was defined as clinically compatible illness and a single serologic titer of >128 by IFA, LA, MA, or IHA or a single titer ≥16 by CF.

References

1. Farhang Azad A, Traub R. Transmission of murine typhus rickettsiae by *Xenopsylla cheopis*, with notes on experimental infection and effects of temperature. Am J Trop Med Hyg. 1985;34:555–63.
2. Massung RF, Davis LE, Slater K, McKechnie DB, Puerzer M. Epidemic typhus meningitis in the southwestern United States. Clin Infect Dis. 2001;32:979–82. http://dx.doi.org/10.1086/319351
3. Boostrom A, Beier MS, Macaluso JA, Macaluso KR, Sprenger D, Hayes J, et al. Geographic association of *Rickettsia felis*–infected opossums with human murine typhus, Texas. Emerg Infect Dis. 2002;8:549–54. http://dx.doi.org/10.3201/eid0806.010350
4. Williams SG, Sacci JB Jr, Schriefer ME, Andersen EM, Fujioka KK, Sorvillo FJ, et al. Typhus and typhuslike rickettsiae associated with opossums and their fleas in Los Angeles County, California. J Clin Microbiol. 1992;30:1758–62.
5. Sorvillo FJ, Gondo B, Emmons R, Ryan P, Waterman SH, Tilzer A, et al. A suburban focus of endemic typhus in Los Angeles County: association with seropositive domestic cats and opossums. Am J Trop Med Hyg. 1993;48:269–73.
6. Dumler JS, Taylor JP, Walker DH. Clinical and laboratory features of murine typhus in south Texas, 1980 through 1987. JAMA. 1991;266:1365–70. http://dx.doi.org/10.1001jama.1991.03470100057033
7. Walker DH, Parks FM, Betz TG, Taylor JP, Muehlberger JW. Histopathology and immunohistologic demonstration of the distribution of *Rickettsia typhi* in fatal murine typhus. Am J Clin Pathol. 1989;91:720–4. http://dx.doi.org/10.1093/ajcp/91.6.720
8. Pratt HD. The changing picture of murine typhus in the United States. Ann N Y Acad Sci. 1958;70:516–27. http://dx.doi.org/10.1111/j.1749-6632.1958.tb35408.x
9. US Census Bureau. 2010 US Census data [cited 2016 May 31]. https://www.census.gov/quickfacts/table/PST045215/48
10. US Census Bureau. Kenedy County population for 2010 [cited 2016 May 31]. https://www.tsl.texas.gov/ref/abouttx/popcnty12010.html
11. Paris DH, Dumler JS. State of the art of diagnosis of rickettsial diseases: the use of blood specimens for diagnosis of scrub typhus, spotted fever group rickettsiosis, and murine typhus. Curr Opin Infect Dis. 2016;29:433–9. http://dx.doi.org/10.1097/QCO.0000000000000298
12. Keysary A, Strenger C. Use of enzyme-linked immunosorbent assay techniques with cross-reacting human sera in diagnosis of murine typhus and spotted fever. J Clin Microbiol. 1997;35:1034–5.
13. Centers for Disease Control and Prevention. Spotted fever rickettsiosis (*Rickettsia* spp.) 2010 case definition [cited 2016 Dec 3]. https://wwwn.cdc.gov/nndss/conditions/spotted-fever-rickettsiosis/case-definition/2010/

Address for correspondence: Kristy O. Murray, Department of Pediatrics, Baylor College of Medicine and Texas Children's Hospital, 1102 Bates Ave, Ste 550, Houston, TX 77030, USA; email: kmurray@bcm.edu

Detection and Molecular Characterization of Zoonotic Poxviruses Circulating in the Amazon Region of Colombia, 2014

Jose A. Usme-Ciro, Andrea Paredes, Diana M. Walteros, Erica Natalia Tolosa-Pérez, Katherine Laiton-Donato, Maria del Carmen Pinzón, Brett W. Petersen, Nadia F. Gallardo-Romero, Yu Li, Kimberly Wilkins, Whitni Davidson, Jinxin Gao, Nishi Patel, Yoshinori Nakazawa, Mary G. Reynolds, P. S. Satheshkumar, Ginny L. Emerson, Andrés Páez-Martínez

During 2014, cutaneous lesions were reported in dairy cattle and farmworkers in the Amazon Region of western Colombia. Samples from 6 patients were analyzed by serologic and PCR testing, and results demonstrated the presence of vaccinia virus and pseudocowpox virus. These findings highlight the need for increased poxvirus surveillance in Colombia.

The *Poxviridae* family comprises large double-stranded DNA viruses that infect a wide range of invertebrate and vertebrate animals, including humans (*1*). Many poxviruses, particularly those belonging to the genus *Orthopoxvirus* (e.g., vaccinia virus [VACV]) and *Parapoxvirus* (e.g., pseudocowpox virus [PCPV]), are considered zoonotic viruses because their infections usually arise from human contact with infected domestic or sylvatic animal species (*2*).

Orthopoxviruses (OPXVs) gained considerable attention in the past because variola (smallpox) virus fatally infected millions of persons worldwide for centuries. However, in 1980, smallpox became the first infectious disease to be eradicated, resulting from vaccination campaigns involving several VACV strains (*3*). VACV has been detected in recurrent zoonotic outbreaks in Brazil, where it has been categorized into 2 well-defined genetic lineages (*4*). VACV has also emerged as a zoonotic virus in India (*5*). In 2011, VACV infections were found in cattle herds during active surveillance in Argentina (*6*). In Colombia, the most recently reported VACV outbreak in 1965–1966 caused disease in ≈8,570 cows and 150 humans and was associated with intensified smallpox eradication campaigns that extended until 1972 (*3,7*).

Parapoxviruses are emerging zoonotic pathogens that can cause infections in humans through direct contact with infected animals, especially domestic and wild ruminants (*1*). Among these viruses, bovine papular stomatitis virus, orf virus, and PCPV are known to cause cutaneous lesions (*2*). Although a parapoxvirus outbreak in imported goats was reported in Colombia in 1983 (*8*), only Brazil and the United States have formal evidence of endemic and zoonotic transmission of these viruses (*9,10*). We describe the clinical features, serologic and molecular diagnosis, and phylogenetic analysis of poxviruses circulating along the Amazon in western Colombia.

The Study

During an active outbreak investigation in February–July 2014, serum and exanthematous lesion samples were collected from 6 patients in the bordering municipalities of Valparaíso (patients 1–5) and Solita (patient 6) in the department of Caquetá (Figure 1; Table) in the Amazon Region of Colombia. Archived serum samples collected in December 2012–April 2013 from 11 patients with exanthematous lesions (from several farms) in the municipality of Valparaíso who consulted the local hospital were also analyzed (Table). In all patients, the incubation period ranged from 4–7 days, after which nodules on the hands or forearms appeared, along with fever, lymphadenopathy, and localized pain. Lesions increased in size and progressed from erythematous macules to papules, vesicles, and pustules that subsequently exhibited bacterial infection by the fourth week of symptom onset. By the fifth and sixth week, lesions progressed to scabs (Figure 1). Lesions appeared mainly in hands with preexisting cuts, abrasions, or other skin barrier defects. Direct contact with lesions from the udders of cattle during milking was reported by all but 1 patient. Patient 5 was a 24-year-old woman who reported no recent contact with infected animals, but her husband was a milker who had exanthematous lesions on his hands 2 weeks before she displayed symptoms.

Author affiliations: Instituto Nacional de Salud, Bogotá, Colombia (J.A. Usme-Ciro, A. Paredes, D.M. Walteros, E.N. Tolosa-Pérez, K. Laiton-Donato, A. Páez-Martínez); Universidad Cooperativa de Colombia, Santa Marta, Colombia (J.A. Usme-Ciro); Laboratorio Departamental de Salud de Caquetá, Caquetá, Colombia (M. del Carmen Pinzón); Centers for Disease Control and Prevention, Atlanta, USA (B.W. Petersen, N.F. Gallardo-Romero, Y. Li, K. Wilkins, W. Davidson, J. Gao, N. Patel, Y. Nakazawa, M.G. Reynolds, P.S. Satheshkumar, G.L. Emerson); Universidad de La Salle, Bogotá (A. Páez-Martínez)

DOI: http://dx.doi.org/10.3201/eid2304.161041

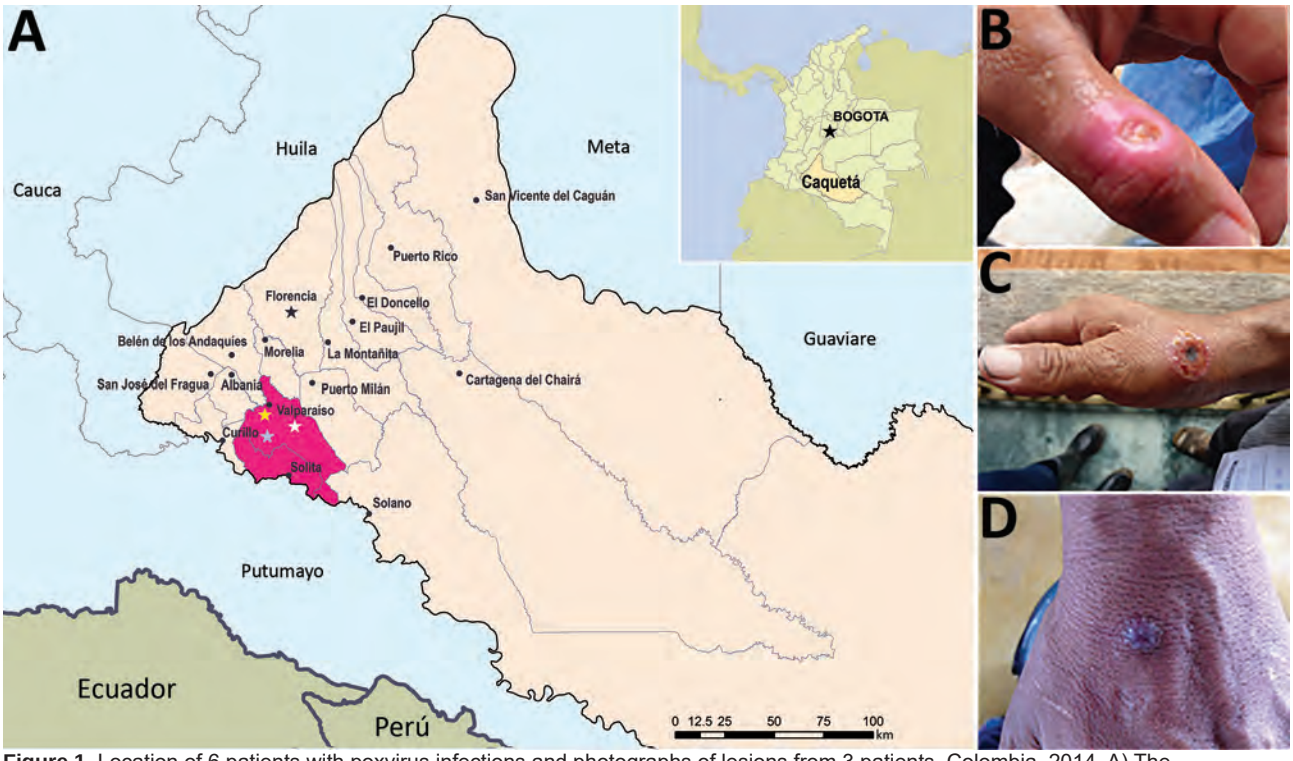

Figure 1. Location of 6 patients with poxvirus infections and photographs of lesions from 3 patients, Colombia, 2014. A) The municipalities of Valparaíso (residence of patients 1–5) and Solita (residence of patient 6) are 36 km apart in the southwestern region of the department of Caquetá. Yellow, white, and blue stars denote locations of patients 2, 3, and 4, respectively. Inset shows location of Caquetá in Colombia. Map source: Departamento Administrativo Nacional de Estadística (http://geoportal.dane.gov.co/). B–D) Exanthematous lesions on the hands of dairy farm workers depicting the varying sizes of lesions and typical evolution of ulcers. Patient 2 (B) tested positive for vaccinia virus, patient 3 (C) had inconclusive results, and patient 4 (D) was positive for parapoxvirus.

All serum samples were tested by ELISA for OPXV IgG and IgM as described (*11*) (online Technical Appendix, https://wwwnc.cdc.gov/EID/article/23/4/16-1041-Techapp1.pdf). An ELISA for detecting parapoxvirus-specific antibodies was not available. Fifteen serum samples were positive for OPXV IgG (Table); 9 were also positive

Table. Orthopoxvirus IgG and IgM antibodies and poxvirus genome detection in lesion and serum samples*

Patient no.	Identification no.	Sex	Age, y	Vaccination status	Municipality	ELISA		Real-time PCR (C_t)	
						IgG†	IgM‡	VACV	Parapoxvirus
1	2014030600020	F	13	Unvaccinated	Valparaíso	Pos (0.176)	Pos (0.408)	Pos (21.8)	Neg
2	2014030600021	F	15	Unvaccinated	Valparaíso	Pos (0.393)	Pos (0.450)	Pos (27.8)	Neg
3	2014030600022	M	46	UNK	Valparaíso	Pos (0.327)	Pos (1.102)	Inc	Inc
4	2014030600023	M	34	Unvaccinated	Valparaíso	Pos (0.166)	Neg	Neg	Pos (36.8)
5	2014042400031 (POX0001)	F	24	Unvaccinated	Valparaíso	Neg	Neg	Pos (21.6)	Neg
6	2014062800100 (POX0002)	M	UNK	UNK	Solita	Neg	Neg	Neg	Pos (35.9)
7	2013050600018	M	26	Unvaccinated	Valparaíso	Pos (0.254)	Pos (0.898)	Neg	Neg
8	2013050600026	M	52	UNK	Valparaíso	Pos (0.213)	Neg	Neg	Neg
9	2013050600019	M	17	Unvaccinated	Valparaíso	Pos (0.261)	Eqi (0.094)	Neg	Neg
10	2013050600020	M	20	Unvaccinated	Valparaíso	Pos (0.384)	Neg	Neg	Neg
11	2013050600021	M	47	UNK	Valparaíso	Pos (0.383)	Pos (0.632)	Neg	Neg
12	2013050600022	M	18	Unvaccinated	Valparaíso	Pos (0.450)	Pos (0.202)	Neg	Neg
13	2013050600027	M	27	Unvaccinated	Valparaíso	Pos (0.224)	Pos (0.243)	Neg	Neg
14	2013050600023	M	24	Unvaccinated	Valparaíso	Pos (0.482)	Neg	Neg	Neg
15	2013050600024	F	12	Unvaccinated	Valparaíso	Pos (0.272)	Pos (0.128)	Neg	Neg
16	2013050600028	M	13	Unvaccinated	Valparaíso	Pos (0.451)	Pos (0.427)	Neg	Neg
17	2013050600025	M	23	Unvaccinated	Valparaíso	Pos (1.651)	Eqi (0.029)	Neg	Neg

*C_t, cycle threshold; eqi, equivocal; inc, inconclusive; neg, negative; pos, positive; UNK, unknown.
†OPXV IgG ELISA titers correspond to a 1:100 dilution of the serum sample.
‡OPXV IgM ELISA titers correspond to a 1:50 dilution of the serum sample.

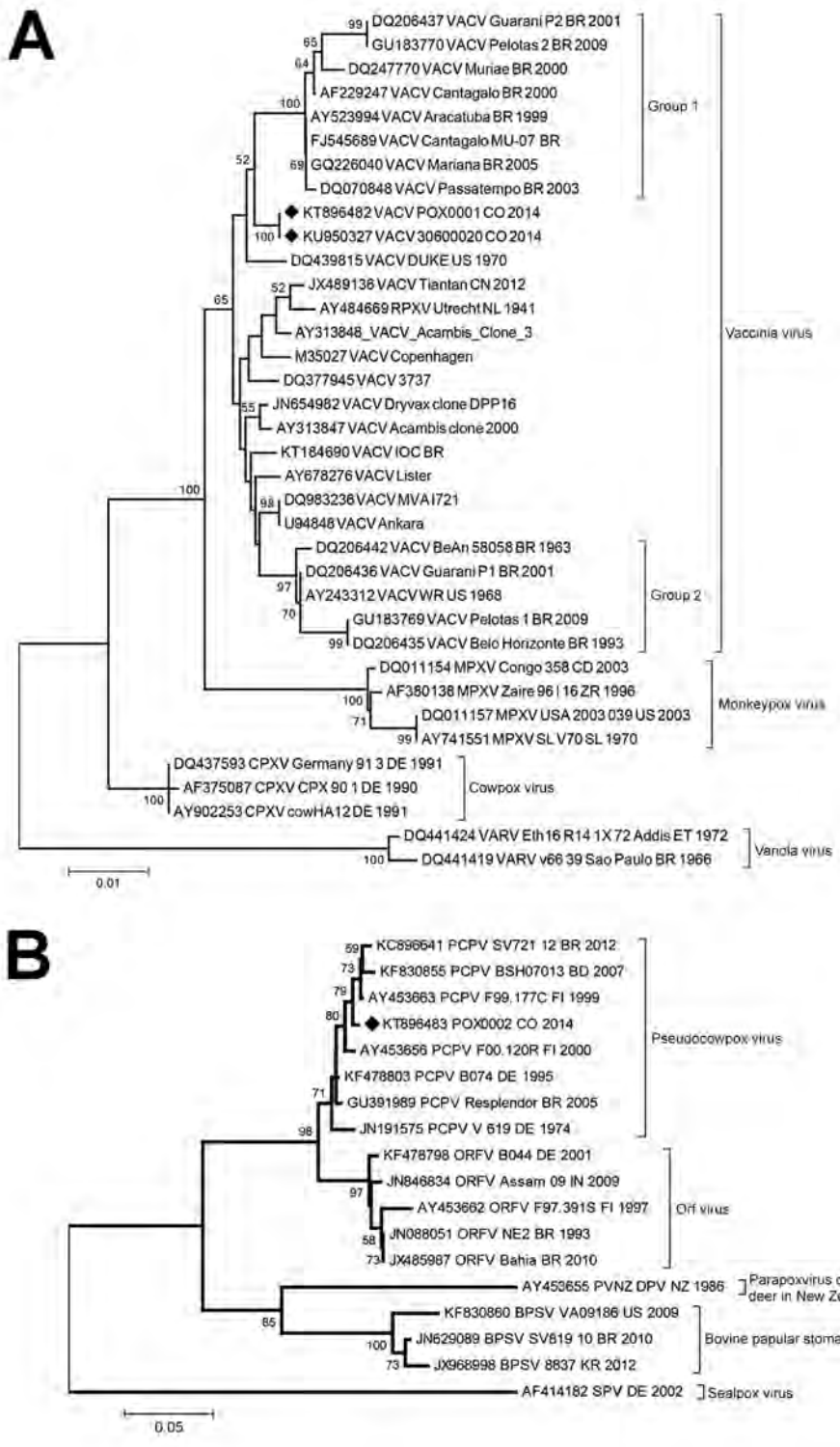

Figure 2. Phylogenetic characterization of orthopoxvirus gene *A56R* and parapoxvirus gene *p37K* of viruses obtained from patient lesion samples from an outbreak in Colombia, 2014. Trees were inferred by the neighbor-joining method. A) Nucleotide sequences of the *A56R* gene (829 bp) of reference orthopoxvirus strains were aligned and used for phylogenetic inference. The evolutionary distances were computed by using the T92+G model (shape: 0.69). Vaccinia virus (VACV) groups 1 and 2 are labeled with brackets. B) Nucleotide sequences of the partial (445 bp) *p37K* gene of reference parapoxvirus strains were aligned and used for phylogenetic inference. The evolutionary distances were computed by using the T92+G model (shape: 0.39). The percentage of replicate trees in which the associated taxa clustered together in the bootstrap test (1,000 replicates) are shown at the nodes. Diamonds indicate poxvirus isolates from Colombia. GenBank accession numbers and further information on the sequences included in the analyses are provided in online Technical Appendix Tables 1, 2 (https://wwwnc.cdc.gov/EID/article/23/4/16-1041-Techapp1.pdf). Scale bars indicate nucleotide substitutions per site. BPSV, bovine papular stomatitis virus; CPXV, cowpox virus; RPXV, rabbitpox virus; MPXV, monkeypox virus; ORFV, orf virus; PCPXV, pseudocowpox virus; PVNZ, parapoxvirus of red deer in New Zealand; SPV, sealpox virus; VARV, variola virus.

for OPXV IgM, which can persist for up to 6 months after primary infection or vaccination (*11*). Reliable vaccination data was not available for these patients; however, on the basis of age, only patients 3, 8, and 11 could have been vaccinated. These 3 patients exhibited detectable OPXV IgG levels, and patients 3 and 11 were also positive for OPXV IgM. These results suggest that these patients had not been vaccinated and that their lesions were caused by recent OPXV exposure. Patients 4, 10, and 14 exhibited detectable OPXV IgG without detectable OPXV IgM. These results suggest

the patients had previous OPXV infections, given that an active parapoxvirus infection was demonstrated in patient 4 and vaccination could be ruled out for patients 10 (a 20-year-old) and 14 (a 24-year-old) based on their age.

DNA was extracted from lesion and serum samples by using the PureLink viral RNA/DNA extraction kit (Invitrogen Inc., Carlsbad, CA, USA) according to the manufacturer's instructions and amplified by using PCR with generic and specific poxvirus primers as previously described (online Technical Appendix) (*12*). OPXV DNA was detected in lesion samples from patients 1, 2, and 5 (Table). For further genetic characterization, the *A56R* (hemagglutinin, 1,134 bp) gene from patients 2 and 5 were amplified by PCR, sequenced (online Technical Appendix), and compared with reference orthopoxvirus *A56R* sequences (online Technical Appendix Table 1). Our phylogenetic analysis confirmed VACV to be the etiologic agent of infection in these patients (Figure 2, panel A). The OPXV isolates detected in our samples were related to group 1 (Passatempo, Aracatuba, Muriae, and other strains from Brazil); however, bootstrap score and branch positioning suggest the strains from Brazil and Colombia diverged long ago or independently arose.

For parapoxvirus detection and characterization, we designed generic and degenerate primers to amplify a partial sequence of the *p37K* (envelope protein B2L, 489 bp) gene by PCR (online Technical Appendix). Parapoxvirus DNA was detected in lesion samples from patients 4 and 6 (Table). Nucleotide sequencing and phylogenetic analysis of the sample from patient 6 showed a close relationship with previously reported PCPV strains circulating in Brazil and worldwide (online Technical Appendix Table 2; Figure 2, panel B).

Conclusions

We found OPXV IgG and IgM in serum samples collected from patients with exanthematous lesions and from those who had such lesions in the past. Molecular methods allowed for the detection and characterization of VACV (3 patients) and PCPV (2 patients). Lesions caused by poxviruses affected the hands and forearms and disappeared within weeks without treatment. However, by limiting the patients' daily activities, the infections had substantial negative impacts on the economies of dairy farmworkers and their local communities.

The disease burden of poxvirus infections in Colombia has not been estimated. However, anecdotal communications and data suggest it might be a serious and increasing health problem because farmworkers and healthcare personnel are not trained to recognize the disease and prevent subsequent transmission. The rapid spread of poxviruses could be facilitated by farmworkers performing daily milking activities at several farms and trading cattle. Also, factors such as human-to-human and fomite transmission, a growing susceptible population, and an unknown animal reservoir might increase the potential risk for infection at the community level. The serious consequences that poxvirus infections could have on immunocompromised persons (*13*), the increased risk for transmission related to the anatomic site of the lesions (*14*), the potential for long-lasting sequelae, and the possibility of the virus evolving into a more virulent strain (*15*) could pose a great threat to individual persons, populations, and public health systems in the near future.

Studies focused on determining the prevalence of poxvirus infections, risk factors for disease, and the geographic distribution of poxvirus strains are needed to understand the disease burden and guide effective prevention and control measures and educational outreach. Analysis and characterization of VACV and PCPV complete genomes could provide clues to explain their emergence and recent evolutionary histories, and research aimed at identifying the domestic animal hosts and wildlife reservoirs of poxviruses could further our understanding of their natural transmission cycles.

Dr. Usme-Ciro was the founder of the Unit of Sequencing and Genomics at the National Institute of Health in Colombia. His research is focused on molecular virology, specifically on molecular epidemiology, evolution and emergence of viruses of public health relevance in Colombia, and the study of viral determinants of disease severity.

References

1. Damon IK. Poxviruses. In: Knipe DM, Howley PM, editors. Fields virology. New York: Lippincott Williams & Wilkins; 2007.
2. Lewis-Jones S. Zoonotic poxvirus infections in humans. Curr Opin Infect Dis. 2004;17:81–9. http://dx.doi.org/10.1097/00001432-200404000-00003
3. Fenner F, Henderson DA, Arita I, Jezek A, Ladnyi ID. Smallpox and its eradication. Geneva: World Health Organization Press; 1988.
4. Oliveira DB, Assis FL, Ferreira PC, Bonjardim CA, de Souza Trindade G, Kroon EG, et al. Group 1 vaccinia virus zoonotic outbreak in Maranhao state, Brazil. Am J Trop Med Hyg. 2013;89:1142–5. http://dx.doi.org/10.4269/ajtmh.13-0369
5. Bhanuprakash V, Venkatesan G, Balamurugan V, Hosamani M, Yogisharadhya R, Gandhale P, et al. Zoonotic infections of buffalopox in India. Zoonoses Public Health. 2010;57:e149–55. http://dx.doi.org/10.1111/j.1863-2378.2009.01314.x
6. Franco-Luiz AP, Fagundes-Pereira A, Costa GB, Alves PA, Oliveira DB, Bonjardim CA, et al. Spread of vaccinia virus to cattle herds, Argentina, 2011. Emerg Infect Dis. 2014;20:1576–8. http://dx.doi.org/10.3201/eid2009.140154
7. Gómez Pando V, Hernán López J, Restrepo A, Forero P. Study of an outbreak of vaccinia in dairy cattle of their milkers [in Spanish]. Bol Oficina Sanit Panam. 1967;63:111–21.
8. Rodríguez G, Moreno O, Mogollón JD, Latorre S, Cortés E. ORF: un brote en cabras importadas. Biomedica. 1983;3:49–57. http://dx.doi.org/10.7705/biomedica.v3i3.1861
9. Schatzmayr HG, Lemos ER, Mazur C, Schubach A, Majerowicz S, Rozental T, et al. Detection of poxvirus in cattle associated with human cases in the state of Rio de Janeiro: preliminary report. Mem Inst Oswaldo Cruz. 2000;95:625–7. http://dx.doi.org/10.1590/S0074-02762000000500007

10. Delhon G, Tulman ER, Afonso CL, Lu Z, de la Concha-Bermejillo A, Lehmkuhl HD, et al. Genomes of the parapoxviruses orf virus and bovine papular stomatitis virus. J Virol. 2004;78:168–77. http://dx.doi.org/10.1128/JVI.78.1.168-177.2004
11. Karem KL, Reynolds M, Braden Z, Lou G, Bernard N, Patton J, et al. Characterization of acute-phase humoral immunity to monkeypox: use of immunoglobulin M enzyme-linked immunosorbent assay for detection of monkeypox infection during the 2003 North American outbreak. Clin Diagn Lab Immunol. 2005;12:867–72.
12. Li Y, Meyer H, Zhao H, Damon IK. GC content-based pan-pox universal PCR assays for poxvirus detection. J Clin Microbiol. 2010;48:268–76. http://dx.doi.org/10.1128/JCM.01697-09
13. Redfield RR, Wright DC, James WD, Jones TS, Brown C, Burke DS. Disseminated vaccinia in a military recruit with human immunodeficiency virus (HIV) disease. N Engl J Med. 1987;316:673–6. http://dx.doi.org/10.1056/NEJM198703123161106
14. Lewis FMT, Chernak E, Goldman E, Li Y, Karem K, Damon IK, et al. Ocular vaccinia infection in laboratory worker, Philadelphia, 2004. Emerg Infect Dis. 2006;12:134–7. http://dx.doi.org/10.3201/eid1201.051126
15. Shchelkunov SN. An increasing danger of zoonotic orthopoxvirus infections. PLoS Pathog. 2013;9:e1003756. http://dx.doi.org/10.1371/journal.ppat.1003756

Address for correspondence: Andrés Páez-Martínez, Departamento de Ciencias Básicas, Universidad de La Salle, Calle 2 Nº 10-70, Bogotá, Colombia; email: apaez@unisalle.edu.co

Reassortment of Influenza A Viruses in Wild Birds in Alaska before H5 Clade 2.3.4.4 Outbreaks

Nichola J. Hill, Islam T.M. Hussein, Kimberly R. Davis, Eric J. Ma, Timothy J. Spivey, Andrew M. Ramey, Wendy Blay Puryear, Suman R. Das, Rebecca A. Halpin, Xudong Lin, Nadia B. Fedorova, David L. Suarez, Walter M. Boyce, Jonathan A. Runstadler

Sampling of mallards in Alaska during September 2014–April 2015 identified low pathogenic avian influenza A virus (subtypes H5N2 and H1N1) that shared ancestry with highly pathogenic reassortant H5N2 and H5N1 viruses. Molecular dating indicated reassortment soon after interhemispheric movement of H5N8 clade 2.3.4.4, suggesting genetic exchange in Alaska or surrounds before outbreaks.

The emergence of highly pathogenic avian influenza (HPAI) A virus subtype H5 of clade 2.3.4.4 in East Asia followed by spread into North America in 2014 highlights the importance of ecologic interactions along the Pacific Rim to the incursion of novel viruses. Introduction of influenza A subtype H5N8 into North America is hypothesized to have occurred through wild bird movement across the Bering Strait (*1*,*2*); the virus then spread through Canada to the continental United States, concurrently infecting wild birds (ducks, geese, passerines, and raptors) and poultry (turkeys and chickens) (*3*). Reassortment of H5N8 with low pathogenic avian influenza (LPAI) A virus in North America generated 3 subtypes (H5N8, H5N2, and H5N1, collectively referred to as H5Nx) that followed different trajectories in local bird populations. HPAI H5N2 became the most widespread in US poultry, prompting the culling of ≈49 million chickens and turkeys in 15 states (*4*). During the outbreaks (November 2014–December 2015), surveillance efforts increased; consequently, later stages of the epidemic were better characterized (*5*,*6*) relative to the beginning. Analysis of wild bird viruses from Alaska preceding outbreaks remains one of the few avenues for elucidating how H5N8 entered and reassorted with North American lineage viruses.

Our sampling of mallards (*Anas platyrhynchos*) from urban ponds in Anchorage, Alaska, during September 2014–April 2015 identified LPAI H5N2 and H1N1 (online Technical Appendix Figure 1, Table 1, https://wwwnc.cdc.gov/EID/article/23/4/16-1668-Techapp1.pdf). These viruses were the closest relatives for 4 of the 8 North American segments that contributed to the H5Nx reassortants based on the time of most recent common ancestry (tMRCA) analysis (online Technical Appendix Figures 2–12). All North American segments of the H5N2 reassortant (basic polymerase protein 1, nucleoprotein, and neuraminidase) shared most recent common ancestry with LPAI H5N2 that circulated in Anchorage mallards and a concurrently sampled wild bird population at Izembek National Wildlife Refuge in western Alaska (*1*) (online Technical Appendix Figures 3, 5, 8, 9). Molecular dating indicated reassortment of H5N8 and LPAI H5N2 (or precursors) shortly after the interhemispheric movement of H5N8. We estimated that ancestors of the H5N2 reassortant emerged among wild birds in Alaska during August 2013–May 2014, based on tMRCAs of multiple segments (Figure 1, panel A), followed by emergence of the H5N2 reassortant during May–September 2014. Our analysis refines the hypothesis of Beringia introduction (*1*,*2*) by indicating that H5N8 reassorted with viruses shed by waterfowl in Alaska (or nearby high latitudes) shortly after introduction into North America (May 2014–October 2014, 95% highest posterior density January 2014–January 2015) (Figure 1, panel A). Accuracy of molecular dating hinges on the availability of virus sequences from relevant hosts, which were lacking from North American poultry and wild birds during the year preceding outbreaks (Figure 1, panel B). Our sampling was fortuitous, being one of the few in Alaska conducted before the outbreaks, underscoring the importance of routine sampling where interhemispheric mixing of viruses occurs with high frequency.

The rapid reassortment of H5N8 clade 2.3.4.4 within North America is premised on the movement of at least a single infected bird across the Bering Strait followed by

Author affiliations: Massachusetts Institute of Technology, Cambridge, Massachusetts, USA (N.J. Hill, I.T.M. Hussein, K.R. Davis, E.J. Ma, W.B. Puryear, J.A. Runstadler); University of Alaska Fairbanks, Alaska, USA (T.J. Spivey); US Geological Survey, Anchorage, Alaska, USA (T.J. Spivey, A.M. Ramey); Vanderbilt University Medical Center, Nashville, Tennessee, USA (S. Das); J. Craig Venter Institute, Rockville, Maryland, USA (R.A. Halpin, X. Lin, N.B. Fedorova); US Department of Agriculture, Athens, Georgia, USA (D.L. Suarez); University of California, Davis, California, USA (W.M. Boyce)

DOI: http://dx.doi.org/10.3201/eid2304.161668

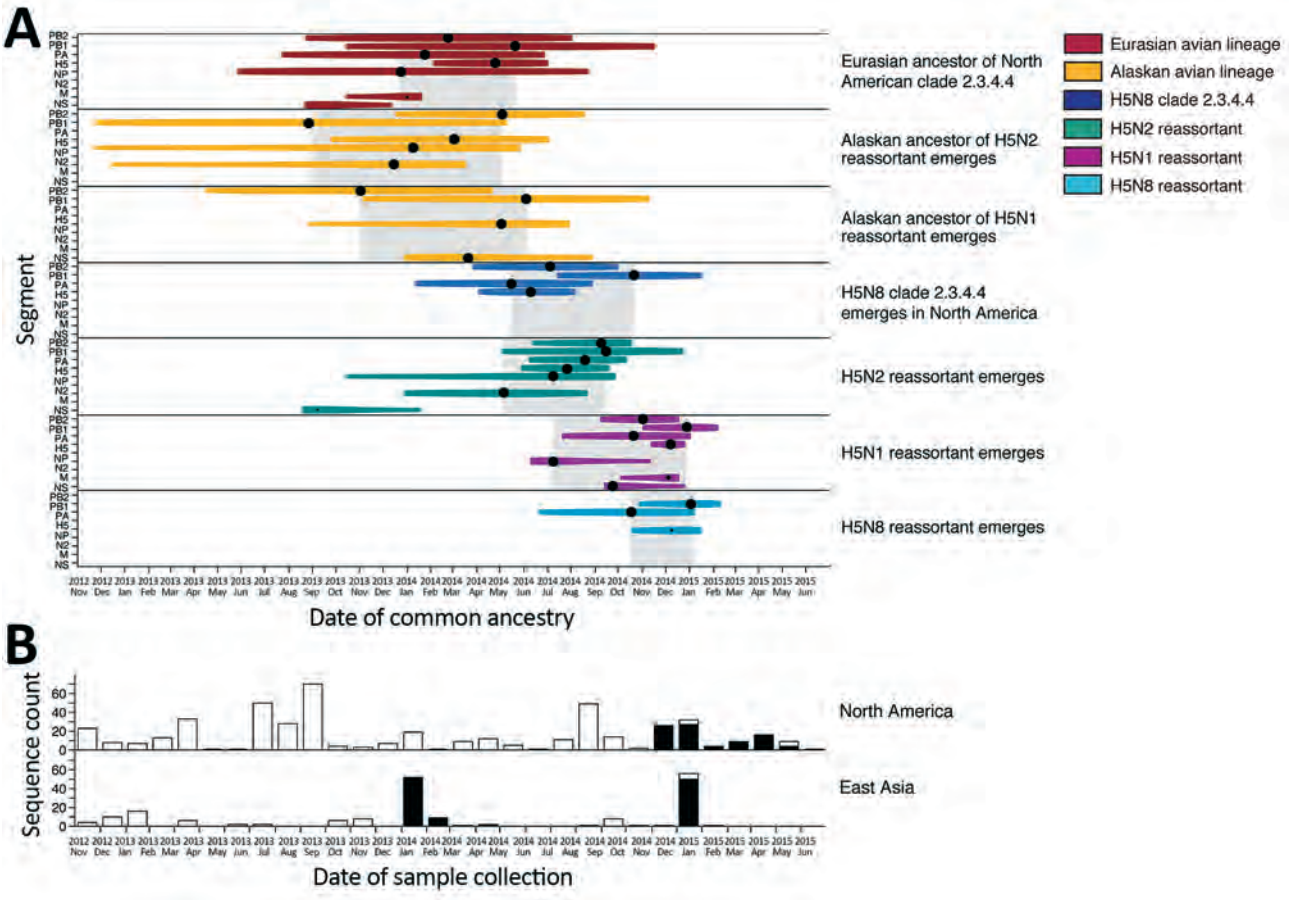

Figure 1. Molecular dating of the emergence of H5 clade 2.3.4.4 influenza A virus in Eurasia and North America and concurrent trends in surveillance effort. A) Events contributing to the evolution of H5 clade 2.3.4.4 estimated using multiple influenza segments. Time of most recent common ancestry (indicated by a black circle) is size-scaled by the posterior probability (0.0–1.0), and the 95% highest posterior density is color-coded by lineage. Gray shading indicates time of most recent common ancestry of multiple segments with a posterior probability >0.85. B) Surveillance effort estimated by the number of hemagglutinin sequences (high and low pathogenicity) available in the Influenza Research Database (https://www.fludb.org). Black bars indicate surveillance effort for H5 clade 2.3.4.4; white bars indicate surveillance effort for other clades. M, matrix gene; N2, neuraminidase 2 gene; NP, nucleoprotein gene; PA, polymerase acidic, PB1, basic polymerase protein 1 gene; PB2, basic polymerase protein 2 gene; tMRCA, time of most recent common ancestry.

infection of a host population at high latitude. Interhemispheric movement during spring 2014 (or earlier) is most plausible given the circulation of the Eurasian ancestor of North American clade 2.3.4.4 during December 2013–May 2014 (95% highest posterior density October 2013–January 2015) (Figure 1, panel A), an event that preceded introduction. The presence of overwintering birds in Alaska, a known area for influenza exchange between East Asia and North America (*7*,*8*), might enhance opportunities for viruses originating in Eurasia to reassort with LPAI in local bird populations. Mallards from this study are a prime example of an overwintering population, occupying urban ponds that remained thawed because of human activity, which allows some birds to remain in southcentral Alaska from September through April, when many migratory waterfowl have since flown south. We found evidence that LPAI H5N2 shed by overwintering mallards from Anchorage (south-central Alaska) and wild birds from Izembek (western Alaska) were highly related and formed monophyletic clades (online Technical Appendix Figures 5, 6, 8–10). This provided evidence of regional dispersal of LPAI in Alaska concurrent with the proposed timing of H5N8 introduction and reassortment.

Anchorage mallards shed viruses that shared ancestry with 2 of 4 North American segments (basic polymerase protein 1 and nonstructural) of the H5N1 reassortant (online Technical Appendix Figures 2, 5, 12). Emergence of the H5N1 reassortant probably occurred after July 2014 (Figure 1, panel A), after the H5N2 reassortant emerged. Molecular dating of tMRCA of H5N8 reassortants was confounded by long branch lengths of parental lineages indicative of unsampled ancestors; however, estimates based

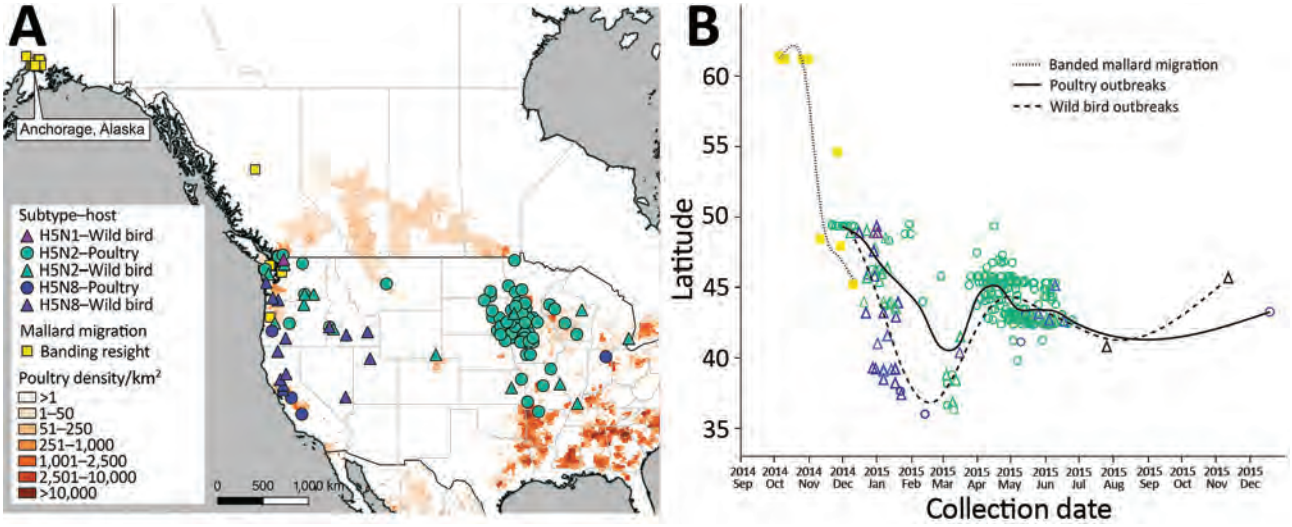

Figure 2. Spatial and temporal distribution of H5 clade 2.3.4.4 influenza A virus outbreaks among wild birds and poultry across North America. A) Spatial distribution of H5 clade 2.3.4.4 influenza A virus outbreaks in wild birds (triangles) and poultry (circles) across North America, color-coded by subtype, relative to poultry density. The location of mallards from Anchorage, Alaska, based on resighting of banded birds, is indicated. B) Temporal distribution of H5 clade 2.3.4.4 influenza A virus detections during the course of the outbreaks relative to the migration of mallards banded in Anchorage.

on 2 segments suggest emergence after October 2014. The H5N1 and H5N8 reassortants possessed a highly similar polymerase acidic segment (online Technical Appendix Figure 6), suggesting a similar evolutionary trajectory of the two subtypes that later diverged. Our tMRCA estimates for H5N1 are consistent with reassortment during or after the breeding season for mallards in Alaska followed by southward dispersal along the Pacific Flyway during autumn (Figure 2). These results suggest that H5N1 is a multiple reassortant that acquired PB1 and NS segments in Alaska (or surrounds) followed by polymerase acidic and neuraminidase 2 from different host populations before detection in Washington (*9*) and Oregon (*4*) in early 2015.

Arrival of mallards banded in Anchorage at the high-density poultry region of the Fraser Valley, British Columbia, Canada, in November 2014 is compatible with the chronology of evolution and subsequent detection of the H5Nx subtypes (Figure 2). The migration chronology of banded mallards might be broadly representative of other dabbling duck species that breed in Alaska, such as the American green-winged teal (*Anas carolinensis*), American wigeon (*Anas americana*), and northern pintail (*Anas acuta*), in which H5Nx was detected at lower latitudes. Consequently, mallards and other waterfowl species probably were involved in the southward dispersal and reassortment of H5Nx followed by spillover to poultry. Observations of wild birds congregating at water bodies on poultry farms in the Fraser Valley support the scenario of indirect transmission from migratory birds to poultry, seeding outbreaks at lower latitudes (*10*). Later divergence of H5N2 into multiple lineages during May–November 2014 (online Technical Appendix Figure 8) implies that outbreaks were seeded by different H5N2 strains, although the mode of dispersal through wild bird migration, farm-to-farm poultry movement, or poultry workers remains unclear.

Since introduction of HPAI H5 of clade 2.3.4.4 into the Pacific Northwest in late 2014, little evidence exists for additional reassortment, despite continued spread of H5N2 and H5N8 until late 2015 (Figure 2, panel B). Lack of further reassortment implies a change from wild bird–mediated dispersal to intermittent spillover between wild birds and poultry or indirect transmission among poultry farms via fomites, wind, or other undetermined vectors. The spatiotemporal pattern of outbreaks in wild birds and poultry appeared correlated during this later phase (Figure 2, panel B). Correlation might be a function of outbreak investigation procedures that require concurrent sampling of poultry and wild birds inhabiting the control zone. However, our phylogenetic analysis lends support for frequent spillover given that lineages of H5Nx were mixed by host, rather than poultry and wild birds clustering separately (online Technical Appendix Figures 4–12). Our analysis and the August 2016 detection of HPAI H5N2 in mallards from Fairbanks, Alaska (*11*), an area lacking commercial poultry, implicates waterfowl as playing an important role in reassortment, spread, and possibly long-term circulation of H5Nx viruses.

This study was supported by the National Institutes of Health Center of Excellence in Influenza Research and Surveillance (contract no. HHSN272201400008C) and the J. Craig Venter

Institute Genomic Centers for Infectious Diseases Program (NIH/NIAID grant no. U19 AI110819).

Capture and processing of wild mallards was approved by the Institutional Animal Care and Use Committee at the University of Alaska Fairbanks (protocol no. 358515-11/662280-3) and was authorized by US Federal Bird Banding and Marking Permits (nos. 08350 and 23191). None of the authors have any financial interests or conflict of interest with this article. Any use of trade names is for descriptive purposes only and does not imply endorsement by the U.S. Government. The content is solely the responsibility of the authors and does not necessarily represent the official views of the NIH.

Dr. Hill is a postdoctoral associate at the Massachusetts Institute of Technology, Cambridge, Massachusetts, USA. Her primary research interests include the ecology and evolution of influenza viruses in natural and man-made systems.

References

1. Ramey AM, Reeves AB, TeSlaa JL, Nashold S, Donnelly T, Bahl J, et al. Evidence for common ancestry among viruses isolated from wild birds in Beringia and highly pathogenic intercontinental reassortant H5N1 and H5N2 influenza A viruses. Infect Genet Evol. 2016;40:176–85. http://dx.doi.org/10.1016/j.meegid.2016.02.035
2. Lee DH, Torchetti MK, Winker K, Ip HS, Song CS, Swayne DE. Intercontinental spread of Asian-origin H5N8 to North America through Beringia by migratory birds. J Virol. 2015;89:6521–4. http://dx.doi.org/10.1128/JVI.00728-15
3. US Department of Agriculture. Avian influenza disease. Animal disease information. Avian health [cited 2016 Aug 5]. https://www.aphis.usda.gov/aphis/ourfocus/animalhealth/animal-disease-information/avian-influenza-disease
4. Lee DH, Bahl J, Torchetti MK, Killian ML, Ip HS, DeLiberto TJ, et al. Highly pathogenic avian influenza viruses and generation of novel reassortants, United States, 2014–2015. Emerg Infect Dis. 2016;22:1283–5. http://dx.doi.org/10.3201/eid2207.160048
5. Krauss S, Stallknecht DE, Slemons RD, Bowman AS, Poulson RL, Nolting JM, et al. The enigma of the apparent disappearance of Eurasian highly pathogenic H5 clade 2.3.4.4 influenza A viruses in North American waterfowl. Proc Natl Acad Sci U S A. 2016;113:9033–8. http://dx.doi.org/10.1073/pnas.1608853113
6. Bevins SN, Dusek RJ, White CL, Gidlewski T, Bodenstein B, Mansfield KG, et al. Widespread detection of highly pathogenic H5 influenza viruses in wild birds from the Pacific Flyway of the United States. Sci Rep. 2016;6:28980. http://dx.doi.org/10.1038/srep28980
7. Pearce JM, Reeves AB, Ramey AM, Hupp JW, Ip HS, Bertram M, et al. Interspecific exchange of avian influenza virus genes in Alaska: the influence of trans-hemispheric migratory tendency and breeding ground sympatry. Mol Ecol. 2011;20:1015–25. http://dx.doi.org/10.1111/j.1365-294X.2010.04908.x
8. Ramey AM, Pearce JM, Ely CR, Guy LM, Irons DB, Derksen DV, et al. Transmission and reassortment of avian influenza viruses at the Asian-North American interface. Virology. 2010;406:352–9. http://dx.doi.org/10.1016/j.virol.2010.07.031
9. Torchetti MK, Killian ML, Dusek RJ, Pedersen JC, Hines N, Bodenstein B, et al. Novel H5 Clade 2.3.4.4 reassortant (H5N1) virus from a green-winged teal in Washington, USA. Genome Announc. 2015;3:e00195–15. http://dx.doi.org/10.1128/genomeA.00195-15
10. Xu W, Berhane Y, Dubé C, Liang B, Pasick J, VanDomselaar G, et al. Epidemiological and evolutionary inference of the transmission network of the 2014 highly pathogenic avian influenza H5N2 outbreak in British Columbia, Canada. Sci Rep. 2016;6:30858. http://dx.doi.org/10.1038/srep30858
11. Lee D, Torchetti MK, Killian M, DeLiberto TJ, Swayne DE. Reoccurrence of avian influenza A(H5N2) virus clade 2.3.4.4 in wild birds, Alaska, USA, 2016. Emerg Infect Dis. 2017;23:365–7. http://dx.doi.org/10.3201/eid2302.161616

Address for correspondence: Jonathan A. Runstadler, Massachusetts Institute of Technology, Building 16-873, 77 Massachusetts Ave, Cambridge, MA 02139, USA; email: jrun@mit.edu

Incidence and Characteristics of Scarlet Fever, South Korea, 2008–2015

Duck Woong Park, Sun-Hee Kim, Jung Wook Park, Min-Ji Kim, Sun Ju Cho, Hye Jung Park, So Hyang Jung, Mi Hee Seo, Yong Seok Lee, Byung Hee Kim, Hyeran Min, Su Ya Lee, Dong Ryong Ha, Eun Sun Kim, Yeongjin Hong,[1] Jae Keun Chung[1]

The incidence rate for scarlet fever in South Korea is rising. During 2008–2015, we collected group A *Streptococcus* isolates and performed *emm* and exotoxin genotyping and disk-diffusion antimicrobial tests. Scarlet fever in South Korea was most closely associated with *emm* types *emm*4, *emm*28, *emm*1, and *emm*3. In 2015, tetracycline resistance started increasing.

Scarlet fever is a common disease caused by group A *Streptococcus* (GAS; also known as *Streptococcus pyogenes*). In the Far East and the United Kingdom, the incidence of scarlet fever has been increasing since 2008 (*1*–*3*), and according to the Infectious Disease Statistics System of Korea, the incidence rate for scarlet fever in South Korea increased from 0.3 cases/100,000 persons in 2008 to 13.7 cases/100,000 persons in 2015 (https://is.cdc.go.kr/dstat/index.jsp).

Several antimicrobial drugs, including β-lactams and tetracyclines, effectively treat scarlet fever, and macrolides and lincosamides can be used in patients with penicillin (β-lactam) allergy (*4*,*5*). However, resistance to erythromycin and clindamycin has been reported for GAS isolates in mainland China and Hong Kong, China (*2*,*3*). The streptococcal M protein and exotoxins are 2 of several virulence factors in GAS (*6*). The streptococcal M protein is a long fimbrial adhesion protein encoded by >220 M protein gene sequence types (*emm* types). Because of the high genetic variability of *emm*, which varies by geographic region, molecular *emm* genotyping is mandatory for epidemiologic investigations of GAS infections (*7*). The incidence of these infections is closely related to variations in the predominance of certain *emm* types (*7*). *spe*A and *spe*C, which are 2 of 11 genes encoding for superantigens found in GAS, are often associated with scarlet fever (*8*). Our objective was to identify the overall trend in the annual incidence and characteristics of scarlet fever in South Korea by studying its upsurge in Gwangju, South Korea, because incidence during the past 8 years was highest for this city (https://is.cdc.go.kr/dstat/index.jsp).

The Study

The incidence of scarlet fever in the Gwangju metropolitan area is the highest among all South Korea cities (61.5 cases/100,000 persons); according to the Korean Disease Web Statistics System, the national incidence from 2008 through 2015 was 36.9 cases/100,000 persons (https://is.cdc.go.kr/dstat/index.jsp). Incidence of scarlet fever in South Korea began to increase in 2011 (Figure 1, panel A), coinciding with an outbreak of scarlet fever in China and Hong Kong. Scarlet fever mainly occurs during the late fall, winter, and early spring. Our study results indicate that the incidence of scarlet fever in South Korea peaks in the winter; however, it also peaked in the summers of 2011 and 2015 (Figure 1, panel B).

During 2008–2015, we collected 1,460 pharyngeal swab samples from patients suspected of having scarlet fever from 8 major hospitals in the Gwangju metropolitan area. We tested the β-hemolytic isolates for susceptibility to bacitracin (0.04 U) and for streptococcal grouping; a total of 705 samples were positive for GAS.

Because variation in the circulating *emm* types could contribute to the incidence of disease and changes in the epidemiology of scarlet fever, we determined the *emm* sequence type for the 705 samples by using a standard protocol (https://www.cdc.gov/streplab/protocol-emm-type.html) (*2*). A total of 11 different *emm* sequence types were identified (Figure 2, panels A and B). *emm*4 (35.6%, 251/705) was the most predominant. The other 3 predominant *emm* types were *emm*28 (14.8%, 104/705), *emm*1 (14.5%, 102/705), and *emm*3 (11.6%, 82/705), and these 4 *emm* types accounted for ≈76.5% (539/705) of all isolates. These results differed from those of previous studies in mainland China and Hong Kong, where the outbreaks of scarlet fever were caused mainly by *emm*12 (*2*,*3*). Our results showed that

Author affiliations: Health and Environment Research Institute of Gwangju, Gwangju, South Korea (D.W. Park, S.-H. Kim, J.W. Park, M.-J. Kim, S.J. Cho, H.J. Park, S.H. Jung, M.H. Seo, Y.S. Lee, D.R. Ha, E.S. Kim, J.K. Chung); Mirae Children's Hospital (NamGu), Gwangju (B.H. Kim); Jungang Children's Hospital, Gwangju (H. Min); Yesarang Pediatric Clinic, Gwangju (S.Y. Lee); Chonnam National University Medical School, Gwangju (D.W. Park, Y. Hong)

DOI: http://dx.doi.org/10.3201/eid2304.160773

[1]These authors contributed equally to this article.

*emm*3 in 2011 (the year incidence began increasing in South Korea) and *emm*1 and *emm*28 in 2015 (the year of a sharp increase in incidence) played major roles in the epidemics in the Gwangju metropolitan area (Figure 2, panel A). To our knowledge, *emm*3 has not been reported to be prevalent in other Asian countries but has been associated with scarlet fever in the United Kingdom (*9*).

Scarlet fever is a toxin-mediated disease (*10*). Therefore, we tested all isolates for the presence of the *spe*A and *spe*C genes by using PCR and previously reported primer pairs and reaction conditions (*8*). We found isolates that harbored *spe*A (57/705, 8.1%), *speC* (249/705, 35.3%), and both (3/705, 0.4%). The exotoxin gene detection rate differed by *emm* gene type. The isolates positive for *spe*A were predominantly *emm*1 (56.1%, 32/57) and *emm*28 (28.1%, 16/57); the other *emm* types made up only 15.8% (9/57). When we examined the reverse association, 31.4% (32/102) of *emm*1 isolates and 15.4% (16/104) of *emm*28 isolates were positive for *spe*A; in contrast, only 1.8% (9/499) of the other *emm* types were positive for *spe*A. The main *emm* types identified in the *spe*C-positive isolates were *emm*4 (68.7%, 171/249), *emm*75 (10.8%, 27/249), and *emm*28 (6.4%, 16/249); 68.1% (171/251) of *emm*4, 67.5% (27/40) of *emm*75, and 15.4% (16/104) of *emm*28 isolates were positive for *spe*C. Only 11.3% (35/310) of the other *emm* types were positive for *spe*C. Therefore, *spe*A and *spe*C exotoxin genes were more prevalent in bacteria of certain *emm* types ($p<0.01$).

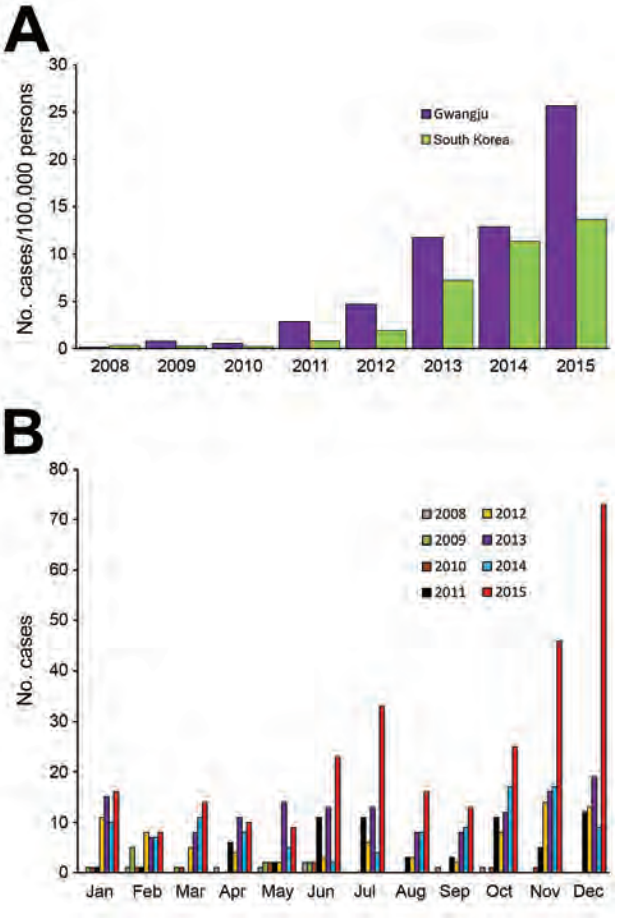

Figure 1. Incidence of scarlet fever in Gwangju, South Korea, 2008–2015. A) The number of cases per 100,000 persons in Gwangju and South Korea. B) Distribution of cases by month of each year.

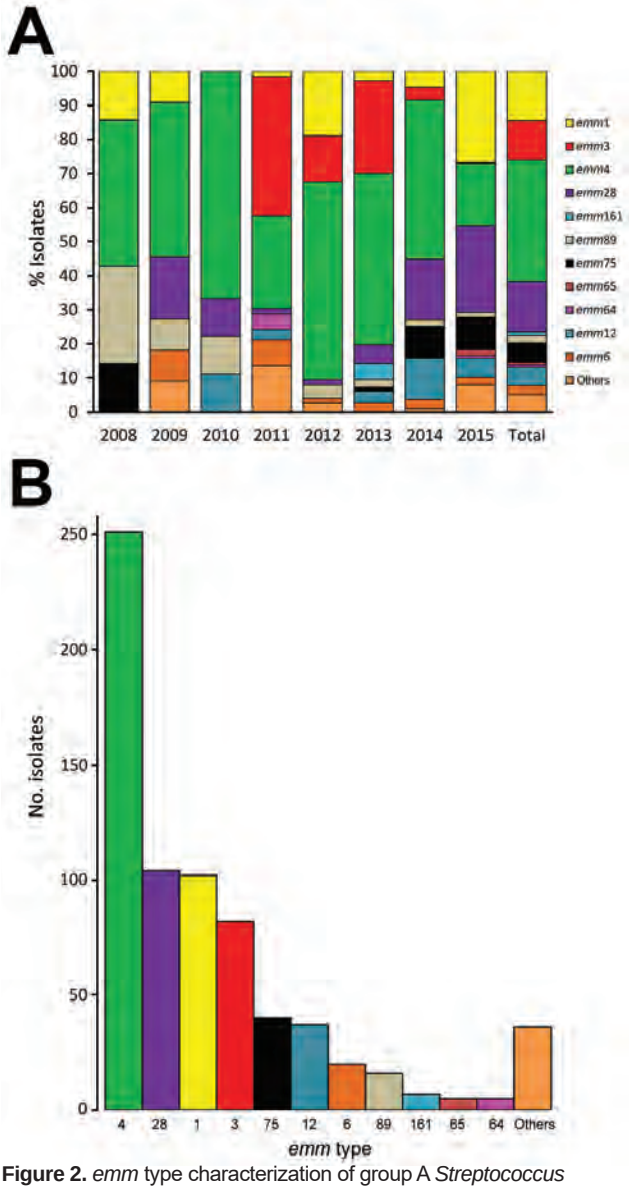

Figure 2. *emm* type characterization of group A *Streptococcus* isolates from patients with scarlet fever, Gwangju, South Korea, 2008–2015. A) Annual fluctuations of *emm* types. Number of isolates by year: 7 in 2008, 11 in 2009, 9 in 2010, 66 in 2011, 74 in 2012, 147 in 2013, 107 in 2014, and 284 in 2015. B) Total number of isolates by *emm* type. Others refers to rarely found *emm* types (*emm*11, *emm*13, *emm*17, *emm*23, *emm*26, *emm*30, *emm*31, *emm*43, *emm*49, *emm*59, *emm*81, *emm*82, *emm*87, *emm*101, *emm*107, *emm*131, *emm*135, *emm*161, *emm*163, *emm*174, *emm*183, *emm*196, *emm*203, *emm*204, *emm*227, *emm*236, and *emm*241).

GAS remains universally susceptible to β-lactams and glycopeptides. However, the rates of resistance against the macrolides and lincosamides used in penicillin-allergic patients have increased (*11*). We performed susceptibility tests by using the disk-diffusion method as recommended by the Clinical and Laboratory Standards Institute (*12*). For all samples collected 2008–2015, the antimicrobial agents chloramphenicol, tetracycline, erythromycin, and clindamycin were tested. Resistance to antimicrobial drugs was detected in 9.1% (64/705) of isolates: 0.3% of the isolates (2/705) showed resistance to chloramphenicol, 7.0% (49/705) to tetracycline, 3.0% (21/705) to erythromycin, and 2.8% (20/705) to clindamycin (Table).

In some isolates, antimicrobial drug resistance is tightly correlated with specific *emm* types (*13*). Resistance to erythromycin, clindamycin, and tetracycline is common in bacteria with the *emm*28 gene. In our study, 18/104 (17.3%) isolates that harbored *emm*28 were resistant to erythromycin, clindamycin, or tetracycline ($p<0.01$). Of all *emm* types, *emm*28 accounted for 71.0% (44/62) of all cases of resistance to these 3 antimicrobial drugs. In our study, 16/44 isolates harboring *emm*28 showed resistance to ≥2 antimicrobials. *emm*28 isolates in France were also found to be associated with multidrug resistance (*13*,*14*). Furthermore, in 2015, we found sharp increases in intermediate tetracycline resistance mainly in isolates harboring *emm*1 (57.9%, 22/38). Tetracycline resistance associated with *emm*12 and *emm*1 isolates was also found in scarlet fever patients in Hong Kong and China (*3*,*15*).

This study has a limitation. We collected samples from only 1 city in South Korea, the Gwangju metropolitan area. Because of the genetic diversity of GAS, our results should not be applied to other countries, even those nearby. However, we do believe that our data are representative of South Korea.

Conclusions

In 2011, rapid increases in the incidence of scarlet fever in South Korea, as well as China and Hong Kong, reflected the beginning of a pandemic in Asia. However, the *emm* types contributing to disease differed from country to country. *emm*4, *emm*28, *emm*1, and *emm*3 were the most common

Table. Characterization of antimicrobial drug resistance according to *emm* types in Gwangju, South Korea, 2008–2015*

Year, antimicrobial drug	*emm* type					
	*emm*1	*emm*4	*emm*12	*emm*28	Others	Total
2008						
Tetracycline	–	1†	–	–	–	1†
2009						
Erythromycin	–	–	–	2	–	2
Clindamycin	–	–	–	2	–	2
Tetracycline	–	–	–	1	–	1
2010						
Erythromycin	–	–	–	1	–	1
Clindamycin	–	–	–	1	–	1
2011						
Erythromycin	–	1	–	1	1†	1/3†
Clindamycin	–	1	–	1	–	2
Tetracycline	–	–	–	1	–	1
2012						
Erythromycin	–	–	–	1	–	1
Clindamycin	–	1	–	1	–	2
Tetracycline	–	1	–	–	–	1
2013						
Chloramphenicol	1	–	–	–	–	1
Erythromycin	1	–	–	2	1†	1/4†
Clindamycin	–	1	–	2	–	3
Tetracycline	–	1	–	1	–	2
2014						
Chloramphenicol	–	–	1†	–	–	1†
Erythromycin	–	–	–	4	–	4
Clindamycin	–	–	–	4	–	4
Tetracycline	–	1†	–	4	–	1/5†
2015						
Erythromycin	–	–	1	5	–	6
Clindamycin	–	–	1	5	–	6
Tetracycline	22/23†	–	1	2/7†	5/7†	29/38†
Isolates, % (no./total)	24.5% (25/102)	3.2% (8/251)	10.8% (4/37)	17.3% (18/104)‡	4.3% (9/211)	9.1% (64/705)
p value	<0.01	<0.01		<0.01		

*Dashes indicate no isolates were drug resistant.
†Intermediate resistance. With fractions, the numerator indicates the number of isolates with intermediate resistance, and the denominator indicates the total number of resistant isolates.
‡Numbers in column do not add up to 18 (the number of isolates) because of multidrug resistance.

emm types associated with scarlet fever in South Korea. Antimicrobial drug resistance in GAS in South Korea is closely associated with *emm*28, and resistance to tetracycline (observed emerging in 2015) is associated with type *emm*1. However, further studies are necessary to characterize the circulating strains and to control and prevent the further spread of scarlet fever.

This study was supported by the infectious disease surveillance project from the Health and Environment Research Institute of Gwangju and the Korea National Institute of Health, South Korea.

Mr. D.W. Park works as a researcher in the Health and Environment Research Institute of Gwangju, Gwangju, South Korea. He is a doctoral candidate studying medicine at Chonnam National University Medical School, Gwangju, South Korea. His primary research interests are human infectious diseases, especially respiratory diseases.

References

1. Guy R, Williams C, Irvine N, Reynolds A, Coelho J, Saliba V, et al. Increase in scarlet fever notifications in the United Kingdom, 2013/2014. Euro Surveill. 2014;19:20749. http://dx.doi.org/10.2807/1560-7917.ES2014.19.12.20749
2. Lau EH, Nishiura H, Cowling BJ, Ip DKM, Wu JT. Scarlet fever outbreak, Hong Kong, 2011. Emerg Infect Dis. 2012;18:1700–2. http://dx.doi.org/10.3201/eid1810.120062
3. Yang P, Peng X, Zhang D, Wu S, Liu Y, Cui S, et al. Characteristics of group A *Streptococcus* strains circulating during scarlet fever epidemic, Beijing, China, 2011. Emerg Infect Dis. 2013;19:909–15. http://dx.doi.org/10.3201/eid1906.121020
4. Cunningham MW. Pathogenesis of group A streptococcal infections. Clin Microbiol Rev. 2000;13:470–511. http://dx.doi.org/10.1128/CMR.13.3.470-511.2000
5. Choi JH, Yang NR, Lee WJ, Lee H, Choi EH, Lee HJ. Distribution of *emm* types among group A *Streptococcus* isolates from children in Korea. Diagn Microbiol Infect Dis. 2015;82:26–31. http://dx.doi.org/10.1016/j.diagmicrobio.2015.01.002
6. Bisno AL, Brito MO, Collins CM. Molecular basis of group A streptococcal virulence. Lancet Infect Dis. 2003;3:191–200. http://dx.doi.org/10.1016/S1473-3099(03)00576-0
7. Steer AC, Law I, Matatolu L, Beall BW, Carapetis JR. Global *emm* type distribution of group A streptococci: systematic review and implications for vaccine development. Lancet Infect Dis. 2009;9:611–6. http://dx.doi.org/10.1016/S1473-3099(09)70178-1
8. Yamaoka J, Nakamura E, Takeda Y, Imamura S, Minato N. Mutational analysis of superantigen activity responsible for the induction of skin erythema by streptococcal pyrogenic exotoxin C. Infect Immun. 1998;66:5020–6.
9. Turner CE, Pyzio M, Song B, Lamagni T, Meltzer M, Chow JY, et al. Scarlet fever upsurge in England and molecular-genetic analysis in North-West London, 2014. Emerg Infect Dis. 2016;22:1075–8. http://dx.doi.org/10.3201/eid2206.151726
10. Silva-Costa C, Carriço JA, Ramirez M, Melo-Cristino J. Scarlet fever is caused by a limited number of *Streptococcus pyogenes* lineages and is associated with the exotoxin genes *ssa, spe*A and *spe*C. Pediatr Infect Dis J. 2014;33:306–10. http://dx.doi.org/10.1097/INF.0000000000000088
11. Plainvert C, Doloy A, Loubinoux J, Lepoutre A, Collobert G, Touak G, et al.; CNR-Strep network. Invasive group A streptococcal infections in adults, France (2006–2010). Clin Microbiol Infect. 2012;18:702–10. http://dx.doi.org/10.1111/j.1469-0691.2011.03624.x
12. Clinical and Laboratory Standards Institute. Performance standards for antimicrobial susceptibility testing; twenty-fifth informational supplement (M100-S25). Wayne (PA): The Institute; 2015.
13. Metzgar D, Zampolli A. The M protein of group A *Streptococcus* is a key virulence factor and a clinically relevant strain identification marker. Virulence. 2011;2:402–12. http://dx.doi.org/10.4161/viru.2.5.16342
14. Mihaila-Amrouche L, Bouvet A, Loubinoux J. Clonal spread of *emm* type 28 isolates of *Streptococcus pyogenes* that are multiresistant to antibiotics. J Clin Microbiol. 2004;42:3844–6. http://dx.doi.org/10.1128/JCM.42.8.3844-3846.2004
15. Davies MR, Holden MT, Coupland P, Chen JH, Venturini C, Barnett TC, et al. Emergence of scarlet fever *Streptococcus pyogenes emm*12 clones in Hong Kong is associated with toxin acquisition and multidrug resistance. Nat Genet. 2015;47:84–7. http://dx.doi.org/10.1038/ng.3147

Address for correspondence: Jae Keun Chung, 149, Hwajeong-ro, Seo-gu, Gwangju, Korea 61986; email: jkchung@korea.kr; Yeongjin Hong, 322, Seoyang-ro, Hwasun-eup. Hwasun-gun Jeonnam, South Korea 58128; email: yjhong@chonnam.ac.kr

Markers of Disease Severity in Patients with Spanish Influenza in the Japanese Armed Forces, 1919–1920

Koichiro Kudo, Toshie Manabe, Shinyu Izumi, Jin Takasaki, Yuji Fujikura, Akihiko Kawana, Kenji Yamamoto

We examined preserved medical charts of 470 Spanish influenza patients (8 with fatal cases) hospitalized at former army hospitals in Japan during 1919–1920. The following factors were associated with longer periods of hospitalization: adventitious discontinuous lung sounds, maximum respiration rate, continuation of high fever after hospital admission, and diphasic fever.

The first and second waves of the Spanish influenza pandemic in Japan affected ≈21 million persons (257,000 deaths) and 2 million persons (127,000 deaths), respectively (*1*). Although available clinical techniques and treatment options for Spanish influenza patients were limited in this era, charts showing detailed records of lung sounds and fever exist and can be used to infer disease severity in affected persons. We aimed to identify physical features, including respiratory sounds, that might be associated with disease severity among patients in Japan who were affected by Spanish influenza during 1919 and 1920.

The Study

We analyzed medical charts preserved at the former First Army Hospital in Tokyo, Japan, and other affiliated hospitals. We previously described the clinical features of Spanish influenza among patients who were hospitalized at several study sites (*2*). Recently, additional records of patients affected by the second wave of disease during 1919–1920 were discovered, and these patients were the subjects of this study.

A total of 470 patients hospitalized during January 1919–January 1920 and diagnosed with Spanish influenza (as "epidemic cold" or "pneumonia due to epidemic cold") fit the criteria for inclusion in the study. All patients were male soldiers or officers in the military of Japan. We collected data concerning patients' general background and physical assessments, including lung sounds and fever charts. Among all patients, 8 (2%) died. We divided the patients who survived (n = 462, 98%) into 3 groups on the basis of hospitalization length: ≤10 days (28%), 11–20 days (34%), and ≥21 days (36%); we compared variables among the 3 groups. High fever was defined as a body temperature ≥38°C, and diphasic fever was defined as a body temperature ≥38°C after the initial fever had decreased to ≤37.5°C. Data on adventitious lung sounds collected during the hospitalization period were classified (on the basis of international classifications) as continuous, discontinuous, bronchial on the chest wall, and friction rub sounds (*3*). The study was approved by the Institutional Review Board of the National Center for Global Health and Medicine, Tokyo, Japan.

Of the 8 patients who died, 6 died within 10 days of hospital admission. Median length of hospitalization was 7 days for nonsurvivors and 16 days for survivors. The proportion of patients with audible adventitious lung sounds was significantly higher among those hospitalized for ≥21 days and among those who did not survive (Table 1). Factors associated with the length of hospitalization in survivors (identified by using a Cox hazard proportional model) included diphasic fever, ≥6 days of continuing high fever from admission, a maximum respiration rate ≥26 breaths/min, and adventitious discontinuous lung sounds (Table 2).

Conclusions

The length of hospitalization of patients with acute infectious diseases, including Spanish influenza, is associated with disease severity. Otherwise healthy soldiers who became patients during the second wave of Spanish influenza in Japan during 1919–1920 were severely affected. Adventitious discontinuous lung sounds, rapid respiration rate, and time-course of fever reflected disease severity during the pandemic. Patients who were severely affected had mainly fulminating fatal cases or experienced secondary bacterial pneumonia.

Severe disease associated with the recent pandemic caused by influenza A(H1N1)pdm09 virus can be attributed to viral pneumonia, superimposition of bacterial pneumonia,

Author affiliations: Koto Hospital, Tokyo, Japan (K. Kudo); Waseda University Organization for Regional and Inter-regional Studies, Tokyo (K. Kudo, T. Manabe); Teikyo University School of Medicine, Tokyo (T. Manabe); Tsukuba University Graduate School of Comprehensive Human Sciences, Ibaraki, Japan (T. Manabe); National Center for Global Health and Medicine, Tokyo (S. Izumi, J. Takasaki, K. Yamamoto); National Defence Medical College, Saitama, Japan (Y. Fujikura, A. Kawana); So-Yu Medical Foundation Institute of Medicine, Tokyo (K. Yamamoto)

DOI: http://dx.doi.org/10.3201/eid2304.152097

Table 1. General characteristics and clinical findings of patients with Spanish influenza during hospitalization, Japan, 1919–1920*

Characteristic/clinical feature	Nonsurvivors, n = 8	Survivors, by hospitalization length, n = 462			
		≤10 d, n = 131	11–20 d, n = 161	≥21 d, n = 170	p value†
Median age, y (IQR)	22 (21–23)	22 (21–28)	21 (20– 27)	21 (20–22)	<0.001‡
Time from onset to first visit, median d (IQR)	2 (1 – 3)	1 (1–1)	1 (0 – 1)	1 (1–2)	0.081‡
Hospitalization, median d (IQR)	7 (6 –14)	8 (6–9)	15 (13 – 17)	32 (25–40)	<0.001‡
Duration of high fever from admission, median d (IQR)	7 (5–14)	3 (2–4)	7 (5 – 8)	10 (7–18)	<0.001‡
≥6 d, no. (%)	6 (75.0)	12 (9.2)	91 (56.5)	123 (72.8)	<0.001§
Maximum respiration rate during hospitalization, median (IQR)	53 (45–60)	24 (21–26)	25 (24–30)	29 (25–33)	<0.001‡
≥26 breaths/min., no. (%)	8 (100.0)	10 (16.4)	34 (39.5)	74 (65.5)	<0.001§
Diphasic fever, no. (%)	0	12 (9.2)	51 (31.7)	111 (65.7)	<0.001§
Adventitious lung sounds, no. (%)					
Discontinuous	8 (100.0)	45 (34.4)	96 (59.6)	141 (82.9)	<0.001§
Continuous	8 (100.0)	75 (57.3)	121 (75.2)	144 (84.7)	<0.001§
Bronchial sounds on chest wall	5 (62.5)	7 (5.3)	13 (8.1)	27 (15.9)	0.002¶
Friction rub	2 (25.0)	2 (1.5)	6 (3.7)	21 (12.4)	<0.001¶
Clinical symptoms, no. (%)					
Upper respiratory tract#	7 (87.5)	126 (96.2)	155 (96.3)	157 (92.4)	0.071§
Dyspnea/tachypnea	8 (100.0)	108 (82.4)	144 (89.4)	159 (93.5)	0.003§
Gastric intestinal	5 (62.5)	26 (19.8)	41 (25.5)	61 (35.9)	0.001§
Psycho/mental**	7 (87.5)	121 (92.4)	150 (93.2)	153 (90.0)	0.273§

*High fever, body temperature of ≥38°C; diphasic fever, body temperature ≥38°C at a time after the initial fever had decreased to ≤37.5°C. IQR, interquartile range;
†p values were calculated for the 3 groups on days of hospitalization of survivors (≤10 d, vs 11 – 20, vs ≥21 d).
‡By Kruskal-Wallis test.
§By χ^2 test.
¶By Fisher exact test.
#Upper respiratory tract symptoms were cough, sputum, and wheezing.
**Psycho/mental denotes psychological and mental disturbances, including anxiety, irritation, delirium, and confusion.

or other underlying conditions (*4*–*6*). Similar factors were likely responsible for severe disease associated with Spanish influenza, despite differences in the viruses themselves and available medical interventions. Therefore, viral pneumonia, superimposed bacterial pneumonia, and underlying conditions were likely associated with the length of hospitalization of our study subjects. Of the patients hospitalized for ≥21 days, 159 (93.5%) had severe respiratory symptoms, 123 (72.8%) experienced ≥6 days of continuous high fever, and most variables examined in this study were significantly higher in accordance with the longer days of the hospitalization group (Table 1). The cause of Spanish influenza was unknown at the time, but viral pneumonia may have developed in the early stages of infection among some patients (*7*–*9*). Viral pneumonia cannot be easily resolved without antiviral agents, as observed among patients with A(H1N1)pdm09 virus infection (*10*,*11*). Another potential explanation for an extended period of high fever is that time is required for eliminating the virus from the body (*5*).

Among the survivors, the respiration rate for patients hospitalized for ≥21 days was significantly higher than that of those who required shorter hospital stays (p<0.001) (Table 1). In addition, a high respiration rate was a risk factor for a lengthy hospital stay (Table 2). According to current medical practice, respiration rate is one of the consistent indicators for CURB-65 (a clinical prediction rule that has been validated for predicting mortality in community-acquired pneumonia by the British Thoracic Society [*12*]) and for severity on the pneumonia severity index of the American Thoracic Society/Infectious Disease Society of America (*13*).

Auscultation of the lungs remains the most useful examination technique for assessing airflow through the tracheal-bronchial tree. Patients with adventitious sounds experienced a longer hospital stay (Table 1). Adventitious discontinuous sounds were a significant risk factor for a lengthy hospitalization (Table 2), suggesting that pneumonia had developed in these patients. Additionally, bronchial sounds, rather than vesicular sounds audible at the chest wall, of the study patients suggest more severe pathophysiologic lung conditions such as severe pneumonia, pulmonary infarction, pulmonary massive bleeding,

Table 2. Risk factors for length of hospitalization among 462 Spanish influenza survivors determined by the Cox proportional hazards model, Japan, 1919–1920*

Risk factor	Hazard ratio (95% CI)	p value
Diphasic fever	1.73 (1.33–2.25)	<0.001
≥6 d of high fever from admission	1.70 (1.29–2.25)	<0.001
≥26 breaths/min on maximum respiration rate	1.57 (1.19–2.06)	<0.001
Adventitious discontinuous lung sounds	1.56 (1.17–2.07)	<0.001

*Diphasic fever, a body temperature ≥38°C at a time after the initial fever had decreased to ≤37.5°C; high fever, body temperature ≥38°C.

and diffuse alveolar damage, which was originally reported by Goodpasture (*7*,*8*). Bronchial sounds were more common among patients who died than among survivors (Table 1). Therefore, severe viral pneumonia may have developed in these patients, and they died shortly after disease onset.

Bacterial pneumonia has been previously reported as a common cause of death among Spanish influenza patients, especially during the second wave of illness (*8*,*14*). Samples from few patients in the study group underwent microbiologic examination. Thus, a diphasic fever might be explained by development of secondary bacterial pneumonia during hospitalization. Patients who experienced diphasic fever and a lengthy hospital stay were believed to have contracted a nosocomial infection (*8*,*9*,*14*).

Although patients with underlying diseases in the influenza pandemic of 2009 exhibited 1 of our identified 3 major prognostic indicators (*4*–*6*), we did not observe this pattern in the patients in our study, who were young soldiers and otherwise healthy and robust. At the time of the Spanish influenza pandemic, specific diagnostic methods and suitable techniques for evaluating disease severity were not available. Laboratory tests and specific treatment options were limited. The preserved medical charts emphasize the importance of providing information on physical assessments, such as body temperature, respiration rate, and lung sounds, to predict disease prognosis.

This study required review of charts handwritten ≈100 years ago, and some areas were unreadable. Because the patients were mainly young male soldiers, generalization of these results to the wider population in Japan who had Spanish influenza is limited. However, the historical documents containing this information are rare, and our results provide valuable information relevant for current and future clinical care of patients affected by pandemic influenza.

Patients experiencing influenza require rapid assessment of disease severity and prompt treatment. Our findings reveal conveniently assessed parameters to aid clinical decision-making, including triage, especially during the rampant stage of pandemic influenza, regardless of the medical resources available.

Acknowledgments

We sincerely thank Junko Sakamoto, Takuro Sasaki, and Fujito Ojika for their valuable assistance.

This study was supported by the Japan Society for the Promotion of Science (JSPS) grant KAKENHI26293115.

Dr. Kudo is a visiting professor at Waseda University and also carries out numerous international research activities as a program officer of Division of Infectious Disease Research, Japan Agency for Medical Research and Development. His primary research interests are influenza and other respiratory infections.

References

1. Ikeda K, Fujitani M, Nadaoka Y, Kamiya N, Hirokado M, Yanagawa Y. Precise analysis of the Spanish influenza in Japan [in Japanese]. Ann Rep Tokyo Metr Inst P.H. 2005;56:369–74.
2. Kawana A, Naka G, Fujikura Y, Kato Y, Mizuno Y, Kondo T, et al. Spanish influenza in Japanese armed forces, 1918–1920. Emerg Infect Dis. 2007;13:590–3. http://dx.doi.org/10.3201/eid1304.060615
3. Murphy RL, Holford SK. Lung sounds. ATS News. 1980;8:24–9.
4. Simonsen L, Spreeuwenberg P, Lustig R, Taylor RJ, Fleming DM, Kroneman M, et al.; GLaMOR Collaborating Teams. Global mortality estimates for the 2009 influenza pandemic from the GLaMOR project: a modeling study. PLoS Med. 2013; 10:e1001558. 10.1371/journal.pmed.1001558 http://dx.doi.org/10.1371/journal.pmed.1001558
5. Writing Committee of the WHO Consultation on Clinical Aspects of Pandemic. Clinical aspects of pandemic 2009 influenza A (H1N1) virus infection. N Engl J Med. 2010;362:1708–19. http://dx.doi.org/10.1056/NEJMra1000449
6. Shieh WJ, Blau DM, Denison AM, Deleon-Carnes M, Adem P, Bhatnagar J, et al. 2009 pandemic influenza A (H1N1): pathology and pathogenesis of 100 fatal cases in the United States. Am J Pathol. 2010;177:166–75. http://dx.doi.org/10.2353/ajpath.2010.100115
7. Goodpasture EW. The significance of certain pulmonary lesions in relation to the etiology of influenza. Am J Med Sci. 1919;158:863–70. http://dx.doi.org/10.1097/ 00000441-191911000-00012
8. Goodpasture EW. Bronchopneumonia due to hemolytic streptococci following influenza. JAMA. 1919;72:724–5. http://dx.doi.org/10.1001/jama.1919.02610100032014
9. Sheng ZM, Chertow DS, Ambroggio X, McCall S, Przygodzki RM, Cunningham RE, et al. Autopsy series of 68 cases dying before and during the 1918 influenza pandemic peak. Proc Natl Acad Sci U S A. 2011;108:16416–21. http://dx.doi.org/10.1073/pnas.1111179108
10. Higuera Iglesias AL, Kudo K, Manabe T, Corcho Berdugo AE, Corrales Baeza A, Alfaro Ramos L, et al. Reducing occurrence and severity of pneumonia due to pandemic H1N1 2009 by early oseltamivir administration: a retrospective study in Mexico. PLoS One. 2011;6:e21838. http://dx.doi.org/10.1371/journal.pone.0021838
11. Muthuri SG, Venkatesan S, Myles PR, Leonardi-Bee J, Al Khuwaitir TS, Al Mamun A, et al.; PRIDE Consortium Investigators. Effectiveness of neuraminidase inhibitors in reducing mortality in patients admitted to hospital with influenza A H1N1pdm09 virus infection: a meta-analysis of individual participant data. Lancet Respir Med. 2014;2:395–404. http://dx.doi.org/10.1016/S2213-2600(14)70041-4
12. British Thoracic Society Standards of Care Committee. BTS guidelines for the management of community acquired pneumonia in adults. Thorax. 2001;56(Suppl 4):IV1–64. http://dx.doi.org/10.1136/thx.56.suppl_4.iv1
13. Niederman MS, Mandell LA, Anzueto A, Bass JB, Broughton WA, Campbell GD, et al.; American Thoracic Society. Guidelines for the management of adults with community-acquired pneumonia. Diagnosis, assessment of severity, antimicrobial therapy, and prevention. Am J Respir Crit Care Med. 2001;163:1730–54. http://dx.doi.org/10.1164/ajrccm.163.7.at1010
14. Morens DM, Taubenberger JK, Fauci AS. Predominant role of bacterial pneumonia as a cause of death in pandemic influenza: implications for pandemic influenza preparedness. J Infect Dis. 2008;198:962–70. http://dx.doi.org/10.1086/591708

Address for correspondence: Koichiro Kudo, Waseda University Organization for Regional and Inter-regional Studies, 2-1-1 Nishi-Shinjuku, Shinjuku-ku, Tokyo 169-0051, Japan; email: kudo@kklabo.gr.jp

Molecular Identification of *Spirometra erinaceieuropaei* Tapeworm in Cases of Human Sparganosis, Hong Kong

Tommy H.C. Tang,[1] Samson S.Y. Wong,[1] Christopher K.C. Lai,[2] Rosana W.S. Poon,[2] Helen S.Y. Chan, Tak Chiu Wu, Yuk-Fai Cheung, Tak-Lap Poon, Yi-Po Tsang, Wai-Lun Tang, Alan K.L. Wu

Human sparganosis is a foodborne zoonosis endemic in Asia. We report a series of 9 histologically confirmed human sparganosis cases in Hong Kong, China. All parasites were retrospectively identified as *Spirometra erinaceieuropaei*. Skin and soft tissue swelling was the most common symptom, followed by central nervous system lesions.

Sparganosis is a parasitic zoonosis endemic in Asia, Europe, and North America. Diphyllobothroid tapeworm under the genus *Spirometra* is the causative agent. Humans can be infected through the consumption of contaminated water or meat from intermediate hosts or through topical application of raw, contaminated poultices to eyes and open wounds. After entry into humans, the plerocercoid larvae (spargana) migrate to different anatomic locations, where they cause space-occupying lesions as they develop into adults. The sites spargana migrate to include skin and soft tissues, muscles, visceral organs, and the central nervous system. Clinical symptoms range from asymptomatic/mild (e.g., subcutaneous swelling) to severe (e.g., seizure and hemiparesis) depending on the site and size of lesions (*1*).

Sparganosis is an emerging zoonotic disease and public health challenge in China, potentially because of the practice of consuming wild frog meat, which is a delicacy in the southern Guangdong province. According to a 2009 survey, >25% of the local wild frogs were infected with spargana (*2*). Most cases of human sparganosis have been found in Asia, with the highest cumulative number in China (online Technical Appendix Table, https://wwwnc.cdc.gov/EID/article/23/4/16-0791-Techapp1.pdf) (*3*). In Hong Kong, the earliest known cases of sparganosis were 2 subcutaneous infections reported in 1962 (*4*), and cases afterward have been sporadic. With advances in molecular sequencing, the identification of sparganum larvae isolated from humans was made possible (*5*,*6*). In this study, we performed molecular sequencing on archived histologic specimens to delineate the parasites down to species level.

Author affiliations: Queen Elizabeth Hospital, Hong Kong, China (T.H.C. Tang, C.K.C. Lai, H.S.Y. Chan, T.C. Wu, Y.-F. Cheung, T.-L. Poon); The University of Hong Kong, Hong Kong (S.S.Y. Wong, R.W.S. Poon); Pamela Youde Nethersole Eastern Hospital, Hong Kong (Y.-P. Tsang, W.-L. Tang, A.K.L. Wu)

DOI: http://dx.doi.org/10.3201/eid2304.160791

The Study

Cases of human sparganosis were identified by searching the clinical, parasitologic, and histopathologic records in the Queen Elizabeth Hospital and the Pamela Youde Nethersole Eastern Hospital in Hong Kong. Archived histopathology specimens showing parasites compatible with plerocercoids were retrieved for further molecular testing. We made 10–15 (depending on the amount of tissue available) 4-μm sections from each paraffin block; the sections were deparaffinized and suspended in sterile, normal saline. Genomic DNA was extracted from formalin-fixed paraffin-embedded tissue by using a DNA minikit (QIAGEN, Hilden, Germany) according to the manufacturer's instructions. The DNA was eluted in 60 μL of elution buffer and used as template for PCR.

Primer sequences used in this study were cox1-F 5′-CGGCTTTTTTTGATCCTTTGGGTGG-3′, cox1-R 5′-GTATCATATGAACAACCTAATTTAC-3′, 28S-F 5′-CACCGAAGC CTGCGGTA-3′, and 28S-R 5′-GAAGGTCGACCTGGTGAA-3′, which targeted specifically to the *cox1* and 28S rRNA genes of *S. erinaceieuropaei* respectively (*7*). The later primers were designed in-house by multiple alignments of different parasite species. The PCR mixture (25 μL) contained DNA, PCR buffer (10 mmol/L Tris-HCl [pH 8.3], 50 mmol/L KCl, 3 mmol/L $MgCl_2$, and 0.01% gelatin), and 200 mmol/L each deoxynucleoside triphosphate (dNTP) and 1.0 U *Taq* polymerase (Applied Biosystems, Foster City, CA, USA). The mixtures were amplified in 60 cycles of 94°C for 1 min, 55°C for 1 min, and 72°C for 1 min with a final extension at 72°C for 10 min in an automated thermal cycler (Applied Biosystems). Standard precautions were taken to avoid PCR contamination, and no false-positive results were observed in negative controls. PCR products were gel purified by using the QIAquick gel extraction kit (QIAGEN). Both strands of the PCR products were sequenced twice with an ABI Prism

[1]These first authors contributed equally to this article.

[2]These authors contributed equally to this article.

3700 DNA analyzer (Applied Biosystems). Sequences of the PCR products were compared with known sequences by BLAST analysis (https://blast.ncbi.nlm.nih.gov).

We constructed a phylogenetic tree using the neighbor-joining method with Kimura's 2-parameter correction with ClustalX 1.83 (http://www.clustal.org). We included in the analysis the 252 bps and 211 bps of the amplicon from the *cox1* gene (GenBank accession nos. KU760072–81) and the 28S rRNA gene (accession nos. KX831668–77) of *S. erinaceieuropaei*, respectively, detected in positive samples. *Strongyloides stercoralis* was used as the outgroup in these analyses.

Seven patients with human sparganosis were identified in Queen Elizabeth Hospital, and 2 patients were identified in the Pamela Youde Nethersole Eastern Hospital. All diagnoses were made from 1999 to 2015 (Table). Eight patients were Chinese; 1 was Filipino, and 4 were male. Patient age at diagnosis was 29–73 (median 49) years. Three patients displayed neurologic symptoms, such as numbness, weakness, or memory impairment, and the other 6 displayed skin and soft tissue involvement. All had progressively enlarging or migratory skin nodules (Table). Additional information on clinical history, histopathology, and magnetic resonance brain imaging of representative cases was collected (online Technical Appendix).

Nine patients had archived histopathologic specimens available for molecular testing. Parasite identification was achieved in all 9 specimens, and they showed 99%–100% and 100% identity with the *cox1* and 28S rRNA gene sequences of *S. erinaceieuropaei*, respectively (Figure, panels A and B).

Conclusions

This study demonstrates that human sparganosis appeared sporadically in Hong Kong. The most common signs of disease were skin and soft tissue nodules followed by intracranial lesions. By molecular sequencing, the tested parasites were *S. erinaceieuropaei.* We were unable to pinpoint the source of infection in most patients; the incubation period can last as long as several months, and early stages of the disease are usually asymptomatic (*8*). Patients might have difficulty recalling specific high-risk exposures. In most industrialized countries, the practice of applying raw frog or snake poultices to open wounds is regarded as unhygienic and becoming obsolete, yet consumption of undercooked frog meat or, less commonly, ingestion of raw snake bile for medicinal purposes is still practiced in Hong Kong. Another possible route of transmission could have been drinking water contaminated with *Spirometra* procercoids.

Subcutaneous sparganosis is the most commonly recognized form of the disease. Because sparganosis is rare, it

Table. Characteristics of cases of human sparganosis, Hong Kong, 1999–2015*

Pt no.	Year	Age, y/sex	Ethnicity	Probable place/mode of infection	Location of lesion	Size of worm or lesion, cm	Clinical features	PEC, $\times 10^9$/L (% total WBC count)
1	1999	67/F	Chinese	Unk/Unk	Right breast	0.15 × 0.1 × 0.7, 0.15 × 0.1 × 0.7, 0.1 × 0.5 × 0.5 (lesions excised)	Right breast mass	NR
2	2000	46/M	Chinese	Unk/Unk	NR	0.15 (worm length)	NR	NR
3	2002	29/F	Chinese	Unk/Unk	Epigastrium of abdominal wall	4 × 2.5 × 2 (lesion excised)	NR	NR
4	2003	63/F	Chinese	Unk/Unk	Left thigh	0.6 (maximum dimension of lesion excised)	Progressive enlarging mass for 2 years	NR
5	2004	44/M	Chinese	Unk/Unk	Right thigh	1.5 × 1.5 (lesion); 0.27 × 0.2 × 0.5 (worm)	Right thigh nodule for 6 months	NR
	2014	55/M		Unk/Unk	Right thigh and suspected left frontal lobe	1.6 × 1.3 × 1.4 (lesion)	Recurrent right thigh nodule; suspicious 2 × 5 × 5 mm T2W/FLAIR hyperintensity with contrast enhancement in left frontal white matter	0.22 (3.7)
6	2005	43/F	Chinese	Unk/Unk	Left breast	0.21 (lesion excised)	Progressive enlarging left breast mass	0.1 (0.7)
7	2011	58/M	Chinese	China/ingestion of frogs and snakes	Left chest wall	3 × 2.5 × 1 (lesion)	Left chest wall mass for 3 years	0.21 (2.5)
8	2013	49/F	Filipino	Unk/Unk	Left parietal lobe	0.17 × 0.12 × 0.23 (lesion)	Right-sided numbness and weakness for 2 days	0.1 (1.1)
9	2015	73/M	Chinese	China/ingestion of frogs	Left thigh	0.5 × 0.5 × 0.1 (lesion excised)	Progressive enlarging left inner thigh mass for 1 year	0.21 (4.2)

*All worms were identified as *Spirometra erinaceieuropaei*. NR, not recorded; PEC, peripheral eosinophil count; Pt, patient; T2W/FLAIR, T2-weighted/fluid attenuation inversion recovery; Unk, unknown; WBC, white blood cell.

is seldom considered during an initial patient assessment, although a migratory nodule might raise the suspicion for a helminthic etiology. Diagnosis of sparganosis needs to be confirmed, normally by studying the excised lesions. Even though serologic tests for sparganosis have been described, these assays are not generally available and their performance requires more evaluation (*9*–*13*). In contrast, the presence of tunnel sign, conglomerated rings, bead-shaped enhancements, or images of parasites of various life stages by computerized tomography or magnetic resonance

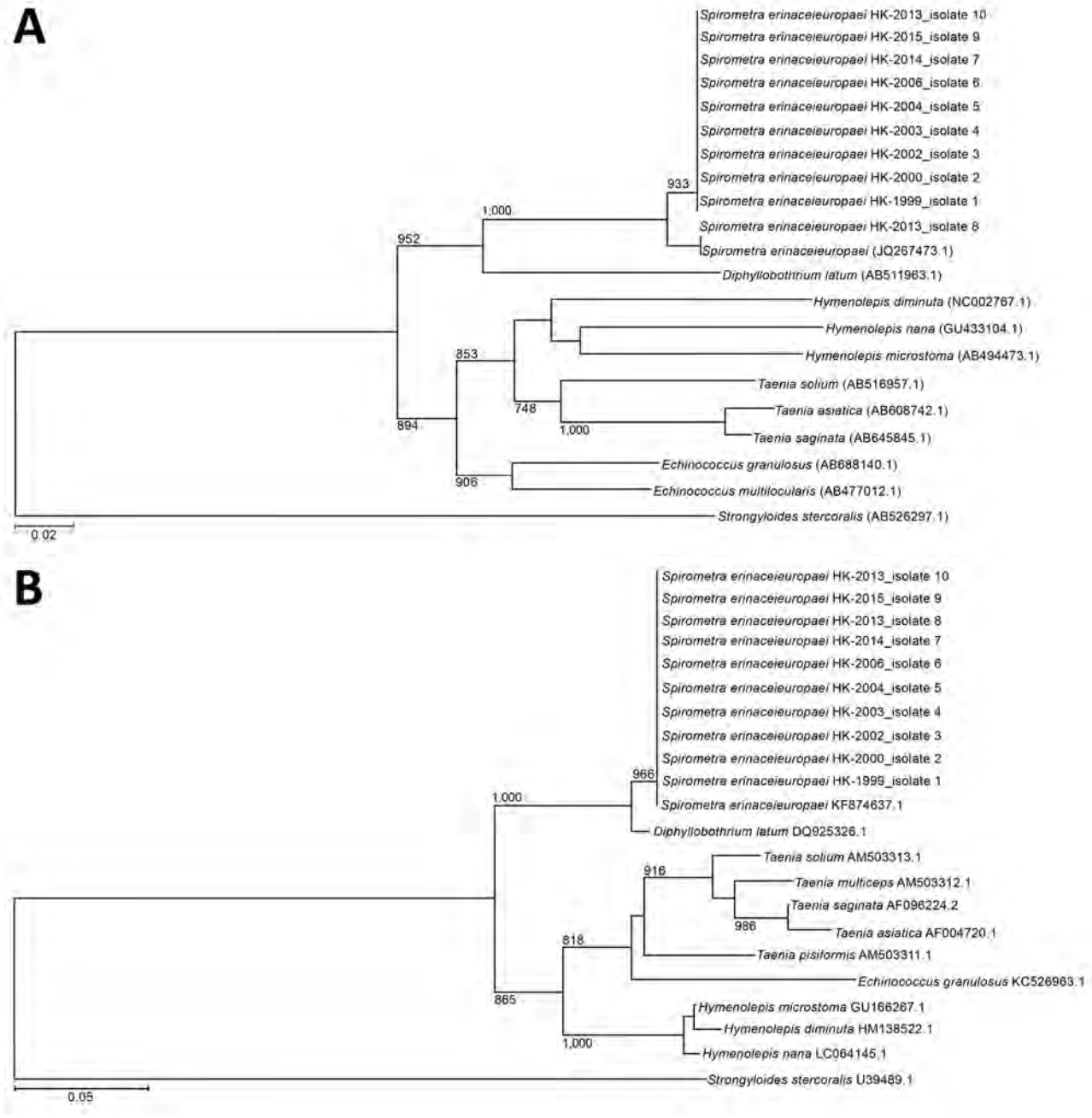

Figure. Phylogenetic analysis of *cox1* and 28S rRNA genes of archived formalin-fixed paraffin-embedded tissues obtained from human sparganosis cases, Hong Kong, 1999–2015. A) A 252-bp sequence from the *cox1* gene (GenBank accession nos. KU760072–81) was included for each isolate. B) A 211-bp sequence from the 28S rRNA gene (accession nos. KX831668–77) was included for each isolate. Trees were constructed by using the neighbor-joining method and rooted with the corresponding sequence in *Strongyloides stercoralis* (accession nos. AB526297.1 and U39489.1 for *cox1* and 28S rRNA genes, respectively). The bootstrap values are shown for nodes that appeared in >70% of the 1,000 replicates. The species used for comparison and their GenBank accession numbers are given in the tree. Scale bars indicate estimated number of substitutions per 50 bases.

imaging are suggestive of sparganosis (*14*). Histopathologic diagnosis of parasitic infections remains a challenge to pathologists in countries where sparganosis is not endemic. Recognizing the different phyla and classes of parasites (i.e., nematodes, cestodes, and trematodes) histologically is usually simple. However, specific identification of the genus and species requires substantial expertise in parasite pathology and morphology. Identification of rare parasites is sometimes impossible because of the lack of detailed morphologic descriptions in the literature. Under such circumstances, molecular studies provide useful information for species identification (*15*). Nevertheless, it is not infallible, especially for rare parasites, because precise species identification depends on gene sequence availability and data accuracy.

Although the parasitic drug praziquantel has wide coverage against several cestodes and trematodes, its efficacy in the treatment of sparganosis remains uncertain. Surgical intervention for complete worm removal should be used whenever feasible.

This study had limitations. We only included information on patients from 2 of the 7 geographic clusters of public hospitals in Hong Kong, and those with asymptomatic subcutaneous lesions most likely did not seek medical attention. The reported number is certainly an underestimate.

Given that human sparganosis is an emerging zoonotic parasitic infection, clinicians may consider it in the differential diagnosis for mass lesions with undetermined etiology. Education of the general public about food safety, including avoiding the consumption of untreated water and undercooked frog and snake meat, is needed.

Acknowledgments

We thank Sherman Lo for providing magnetic resonance imaging brain scans.

Dr. Tang is the associate consultant of the Division of Infectious Diseases in the Department of Medicine at Queen Elizabeth Hospital. His research interests are emerging infectious diseases, infections in immunocompromised hosts, infectious disease epidemiology, and global health.

References

1. Liu Q, Li MW, Wang ZD, Zhao GH, Zhu XQ. Human sparganosis, a neglected food borne zoonosis. Lancet Infect Dis. 2015;15:1226–35. http://dx.doi.org/10.1016/S1473-3099(15)00133-4
2. Li MW, Lin HY, Xie WT, Gao MJ, Huang ZW, Wu JP, et al. Enzootic sparganosis in Guangdong, People's Republic of China. Emerg Infect Dis. 2009;15:1317–8. http://dx.doi.org/10.3201/eid1508.090099
3. Zhang X, Cui J, Liu LN, Jiang P, Wang H, Qi X, et al. Genetic structure analysis of *Spirometra erinaceieuropaei* isolates from central and southern China. PLoS One. 2015;10:e0119295. http://dx.doi.org/10.1371/journal.pone.0119295
4. Huang CT, Kirk R. Human sparganosis in Hong Kong. J Trop Med Hyg. 1962;65:133–8.
5. Boonyasiri A, Cheunsuchon P, Suputtamongkol Y, Yamasaki H, Sanpool O, Maleewong W, et al. Nine human sparganosis cases in Thailand with molecular identification of causative parasite species. Am J Trop Med Hyg. 2014;91:389–93. http://dx.doi.org/10.4269/ajtmh.14-0178
6. Jeon HK, Park H, Lee D, Choe S, Kim KH, Huh S, et al. Human Infections with *Spirometra decipiens* plerocercoids identified by morphologic and genetic analyses in Korea. Korean J Parasitol. 2015;53:299–305. http://dx.doi.org/10.3347/kjp.2015.53.3.299
7. Koonmee S, Intapan PM, Yamasaki H, Sugiyama H, Muto M, Kuramochi T, et al. Molecular identification of a causative parasite species using formalin-fixed paraffin embedded (FFPE) tissues of a complicated human pulmonary sparganosis case without decisive clinical diagnosis. Parasitol Int. 2011;60:460–4. http://dx.doi.org/10.1016/j.parint.2011.07.018
8. Tappe D, Berger L, Haeupler A, Muntau B, Racz P, Harder Y, et al. Case report: molecular diagnosis of subcutaneous *Spirometra erinaceieuropaei* sparganosis in a Japanese immigrant. Am J Trop Med Hyg. 2013;88:198–202. http://dx.doi.org/10.4269/ajtmh.2012.12-0406
9. Yeo IS, Yong TS, Im K. Serodiagnosis of human sparganosis by a monoclonal antibody-based competition ELISA. Yonsei Med J. 1994;35:43–8. http://dx.doi.org/10.3349/ymj.1994.35.1.43
10. Cui J, Li N, Wang ZQ, Jiang P, Lin XM. Serodiagnosis of experimental *Sparganum* infections of mice and human sparganosis by ELISA using ES antigens of *Spirometra mansoni* spargana. Parasitol Res. 2011;108:1551–6. http://dx.doi.org/10.1007/s00436-010-2206-2
11. Rahman SMM, Kim JH, Hong ST, Choi MH. Diagnostic efficacy of a recombinant cysteine protease of *Spirometra erinacei* larvae for serodiagnosis of sparganosis. Korean J Parasitol. 2014;52:41–6. http://dx.doi.org/10.3347/kjp.2014.52.1.41
12. Liu LN, Zhang X, Jiang P, Liu RD, Zhou J, He RZ, et al. Serodiagnosis of sparganosis by ELISA using recombinant cysteine protease of *Spirometra erinaceieuropaei* spargana. Parasitol Res. 2015;114:753–7. http://dx.doi.org/10.1007/s00436-014-4270-5
13. Liu LN, Wang ZQ, Zhang X, Jiang P, Qi X, Liu RD, et al. Characterization of *Spirometra erinaceieuropaei* plerocercoid cysteine protease and potential application for serodiagnosis of sparganosis. PLoS Negl Trop Dis. 2015;9:e0003807. http://dx.doi.org/10.1371/journal.pntd.0003807
14. Lo Presti A, Aguirre DT, De Andrés P, Daoud L, Fortes J, Muñiz J. Cerebral sparganosis: case report and review of the European cases. Acta Neurochir (Wien). 2015;157:1339–43, discussion 1343. http://dx.doi.org/10.1007/s00701-015-2466-9
15. Wong SSY, Fung KSC, Chau S, Poon RWS, Wong SCY, Yuen KY. Molecular diagnosis in clinical parasitology: when and why? Exp Biol Med (Maywood). 2014;239:1443–60. http://dx.doi.org/10.1177/1535370214523880

Address for correspondence: Tommy H.C. Tang, Division of Infectious Diseases, Department of Medicine, Queen Elizabeth Hospital, 30 Gascoigne Rd, Hong Kong, China; email: thc061@gmail.com

Zika Virus Seroprevalence, French Polynesia, 2014–2015

Maite Aubry, Anita Teissier, Michael Huart, Sébastien Merceron, Jessica Vanhomwegen, Claudine Roche, Anne-Laure Vial, Sylvianne Teururai, Sébastien Sicard, Sylvie Paulous, Philippe Desprès, Jean-Claude Manuguerra, Henri-Pierre Mallet, Didier Musso, Xavier Deparis, Van-Mai Cao-Lormeau

During 2013–2014, French Polynesia experienced an outbreak of Zika virus infection. Serosurveys conducted at the end of the outbreak and 18 months later showed lower than expected disease prevalence rates (49%) and asymptomatic:symptomatic case ratios (1:1) in the general population but significantly different prevalence rates (66%) and asymptomatic:symptomatic ratios (1:2) in schoolchildren.

Zika virus (family *Flaviviridae*, genus *Flavivirus*), an arthropodborne pathogen, is transmitted to humans by *Aedes* spp. mosquitoes, but nonvectorborne transmission (i.e., maternofetal and sexual transmission and transmission via blood transfusion) has also been reported (*1*). Infection by Zika virus most commonly causes mild disease consisting of fever, rash, arthralgia, headache, and conjunctivitis (*1*), but severe neurologic complications, such as Guillain-Barré syndrome in adults (*2*) and microcephaly in fetuses and newborns (*3*), have been described.

Zika virus emerged for the first time in 2007 on Yap Island, Federated States of Micronesia, in the Pacific region (*4*). Six years later, Zika virus caused an explosive outbreak in French Polynesia (*5*), and the virus then spread across the Pacific region (*6*). During October 2013–April 2014 in French Polynesia, an estimated 32,000 persons (11.5% of the population) visited healthcare facilities because of clinical symptoms suggestive of Zika virus infection (*1*,*7*). A retrospective serosurvey conducted on blood collected from donors before the outbreak confirmed that Zika virus had not previously circulated in French Polynesia (*8*). We conducted a study to assess Zika virus seroprevalence among the French Polynesia population after the virus emerged in the country.

The Study

French Polynesia comprises 119 islands distributed among 5 archipelagos (Society, Tuamotu, Marquesas, Australs, and Gambier). The population of ≈270,000 inhabitants lives on 74 islands (2012 census; http://www.ispf.pf/docs/default-source/publi-pr/POP_LEGALE_2012_PF.pdf?sfvrsn=2). During February and March 2014, we conducted a cluster sampling among the general population living in the 5 archipelagos. We randomly recruited a total of 196 participants on the most inhabited islands of each archipelago: Tahiti and Moorea (Society), Rangiroa and Makemo (Tuamotu), Nuku Hiva and Hiva Oa (Marquesas), Rurutu (Australs), and Rikitea (Gambier) (Figure). Because >85% of the inhabitants of French Polynesia live on the Society Islands, we conducted a second cluster sampling among 700 participants recruited on Tahiti and Moorea during September–November 2015. In addition, 476 schoolchildren initially recruited for a dengue serosurvey on Tahiti during May and June 2014 were included in the study.

All participants were asked to declare whether they had clinical manifestations suggestive of past Zika infection. Adults provided written informed consent before enrollment, and parents or guardians gave consent for their children. Participants' blood samples and personal data were anonymized before processing, and the study was approved by the Ethics Committee of French Polynesia (no. 60/CEPF 06/27/2013).

We used a recombinant antigen–based indirect ELISA to detect Zika virus IgG in blood samples collected in 2014 from the general population and schoolchildren (*8*). We also tested serum samples from the general population by microsphere immunoassay (MIA), using the same recombinant antigens as for the ELISA (*2*,*8*). Among the 196 serum samples from the general population, 80% tested positive for Zika virus IgG by both assays ($\kappa = 0.51$, indicating good agreement between ELISA and MIA

Author affiliations: Institut Louis Malardé, Papeete, Tahiti, French Polynesia (M. Aubry, A. Teissier, C. Roche, S. Teururai, D. Musso, V.-M. Cao-Lormeau); Centre d'Épidémiologie et de Santé Publique des Armées, Marseille, France (M. Huart, S. Sicard, X. Deparis); Unité Mixte de Recherche Sciences Economiques et Sociales de la Santé et Traitement de l'Information Médicale, Marseille (M. Huart, S. Sicard, X. Deparis); Institut de la Statistique de la Polynésie Française, Papeete (S. Merceron); Institut Pasteur, Paris, France (J. Vanhomwegen, S. Paulous, J.-C. Manuguerra); Direction Départementale de la Cohésion Sociale et de la Protection des Populations, Yonne, France (A.-L. Vial); Direction de la Santé de la Polynésie Française, Papeete (A.-L. Vial, H.-P. Mallet); Université de La Réunion and UMR PIMIT, Sainte Clotilde, France (P. Desprès)

DOI: http://dx.doi.org/10.3201/eid2304.161549

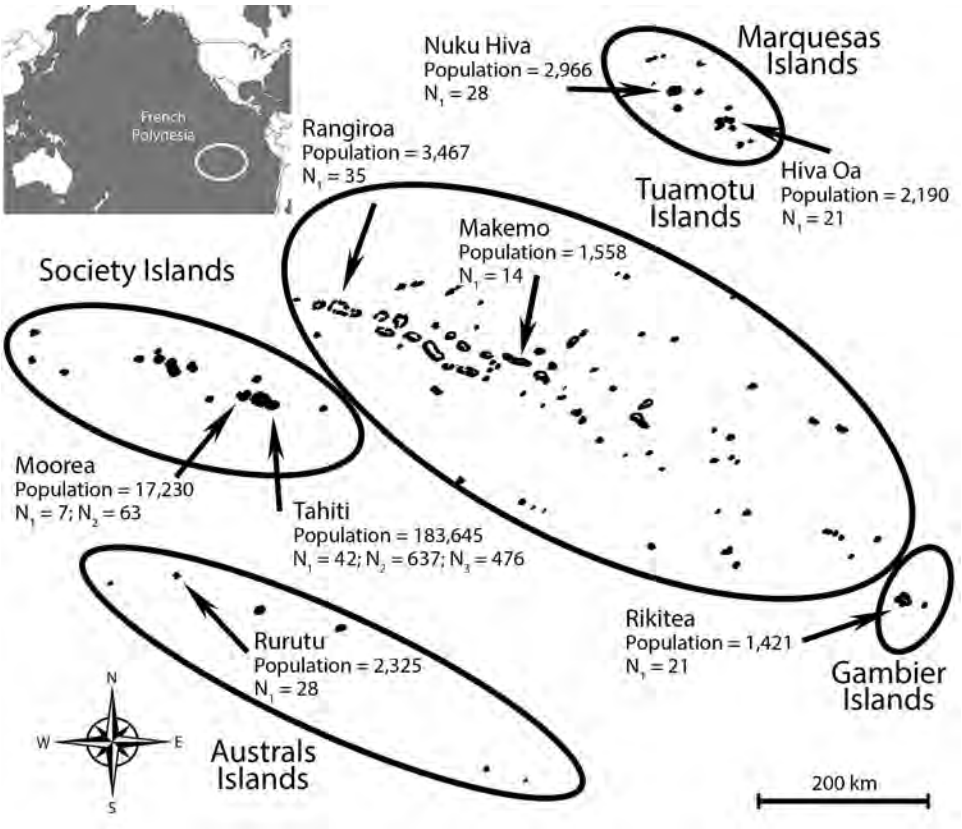

Figure. Geographic distribution of participants recruited for a study of the postemergence seroprevalence of Zika virus infections in French Polynesia, 2014–2015. N_1 and N_2 indicate areas of recruitment among the general population during February and March 2014 and September–November 2015, respectively; N_3 indicates areas of recruitment among schoolchildren during May and June 2014. The total population and number of recruited participants is shown for each area. Lines delineate the 5 archipelagos that comprise French Polynesia (Marquesas, Society, Tuamotu, Gambier, and Australs). Inset map at upper left shows location of French Polynesia in the Pacific Ocean (white circle).

results). Blood samples collected in 2015 were tested by MIA only.

Zika virus seroprevalence rates and proportions of asymptomatic infections were 49% (95% CI 42%–57%) and 43% (95% CI 33%–53%), respectively, for participants from the general population sampled in 2014 and 66% (95% CI 60%–71%) and 29% (95% CI 24%–34%), respectively, for schoolchildren sampled in 2014 (Table). Seroprevalence rates and proportions of asymptomatic infections were 22% (95% CI 16%–28%) and 53% (95% CI 45%–61%), respectively, for participants recruited in 2015 (Table).

Conclusions

During the October 2013–April 2014 Zika infection outbreak in French Polynesia, ≈11.5% of the population sought medical care for symptoms suggestive of Zika infection (*1*,*7*); however, serosurveys at the end of the outbreak showed a Zika virus seroprevalence rate of 49% (95% CI 42%–57%), suggesting that most infected persons did not seek medical care. The finding that 43% (95% CI 33%–53%) of the participants had Zika virus IgG without self-reported symptoms reflects an estimated asymptomatic to symptomatic ratio of 1:1. These results suggest that infected persons did not consult medical care staff because

Table. Zika virus seroprevalence among persons randomly recruited from the general population and among schoolchildren immediately after and 18 months after a Zika outbreak, French Polynesia, 2014 and 2015*

Sampled population, time of sampling, location of sampling	Median age (range), y	No. symptomatic/no. positive (% [95% CI])	No. asymptomatic/no. positive (% [95% CI])	Total no. seropositive/total no. tested (% [95% CI])
General population				
February–March 2014				
Society Islands	47 (13–77)	8/18 (44 [26–69])	10/18 (56 [33–79])	18/49 (37 [26–47])
Tuamotu Islands	39 (7–86)	12/22 (55 [34–75])	10/22 (45 [25–66])	22/49 (45 [38–52])
Marquesas Islands	45 (10–82)	16/28 (57 [39–75])	12/28 (43 [24–61])	28/49 (57 [47–68])
Austral–Gambier Islands	38 (7–84)	19/29 (66 [48–83])	10/29 (34 [17–52])	29/49 (59 [39–80])
Total	41 (7–86)	55/97 (57 [47–67])	42/97 (43 [33–53])	97/196 (49 [42–57])
September–November 2015				
Society Islands	43 (4–88)	73/154 (47 [40–55])	81/154 (53 [45-61])	154/700 (22 [16–28])
Schoolchildren				
May–June 2014				
Society Islands	11 (6–16)	221/312 (71 [66–76[)	91/312 (29 [24–34])	312/476 (66 [60–71])

*CIs were calculated taking into account the cluster sampling design (*9*) and using the Fisher exact test.

the infection was mild or asymptomatic, as previously described (*10*). Of the 5 French Polynesia archipelagos, the Society Islands had the lowest seroprevalence rate (37% [95% CI 26%–47%]) and the Australs–Gambier Islands the highest (59% [95% CI 39%–80%]); however, seroprevalence among the archipelagos did not differ substantially, suggesting that no matter their location, study participants had similar Zika virus transmission exposure.

Eighteen months after the end of the outbreak, the Zika virus seroprevalence rate and proportion of asymptomatic infections among 700 persons on the Society Islands were 22% (95% CI 16%–28%) and 53% (95% CI 45%–61%), respectively, not substantially different from those during the first cluster sampling in the same islands (37% [95% CI 26%–47%] and 56% [95% CI 33%–79%], respectively). The finding that the Zika virus seroprevalence rate did not increase between the 2 sampling periods suggests that the virus did not actively circulate after the end of the outbreak. In contrast, the decrease in the Zika virus seroprevalence rate, even if not significant, suggests that Zika virus IgG titers may drop over time.

Within 2 months after the end of the outbreak, the Zika virus seroprevalence rate among schoolchildren (6–16 [median 11] years of age) on Tahiti was substantially higher than that among the general population (4–88 [median 43] years of age) (66% [95% CI 60%–71%] vs. 22% [95% CI 16%–28%], respectively). In contrast, the proportion of asymptomatic Zika virus infections was substantially lower among schoolchildren (29% [95% CI 24%–34%]) than among the general population (53% [95% CI 45%–61%]). Dengue virus (DENV) may provide cross-protection against Zika infection; thus, the higher DENV IgG seroprevalence among adults may explain why fewer adults than children were infected by Zika virus (*8*,*11*–*13*). The lower asymptomatic rate in children may have 2 additional explanations: the reporting of symptoms among children may have been compounded by the relatively higher frequency of febrile rash illness due to other viral infections, and sampling among children was conducted at the tail end of the outbreak, so they would likely remember symptoms more clearly than the population surveyed 18 months after the outbreak.

In the 3 groups tested, no difference was seen by sex in the seroprevalence rate or the proportion of asymptomatic infections. However, because the sampling scheme was not initially designed to compare data by sexes, data could not be extrapolated to the population level.

Our findings show that <50% of the population of French Polynesia had detectable Zika virus IgG. This seroprevalence rate is much lower than the 86% attack rate estimated by Kucharski et al. (*14*) using a model that assumed the French Polynesia population was 100% susceptible to Zika virus infection. However, in a setting where DENVs are highly prevalent (*8*), the possibility of cross-protecting immunity preventing infection from Zika virus (*12*,*13*) cannot be excluded. The attack rate and the asymptomatic:symptomatic ratio in French Polynesia were also lower than those described for the 2007 outbreak on Yap Island (73% and 4:1, respectively) (*4*); this finding supports the perception that the drivers of Zika virus transmission vary depending on geographic context. For other flaviviruses, such as DENV, previous model-based studies showed that the herd immunity threshold required to block viral transmission is ≈50%–85% (*15*). Thus, if Zika virus has the same epidemiologic characteristics as DENV, the seroprevalence rate of 49% would not be sufficient to prevent another outbreak.

Acknowledgments

We are grateful to Eliane Mama, Sylvia Fontanel, and Jean-Paul Pescheux for their help in collecting blood samples and to Teheipuaura Mariteragi-Helle for her technical support. We thank the administrators and health authorities of each French Polynesia archipelago and the mayors, municipal staff, practitioners, and nurses in the islands selected for the study for their support in recruiting participants and sending blood samples to the Institut Louis Malardé. We also thank the minister for education of French Polynesia; the Direction de l'enseignement primaire and the Direction de l'enseignement secondaire in French Polynesia; and the directors, teachers and nurses of the elementary and junior high schools selected for the study for their participation in recruiting schoolchildren and collecting blood samples. We especially thank all of the participants.

This study received funding from the Contrat de Projet Etat-Pays (convention no. 7331/MSS/DSP du 31/08/12 modifiée) and from the French Government's Investissement d'Avenir Programme (Labex Integrative Biology of Emerging Infectious Diseases, IBEID, grant no. ANR-10-LABX-62-IBEID).

Dr. Aubry is a research scientist at the Institut Louis Malardé, Tahiti, French Polynesia. Her research interests include arboviruses epidemiology and genetic evolution in the Pacific region.

References

1. Musso D, Gubler DJ. Zika Virus. Clin Microbiol Rev. 2016;29:487–524. http://dx.doi.org/10.1128/CMR.00072-15
2. Cao-Lormeau VM, Blake A, Mons S, Lastère S, Roche C, Vanhomwegen J, et al. Guillain-Barré Syndrome outbreak associated with Zika virus infection in French Polynesia: a case-control study. Lancet. 2016;387:1531–9. http://dx.doi.org/10.1016/S0140-6736(16)00562-6
3. Cauchemez S, Besnard M, Bompard P, Dub T, Guillemette-Artur P, Eyrolle-Guignot D, et al. Association between Zika virus and microcephaly in French Polynesia, 2013-15: a retrospective study. Lancet. 2016;387:2125–32. http://dx.doi.org/10.1016/S0140-6736(16)00651-6
4. Duffy MR, Chen TH, Hancock WT, Powers AM, Kool JL, Lanciotti RS, et al. Zika virus outbreak on Yap Island, Federated States of Micronesia. N Engl J Med. 2009;360:2536–43. http://dx.doi.org/10.1056/NEJMoa0805715

5. Cao-Lormeau VM, Roche C, Teissier A, Robin E, Berry A-L, Mallet H-P, et al. Zika virus, French Polynesia, South Pacific, 2013. Emerg Infect Dis. 2014;20:1085–6. http://dx.doi.org/10.3201/eid2011.141380
6. Musso D, Nilles EJ, Cao-Lormeau VM. Rapid spread of emerging Zika virus in the Pacific area. Clin Microbiol Infect. 2014;20:O595–6. http://dx.doi.org/10.1111/1469-0691.12707
7. Mallet HP, Vial AL, Musso D. Bilan de l'épidémie à virus Zika survenue en Polynésie française entre octobre 2013 et mars 2014. De la description de l'épidémie aux connaissances acquises après l'évènement. Bulletin épidémiologique hebdomadaire. 2016;20–21:367–73.
8. Aubry M, Finke J, Teissier A, Roche C, Broult J, Paulous S, et al. Seroprevalence of arboviruses among blood donors in French Polynesia, 2011-2013. Int J Infect Dis. 2015;41:11–2. http://dx.doi.org/10.1016/j.ijid.2015.10.005
9. Spiegel A, Moulia-Pelat J, Daumerie D, Merlin M, Baudon D. Le sondage en grappe type OMS : méthodes pratiques en épidémiologie descriptive. Med Afr Noire. 1989;36:740–5.
10. Musso D, Nhan T, Robin E, Roche C, Bierlaire D, Zisou K, et al. Potential for Zika virus transmission through blood transfusion demonstrated during an outbreak in French Polynesia, November 2013 to February 2014. Euro Surveill. 2014;19:2pii=0761.
11. Chungue E, Marché G, Plichart R, Boutin JP, Roux J. Comparison of immunoglobulin G enzyme-linked immunosorbent assay (IgG-ELISA) and haemagglutination inhibition (HI) test for the detection of dengue antibodies. Prevalence of dengue IgG-ELISA antibodies in Tahiti. Trans R Soc Trop Med Hyg. 1989;83:708–11. http://dx.doi.org/10.1016/0035-9203(89)90404-5
12. Dejnirattisai W, Supasa P, Wongwiwat W, Rouvinski A, Barba-Spaeth G, Duangchinda T, et al. Dengue virus sero-cross-reactivity drives antibody-dependent enhancement of infection with zika virus. Nat Immunol. 2016;17:1102–8. http://dx.doi.org/10.1038/ni.3515
13. Priyamvada L, Quicke KM, Hudson WH, Onlamoon N, Sewatanon J, Edupuganti S, et al. Human antibody responses after dengue virus infection are highly cross-reactive to Zika virus. Proc Natl Acad Sci U S A. 2016;113:7852–7. http://dx.doi.org/10.1073/pnas.1607931113
14. Kucharski AJ, Funk S, Eggo RM, Mallet H-P, Edmunds WJ, Nilles EJ. Transmission dynamics of Zika virus in island populations: a modelling analysis of the 2013–14 French Polynesia outbreak. PLoS Negl Trop Dis. 2016;10:e0004726. http://dx.doi.org/10.1371/journal.pntd.0004726
15. Johansson MA, Hombach J, Cummings DA. Models of the impact of dengue vaccines: a review of current research and potential approaches. Vaccine. 2011;29:5860–8. http://dx.doi.org/10.1016/j.vaccine.2011.06.042

Address for correspondence: Maite Aubry, Institut Louis Malardé, PO Box 30, 98713 Papeete, Tahiti, French Polynesia; email: maubry@ilm.pf

etymologia

Sparganosis [spahr"ge-no'sis]

Ronnie Henry

Sparganosis refers to tissue infection with the pleurocercoid larvae of the genera *Diphyllobothrium* (from the Greek *di* ["two"] + *phyllon* ["leaf"] + *bothrion* ["pit"]) or *Spirometra* (from the Greek *speira* ["coil"] + *metra* ["uterus"]). *Sparganum* (from the Greek *sparganon* ["swaddling clothes"]) was originally described in 1854 by Diesing as a separate species but is now used generically to describe the larval stage of these cestodes.

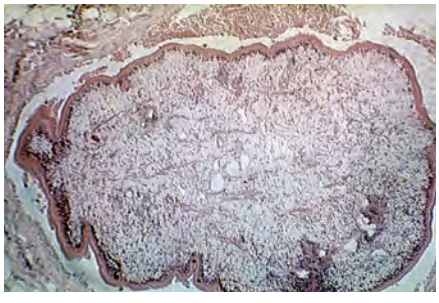

Histopathology of *Sparganum proliferum* infection. Public Image Health Library, Center for Disease Control, 1962.

The first human case was reported by Sir Patrick Manson in China in 1882, and 2 species (*S. mansoni* and *S. mansonoides*) are named for him. Sparganosis is most common in Asia where frogs or snakes are more commonly eaten or where traditional medicinal practices call for the use of raw frog or snake meat in poultices, although recent reports indicate it occurs in in some populations in Africa.

Sources

1. Dorland's Illustrated Medical Dictionary. 32nd ed. Philadelphia: Elsevier Saunders; 2012.
2. Eberhard ML, Thiele EA, Yembo GE, Yibi MS, Cama VA, Ruiz-Tiben E. Thirty-seven human cases of sparganosis from Ethiopia and South Sudan caused by *Spirometra* spp. Am J Trop Med Hyg. 2015;93:350–5. http://dx.doi.org/10.4269/ajtmh.15-0236
3. Fantham HB, Stephens JW, Theobald FV. The animal parasites of man. New York: William Wood and Company; 1920.
4. Lescano AG, Zunt J. Other cestodes: sparganosis, coenurosis and *Taenia crassiceps* cysticercosis. Handb Clin Neurol. 2013;114:335–45. http://dx.doi.org/10.1016/B978-0-444-53490-3.00027-3

Address for correspondence: Ronnie Henry, Centers for Disease Control and Prevention, 1600 Clifton Rd NE, Mailstop E03, Atlanta, GA 30329-4027, USA; email: boq3@cdc.gov

DOI: http://dx.doi.org/10.3201/eid2304.ET2304

Persistent Arthralgia Associated with Chikungunya Virus Outbreak, US Virgin Islands, December 2014–February 2016

Leora R. Feldstein, Ali Rowhani-Rahbar, J. Erin Staples, Marcia R. Weaver, M. Elizabeth Halloran, Esther M. Ellis

After the 2014–2015 outbreak of chikungunya virus in the US Virgin Islands, we compared the prevalence of persistent arthralgia among case-patients and controls. Prevalence was higher in case-patients than controls 6 and 12 months after disease onset. Continued vaccine research to prevent acute illness and long-term sequelae is essential.

Autochthonous transmission of chikungunya virus (CHIKV) was first reported in the Americas in December 2013 on the island of Saint Martin, and by early 2016, the virus had spread to 45 countries in the Caribbean and Central, South, and North America (*1*,*2*). Acute symptoms of CHIKV infection often resolve within 7–10 days (*3*). However, 7%–79% of case-patients from previous outbreaks have reported persistent arthralgia for months after infection (*4*–*8*). Persistent arthralgia associated with CHIKV illness has been assessed in persons in Southeast Asia, South America, and Europe but not in the Caribbean (*4*,*9*).

The US Virgin Islands (USVI), one of many regions in the Caribbean affected by the CHIKV epidemic, identified its first locally acquired case in June 2014 (*10*). USVI subsequently reported nearly 2,000 suspected CHIKV cases before the last laboratory-confirmed case was reported in February 2015 (*11*). To determine the prevalence of CHIKV-associated persistent arthralgia in USVI, we compared the prevalence of persistent arthralgia among CHIKV case-patients and nonsymptomatic controls during December 2014–February 2016.

Author affiliations: Fred Hutchinson Cancer Research Center, Seattle, Washington, USA (L.R. Feldstein, M.E. Halloran); University of Washington, Seattle (A. Rowhani-Rahbar, M.R. Weaver, M.E. Halloran); Centers for Disease Control and Prevention, Fort Collins, Colorado, USA (J.E. Staples); US Virgin Islands Department of Health, Saint Croix, US Virgin Islands (E.M. Ellis)

DOI: http://dx.doi.org/10.3201/eid2304.161562

The Study

A confirmed case-patient was defined as a USVI resident of any age with acute onset of fever (≥38°C) and severe arthralgia or arthritis not explained by another medical condition plus 1 of the following: 1) CHIKV RNA in blood, as determined using reverse transcription PCR, or 2) CHIKV-specific IgM antibodies in serum, as determined using ELISA in conjunction with either CHIKV-specific neutralizing antibodies using plaque reduction neutralization test with a 90% cutoff or CHIKV-specific IgG using ELISA (*10*). Confirmed case-patients captured by the USVI Department of Health surveillance system were invited via telephone to participate in a follow-up investigation at 6 and 12 months after acute illness; a total of 165 case-patients were recruited. Verbal informed consent was obtained at the start of each interview.

At the 12-month follow-up, we concurrently enrolled a nonsymptomatic control group. Members of the control group were recruited from the emergency department waiting room of a hospital or from a health clinic in USVI; the group comprised 167 USVI residents of any age. Persons were not eligible for the control group if they reported symptoms consistent with CHIKV disease (i.e., concurrent fever and acute joint pain) or responded "yes" to being tested for CHIKV and test results were positive. All controls were offered free CHIKV IgG testing and were excluded from analysis if positive (online Technical Appendix Table 1, https://wwwnc.cdc.gov/EID/article/23/4/16-1562-Techapp1.pdf).

At 6 and 12 months, we interviewed case-patients about presence, frequency, and anatomic location of arthralgia after acute CHIKV infection. We defined persistent arthralgia as joint pain occurring at least once per week within 1 month before the interview. We asked case-patients whether they had a history of arthritis (defined as doctor-diagnosed arthritis before CHIKV illness). At the 12-month interview, we asked case-patients whether they had difficulty performing everyday activities (i.e., walking, climbing stairs, lifting heavy objects, getting in and out of cars, opening jars). We interviewed the control group only once, using the same 12-month questionnaire that we used for case-patients. The University of the Virgin Islands and the University of Washington ethics committees approved this study.

Table 1. Prevalence and prevalence ratios of persistent arthralgia and impaired physical functionality among residents in a study of persistent arthralgia after a chikungunya virus outbreak, US Virgin Islands, December 2014–February 2016*

Variable	Prevalence difference (95% CI)	p value	Prevalence ratio (95% CI)	p value
Persistent arthralgia				
6 month analysis*	0.32 (0.24–0.40)	<0.001	2.90 (1.90–4.43)	<0.001
12 month analysis*	0.19 (0.11–0.28)	0.001	2.51 (1.71–3.69)	<0.001
Difficulty performing daily activities				
Walking	0.11 (0.03–0.18)	0.007	1.77 (1.06–2.95)	0.028
Climbing stairs	0.12 (0.05–0.19)	0.001	1.81 (1.15–2.86)	0.011
Lifting heavy objects	0.04 (–0.02–0.11)	0.209	1.68 (0.96–2.97)	0.072
Getting in and out of cars	0.09 (0.03–0.14)	0.001	2.65 (1.32–5.32)	0.006
Opening jars	0.15 (0.07–0.23)	<0.001	2.24 (1.28–3.91)	0.005

*Adjusted for age group, sex, and self-reported history of arthritis.

At each time point, we ran 2 independent regression models. We constructed generalized linear models, using the binomial family with robust variance estimators, to estimate prevalence differences and prevalence ratios. We included age grouping (≤35, 36–55, and >55 years), sex, and self-reported history of arthritis in the models. We used 2-sample *t*-tests with unequal variances to determine differences in arthralgia prevalence by affected joint sites. We used Stata 14.0 (StataCorp LLC, College Station, TX, USA) for the analysis.

Six months after disease onset, the difference in persistent arthralgia prevalence between case-patients and controls was 32% (95% CI 24%–40%), after adjusting for age, sex, and self-reported history of arthritis; 12 months after onset, the difference was 19% (95% CI 11%–28%) (Table 1). At 6 months, case-patients reported higher prevalence of foot-specific joint pain (28%, 95% CI 11%–44%), and at 12 months, controls reported higher prevalence of knee-specific pain (29%, 95% CI 8%–50%) (Figure 1). At 12 months, we found no statistically significant differences by joint site between case-patients and controls (Figure 2).

After we adjusted for age, sex, and self-reported history of arthritis, case-patients were 1.77 (95% CI 1.06–2.95) times more likely than controls to have difficulty walking and 1.81 (95% CI 1.15–2.86) times more likely to have difficulty climbing stairs (Table 1). Case-patients were also 2.65 (95% CI 1.32–5.32) times more likely to have difficulty getting in and out of cars and 2.24 (95% CI 1.28–3.91) times more likely to have difficulty opening jars.

Conclusions

Although acute symptoms of CHIKV infection are well-documented (*12*), information on the prevalence of long-term sequelae remains limited to observational studies, many of which lack comparator groups (*4*). From our year-long study of 165 case-patients and 167 controls, we found an almost 3-fold increased risk for persistent arthralgia in CHIKV case-patients at 6 and 12 months after illness onset. At 12 months, case-patients were significantly (p<0.01) more likely than controls to report difficulty performing daily activities. Our unadjusted persistent arthralgia estimates at 6 (44%) and 12 (33%) months (Table 2) fall within the pooled estimate from a metaanalysis (40%, 95% CI 31%–49%) (*4*).

Consistent with findings in previous studies, case-patients in our study reported a higher prevalence of foot-specific joint pain, (*6*,*8*,*13*,*14*). Furthermore, a higher proportion of case-patients reported the presence of persistent arthralgia and of more severe arthralgia in the morning; this finding is consistent with those from previous studies reporting a high prevalence of morning stiffness among case-patients (*6*,*8*).

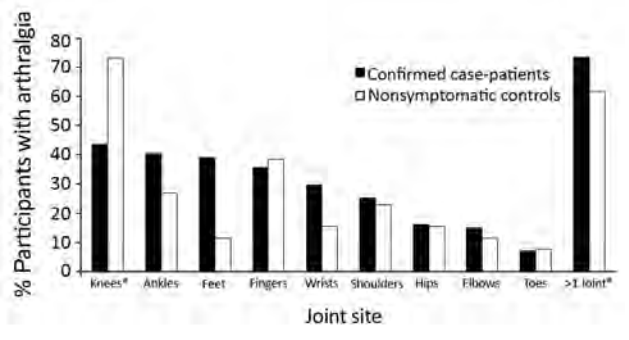

Figure 1. Arthralgia reported by joint site among confirmed chikungunya virus case-patients 6 months after illness onset and by nonsymptomatic controls enrolled at the time of the 12-month follow-up for case-patients, US Virgin Islands, December 2014–February 2016. *Statistically significant differences (p<0.01) between case-patients and controls.

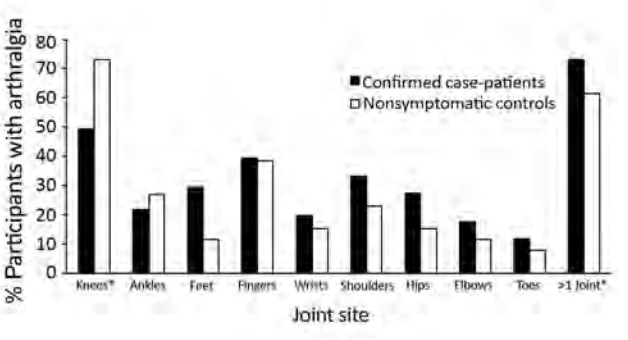

Figure 2. Arthralgia reported by joint site among confirmed chikungunya virus case-patients 12 months after illness onset and by nonsymptomatic controls enrolled at the time of the 12-month follow-up for case-patients, US Virgin Islands, December 2014–February 2016. No statistically significant differences were found between case-patients and controls.

Table 2. Demographic and physical characteristics among residents in a study of persistent arthralgia after a chikungunya virus outbreak, US Virgin Islands, December 2014–February 2016*

Variable	No. (%) chikungunya virus case-patients		No. (%) nonsymptomatic controls at 12-month case-patient follow-up, N = 167*
	6 months after symptom onset, N = 165	12 months after symptom onset, N = 128	
Median age (range), y	52 (1-96)	52 (1-92)	35 (2-78)
Sex			
F	108 (65)	82 (64)	108 (65)
M	57 (35)	46 (36)	59 (35)
Employed or a student	96 (58)	73 (57)	125 (75)
History of self-reported arthritis	37 (22)	30 (23)	28 (17)
Annual household income <US$50,000	–	82 (64)	121 (72)
Joint pain day of interview	59 (36)	34 (27)	14 (8)
Joint pain within month of interview	87 (53)	51 (40)	26 (16)
Difficulty performing daily activities			
Walking	–	36 (28)	20 (12)
Climbing stairs	–	40 (31)	20 (12)
Lifting heavy objects	–	27 (21)	16 (10)
Getting in and out of cars	–	27 (21)	10 (6)
Opening jars	–	33 (26)	13 (8)
Sleeping	27 (31)	19 (37)	8 (29)
Health somewhat/much worse after 1 y	–	28 (22)	16 (10)
Subsample of participants reporting joint pain within mo of interview	N = 87	N = 51	N = 26
Persistent arthralgia	72 (44)	42 (33)	20 (12)
Joint pain frequency			
Daily	42 (48)	28 (55)	13 (50)
2–3 times/wk	17 (20)	8 (16)	5 (19)
1 time/wk	13 (15)	6 (12)	2 (8)
<1 time/wk	12 (14)	9 (18)	6 (23)
Not known	3 (3)	0	0
Symmetrical joint pain	27 (31)	14 (27)	7 (27)
Joint pain time of day			
Morning	16 (18)	12 (24)	2 (8)
Day	10 (11)	5 (10)	1 (4)
Night	11 (13)	6 (12)	5 (19)
Morning and night	5 (6)	2 (4)	1 (4)
Present at all times or activity dependent	43 (49)	23 (45)	15 (58)
Not known	2 (2)	3 (6)	2 (8)
Worst time of day for joint pain			
Morning	29 (33)	21 (41)	3 (12)
Day	9 (10)	7 (14)	1 (4)
Night	20 (23)	8 (16)	8 (31)
Morning and night	3 (3)	3 (6)	0
Present at all times or activity dependent	23 (26)	8 (16)	12 (46)
Not known	3 (3)	4 (8)	2 (8)

*Values are no. (%) except as indicated. –,data not obtained.

Our comparative study had limitations, which may have influenced our findings. First, due to missing or incorrect contact information (online Technical Appendix Table 2), the study sample represents only 36% of eligible confirmed CHIKV case-patients and thus might not be representative of all USVI residents with CHIKV disease. Second, controls were younger than case-patients and were interviewed only once. Thus, we may have overestimated persistent arthralgia among case-patients due to progression of osteoarthritis associated with increased age and may have underestimated persistent arthralgia among controls. However, a BRFSS (Behavioral Risk Factor Surveillance System) survey indicated that 15% (95% CI 14%–17%) of adult USVI residents reported having arthritis (*15*), a percentage consistent with our estimated persistent arthralgia prevalence among controls (17%). Third, we did not test all controls for CHIKV IgG; thus, some controls with asymptomatic CHIKV infection may have been included in the analysis. However, prevalence differences were similar when we included controls who were asymptomatic but IgG-positive (n = 12). Last, most case-patients knew their diagnosis, which may have influenced their reporting of persistence arthralgia, and case-patients with persistent arthralgia may have been more inclined to participate in the interviews. As a result of these limitations, we may have overestimated the association between persistent arthralgia and CHIKV disease up to 1 year after illness onset.

Our results emphasize that, in the USVI, CHIKV illness was associated with persistent arthralgia and difficulty with daily activities 1 year after disease onset. These

findings highlight the need for therapeutic and vaccine research to manage and prevent acute illness and long-term sequelae associated with CHIKV infection. The results also underscore the need for studies to identify risk factors for long-term sequelae of CHIKV illness, to estimate the burden of persistent arthralgia after acute illness, and to understand the effect of persistent arthralgia on quality of life.

Acknowledgments

Assistance with data collection was provided by Michael Johansson, Christina Sancken, Zachary Heth and Elyse Phillips. Diagnostic expertise and assistance was generously provided by the Centers for Disease Control and Prevention.

This work was supported by the National Institutes of Health National Institute of Allergy and Infectious Disease (R37-AI032042), and National Institute of General Medical Sciences (U54 GM111274) and by the US Virgin Islands Department of Health.

Dr. Feldstein is a postdoctoral research fellow at Fred Hutchinson Cancer Research Center. Her research focuses on the epidemiology of emerging and neglected tropical diseases.

References

1. Pan American Health Organization, World Health Organization. Chikungunya: statistics data. Geographic distribution, 2016 [cited 2016 Sep 9]. http://www.paho.org/hq/index.php?option=com_topics&view=readall&cid=5927&Itemid=40931&lang=en
2. Centers for Disease Control and Prevention. Chikungunya virus. Geographic distribution [cited 2016 May 3]. http://www.cdc.gov/chikungunya/geo/index.html
3. Staples JE, Breiman RF, Powers AM. Chikungunya fever: an epidemiological review of a re-emerging infectious disease. Clin Infect Dis. 2009;49:942–8.
4. Rodríguez-Morales AJ, Cardona-Ospina JA, Fernanda Urbano-Garzón S, Sebastian Hurtado-Zapata J. Prevalence of post-chikungunya infection chronic inflammatory arthritis: a systematic review and meta-analysis. Arthritis Care Res (Hoboken). 2016;68:1849–58.
5. Javelle E, Ribera A, Degasne I, Gaüzère B-A, Marimoutou C, Simon F. Specific management of post-chikungunya rheumatic disorders: a retrospective study of 159 cases in Reunion Island from 2006-2012. PLoS Negl Trop Dis. 2015;9:e0003603.
6. Schilte C, Staikowsky F, Couderc T, Madec Y, Carpentier F, Kassab S, et al. Chikungunya virus-associated long-term arthralgia: a 36-month prospective longitudinal study. PLoS Negl Trop Dis. 2013;7:e2137.
7. Mohd Zim MA, Sam I-C, Omar SFS, Chan YF, AbuBakar S, Kamarulzaman A. Chikungunya infection in Malaysia: comparison with dengue infection in adults and predictors of persistent arthralgia. J Clin Virol. 2013;56:141–5.
8. Sissoko D, Malvy D, Ezzedine K, Renault P, Moscetti F, Ledrans M, et al. Post-epidemic Chikungunya disease on Reunion Island: course of rheumatic manifestations and associated factors over a 15-month period. PLoS Negl Trop Dis. 2009;3:e389.
9. Rodriguez-Morales AJ, Gil-Restrepo AF, Ramírez-Jaramillo V, Montoya-Arias CP, Acevedo-Mendoza WF, Bedoya-Arias JE, et al. Post-chikungunya chronic inflammatory rheumatism: results from a retrospective follow-up study of 283 adult and child cases in La Virginia, Risaralda, Colombia. F1000 Res. 2016;5:360.
10. Ellis E. Chikungunya surveillance weekly report. St. Croix (US Virgin Islands): US Virgin Islands Department of Health; 2015.
11. Feldstein LR, Ellis EM, Rowhani-Rahbar A, Halloran ME, Ellis BR. The first reported outbreak of chikungunya in the US Virgin Islands, 2014–2015. Am J Trop Med Hyg. 2016;95:885–9.
12. Pialoux G, Gaüzère B-A, Jauréguiberry S, Strobel M. Chikungunya, an epidemic arbovirus. Lancet Infect Dis. 2007;7:319–27.
13. Moro ML, Grilli E, Corvetta A, Silvi G, Angelini R, Mascella F, et al.; Study Group "Infezioni da Chikungunya in Emilia-Romagna". Long-term chikungunya infection clinical manifestations after an outbreak in Italy: a prognostic cohort study. J Infect. 2012;65:165–72.
14. Soumahoro M-K, Gérardin P, Boëlle P-Y, Perrau J, Fianu A, Pouchot J, et al. Impact of chikungunya virus infection on health status and quality of life: a retrospective cohort study. PLoS One. 2009;4:e7800.
15. Centers for Disease Control and Prevention. BRFSS prevalence and trends data, 2010 [cited 2015 Jul 22]. https://www.cdc.gov/brfss/brfssprevalence/index.html

Address for correspondence: Leora R. Feldstein, Fred Hutchinson Cancer Research Center, 1100 Fairview Ave N, Seattle, WA 98109, USA; email: lrfeldst@uw.edu

Assessing Sensitivity and Specificity of Surveillance Case Definitions for Zika Virus Disease

Angela Chow, Hanley Ho, Mar-Kyaw Win, Yee-Sin Leo

We evaluated performance of 5 case definitions for Zika virus disease surveillance in a human cohort during an outbreak in Singapore, August 26–September 5, 2016. Because laboratory tests are largely inaccessible, use of case definitions that include rash as a required clinical feature are useful in identifying this disease.

Zika virus infections in humans were first reported in Nigeria, Uganda, and Tanganyika (now Tanzania) in 1951–1952 (*1*,*2*). Until 2006, sporadic cases and small clusters of Zika virus infections were reported (*3*). In 2007, the first major outbreak occurred on Yap Island, where ≈1/5 infected persons were symptomatic, predominantly with rash, fever, arthralgia, and conjunctivitis (*4*). In a recent outbreak in Brazil in 2015, similar signs and symptoms predominated (*5*). Rash (67%), fever (64%), arthralgia (29%), myalgia (24%), headache (22%), and conjunctivitis (21%) were the 6 most common signs and symptoms reported during January 1964–February 2016 (*3*).

Unlike dengue virus (a related flavivirus), Zika virus was not considered to be a major pathogen until recent reports of its association with Guillain-Barré syndrome and microcephaly (*6*). Thus, there is little information on the performance of surveillance case definitions for detection of Zika virus disease.

Responding to the rapidly evolving Zika virus epidemic to guide surveillance for Zika virus disease, the US Centers for Disease Control and Prevention worked with the Council of State and Territorial Epidemiologists (CSTE) to approve an interim definition in February 2016 and a final case definition in June 2016 for noncongenital Zika virus disease as >1 of the following signs or symptoms: acute onset of fever, maculopapular rash, arthralgia, and conjunctivitis (*7*). The interim case definition (February 2016) of the World Health Organization (WHO) for suspected Zika virus disease includes rash or fever and >1 of the following signs or symptoms: arthralgia, arthritis, and conjunctivitis (nonpurulent/hyperemic) (*8*). The case definition of the European Centre for Disease Prevention and Control (ECDC) includes rash and optional symptoms in the WHO definition plus myalgia (*9*). The case definition of the Pan American Health Organization (PAHO) includes rash and ≥2 of the following signs or symptoms: fever, conjunctivitis (nonpurulent/hyperemic), arthralgia, myalgia, and periarticular edema (*10*).

The first outbreak of Zika virus disease in Singapore occurred in August 2016 (*11*). Singapore is a densely populated tropical country to which dengue fever is endemic. With the identification of the first local case of Zika virus disease, the Singapore Ministry of Health (MOH) initiated active case finding (*12*,*13*). The MOH recommended Zika virus screening for persons with fever and maculopapular rash, and 1 of the following: arthralgia, myalgia, headache, and nonpurulent conjunctivitis.

Clinical criteria for disease surveillance are a balancing act for satisfying 2 potentially conflicting needs: sensitivity and specificity. A more sensitive case definition will identify a larger proportion of true cases, but at the cost of finding a large number of cases from other causes. In comparison, a more specific case definition will provide a more accurate description of true cases, but at the expense of missing true cases (*14*).

The Study

We evaluated the performance of surveillance case definitions for Zika virus disease recommended by the CSTE, WHO, PAHO, ECDC, and the Singapore MOH by using a cohort of 359 adult patients with suspected Zika virus disease who came to the Institute of Infectious Diseases and Epidemiology, Tan Tock Seng Hospital, Singapore, the national referral center for Zika virus disease during the containment phase of the Zika virus outbreak during August 26– September 5, 2016. All adults living or working in the outbreak area who were sick and had symptoms that partially or fully met the MOH definition were screened for Zika virus disease.

At their first visit to the hospital, all patients had their signs and symptoms documented, and blood and urine samples were obtained for detection of Zika virus nucleic acids by reverse transcription PCR (RT-PCR) (*15*). Parallel testing in the hospital laboratory and at the National Public Health Laboratory (Singapore) was conducted to maximize sensitivity and negative predictive values to rule out Zika virus infection.

A total of 42.0% of the cohort had Zika virus infection confirmed in blood (4%), urine (36%), or both (60%) samples (Table 1). Most (80%) infected and noninfected

Author affiliation: Tan Tock Seng Hospital, Singapore

DOI: http://dx.doi.org/10.3201/eid2304.161716

Table 1. Clinical characteristics of an adult cohort with suspected Zika virus disease, Singapore, August 26–September 5, 2016*

Characteristic	Zika virus positive, n = 149	Zika virus negative, n = 210
Demographic data		
Mean age, y (SD)	38.1 (14.2)	34.2 (12.1)
Sex		
M	92 (61.7)	129 (61.4)
F	57 (38.3)	81 (38.6)
Ethnicity		
Chinese	109 (73.2)	122 (58.1)
Malay	15 (10.1)	17 (8.1)
Indian	9 (6.0)	24 (11.4)
Other	16 (10.7)	47 (22.4)
Singapore residents	113 (75.8)	131 (62.4)
Signs and symptoms at presentation		
Rash	139 (93.3)	94 (44.8)
Fever	118 (79.2)	181 (86.2)
Myalgia	63 (42.3)	124 (59.1)
Headache	35 (23.5)	75 (35.7)
Conjunctivitis	35 (23.5)	32 (15.2)
Arthralgia	34 (22.8)	50 (23.8)
Pruritis	17 (11.4)	17 (8.1)
Any gastrointestinal symptom†	10 (6.7)	25 (11.9)
Fulfilled case definition		
United States‡	149 (100.0)	206 (98.1)
World Health Organization§	57 (38.3)	64 (30.5)
PAHO¶	73 (49.0)	50 (23.8)
ECDC#	83 (55.7)	55 (26.2)
Singapore Ministry of Health**	81 (54.4)	51 (24.3)

*Values are no. (%) except as indicated. ECDC, European Centre for Disease Prevention and Control; PAHO, Pan American Health Organization.
†Nausea, vomiting, diarrhea, or abdominal pain.
‡Definition used in the United States (interim, February 2016; confirmed, June 2016) states that clinical criteria for noncongenital Zika virus disease are defined as >1 of the following: acute onset of fever, maculopapular rash, arthralgia, and conjunctivitis.
§Interim case definition (February 12, 2016) includes rash or fever and >1 of the following signs or symptoms: arthralgia or arthritis, or conjunctivitis (nonpurulent/hyperemic).
¶Interim case definition (April 1, 2016) includes rash with >2 of the following signs or symptoms: fever, conjunctivitis (nonpurulent/hyperemic), arthralgia, myalgia, or periarticular edema.
#Interim case definition (March 17, 2016) includes rash with or without fever and >1 of the following signs or symptoms: arthralgia, myalgia, or conjunctivitis (nonpurulent/hyperemic).
**Case definition (August 2016) includes fever and rash and >1 of the following symptoms: headache, myalgia, arthralgia, or nonpurulent conjunctivitis.

patients were tested ≤5 days after illness onset (infected patients, mean 3.6 days; noninfected patients, mean 4.6 days). Infected and noninfected patients were similar in age and sex. No female patients were pregnant. Among Zika virus–infected patients, rash (93.3%) was the most common symptom, followed by fever (79.2%) and myalgia (42.3%). Headache, arthralgia, and conjunctivitis were reported in <25% patients with Zika virus disease. Pruritus (11.4%) and gastrointestinal symptoms (6.7%) were relatively uncommon. For patients not infected with Zika virus, fever (86.2%) was the most common symptom, followed by myalgia (59.1%) and rash (44.8%).

The case definition recommended by CSTE for use in the United States (US definition) had a sensitivity of 100% and a specificity of 2% in detecting Zika virus in the cohort (Table 2). The WHO case definition had the lowest sensitivity (38%). The Singapore MOH case definition had a sensitivity of 54% and a high specificity of 76%, and performed well in diagnosing Zika virus disease (positive likelihood ratio [LR+] 2.2, 95% CI 1.7–3.0). The performances of PAHO (LR+ 2.1, 95% CI 1.5–2.8) and ECDC (LR+ 2.1, 95% CI 1.6–2.8) case definitions were similar.

Conclusions

Despite increasing incidence of Zika virus disease and its spread across the Americas and Asia, there is no internationally adopted common clinical criteria for the surveillance of this disease. We report a large outbreak

Table 2. Performance of case definitions for diagnosing Zika virus infection in a human cohort during an outbreak, Singapore, August 26–September 5, 2016*

Case definition	Sensitivity, %	Specificity, %	PPV, %	NPV, %	LR+ (95% CI)	LR– (95% CI)
United States	100	2	42	100	1.02 (1.00–1.04)	0
WHO	38	70	47	61	1.3 (0.9–1.7)	0.9 (0.8–1.0)
PAHO	49	76	59	68	2.1 (1.5–2.8)	0.7 (0.6–0.8)
ECDC	56	74	60	70	2.1 (1.6–2.8)	0.6 (0.5–0.7)
Singapore MOH	54	76	61	70	2.2 (1.7–3.0)	0.6 (0.5–0.7)

*ECDC, European Centre for Disease Prevention and Control; LR, likelihood ratio; MOH, Ministry of Health; NPV, negative predictive value; PAHO, Pan American Health Organization; PPV, positive predictive value; WHO, World Health Organization; +, positive; –, negative.

cohort of patients with suspected Zika virus infection and comprehensive documentation of clinical symptoms and parallel RT-PCR conducted on blood and urine samples for these patients by 2 laboratories. Evaluation of the performance of surveillance case definitions in such a cohort would provide useful findings that would contribute to development of guidance for Zika virus disease surveillance.

Diagnosis of Zika virus disease remains suboptimal because of limited availability of confirmatory testing by RT-PCR during acute illness and cross-reactivity of serologic tests for Zika virus with other co-circulating flaviviruses (*3*,*4*). Thus, a good discriminatory clinical criteria for disease surveillance is crucial for prevention and control of Zika virus transmission.

The US case definition would identify all Zika virus infections and be useful for prevention of autochthonous transmission by imported cases. However, because this definition is not specific, considerable resources would be required for confirmatory testing of identified cases. The definition requires laboratory testing to report a case. Thus, sensitivity of the definition is most likely appropriate in the US setting. Conversely, the WHO case definition might miss 60% of Zika virus infections. For Zika virus disease surveillance in the absence of commercially available diagnostic laboratory tests, case definitions incorporating rash as a required clinical criteria, such as the PAHO, ECDC, and Singapore MOH case definitions, would be useful (LR+ >2), although ≈50% (range 44%–51%) of cases of Zika virus disease could be missed.

The main limitation of this study is that it included only adults. However, the small number of children infected with Zika virus during the containment phase of the outbreak in Singapore had symptoms similar to those for adults (A. Chow et al., unpub. data). Some Zika virus infections could have been misclassified as noninfections because RT-PCR could have missed infections late in the illness course or after development of antibodies against Zika virus.

In conclusion, we evaluated the performance of 5 case definitions for Zika virus disease surveillance. In the current effort to halt transmission of this virus worldwide, and with laboratory tests being largely inaccessible, use of surveillance case definitions that include rash as a required clinical criteria would provide a high yield in identifying Zika virus disease.

Dr. Chow is a preventive medicine physician at and head of the Department of Clinical Epidemiology, Institute of Infectious Diseases and Epidemiology, Tan Tock Seng Hospital, Singapore. Her primary research interest is infectious disease epidemiology.

References

1. MacNamara FN. Zika virus: a report on three cases of human infection during an epidemic of jaundice in Nigeria. Trans R Soc Trop Med Hyg. 1954;48:139–45 10.1016/0035-9203(54)90006-1.
2. Smithburn KC. Neutralizing antibodies against certain recently isolated viruses in the sera of human beings residing in east Africa. J Immunol. 1952;69:223–34.
3. Plourde AR, Bloch EM. A literature review of Zika virus. Emerg Infect Dis. 2016;22:1185–92 10.3201/eid2207.151990.
4. Duffy MR, Chen TH, Hancock WT, Powers AM, Kool JL, Lanciotti RS, et al. Zika virus outbreak on Yap Island, Federated States of Micronesia. N Engl J Med. 2009;360:2536–43 10.1056/NEJMoa0805715.
5. Brasil P, Calvet GA, Siqueira AM, Wakimoto M, de Sequeira PC, Nobre A, et al. Zika virus outbreak in Rio de Janeiro, Brazil: clinical characterization, epidemiological and virological aspects. PLoS Negl Trop Dis. 2016;10:e0004636 10.1371/journal.pntd.0004636.
6. Paploski IA, Prates AP, Cardoso CW, Kikuti M, Silva MM, Waller LA, et al. Time lags between exanthematous illness attributed to Zika virus, Guillain-Barré syndrome, and microcephaly, Salvador, Brazil. Emerg Infect Dis. 2016;22:1438–44 10.3201/eid2208.160496.
7. Centers for Disease Control and Prevention. Zika virus disease and Zika virus infection, 2016 case definition, approved June 2016 [cited 2016 Oct 11]. https://wwwn.cdc.gov/nndss/conditions/zika-virus-disease-and-zika-virus-congenital-infection/case-definition/2016/
8. World Health Organization. Zika virus disease: interim case definition. Feb 12, 2016 [cited 2016 Oct 11]. http://www.who.int/csr/disease/zika/case-definition/en/
9. European Centre for Disease Control and Prevention. Zika virus infection: case definition, Jul 21, 2016 [cited 2016 Oct 11]. http://ecdc.europa.eu/en/healthtopics/zika_virus_infection/patient-case-management/Pages/case-definition.aspx
10. Pan American Health Organization. Zika case definitions. Apr 1, 2016 [cited 2016 Nov 19]. http://www.paho.org/hq/index.php?option=com_content&view=article&id=11117:2015-zika-case-definitions-&Itemid=41532&lang=en
11. Sadarangani SP, Hsu LY. The 2016 outbreak of Zika in Singapore. Ann Acad Med Singapore. 2016;45:381–2.
12. Maurer-Stroh S, Mak TM, Ng YK, Phuah SP, Huber RG, Marzinek JK, et al. South-east Asian Zika virus strain linked to cluster of cases in Singapore, August 2016. Euro Surveill. 2016;21:30347. 10.2807/1560-7917.ES.2016.21.38.30347 http://dx.doi.org/10.2807/1560-7917.ES.2016.21.38.30347
13. Ministry of Health Singapore. First case of locally transmitted Zika virus infection. Aug 27, 2016 [cited 2016 Oct 11]. https://www.moh.gov.sg/content/moh_web/home/pressRoom/pressRoomItemRelease/2016/first-case-of-locally-transmitted-zika-virus-infection.html
14. Giesecke J. Modern infectious disease epidemiology. New York: Oxford University Press; 2002.
15. Lanciotti RS, Kosoy OL, Laven JJ, Velez JO, Lambert AJ, Johnson AJ, et al. Genetic and serologic properties of Zika virus associated with an epidemic, Yap State, Micronesia, 2007. Emerg Infect Dis. 2008;14:1232–9 10.3201/eid1408.080287.

Address for correspondence: Angela Chow, Institute of Infectious Diseases and Epidemiology, Tan Tock Seng Hospital, 11 Jalan Tan Tock Seng, Singapore; email: angela_chow@ttsh.com.sg

Detection of Zika Virus in Desiccated Mosquitoes by Real-Time Reverse Transcription PCR and Plaque Assay

Kristen L. Burkhalter, Harry M. Savage

We assayed Zika virus–infected mosquitoes stored at room temperature for ≤30 days for live virus by using plaque assay and virus RNA by using real-time reverse transcription PCR. Viable virus was detected in samples stored ≤10 days, and virus RNA was detected in samples held for 30 days.

Laboratory detection of Zika virus in field-collected mosquitoes is often accomplished by using molecular methods, such as reverse transcription PCR (RT-PCR) or virus isolation protocols. Sample handling conditions recommended for these assays include maintaining a cold chain from field to laboratory to preserve live virus and mitigate degradation of virus RNA.

Ideally, mosquitoes should be stored and shipped to a diagnostic laboratory at a temperature of −70°C or below. However, in some locations, an optimal cold chain is difficult to maintain when shipping the specimens because of unavailability of a liquid nitrogen or dry ice supplier. We tested Zika virus–infected mosquitoes that had been stored at room temperature for ≤30 days by using real-time RT-PCR to determine the rate of recovery of virus RNA and Vero cell plaque assays to determine the rate of recovery of infectious virus.

The Study

Female, laboratory-reared *Aedes aegypti* (REXD strain) mosquitoes were intrathoracically inoculated with 0.3 μL of ≈4.7 $\log_{10}$ PFU/mL of Zika virus (MR766 strain) as described (*1*). Inoculated mosquitoes were incubated for 7 days at 26°C and a relative humidity of 80% during a 16:8 h photoperiod, then killed by freezing overnight at −80°C. Nine mosquitoes were retained at −80°C until the end of the experiment to serve as controls (referred to as day 0). The remaining mosquitoes were kept in an open petri dish at room temperature (21°C) and a relative humidity of 50% during a 16:8 h photoperiod until collected. Six mosquitoes were collected every other day, from day 2 through day 30, and stored at −80°C until tested.

Author affiliation: Centers for Disease Control and Prevention, Fort Collins, Colorado, USA

DOI: http://dx.doi.org/10.3201/eid2304.161772

Mosquitoes were homogenized individually in 500 μL of cell culture medium/bovine albumin by vortexing with 1 copper-clad steel bead, and centrifuged for 3 min at 1,700 × *g*. We extracted virus RNA from a 100-μL aliquot of the resulting supernatant by using the QIAmp Virus BioRobot 9604 Kit and a BioRobot Universal System (QIAGEN, Valencia, CA, USA) according to the manufacturer's protocol. Real-time RT-PCR (sensitivity limit 25 RNA copies) (*2*) was performed by using a Quantitect Probe RT-PCR Kit (QIAGEN) and primers specific for the envelope region of the Zika virus genome, according to the manufacturer's instructions. Samples with a cycle threshold (C_t) ≤38 were considered positive. In addition, day 0 control mosquitoes that had been stored at −80°C and all mosquitoes collected on days 2–30 were assayed for viable virus by using Vero plaque assay cell culture as described (*3*).

Vero cell plaque assay results for day 0 samples, which were frozen until testing and served as controls, had expected virus titers (range 6.3–6.8 $\log_{10}$ PFU/mL) (Table). Viable virus was recovered from 6/6 (100.0%) pools collected on day 2, 2/6 (33.3%) pools collected on day 4, 1/6 (16.6%) pools collected on day 6, and 1/6 (16.6%) pools collected on day 10. Titers of viable virus recovered from individual desiccated mosquitoes at days 2–10 ranged from 1.69 to 2.6 $\log_{10}$ PFU/mL (Table). The remaining replicates from days 4, 6, and 10, and all replicates from day 8 and days 12–30 did not produce plaques. A similar study with dried Zika virus stock stored at room temperature for 4.5 days showed that virus was still infectious after reconstitution at 3.5 days (*4*), which correlates with our findings for desiccated mosquitoes.

Although virus titers of desiccated mosquitoes had been reduced, evidence of residual infectivity indicates that precautions, such as use of proper personal protective equipment and appropriate biosafety protocols, are required when handling field-collected samples regardless of storage conditions because these samples might contain viable virus. The large reduction of infectivity in desiccated samples collected on days 2–10 and the complete reduction of infectivity in samples beyond day 10 confirm that a cold chain is required if infectious virus retrieval is the goal of the field collection effort.

Maintaining a cold chain is less critical for detecting Zika virus RNA in mosquito pools. Real-time RT-PCR

Table. Zika virus titers for infected mosquitoes stored at room temperature (21°C) and collected every other day for 2–30 days and control samples*

Day of collection	No. samples with live virus/no. tested (%)	Mean titer, log_{10} PFU/mL (95% CI)
0	9/9 (100.0)	6.62 (6.52–6.72)
2	6/6 (100.0)	2.3 (2.06–2.54)
4	2/6 (33.3)	1.85 (0.63–3.07)
6	1/6 (16.6)	1.69
8	0/6 (0)	NA
10	1/6 (16.6)	2.5
12–30	0/6 per day (0)	NA

*Control samples (day 0) were stored at –80°C until testing. NA, not applicable.

C_t values for day 0 control samples ranged from 23.9 to 29.1 (Figure). Although C_t values of desiccated samples increased over the 30-day holding period, all samples from each time point were positive (C_t <38), with the exception of 1 sample from day 18 from which virus RNA could not be detected (Figure). Stability of virus RNA from either mosquito samples or lyophilized virus held at room temperature has been demonstrated for other arboviruses, including West Nile, chikungunya, yellow fever, and Venezuelan equine encephalitis viruses (*5*–*7*). Future evaluations that include variable temperature, lighting conditions, and humidity would elucidate how diverse conditions encountered in the field affect recovery of Zika virus RNA.

Conclusions

Results from this study suggest that, although Zika virus RNA in samples kept at room temperature degrades with time, qualitative detection by real-time RT-PCR is possible for up to 30 days. Although agencies should strive to implement recommended protocols and maintain a cold chain, this is not always possible when performing field-based entomologic arbovirus surveillance, particularly in remote areas where dry ice and ultralow freezers are absent. If the goal of a surveillance program is to determine the infection rate in mosquito populations as efficiently as possible, and is not focused on recovery of live virus, storage and shipment from the field to the testing laboratory under less than optimal conditions would be sufficient for virus detection by using real-time RT-PCR.

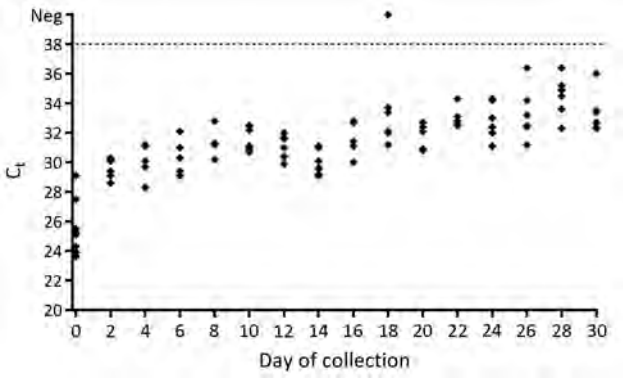

Figure. Real-time reverse transcription PCR cycle threshold (C_t) values for mosquitoes infected with Zika virus and stored at room temperature (21°C) for 2–30 days and for control samples (day 0) stored at –80°C until testing. Samples with a C_t ≤38 (dashed line) were considered positive. Each diamond indicates a mosquito pool. Neg, negative.

Acknowledgment

We thank Mark Schmaedick for asking the question that led to this study.

Ms. Burkhalter is a microbiologist at the Division of Vector-Borne Diseases, National Center for Emerging and Zoonotic Infectious Diseases, Centers for Disease Control and Prevention, Fort Collins, CO. Her research interests include development and optimization of methods to improve detection of arboviruses in environmental samples and providing support for public health partners of the Centers for Disease Control and Prevention.

Dr. Savage is chief of Ecology Entomology Activity, Division of Vector-Borne Diseases, National Center for Emerging and Zoonotic Infectious Diseases, Centers for Disease Control and Prevention, Fort Collins, CO. His research interests include vector surveillance and control, vector biology, and transmission dynamics of arboviruses.

References

1. Rosen L, Gubler D. The use of mosquitoes to detect and propagate dengue viruses. Am J Trop Med Hyg. 1974;23:1153–60.
2. Lanciotti RS, Kosoy OL, Laven JJ, Velez JO, Lambert AJ, Johnson AJ, et al. Genetic and serologic properties of Zika virus associated with an epidemic, Yap State, Micronesia, 2007. Emerg Infect Dis. 2008;14:1232–9. http://dx.doi.org/10.3201/eid1408.080287
3. Beaty BJ, Calisher CH, Shope RS. Diagnostic procedures for viral, rickettsial and chlamydial infections. In: Lennete ET, Lennete DA, editors. Arbovirology. 7th ed. Washington (DC): American Public Health Association; 1995. p. 189–212.
4. Müller JA, Harms M, Schubert A, Jansen S, Michel D, Mertens T, et al. Inactivation and environmental stability of Zika virus. Emerg Infect Dis. 2016;22:1685–7. http://dx.doi.org/10.3201/eid2209.160664
5. Turell MJ, Spring AR, Miller MK, Cannon CE. Effect of holding conditions on the detection of West Nile viral RNA by reverse transcriptase-polymerase chain reaction from mosquito (Diptera: Culicidae) pools. J Med Entomol. 2002;39:1–3. http://dx.doi.org/10.1603/0022-2585-39.1.1
6. Guzman H, Ding X, Xiao SY, Tesh RB. Duration of infectivity and RNA of Venezuelan equine encephalitis, West Nile, and yellow fever viruses dried on filter paper and maintained at room temperature. Am J Trop Med Hyg. 2005;72:474–7.
7. Andrews ES, Turell MJ. Effect of holding conditions on the detection of chikungunya and Venezuelan equine encephalitis viruses in mosquito pools. J Am Mosq Control Assoc. 2016;32:51–4. http://dx.doi.org/10.2987/moco-32-01-51-54.1

Address for correspondence: Kristen L. Burkhalter, Centers for Disease Control and Prevention, 3156 Rampart Rd, Fort Collins, CO 80521, USA; email: ktb3@cdc.gov

Surveillance and Testing for Middle East Respiratory Syndrome Coronavirus, Saudi Arabia, April 2015–February 2016

Abdulaziz A. Bin Saeed, Glen R. Abedi, Abdullah G. Alzahrani, Iyad Salameh, Fatima Abdirizak, Raafat Alhakeem, Homoud Algarni, Osman A. El Nil, Mutaz Mohammed, Abdullah M. Assiri, Hail M. Alabdely, John T. Watson, Susan I. Gerber

Saudi Arabia has reported >80% of the Middle East respiratory syndrome coronavirus (MERS-CoV) cases worldwide. During April 2015–February 2016, Saudi Arabia identified and tested 57,363 persons (18.4/10,000 residents) with suspected MERS-CoV infection; 384 (0.7%) tested positive. Robust, extensive, and timely surveillance is critical for limiting virus transmission.

Middle East respiratory syndrome (MERS) coronavirus (CoV) causes severe respiratory illness in humans, with death occurring in >35% of reported cases (*1*). MERS has been documented among persons with close contact with known case-patients in healthcare (*2*) and household (*3*) settings and among persons with recent contact with dromedaries (*4*). Proper clinical management of persons with suspected MERS-CoV infection who seek care in a healthcare setting relies upon adherence to recommended infection-control precautions (*5*), which in turn depends upon the early recognition of cases.

The International Health Regulations Emergency Committee of the World Health Organization reported that data sharing for this disease, including sharing of surveillance results, "remains limited and has fallen short of expectations" (*6*). To determine the extent of MERS surveillance in Saudi Arabia, we reviewed electronic surveillance data collected during April 1, 2015–February 1, 2016, to describe trends in surveillance for MERS and to compare demographic and clinical features among persons tested.

The Study

In Saudi Arabia, persons who should be tested for MERS-CoV include suspect case-patients who meet at least 1 of 4 case definition categories (online Technical Appendix Table, https://wwwnc.cdc.gov/EID/article/23/4/16-1793-Techapp1.pdf). In brief, the categories are persons with community-acquired pneumonia (category I); healthcare-associated pneumonia (II); symptoms after exposure to a MERS-CoV case-patient (III); or unexplained febrile illness (IV). The case definition was revised in May 2014 (*7*); additional refinements were made in June 2015 (*8*). The 2015 definition included changes to the approach for testing children ≤14 years of age with nonsevere illness (testing is reserved for children with exposure to camels or camel products or to a confirmed or suspected MERS case-patient). In addition to suspected cases, testing is recommended for close contacts of persons with confirmed MERS-CoV infection, regardless of symptoms, and can also be requested at the discretion of an infectious disease consultant. Tests are performed on respiratory specimens at 5 regional laboratories using real-time PCR (*9*).

Since March 7, 2015, official reporting of cases referred for MERS-CoV testing in Saudi Arabia has exclusively been documented through the Health Electronic Surveillance Network (HESN). When a suspected case-patient is identified for testing, the referring hospital reports demographic and basic clinical data to HESN (Figure 1). After specimens are

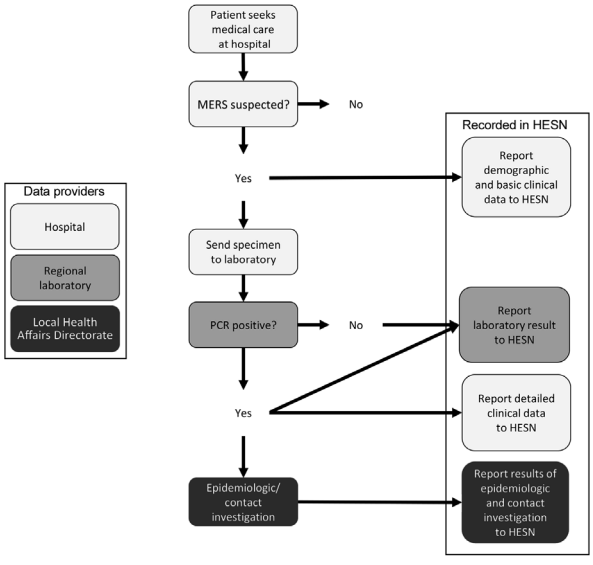

Figure 1. Reporting pathway for data regarding persons tested for Middle East respiratory syndrome coronavirus infection to the Health Electronic Surveillance Network (HESN), Saudi Arabia, 2014–2016.

Author affiliations: Ministry of Health, Riyadh, Saudi Arabia (A.A. Bin Saeed, A.G. Alzahrani, I. Salameh, R. Alhakeem, H. Algarni, O.A. El Nil, M. Mohammed, A.M. Assiri, H.M. Alabdely); Centers for Disease Control and Prevention, Atlanta, Georgia, USA (G.R. Abedi, F. Abdirizak, J.T. Watson, S.I. Gerber).

DOI: http://dx.doi.org/10.3201/eid2304.161793

submitted and testing completed, the regional laboratory reports the result to HESN. For positive cases, the referring hospital submits additional clinical information, and the local Health Affairs Directorate (HAD) initiates an investigation of exposures and contacts. For negative test results, no further action is taken in HESN. Surveillance activities occur in each of the 20 local HADs and among Hajj pilgrims. We analyzed demographic, clinical, and laboratory data for persons reported to HESN during April 1, 2015–February 1, 2016, in aggregate and by HAD using Microsoft Excel 2013 (Microsoft Corp., Redmond, WA, USA) and SAS version 9.3 (SAS Institute, Inc., Cary, NC, USA).

A total of 57,363 suspected MERS case-patients were identified and tested during the study period; 384 (0.7%) tested positive (Table 1). Among those for whom nationality and sex were known, 70.3% were Saudi (compared with 67.3% of the general population) and 54.3% were male. Rates of positivity among those with known age differed by age group; highest and lowest rates were among persons 50–65 and ≤14 years of age, respectively (Table 1). The month with the highest number of tested persons was November 2015 (n = 9,197) (Figure 2), and the month with the highest percentage of positive tested persons was August 2015 (3.4% of 4,770 tested persons).

Among tested persons for whom the reason for testing was known, 89.0% met the clinical case definition for suspected MERS (Table 1). The remaining 11.0% were those recommended for testing by an infectious disease consultant and asymptomatic contacts of confirmed case-patients. More than half of those tested (60.2%) met the category I definition (community-acquired pneumonia) for a suspected case-patient; 0.3% tested positive. The highest positivity

Table 1. Demographic characteristics of persons tested for Middle East respiratory syndrome coronavirus, Saudi Arabia, April 1, 2015–February 1, 2016

Characteristic	No. (%) confirmed	No. (%) not confirmed	No. (%) total	% Positive
Overall	384	56,979	57,363	0.7
Sex				
F	156 (40.8)	25,863 (45.7)	26,019 (45.7)	0.6
M	226 (59.2)	30,718 (54.3)	30,944 (54.3)	0.7
Total	382	56,581	56,963	0.7
Nationality				
Saudi	246 (69.7)	34,628 (70.3)	34,874 (70.3)	0.7
Non Saudi	107 (30.3)	14,604 (29.7)	14,711 (29.7)	0.7
Total	353	49,232	49,585	0.7
Reason for testing				
Suspected case*	286 (77.1)	47,592 (89.1)	47,878 (89.0)	0.6
Category I	87 (23.5)	32,284 (60.5)	32,371 (60.2)	0.3
Category II	67 (18.1)	2,662 (5.0)	2,729 (5.1)	2.5
Category III	107 (28.8)	4,669 (8.7)	4,776 (8.9)	2.2
Category IV	25 (6.7)	7,977 (14.9)	8,002 (14.9)	0.3
Recommended by infectious disease consultant	66 (17.8)	3,256 (6.1)	3,322 (6.2)	2.0
Patient asymptomatic	19 (5.1)	2,555 (4.8)	2,574 (4.8)	0.7
Total	371	53,403	53,774	0.7
Month of report				
April 2015	10 (2.6)	4,953 (8.7)	4,963 (8.7)	0.2
May 2015	54 (14.1)	4,414 (7.7)	4,468 (7.8)	1.2
June 2015	24 (6.3)	3,090 (5.4)	3,114 (5.4)	0.8
July 2015	24 (6.3)	2,634 (4.6)	2,658 (4.6)	0.9
August 2015	160 (41.7)	4,610 (8.1)	4,770 (8.3)	3.4
September 2015	66 (17.2)	6,520 (11.4)	6,586 (11.5)	1.0
October 2015	28 (7.3)	7,568 (13.3)	7,596 (13.2)	0.4
November 2015	6 (1.6)	9,191 (16.1)	9,197 (16.0)	0.1
December 2015	5 (1.3)	7,280 (12.8)	7,285 (12.7)	0.1
January 2016	6 (1.6)	6,487 (11.4)	6,493 (11.3)	0.1
February 2016	1 (0.3)	232 (0.4)	233 (0.4)	0.4
Total	384	56,979	57,363	0.7
Age, y				
0–14	10 (2.6)	8,022 (14.2)	8,032 (14.1)	0.1
15–34	97 (25.4)	17,621 (31.1)	17,718 (31.1)	0.5
35–49	82 (21.5)	10,201 (18.0)	10,283 (18.0)	0.8
50–65	109 (28.5)	10,082 (17.8)	10,191 (17.9)	1.1
≥66	84 (22.0)	10,692 (18.9)	10,776 (18.9)	0.8
Total	382	56,618	57,000	

*Categories: I, acute respiratory illness with clinical and/or radiologic evidence of pulmonary parenchymal disease (pneumonia or acute respiratory distress syndrome); II, a hospitalized patient with healthcare associated pneumonia based on clinical and radiological evidence; III, upper or lower respiratory illness within 2 weeks after exposure to a confirmed or probable case of MERS-CoV; IV, unexplained acute febrile (≥38°C) illness, and body aches, headache, diarrhea, or nausea/vomiting, with or without respiratory symptoms, and leukopenia (white blood cell count <3.5 × 10^9/L) and thrombocytopenia (platelets <150 × 10^9/L). Descriptions are from the Saudi Arabia Ministry of Health MERS-CoV Case Definition and Surveillance Guidance–Updated June 2015 (http://www.moh.gov.sa/en/CCC/Regulations/Case%20Definition.pdf).

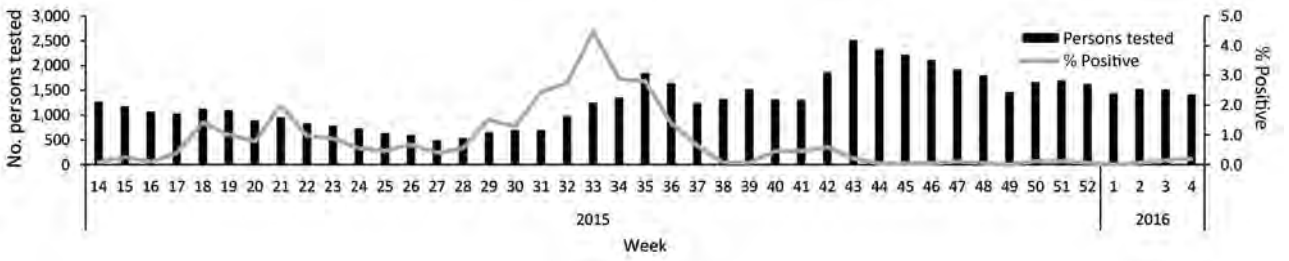

Figure 2. Number persons tested and percent positive for Middle East respiratory syndrome coronavirus, Saudi Arabia, April 1, 2015–February 1, 2016.

rate, 2.5%, was among persons meeting the category II definition for a suspected case-patient (healthcare-associated pneumonia). Among all persons with presumed exposure to MERS case-patients (persons meeting categories II, III and asymptomatic contacts of confirmed case-patients), the positivity rate was 1.9%. Among the 185 confirmed case-patients with available occupational information, 35 (18.9%) were healthcare workers (data not shown).

Most tested persons were reported in the course of routine surveillance through a local HAD. Nationwide, 18.4 persons/10,000 inhabitants were tested, and 1.2/100,000 were MERS-CoV–positive (*10*) (Table 2). Rates of testing and positivity varied by HAD; the highest testing rates were in Ahsa HAD, followed by Riyadh HAD. Najran HAD had the highest percentage of positive persons (Table 2).

In addition, surveillance during the annual Hajj pilgrimage included 888 tested persons during September 2015, representing 4.5 tested persons/10,000 among 1,952,817 pilgrims. None tested positive for MERS-CoV.

Among 8,032 children ≤14 years of age, 10 (0.1%) tested positive, including 5 who were <1 year of age. At least 7 of the 10 children were tested because of exposure to a MERS case-patient. The number of tests among children ≤14 years of age temporarily dropped after the case definition revision in June 2015, which introduced more stringent criteria for testing.

Conclusions

Surveillance and testing for MERS-CoV infection is extensive and widespread in Saudi Arabia. During our study, an average of >5,000 persons per month were identified as being at high risk for infection due to clinical or epidemiologic criteria and were subsequently tested. MERS was first recognized in 2012, and as of November 3, 2016, Saudi Arabia has reported 80.9% of the cases reported worldwide (*11*); this distinction may be partly due to the country's robust implementation of surveillance practices and the ready availability

Table 2. Middle East respiratory syndrome cases by local Health Affairs Directorate and among Hajj pilgrims, Saudi Arabia, April 1, 2015–February 1, 2016*

Surveillance population	Population	No. positive/no. tested	No. tested/10,000 population	No. confirmed cases/100,000 population	% Positive
Local Health Affairs Directorate					
Riyadh	7,717,467	276/22,322	28.9	3.6	1.2
Jeddah	4,224,568	10/6,606	15.6	0.2	0.2
Eastern	3,019,461	2/7,319	24.2	0.1	0
Makkah	2,111,127	2/3,729	17.7	0.1	0.1
Madinah	2,012,749	8/2,258	11.2	0.4	0.4
Asir	1,766,212	6/1,730	9.8	0.3	0.3
Jazan	1,533,496	0/790	5.2	0	0
Qasim	1,370,727	5/1,091	8.0	0.4	0.5
Taif	1,257,888	7/1,866	14.8	0.6	0.4
Ahsa	1,193,373	57/5,359	44.9	4.8	1.1
Tabuk	887,383	1/732	8.2	0.1	0.1
Hail	670,468	0/685	10.2	0	0
Najran	568,631	10/494	8.7	1.8	2.0
Baha	461,360	0/184	4.0	0	0
Hafr al-Batin	437,349	0/145	3.3	0	0
Bisha	379,521	0/227	6.0	0	0
Northern Borders	359,297	0/240	6.7	0	0
Jauf	329,277	0/390	11.8	0	0
Qunfudha	304,392	0/183	6.0	0	0
Qurayat	165,629	0/122	7.4	0	0
Total	30,770,375	384/56,472	18.4	1.2	0.7
Hajj pilgrims					
Total	1,952,817	0/888	4.5	0	0

*Population data from (*10*).

of testing, which is facilitated by HESN. We found few other published descriptions of surveillance practices for MERS-CoV (*12*,*13*).

Confirmed MERS case-patients represented <1% of all tested persons in Saudi Arabia. Most tests were conducted for persons with community-acquired pneumonia, among whom the positivity rate was predictably low. Positivity rates were highest among persons tested because of presumed exposure to MERS case-patients (i.e., those tested because of healthcare-acquired pneumonia or onset of symptoms following contact with a confirmed case-patient).

Only 0.1% of children ≤14 years of age tested positive for MERS-CoV; this was the lowest rate among all age groups. Most MERS-CoV–positive children ≤14 years of age were tested because of high-risk exposures, not because they met clinical criteria. Although the proportion of positive tests was highest among persons ≥35 years of age, the number of tests was highest among persons 18–34 years of age, perhaps because of widespread testing of healthcare workers during outbreaks.

The largest number of tests was conducted in November, coinciding with the winter respiratory virus season. In comparison, the proportion of positive tests peaked in May and August, coinciding with outbreaks that occurred in Ahsa (*14*) and Riyadh (*15*), respectively.

Our analysis had limitations. Variations were probably present in the reporting practices of the various data reporters, in the clinical diagnostic practices used across Saudi Arabia, and among investigation teams. Such variations could affect the completeness, accuracy, and timeliness of the data used for this assessment.

Surveillance and testing for MERS-CoV throughout Saudi Arabia is extensive, as documented by HESN; in a single month during this study, >9,000 patients at high risk for MERS were investigated. A continued robust approach to the early detection of patients with MERS is critical for the prompt implementation of infection-control precautions and the prevention of healthcare-associated transmission of MERS-CoV.

Dr. Bin Saeed served as Deputy Minister for Preventive Health at the Saudi Arabia Ministry of Health from October 2014 through October 2016 and is currently a professor of epidemiology in the Department of Family and Community Medicine at King Saud University College of Medicine in Riyadh. His research interests include epidemiologic methodologies, infection control, and outbreak investigations.

References

1. Situation update on Middle East respiratory syndrome coronavirus September–October 2016. MERS situation update 2016 Oct 2016 [cited 2016 Dec 21]. http://www.emro.who.int/images/stories/csr/documents/MERS-CoV_Sep_October_2016.pdf?ua=1
2. Oboho IK, Tomczyk SM, Al-Asmari AM, Banjar AA, Al-Mugti H, Aloraini MS, et al. 2014 MERS-CoV outbreak in Jeddah—a link to health care facilities. N Engl J Med. 2015;372:846–54. http://dx.doi.org/10.1056/NEJMoa1408636
3. Drosten C, Meyer B, Müller MA, Corman VM, Al-Masri M, Hossain R, et al. Transmission of MERS-coronavirus in household contacts. N Engl J Med. 2014;371:828–35. http://dx.doi.org/10.1056/NEJMoa1405858
4. Alraddadi BM, Watson JT, Almarashi A, Abedi GR, Turkistani A, Sadran M, et al. Risk factors for primary Middle East respiratory syndrome coronavirus illness in humans, Saudi Arabia, 2014. Emerg Infect Dis. 2016;22:49–55. http://dx.doi.org/10.3201/eid2201.151340
5. World Health Organization. Infection prevention and control during health care for probable or confirmed cases of novel coronavirus (nCoV) infection. Interim guidance, 6 May 2013 [cited 2016 Dec 21]. http://www.who.int/csr/disease/coronavirus_infections/IPCnCoVguidance_06May13.pdf?ua=1
6. World Health Organization. WHO statement on the tenth meeting of the IHR Emergency Committie regarding MERS, 3 Sep 2016 [cited 2016 Nov 3]. http://www.who.int/mediacentre/news/statements/2015/ihr-emergency-committee-mers/en/
7. Madani TA. Case definition and management of patients with MERS coronavirus in Saudi Arabia. Lancet Infect Dis. 2014;14:911–3. http://dx.doi.org/10.1016/S1473-3099(14)70918-1
8. Command and Control Center. Ministry of Health Kingdom of Saudi Arabia, Scientific Advisory Board. Infection prevention and control guidelines for Middle East respiratory syndrome coronavirus (MERS-CoV) infection. 3rd edition. June 2015 [cited 2016 Dec 21]. http://www.moh.gov.sa/en/CCC/Regulations/2015%20update.pdf
9. World Health Organization. Laboratory testing for Middle East respiratory syndrome coronavirus (MERS-CoV). Interim guidance, updated June 2015. WHO/MERS/LAB/15.1 [cited 2016 Dec 21]. http://apps.who.int/iris/bitstream/10665/176982/1/WHO_MERS_LAB_15.1_eng.pdf
10. Ministry of Health. Kingdom of Saudi Arabia. Statistics book. Statistical book for the year 1435. 2015 [cited 2016 Mar 23]. http://www.moh.gov.sa/en/ministry/statistics/book/pages/default.aspx
11. World Health Organization. Confirmed global cases of MERS-CoV reported to WHO as of 14 Oct 2016 [cited 2016 Oct 17]. http://www.who.int/emergencies/mers-cov/14-october-2016-epicurve.png?ua=1
12. Al Hosani FI, Pringle K, Al Mulla M, Kim L, Pham H, Alami NN, et al. Response to emergence of Middle East respiratory syndrome coronavirus, Abu Dhabi, United Arab Emirates, 2013–2014. Emerg Infect Dis. 2016;22:1162–8. http://dx.doi.org/10.3201/eid2207.160040
13. Schneider E, Chommanard C, Rudd J, Whitaker B, Lowe L, Gerber SI. Evaluation of patients under investigation for MERS-CoV infection, United States, January 2013–October 2014. Emerg Infect Dis. 2015;21:1220–3. http://dx.doi.org/10.3201/eid2107.141888
14. El Bushra HE, Abdalla MN, Al Arbash H, Alshayeb Z, Al-Ali S, Latif ZA, et al. An outbreak of Middle East respiratory syndrome (MERS) due to coronavirus in Al-Ahssa region, Saudi Arabia, 2015. East Mediterr Health J. 2016;22:468–75.
15. Balkhy HH, Alenazi TH, Alshamrani MM, Baffoe-Bonnie H, Arabi Y, Hijazi R, et al. Description of a hospital outbreak of Middle East respiratory syndrome in a large tertiary care hospital in Saudi Arabia. Infect Control Hosp Epidemiol. 2016;37:1147–55. http://dx.doi.org/10.1017/ice.2016.132

Address for correspondence: Glen R. Abedi, Centers for Disease Control and Prevention; 1600 Clifton Rd NE, Mailstop A34, Atlanta, GA 30329-4027, USA; email: gabedi@cdc.gov

Antiviral Drug–Resistant Influenza B Viruses Carrying H134N Substitution in Neuraminidase, Laos, February 2016

Tatiana Baranovich, Phengta Vongphrachanh, Pakapak Ketmayoon, Thongchanh Sisouk, Khampheng Chomlasack, Viengphone Khanthamaly, Ha Thuy Nguyen, Vasiliy P. Mishin, Henju Marjuki, John R. Barnes, Rebecca J. Garten, James Stevens, David E. Wentworth, Larisa V. Gubareva

In February 2016, three influenza B/Victoria/2/87 lineage viruses exhibiting 4- to 158-fold reduced inhibition by neuraminidase inhibitors were detected in Laos. These viruses had an H134N substitution in the neuraminidase and replicated efficiently in vitro and in ferrets. Current antiviral drugs may be ineffective in controlling infections caused by viruses harboring this mutation.

Influenza B viruses cause annual epidemics and contribute to ≈30% of influenza-associated deaths among children in the United States (*1*). Two lineages, B/Victoria/2/87 and B/Yamagata/16/88, have been co-circulating globally in recent years (*2*,*3*). Neuraminidase (NA) inhibitors (NAIs) are the only drugs available for treating influenza B virus infections, but NA mutations that emerge during treatment or due to natural variance can diminish the usefulness of NAIs.

The Study

For this study, the National Center for Laboratory and Epidemiology in Vientiane, Laos, a member of the World Health Organization Global Influenza Surveillance and Response System, provided influenza A and B viruses to the World Health Organization Collaborating Center at the Centers for Disease Control and Prevention (CDC) in Atlanta, Georgia, USA; the viruses had been collected during October 1, 2015–February 29, 2016. We propagated the viruses and then used the CDC standardized NA inhibition assay to assess their susceptibility to NAIs (*4*). Compared with the median 50% inhibitory concentration (IC_{50}) values for B-Victoria lineage viruses, IC_{50} values for 2 of the 24 B-Victoria lineage viruses, B/Laos/0406/2016 and B/Laos/0525/2016, were elevated for zanamivir (129- to 158-fold), oseltamivir (4-fold), peramivir (72- to 74-fold), and laninamivir (41- to 42-fold) (Table 1). These results were interpreted as highly reduced inhibition by zanamivir, normal inhibition by oseltamivir, and reduced inhibition by peramivir and laninamivir (Table 1) (*5*).

This interpretation is useful but obscures the higher median oseltamivir IC_{50} value (9.67 nmol/L vs. 0.42–1.47 nmol/L for other NAIs; Table 1) and the lower potency of oseltamivir in inhibiting NA activity of influenza B viruses (*4*,*7*). Moreover, reports from clinical studies indicate a lesser susceptibility of influenza B viruses to oseltamivir than to zanamivir (*7*–9). Although the laboratory criteria defining clinically relevant NAI resistance are not established, the inhibitory profiles of these 2 viruses suggest resistance to ≥1 antiviral drugs. NA sequence analysis revealed that both viruses had an amino acid substitution, histidine (H)→asparagine (N), at the highly conserved residue 134 (NA-H134N) (*6*); the presence of H134N in the respiratory specimens was confirmed by pyrosequencing (Figure 1) (*10*). NA-H134Y was previously reported in influenza B virus displaying reduced inhibition by peramivir (*11*). The inhibition profile of influenza B viruses bearing NA-H134N resembles that of influenza A(H1N1) viruses carrying NA-Q136R (residue 134 in influenza B NA corresponds to 136 in N1 numbering) (*12*). Residue 134 (136) has been implicated in the conformational change of the 150-loop, which may adversely affect the interaction between the NA active site and NAIs, especially those containing the guanidyl group (online Technical Appendix Figure, https://wwwnc.cdc.gov/EID/article/23/4/16-1876-Techapp1.pdf).

To expand testing, the Laos National Center for Laboratory and Epidemiology provided 40 additional specimens

Author affiliations: Carter Consulting, Inc., Atlanta, Georgia, USA (T. Baranovich); World Health Organization Collaborating Center for Surveillance, Epidemiology and Control of Influenza, Atlanta (T. Baranovich, V. Khanthamaly, H.T. Nguyen, V.P. Mishin, H. Marjuki, J.R. Barnes, R.J. Garten, J. Stevens, D.E. Wentworth, L.V. Gubareva); Centers for Disease Control and Prevention, Atlanta (T. Baranovich, V. Khanthamaly, H.T. Nguyen, V.P. Mishin, H. Marjuki, J.R. Barnes, R.J. Garten, J. Stevens, D.E. Wentworth, L.V. Gubareva); National Center for Laboratory and Epidemiology, Vientiane, Laos (P. Vongphrachanh, P. Ketmayoon, T. Sisouk, K. Chomlasack); World Health Organization Emerging Disease Surveillance and Response Unit, Vientiane, Laos (P. Ketmayoon); Battelle Memorial Institute, Atlanta (H.T. Nguyen)

DOI: http://dx.doi.org/10.3201/eid2304.161876

Table 1. Neuraminidase inhibitor susceptibility of influenza B viruses isolated from human respiratory specimens. Laos, 2016*

Virus isolate	NA amino acid change§	Mean IC_{50} ± SD, nmol/L (fold change)†‡				Date specimen collected	GISAID accession no.
		Zanamivir	Oseltamivir¶	Peramivir	Laninamivir		
B/Laos/0080/2016	H134	1.09 ± 0.16 (1)	14.48 ± 1.76 (1)	0.36 ± 0.05 (1)	1.15 ± 0.02 (1)	14 Jan	EPIISL 222862
B/Laos/0406/2016	H134N	148.36 ± 14.40 (**129**)	37.87 ± 1.96 (4)	31.09 ± 3.70 (**74**)	62.43 ± 4.66 (**42**)	9 Feb	EPIISL 230596
B/Laos/0525/2016	H134N	176.03 ± 11.14 (**158**)	37.55 ± 5.60 (4)	30.25 ± 2.90 (**72**)	60.12 ± 2.38 (**41**)	15 Feb	EPIISL 230599
B/Laos/0654/2016	H134N	151.95 ± 16.30 (**138**)	35.06 ± 5.08 (4)	31.29 ± 0.24 (**75**)	61.53 ± 1.03 (**42**)	25 Feb	EPIISL 230600

*Viruses were isolated and propagated on MDCK cells. Susceptibility was determined using a fluorescence-based neuraminidase (NA) inhibition assay.
†IC_{50} values (NA inhibitor concentration needed to reduce NA activity by 50%) represent mean ± SD from 3 independent experiments.
‡Fold change compared with the median IC_{50} value determined for influenza B-Victoria lineage viruses (n = 430) that were circulating worldwide during the 2015–16 influenza season. Median IC_{50} values are 1.11, 9.67, 0.42, and 1.47 nM for zanamivir, oseltamivir, peramivir, and laninamivir, respectively. Bold indicates fold increases that correspond to reduced inhibition (5- to 50-fold) or to highly reduced (>50-fold) inhibition by a NAI, as outlined by the World Health Organization Expert Working Group of the Global Influenza Surveillance and Response System for Surveillance on Antiviral Susceptibility (*5*).
§Amino acid residue 134 in influenza type B NA corresponds to residue Q136 in N1 and N2 NA amino acid numbering (*6*).
¶Oseltamivir carboxylate was used in NA inhibition assay.

that were positive for B-Victoria lineage virus by real-time reverse transcription PCR (*13*), bringing the total number tested to 64. The specimens were collected during October 2015–April 2016 in Champasack (n = 41), Vientiane (n = 12), Luangprabang (n = 7), and Saravanh (n = 5) Provinces from 28 male and 37 female patients (median age 7 [range 0–67] years). Pyrosequencing revealed NA-H134N in 1 specimen; the respective isolate, B/Laos/0654/2016, displayed the expected NA inhibition profile (Table 1). In total, we found the NA-H134N substitution in 3 (4.6%) of the 65 tested B-Victoria viruses. Analysis of NA sequences deposited to the GISAID database (http://www.gisaid.org) revealed that among 8,601 sequences of influenza B viruses collected worldwide during October 2014–September 2016, only 3 other sequences contained a substitution at H134 (2 harbored H134Y and 1 H134L); the 3 sequences were for B-Victoria lineage viruses.

Epidemiologic data revealed that the NA-H134N viruses were collected from a young woman, a young man, and a 3-year-old girl residing in 2 distant provinces (Table 2). The 3 infections occurred 6–10 days apart in February 2016, and 1 of the patients received medical care for severe acute respiratory illness. No epidemiologic links were identified among the 3 patients infected with the drug-resistant viruses, and patients had no documented exposure to NAIs.

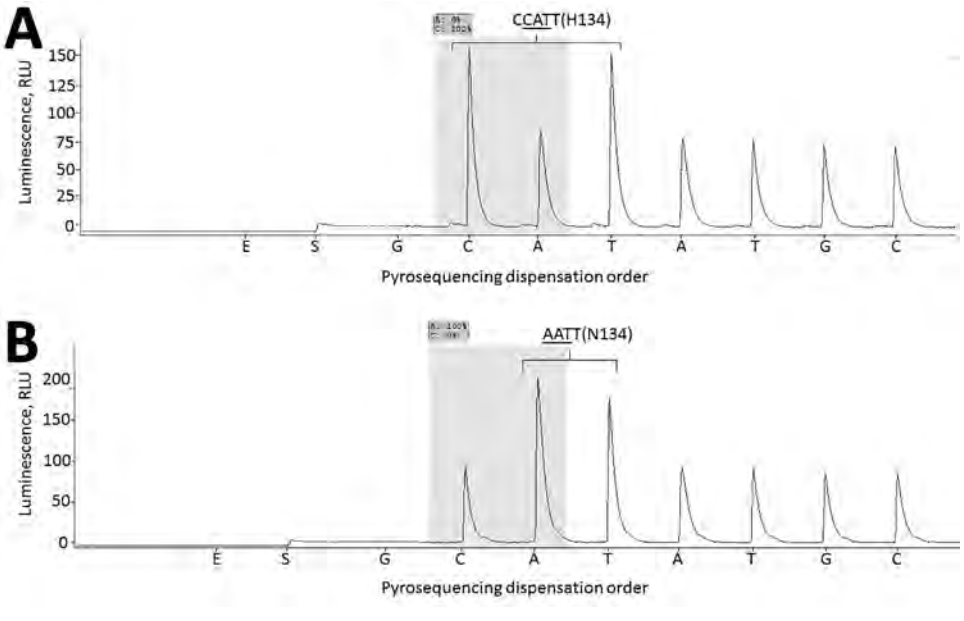

Figure 1. Neuraminidase gene segment (nts 399–497) of influenza B/Laos/0080/2016 virus carrying NA-H134 (A) and B/Laos/0654/2016, NA-N134 (B). RNA extracted from respiratory specimens was used for reverse transcription PCR (RT-PCR) amplification. Two primers, NA-B-242F (5′-CATACCCGCGTTTAT CTTGC-3′, forward primer) and NA-B-426Rb (biotin-5′-CTGTCTCCTCTTGTTCC ATTGTAG-3′, reverse biotinylated primer) were used in RT-PCR, essentially as described previously (*10*); primer NA-B-378Fs (5′-TGCAAACACTTTG CTTTAAC-3′) was used for pyrosequencing. Underlining indicates nucleotide triplet encoding amino acid residue 134. Shading indicates the nucleotides used to determine the proportion of H134 and N134 neuraminidase variants. Pyrosequencing dispensation order: E-Enzyme mixture; S-substrate mixture; G, C, A and T – nucleotides dGTP, dCTP; dATPαS and dTTP, correspondingly.

Table 2. NA-H134N substitution–containing influenza B viruses that caused confirmed infection among 3 persons, Laos, February 2016*

Virus name, passage history§	Amino acid change in virus genes†						Patient information			
	NA		HA	M1		NS1‡	Age, y/sex	Clinical pres.	Location, province	Date specimen collected
	H134¶	D390	V225	E73	H159	V220				
B/Laos/0406/2016							22/F	SARI	Vientiane	Feb 9
Original	N	D/E	–	–	Q	–				
C2	N	D/E	–	E/G	Q	–				
B/Laos/0525/2016							23/M	ILI	Champasack	Feb 15
Original	N	–	A	–	Q	–				
C2	N	–	A	–	Q	–				
B/Laos/0654/2016							3/F	ILI	Champasack	Feb 25
Original	N	–	–	–	Q	I				
C1	N	–	–	–	Q	I				

*HA, hemagglutinin; ILI, influenza-like illness; M1, matrix protein 1; NA, neuraminidase; NS1, nonstructural protein 1; Pres., presentation; SARI, severe acute respiratory illness; –, indicates same amino acid residue as in the consensus sequence of B-Victoria viruses that were circulating in Laos during the 2015–16 influenza season.
†Strain-specific amino acid sequence numbering is used. Sequences for all 8 gene segments were generated using the MiSeq sequencing system (Illumina Inc., San Diego, CA, USA) (*14*) (online Technical Appendix Table 1, https://wwwnc.cdc.gov/EID/article/23/4/16-1876-Techapp1.pdf). Data are amino acid differences in protein-coded regions of NA, HA, M1, and NS1 genes compared with the consensus sequence. Not shown: synonymous nucleotide mutations that were common for the NA-H134N viruses: PB1-c93t, PB1-g1930a, and HA-g1520a. In addition, NA-H134N viruses differed from each other by the following synonymous nucleotide mutations: B/Laos/0406/2016 possessed NS1-g345a, B/Laos/0525/2016 possessed NA-t762a, NS1-a561g, and B/Laos/0654/2016 possessed NS2-g186a.
‡Corresponds to position 219 in NS1 protein numbering used by Ma et al. (*15*).
§Original indicates specimen collected from patient; C1 and C2 indicates virus propagated 1 or 2 times on MDCK cells.
¶Presence of the NA-H134N substitution in the original respiratory specimens was confirmed by a pyrosequencing assay (Figure 1; online Technical Appendix Table 2).

The 3 drug-resistant viruses were genetically similar to other B-Victoria lineage viruses circulating in Laos during 2015–2016. Besides having the NA-H134N amino acid substitution, these viruses also shared the M1-H159Q amino acid substitution not identified in other virus sequences (Table 2). Also, these viruses have 3 synonymous nucleotide mutations: PB1-c93t, PB1-g1930a, and HA-g1520a. In addition, B/Laos/0406/2016, B/Laos/0525/2016, and B/Laos/0654/2016 harbored substitutions NA-D390D/E, HA-V225A, and NS1-V220I, respectively (Table 2). An analysis of influenza B NS1 sequences available in the GISAID database (as of September 12, 2016) indicated that NS1-V220I is rare, present in only 7 (0.1%) of 10,405 sequences. Taken together, the geographic distance between the sites where the drug-resistant viruses were collected and the differences in their genomes point toward the possibility of influenza NA-H134N viruses circulating in Laos communities.

Results of the NA inhibition assay showed that NA-H134N impairs binding of NAIs to the active site of the enzyme. To determine whether this change also affects other properties (e.g., thermostability) of the enzyme, we incubated 3 H134N viruses at elevated temperatures for 15 min and then assessed their NA activity (Figure 2, panel A). The H134N substitution reduced the thermostability of the enzyme. This was evident from the undetectable activity levels starting at 47.5°C, which was 7.5°C lower than that for the control virus, B/Laos/0880/2016, with H134 ($p<0.001$) (Figure 2, panel A).

To assess the replicative fitness of NA-H134N viruses, we used primary human differentiated normal human bronchial epithelial (NHBE) cells, a cell culture system that morphologically and functionally recapitulates the human airway. The NA-H134N viruses displayed ≈1–2 $\log_{10}$ lower titers at 24–72 h after inoculation (Figure 2, panel B). Although, the virus yield reduction (area under the curve) was evident for 2 of the NA-H134N viruses (AUC_{2-72} [$p<0.05$]) (Figure 2, panel B), the difference was not statistically significant for B/Laos/0654/2016 (Figure 2, panel B). The growth kinetics data in differentiated NHBE cells indicate an attenuated phenotype for NA-H134N viruses in vitro. Unlike the other 2 drug-resistant viruses, B/Laos/0654/2016 had substitution NS1-V220I, which resides at the recently discovered second RNA binding site of the NS1 protein of influenza B viruses (*15*). This finding suggests a possible compensatory effect of NS1-V220I on the in vitro replicative capacity of B/Laos/0654/2016.

We assessed the replicative fitness of drug-resistant B/Laos/0654/2016 in three 4- to 6-month-old male ferrets (*Mustela putorius furo*) (Triple F Farms, Sayre, PA, USA) that were serologically negative by HI assay for currently circulating influenza A(H1N1)pdm09, A(H3N2), and B viruses. At 48 h after inoculation with virus (10^4 50% tissue culture infectious dose/mL), ferrets displayed fever (≥1.5°C above baseline) that lasted 21.8 ± 5.1 h on average. Virus shedding lasted 6 days; nasal wash virus titers, which were determined daily, were 4.2 ± 0.4; 6.0 ± 0.2; 4.8 ± 0.4, 4.7 ± 0.4, 4.7 ± 0.6, and 2.8 ± 0.4 $\log_{10}$ 50% tissue culture infectious doses/mL, respectively. These data suggest that the drug-resistant virus can replicate to high titers in the upper respiratory tract of ferrets and induce persistent fever.

Conclusions

In February 2016, we detected 3 influenza B viruses in Laos bearing a rare NA-H134N substitution. Current antiviral medications may not effectively control infections

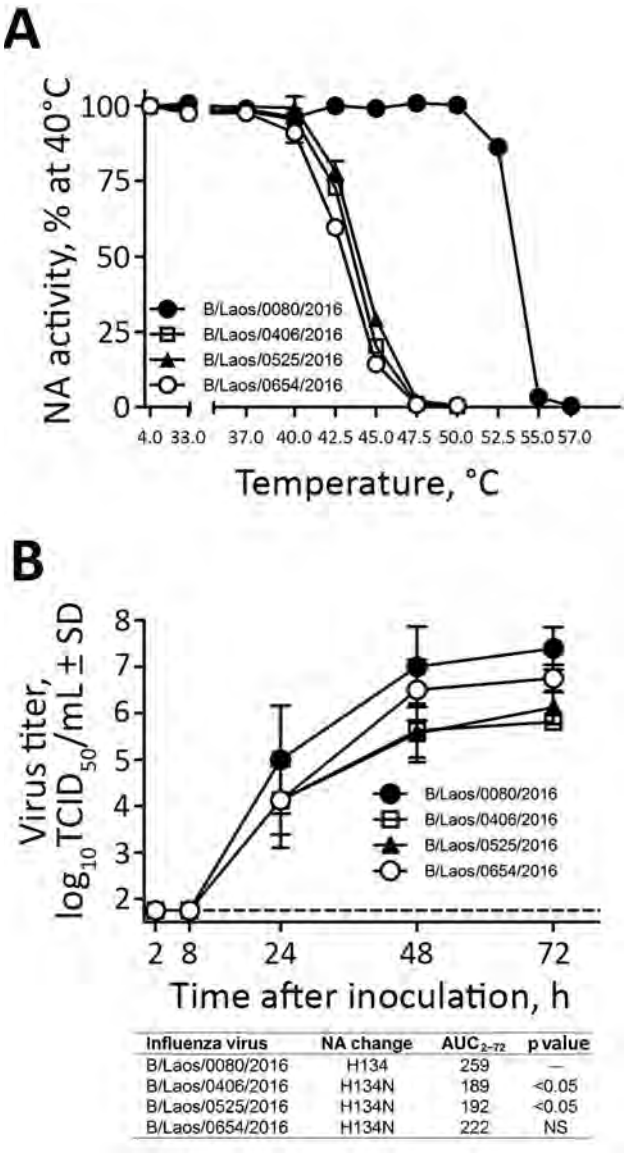

Influenza virus	NA change	$AUC_{2–72}$	p value
B/Laos/0080/2016	H134	259	—
B/Laos/0406/2016	H134N	189	<0.05
B/Laos/0525/2016	H134N	192	<0.05
B/Laos/0654/2016	H134N	222	NS

Figure 2. Characterization of influenza B viruses detected in Laos, February 2016. A) Thermostability of neuraminidase (NA) determined after viruses were incubated for 15 min at 4°C or at 30°C–57°C. NA enzyme activity was determined by a fluorescence-based assay (*4*). B) Replication kinetics of influenza B viruses in fully differentiated human primary NHBE cells that were inoculated with the designated viruses (multiplicity of infection 0.001). Apical washes were taken at indicated times after inoculation, and virus titers were determined on MDCK cells. The area under the virus titer curve from 2 to 72 h after inoculation ($AUC_{2–72}$) was determined and compared with that of the control virus by repeated-measures analysis of variance with the Dunnett posttest, using GraphPad Prism 5 software (GraphPad Software, La Jolla, CA, USA). Dashed line represents the limit of detection of the assay (1.75 log_{10} 50% tissue culture infectious dose [$TCID_{50}$/mL]). Values shown are means and SDs from 2 independent experiments performed in duplicates (n = 4). Error bars represent SDs. NS, not significant.

caused by such viruses. Virus harboring NA-H134N and NS1-V220I replicated efficiently in NHBE cells and in the ferret upper respiratory tract. Studies to ascertain the effect of NA-H134N and NS1-V220I on influenza B virus virulence and transmissibility in a mammalian host are needed.

Acknowledgments

We thank the laboratories that and clinicians who submit specimens and isolates to the World Health Organization Collaborating Center for Influenza in Atlanta, Georgia, USA. We greatly value the technical assistance provided by Michelle Adamczyk, Lori Lollis, Juan De la Cruz, Anton Chesnokov, and members of Reference and Genomic Teams in the Virology, Surveillance and Diagnosis Branch, Influenza Division, National Center for Immunization and Respiratory Diseases, Centers for Disease Control and Prevention. We thank Hoffmann-La Roche Ltd, Switzerland, for providing oseltamivir carboxylate, the active form of the ethyl ester prodrug oseltamivir phosphate; GlaxoSmithKline, Australia, for providing zanamivir; BioCryst Pharmaceuticals, USA, for providing peramivir; and Biota, Australia, for providing laninamivir.

This study was funded by the Centers for Disease Control and Prevention.

Dr. Baranovich worked in the Influenza Division, National Center for Immunization and Respiratory Diseases, Centers for Disease Control and Prevention, during the conduct of this study. Her research interests include the molecular mechanisms of influenza virus resistance to antiviral medications and the effect of resistance mutations on viral fitness and evolution.

References

1. Burnham AJ, Baranovich T, Govorkova EA. Neuraminidase inhibitors for influenza B virus infection: efficacy and resistance. Antiviral Res. 2013;100:520–34. http://dx.doi.org/10.1016/j.antiviral.2013.08.023
2. Budd A, Blanton L, Kniss K, Smith S, Mustaquim D, Davlin SL, et al. Update: influenza activity—United States and worldwide, May 22–September 10, 2016. MMWR Morb Mortal Wkly Rep. 2016;65:1008–14. http://dx.doi.org/10.15585/mmwr.mm6537a5
3. Davlin SL, Blanton L, Kniss K, Mustaquim D, Smith S, Kramer N, et al. Influenza activity—United States, 2015–16 season and composition of the 2016–17 influenza vaccine. MMWR Morb Mortal Wkly Rep. 2016;65:567–75. http://dx.doi.org/10.15585/mmwr.mm6522a3
4. Okomo-Adhiambo M, Mishin VP, Sleeman K, Saguar E, Guevara H, Reisdorf E, et al. Standardizing the influenza neuraminidase inhibition assay among United States public health laboratories conducting virological surveillance. Antiviral Res. 2016;128:28–35. http://dx.doi.org/10.1016/j.antiviral.2016.01.009
5. World Health Organization. Meetings of the WHO working group on surveillance of influenza antiviral susceptibility—Geneva, November 2011 and June 2012. Wkly Epidemiol Rec. 2012;87:369–74.
6. Colman PM, Hoyne PA, Lawrence MC. Sequence and structure alignment of paramyxovirus hemagglutinin-neuraminidase with influenza virus neuraminidase. J Virol. 1993;67:2972–80.

7. Kawai N, Ikematsu H, Iwaki N, Maeda T, Satoh I, Hirotsu N, et al. A comparison of the effectiveness of oseltamivir for the treatment of influenza A and influenza B: a Japanese multicenter study of the 2003–2004 and 2004–2005 influenza seasons. Clin Infect Dis. 2006;43:439–44. http://dx.doi.org/10.1086/505868
8. Monto AS, McKimm-Breschkin JL, Macken C, Hampson AW, Hay A, Klimov A, et al. Detection of influenza viruses resistant to neuraminidase inhibitors in global surveillance during the first 3 years of their use. Antimicrob Agents Chemother. 2006;50:2395–402. http://dx.doi.org/10.1128/AAC.01339-05
9. Sugaya N, Mitamura K, Yamazaki M, Tamura D, Ichikawa M, Kimura K, et al. Lower clinical effectiveness of oseltamivir against influenza B contrasted with influenza A infection in children. Clin Infect Dis. 2007;44:197–202. http://dx.doi.org/10.1086/509925
10. Sheu TG, Deyde VM, Garten RJ, Klimov AI, Gubareva LV. Detection of antiviral resistance and genetic lineage markers in influenza B virus neuraminidase using pyrosequencing. Antiviral Res. 2010;85:354–60. http://dx.doi.org/10.1016/j.antiviral.2009.10.022
11. Takashita E, Meijer A, Lackenby A, Gubareva L, Rebelo-de-Andrade H, Besselaar T, et al. Global update on the susceptibility of human influenza viruses to neuraminidase inhibitors, 2013–2014. Antiviral Res. 2015;117:27–38. http://dx.doi.org/10.1016/j.antiviral.2015.02.003
12. Little K, Leang SK, Butler J, Baas C, Harrower B, Mosse J, et al. Zanamivir-resistant influenza viruses with Q136K or Q136R neuraminidase residue mutations can arise during MDCK cell culture creating challenges for antiviral susceptibility monitoring. Euro Surveill. 2015;20:30060. http://dx.doi.org/10.2807/1560-7917.ES.2015.20.45.30060
13. Centers for Disease Control and Prevention. Human influenza virus real-time RT-PCR detection and characterization panel. 510(k) summary. 2008. http://www.accessdata.fda.gov/cdrh_docs/pdf8/k080570.pdf.
14. Zhou B, Donnelly ME, Scholes DT, St George K, Hatta M, Kawaoka Y, et al. Single-reaction genomic amplification accelerates sequencing and vaccine production for classical and swine origin human influenza a viruses. J Virol. 2009;83:10309–13. http://dx.doi.org/10.1128/JVI.01109-09
15. Ma LC, Guan R, Hamilton K, Aramini JM, Mao L, Wang S, et al. A second RNA-binding site in the NS1 protein of influenza B virus. Structure. 2016;24:1562–72. http://dx.doi.org/10.1016/j.str.2016.07.001

Address for correspondence: Larisa V. Gubareva, Centers for Disease Control and Prevention, 1600 Clifton Rd NE, Mailstop G16, Atlanta, GA 30329-4027, USA; email: lgubareva@cdc.gov

Characterization of Highly Pathogenic Avian Influenza Virus A(H5N6), Japan, November 2016

Masatoshi Okamatsu,[1] Makoto Ozawa,[1] Kosuke Soda,[1] Hiroki Takakuwa,[1] Atsushi Haga, Takahiro Hiono, Aya Matsuu, Yuko Uchida, Ritsuko Iwata, Keita Matsuno, Masakazu Kuwahara, Toshiyo Yabuta, Tatsufumi Usui, Hiroshi Ito, Manabu Onuma, Yoshihiro Sakoda, Takehiko Saito, Koichi Otsuki, Toshihiro Ito, Hiroshi Kida

Highly pathogenic avian influenza viruses (HPAIVs) A(H5N6) were concurrently introduced into several distant regions of Japan in November 2016. These viruses were classified into the genetic clade 2.3.4.4c and were genetically closely related to H5N6 HPAIVs recently isolated in South Korea and China. In addition, these HPAIVs showed further antigenic drift.

Since their emergence in ≈2010–11 in China (*1*), highly pathogenic avian influenza viruses (HPAIVs) that have the hemagglutinin (HA) genes of the H5 subtype classified into the genetic clade 2.3.4.4 have threatened global bird species, including wild birds and poultry, as well as humans. Although the H5 HA genes of these viruses are closely related, the subtypes of their neuraminidase (NA) genes vary widely. These new H5 HPAIVs with NA genes of various subtypes, the so-called H5Nx viruses, have spread globally, most likely because of their host preference for waterfowl, similar to the previous H5N1 HPAIVs (*2*–*4*). During the winter season 2014–15, H5N8 HPAIVs were isolated from wild birds and chickens in western Japan (*5*–*7*). In November 2016, HPAIVs of the H5N6 subtype were isolated in 3 geographically distant regions of Japan. We report the genetic and antigenic characteristics of 6 H5N6 HPAIVs.

Author affiliations: Hokkaido University, Sapporo Japan (M. Okamatsu, T. Hiono, K. Matsuno, Y. Sakoda, H. Kida); Kagoshima University, Kagoshima, Japan (M. Ozawa, A. Matsuu); Yamaguchi University, Yamaguchi, Japan (M. Ozawa, A. Matsuu); Tottori University, Tottori, Japan (K. Soda, T. Usui, H. Ito, K. Otsuki, T. Ito); Kyoto Sangyo University, Kyoto, Japan (H. Takakuwa, T. Yabuta, K. Otsuki); Matsuoka Research Institute for Science, Koganei, Tokyo, Japan (M. Kuwahara); National Agriculture and Food Research Organization, Tsukuba, Japan (Y. Uchida, T. Saito); National Institute for Environmental Studies, Tsukuba (A. Haga, R. Iwata, M. Onuma)

DOI: http://dx.doi.org/10.3201/eid2304.161957

The Study

The first suspected case of an HPAI outbreak in Japan during winter 2016–17 was reported from Akita Prefecture in northern Japan (Figure 1). A black swan (*Cygnus atratus*) in a zoo that died on November 15, 2016, tested positive for influenza virus antigen by a rapid diagnostic test. While this bird's specimens underwent further analysis, another influenza virus was isolated from a water sample collected at an overwintering site of migratory birds in Kagoshima Prefecture at the southern tip of Japan on November 14, 2016 (Table 1). This isolate, A/environment/Kagoshima/KU-ngr-I/2016 (H5N6), was confirmed to be an H5N6 subtype having multiple basic amino acid residues, PLRERRRKR/GLF, at the cleavage site in the HA protein, which is characteristic of HPAIVs, by conventional reverse transcription PCR and Sanger sequencing. Subsequently, an isolate from the first black swan, A/black swan/Akita/1/2016 (H5N6), also was confirmed to be an H5N6 HPAIV, showing that all 3 chickens inoculated intranasally with $10^{8.4}$ of 50% egg infectious dose of the virus died within 2 days. In addition, a fecal sample of a common teal (*Anas crecca*) collected at an overwintering site of migratory birds in Tottori Prefecture in the middle of Japan on November 15, 2016, was reported to harbor an H5N6 HPAIV, A/teal/Tottori/1/2016 (H5N6) (Table 1). The isolation sites of these 3 H5N6 HPAIVs are distant (Figure 1), although the sample collection dates were close (Table 1). These 3 cases were followed by several reports of H5N6 HPAIVs, including A/black swan/Akita/2/2016 (H5N6), A/northern pintail/Tottori/b37/2016 (H5N6), and A/crane/Kagoshima/KU-4/2016 (H5N6), in Japan (Table 1). As of December 4, a total of 31 confirmed cases in wild birds had been reported to the Ministry of Environment (http://www.env.go.jp/nature/dobutsu/bird_flu/index.html), and 4 cases at poultry farms were confirmed in Japan (*8*).

To clarify the genetic background of the H5N6 HPAIVs concurrently introduced into several distant regions of Japan, we determined the complete genome sequences of 5 of our isolates: A/black swan/Akita/1/2016 (H5N6) (GenBank/DDBJ/EMBL accession

[1]These authors contributed equally to this article.

Figure 1. Locations of confirmed highly pathogenic avian influenza virus A(H5N6) infections in Akita, Tottori, and Kagoshima Prefectures, Japan, 2016.

nos. LC198525–LC198532), A/teal/Tottori/1/2016 (H5N6) (GenBank/DDBJ/EMBL accession nos. LC199865–LC199872), A/northern pintail/Tottori/b37/2016 (H5N6) (GenBank/DDBJ/EMBL accession nos. LC200414-LC200421), A/environment/Kagoshima/KU-ngr-I/2016 (H5N6) (GISAID EpiFlu [http://platform.gisaid.org/], GenBank/DDBJ/EMBL accession nos. EPI861582–EPI861589), and A/crane/Kagoshima/KU-4/2016 (H5N6) (GenBank/DDBJ/EMBL accession nos. EPI867577–EPI867584) by Sanger and/or Illumina Miseq next-generation sequencing. These 5 isolates were almost genetically identical. Even among the HA genes, which are the most frequently mutated ones among the 8 gene segments, only 3–8 nt mutations, including 3 nonsynonymous mutations, were detected compared with the earliest strain, A/northern pintail/Tottori/b37/2016 (H5N6) (online Technical Appendix Table, https://wwwnc.cdc.gov/EID/article/23/4/16-1957-Techapp1.pdf). Thus, the 5 isolates would share a close common ancestor.

The phylogenetic tree analysis of the HA gene revealed that our isolates are classified into the genetic clade 2.3.4.4c and clustered with the recent H5N6 HPAIV isolates from wild and domestic birds and humans in China, in addition to an isolate South Korea, A/Mandarin duck/Korea/K16-187-3/2016 (H5N6) (Figure 2, panel A), on the basis of a recent classification in clade 2.3.4.4 (*9*,*10*). The NA genes of our isolates also form a single cluster together with the H5N6 HPAIV isolates from China into group C in the phylogenetic tree (Figure 2, panel B). In addition, the remaining 6 genes were genetically close to the recent H5N6 HPAIV isolates from China in the corresponding phylogenetic trees (online Technical Appendix Figure 1), except for the polymerase basic 1 genes, which are most closely related to the counterpart of A/duck/Guangdong/S4040/2011 (H4N2) that was isolated from a domestic duck at a live bird market in China (*11*). Thus, the H5N6 HPAIV isolates would be derived from a reassortant that arose between an H5N6 HPAIV recently circulating in wild birds, poultry, or both in East Asia and in low pathogenicity avian influenza virus circulating in poultry in China. The genetic background of the H5N6 HPAIV isolates in this study is similar to the recent South Korea H5N6 virus collected in October 2016 and clearly different from that of recent H5Nx HPAIVs in Russia (*10*), Western European countries, and Alaska (*8*).

Our putative amino acid sequence comparison revealed that a leucine residue at position 134 in the HA protein (H3 numbering) was deleted, unlike that with the closest relative A/feline/Guangdong/1/2015 (H5N6) (online Technical Appendix Figure 2). Our isolates have the amino acid sequence QQG at positions 226–228, which are located at the receptor-binding site in the HA protein, although the corresponding amino acid sequences of the previous H5 viruses are QSG or QRG (online Technical Appendix Figure 2). These findings suggest that the receptor specificity of our H5N6 HPAIV isolates might be altered from their parental viruses (*12*,*13*). We also found 11 aa deletions in the stalk region of the NA protein, unlike that of A/duck/Vietnam/HU1–1151/2014 (H5N6), a representative virus strain of an N6 NA gene-based group D (online Technical Appendix Figure 3), which belongs to a different cluster of the clade 2.3.4.4.

For HA antigenic characterization, we investigated the reactivity of chicken antiserum raised against several H5 isolates to our H5N6 HPAIV isolates using the hemagglutination inhibition test (*14*). We selected 1 reference virus strain,

Table 1. Details of highly pathogenic avian influenza virus A(H5N6) infections, Japan, November 2016

Date of report	Date of sample collection	Sample (species of bird)	Isolate
Nov 18	Nov 14	Water at an overwintering site	A/environment/Kagoshima/KU-ngr-I/2016 (H5N6)
Nov 21	Nov 15	Dead exhibition bird in a zoo (black swan)	A/black swan/Akita/1/2016 (H5N6)
Nov 21	Nov 6	Wild birds' feces (northern pintail)	A/northern pintail/Tottori/b37/2016 (H5N6)
Nov 21	Nov 15	Wild birds' feces (teal)	A/teal/Tottori/1/2016 (H5N6)
Nov 21	Nov 17	Dead exhibition bird in a zoo (black swan)	A/black swan/Akita/2/2016 (H5N6)
Nov 22	Nov 18	Dead wild bird (hooded crane)	A/crane/Kagoshima/KU-4/2016 (H5N6)

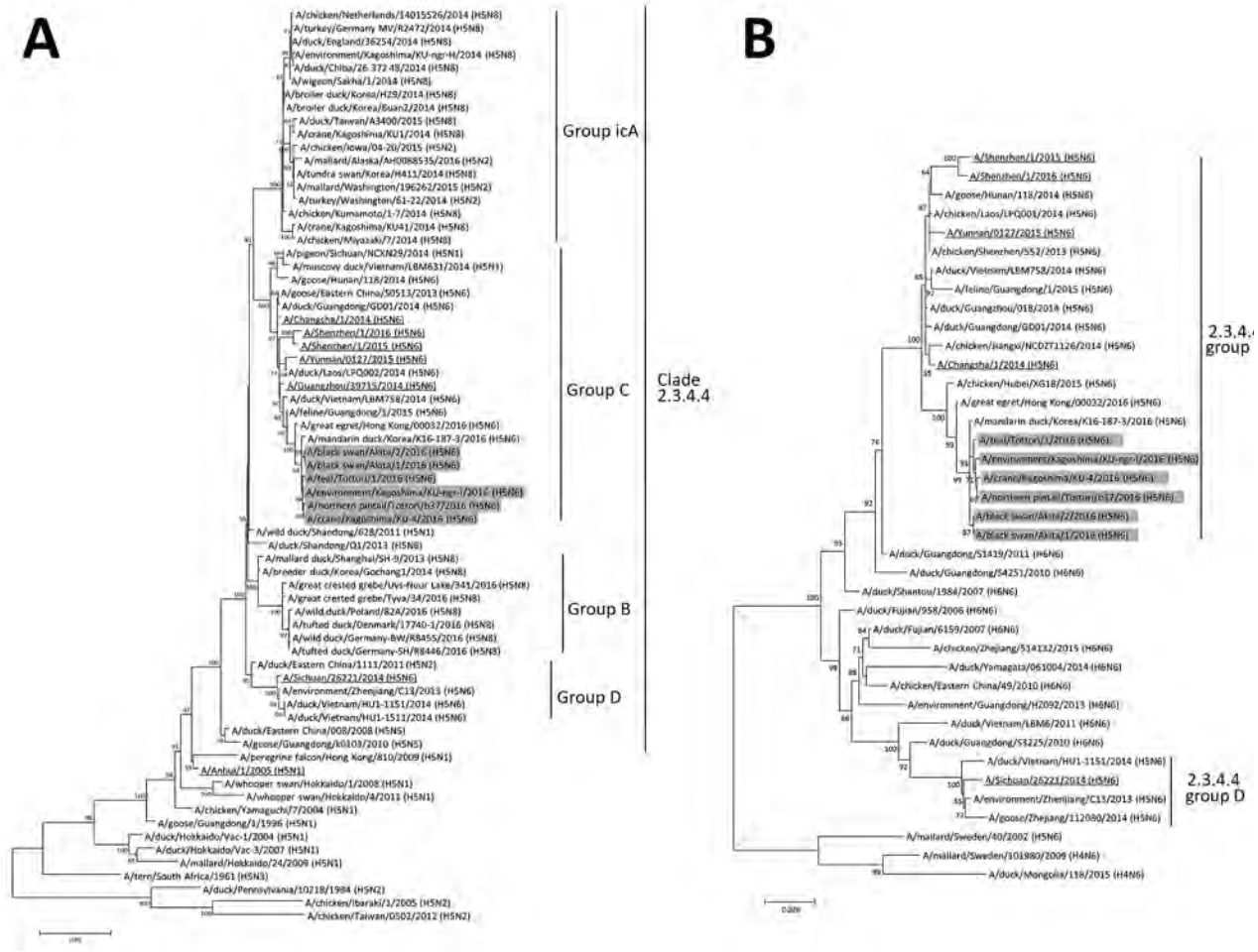

Figure 2. Phylogenetic trees of the HA and NA gene segments of highly pathogenic avian influenza virus A(H5N6) isolated in Japan. The nucleotide sequences of the H5 HA (A) and N6 NA (B) genes were analyzed by the maximum-likelihood method along with the corresponding genes of reference strains using MEGA 7.0 software (http://www.megasoftware.net/). Horizontal distances are proportional to the minimum number of nucleotide differences required to join nodes and sequences. Numbers at the nodes indicate the probability of confidence levels in a bootstrap analysis with 1,000 replications. Gray indicates viruses isolated in this study; underlining indicates viruses isolated in humans. The H5 HA gene sequences are classified into genetic clades as defined by Lee et al. (*9*). Scale bars indicate nucleotide substitutions per site. HA, hemagglutinin; NA, neuraminidase.

A/black swan/Akita/1/2016 (H5N6), and prepared single immunized chicken antiserum against the virus because of the limited variation of the nucleotide sequences in the HA genes among our 6 H5N6 HPAIV isolates. Antibody titer of antiserum of A/black swan/Akita/1/2016 (H5N6) were 16–32-fold higher against homologous virus than against the other strains (Table 2). The reactivity of the antiserum of A/chicken/Kumamoto/1-7/2014 (H5N8), whose HA gene belongs to the genetic clade 2.3.4.4, to A/black swan/Akita/1/2016 (H5N6) was 4-fold lower than that of the antiserum to the homologous combination. Moreover, none of the antiserum samples tested reacted strongly with A/black swan/Akita/1/2016 (H5N6) except for the homologous antiserum. These results indicate that the HA antigenicity of the H5N6 HPAIVs recently introduced in Japan differ appreciably from those of the previous H5Nx viruses.

Conclusions

We isolated 6 H5N6 HPAIVs from dead birds, fecal samples of migratory birds, and environmental water sample in 3 distant regions of Japan in November 2016. A genetic analysis showed that these isolates were genetically closely related to H5N6 HPAIVs recently isolated in China except for the polymerase basic 1 gene segment. The HA antigenicity of our H5N6 HPAIVs was demonstrated to have drifted further than viruses belonging to the same genetic clade 2.3.4.4. To prevent the spread of HPAIVs by wild birds, prompt elimination of HPAIVs is urgently needed in countries in Asia.

Table 2. Antigenic analyses of H5 influenza viruses with antiserum*

Virus lineage/clade	Virus	Hemagglutination inhibition titers of the antiserum						
		Mal/Hok (H5N1)	Ws/Hok (H5N1)	Pf/HK (H5N1)	Ck/Kum (H5N8)	B. swan/ Akita (H5N6)	Ck/Yam (H5N1)	Ck/Ibr (H5N2)
Eurasian								
–	Mal/Hok/24/2009 (H5N1)†	1,280	80	40	1,280	16	1,280	1,280
2.3.2.1	Ws/Hok/1/2008 (H5N1)	40	640	40	640	8	640	<20
2.3.4	Pf/HK/810/2009 (H5N1)	<20	20	2,560	20	8	80	<20
2.3.4.4 icA	Ck/Kumamoto/1-7/2014 (H5N8)	20	20	320	640	16	80	<20
2.3.4.4c	**B. swan/Akita/1/2016 (H5N6)**	<20	<20	80	160	256	80	<20
2.5	Ck/Yamaguchi/7/2004 (H5N1)	320	320	80	80	16	5,120	320
North American	Ck/Ibaraki/1/2005 (H5N2)	320	20	<20	<20	16	1,280	20,480

*Dash indicates virus does not belong to clade classification. Bold indicates virus isolated in this study. Underline indicates homologous titers. B. swan, black swan; Ck, chicken; HK, Hong Kong; Hok, Hokkaido; Mal, mallard; Pf, peregrine falcon; Ws, whooper swan.
†Low pathogenic avian influenza viruses isolated from mallard (*15*) and chicken in Japan.

Acknowledgments

We thank Mizuho Suzuki, Aiko Ohnuma, Junki Maruyama, Ayato Takada, Satoshi Saito, Hiroichi Ozaki, Toshiyuki Murase, Tsuyoshi Yamaguchi, Natsuko Nishi, Kaori Tokorozaki, Shigehisa Toda, Satoru Taura, Kotaro Kawabe, Atsushi Nishitani, and Naoko Maruta for their technical assistance. We thank the Ministry of the Environment, the Prefecture of Akita, the Prefecture of Tottori, and the City of Izumi for their kind cooperation.

This work was supported by a grant from the Project of the National Agriculture and Food Research Organization Bio-oriented Technology Research Advancement Institution (Integration Research for Agriculture and Interdisciplinary Fields) and by a grant for contracted research activity for crane conservation with the City of Izumi, Japan. This research was partially supported by the Japan Initiative for Global Research Network on Infectious Diseases from Japan's Ministry of Education, Culture, Sport, Science and Technology, and Japan Agency for Medical Research and Development and by grants for Scientific Research on Innovative Areas from the Ministry of Education, Culture, Science, Sports and Technology of Japan (JP16H06431, JP16H06429, and JP16K21723). This research was commissioned by the Kagoshima Crane Conservation Committee.

Dr. Okamatsu is an associate professor at the Graduate School of Veterinary Medicine, Hokkaido University, Sapporo, Japan. His primary research interests are interspecies transmission and pathogenecity of influenza viruses.

References

1. Smith GJ, Donis RO; World Health Organization/World Organisation for Animal Health/Food and Agriculture Organization (WHO/OIE/FAO) H5 Evolution Working Group. Nomenclature updates resulting from the evolution of avian influenza A(H5) virus clades 2.1.3.2a, 2.2.1, and 2.3.4 during 2013–2014. Influenza Other Respi Viruses. 2015;9:271–6. http://dx.doi.org/10.1111/irv.12324 PMID: 25966311
2. Claes F, Morzaria SP, Donis RO. Emergence and dissemination of clade 2.3.4.4 H5Nx influenza viruses—how is the Asian HPAI H5 lineage maintained. Curr Opin Virol. 2016;16:158–63. http://dx.doi.org/10.1016/j.coviro.2016.02.005
3. Global Consortium for H5N8 and Related Influenza Viruses. Role for migratory wild birds in the global spread of avian influenza H5N8. Science. 2016;354:213–7. http://dx.doi.org/10.1126/science.aaf8852
4. Bi Y, Chen Q, Wang Q, Chen J, Jin T, Wong G, et al. Genesis, evolution and prevalence of H5N6 avian influenza viruses in China. Cell Host Microbe. 2016;20:810–21. http://dx.doi.org/10.1016/j.chom.2016.10.022
5. Ozawa M, Matsuu A, Tokorozaki K, Horie M, Masatani T, Nakagawa H, et al. Genetic diversity of highly pathogenic H5N8 avian influenza viruses at a single overwintering site of migratory birds in Japan, 2014/15. Euro Surveill. 2015;20:21132. http://dx.doi.org/10.2807/1560-7917.ES2015.20.20.21132
6. Usui T, Soda K, Tomioka Y, Ito H, Yabuta T, Takakuwa H, et al. Characterization of clade 2.3.4.4 H5N8 highly pathogenic avian influenza viruses from wild birds possessing atypical hemagglutinin polybasic cleavage sites. Virus Genes. 2016. http://dx.doi.org/10.1007/s11262-016-1399-6
7. Tanikawa T, Kanehira K, Tsunekuni R, Uchida Y, Takemae N, Saito T. Pathogenicity of H5N8 highly pathogenic avian influenza viruses isolated from a wild bird fecal specimen and a chicken in Japan in 2014. Microbiol Immunol. 2016;60:243–52. http://dx.doi.org/10.1111/1348-0421.12369
8. World Organization for Animal Health. Update on highly pathogenic avian influenza in animals (type H5 and H7) [cited 2016 Dec 4]. http://www.oie.int/en/animal-health-in-the-world/update-on-avian-influenza/2016/
9. Lee DH, Bahl J, Torchetti MK, Killian ML, Ip HS, DeLiberto TJ, et al. Highly pathogenic avian influenza viruses and generation of novel reassortants, United States, 2014–2015. Emerg Infect Dis. 2016;22:1283–5. http://dx.doi.org/10.3201/eid2207.160048
10. Lee DH, Sharshov K, Swayne DE, Kurskaya O, Sobolev I, Kabilov M, et al. Novel reassortant clade 2.3.4.4 avian influenza A(H5N8) virus in wild aquatic birds, Russia, 2016. Emerg Infect Dis. 2017;23:359–60. http://dx.doi.org/10.3201/eid2302.161252
11. Jiao P, Cao L, Yuan R, Wei L, Song Y, Shen D, et al. Complete genome sequence of an H10N8 avian influenza virus isolated from a live bird market in southern China. J Virol. 2012;86:7716. http://dx.doi.org/10.1128/JVI.00959-12
12. Guo H, de Vries E, McBride R, Dekkers J, Peng W, Bouwman KM, et al. Highly pathogenic influenza A(H5Nx) viruses with altered H5 receptor-binding specificity. Emerg Infect Dis. 2017;23:220–31. http://dx.doi.org/10.3201/eid2302.161072
13. Hiono T, Okamatsu M, Igarashi M, McBride R, de Vries RP, Peng W, et al. Amino acid residues at positions 222 and 227 of the hemagglutinin together with the neuraminidase determine binding of H5 avian influenza viruses to sialyl Lewis X. Arch Virol. 2016;161:307–16. http://dx.doi.org/10.1007/s00705-015-2660-3

14. Hiono T, Ohkawara A, Ogasawara K, Okamatsu M, Tamura T, Chu DH, et al. Genetic and antigenic characterization of H5 and H7 influenza viruses isolated from migratory water birds in Hokkaido, Japan and Mongolia from 2010 to 2014. Virus Genes. 2015;51:57–68. http://dx.doi.org/10.1007/s11262-015-1214-9
15. Yamamoto N, Sakoda Y, Motoshima M, Yoshino F, Soda K, Okamatsu M, et al. Characterization of a non-pathogenic H5N1 influenza virus isolated from a migratory duck flying from Siberia in Hokkaido, Japan, in October 2009. Virol J. 2011;8:65. http://dx.doi.org/10.1186/1743-422X-8-65

Address for correspondence: Yoshihiro Sakoda, Laboratory of Microbiology, Department of Disease Control, Graduate School of Veterinary Medicine, Hokkaido University, North 18, West 9, Kita-ku, Sapporo, Hokkaido 060-0818, Japan; email: sakoda@vetmed.hokudai.ac.jp

Severe Thrombocytopenia after Zika Virus Infection, Guadeloupe, 2016

Timothée Boyer Chammard, Kinda Schepers, Sébastien Breurec, Thierry Messiaen, Anne-Laure Destrem, Matthieu Mahevas, Adrien Soulillou, Ludovic Janaud, Elodie Curlier, Cécile Herrmann-Storck, Bruno Hoen

Severe thrombocytopenia during or after the course of Zika virus infection has been rarely reported. We report 7 cases of severe thrombocytopenia and hemorrhagic signs and symptoms in Guadeloupe after infection with this virus. Clinical course and laboratory findings strongly suggest a causal link between Zika virus infection and immune-mediated thrombocytopenia.

Zika virus is an arthropod-borne flavivirus transmitted by mosquitoes. The most common signs and symptoms of Zika virus infection include pruritic rash, headache, arthralgia, myalgia, nonpurulent conjunctivitis, and low-grade fever (*1*). Signs and symptoms of Zika virus infection are usually mild. Rare complications, including birth defects, mainly microcephaly (*2*), and neurologic complications, such as Guillain-Barré syndrome, meningoencephalitis, and acute myelitis, might occur and have been reported during recent outbreaks (*3*–*6*). However, severe forms requiring hospitalization are uncommon, and lethality is low (*1*). In most cases, initial laboratory findings are nonspecific and whole blood cell counts are often within reference ranges (*7*). Mild-to-moderate thrombocytopenia has been rarely described (*8*,*9*), and severe thrombocytopenia has been reported only recently as an uncommon manifestation (*10*–*14*).

The Study

We report severe thrombocytopenia (i.e., platelet count $<50 \times 10^9$/L) (*15*), which developed during or after the course of acute Zika virus infection in 7 patients who were admitted to the Guadeloupe University Hospital, French West Indies, during May–August 2016. This period coincides with the peak of a Zika outbreak in Guadeloupe.

The 7 patients (5 women and 2 men, mean age 43 years, range 15–74 years) had petechial purpura in the lower limbs (Table). Five of the patients also had additional bleeding signs and symptoms (gingival bleeding, epistaxis, oral hemorrhagic mucosal blisters, and hematuria). These manifestations prompted us to perform blood tests, which showed isolated thrombocytopenia. Results of physical examinations were otherwise unremarkable. All 7 patients had a typical Zika virus infection (median 5 days, range 2–18 days) before diagnosis of thrombocytopenia. Median minimum platelet count was 2×10^9/L (range 1×10^9/L–17×10^9/L). Results of peripheral blood smears were unremarkable for all patients.

We evaluated patients for a differential diagnosis of isolated severe thrombocytopenia. None had recently received a new medication or vaccination or had traveled to an area to which malaria is endemic. No underlying conditions, such as autoimmune or lymphoproliferative disorders, were known or identified for any patient. Four patients had nonsignificantly positive antinuclear antibody titers (1:80–1:160). None of these patients had signs or symptoms of connective tissue disease.

Serologic test results for HIV and hepatitis B virus were negative for all 7 patients. Two of 7 patients had positive serologic results for hepatitis C virus; these 2 patients had negative results for hepatitis C virus RNA in plasma. Serologic test results ruled out diagnoses of acute leptospirosis, cytomegalovirus infection, and Epstein-Barr virus infection for all 7 patients. Six of 7 patients showed negative results for parvovirus B19 infection (1 patient was not tested). We did not test patients for chikungunya virus because this virus had not been detected in Guadeloupe since January 2015.

We tested patients for infection with Zika virus and dengue virus (DENV) by using reverse transcription PCR (RT-PCR) for urine samples ≤6 days of onset of purpura. Results of RT-PCR were positive for Zika virus and negative for DENV for all patients. In addition, results of serum tests for DENV nonstructural protein 1 were negative for all patients. IgG against DENV was detected in 6 of the 7 patients.

A diagnosis of acute immune mediated thrombocytopenia (ITP) was made for all 7 patients. Because of thrombocytopenia severity, all patients received steroid therapy

Author affiliations: Centre Hospitalier Universitaire, Pointe-à-Pitre, France (T. Boyer Chammard, K. Schepers, S. Breurec, T. Messiaen, A.-L. Destrem, A. Soulillou, L. Janaud, E. Curlier, C. Herrmann-Storck, B. Hoen); Institut National de la Santé et de la Recherche Médicale, Pointe-à-Pitre (K. Schepers, B. Hoen); Institut Pasteur de Guadeloupe, Pointe-à-Pitre (S. Breurec); Université des Antilles, Pointe-à-Pitre (S. Breurec, B. Hoen); Centre Hospitalier Universitaire Henri Mondor, Créteil, France (M. Mahevas)

DOI: http://dx.doi.org/10.3201/eid2304.161967

Table. Characteristics of 16 patients with severe thrombocytopenia associated with Zika virus infection*

Pt no./ age, y/sex	Country	Hemorrhagic signs and symptoms	Min platelet count, × 10^9/L	Days to min platelet count†	RT-PCR result				Steroid therapy	IVIG	Outcome	Reference
					Zika virus		DENV					
					Urine	Plas	Urine	Plas				
1/38/F	Guadeloupe	Yes	17	3	+	–	–	–	Yes	No	Recovered	This study
2/58/F	Guadeloupe	Yes	3	6	+	+	–	–	Yes	Yes	Recovered	This study
3/15/F	Guadeloupe	Yes	2	19	+	+	–	–	Yes	No	Recovered	This study
4/36/M	Guadeloupe	Yes	5	8	+	–	–	–	Yes	No	Recovered	This study
5/74/F	Guadeloupe	Yes	1	5	+	–	–	–	Yes	No	Recovered	This study
6/46/F	Guadeloupe	Yes	1	12	+	Unk	–	Unk	Yes	Yes	Recovered	This study
7/35/M	Guadeloupe	Yes	1	4	+	–	–	–	Yes	Yes	Recovered	This study
8/54/F	Suriname	Yes	10	29	+	–	–	Unk	No	Yes	Recovered	(*10*)
9/2/F	Colombia	Yes	<14	Unk	Unk	+	Unk	–	Unk	Unk	Died	(*11*)
10/30/F	Colombia	Yes	<14	Unk	Unk	+	Unk	–	Unk	Unk	Died	(*11*)
11/72/F	Colombia	Yes	<14	Unk	Unk	+	Unk	–	Unk	Unk	Died	(*11*)
12/72/M	Puerto Rico	Yes	1	5	Unk	+	Unk	–	No	No	Died	(*13*)
13/38/M	Puerto Rico	Yes	2	7	–	–	Unk	–	Yes	Yes	Recovered	(*13*)
14/26/F	Martinique	Yes	2	8	+	–	Unk	–	Yes	No	Recovered	(*14*)
15/21/M	Martinique	Yes	3	7	+	–	Unk	–	Yes	No	Recovered	(*14*)
16/30/F	Colombia	No	9	4	+	–	Unk	Unk	No	No	Recovered	(*12*)

*DENV, dengue virus; IVIG, intravenous immune globulins; min, minimum; plas, plasma; pt, patient; unk, unknown.
†From Zika onset.

with either prednisone or methylprednisolone at an initial dosage of 1–2 mg/kg/day. Three patients also received intravenous immune globulins (IVIG). Two patients received platelet transfusions. Except for patient 2, platelet counts returned to reference ranges ≤15 days after treatment initiation for all patients. After ≥2 months without treatment, no relapse was observed in any patient. We provide additional information on the atypical clinical course that was observed for 3 of the patients.

Patient 1 had a history of refractory ITP. She had been treated for primary ITP during 2004–2007 with steroids and IVIG, followed by vinblastine and danazol, and eventually splenectomy, which was curative. In 2014, an acute chikungunya virus infection caused a relapse of ITP, which fully responded to a short-course steroid treatment. During 2014–2016, she remained asymptomatic and had a platelet count >100 × 10^9/L. In May 2016, she was hospitalized 2 days after onset of a typical Zika virus infection. The patient had petechiae in the upper and lower limbs and a platelet count of 17 × 10^9/L. Her clinical course rapidly became favorable after steroid therapy, and she had a platelet count of 172 × 10^9/L by day 5 of steroid therapy. She was the only patient who did not have IgG against DENV.

Patient 2 responded only partially to steroids and IVIG and had a maximum platelet count of 92 × 10^9/L at day 14 after treatment initiation. While she was underdoing tapering of steroid treatment, palate petechiae appeared on day 39 (platelet count 9 × 10^9/L). Prednisone (1 mg/kg/day) was given for 10 days and was followed by a sustained recovery of the platelet count.

Patient 7 had severe hemorrhagic manifestations (gross hematuria and oral hemorrhagic blisters) and platelet count of 1 × 10^9/L. He was hospitalized in an intensive care unit and received steroid therapy, IVIG, and platelet transfusion. The patient showed a full response to treatment (platelet count 169 × 10^9/L at day 7 of treatment).

Conclusions

From the beginning of the current Zika outbreak in the Americas to November 2016, nine case-patients with severe Zika virus–associated thrombocytopenia have been reported, 1 in Suriname (*10*), 4 in Colombia (*11*,*12*), 2 in Puerto Rico (*13*), and 2 in Martinique (*14*). We report information for these 9 case-patients and the 7 patients we analyzed in Guadeloupe (Table).

The 16 patients had similar characteristics. First, all had severe and profound thrombocytopenia (platelet counts <20 × 10^9/L). Second, probably as a consequence of thrombocytopenia, hemorrhagic manifestations developed in all but 1 patient. Third, thrombocytopenia was present shortly after acute Zika virus infection, and Zika virus RNA was still detected in urine from 11 of the 12 patients for whom RT-PCR for Zika virus was performed.

Overall, despite the severity of thrombocytopenia, the outcome was generally favorable after conventional steroid treatment with or without IVIG. Among the 4 patients who died, only 1 patient had isolated thrombocytopenia; this patient died of hemorrhagic complications (*13*). The other 3 patients had various systemic signs and symptoms and thrombocytopenia; thrombocytopenia was the direct cause of death for only 1 patient (*11*).

For the 7 patients in Guadeloupe, we were able to exclude all other main causes of isolated severe thrombocytopenia, especially DENV infection. Because all 7 patients still had a positive RT-PCR result for Zika virus in urine when thrombocytopenia was diagnosed, we can reasonably assume that ITP was secondary to Zika virus infection. As reported for other viruses, Zika virus–associated

ITP might result from stimulation of the immune system, which usually decreases after clearance of viral replication. The mechanism of thrombocytopenia was probably different in patients 1 and 16 (*12*), in whom thrombocytopenia appeared as a relapse of previous ITP.

In conclusion, thrombocytopenia is a rare complication of Zika virus infection. Our observations strongly suggest a causal relationship between Zika virus infection and ITP. Therefore, Zika virus should be included in the list of viruses that might trigger immune-mediated severe thrombocytopenia.

Dr. Boyer Chammard is a physician in the Department of Infectious Diseases, Dermatology, and Internal Medicine, University Medical Center of Guadeloupe, Pointe-à-Pitre, France. His research interests include arboviruses, tropical medicine, and HIV infection.

References

1. Brasil P, Calvet GA, Siqueira AM, Wakimoto M, de Sequeira PC, Nobre A, et al. Zika virus outbreak in Rio de Janeiro, Brazil: clinical characterization, epidemiological and virological aspects. PLoS Negl Trop Dis. 2016;10:e0004636. http://dx.doi.org/10.1371/journal.pntd.0004636
2. de Araújo TV, Rodrigues LC, de Alencar Ximenes RA, de Barros Miranda-Filho D, Montarroyos UR, de Melo AP, et al.; investigators from the Microcephaly Epidemic Research Group; Brazilian Ministry of Health; Pan American Health Organization; Instituto de Medicina Integral Professor Fernando Figueira; State Health Department of Pernambuco. Association between Zika virus infection and microcephaly in Brazil, January to May 2016: preliminary report of a case-control study. Lancet Infect Dis. 2016 Sep 15;pii: S1473-3099(16)30318-8.
3. Dos Santos T, Rodriguez A, Almiron M, Sanhueza A, Ramon P, de Oliveira WK, et al. Zika virus and the Guillain-Barré syndrome: case series from seven countries. N Engl J Med. 2016;375:1598–601. http://dx.doi.org/10.1056/NEJMc1609015
4. Carteaux G, Maquart M, Bedet A, Contou D, Brugières P, Fourati S, et al. Zika virus associated with meningoencephalitis. N Engl J Med. 2016;374:1595–6. http://dx.doi.org/10.1056/NEJMc1602964
5. Rozé B, Najioullah F, Signate A, Apetse K, Brouste Y, Gourgoudou S, et al.; Neuro-Zika Working Group of Martinique. Zika virus detection in cerebrospinal fluid from two patients with encephalopathy, Martinique, February 2016. Euro Surveill. 2016;21.
6. Mécharles S, Herrmann C, Poullain P, Tran T-H, Deschamps N, Mathon G, et al. Acute myelitis due to Zika virus infection. Lancet. 2016;387:1481. http://dx.doi.org/10.1016/S0140-6736(16)00644-9
7. Plourde AR, Bloch EM. A literature review of Zika virus. Emerg Infect Dis. 2016;22:1185–92. http://dx.doi.org/10.3201/eid2207.151990
8. Zammarchi L, Stella G, Mantella A, Bartolozzi D, Tappe D, Günther S, et al. Zika virus infections imported to Italy: clinical, immunological and virological findings, and public health implications. J Clin Virol. 2015;63:32–5. http://dx.doi.org/10.1016/j.jcv.2014.12.005
9. Kutsuna S, Kato Y, Takasaki T, Moi M, Kotaki A, Uemura H, et al. Two cases of Zika fever imported from French Polynesia to Japan, December 2013 to January 2014. Euro Surveill. 2014;19:20683. http://dx.doi.org/10.2807/1560-7917.ES2014.19.4.20683
10. Karimi O, Goorhuis A, Schinkel J, Codrington J, Vreden SGS, Vermaat JS, et al. Thrombocytopenia and subcutaneous bleedings in a patient with Zika virus infection. Lancet. 2016;387:939–40. http://dx.doi.org/10.1016/S0140-6736(16)00502-X
11. Sarmiento-Ospina A, Vásquez-Serna H, Jimenez-Canizales CE, Villamil-Gómez WE, Rodriguez-Morales AJ. Zika virus associated deaths in Colombia. Lancet Infect Dis. 2016;16:523–4. http://dx.doi.org/10.1016/S1473-3099(16)30006-8
12. Zea-Vera AF, Parra B. Zika virus (ZIKV) infection related with immune thrombocytopenic purpura (ITP) exacerbation and antinuclear antibody positivity. Lupus. 2016 Sep 30;pii: 0961203316671816.
13. Sharp TM, Muñoz-Jordán J, Perez-Padilla J, Bello-Pagán MI, Rivera A, Pastula DM, et al. Zika virus infection associated with severe thrombocytopenia. Clin Infect Dis. 2016;63:1198–201.
14. Chraïbi S, Najioullah F, Bourdin C, Pegliasco J, Deligny C, Résière D, et al. Two cases of thrombocytopenic purpura at onset of Zika virus infection. J Clin Virol. 2016;83:61–2. http://dx.doi.org/10.1016/j.jcv.2016.08.299
15. Williamson DR, Albert M, Heels-Ansdell D, Arnold DM, Lauzier F, Zarychanski R, et al.; PROTECT collaborators; Canadian Critical Care Trials Group; Australian and New Zealand Intensive Care Society Clinical Trials Group. Thrombocytopenia in critically ill patients receiving thromboprophylaxis: frequency, risk factors, and outcomes. Chest. 2013;144:1207–15. http://dx.doi.org/10.1378/chest.13-0121

Address for correspondence: Bruno Hoen, Department of Infectious Diseases, Dermatology, and Internal Medicine, University Medical Center of Guadeloupe, BP 465, 97159 Pointe-à-Pitre CEDEX, France; email: bruno.hoen@chu-guadeloupe.fr

Significant Decrease in Pertactin-Deficient *Bordetella pertussis* Isolates, Japan

Yukihiro Hiramatsu, Yusuke Miyaji, Nao Otsuka, Yoshichika Arakawa, Keigo Shibayama, Kazunari Kamachi

Prevalence of pertactin-lacking *Bordetella pertussis* isolates has been observed worldwide. In Japan, however, we found that the frequency of pertactin-deficient isolates in 2014–2016 (8%) was significantly lower than the frequency in 2005–2007 (41%), 2008–2010 (35%), and 2011–2013 (25%). This reduction was closely associated with changes in genotypes.

Bordetella pertussis, a highly communicable, gram-negative coccobacillus, is the etiologic agent of pertussis (whooping cough), an acute respiratory infection that leads to severe illness in children. Vaccination is the most effective method for preventing and controlling pertussis. In Japan, acellular pertussis vaccines (ACVs) were introduced in 1981. Pertussis toxin and filamentous hemagglutinin derived from *B. pertussis* are the major antigens in ACVs in Japan, and certain ACVs also contain pertactin and fimbriae (*1*). Pertactin is believed to play a role in adherence to human epithelial cells (*2*); however, *B. pertussis* isolates that lack pertactin production have been identified in several countries where ACVs have been introduced (*3*–*7*). In Japan, pertactin-deficient isolates have increased significantly since the early 2000s, resulting in a high prevalence of these isolates (*5*,*8*). Recent studies have demonstrated that pertactin-deficient strains could colonize the respiratory tract more effectively than pertactin-producing strains in ACV-vaccinated mice (*9*,*10*). Supporting these results, an epidemiologic study suggested that ACV-vaccinated persons are more susceptible to pertactin-deficient strains than to pertactin-producing strains (*11*). These reports imply that pertactin-deficient strains have increased fitness in humans who have been vaccinated with ACVs and that their expansion may reduce the effectiveness of ACVs. We assessed trends in the frequency of pertactin-deficient isolates in Japan and further investigated their genotypes using multilocus variable-number tandem-repeat analysis (MLVA).

Author affiliations: National Institute of Infectious Diseases, Tokyo, Japan (Y. Hiramatsu, Y. Miyaji, N. Otsuka, K. Shibayama, K. Kamachi); St. Marianna University School of Medicine, Kawasaki, Japan (Y. Miyaji); Nagoya University Graduate School of Medicine, Nagoya, Japan (Y. Arakawa)

DOI: http://dx.doi.org/10.3201/eid2304.161575

The Study

We studied 232 *B. pertussis* clinical isolates collected from January 2005 through June 2016 in Japan. All isolates were derived from epidemiologically unrelated cases of pertussis. Pertactin production and MLVA types (MTs) of 111 isolates collected during 2005–2012 were previously determined by immunoblotting and MLVA typing, respectively (*5*,*8*). For our study, we extended these analyses to additional isolates collected during 2008–2016 (n = 121).

We determined the temporal trend in the frequency of pertactin-deficient isolates by 3-year periods (Figure, panel A). Percentages were 41% in 2005–2007 (n = 39 isolates), 35% in 2008–2010 (n = 43), 25% in 2011–2013 (n = 97), and 8% in 2014–2016 (n = 53). A significant decrease in the frequency of pertactin-deficient isolates was observed from 2005–2007 to 2014–2016 ($p<0.05$ by Fisher exact test).

Among the 232 *B. pertussis* isolates, 25 MTs were identified; MT27 and MT186 isolates were predominant, and other MT isolates were found at low frequencies (online Technical Appendix Table 1, http://wwwnc.cdc.gov/EID/article/23/4/16-1575-Techapp1.pdf). The frequency of MT27 isolates increased significantly over time (Figure 1, panel B): 28% in 2005–2007, 44% in 2008–2010, 70% in 2011–2013, and 77% in 2014–2016. In contrast, the frequency of MT186 isolates decreased: 31% in 2005–2007, 44% in 2008–2010, 21% in 2011–2013, and 6% in 2014–2016. We also observed a substitution of the major genotype in the *B. pertussis* population from MT186 to MT27.

Of 59 pertactin-deficient *B. pertussis* isolates collected during 2005–2016, 45 (76.3%) were MT186 isolates, whereas 2 (3.4%) represented MT27 and 12 (20.3%) other MT isolates (MT194, MT224–226, MT314–316) (Table). Notably, 45 (83.3%) of 54 MT186 isolates were pertactin-deficient, whereas only 2 (1.4%) of 139 MT27 isolates were pertactin-deficient. This finding indicates that pertactin-deficient isolates predominate among the MT186 strain but are rare among the MT27 strain.

We previously showed that pertactin-deficient isolates in Japan were generated by 2 different mutations: an 84-bp deletion of the *prn* gene signal sequence (ΔSS) and an IS*481* insertion at nucleotide position 1598 in *prn* (1598–1599::IS*481*) (*5*). Thus, to confirm the molecular basis for the loss of pertactin production, pertactin-deficient isolates (n = 26) that were newly identified in this study underwent PCR screening with 2 primer sets (online Technical Appendix Table 2). We summarized the molecular mechanisms of loss of pertactin production in 59 pertactin-deficient isolates

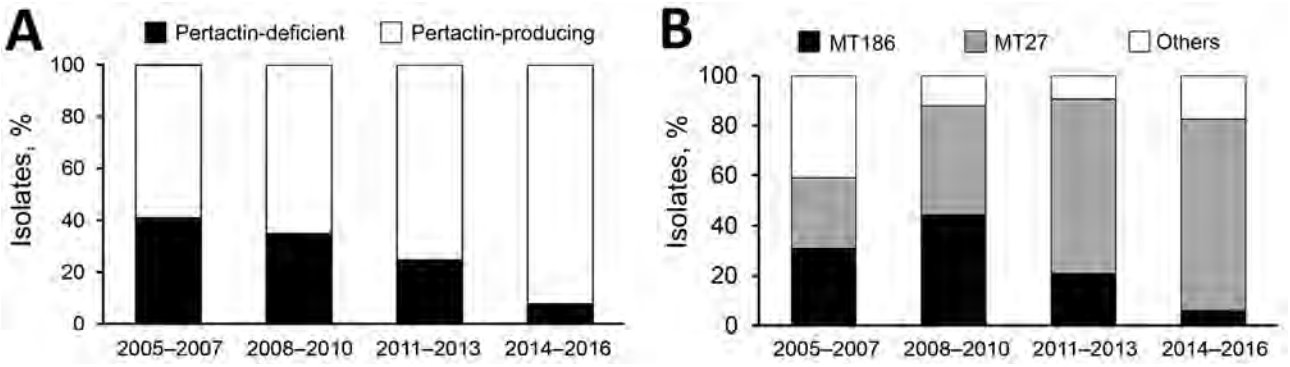

Figure. Temporal trends in the frequency of pertactin-deficient isolates and changes in multi-locus variable-number tandem repeat analysis types (MTs) in the *Bordetella pertussis* population in Japan. Pertactin production (A) and MTs (B) were analyzed for 232 *B. pertussis* isolates collected from January 2005 through June 2016. The frequencies of pertactin-deficient isolates and 2 major MTs (MT27 and MT186) are shown by time period. For convenience, minor MTs (MT194, MT224–226, and MT314–316) are included as "others."

(Table); the ΔSS mutation was detected in 43 (72.9%) MT186 isolates and in 11 (18.6%) other MT isolates. In contrast, the 1598–1599::IS*481* mutation was detected in 2 (3.4%) MT186 isolates and 1 other MT isolate (1.7%, MT226). Two MT27 isolates (BP394 and BP533) do not have either of these mutations. Instead, BP533 isolates (1.7%) have an IS*481* insertion at nucleotide position 245 (245–246::IS*481*; GenBank accession no. KC445198), and BP394 (1.7%) isolates exhibit transcriptional down-regulation of *prn* gene expression (online Technical Appendix Figure 1).

Conclusions

The expansion of pertactin-deficient *B. pertussis* isolates has been reported worldwide (*3*–*8*). However, we observed a significant decrease in pertactin-deficient isolates within the *B. pertussis* population in Japan, caused by a genotypic replacement from the pertactin-deficient MT186 strain to the pertactin-producing MT27 strain.

The most likely explanation for the prevalence of pertactin-deficient strains is vaccine-driven strain evolution, because pertactin is a component of ACVs. No pertactin-deficient isolates have been detected in Denmark, where an ACV that does not contain pertactin is used, and pertactin-deficient strains exhibit a selective advantage against ACV-induced immunity (*7*,*9*–*11*). In Japan, 5 brands of the diphtheria–tetanus–acellular pertussis vaccine (DTaP) had been used to control pertussis for many years. These DTaPs had different formulations of components; only 3 contained the pertactin antigen (*1*). When the DTaP vaccine was replaced, however, 2 brands of combined DTaP–inactivated poliovirus (DTaP-IPV) vaccine that did not contain pertactin were introduced in November 2012. Therefore, most Japanese children ≤4 years of age do not have immunity to pertactin; consequently, the selective pressure for pertactin-deficient strains in the host environment has recently been reduced. This effect may be responsible for the recent decline in pertactin-deficient isolates and further supports the hypothesis that pertactin-deficient strains are selected on the basis of host immunity to pertactin. Notably, a new brand of DTaP-IPV vaccine containing pertactin was also introduced in December 2015 in Japan. If the hypothesis of vaccine-driven evolution is correct, pertactin-deficient isolates should increase again in Japan in the near future. Thus, continued surveillance of pertactin-deficient isolates is of particular value.

We demonstrated that genotypic replacement from MT186 to MT27 has taken place among recent *B. pertussis* isolates in Japan: MT27 is a triple-locus variant of MT186. MT186 strains carry the pertussis-toxin promoter allele *ptxP1*, whereas MT27 strains carry the allele *ptxP3* (*8*). *B. pertussis* strains carrying *ptxP3* (i.e., MT27) produce more of several virulence factors than do *ptxP1* (i.e., MT186) strains (*12*,*13*). The population of MT27 strains carrying *ptxP3* has increased worldwide (*14*,*15*), although a low frequency of *ptxP1* isolates was observed in Japan (*8*), suggesting that MT27 strains are associated with the recent pertussis resurgence. It is possible, therefore, that the genotypic replacement in the *B. pertussis* population may have resulted from the expansion of the more virulent *ptxP3* (i.e., MT27) strains. In addition, given that pertactin-deficient MT27 isolates are rare, this genotypic replacement

Table. Molecular mechanisms of loss of pertactin production in 59 pertactin-deficient *Bordetella pertussis* isolates, Japan, 2005–2016*

Reason for loss of pertactin	No. (%) MTs		
	MT27	MT186	Others†
ΔSS	0	43 (72.9)	11 (18.6)
1598–1599::IS481	0	2 (3.4)	1 (1.7)
245–246::IS481	1 (1.7)	0	0
Transcriptional downregulation	1 (1.7)	0	0
Total	2 (3.4)	45 (76.3)	12 (20.3)

*MT, types determined by using multilocus variable-number tandem-repeat analysis.
†For convenience, minor MTs (MT194, MT224–226, and MT314–316) are included in this category.

may have contributed to the recent decrease in pertactin-deficient isolates in Japan.

In Japan, most pertactin-deficient isolates carry a deletion of the *prn* signal sequence (ΔSS), which has been found primarily in MT186 isolates carrying the *prn1* allele (online Technical Appendix Table 1). In other countries, a common *prn* mutation includes an insertion of IS*481* into the *prn2* allele (*4*,*6*,*7*). In this study, we identified 2 pertactin-deficient MT27 isolates carrying the *prn2* allele, due to the IS*481* insertion (245–246::IS*481*) and the transcriptional down-regulation of the *prn* gene. These pertactin-deficient isolates were previously identified in Europe and the United States (*6*,*7*). One possible explanation for the appearance of pertactin-deficient MT27 isolates is that they were imported from other countries.

This study was supported by the following funding sources: Research on Emerging and Re-emerging Infectious Diseases from the Ministry of Health, Labor, and Welfare of Japan; Research Program on Emerging and Re-emerging Infectious Diseases from the Japan Agency for Medical Research and Development.

Dr. Hiramatsu is a research scientist at the National Institute of Infectious Diseases in Tokyo, Japan. His research interests focus on the epidemiology, pathogenesis, and development of pertussis vaccines.

References

1. Okada K, Komiya T, Yamamoto A, Takahashi M, Kamachi K, Nakano T, et al. Safe and effective booster immunization using DTaP in teenagers. Vaccine. 2010;28:7626–33. http://dx.doi.org/10.1016/j.vaccine.2010.09.050
2. Leininger E, Roberts M, Kenimer JG, Charles IG, Fairweather N, Novotny P, et al. Pertactin, an Arg-Gly-Asp-containing *Bordetella pertussis* surface protein that promotes adherence of mammalian cells. Proc Natl Acad Sci U S A. 1991;88:345–9. http://dx.doi.org/10.1073/pnas.88.2.345
3. Bouchez V, Brun D, Cantinelli T, Dore G, Njamkepo E, Guiso N. First report and detailed characterization of *B. pertussis* isolates not expressing pertussis toxin or pertactin. Vaccine. 2009;27:6034–41. http://dx.doi.org/10.1016/j.vaccine.2009.07.074
4. Lam C, Octavia S, Ricafort L, Sintchenko V, Gilbert GL, Wood N, et al. Rapid increase in pertactin-deficient *Bordetella pertussis* isolates, Australia. Emerg Infect Dis. 2014;20:626–33. http://dx.doi.org/10.3201/eid2004.131478
5. Otsuka N, Han HJ, Toyoizumi-Ajisaka H, Nakamura Y, Arakawa Y, Shibayama K, et al. Prevalence and genetic characterization of pertactin-deficient *Bordetella pertussis* in Japan. PLoS One. 2012;7:e31985. http://dx.doi.org/10.1371/journal.pone.0031985
6. Pawloski LC, Queenan AM, Cassiday PK, Lynch AS, Harrison MJ, Shang W, et al. Prevalence and molecular characterization of pertactin-deficient *Bordetella pertussis* in the United States. Clin Vaccine Immunol. 2014;21:119–25. http://dx.doi.org/10.1128/CVI.00717-13
7. Zeddeman A, van Gent M, Heuvelman CJ, van der Heide HG, Bart MJ, Advani A, et al. Investigations into the emergence of pertactin-deficient *Bordetella pertussis* isolates in six European countries, 1996 to 2012. Euro Surveill. 2014;19:20881. http://dx.doi.org/10.2807/1560-7917.ES2014.19.33.20881
8. Miyaji Y, Otsuka N, Toyoizumi-Ajisaka H, Shibayama K, Kamachi K. Genetic analysis of *Bordetella pertussis* isolates from the 2008-2010 pertussis epidemic in Japan. PLoS One. 2013;8:e77165. http://dx.doi.org/10.1371/journal.pone.0077165
9. Hegerle N, Dore G, Guiso N. Pertactin deficient *Bordetella pertussis* present a better fitness in mice immunized with an acellular pertussis vaccine. Vaccine. 2014;32:6597–600. http://dx.doi.org/10.1016/j.vaccine.2014.09.068
10. Safarchi A, Octavia S, Luu LD, Tay CY, Sintchenko V, Wood N, et al. Pertactin negative *Bordetella pertussis* demonstrates higher fitness under vaccine selection pressure in a mixed infection model. Vaccine. 2015;33:6277–81. http://dx.doi.org/10.1016/j.vaccine.2015.09.064
11. Martin SW, Pawloski L, Williams M, Weening K, DeBolt C, Qin X, et al. Pertactin-negative *Bordetella pertussis* strains: evidence for a possible selective advantage. Clin Infect Dis. 2015;60:223–7. http://dx.doi.org/10.1093/cid/ciu788
12. King AJ, van der Lee S, Mohangoo A, van Gent M, van der Ark A, van de Waterbeemd B. Genome-wide gene expression analysis of *Bordetella pertussis* isolates associated with a resurgence in pertussis: elucidation of factors involved in the increased fitness of epidemic strains. PLoS One. 2013;8:e66150. http://dx.doi.org/10.1371/journal.pone.0066150
13. Mooi FR, van Loo IH, van Gent M, He Q, Bart MJ, Heuvelman KJ, et al. *Bordetella pertussis* strains with increased toxin production associated with pertussis resurgence. Emerg Infect Dis. 2009;15:1206–13. http://dx.doi.org/10.3201/eid1508.081511
14. Schmidtke AJ, Boney KO, Martin SW, Skoff TH, Tondella ML, Tatti KM. Population diversity among *Bordetella pertussis* isolates, United States, 1935–2009. Emerg Infect Dis. 2012;18:1248–55. http://dx.doi.org/10.3201/eid1808.120082
15. van Gent M, Heuvelman CJ, van der Heide HG, Hallander HO, Advani A, Guiso N, et al. Analysis of *Bordetella pertussis* clinical isolates circulating in European countries during the period 1998–2012. Eur J Clin Microbiol Infect Dis. 2015;34:821–30. http://dx.doi.org/10.1007/s10096-014-2297-2

Address for correspondence: Yukihiro Hiramatsu, Department of Bacteriology II, National Institute of Infectious Diseases, 4-7-1 Gakuen, Musashimurayama, Tokyo 208-0011, Japan; email: yhira@nih.go.jp

Increased Proinflammatory Cytokine Levels in Prolonged Arthralgia in Ross River Virus Infection

Dennis Tappe, José Vicente Pérez-Girón,[1] Sergio Gómez-Medina, Stephan Günther, César Muñoz-Fontela, Jonas Schmidt-Chanasit

Author affiliations: Bernhard Nocht Institute for Tropical Medicine, Hamburg, Germany (D. Tappe, S. Günther, C. Muñoz-Fontela, J. Schmidt-Chanasit); German Centre for Infection Research, Hamburg (D. Tappe, S. Günther, C. Muñoz-Fontela, J. Schmidt-Chanasit); Leibniz Institute for Experimental Virology, Hamburg (J.V. Pérez-Girón, S. Gómez-Medina, C. Muñoz-Fontela)

DOI: http://dx.doi.org/10.3201/eid2304.160466

Ross River virus, a mosquitoborne alphavirus, causes epidemic polyarthritis in Australia and the Pacific region. We analyzed serum cytokine, chemokine, and growth factor levels in travelers returning to Germany from Australia. Serum samples showed elevated concentrations in the acute phase of the illness and, more pronounced, in the long-lasting convalescent phase.

Ross River virus (RRV) is a mosquitoborne alphavirus endemic to Australia and the Pacific region. The virus is transmitted by various *Aedes* and *Culex* spp. mosquito species; macropods are the natural reservoir (*1*). RRV causes epidemic polyarthritis, with several thousand cases noted annually in Australia (*1*). Large outbreaks occurred during 1979–1980 on South Pacific islands. Infections in travelers, however, are rare (*2*). Epidemic polyarthritis is a self-limiting febrile arthralgia syndrome that closely resembles chikungunya and Mayaro fever. Acute-onset symmetric polyarthritis, most often affecting the fingers, wrists, ankles, and knees, is the predominant clinical presentation. Rash, myalgia, fatigue, and fever are present in half of patients (*1*). Joint effusions are common, and arthralgia can be long-lasting (months to years), and recurring.

The clinical disease, diagnostic procedures, and epidemiology of RRV have been well described, but immunologic parameters in humans and their usefulness in the clinical follow-up of patients warrant further investigation. Therefore, we investigated travelers returning to Germany from Australia with epidemic polyarthritis resulting from RRV infection.

We analyzed 20 serum samples from 16 patients (7 men, 9 women; age range 20–67 years [median 38 years]) who had serologic evidence for acute or recent RRV infection, as confirmed by indirect immunofluorescence assay and virus neutralization assay (*2*) (Table). All patients had acquired the infection during travel in Australia. We obtained serum samples at different times after symptom onset (3 days–16 weeks) and classified them as either acute (taken ≤30 days after symptom onset; n = 7) or convalescent with symptomatic arthralgia (taken >30 days after disease onset; n = 13). After we obtained written consent from the patients, we subjected the serum samples to multiplex cytokine analyses. In parallel with the RRV patients, we tested 20 serum samples from healthy blood donors.

Compared with concentrations in samples from healthy controls, concentrations in samples from patients in the acute phase of RRV infection showed noticeably elevated concentrations of serum interleukin (IL) 4 and 7; granulocyte-macrophage colony stimulating factor (GM-CSF); regulated on activation, normal T cell expressed and secreted (RANTES); interferon-γ–induced protein 10 (IP-10); and vascular endothelial growth factor (VEGF). We also saw a notable decrease in eotaxin levels in acute-phase samples. In samples from patients in the arthralgic convalescent phase, we noted increases in IL-1β, IL-4, IL-6, IL-8, IL-9, IL-13, IL-15, GM-CSF, interferon-γ, tumor necrosis factor-α (TNF-α), RANTES, basic fibroblast growth factor (bFGF), macrophage inflammatory protein 1α (MIP1α), and VEGF in comparison to healthy controls. Substantial elevations in the convalescent phase when compared with the acute phase were recorded for levels of bFGF and MIP1α, and a marked decrease was seen in IP-10 concentrations.

Cytokine and chemokine levels were generally higher in the convalescent phase than in the acute phase, with individual exceptions (online Technical Appendix, https://wwwnc.cdc.gov/EID/article/23/4/16-0466-Techapp1.pdf). No notable changes in either phase were seen for IL-1RA, IL-2, IL-5, IL-10, IL-12p70, IL-17, granulocyte colony-stimulating factor, monocyte chemotactic protein 1, and platelet-derived growth factor β polypeptide levels (data not shown), and macrophage inflammatory protein 1β concentrations.

Similar to chikungunya and Mayaro fever, the most prominent clinical symptom of RRV infection is long-lasting arthralgia. Nearly 60% of patients reported persisting pain after 2–3 years (*1*). RRV RNA has been detected in synovial fluid up to 5 weeks after symptom onset (*3*), suggesting ongoing viral replication and inflammation (*4*). In the RRV-infected travelers examined in this study, the increased proinflammatory cytokine serum concentrations during the prolonged arthralgic convalescence phase strengthen the hypothesis of persisting inflammation of the joints. In patients and in a murine model, macrophage-derived TNF-α, interferon-γ, and IL-6 were elevated in synovial fluid during RRV disease (*5*), as we have shown here in serum.

[1]Deceased.

Table. Returning travelers from Australia infected with Ross River virus included in study of cytokine levels during acute and convalescent disease phases, Germany

Patient no.	Age, y/sex	Timing of cytokine level testing after symptom onset	IgM titer*	IgG titer*
1	33/M	8 wk	1:320	1:320
2	67/F	7 wk	1:80	1:1,280
3	55/F	4 wk	1:2,560	1:1,280
4	24/M	10 and 13 wk	1:320 each	1:2,560
5	29/F	6 wk	1:2560	1:10,240
6	21/F	6 wk	1:80	1:1,280
7	46/M	5 d	1:2,560	1:80
8	31/F	1 wk	1:10,240	1:160
9	32/F	2 wk	1:81,900	1:327,680
10	51/F	4 and 8 wk	1:320 and 1:160	1:2,560 and 1:640
11	20/F	6 wk	1:320	1:2,560
12	47/M	8 wk	1:160	1:320
13	32/M	16 wk	1:20	1:160
14	43/F	8 wk	1:320	1:2,560
15	53/M	3 d, 2 wk, and 9 wk	1:320, 1:10,240, and 1:640	1:20, 1:1,280, and 1:320
16	49/F	6 wk	1:1,280	1:2,560

*By indirect immunofluorescence testing; reference value <1:20 (*2*).

Furthermore, increased levels of IL-1β, IL-6, IL-15, MIP1α, and GM-CSF, as seen in our study, have been described in the clinically similar chikungunya (*6*). Elevated levels of RANTES (and IP-10 initially) indicate T-cell activation, possibly reflecting ongoing viral replication in the joints, also as described in chikungunya (*6*). A similar effect could recently be demonstrated in Mayaro fever patients with prolonged arthralgia (*7*).

In conclusion, cytokine level testing in alphavirus infections with prolonged arthralgia may aid monitoring patient symptoms. This information is particularly valuable when clinical signs of arthritis, such as joint swelling and redness, are no longer present, and standard serum inflammatory parameters are within reference ranges. Low-grade inflammation in persistent alphavirus-induced arthritis might place patients at risk for bone loss and fractures (*8*). Levels of RANKL (receptor activator of nuclear factor κB ligand), which were not determined in our study, were recently shown to be elevated in RRV infection and associated with increased osteoclast formation (*9*).

The pattern of cytokine concentration elevations we demonstrated for patients with epidemic polyarthritis is similar to what has recently been described for patients with Mayaro fever (*7*) and chikungunya (*6*,*10*). Our data broaden the knowledge of alphavirus pathogenesis in arthralgia syndromes; however, more immunological investigations, including human T-cell analyses, are needed.

Acknowledgments

We thank Birgit Hüsing, Corinna Thomé, and Alexander Schlaphof for their excellent technical assistance.

Dr. Tappe is a clinical microbiologist at the National Reference Center for Tropical Diseases, Bernhard Nocht Institute, Hamburg, Germany. His research interests focus on the immune response in viral and rickettsial diseases.

References

1. Harley D, Sleigh A, Ritchie S. Ross River virus transmission, infection, and disease: a cross-disciplinary review. Clin Microbiol Rev. 2001;14:909–32. http://dx.doi.org/10.1128/CMR.14.4.909-932.2001
2. Tappe D, Schmidt-Chanasit J, Ries A, Ziegler U, Müller A, Stich A. Ross River virus infection in a traveller returning from northern Australia. Med Microbiol Immunol (Berl). 2009;198:271–3. http://dx.doi.org/10.1007/s00430-009-0122-9
3. Soden M, Vasudevan H, Roberts B, Coelen R, Hamlin G, Vasudevan S, et al. Detection of viral ribonucleic acid and histologic analysis of inflamed synovium in Ross River virus infection. Arthritis Rheum. 2000;43:365–9. http://dx.doi.org/10.1002/1529-0131(200002)43:2<365::AID-ANR16>3.0.CO;2-E
4. Suhrbier A, La Linn M. Clinical and pathologic aspects of arthritis due to Ross River virus and other alphaviruses. Curr Opin Rheumatol. 2004;16:374–9. http://dx.doi.org/10.1097/01.bor.0000130537.76808.26
5. Lidbury BA, Rulli NE, Suhrbier A, Smith PN, McColl SR, Cunningham AL, et al. Macrophage-derived proinflammatory factors contribute to the development of arthritis and myositis after infection with an arthrogenic alphavirus. J Infect Dis. 2008;197:1585–93. http://dx.doi.org/10.1086/587841
6. Ng LF, Chow A, Sun YJ, Kwek DJ, Lim PL, Dimatatac F, et al. IL-1β, IL-6, and RANTES as biomarkers of chikungunya severity. PLoS One. 2009;4:e4261. http://dx.doi.org/10.1371/journal.pone.0004261
7. Tappe D, Pérez-Girón JV, Just-Nübling G, Schuster G, Gómez-Medina S, Günther S, et al. Sustained elevated cytokine levels during recovery phase of Mayaro virus infection. Emerg Infect Dis. 2016;22:750–2. http://dx.doi.org/10.3201/eid2204.151502
8. Chen W, Foo SS, Sims NA, Herrero LJ, Walsh NC, Mahalingam S. Arthritogenic alphaviruses: new insights into arthritis and bone pathology. Trends Microbiol. 2015;23:35–43. http://dx.doi.org/10.1016/j.tim.2014.09.005
9. Chen W, Foo SS, Rulli NE, Taylor A, Sheng KC, Herrero LJ, et al. Arthritogenic alphaviral infection perturbs osteoblast function and triggers pathologic bone loss. Proc Natl Acad Sci U S A. 2014;111:6040–5. http://dx.doi.org/10.1073/pnas.1318859111
10. Chow A, Her Z, Ong EK, Chen JM, Dimatatac F, Kwek DJ, et al. Persistent arthralgia induced by chikungunya virus infection is associated with interleukin-6 and granulocyte macrophage colony-stimulating factor. J Infect Dis. 2011;203:149–57. http://dx.doi.org/10.1093/infdis/jiq042

Address for correspondence: Dennis Tappe, Bernhard Nocht Institute for Tropical Medicine, Bernhard-Nocht-Str. 74, 20359 Hamburg, Germany; email: tappe@bnitm.de

Peste des Petits Ruminants Virus in Vulnerable Wild Small Ruminants, Iran, 2014–2016

Mahmoud Marashi, Siamak Masoudi, Majid Kharazian Moghadam, Hossein Modirrousta, Mahyar Marashi, Masoumeh Parvizifar, Majid Dargi, Mahyar Saljooghian, Farbod Homan, Bernd Hoffmann, Claudia Schulz, Elke Starick, Martin Beer, Sasan Fereidouni

Author affiliations: Department of Environment, Tehran, Iran (M. Marashi, S. Masoudi, M.K. Moghaddam, M. Marashi, M. Parvizifar, M. Dargi, M. Saljooghian, F. Homan); Razi Research Institute, Karaj, Iran (H. Modirrousta); Friedrich-Loeffler-Institute, Insel Riems, Germany (B. Hoffmann, C. Schulz, E. Starick, M. Beer); University of Veterinary Medicine Hannover, Hannover, Germany (C. Schulz); University of Veterinary Medicine Vienna, Vienna, Austria (S. Fereidouni)

DOI: http://dx.doi.org/10.3201/eid2304.161218

In 2014–2016, >1,000 wild goats and sheep in 4 northern and central provinces of Iran died from peste des petits ruminants virus (PPRV) infection. Partial nucleoprotein sequencing of PPRV from 3 animals showed a close relationship to lineage 4 strains from China. Control measures are needed to preserve vulnerable ruminant populations.

Peste des petits ruminants virus (PPRV; family *Paramyxoviridae*, genus *Morbillivirus*) causes a highly contagious disease with a high death rate in wild and domestic small ruminants. Four PPRV lineages (L1–L4) exist in Africa and Asia (*1*). The disease was initially recorded in Iran in 1995 (*2*) and subsequently spread throughout the country (*3*). PPRV-L4 infections are endemic in Iran and several neighboring countries (*4*,*5*).

Wild goats (*Capra aegagrus*) and sheep (*Ovis orientalis*), which have become extinct in several West Asia countries, are considered vulnerable species in Iran (*6*,*7*). Although PPRV-associated outbreaks among these ruminants have been suspected since 2000, the virus was not isolated or characterized at that time. In 2001, at least 1,500 wild goats and gazelles (*Gazella subgutturosa*) with clinical signs similar to those caused by PPRV infection died in Kavir National Park (Figure; online Technical Appendix Table, https://wwwnc.cdc.gov/EID/article/23/4/16-1218-Techapp1.pdf). An estimated 25%–40% of the wild goat population in the park was deemed lost as a result of the disease. In 2011, PPRV was the suspected cause of 550–700 deaths among wild sheep in Sarigol National Park (Figure); laboratory investigations using conventional reverse transcription PCR (RT-PCR) confirmed PPRV infection in several dead animals (Iran veterinary organization, pers. comm., 2011 Sep 26).

Beginning in September 2014, park rangers reported and field investigations substantiated mass deaths among wild goats in Bamou National Park (Figure). Clinical signs in affected animals were similar to those reported in wild small ruminants in 2011, and samples we tested from 5 dead goats were positive for PPRV by RT-PCR (online Technical Appendix). In April 2015, a new outbreak started in Haftad Qolleh Arak (Figure) and continued until mid-May, resulting in the death of 428 wild goats and 30 wild sheep. Three more outbreaks occurred in 2015: the first started in August in Kharmaneh-sar Tarom; the second in September in the Alamout Protected Area, 150 km from the previous outbreak in Kharmaneh-sar Tarom; and the third in November in the Taleghan Protected Area, 100 km away from the previous outbreak in Alamout Protected Area (Figure; online Technical Appendix Table).

The last reported outbreak started in April 2016 in Khojir, a national park close to a dam that serves as a water source for wild animals (Figure). In 2015, a total of 110 wild goats and sheep were counted in the park, and by May, 1, 2016, ≈85 were found dead (online Technical Appendix Table).

We detected PPRV genome in 6 oral swab samples and 7 blood and lymph node samples from dead ruminants by using conventional RT-PCR and in 3 oral swab samples by using real-time RT-PCR (quantification cycles 31–34) (online Technical Appendix). In addition, we performed partial nucleocapsid gene sequencing of 3 PPRV isolates from 2015; results showed 100% pairwise nt identity among the isolates (online Technical Appendix). The strains shared highest nt identity (99.4%) with PPRV-L4 strains that were circulating in domestic or wild small ruminants in northwestern and southeastern China during 2013–2015 (*8*) (online Technical Appendix Figure); they were more distantly related to PPRV-L4 strains previously reported from outbreaks in Iran and neighboring countries (*9*,*10*).

Field investigations and laboratory analyses indicated that PPRV was the cause of mass die-offs of wild goats and sheep during 2014–2016 in several national parks in Iran. A risk assessment of PPRV infection in several developing countries in Africa and the Middle East and on the Indian Peninsula indicated that 63% of small ruminant populations

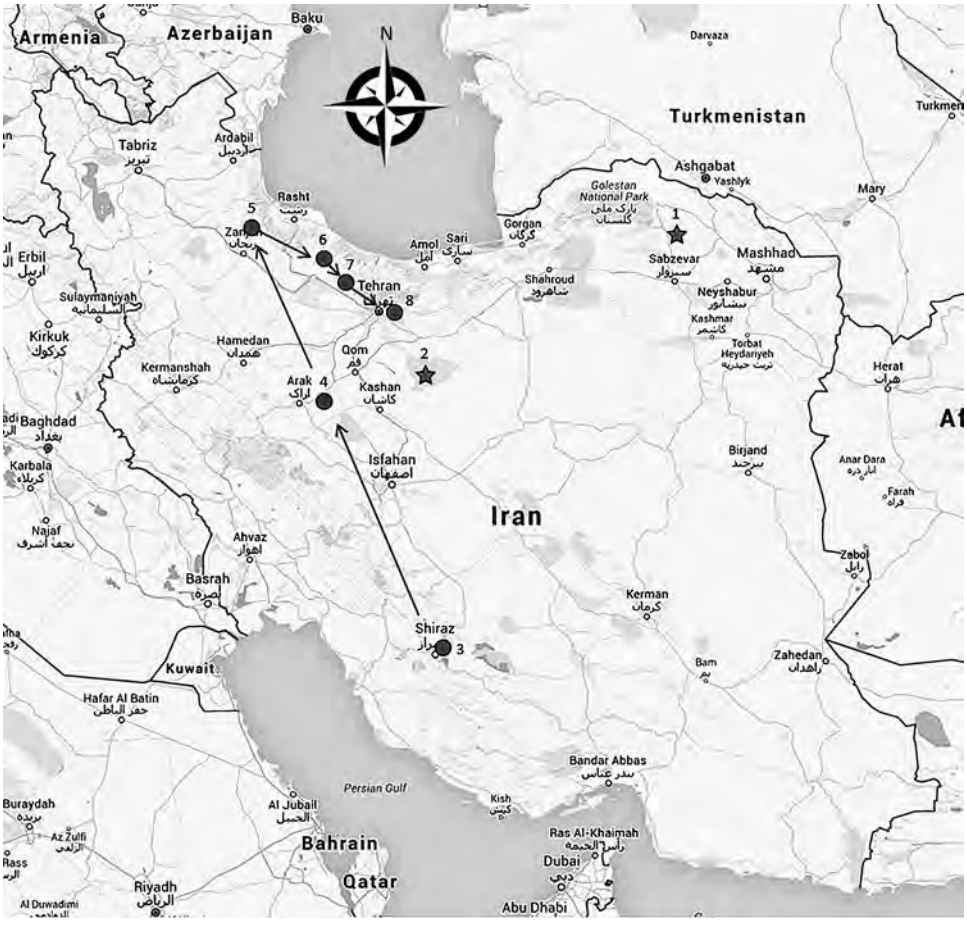

Figure. Geographic distribution of peste des petits ruminants virus outbreaks in Iran since 2000. Stars indicate outbreaks that occurred in 2000 and 2011; circles indicate outbreaks investigated during this study in 2014–2016. Arrows indicate chronologic order of the outbreaks: 1, Sarigol National Park; 2, Kavir National Park; 3, Bamou National Park; 4, Haftad-qolleh; 5, Kharmaneh Sar Tarom; 6, Alamout Protected Area; 7, Taleghan Protected Area; 8, Khojir National Park. Map generated using Google Maps (interactive map available at https://www.google.com/maps/d/viewer?mid=1GsluO7SZ2z_SBUawdPHsDF6s7ww). Details on the number of animals and dates of outbreaks are available in the online Technical Appendix Table (https://wwwnc.cdc.gov/EID/article/23/4/16-1218-Techapp1.pdf).

are at risk for infection (*4*). Legal and illegal movement of domestic small ruminants into wildlife territories over short and long distances, within and across borders, increases the possibility of transmission of various pathogens, including PPRV, to wild small ruminants, which may threaten vulnerable species. Transboundary circulation between China and Kazakhstan was recently shown for PPRV strains closely related to the PPRV Iran/2015 strains, suggesting that these closely related strains have been circulating in central and western Asia for a few years (*5*).

Clinical signs similar to those caused by PPRV infection were observed in domestic small ruminants in villages around the Kharmaneh-sar Tarom region before deaths were noted among wild goats in the area, and the samples collected from domestic animals tested positive for PPRV. It is unknown whether PPRV-infected wild small ruminants may contribute to PPRV spread by spillback to domestic small ruminants.

Comprehensive field studies of PPRV infection in domestic and wild small ruminants are necessary to evaluate the occurrence and origin of PPRV infections and of different PPRV strains in domestic and wild small ruminants in Iran. Emerging PPRVs can potentially spread to all susceptible small ruminant populations in the region and cause extinction of local subpopulations. Furthermore, control measures, such as vaccination against PPRV and movement control of domestic small ruminants around protected areas, would facilitate the preservation of vulnerable wild small ruminant populations and reduce the economic effect of PPRV infection on small ruminant production in affected regions.

Dr. Marashi is a veterinary officer at the Department of Environment in Tehran, Iran. His primary research areas are wildlife health and diseases and epidemiologic investigation of wildlife outbreaks.

References

1. Parida S, Muniraju M, Mahapatra M, Muthuchelvan D, Buczkowski H, Banyard AC. Peste des petits ruminants. Vet Microbiol. 2015;181:90–106. http://dx.doi.org/10.1016/j.vetmic.2015.08.009
2. Radostits OM, Gay CC, Blood DC, Hinchcliff KW. Veterinary Medicine, 9th ed, London: W.B. Saunders Co; 2000. p. 1072–9.
3. Bazarghani TT, Charkhkar S, Doroudi J, Bani Hassan E. A review on peste des petits ruminants (PPR) with special reference to PPR in Iran. Journal of Veterinary Medicine, Series B. 2006;53(Suppl 1):17–8. http://dx.doi.org/10.1111/j.1439-0450.2006.01014.x

4. Libeau G, Diallo A, Parida S. Evolutionary genetics underlying the spread of peste des petits ruminants virus. Animal Frontiers. 2014;4:14–20. http://dx.doi.org/10.2527/af.2014-0003
5. Kock RA, Orynbayev MB, Sultankulova KT, Strochkov VM, Omarova ZD, Shalgynbayev EK, et al. Detection and genetic characterization of lineage IV peste des petits ruminant virus in Kazakhstan. Transbound Emerg Dis. 2015;62:470–9. http://dx.doi.org/10.1111/tbed.12398
6. International Union for Conservation of Nature and Natural Resources. The IUCN red list of threatened species. *Capra aegagrus* [cited 2016 Jul 15]. http://dx.doi.org/10.2305/IUCN.UK.2008.RLTS.T3786A10076632.en
7. International Union for Conservation of Nature and Natural Resources. The IUCN red list of threatened species. *Ovis orientalis* [cited 2016 Jul 15]. http://dx.doi.org/10.2305/IUCN.UK.2008.RLTS.T15739A5076068.en
8. Zhu Z, Zhang X, Adili G, Huang J, Du X, Zhang X, et al. Genetic characterization of a novel mutant of peste des petits ruminants virus isolated from *Capra ibex* in China during 2015. BioMed Res Int. 2016;2016:7632769. http://dx.doi.org/10.1155/2016/7632769
9. Hoffmann B, Wiesner H, Maltzan J, Mustefa R, Eschbaumer M, Arif FA, et al. Fatalities in wild goats in Kurdistan associated with Peste des Petits Ruminants virus. Transbound Emerg Dis. 2012; 59:173–6. http://dx.doi.org/10.1111/j.1865-1682.2011.01270.x
10. Bailey D, Banyard A, Dash P, Ozkul A, Barrett T. Full genome sequence of peste des petits ruminants virus, a member of the *Morbillivirus* genus. Virus Res. 2005;110:119–24. http://dx.doi.org/10.1016/j.virusres.2005.01.013

Address for correspondence: Sasan Fereidouni, Conservation Medicine, Research Institute of Wildlife Ecology University of Veterinary Medicine Vienna, Savoyenstrasse 1, Vienna, Austria; email: sasan.fereidouni@vetmeduni.ac.at

Discussion of Average versus Extreme Case Severity in Pandemic Risk Communications

Brian J. Zikmund-Fisher, Aaron M. Scherer, Megan Knaus, Enny Das, Angela Fagerlin

Author affiliations: University of Michigan, Ann Arbor, Michigan, USA (B.J. Zikmund-Fisher, A.M. Scherer, M. Knaus); University of Iowa, Iowa City, Iowa, USA (A.M. Scherer); Radboud University Nijmegen, Nijmegen, The Netherlands (E. Das); University of Utah, Salt Lake City, Utah, USA (A. Fagerlin); Salt Lake City VA Center for Informatics Decision Enhancement and Surveillance, Salt Lake City (A. Fagerlin)

DOI: http://dx.doi.org/10.3201/eid2304.161600

To investigate determinants of the public's perceptions of disease threat, in 2015 we conducted a randomized survey experiment in the Netherlands. Adults who read a mock news article describing average or extreme outcomes from a hypothetical influenza pandemic were more influenced by average than by extreme case information. Presenting both types of information simultaneously appeared counterproductive.

When pandemics strike, clear and timely communication is essential to raising public awareness of disease threat and motivating preventive behaviors (*1*). Yet, in most pandemics, the experience of affected persons is heterogeneous: a subset of persons have severe symptoms or sequelae, whereas most affected persons have much milder symptoms or sequelae. This heterogeneity creates a dilemma: Should communications about new infectious disease threats emphasize the character and severity of modal cases, which represents what most persons will experience, or should they focus on the severity of extreme cases to make clear the potential threat, even if that threat is highly unlikely? Both types of information are clearly important. Yet, risk messages are inherently difficult to understand, and providing multiple types of information simultaneously might undermine the public's understanding of a threat. Simplicity of message enables communications to stick with target audiences, and limiting communications to fewer, clearly contextualized, issues can increase efficacy (*2*,*3*).

To begin to address this communications dilemma, during 2015 we conducted a randomized survey experiment with adult residents of the Netherlands who participate in an online panel administered by Survey Sampling International (https://www.surveysampling.com/). We established quotas for age and sex that approximated the distributions of these characteristics in the population of the Netherlands (online Technical Appendix, https://wwwnc.cdc.gov/EID/article/23/4/16-1600-Techapp1.pdf). Upon completing the survey, participants received modest prizes.

Participants read a mock news article about a new pandemic (referred to as H7N3 influenza) spreading within the Netherlands. We randomly varied how the article discussed the average case severity, which was 1) not discussed, 2) described as mild (moderate fever and cough; generally goes away by itself), or 3) described as moderately severe (high fever, cough, vomiting; generally requires intravenous medication and hospitalization). We also independently varied the description of extreme cases, which were 1) not discussed, 2) described as (relatively) mild (requiring 1–2 days of hospitalization because of difficulty breathing, dizziness, and persistent coughing), or 3) described as moderately severe (requiring hospitalization [and causing 1 death] because of difficulty breathing, dizziness, severe coughing, and fluid in the lungs). This randomization resulted in a 3 × 3 between-subjects factorial design. Following guidelines for effective health messages (*4*), all articles

Table. Differences in ratings of worry and vaccination intentions compared with ratings when no information was provided about a hypothetical influenza pandemic, the Netherlands, 2015*

	Extreme case scenario		
Average case scenario	No Information	Mild severity	Moderate severity
No information			
Worry if symptoms	Reference	–0.01	+0.20
Worry about extreme	Reference	+0.07	+0.13
Vaccination intentions	Reference	–0.16	+0.18
Mild severity			
Worry if symptoms	–0.23	–0.08	–0.07
Worry about extreme	–0.07	–0.01	+0.01
Vaccination intentions	–0.25	–0.18	–0.12
Moderate severity			
Worry if symptoms	+0.26	+0.18	+0.17
Worry about extreme	+0.22	+0.13	+0.13
Vaccination intentions	+0.21	+0.05	–0.06

+, increased worry; –, decreased worry.

included a (fixed) efficacy message, instructing readers to cover their mouths for coughs and sneezes and wash hands frequently to prevent disease spread (online Technical Appendix). This design received exempt status approval from the University of Michigan Medical Institutional Review Board (Ann Arbor, MI, USA).

Our analyses focused on 3 questions: how much respondents would worry if symptoms developed, how much they would worry about extreme effects if they contracted the disease, and participants' vaccination intentions if a vaccine were available. All questions were 5-point Likert scales, where higher values represented greater worry or intent to vaccinate. Although absolute rates of concern and vaccination intentions are not generalizable from the hypothetical scenario, significant differences among the experimental conditions should be. We conducted 3 × 3 analyses of variance and ordered logistic regression analyses of each outcome with variables for each level of average and/or extreme case information (not present, mild, moderate). The results showed close correspondence, so for simplicity we report only analysis of variance results.

A total of 2,695 participants completed the survey and answered the 3 primary outcome questions. Average age was 49.2 (SD ± 15.6; range 18–96) years, and 49.8% of respondents reported being female.

Overall, respondents were most sensitive to descriptions of average case severity: worry if symptoms: $F(2,2686) = 20.87$, $p<0.001$; worry about extreme: $F(2,2686) = 6.16$, $p = 0.002$; vaccination intentions: $F(2,2686) = 7.56$, $p<0.001$. By contrast, the main effect of extreme case information was nonsignificant in all 3 analyses ($0.16<p<0.77$). However, we noticed evidence of an interaction effect for vaccination intentions ($F[2,2686] = 3.23$, $p = 0.01$).

The main effect of average case information was clearly visible among respondents receiving no information about extreme cases (Table, first column). Yet, the effect of average case information appears muted (less variance) when extreme case descriptions were also presented. In fact, if participants were told that the average case was moderately severe (Table, bottom row), adding extreme case information (either severity level) did not increase worry or vaccination intentions, and the trend is negative.

Our data suggest that information about average cases and extreme cases did not have additive effects on participants' responses. We observed the strongest effects (positive and negative) of average case information when information about extreme cases was not provided. Providing average case information might inhibit consideration of just how serious the disease could be. Average case information also might have higher personal relevance to the public because extreme cases are more easily discounted. If so, public health communications about new threats should avoid presenting both types of information simultaneously.

Funding for this research was provided to A.F. from the European Union's Seventh Framework Programme for research, technological development, and demonstration under grant agreement #278763. The funding agreement ensured the authors' independence in designing the study, in the collection, analysis, and reporting of the data, and in the decision to submit the article for publication.

Dr. Zikmund-Fisher is associate professor of Health Behavior and Health Education at the University of Michigan School of Public Health. His research focuses on determinants of health risk perceptions and designing effective health risk communications.

References

1. Bults M, Beaujean DJMA, Richardus JH, Voeten HACM. Perceptions and behavioral responses of the general public during the 2009 influenza A (H1N1) pandemic: a systematic review. Disaster Med Public Health Prep. 2015;9:207–19. http://dx.doi.org/10.1017/dmp.2014.160
2. Peters E, Dieckmann N, Dixon A, Hibbard JH, Mertz CK. Less is more in presenting quality information to consumers. Med Care Res Rev. 2007;64:169–90. http://dx.doi.org/10.1177/1077558707064020301
3. Zikmund-Fisher BJ. The right tool is what they need, not what we have: a taxonomy of appropriate levels of precision in patient risk

communication. Med Care Res Rev. 2013;70(Suppl):37S–49S. http://dx.doi.org/10.1177/1077558712458541
4. Peters G-JY, Ruiter RAC, Kok G. Threatening communication: a critical re-analysis and a revised meta-analytic test of fear appeal theory. Health Psychol Rev. 2013;7(Suppl 1):S8–31. http://dx.doi.org/10.1080/17437199.2012.703527

Address for correspondence: Brian J. Zikmund-Fisher, Department of Health Behavior and Health Education, University of Michigan, 1415 Washington Heights, Ann Arbor, MI 48109-2029, USA; email: bzikmund@umich.edu

West Nile Virus Seroprevalence, Connecticut, USA, 2000–2014

Megan E. Cahill, Yi Yao, David Nock, Philip M. Armstrong, Theodore G. Andreadis, Maria A. Diuk-Wasser, Ruth R. Montgomery

Author Affiliations: Yale University School of Public Health, New Haven, Connecticut, USA (M.E. Cahill); Yale University School of Medicine, New Haven (Y. Yao, D. Nock, R.R. Montgomery); The Connecticut Agricultural Experiment Station, New Haven (P.M. Armstrong, T.G. Andreadis); Columbia University, New York, New York, USA (M.A. Diuk-Wasser)

DOI: http://dx.doi.org/10.3201/eid2304.161669

West Nile virus (WNV) infection is mainly asymptomatic but can be severe in elderly persons. As part of studies on immunity and aging in Connecticut, USA, we detected WNV seroconversion in 8.5% of nonimmunosuppressed and 16.8% of immunosuppressed persons. Age was not a significant seroconversion factor. Our findings suggest that immune factors affect seroconversion.

Since the 1999 emergence of West Nile virus (WNV) in North America, >43,000 cases of disease and 1,884 deaths have been reported (*1*); overall infections are estimated at ≈3 million (*2*). Although WNV infections can be asymptomatic, they can also cause severe neuroinvasive disease, especially among infants, immunocompromised persons, and elderly persons (*3*). Control of WNV infection involves innate immune pathways that mediate initial recognition and regulation of viral replication and adaptive immune responses that provide long-term protection (*3*). Spatial distribution analysis and mosquito surveillance studies have confirmed that WNV is endemic to Connecticut, USA (*1*,*4*).

We compared seroprevalence and demographics for 890 nonimmunosuppressed and 173 immunosuppressed adults enrolled in a study on immunity in aging (approved by the Human Investigations Committee of Yale University) (*5*) with those of symptomatic WNV case-patients reported to the Connecticut Department of Health (DPH) during 2000–2014. DPH-reported symptomatic case-patients (n = 116) sought medical attention and had a positive WNV laboratory test result (*1*). None of the asymptomatic participants were reported to DPH as WNV case-patients. Immunosuppressed participants followed an immunosuppressive medication regimen or had a diagnosis of rheumatoid arthritis (*5*). For all participants, we assessed previous exposure to WNV by immunoblot for WNV envelope protein (*6*). Seroconversion to WNV was distinguished from cross-reactivity to other flaviviruses by rescreening all positive serum against a recombinant WNV-specific mutant envelope protein that lacks the conserved cross-reactive fusion loop epitope (*7*).

We compared demographic characteristics of participant groups by using the Student *t*-test for continuous variables and χ^2 and Fisher exact tests for categorical variables; $p<0.05$ indicated statistical significance. Analysis was completed with SAS software version 9.3 (SAS Institute, Cary, NC, USA) and Prism 6 (GraphPad Software, Inc., La Jolla, CA, USA).

Immunoblot detected evidence of WNV exposure in 76 (8.5%) of the 890 nonimmunosuppressed participants (Table). These seropositive participants reported neither symptoms nor diagnosis of WNV infection and are considered to have had asymptomatic infections. Timing of asymptomatic infections could not be determined, but antibodies against WNV are durable and do not differ between asymptomatic and symptomatic adults (*8*).

Although age is a critical risk factor for severe WNV infection (*3*,*9*), the mean age of seropositive and seronegative nonimmunosuppressed participants did not differ significantly (Table). The rate of asymptomatic seroconversion did not vary significantly among the 890 persons in 3 age groups: <35 years (42/421), 35–65 years (7/121), and >65 years (27/348) ($p = 0.338$). Seroconversion rates did not differ significantly by patient sex but were significantly elevated among those in self-identified Hispanic groups ($p<0.0001$), possibly because of different exposure histories. The similar age distribution among asymptomatic seroconverters suggests that the observed age-associated susceptibility to clinically apparent disease may result from other factors, including individual host factors and dysregulation in immune responses (*6*,*10*).

Among 173 immunosuppressed adults, 29 (16.8%) showed evidence of exposure to WNV (Table), resulting in 2.16 times the odds of positive immunoblot result than for nonimmunosuppressed adults (76/890, 8.5%; $p = 0.002$).

Table. Seroconversion rates among participants in study of West Nile virus, Connecticut, USA, 2000–2014*

Participant	Asymptomatic				Symptomatic, DPH case-patients 2000–2014, n = 116
	Not immunosuppressed		Immunosuppressed		
	Seropositive, n = 76	Seronegative, n = 814	Seropositive, n = 29	Seronegative, n = 144	
Age, y, mean ± SEM	45.7 ± 2.7	48.6 ± 0.8	43.55 ± 2.5	48.48 ± 1.2	56.6 ± 1.7†
Female, %	52.6	61.1	82.8	76.4	44.0
Hispanic, %	7.9	4.1	55.2	16.7‡	Data not available
White, %	59.2	81.7§	75.9	75.0	Data not available

*DPH, Connecticut Department of Public Health.
†Mean age for DPH case-patients differed statistically from that for seropositive nonimmunosuppressed (p<0.001) and seropositive immunosuppressed (p<0.001) participants.
‡Difference in percentage of Hispanics within the seropositive and seronegative categories of the immunosuppressed population (p<0.0001).
§Difference in percentage of participants self-identifying as white within the seropositive and seronegative categories of the nonimmunosuppressed population (p<0.0001).

Seroconversion rates among immunosuppressed persons did not differ statistically according to sex or age. The seroconversion rate was higher among immunosuppressed Hispanics (16/40, 40.0%) than non-Hispanics (13/132, 9.8%) (p<0.0001). Because the immunosuppression status of DPH-reported case-patients was not available, we could not further explore a role for immunosuppression in the occurrence of WNV infection among these patients. Immunosuppression carries unique risks for infectious diseases; thus, the higher rate of seroconversion among immunosuppressed participants may be a consequence of underlying medical conditions or medication regimens.

The mean age for asymptomatic seropositive adults, nonimmunosuppressed and immunosuppressed, was lower than that for DPH-reported symptomatic case-patients (Table; p = 0.0004). The 2 groups did not vary significantly according to sex (p = 0.30). Because racial data for DPH-reported case-patients was not available, no comparison by race was possible. Comparison of geocoded household locations of all study participants and DPH case-patients showed an overlapping distribution of nonimmunosuppressed and immunosuppressed asymptomatic seroconverters and DPH case-patients (online Technical Appendix Figure, https://wwwnc.cdc.gov/EID/article/23/4/16-1669-Techapp1.pdf). Although only a surrogate for location where infection was acquired, this mapping provides no support for localized pockets of increased disease susceptibility.

We provide evidence of WNV exposure in Connecticut among 1,063 adults who differed by age, sex, race, and immunosuppression status. Among nonimmunosuppressed asymptomatic participants, age was not a significant factor with regard to WNV seroconversion. However, mean age of symptomatic case-patients was older than that of asymptomatic seropositive participants, indicating that age remains a factor in disease susceptibility (*9*). Age has a well-documented role in decreased immune cell function and increased susceptibility to infectious diseases, including WNV (*9*,*10*); dysregulation of immune responses with elevated cytokine levels may contribute to development of severe disease. The higher WNV seroprevalence among immunosuppressed adults strongly suggests a key role for immune factors in seroconversion.

Ongoing research seeks to further define the immune system attributes that lead to increased risk for higher WNV disease severity; active areas of interest include genomic, transcriptional, and immune- and age-related variable responses (*6*,*8*,*9*). In addition to environmental conditions that affect vector abundance, our study suggests that individual variation, such as immune status, may be a key driver for susceptibility to infection and disease severity and for differing seroconversion rates among neighbors.

Acknowledgments

We are grateful to Barbara Siconolfi, Sui Tsang, and Qiong Zhang for sample collection and helpful discussions. We thank Michael Diamond for his kind gift of recombinant WNV-specific mutant envelope protein.

This work was supported in part by awards from the National Institutes of Health (HHS N272201100019C and AI08992), the Centers for Disease Control and Prevention (U50/CCU116806-01-1), the US Department of Agriculture (58- 6615-1-218, CONH00768, and CONH00773), and the Multistate Research Project (NE1043).

All procedures contributing to this work comply with the ethical standards of the relevant national and institutional committees on human experimentation and with the Helsinki Declaration of 1975, as revised in 2008. Certain data used in this study were obtained from the Connecticut DPH, which approved this study.

Ms. Cahill is a candidate for a PhD degree in the epidemiology of microbial diseases at the Yale School of Public Health. She is interested in biology and viral disease susceptibility.

References

1. Centers for Disease Control and Prevention. West Nile virus, final cumulative maps & data for 1999–2014 [cited 2016 Apr 6]. http://www.cdc.gov/westnile/statsMaps/cumMapsData.html
2. Petersen LR, Carson PJ, Biggerstaff BJ, Custer B, Borchardt SM, Busch MP. Estimated cumulative incidence of West Nile virus infection in US adults, 1999–2010. Epidemiol Infect. 2013;141:591–5. http://dx.doi.org/10.1017/S0950268812001070

3. Suthar MS, Pulendran B. Systems analysis of West Nile virus infection. Curr Opin Virol. 2014;6:70–5. http://dx.doi.org/10.1016/j.coviro.2014.04.010
4. Diuk-Wasser MA, Brown HE, Andreadis TG, Fish D. Modeling the spatial distribution of mosquito vectors for West Nile virus in Connecticut, USA. Vector Borne Zoonotic Dis. 2006;6:283–95. http://dx.doi.org/10.1089/vbz.2006.6.283
5. Dunne DW, Shaw A, Bockenstedt LK, Allore HG, Chen S, Malawista SE, et al. Increased TLR4 expression and downstream cytokine production in immunosuppressed adults compared to non-immunosuppressed adults. PLoS One. 2010;5:e11343. http://dx.doi.org/10.1371/journal.pone.0011343
6. Qian F, Goel G, Meng H, Wang X, You F, Devine L, et al. Systems immunology reveals markers of susceptibility to West Nile virus infection. Clin Vaccine Immunol. 2015;22:6–16. http://dx.doi.org/10.1128/CVI.00508-14
7. Chabierski S, Barzon L, Papa A, Niedrig M, Bramson JL, Richner JM, et al. Distinguishing West Nile virus infection using a recombinant envelope protein with mutations in the conserved fusion-loop. BMC Infect Dis. 2014;14:246. http://dx.doi.org/10.1186/1471-2334-14-246
8. Qian F, Thakar J, Yuan X, Nolan M, Murray KO, Lee WT, et al. Immune markers associated with host susceptibility to infection with West Nile virus. Viral Immunol. 2014;27:39–47. http://dx.doi.org/10.1089/vim.2013.0074
9. Montgomery RR. Age-related alterations in immune responses to West Nile virus infection. Clin Exp Immunol. 2017;187:26–34.
10. Shaw AC, Goldstein DR, Montgomery RR. Age-dependent dysregulation of innate immunity. Nat Rev Immunol. 2013;13:875–87. http://dx.doi.org/10.1038/nri3547

Address for correspondence: Ruth R. Montgomery, Department of Internal Medicine, Yale University School of Medicine, 300 Cedar St/TAC S413, New Haven, CT 06520-8031, USA; email: ruth.montgomery@yale.edu

mcr-1 in *Enterobacteriaceae* from Companion Animals, Beijing, China, 2012–2016

Lei Lei,[1] Yang Wang,[1] Stefan Schwarz, Timothy R. Walsh, Yanran Ou, Yifan Wu, Mei Li, Zhangqi Shen

Author affiliations: China Agricultural University, Beijing, China (L. Lei, Y. Wang, Y. Ou, Y. Wu, M. Li, Z. Shen); Freie Universität Berlin, Berlin, Germany (S. Schwarz); Cardiff University, Cardiff, Wales, UK (T.R. Walsh, M. Li); Iowa State University, Ames, Iowa, USA (Z. Shen)

DOI: http://dx.doi.org/10.3201/eid2304.161732

[1]These authors contributed equally to this article.

To investigate the prevalence of the recently emerging colistin resistance gene *mcr-1* in *Enterobacteriaceae* among companion animals, we examined 566 isolates collected from cats and dogs in Beijing, China, during 2012–2016. Of these isolates, 49 (8.7%) were *mcr-1*–positive.

Multidrug-resistant and extensively drug-resistant gram-negative bacteria are a major threat to public health worldwide (*1*,*2*). The recent rapid dissemination of carbapenem-resistant *Enterobacteriaceae* has worsened this situation and further narrowed treatment options for infections caused by these bacteria (*3*). Colistin is a last-resort drug for treating carbapenem-resistant *Enterobacteriaceae* infections (*4*). In 2016, we identified the mobile colistin resistance gene *mcr-1* (*1*). Soon after its description, *mcr-1* was observed in *Enterobacteriaceae* from humans and food-producing animals in >30 countries on 5 continents (*5*).

A 2016 article reported that a 50-year-old man who worked in a pet store tested positive for *mcr-1*–harboring *E. coli* (*6*). Investigation identified 6 multidrug-resistant *mcr-1*–producing *E. coli* isolates in samples from 4 dogs and 2 cats in the pet store, indicating that the pathogens can be transmitted between humans and companion animals. So far, the prevalence of *mcr-1*-containing *Enterobacteriaceae* in companion animals is largely unknown. In our study, we focused on estimating the prevalence of *mcr-1* in *Enterobacteriaceae* of companion animal origin in Beijing, China, during 2012–2016, and investigated the presence of the *mcr-1* gene in pet foods purchased there.

In Beijing, the total number of registered dogs and cats is ≈1.2 million. We collected samples from both healthy and sick dogs and cats in Veterinary Teaching Hospital of China Agricultural University.

A total of 566 nonduplicate *Enterobacteriaceae* strains were isolated from 1,439 nasal and rectal swab samples collected from 1,254 dogs and 185 cats during 2012–2016. We also isolated 25 *Enterobacteriaceae* from 32 nasal swab samples from the pet owners. Because the food chain is among the main routes for humans and companion animals to acquire foodborne pathogens, we collected a small sample of pet foods (dog food, n = 30; cat food, n = 5) containing chicken as the main ingredient in Beijing during June–August 2016.

The species of all *Enterobacteriaceae* were determined by 16S rDNA sequencing and matrix-assisted laser desorption/ionization time-of-flight mass spectrometry of specimens cultured on brain–heart infusion agar plates containing 2 μg/mL colistin. A total of 79/566 (14.0%) of the *Enterobacteriaceae* isolates from companion animals were resistant to colistin: 56 *E. coli*, 16 *Klebsiella pneumoniae*, 5 *Enterobacter cloacae*, 1 *Enterobacter aerogenes*, and 1 *Shigella* spp. PCR amplification of *mcr-1* indicated that 8.7% (49/566) of *Enterobacteriaceae* and 62.0% (49/79)

of colistin-resistant isolates harbored the *mcr-1* gene, 47 *E. coli* and 2 *K. pneumoniae*. Only 1 *E. coli* isolate from a pet owner was colistin-resistant and *mcr-1*–positive. The proportions of *mcr-1*–containing *E. coli* per year ranged from 6.1% to 14.3% (Figure).

We examined the susceptibility of colistin-resistant *E. coli* to 8 other antimicrobial agents by agar dilution, according to the recommendations of Clinical and Laboratory Standards Institute (*7*). The *mcr-1*–carrying *E. coli* exhibited high resistance rates to ampicillin (97.9%), cefotaxime (91.5%), chloramphenicol (89.4%), and gentamicin (85.1%) (online Technical Appendix Table 1, http://wwwnc.cdc.gov/EID/article/23/4/16-1732-Techapp1.pdf) but were susceptible to imipenem. The *mcr-1*–positive *E. coli* were more often resistant to amoxicillin/clavulanate, ampicillin, and chloramphenicol than were the *mcr-1*–negative *E. coli* ($p<0.05$) (online Technical Appendix Table 1).

All 57 colistin-resistant *E. coli* were subjected to XbaI pulsed-field gel electrophoresis (PFGE). The 55 colistin-resistant *E. coli* strains (2 nontypeable strains were excluded) were subdivided into 33 patterns and grouped into 31 clusters (A–Z, AB–AF) (online Technical Appendix Figure). The diversity and similarity of PFGE patterns of *E. coli* from different origins suggested that the dissemination of *mcr-1* was possibly related to both clonal expansion and horizontal transmission.

Of note, the 1 *E. coli* colistin-resistant, *mcr-1*–positive isolate from a pet owner had the same PFGE pattern as 5 isolates from dogs and cats. Multilocus sequence typing linked these 6 strains to sequence type 101. These results suggest that *E. coli* strains can be exchanged between companion animals and humans.

The PCR and sequence analysis of the pet food samples showed that 7 of 35 samples were positive for *mcr-1*. Companies in China produced 5 of these foods; the other 2 were from Italy and Belgium (online Technical Appendix Table 2). These results suggest that pet foods may be a source from which intestinal bacteria of companion animals can acquire the *mcr-1* gene.

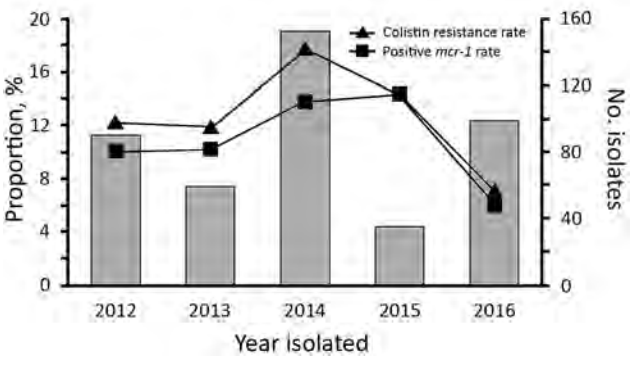

Figure. Proportion of colistin resistance and *mcr-1* in *Escherichia coli* of companion animal origin, Beijing, China, 2012–2016.

Currently, colistin is not used to treat companion animals in China. The companion animals included in this study were from an urban area of Beijing, so they had minimal or no contact with food-producing animals in which colistin may have been used. Because we found *mcr-1* in pet foods, we speculate that the pet food industry may be a source of *mcr-1* among companion animals. Because of frequent and close contact between humans and companion animals, our study proposes that opportunities exist to transmit colistin-resistant *Enterobacteriaceae* to and from both groups. Thus, colistin-resistant *Enterobacteriaceae* from companion animals may represent a potential risk to human health. Further surveillance and control efforts are needed to reduce colistin-resistant and *mcr-1*–containing *Enterobacteriaceae* in companion animals and food-producing animals.

This work was supported in part by National Natural Science Foundation of China (nos. 31672604, 31422055 and 81661138002). T.R. Walsh was also supported by MRC grant DETER-XDR-CHINA (MR/P007295/1).

Ms. Lei is a PhD student in the College of Veterinary Medicine, China Agricultural University. Her main interest is the prevalence of antibiotic resistance in enteric bacteria.

References

1. Liu YY, Wang Y, Walsh TR, Yi LX, Zhang R, Spencer J, et al. Emergence of plasmid-mediated colistin resistance mechanism MCR-1 in animals and human beings in China: a microbiological and molecular biological study. Lancet Infect Dis. 2016;16:161–8. http://dx.doi.org/10.1016/S1473-3099(15)00424-7
2. van der Bij AK, Pitout JD. The role of international travel in the worldwide spread of multiresistant Enterobacteriaceae. J Antimicrob Chemother. 2012;67:2090–100. http://dx.doi.org/10.1093/jac/dks214
3. Temkin E, Adler A, Lerner A, Carmeli Y. Carbapenem-resistant Enterobacteriaceae: biology, epidemiology, and management. Ann N Y Acad Sci. 2014;1323:22–42. http://dx.doi.org/10.1111/nyas.12537
4. Michalopoulos AS, Tsiodras S, Rellos K, Mentzelopoulos S, Falagas ME. Colistin treatment in patients with ICU-acquired infections caused by multiresistant Gram-negative bacteria: the renaissance of an old antibiotic. Clin Microbiol Infect. 2005;11: 115–21. http://dx.doi.org/10.1111/j.1469-0691.2004.01043.x
5. Schwarz S, Johnson AP. Transferable resistance to colistin: a new but old threat. J Antimicrob Chemother. 2016;71:2066–70. http://dx.doi.org/10.1093/jac/dkw274
6. Zhang XF, Doi Y, Huang X, Li HY, Zhong LL, Zeng KJ, et al. Possible transmission of *mcr-1*-harboring *Escherichia coli* between companion animals and human. Emerg Infect Dis. 2016;22: 1679–81. http://dx.doi.org/10.3201/eid2209.160464
7. Clinical and Laboratory Standards Institute. Performance standards for antimicrobial disk and dilution susceptibility tests for bacteria isolated from animals; 3rd ed (VET01S). Wayne (PA): The Institute; 2005.

Address for correspondence: Zhangqi Shen, Beijing Advanced Innovation Center for Food Nutrition and Human Health, College of Veterinary Medicine, 2 Yuanmingyuan West Rd, Beijing 100193, China; email: szq@cau.edu.cn

Bartonella-Associated Transverse Myelitis

Parham Sendi, Cedric Hirzel, Andreas Bloch, Urs Fischer, Natalie Jeannet, Livia Berlinger, Heinz Krestel

Author affiliations: Bern University Hospital, Bern, Switzerland; University of Bern, Bern; Bioanalytica AG, Luzern, Switzerland

DOI: http://dx.doi.org/10.3201/eid2304.161733

Each year in the United States, 500 patients are hospitalized for cat-scratch disease, caused by *Bartonella henselae* infection. We report a case of rare but serious neurologic *B. henselae* infection. When typical features of cat-scratch disease occur with neurologic findings, *Bartonella* infection should be suspected and diagnostic testing should be performed.

In a recent epidemiologic study, Nelson et al. (*1*) estimated that each year in the United States, 500 patients are hospitalized for cat-scratch disease (CSD), caused by *Bartonella henselae* infection. Typical disease presentation includes enlarged lymph nodes proximal to the site of organism inoculation. *B. henselae* can disseminate and infect various organs, including the central nervous system (CNS). For patients with neurologic involvement, laboratory diagnosis can be challenging.

In 2015, a previously healthy 46-year-old woman was referred to Bern University Hospital, Bern, Switzerland, for suspected acute ischemic stroke; she was experiencing dysarthria, aphasia, dysphagia, paresthesia, and weakness in both legs. She reported no travel history or recent vaccination but reported having had contact with her neighbor's cat.

Physical examination revealed blood pressure 130/80 mm Hg and heart rate 100 beats/min. Also noted were flaccid paralysis of the lower extremities (manual muscle testing score 4, dorsal and plantar flexion of the foot; manual muscle testing score 2, flexion and extension of the thighs), dysarthria, peripheral facial paralysis, and gaze-evoked nystagmus. Serum leukocyte count was 7.2×10^9 cells/L (without a left shift of neutrophils), and serum C-reactive protein level was 8 mg/L (reference <5 mg/L). Magnetic resonance images of the brain showed no abnormalities, but those of the spinal cord showed longitudinal lesions consistent with transverse myelitis (Figure). Analyses of cerebrospinal fluid (CSF) revealed a cell count of 167/μL (98% mononuclear cells) and elevated levels of protein (1.1 g/L) and lactate (2.4 mmol/L). The CSF/serum ratio of albumin indicated a blood–CSF barrier dysfunction. Thus, a diagnosis of meningoencephalitis and acute transverse myelitis was made.

Initial treatment consisted of corticosteroids and empirically prescribed antiinfective therapy with acyclovir, amoxicillin, and ceftriaxone. After 5 days of incubation,

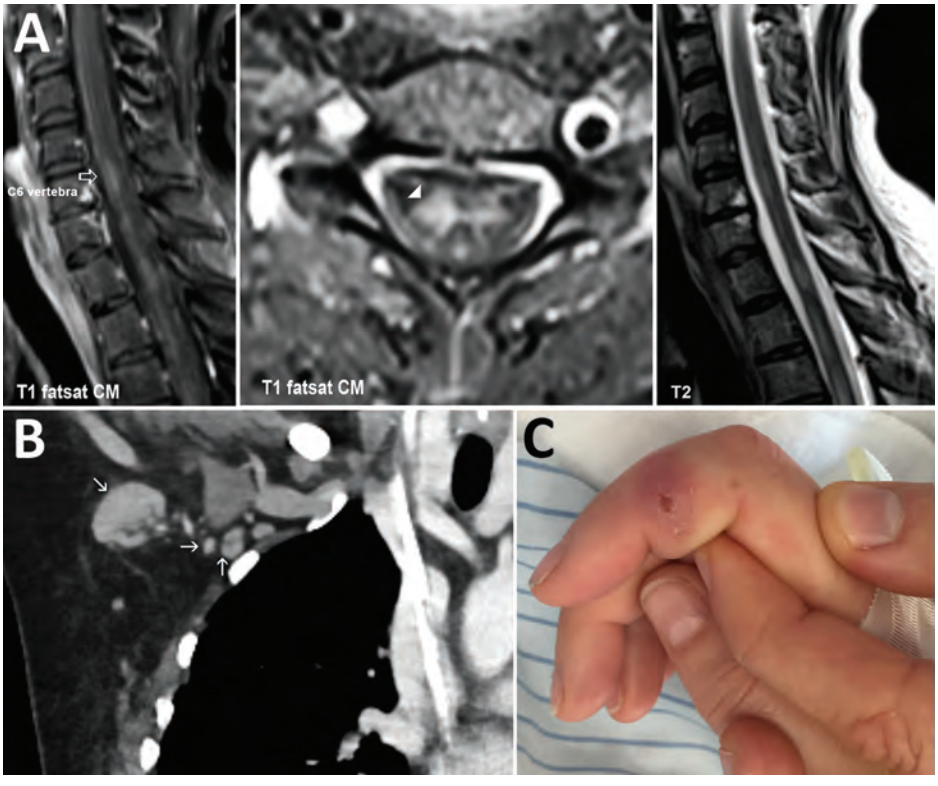

Figure. Images of woman with transverse myelitis and *Bartonella henselea* infection. A) Magnetic resonance image of the spine showing transverse myelitis (arrowhead). Fat-saturated (fs) T1-weighted image with contrast medium (cm), sagittal plane (left panel) and axial plane (middle panel). T2-weighted image, sagittal plane (right panel). B) Coronal view of computed tomography image of the chest, showing right axillar lymphadenopathy (arrows). C) Right index finger, showing a persistent ulcer from a cat scratch.

CSF samples showed no microorganism growth; however, specific culture techniques for *Bartonella* spp. were not used because lumbar puncture had been performed before CSD was suspected. PCR results were negative for herpes simplex virus 1/2, varicella zoster virus, cytomegalovirus, Epstein-Barr virus, and enterovirus. Serologic test results were negative for *Borrelia burgdorferi, Treponema pallidum, Mycoplasma pneumoniae*, tickborne encephalitis virus, *Toxoplasma gondii*, and HIV, as were results for *Cryptococcus neoformans* serum antigen testing. Results of a multiplex PCR for respiratory viruses and *M. pneumoniae* in a nasopharyngeal swab sample were negative. Therefore, empirical treatment with antiviral and antibiotic agents was stopped. Because no infectious etiology was found, the differential diagnosis included vasculitis and neoplastic and paraneoplastic disorders. The clinical findings and high CSF cell count argued against multiple sclerosis. Test results were negative for autoantibodies (antinuclear antibodies; c and p antineutrophil cytoplasmic antibodies; double-stranded DNA antibodies; and antiphospholipid, onconeural, and neuromyelitis optica [antiaquaporin 4] autoantibodies).

Computed tomography of the chest and abdomen showed no evidence of neoplasia but did show enlarged right-sided axillary lymph nodes (Figure). This result, together with a visible scratch on the patient's right index finger (Figure) and a history of contact with the neighbor's cat, was highly suggestive of CSD. The PCR result for *B. henselae* (online Technical Appendix, https://wwwnc.cdc.gov/EID/article/23/4/16-1733-Techapp1.pdf) in a biopsy sample from the right index finger was positive, as was the result of an indirect immunofluorescence assay for *B. henselae* IgG (titer 1:512). After being asked, the patient reported having been scratched by the cat 6 weeks earlier and having felt enlarged axillary lymph nodes 4 weeks before admission. The PCR result for *B. henselae* in CSF was negative. Intrathecal antibody production was not elevated, and the specific CSF/serum ratio for IgG against *Bartonella* was negative, although the laboratory method for the latter is not standardized. CSD-associated transverse myelitis was postulated. Doxycycline was given for 3 weeks and continued with tapering doses of corticosteroids. The patient improved, but at follow-up examination 6 months after discharge, she reported residual neurologic symptoms, including fatigue, chronic headache, radicular neuropathic pain, and slight gait unsteadiness. *B. henselae* IgG titer was 1:64.

For this patient, the classic features of CSD were present, and laboratory diagnosis of CSD was made by 2 methods. Nonetheless, we detected neither *Bartonella* antigens in CSF via PCR nor significant intrathecal production of antibodies against *Bartonella*. Thus, we cannot rule out coincidental CSD and idiopathic inflammatory myelitis. However, in the latter disease, the CSF cell count is typically markedly lower and the myelitis less extensive than was observed for this patient. Moreover, the consistent time course of the disease, lack of an alternative diagnosis, and similarity to other clinical courses suggest CSD-associated transverse myelitis (*2*). In previously published cases of patients with CNS manifestations and CSD, laboratory diagnosis was not made from CSF samples (*2*–*6*). Therefore, it is uncertain whether the pathogenesis of myelitis is the result of direct invasion of the spinal cord by *B. henselae* or an immune-mediated postinfectious process (*2*).

Our report and others (*2*–*6*) demonstrate that diagnosis of *B. henselae* CNS disease is currently based on neurologic symptoms and findings after a cat scratch, not on laboratory diagnosis of CSF or CNS biopsy samples. Nonetheless, for suspected cases of CSD, laboratory studies from serum or skin lesion samples should be used for confirmation.

Acknowledgment

We are indebted to Martin Altwegg for his contribution to the development of *Bartonella* PCR assays.

Dr. Sendi is an attending physician and lecturer in infectious diseases at Bern University Hospital and the University of Bern, Switzerland. His research interests are group B *Streptococcus* in nonpregnant adults, infections of the locomotor apparatus, and infectious diseases in neurology.

References

1. Nelson CA, Saha S, Mead PS. Cat-scratch disease in the United States, 2005–2013. Emerg Infect Dis. 2016;22:1741–6. http://dx.doi.org/10.3201/eid2210.160115
2. Baylor P, Garoufi A, Karpathios T, Lutz J, Mogelof J, Moseley D. Transverse myelitis in 2 patients with *Bartonella henselae* infection (cat scratch disease). Clin Infect Dis. 2007;45:e42–5. http://dx.doi.org/10.1086/519998
3. Marra CM. Neurologic complications of *Bartonella henselae* infection. Curr Opin Neurol. 1995;8:164–9. http://dx.doi.org/10.1097/00019052-199506000-00002
4. Carman KB, Yimenicioglu S, Ekici A, Yakut A, Dinleyici EC. Co-existence of acute transverse myelitis and Guillain-Barré syndrome associated with *Bartonella henselae* infection. Paediatr Int Child Health. 2013;33:190–2. http://dx.doi.org/10.1179/2046905512Y.0000000044
5. Massei F, Gori L, Taddeucci G, Macchia P, Maggiore G. *Bartonella henselae* infection associated with Guillain-Barré syndrome. Pediatr Infect Dis J. 2006;25:90–1. http://dx.doi.org/10.1097/01.inf.0000195642.28901.98
6. Vermeulen MJ, Rutten GJ, Verhagen I, Peeters MF, van Dijken PJ. Transient paresis associated with cat-scratch disease: case report and literature review of vertebral osteomyelitis caused by *Bartonella henselae*. Pediatr Infect Dis J. 2006;25:1177–81. http://dx.doi.org/10.1097/01.inf.0000246807.14916.d3

Address for correspondence: Parham Sendi, Department of Infectious Diseases, Bern University Hospital and Institute for Infectious Diseases, University of Bern, Switzerland; email: parham.sendi@ifik.unibe.ch

Ebola Virus RNA in Semen from an HIV-Positive Survivor of Ebola

Lawrence J. Purpura,[1] Emerson Rogers,[1] April Baller, Stephen White, Moses Soka, Mary J. Choi, Nuha Mahmoud, Christine Wasunna, Moses Massaquoi, Jomah Kollie, Straker Dweh, Philip Bemah, Victor Ladele, Jonathan Kpaka, Mary Jawara, Margaret Mugisha, Onyekachi Subah, Mylene Faikai, Jeff A. Bailey, Pierre Rollin, Barbara Marston, Tolbert Nyenswah, Alex Gasasira, Barbara Knust, Stuart Nichol, Desmond Williams

Author affiliations: Centers for Disease Control and Prevention, Atlanta, Georgia, USA (L.J. Purpura, M.J. Choi, P. Rollin, B. Marston, B. Knust, S. Nichol, D. Williams); Ministry of Health, Monrovia, Liberia (E. Rogers, M. Soka, M. Massaquoi, P. Bemah, T. Nyenswah); World Health Organization, Monrovia (A. Baller, N. Mahmoud, J. Kollie, V. Ladele, M. Mugisha, A. Gasasira); Academic Consortium Combating Ebola in Liberia, Monrovia (S. White, C. Wasunna, S. Dweh, J. Kapka, O. Subah, J.A. Bailey); Men's Health Screening Program, Monrovia (M. Jawara, M. Faikai)

DOI: http://dx.doi.org/10.3201/eid2304.161743

Ebola virus is known to persist in semen of male survivors of Ebola virus disease (EVD). However, maximum duration of, or risk factors for, virus persistence are unknown. We report an EVD survivor with preexisting HIV infection, whose semen was positive for Ebola virus RNA 565 days after recovery from EVD.

In March 2015 in Liberia, unprotected sexual intercourse was strongly suspected in the transmission of Ebola virus disease (EVD) from a male survivor of EVD to his female partner (*1*). Results of Ebola RNA sequence analysis for a semen sample from the survivor 199 days after onset of illness and blood samples from the female patient were consistent with direct transmission.

In July 2015, the Liberian Ministry of Health established the Men's Health Screening Program to offer semen testing for Ebola virus and behavioral counseling on safe sexual practices to male survivors of EVD to the Ebola response (*2*). We report a survivor of EVD who had a preexisting HIV infection whose semen was positive for Ebola virus RNA 565 days after recovering from this disease.

[1]These authors contributed equally to this article.

On August 27, 2014, a 48-year-old man with a history of HIV infection who was receiving antiretroviral therapy was admitted to an Ebola treatment unit (ETU) in Monrovia, Liberia, with a 1-week history of fever, chills, and weakness and a 2-day history of vomiting and diarrhea. The next day, he had a positive result for Ebola virus in blood by real-time reverse transcription PCR (RT-PCR), with a cycle threshold (C_t) of 32.39. While in the ETU, he continued his antiretroviral therapy. The patient was discharged on September 8, 2014, after showing a negative result for Ebola virus in blood by RT-PCR.

When the patient was first given a diagnosis of infection with HIV-1 in October 2009 (CD4 cell count 46/μL) (Figure), he was given ART with zidovudine/lamivudine/nevirapine and trimethoprim/sulfamethoxazole for prophylaxis against opportunistic infections. On March 25, 2010, he was given a diagnosis of co-infection with HIV-1 and HIV-2, and his ART regimen was changed to zidovudine/lamivudine/lopinavir plus ritonavir because HIV-2 strains are typically resistant to non-nucleoside reverse transcription inhibitors, such as nevirapine. His CD4 cell count 4 months before admission to the ETU was 459/μL on April 24, 2014. His only measured CD4 cell count after recovery

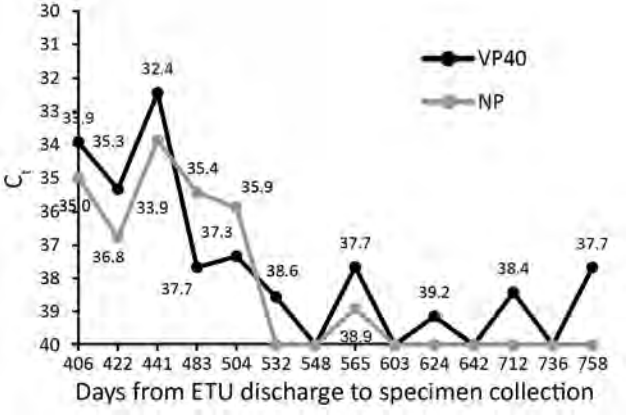

Figure. Ebola virus RNA detected by RT-PCR in semen samples from an HIV-positive survivor (48-year-old man) of Ebola virus disease, Monrovia, Liberia, 2009–2016. RT-PCR cycle threshold (C_t) values for Ebola virus VP40 and NP gene targets are reported by days from the patient's discharge from the ETU to collection of a semen specimen. A gene target is considered detected if the C_t is <40. If gene amplification is not demonstrated within 40 cycles, then the gene target is considered undetectable and no C_t is reported. All undetectable results are indicated as C_t values of 40. CD4 cell counts per microliter were 46 on October 20, 2009; 48 on November 12, 2009; 358 on March 25, 2010; 358 on April 22, 2010; 563 on November 22, 2010; 824 on January 22, 2013; 459 on April 24, 2014; and 529 on August 9, 2016. The patient had a CD4 cell count of 529/μL 699 days after discharge from the Ebola treatment unit. On November 12, 2009, the patient was given an ART regimen of zidovudine/lamivudine/nevirapine. On April 22, 2010, the ART regimen changed to zidovudine/lamivudine/lopinavir plus ritonavir. ART, antiretroviral therapy; C_t, cycle threshold; ETU, Ebola treatment unit; NP, nucleoprotein, RT-PCR, reverse transcription PCR; VP40; viral structural protein 40.

from EVD was 529/μL on August 9, 2016. He reported compliance with his ART regimen and denied any serious illness since the time of his HIV diagnosis.

The patient enrolled in the Men's Health Screening Program on October 21, 2015. Per program protocol, his semen was tested every 4 weeks for Ebola virus by RT-PCR using described methods (*2*). Specimens are considered positive if viral structural protein 40 gene and nucleoprotein gene targets of Ebola virus have C_t values <40, and indeterminate if only 1 gene target has a C_t <40. Since his enrollment in the program, the semen of the patient has been positive for Ebola virus RNA up to 565 days after he was discharged from the ETU. C_t values plateaued to indeterminate for samples up to 758 days after discharge (Figure). Although detection of Ebola virus RNA by RT-PCR does not necessarily indicate the presence of infectious virus, a previous study reported Ebola virus infectivity by RT-PCR–positive human semen samples in immunodeficient mice (*3*).

The prolonged period during which Ebola virus RNA was detected in this patient adds to evidence (*2*–*4*) that there is heterogeneity in duration of Ebola virus persistence in semen among survivors of EVD. Although etiology of this heterogeneity is unclear, possible explanations for this patient include age-associated effects (*2*), attenuated clearance caused by dual HIV infection, immunosuppression from etiologies other than HIV, severity of acute illness, or unknown host genetic factors. Although the patient had an adequate CD4 cell count, chronic inflammation, immune system dysregulation, and accelerated immunoscenescence in well-controlled HIV patients have been described and are clinically manifested as early cardiovascular disease, neurocognitive disorders, metabolic syndrome, and non–AIDS-associated cancers (*5*). Therefore, co-infection with HIV might play a role in persistence of Ebola virus in semen, despite an adequate clinical response to ART.

Because HIV infection is treatable and testing is readily available in West Africa, semen testing programs for Ebola virus should consider offering HIV testing to male survivors of EVD with persistently detectable Ebola virus in semen. Furthermore, HIV care was interrupted during the Ebola outbreak in West Africa because of closure of clinics and interruption of ART distribution (*6*). This case- patient had a favorable outcome for EVD despite being HIV positive, which emphasizes the need for continuing treatment for HIV infection in the setting of a large-scale Ebola outbreak. In addition, this case highlights the need for a better understanding of the role that co-infection with HIV might play in persistent detection of Ebola virus RNA in male survivors of EVD.

Dr. Purpura is an Epidemic Intelligence Service Officer in the National Center for Emerging and Zoonotic Infectious Diseases, Centers for Disease Control and Prevention, Atlanta, GA. His research interests include filoviruses and other viruses that cause hemorrhagic fevers.

References

1. Mate SE, Kugelman JR, Nyenswah TG, Ladner JT, Wiley MR, Cordier-Lassalle T, et al. Molecular evidence of sexual transmission of Ebola virus. N Engl J Med. 2015;373:2448–54. http://dx.doi.org/10.1056/NEJMoa1509773
2. Soka MJ, Choi MJ, Baller A, White S, Rogers E, Purpura LJ, et al. Prevention of sexual transmission of Ebola in Liberia through a national semen testing and counselling programme for survivors: an analysis of Ebola virus RNA results and behavioural data. Lancet Glob Health. 2016;4:e736–43. http://dx.doi.org/10.1016/S2214-109X(16)30175-9
3. Sissoko D, Duraffour S, Kerber R, Kolie JS, Beavogui AH, Camara AM, et al. Persistence and clearance of Ebola virus RNA from seminal fluid of Ebola virus disease survivors: a longitudinal analysis and modelling study. Lancet Glob Health. 2017;5:e80–8. http://dx.doi.org/10.1016/S2214-109X(16)30243-1
4. Diallo B, Sissoko D, Loman NJ, Bah HA, Bah H, Worrell MC, et al. Resurgence of Ebola virus disease in Guinea linked to a survivor with virus persistence in seminal fluid for more than 500 days. Clin Infect Dis. 2016;63:1353–6. http://dx.doi.org/10.1093/cid/ciw601
5. Deeks SG. HIV infection, inflammation, immunosenescence, and aging. Annu Rev Med. 2011;62:141–55. http://dx.doi.org/10.1146/annurev-med-042909-093756
6. Hira S, Piot P. The counter effects of the Ebola epidemic on control and treatment of HIV/AIDS, tuberculosis, and malaria in West Africa. AIDS. 2016;30:2555–9. http://dx.doi.org/10.1097/QAD.0000000000001231

Address for correspondence: Lawrence J. Purpura, Centers for Disease Control and Prevention, 1600 Clifton Rd NE, Mailstop A30, Atlanta, GA 30329-4027, USA; email: yxp0@cdc.gov

Treatment Failure of Dihydroartemisinin/Piperaquine for *Plasmodium falciparum* Malaria, Vietnam

Bui Quang Phuc, Charlotte Rasmussen, Tran Thanh Duong, Le Than Dong, Mai Anh Loi, Didier Ménard, Joel Tarning, Dorina Bustos, Pascal Ringwald, Gawrie Loku Galappaththy, Nguyen Quang Thieu

Author affiliations: National Institute of Malariology, Parasitology, and Entomology, Hanoi, Vietnam (B.Q. Phuc, T.T. Duong, M.A. Loi, N.Q. Thieu); World Health Organization, Geneva, Switzerland (C. Rasmussen, D. Bustos, P. Ringwald, G.L. Galappaththy); Institute of Malariology, Parasitology, and Entomology, Ho Chi Minh, Vietnam (L.T. Dong); Institut Pasteur, Phnom Penh, Cambodia (D. Ménard); Mahidol University, Bangkok, Thailand (J. Tarning)

DOI: http://dx.doi.org/10.3201/eid2304.161872

We conducted a study in Binh Phuoc, Vietnam, in 2015 on the therapeutic efficacy of dihydroartemisinin/piperaquine for *Plasmodium falciparum* malaria. A high number of treatment failures (14/40) was found, and piperaquine resistance in Vietnam was confirmed. A change in the malaria treatment policy for Vietnam is in process.

The high failure rate of artemisinin-based combination therapy in the treatment of uncomplicated *Plasmodium falciparum* malaria has been a growing concern in the Greater Mekong Subregion of Southeast Asia. High numbers of treatment failures were reported for dihydroartemisinin/piperaquine in Cambodia (*1*), but efficacy of this drug has remained high in Vietnam since its introduction in 2003. We investigated dihydroartemisinin/piperaquine efficacy in the treatment of uncomplicated *P. falciparum* malaria in Binh Phuoc Province, Vietnam, during August–December 2015. We looked for molecular markers of drug resistance and determined piperaquine blood levels in treated patients to assess if piperaquine resistance was present in Vietnam. This study was approved by the ethics boards of the Ministry of Health in Vietnam and the Western Pacific Regional Office of the World Health Organization.

The National Institute of Malariology, Parasitology, and Entomology conducted this study as part of routine surveillance on drug efficacy following the 2009 World Health Organization protocol (*2*). After obtaining written consent, patients (age of inclusion, 2–60 years) were enrolled and given dihydroartemisinin/piperaquine (Pharbaco, Hanoi, Vietnam) at a target dosage of 2.4 mg/kg for dihydroartemisinin and 18 mg/kg for piperaquine once a day for 3 days. Patients with treatment failures were subsequently given quinine hydrochlorate (30 mg/kg/d) and doxycycline (3 mg/kg/d) for 7 days. Primary endpoint was adequate clinical and parasitologic response (ACPR) on day 42; PCR genotyping, comparing day 0 and day of failure samples, was used to distinguish recrudescence from reinfection with another strain (*2*). Dried blood spots were collected on day 0 and analyzed for mutations in the *K13* propeller domain (*3*), *Pfmdr1* copy number (*4*), and *Pfplasmepsin2* (*PfPM2*) copy number (*5*), which are markers associated with artemisinin, mefloquine, and piperaquine resistance, respectively. By using a previously established relationship between capillary whole blood and venous plasma, piperaquine plasma concentrations were calculated from blood spots collected day 7 (*6*). Sequencing was done by the Institut Pasteur in Cambodia, and the piperaquine blood levels were assessed by the Mahidol Oxford Tropical Medicine Research Unit in Thailand.

Forty-six patients with uncomplicated *P. falciparum* malaria were enrolled; 44 were followed until day 42, and 2 were lost to follow-up after day 14. Mean age of enrolled patients was 26.9 (range 14–53) years, and 93% (43/46) were male. Geometric mean parasitemia on day 0 was 17,759 (range 1,514–97,454)/μL.

On day 3, half (23/46) of patients were parasitemic. On day 42, a total of 65% (26/40, 95% CI 48.3%–79.4%) had an ACPR, and 35% (14/40) had recrudescence; 4 were withdrawn because they became reinfected.

Artemisinin resistance is defined as delayed parasite clearance and is associated with mutations in the *K13* propeller domain, the most prevalent being the C580Y mutation in the eastern Greater Mekong Subregion (*7*). *K13* analysis of 42 samples (4 were excluded because of uninterpretable results) from our study showed that 90.5% (38/42) were C580Y and 9.5% (4/42) were wild-type. This C580Y prevalence is higher than that reported in a previous study done in Binh Phuoc in 2014, in which 34.5% of samples had the C580Y mutation (B.Q. Phuc, unpub. data).

Analysis of *PfPM2* showed that 25/46 (54.3%) samples had multiple copies of the gene. Of the 42 samples with known *K13* types, 22 (52.4%) had both C580Y and *PfPM2* amplifications. The remaining 3 had unknown *K13* types. All 46 samples had a single copy of *Pfmdr1*, indicating that all parasites were sensitive to mefloquine (*4*).

The average day 7 piperaquine plasma concentration (n = 42) was 35.7 (range 11.1–71.0) ng/mL. In 57.1% (24/42) of patients, this concentration was at or above the cutoff value (30 ng/mL) associated with adequate piperaquine exposure (*1*). For patients with ACPRs, the average concentration was 36.9 (range 17.2–71.0) ng/mL, and 57.7% (15/26) were adequately exposed. For patients that had recrudescence, the average concentration was 39.5 (range 12.4–65.7) ng/mL, and 72.7% (8/11) were adequately exposed.

Of the 14 patients who experienced recrudescence, 10 had parasites with the C580Y mutation and *PfPM2* amplifications, 3 had parasites with the C580Y mutation only, and 1 had parasites with an unknown *K13* type and *PfPM2* amplifications. *K13* mutations (found during routine surveillance conducted over the last 5 years in Vietnam) alone did not lead to dihydroartemisinin/piperaquine failures. The association between the presence of molecular markers and recrudescence is confounded by various factors, including parasite load, immunity, and drug levels. Of the 3 patients who had recrudescence and were infected with *P. falciparum* without *PfPM2* amplifications, 2 had inadequate piperaquine levels. Of the 11 patients who had recrudescence and an infection with *P. falciparum* with *PfPM2* amplifications, 7 had adequate piperaquine levels. Low piperaquine blood levels, irrespective of the presence of *PfPM2* amplifications, might play a role in some treatment failures. Treatment failures in cases with *PfPM2* amplification–positive parasites and adequate piperaquine exposure support the presence of piperaquine resistance in Vietnam.

Our results show that 1 *K13* mutation has become dominant and that piperaquine resistance is present in Vietnam. A change in the malaria treatment policy to treat with artesunate/mefloquine in Binh Phuoc Province is underway.

Acknowledgments

The authors would like to express their appreciation to all of the study patients.

This study was supported by the Bill and Melinda Gates Foundation and the US Agency for International Development via the World Health Organization.

The authors declare that there is no conflict of interest regarding the publication of this paper. D.B., C.R., G.G., and P.R. are staff members of the World Health Organization. D.B., C.R., G.G., and P.R. are solely responsible for views expressed in this publication, and they do not necessarily represent decisions, policies, or views of the World Health Organization.

Dr. Phuc is an associate professor and the Chief of the Department of Clinical Research, National Institute of Malariology, Parasitology, and Entomology, Hanoi, Vietnam. His primary research interests are clinical trials and drug efficacy in malaria.

References

1. Leang R, Taylor WR, Bouth DM, Song L, Tarning J, Char MC, et al. Evidence of *Plasmodium falciparum* malaria multidrug resistance to artemisinin and piperaquine in western Cambodia: dihydroartemisinin-piperaquine open-label multicenter clinical assessment. Antimicrob Agents Chemother. 2015;59:4719–26. http://dx.doi.org/10.1128/AAC.00835-15
2. World Health Organization. Methods for surveillance of antimalarial drug efficacy. Geneva: The World Health Organization; 2009.
3. Ariey F, Witkowski B, Amaratunga C, Beghain J, Langlois A-C, Khim N, et al. A molecular marker of artemisinin-resistant *Plasmodium falciparum* malaria. Nature. 2014;505:50–5. http://dx.doi.org/10.1038/nature12876
4. Sidhu AB, Uhlemann AC, Valderramos SG, Valderramos JC, Krishna S, Fidock DA. Decreasing *pfmdr1* copy number in *plasmodium falciparum* malaria heightens susceptibility to mefloquine, lumefantrine, halofantrine, quinine, and artemisinin. J Infect Dis. 2006;194:528–35. http://dx.doi.org/10.1086/507115
5. Witkowski B, Duru V, Khim N, Ross LS, Saintpierre B, Beghain J, et al. A surrogate marker of piperaquine-resistant *Plasmodium falciparum* malaria: a phenotype-genotype association study. Lancet Infect Dis. 2016;S1473-3099(16)30415-7.
6. Ashley EA, Stepniewska K, Lindegardh N, Annerberg A, Tarning J, McGready R, et al. Comparison of plasma, venous and capillary blood levels of piperaquine in patients with uncomplicated *falciparum* malaria. Eur J Clin Pharmacol. 2010;66:705–12. http://dx.doi.org/10.1007/s00228-010-0804-7
7. Ménard D, Khim N, Beghain J, Adegnika AA, Shafiul-Alam M, Amodu O, et al.; KARMA Consortium. A worldwide map of *Plasmodium falciparum* K13-propeller polymorphisms. N Engl J Med. 2016;374:2453–64. http://dx.doi.org/10.1056/NEJMoa1513137

Address for correspondence: Charlotte Rasmussen, World Health Organization, Ave Appia, Geneve 1211, Switzerland; email: rasmussenc@who.int

Novel Reassortant Highly Pathogenic Avian Influenza (H5N8) Virus in Zoos, India

Shanmugasundaram Nagarajan,[1] Manoj Kumar,[1] Harshad V. Murugkar, Sushil Tripathi, Shweta Shukla, Sonam Agarwal, Garima Dubey, Raunaq Singh Nagi, Vijendra Pal Singh, Chakradhar Tosh

Author affiliation: Indian Council of Agricultural Research–National Institute of High Security Animal Diseases, Bhopal, India

DOI: http://dx.doi.org/10.3201/eid2304.161886

Highly pathogenic avian influenza (H5N8) viruses were detected in waterfowl at 2 zoos in India in October 2016. Both viruses were different 7:1 reassortants of H5N8 viruses isolated in May 2016 from wild birds in the Russian Federation and China, suggesting virus spread during southward winter migration of birds.

Since 1996, the hemagglutinin (HA) gene of subtype H5N1 highly pathogenic avian influenza (HPAI) viruses has evolved into multiple phylogenetic clades (*1*). During 2010, subtype H5N8 virus, bearing an H5N1 backbone and polymerase basic (PB) protein 1 (PB1), nucleoprotein (NP), and neuraminidase (NA) genes from non-H5N1 virus, emerged in China (*2*). In January 2014, a novel reassortant HPAI (H5N8) virus was detected in poultry and wild birds in South Korea (*3*) and subsequently spread to other counties in Asia and Europe before reaching North America by the end of 2014 (*4*). Because the H5N8-associated outbreaks coincided with bird migration routes, movement of wild waterfowl was suspected in intercontinental spread (*5*). Therefore, understanding the source and spread of the virus is a critical requirement for guidance of control measures. We report analysis of the genome of HPAI (H5N8) viruses isolated from waterfowl (domestic duck [*Anas platyrhynchos domesticus*] and painted stork [*Mycteria leucocephala*]) at 2 zoos in India in October 2016.

Twenty avian influenza viruses were isolated from 83 samples from National Zoological Park, Delhi, and Gandhi Zoological Park, Gwalior, Madhya Pradesh, India, in October 2016. The viruses were subtyped as H5N8 using reverse transcription PCR and real-time RT-PCR (online Technical Appendix 1, https://wwwnc.cdc.gov/EID/article/23/4/16-1886-Techapp1.pdf). One representative isolate each from Delhi (A/duck/India/10CA01/2016) and Madhya Pradesh (A/painted stork/India/10CA03/2016) were processed for pathogenic and molecular characterization. A detailed

[1]These authors contributed equally to this article.

description of the methods for the intravenous pathogenicity index test and genetic analysis used are provided in online Technical Appendix 1. Nucleotide sequences were deposited in the GISAID EpiFlu database (http://www.gisaid.org) under accession nos. EP1858833–EP1858848.

Both isolates were highly pathogenic based on amino acid sequence at the HA cleavage region (PLREKRRKR/GLF), which was corroborated by using an intravenous pathogenicity index test of 3.00 (Delhi isolate) and 2.96 (Madhya Pradesh isolate). Amino acid markers in the neuraminidase protein and matrix protein 2 indicated sensitivity to neuraminidase inhibitors and amantadines. Markers for mammalian virulence and poultry adaptation, such as E627K and D701N in PB2 and amino acid deletion in nonstructural protein (NS) 1 (position 80–84), were absent in the H5N8 viruses. However, 42S and 13P mutations in NS and PB1 genes (*6*) associated with increased virulence of the virus to mice were present. The PB1-F2 protein was truncated because of nucleotide mutation C35A, leading to premature termination after 11 aa.

Except the polymerase acidic (PA) and NP genes, all other gene segments of both isolates shared high nucleotide identity, ranging from 99.2% to 99.5%. The nucleotide identity of the PA and NP gene was 95.8% and 94.8%, respectively, suggesting involvement of 2 gene pools of H5N8 virus in the waterfowl outbreaks at Delhi and Madhya Pradesh.

In the HA gene phylogeny, the India isolates clustered with H5N8 viruses from other countries in Asia and Europe within group B (intercontinental group B) (online Technical Appendix 1 Figures 1–8). A similar grouping pattern was observed in the neuraminidase and nonstructural (NS) gene phylogenies. Further, within intercontinental group B, the isolates shared >99% nucleotide sequence identity with H5N8 viruses isolated in Uvs-Nuur Lake (located at the Mongolia–Russia border) and Qinghai Lake, China, in May 2016 (online Technical Appendix 1 Table 2). However, PB1, PB2, and matrix protein genes grouped with low pathogenic avian influenza (LPAI) viruses isolated in Eurasia and H5N8 viruses isolated in Qinghai Lake, Uvs-Nuur Lake, and Tyva Republic (Russian Federation).

In the PA phylogeny, although the Delhi virus grouped with LPAI viruses isolated in Mongolia and Vietnam and viruses isolated in Qinghai Lake, Uvs-Nuur Lake, and Tyva Republic, the Madhya Pradesh virus shared close relationship with LPAI viruses from Eurasia. In the NP gene phylogeny, although the Delhi virus shared close relationship with the Eurasia group of LPAI viruses, whereas the Madhya Pradesh virus and H5N8 viruses from Qinghai Lake, Uvs-Nuur Lake, and Tyva Republic are closely related to the Eurasia 2 LPAI viruses. These results suggest that both isolates are 7:1 reassortant of the Tyva Republic and Uvs-Nuur Lake H5N8 viruses reported previously (*7*) with different gene constellations. A median-joining network analysis indicated that, even though the contemporary H5N8 viruses isolated from wild birds in Qinghai Lake, Uvs-Nuur Lake, and Tyva Republic are not the direct ancestors, closely related precursor gene pools are source of the H5N8 viruses that caused outbreaks in waterfowls at the 2 zoos in India (online Technical Appendix 1 Figure 9).

The outbreak in waterfowls at both zoos coincided with winter migration of birds to India (September–March). The Uvs-Nuur Lake is an important habitat for 46 resident waterfowl species and 215 different species of birds migrating southward from Siberia (*8*). Therefore, different waves of migration of the wild birds might be the source of introduction of the H5N8 virus at the 2 zoos in India, as suggested by the observed spread of H5N1 clade 2.2 and 2.3.2.1c viruses (*9*,*10*).

Acknowledgments

We are thankful to the Indian Council of Agricultural Research, New Delhi, and the Indian Council of Agricultural Research–National Institute of High Security Animal Diseases, Bhopal, for providing necessary facilities to carry out this work. We are thankful to the Directors of Animal Husbandry Department of Delhi and Madhya Pradesh states in India for sharing the clinical samples used as part of this study. We gratefully acknowledge the authors and the originating and submitting laboratories for the sequences from the Global Initiative on Sharing Avian Influenza Data EpiFlu database (online Technical Appendix 2, https://wwwnc.cdc.gov/EID/article/23/4/16-1886-Techapp2.xlsx).

We acknowledge funding by the Department of Animal Husbandry, Dairying and Fisheries, Ministry of Agriculture and Farmers Welfare, Government of India under Central Disease Diagnostic Laboratory Grant.

Dr. Nagarajan is senior scientist at Indian Council of Agricultural Research–National Institute of High Security Animal Diseases, Bhopal, India. His research interests are focused on surveillance, development of diagnostics, molecular epidemiology, and pathogenesis of avian influenza.

References

1. WHO/OIE/FAO H5N1 Evolution Working Group. Continued evolution of highly pathogenic avian influenza A(H5N1): updated nomenclature. Influenza Other Respi Viruses. 2012;6:1–5. http://dx.doi.org/10.1111/j.1750-2659.2011.00298.x
2. Zhao K, Gu M, Zhong L, Duan Z, Zhang Y, Zhu Y, et al. Characterization of three H5N5 and one H5N8 highly pathogenic avian influenza viruses in China. Vet Microbiol. 2013;163:351–7. http://dx.doi.org/10.1016/j.vetmic.2012.12.025
3. Lee YJ, Kang HM, Lee EK, Song BM, Jeong J, Kwon YK, et al. Novel reassortant influenza A(H5N8) viruses, South Korea, 2014. Emerg Infect Dis. 2014;20:1087–9. http://dx.doi.org/10.3201/eid2006.140233
4. World Organization for Animal Health. Summary of immediate notifications and follow-ups—2014: highly path. avian influenza [cited 2016 Dec 3]. http://www.oie.int/wahis_2/public/wahid.php/Diseaseinformation/Immsummary

5. Lee DH, Torchetti MK, Winker K, Ip HS, Song CS, Swayne DE. Intercontinental spread of Asian-origin H5N8 to North America through Beringia by migratory birds. J Virol. 2015;89:6521–4. http://dx.doi.org/10.1128/JVI.00728-15
6. Gabriel G, Dauber B, Wolff T, Planz O, Klenk HD, Stech J. The viral polymerase mediates adaptation of an avian influenza virus to a mammalian host. Proc Natl Acad Sci U S A. 2005;102:18590–5. http://dx.doi.org/10.1073/pnas.0507415102
7. Lee D-H, Sharshov K, Swayne DE, Kurskaya O, Sobolev I, Kabilov M, et al. Novel reassortant clade 2.3.4.4 highly pathogenic avian influenza A(H5N8) virus in wild aquatic birds, Russia, 2016. Emerg Infect Dis. 2017 Feb 15 [Epub ahead of print]. https://dx.doi.org/10.3201/eid2302.161252
8. Florin BM. Uvs Nuur, Lake. In: Robert W. H. ed. Biomes and Ecosystems. Vol. 4. Amenia (NY): Salem Press; 2013. p. 1260–1.
9. Chen H, Smith GJ, Zhang SY, Qin K, Wang J, Li KS, et al. Avian flu: H5N1 virus outbreak in migratory waterfowl. Nature. 2005;436:191–2. http://dx.doi.org/10.1038/nature03974
10. United Nations Food and Agriculture Organization. H5N8 highly pathogenic avian influenza (HPAI) of clade 2.3.4.4 detected through surveillance of wild migratory birds in the Tyva Republic, the Russian Federation—potential for international spread [cited 2016 Dec 3]. http://www.fao.org/3/a-i6113e.pdf

Address for correspondence: Chakradhar Tosh, ICAR-National Institute of High Security Animal Diseases, Anand Nagar, Bhopal 462022, India; email: chakradhar.tosh@icar.gov.in

Acute Tetraplegia Caused by Rat Bite Fever in Snake Keeper and Transmission of *Streptobacillus moniliformis*

Tobias Eisenberg,[1] Simon Poignant,[1] Youenn Jouan, Ahmad Fawzy, Werner Nicklas, Christa Ewers, Laurent Mereghetti, Antoine Guillon

Author affiliations: Hessian State Laboratory, Giessen, Germany (T. Eisenberg, A. Fawzy); Centre Hospitalier Universitaire de Tours, Tours, France (S. Poignant, Y. Jouan, L. Mereghetti, A. Guillon); Université François Rabelais, Tours (S. Poignant, Y. Jouan, L. Mereghetti, A. Guillon); Cairo University, Giza, Egypt (A. Fawzy); Justus-Liebig-University, Giessen (A. Fawzy, C. Ewers); German Cancer Research Center, Heidelberg, Germany (W. Nicklas)

DOI: http://dx.doi.org/10.3201/eid2304.161987

We report acute tetraplegia caused by rat bite fever in a 59-year old man (snake keeper) and transmission of *Streptobacillus moniliformis*. We found an identical characteristic bacterial pattern in rat and human samples, which validated genotyping-based evidence for infection with the same strain, and identified diagnostic difficulties concerning infection with this microorganism.

Human infections by *Streptobacillus moniliformis* are assumed to be caused by rats on the basis of epidemiologic information. We provide genotyping-based evidence for infection with the same bacterial strain in rat and human samples and highlight diagnostic difficulties concerning this microorganism and its potential for life-threatening consequences.

A 59-year-old man was admitted to Centre Hospitalier Universitaire de Tours (Tours, France) because he was unable to stand and had acute progressive onset of dyspnea and a 15-day history of fever and arthralgia (left knee, right wrist) but no signs of rash. He was sedated, mechanically ventilated, and admitted to the intensive care unit. The patient had a temperature of 39°C, a pulse rate of 63 beats/min, and a blood pressure of 126/68 mm Hg.

After discontinuation of sedation, physical examination showed cervical pain, flaccid tetraplegia, and sensitivity at the T4 level. His knees and left wrist were swollen and had joint effusions. There was little available information for the patient because he could not speak and had no known social contacts. Blood tests showed an increased leukocyte count (15×10^9 cells/L), predominantly neutrophils, and an increased C-reactive protein level (125 mg/L).

The patient was given antimicrobial drugs (amoxicillin and cloxacillin) after blood and synovia (knee) sampling. Cervical magnetic resonance imaging showed C5–T1 vertebral osteomyelitis and an epidural abscess with consecutive compression of the spinal cord (C5–T1) (Figure). Surgical spinal decompression and vertebral stabilization were not attempted because of extensiveness of injury and flaccid tetraplegia. Transthoracic and transesophageal echocardiograms showed no features of endocarditis. Blood cultures showed negative results. Joint effusions contained a culture-negative inflammatory liquid and uric acid crystals. The patient was given a tracheotomy and continuously ventilated.

A final diagnosis was obtained by sequencing the 16S rRNA gene obtained directly from synovia. An 897-nt partial 16S rRNA sequence showed 99.0% identity with sequences of *S. moniliformis* (GenBank accession nos. JQ087393 and CP001779).

The patient was a snake keeper who bred rats for snake food. He reported snake bites but not rat bites. We sampled his snakes (*Boa constrictor* and *Elaphe* sp.) and 1 of his feeder rats (*Rattus norvegicus*) by obtaining swab and biopsy specimens from oral cavities of all animals. All cultures were polymicrobial. We used desorption/ionization time-of-flight mass spectrometry (Bruker Daltonique,

[1]These authors contributed equally to this article.

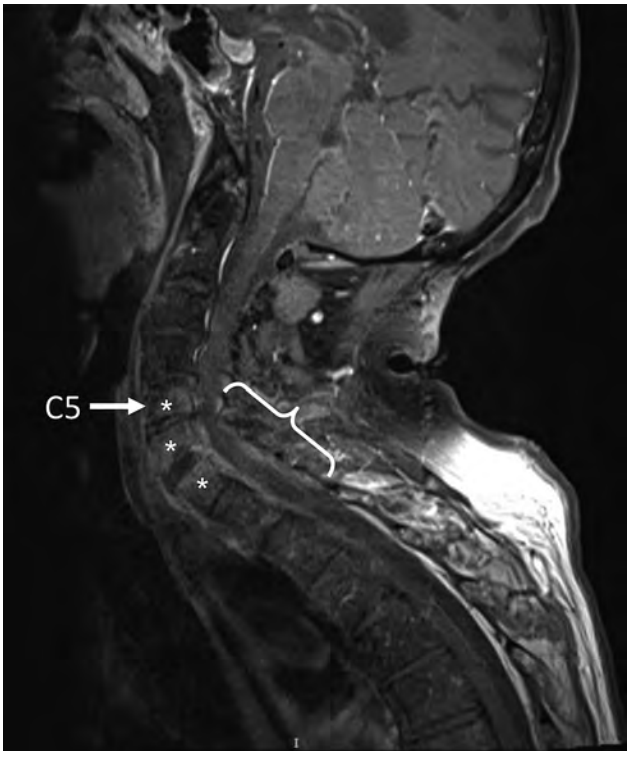

Figure. Fat-saturated, contrast-enhanced T1-weighted magnetic resonance image of the spine of a 59-year-old man (snake keeper) with rat bite fever. Sagittal view of the cervical spine shows spondylodiscitis (*) and an epidural absess with C5–T1 compression (brace). Preexisting spinal degeneration was observed and was probably a promoting factor for spinal compression.

Wissembourg, France) to identify isolated bacteria but failed to identify *S. moniliformis*.

Synovia and serum samples from the patient and oral swab and biopsy specimens from animals were subjected to three 16S rRNA gene–based PCRs that were genus specific, rather than *S. moniliformis* specific (*1*). Synovia from the patient and 2 swab and 2 biopsy specimens from the same rat, but none of the oral samples from snakes, were positive. This result suggested rat bite fever. However, diagnosis of rat bite fever on the basis of partial 16S rRNA gene sequencing might be uncertain (*1*).

We tested the same samples by using *S. moniliformis*–specific multilocus variant analysis (MLVA) (*2*) to identify the bacterial transmission chain. Results were consistent with those for PCR and identified 2 MLVA genotypes of *S. moniliformis* in rat oral samples. Conversely, genomic information obtained for human synovia showed only 1 of these patterns, indicating a clonal relationship with 1 of the rat bacterial strains. Serum from the patient obtained on day 1 after hospitalization contained antibodies against *S. moniliformis* when tested by bead-based multiplex serologic analysis and indirect immunofluorescence.

Rat bite fever is an underdiagnosed worldwide zoonosis closely associated with bites of rats or close contact with them. Snakes that eat rats might serve, at least temporarily, as reservoirs for human infection. Thus, we attempted to detect the rat bite fever organism in oral and biopsy specimens from the patient's snakes by using different PCRs (including a quantitative PCR that has an analytical sensitivity of 10 DNA molecules). All results were negative.

Four studies reported rat bite fever associated with keeping reptiles, but definitive transmission could not be proven in these instances, in which infections seemed more likely to be introduced by feeder rats (*3*–*6*). Regular contact with prey rats might be a general risk factor, and being bitten by a snake shortly after it fed on a prey rat might have the same consequences as a rat bite. In our study, we identified and typed the involved clone by using a recently developed, species-specific, culture-independent MLVA scheme (http://microbesgenotyping.i2bc.paris-saclay.fr/databases/public).

We showed that a rat might be simultaneously colonized by >1 clone of *S. moniliformis* and demonstrated identical strains in the human patient and the reservoir host (online Technical Appendix Figure, https://wwwnc.cdc.gov/EID/article/23/4/16-1987-Techapp1.pdf). The infectious genotype has been designated as LHL18 on the basis of the novel allele combination 17-3-16.

We demonstrated the presence of an identical characteristic *S. moniliformis* bacterial pattern in rat and human samples, which validated genotyping-based evidence for infection with the same strain. Our case highlights diagnostic difficulties concerning this microorganism and supports tropism of this bacteria for synovial tissue and its potential for life-threatening consequences.

Acknowledgments

We thank the patient for providing written permission to publish this report; Kathkeen Gaillot and Isabelle Griffoul for help in interpreting magnetic resonance imaging results; and Chrystophe Aubert and Elodie Theyssandier for handling snakes.

S.P., Y.J., and A.G. provided care for the patient; T.E., A.F., W.N., C.E., and L.M. performed the microbiological analyses; and T.E., S.P., and A.G. wrote the report.

Dr. Eisenberg is a veterinary specialist in microbiology and team supervisor of the bacteriology department, Hessian State Laboratory, Giessen, Germany. His primary research interests are rat bite fever, other infectious diseases in zoo animals and wildlife, and zoonoses.

References

1. Eisenberg T, Ewers C, Rau J, Akimkin V, Nicklas W. Approved and novel strategies in diagnostics of rat bite fever and other *Streptobacillus* infections in humans and animals. Virulence. 2016;7:630–48. http://dx.doi.org/10.1080/21505594.2016.1177694

2. Eisenberg T, Fawzy A, Nicklas W, Semmler T, Ewers C. Phylogenetic and comparative genomics of the family *Leptotrichiaceae* and introduction of a novel fingerprinting MLVA for *Streptobacillus moniliformis.* BMC Genomics. 2016;17:864. http://dx.doi.org/10.1186/s12864-016-3206-0
3. Dendle C, Woolley IJ, Korman TM. Rat-bite fever septic arthritis: illustrative case and literature review. Eur J Clin Microbiol Infect Dis. 2006;25:791–7. http://dx.doi.org/10.1007/s10096-006-0224-x
4. Gilroy SA, Khan MU. Rat bite fever: case report and review of the literature. Infectious Diseases in Clinical Practice. 2002;11:403–5. http://dx.doi.org/10.1097/00019048-200209000-00007
5. Irvine L, Wills T. *Streptobacillus moniliformis*: a mouse trying to become a rat. Clinical Microbiology Newsletter. 2006;28:118–20. http://dx.doi.org/10.1016/j.clinmicnews.2006.07.002
6. Trigo-Daporta M, Cortizo-Vidal S, Pallarés-González Á, García-Campello M. Fever and rash in the owner of exotic pets [in Spanish]. Enferm Infecc Microbiol Clin. 2011;29:311–2. http://dx.doi.org/10.1016/j.eimc.2010.07.019

Address for correspondence: Antoine Guillon, Centre Hospitalier Regional Universitaire de Tours, 2 Blvd Tonnelle, Tours 37044, France; email: antoine.guillon@univ-tours.fr

Malaria in Children Adopted from the Democratic Republic of the Congo

Elena Chiappini, Sara Sollai, Maurizio de Martino, Luisa Galli

Author affiliation: Meyer University Hospital, Florence University, Florence, Italy

DOI: http://dx.doi.org/10.3201/eid2304.161777

Data are lacking regarding asymptomatic and symptomatic malaria prevalence in internationally adopted children. Among 20 children from Democratic Republic of the Congo evaluated in Florence, Italy, in April 2016, malaria prevalence was 80%; 50% of infected children had symptomatic malaria. Adopted children from areas of high malaria endemicity should be screened for malaria.

The Democratic Republic of the Congo (DRC) banned adoption of children by parents from other countries in 2013. In February 2016, the ban was removed, and several hundred children were allowed to join families in Europe and in the United States. The first group of children from DRC arrived in Italy in April 2016, and 20 children were referred to the Center for Internationally Adopted Children at Meyer University Hospital, Florence, Italy. All children underwent the standard infectious disease screening tests recommended by the American Academy of Pediatrics, including those for tuberculosis (by tuberculin skin test and interferon-γ release assay) and intestinal parasites (by fecal testing for ova, parasites, and antigen test for *Giardia* spp.) and serologic tests for *Toxocara canis, Strongyloides* spp., hepatitis B and C viruses, HIV-1/2 viruses, and *Treponema pallidum* (syphilis) (*1*).

Eight children who were exhibiting fever were admitted to the hospital and received a diagnosis of malaria soon after their arrival in Italy. For malaria testing, PCR and microscopy were performed on thin and thick smears. Parasitemia level was determined by counting the parasitized erythrocytes among the 500–2,000 erythrocytes on the thin smear and calculating the percentage.

The remaining children from DRC were screened, and another 8 children were found to be infected. Thus, malaria was diagnosed in 16 children (10 were boys; median age 7 years [range 4–10 years]), and malaria prevalence was 80% (16/20). *Plasmodium falciparum* infection was documented in 15 cases, whereas a mixed infection (*P. falciparum* and *P. ovale*) was observed in 1 child. All children underwent treatment with intravenous quinine plus artesunate or oral dihydroartemisinin/piperaquine (*2*). Intravenous treatment was administered to 1 child who had severe malaria (generalized seizures) and to 5 children with a parasitemia level ≥2% or who exhibited vomiting and therefore were unable to take oral medications reliably (*2*). Because intravenous artesunate is unlicensed in Europe but is available in our center, we obtained written informed consent for its use from the patients' parents before administration. The study received approval by Meyer University Hospital Ethics Committee.

Other studies have assessed the prevalence of malaria in internationally adopted children. Among a population of 182 children in France, when Blanchi et al. screened for the children originating from malaria-endemic zones who were exhibiting fever, splenomegaly, or both for malaria, they found 2 infected children (*3*). More recently, Adebo et al. screened 52 children arriving in the United States from Ethiopia for malaria and reported 7 (13.5%) children with asymptomatic malaria (*4*). These authors suggested that screening be conducted of children coming from malaria-endemic areas with noted risk factors, such as splenomegaly (*4*). Anemia (hemoglobin levels <11 g/dL) could be another risk factor for malaria but, because it is common in this population, it was not considered in the study by Adebo et al. (*4*). However, in our population, we found that tests for parasitemia were positive for 6 children without splenomegaly or hepatomegaly and for 1 child who had neither anemia (<11 g/dL), hepatomegaly, nor splenomegaly. Therefore, using clinical features to select children who should undergo the screening may be challenging.

Given the paucity of literature data regarding malaria prevalence in internationally adopted children, testing by PCR, microscopy, or both, followed by treatment of infected children, would be preferable to the empiric treatment, considering the costs and possible adverse effects of antimarial drugs. Moreover, the preferable screening strategy is not apparent. We did not observe any discrepancy between microscopy and PCR results; however, a higher sensitivity by PCR has been reported (*4*,*5*). In contrast, some experts prefer testing by microscopy examination because PCR techniques are not sufficiently standardized or validated to be used for routine clinical diagnosis (*2*).

In our dataset, malaria prevalence was substantially higher than that previously reported (*4*). This finding may be due to the particular situation of these children and to orphanage conditions (i.e., lack of mosquito nets). Moreover, it should be noted that, to date, 3 countries— DRC, Nigeria, and India—account for 40% of all estimated malaria cases in the world (*6*). Also, a high prevalence of asymptomatic malaria in DRC has been reported, in ≈15% of children (*7*,*8*).

Our results should be interpreted with caution, given the small dataset, but they should alert pediatricians regarding the importance of assessing malaria risk in children who have been adopted internationally. The degree of malaria endemicity in the child's area of origin may be considered in the decision to screen asymptomatic children adopted in non–malaria-endemic countries. In particular, children who come from areas of high malaria endemicity, such as DRC, deserve a careful screening, even in the absence of any sign or symptom.

Dr. Chiappini is an associate professor of pediatrics at the University of Florence. She is also the head of the unit for internationally adopted children at Meyer University Hospital in Florence. Her research interests focus on pediatric infectious diseases, including HIV infection, tuberculosis, and malaria.

References

1. American Academy Pediatrics Committee on Infectious Diseases. Medical evaaluation of internationally adopted children for infectious disease. In: Pickering LK, Baker CJ, Kimberlin DW, editors. Red book: report of the Committee on Infectious Diseases. 29th ed. Elk Grove Village (IL): The Academy; 2012. p. 192–200.
2. Lalloo DG, Shingadia D, Bell DJ, Beeching NJ, Whitty CJ, Chiodini PL; PHE Advisory Committee on Malaria Prevention in UK Travellers. UK malaria treatment guidelines 2016. J Infect. 2016;72:635–49. http://dx.doi.org/10.1016/j.jinf.2016.02.001
3. Blanchi S, Chabasse D, Pichard E, Darviot E, de Gentile L. Post-international adoption medical follow-up at the Angers university hospital between 2009 and 2012. Med Mal Infect. 2014;44:69–75. http://dx.doi.org/10.1016/j.medmal.2013.12.003
4. Adebo SM, Eckerle JK, Andrews ME, Howard CR, John CC. Asymptomatic malaria and other infections in children adopted from Ethiopia, United States, 2006–2011. Emerg Infect Dis. 2015;21:1227–9. http://dx.doi.org/10.3201/eid2107.141933
5. Menge DM, Ernst KC, Vulule JM, Zimmerman PA, Guo H, John CC. Microscopy underestimates the frequency of *Plasmodium falciparum* infection in symptomatic individuals in a low transmission highland area. Am J Trop Med Hyg. 2008;79:173–7.
6. World Health Organization. WHO malaria report 2012 [cited 2016 Oct 31]. https://www.k4health.org/sites/default/files/who_malaria_report_2012.pdf
7. Maketa V, Mavoko HM, da Luz RI, Zanga J, Lubiba J, Kalonji A, et al. The relationship between *Plasmodium* infection, anaemia and nutritional status in asymptomatic children aged under five years living in stable transmission zones in Kinshasa, Democratic Republic of Congo. Malar J. 2015;14:83. http://dx.doi.org/10.1186/s12936-015-0595-5
8. Myumbi DM, Bobanga TL, Melin P, De Mol P, Kayembe JM, Situakibanza HN, et al. The prevalence of *Plasmodium falciparum* infection in asymptomatic individuals from the Democratic Republic of Congo. Malar Res Treat. 2016; 2016:5405802.

Address for correspondence: Elena Chiappini, Infectious Disease Unit, Meyer University Hospital, Department of Health Science, Florence University, Viale Pieraccini, 24, Florence, Italy; email: elena.chiappini@unifi.it

LETTER

Cord Blood Sample Screening for Evidence of Maternal Chagas Disease

Susan P. Montgomery, Susan L. Stramer

Author affiliations: Centers for Disease Control and Prevention, Atlanta, Georgia, USA (S.P. Montgomery); American Red Cross, Gaithersburg, Maryland, USA (S.L. Stramer)

DOI: http://dx.doi.org/10.3201/eid2304.161287

To the Editor: The article by Edwards et al. (*1*) contained several errors regarding testing, results, and interpretation of results. The authors incorrectly described the testing performed for the cord blood samples. The American Red Cross (ARC) National Testing Laboratory (NTL) (identified as the "American Red Cross National Donor Testing Laboratory" in the article) has never performed indirect hemagglutination assay testing, a method not licensed by the Food and Drug Administration (FDA) for detection of antibodies to *Trypanosoma cruzi*. In fact, the laboratory used a combination of testing algorithms during 2007–2014, the period of the study, involving 2 different FDA-licensed screening tests and a combination of research and licensed supplemental tests. Each algorithm had varying positive predictive values, ranging from <10% to >50%. The laboratory

algorithm from January 2007 to the end of August 2011 included the FDA-licensed Ortho *T. cruzi* enzyme immunoassay (EIA) (Ortho-Clinical Diagnostics, Inc., Raritan, NJ, USA), followed by a research radioimmunoprecipitation assay (RIPA) for supplemental testing of all repeat reactive donations.

On September 1, 2011, the laboratory began using the FDA-licensed PRISM Chagas chemiluminescent immunoassay (Abbott Laboratories, Abbott Park, IL, USA) for donor screening, followed by a combination of RIPA and the Ortho EIA for supplemental testing. On July 30, 2012, the laboratory switched from the RIPA to the FDA-licensed Abbott enzyme strip assay (ESA) (Abbott Laboratories) for supplemental testing, maintaining concurrent testing with the Ortho EIA (*2*). The ARC NTL notified all customers of changes in laboratory testing algorithms.

The results reported in the article do not match those recorded at the ARC NTL. The authors describe 25 samples that tested reactive by indirect hemagglutination and that 19 of those were positive by supplemental RIPA testing. In addition to the incorrect tests described, reported results do not correspond to laboratory records. Reviewing the ARC NTL testing results for the Carolinas Cord Blood Bank facility codes, we found that 34 unique samples tested repeat reactive from October 9, 2007, through October 13, 2014. Of these 34 samples, 11 were positive on supplemental RIPA testing and none were ESA positive; testing with RIPA or ESA was dependent on the algorithm in place at the time. Of the 11 samples that were reactive in screening tests and showed positive results in supplemental tests, 2 positives were identified from October–November 2007, 1 from November 2008, 5 from June 2009–January 2010, 2 from May–June 2010, and 1 from 2012 (which does not correspond to the data in the figure or patterns described in the discussion). An additional 4 screening test repeat reactive donations were tested during 2015–2016, with 1 ESA positive but Ortho EIA nonreactive.

Test results of submissions from other facility codes for Duke University were reviewed to see whether any positive samples were submitted from a different North Carolina laboratory; we found 10 additional screening test repeat reactive donations, but none had positive results by supplemental testing. We do not know whether testing of cord blood samples was performed by another laboratory; only the ARC NTL was described in the methods of this study.

Much of the interpretation of results was misleading. The authors considered any screening test positive result as being sufficient for confirmation of infection. To be meaningful, all samples with reactive results should be tested further, and only those with reactive or positive results by at least 2 different tests considered for any investigation of epidemiologic trends. Furthermore, a single serologic screening test reactive result confirmed as positive, though useful for blood donor management, does not define a confirmed diagnosis of Chagas disease (*3*).

The authors' use of the term incidence does not agree with the epidemiologic definition of that term. The authors state, "The incidence of confirmed Chagas disease among mothers who donated their neonate's cord blood varied over time," "The incidence of Chagas disease varied over time," and "A strength of this study is its large sample size, particularly because the incidence of this disease is low." However, no incident *T. cruzi* infections were identified by their study. No evidence of acute infection was presented. All mothers who donated cord blood were chronically infected; the testing of their samples revealed the prevalence of positive results among the samples tested in a given period (had the numbers used been accurate, which they were not). This distinction is key because acute infections are more likely to be transmitted through blood transfusion and patients' infections are more likely to be successfully cured by antitrypanosomal treatment during the acute phase of infection, before development of cardiac manifestations.

Preventing and controlling congenital Chagas disease is a serious public health issue; the screening of mothers at risk for transmitting *T. cruzi* infection to their babies is considered key to accomplishing these factors. The evidence base to support screening recommendations must be high-quality and accurate. Other studies have emphasized this risk in the US population, particularly in Latin American immigrant mothers (*4*), but further evidence is needed to guide policy recommendations. The report of Edwards et al. (*1*) could be a contribution to this needed evidence base, but only if reported data are accurate and appropriately interpreted.

References

1. Edwards JM, Gilner JB, Hernandez J, Kurtzberg J, Heine RP. Chagas disease screening in maternal donors of publicly banked umbilical cord blood, United States. Emerg Infect Dis. 2016;22:1468–70. http://dx.doi.org/10.3201/eid2208.151622
2. US Food and Drug Administration. Guidance for industry: use of serological tests to reduce the risk of transmission of *Trypanosoma cruzi* infection in whole blood and blood components intended for transfusion, December 2010 [cited 2016 Aug 3]. http://www.fda.gov/downloads/BiologicsBloodVaccines/GuidanceComplianceRegulatoryInformation/Guidances/Blood/UCM235960.pdf
3. Bern C, Montgomery SP, Herwaldt BL, Rassi A Jr, Marin-Neto JA, Dantas RO, et al. Evaluation and treatment of Chagas disease in the United States: a systematic review. JAMA. 2007;298:2171–81. http://dx.doi.org/10.1001/jama.298.18.2171
4. Edwards MS, Rench MA, Todd CW, Czaicki N, Steurer FJ, Bern C, et al. Perinatal screening for Chagas disease in southern Texas. J Pediatric Infect Dis Soc. 2015;4:67–70. http://dx.doi.org/10.1093/jpids/pit056

Address for correspondence: Susan P. Montgomery, Centers for Disease Control and Prevention, 1600 Clifton Road NE, Mailstop A06, Atlanta, GA 30329-4027; email: smontgomery@cdc.gov

One Health and the Politics of Antimicrobial Resistance

Laura H. Kahn John Hopkins University Press, Baltimore, MD, USA; ISBN-10: 142142004X; ISBN-13: 978-1421420042; Pages: 200; Price: $30.00

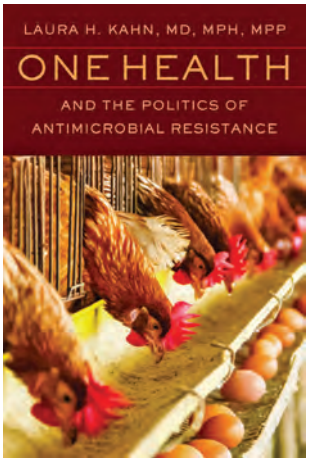

The use of antimicrobial drugs in food-producing animals can result in antimicrobial drug–resistant infections in humans. A good example is the use of fluoroquinolone in poultry and the emergence of fluoroquinolone-resistant *Campylobacter* infections among humans. However, topics of intense debate include the widespread use of antimicrobial drugs in animals, the extent to which antimicrobial drug use in animals affects human health, what drugs used in animals could be cause for concern to humans, and how to prevent overall risks to human health.

The issue is complex from both policy and science perspectives. Antimicrobial drugs are used to raise all types of food-producing animals, but detailed drug use data are still lacking, making efforts to change drug use practices particularly challenging. In addition, because mobile genetic elements can confer new resistance on bacteria that already have complex ecology, there is often a lack of direct evidence to link the use of a particular antimicrobial drug to a specific resistant organism in humans.

Policies that drive antimicrobial drug use, or lack of use, in animals can have profound effects on the health of the world's population, the health of the agricultural industry, and the world's food supply. However, even those well-versed in the topic of antimicrobial drug resistance find the issues of antimicrobial drug use in food-producing animals to be confusing and loaded with contrary political opinions on the significance of the public health threat and how best to address it.

Laura H. Kahn's book One Health and the Politics of Antimicrobial Resistance should be considered an essential primer for anyone who chooses to grapple with this challenging but crucial public health issue. The book is a concise summary of events and milestones that have been driving forces in the use of antimicrobial drugs for food production efforts and objectively outlines the effect these efforts have had on the problem of drug resistance. For example, few are aware of the effect World War II had on supply chains of traditional animal feed supplements such as cod liver oil and fishmeal. In the United States, this interruption resulted in the transition to using antimicrobial drugs to boost the growth of food-producing animals. The author not only provides the US perspective but also describes the history of antimicrobial drug use in Europe, the steps these countries have taken to curb the tide of drug resistance, and where progress has been made. An example is the decrease in vancomycin-resistant enterococci carriage among healthy people in the Netherlands and Germany after avoparcin was banned.

The author demonstrates her command of both the politics and the science of establishing medication guidelines throughout the book and approaches the subject with professional objectivity. In the concluding chapter, she provides concrete recommendations for policy, surveillance systems, and scientific research to understand and prevent antimicrobial resistance from a One Health perspective.

Jean B. Patel

Author affiliation: Centers for Disease Control and Prevention, Atlanta, Georgia, USA

DOI: http://dx.doi.org/10.3201/eid2304.161871

Address for correspondence: Jean B. Patel, Centers for Disease Control and Prevention, 1600 Clifton Rd NE, Mailstop C12, Atlanta, GA 30329-4027, USA; email: JPatel1@cdc.gov

Corrections

Vol. 22, No. 11

The name of author Massimo Ciccozzi was misspelled in Mayaro Virus in Child with Acute Febrile Illness, Haiti, 2015 (J. Lednicky et al.). The article has been corrected online (https://wwwnc.cdc.gov/eid/article/22/11/16-1015_article).

Vol. 23, No. 1

The GenBank accession no. KX757840 was listed incorrectly in Puumala Virus in Bank Voles, Lithuania (P. Straková et al.). The article has been corrected online (https://wwwnc.cdc.gov/eid/article/23/1/16-1400_article).

Vol. 23, No. 3

The name of author Apurva Narechania was misspelled in *Mycobacterium tuberculosis* Infection among Asian Elephants in Captivity (G. Simpson et al.). The article has been corrected online (https://wwwnc.cdc.gov/eid/article/23/3/16-0726_article).

Joseph Stella (1877–1946), ***Spring*** **(*The Procession*)** (detail), c. 1914–1916. Oil on canvas, 75 5/16 in x 40 3/16 in / 191.3 x 102.1 cm. Gift of Collection Société Anonyme, Yale University Art Gallery, New Haven, Connecticut, USA.

The Exploding Aliveness of the World

Byron Breedlove and Paul M. Arguin

When Joseph Stella journeyed to New York City from his native Italy in 1896, he intended to study medicine. Stella instead pursued art, which he studied at the Art Students League of New York under William Merritt Chase. During 1905–1909, Stella illustrated magazines, and he continued to draw throughout a career marked by numerous shifts in his style and approach to art. According to a brief bio from the Phillips Collection website, Stella "began as an academic realist, but his mature work is in a modernist style, notable for its sweeping and dynamic lines."

During a return visit to Italy in 1909, Stella had his initial brush with modernism, specifically with the Italian Futurist school of painting. According to art critic Holland Carter, "Color entered his art with a bang when he was introduced to Italian Futurism." Not long after returning to New York from Europe, Stella became immersed in

Author affiliation: Centers for Disease Control and Prevention, Atlanta, Georgia, USA

DOI: http://dx.doi.org/10.3201/eid2304.AC2304

modernism, and he is now viewed as a principal figure in American Modernism.

"Spring (The Procession)" this month's cover image, a painting bursting with innumerable dazzling slivers of color, is considered among Stella's finest works. The artist concentrates dark blue, gold, green, and red shards in the lower quarter, suggesting the interactions of biological and chemical processes following the spring thaw. Swirls of pale yellow accented with bursts of green, blue, and gold near the painting's center reflect the showiness of an early spring garden as the first flowers, shoots, and leaves appear, hungry insects and birds take wing, and lizards and amphibians awaken from their winter torpor. Green, the most common color in nature, dominates Stella's celebration of renewal. According to art critic Richard Nilsen, "He was one of those painters, like Van Gogh, who yearned to express the exploding aliveness of the world, a man with a visionary sense of cosmic energy."

"The exploding aliveness of the world" that fuels artistic creativity also finds full expression in dynamic microscopic realms teeming with unfathomable numbers of viruses, bacteria, fungi, prions, and protozoa that lead to an incredible variety of pathologic consequences when infecting their hosts. An editorial in *Nature Reviews Microbiology*, which attempts to quantify some of those numbers used to give perspective to this microscopic world, provides this frame of reference for viruses: "Astronomy is a field that is used to dealing with large numbers, but these can be dwarfed when compared with life on the microbial scale. For instance, if all the 1×10^{31} viruses on earth were laid end to end, they would stretch for 100 million light years." And that is just the viruses!

That only some 1,400 recognized microbes are known to be pathogenic to humans should not be considered reassuring. Since the 1980s, nearly 40 new pathogens have been identified as causes of disease in humans. HIV, Ebola virus, MERS coronavirus, SARS coronavirus, West Nile virus, and Zika virus are among the high-profile viruses that have emerged from the confluence of ecologic forces. Potential new exposure to these previously quiescent microbes can result from human incursion and settlement in remote and rural areas, food production and importation practices, and prevailing planetary weather and temperature.

Comparable to the exuberance of spring, the emergence of microbes is often a spectacular display of the power of nature. Similar to the explosion of springtime pollen, some emerging infections declare their presence with large outbreaks that are impossible to miss. Others are insidiously tenacious, going unnoticed until entrenched like flowing waves of kudzu. Even familiar foes such as *Staphylococcus aureus, Enterobacteriaceae*, and mycobacteria emerge in their own surprising new slivers of color with the development of multiple and extensively drug-resistant varieties.

It has been 25 years since the publication of *Emerging Infections: Microbial Threats to Health in the United States* and 14 years since the publication of *Microbial Threats to Health: Emergence, Detection, and Response*. Those influential reports—which represent the insights of Joshua Lederberg, Robert Shope, and their colleagues—from the Institute of Medicine (now National Academy of Medicine) Committee on Emerging Microbial Threats offered far-reaching recommendations and galvanized support for research and public health action to address the challenges posed by new, emerging, and reemerging infectious diseases. Our success, now and in the future, depends on having a fully functioning national and global public health surveillance system, supported with epidemiologic and laboratory capacity, being able to rapidly share and communicate information.

Springtime is when we see the results of the seeds we have sown. The time and attention given to tending to our backyard gardens, our larger communities, our public health infrastructure, and our approach to addressing emerging infections will be apparent and on display when that inevitable exploding aliveness occurs. Stella's intoxicating depiction of spring may serve to remind us that we must not become complacent, but that we must constantly renew our focus, thinking, and approaches to addressing emerging infections.

Bibliography

1. American Art. The Phillips Collection. Biography Joseph Stella (1877–1946) [cited 2017 Feb 8]. http://www.phillipscollection.org/research/american_art/bios/stella_j-bio.htm
2. Bowdoin College Museum of Art. Modernism at Bowdoin: American paintings from 1900 to 1940. Brunswick (ME): The Museum; 2011. p. 18.
3. Cotter H. Review/art; painterly synthesis of a wanderer's life review [cited 2017 Feb 8]. http://www.nytimes.com/1994/04/22/arts/review-art-painterly-synthesis-of-a-wanderer-s-life.html
4. Microbiology by numbers. Nat Rev Microbiol. 2011;9:628. http://dx.doi.org/10.1038/nrmicro2644
5. Doucleff M, Greenhalgh J. Why killer viruses are on the rise [cited 2017 Feb 14]. http://www.npr.org/sections/goatsandsoda/2017/02/14/511227050/why-killer-viruses-are-on-the-rise
6. Lederberg J, Shope RE, Oaks SC Jr, editors. Emerging infections: microbial threats to health in the United States. October 1992 [cited 2017 Feb 10]. http://www.nap.edu/catalog/2008/emerging-infections-microbial-threats-to-health-in-the-united-states
7. Institute of Medicine Committee on Emerging Microbial Threats to Health in the 21st Century. Smolinski MS, Hamburg MA, Lederberg J, editors. Microbial threats to health: emergence, detection, and response. 2003 [cited 2017 Feb 27]. https://www.ncbi.nlm.nih.gov/books/NBK221486/
8. Nilsen R. Joseph Stella's flowers [cited 2017 Mar 3]. https://richardnilsen.com/tag/joseph-stellas-flowers/
9. Woolhouse ME, Gowtage-Sequeria S. Host range and emerging and reemerging pathogens. Emerg Infect Dis. 2005;11:1842–7. http://dx.doi.org/10.3201/eid1112.050997

Address for correspondence: Byron Breedlove, EID Journal, Centers for Disease Control and Prevention, 1600 Clifton Rd NE, Mailstop C19, Atlanta, GA 30329-4027, USA; email: wbb1@cdc.gov

EMERGING INFECTIOUS DISEASES®

Upcoming Issue

- Risk for Hantavirus Pulmonary Syndrome, United States, 1993–2015
- Control of Malaria Mosquito Vectors by Insecticide-Treated Combinations of Window Screens and Eave Baffles
- Insecticide-Treated Nets in the Protection Against Insecticide-Resistant Mosquito Vectors of Malaria, Western Kenya
- Prevention of Chronic Hepatitis B after 3 Decades of Escalating Vaccination Policy, China
- Increased Neurotropic Threat from *Burkholderia pseudomallei* Strains with a *B. mallei*–Like Variation in the *bimA* Motility Gene, Australia
- Exposure Risk for Infection and Lack of Human-to-Human Transmission of *Mycobacterium ulcerans* Disease, Australia
- Amoxicillin and Ceftriaxone as Treatment Alternatives to Penicillin for Maternal Syphilis
- Macrolide and Fluoroquinolone Resistance in *Mycoplasma genitalium*
- Reassortant Clade 2.3.4.4 Avian Influenza A(H5N6) Virus in a Wild Mandarin Duck, South Korea, 2016
- Regional Transmission of *Salmonella* Paratyphi A, China, 1998–2012
- Management of 2 Cases of *Bartonella* Prosthetic Valve Endocarditis without Cardiac Surgery
- Persistence of Zika Virus in Breast Milk after Infection in Late Stage of Pregnancy
- Colistin Resistance in ESBL-Producing *Klebsiella pneumoniae*, France
- *Borrelia turicatae* Infection in Febrile Soldier, Texas, USA
- CTX-M-27–Producing *Escherichia coli* of Sequence Type 131 and Clade C1-M27 in France
- Antimicrobial Drug Resistance among Refugees from Syria, Jordan
- Translating Real-Time Infectious Disease Modeling into Routine Public Health Practice

Complete list of articles in the May issue at http://www.cdc.gov/eid/upcoming.htm

Upcoming Infectious Disease Activities

June 1–5, 2017
ASM
American Society for Microbiology
New Orleans, LA, USA
http://www.showsbee.com/fairs/25161-ASM-Microbe-2017.html

June 4–8, 2017
Council of State and Territorial Epidemiologists
2017 Annual Conference
Boise, ID, USA
http://www.csteconference.org/2017/

June 11–14 2017
APHL
Association of Public Health Laboratories
Providence, RI, USA
https://www.aphl.org/conferences/annualmeeting/Pages/default.aspx

June 19–21 2017
Transmission of Respiratory Viruses
Harbour Grand Hong Kong
https://transmission2017.med.hku.hk/mass_email.html

September 10–12, 2017
International Peer Review Congress
Chicago, Il, USA
http://www.peerreviewcongress.org/index.html

October 4–8, 2017
ID Week
San Diego, CA, USA
http://www.idweek.org/past-and-future-events/

November 4–8, 2017
APHA
American Public Health Association
Atlanta, GA, USA
https://www.apha.org/annualmeeting

To submit an announcement, send an email message to EIDEditor (eideditor@cdc.gov). Include the date of the event, the location, the sponsoring organization(s), and a website that readers may visit or a telephone number or email address that readers may contact for more information.

Announcements may be posted on the journal Web page only, depending on the event date.

Earning CME Credit

To obtain credit, you should first read the journal article. After reading the article, you should be able to answer the following, related, multiple-choice questions. To complete the questions (with a minimum 75% passing score) and earn continuing medical education (CME) credit, please go to http://www.medscape.org/journal/eid. Credit cannot be obtained for tests completed on paper, although you may use the worksheet below to keep a record of your answers.

You must be a registered user on http://www.medscape.org. If you are not registered on http://www.medscape.org, please click on the "Register" link on the right hand side of the website.

Only one answer is correct for each question. Once you successfully answer all post-test questions, you will be able to view and/or print your certificate. For questions regarding this activity, contact the accredited provider, CME@medscape.net. For technical assistance, contact CME@medscape.net. American Medical Association's Physician's Recognition Award (AMA PRA) credits are accepted in the US as evidence of participation in CME activities. For further information on this award, please go to https://www.ama-assn.org. The AMA has determined that physicians not licensed in the US who participate in this CME activity are eligible for AMA PRA Category 1 Credits™. Through agreements that the AMA has made with agencies in some countries, AMA PRA credit may be acceptable as evidence of participation in CME activities. If you are not licensed in the US, please complete the questions online, print the AMA PRA CME credit certificate, and present it to your national medical association for review.

Article Title

Neurologic Complications of Influenza B Virus Infection in Adults, Romania

CME Questions

1. Your patient is a 29-year-old woman with headache and influenza B virus infection. According to the case series from a tertiary facility in Romania by Popescu and colleagues, which of the following statements about clinical and neurologic manifestations of influenza B virus infection in adults is most accurate?

A. Most patients with neurologic manifestations of influenza B were elderly and had multiple previous comorbidities and/or neurologic diseases
B. Half of patients with neurologic manifestations of influenza B had been vaccinated against influenza
C. Cerebellar ataxia was the most common neurologic presentation
D. Influenza B virus should be considered as an etiologic factor in encephalitis in adults as well as in children and adolescents

2. According to the case series from a tertiary facility in Romania by Popescu and colleagues, which of the following statements about treatment and course of influenza B virus infection in adults with neurologic complications is correct?

A. There were no fatalities
B. Respiratory complications and life-threatening respiratory failure were common
C. Neuraminidase inhibitors are less effective against influenza B than influenza A viruses
D. Most adults received oseltamivir, 75 mg twice daily, within the first 48 hours of disease onset

3. According to the case series from a tertiary facility in Romania by Popescu and colleagues, which of the following statements about laboratory and neuroimaging findings of influenza B virus infection in adults with neurologic complications is correct?

A. Viral sequencing identified influenza virus B (Yam)-lineage clade 3, representative of B/Phuket/3073/2013, in 4 patients
B. Cerebrospinal fluid (CSF) samples were positive for viral nucleic acids in 4 patients
C. All patients had abnormal brain imaging results
D. All patients had CSF pleocytosis

Earning CME Credit

To obtain credit, you should first read the journal article. After reading the article, you should be able to answer the following, related, multiple-choice questions. To complete the questions (with a minimum 75% passing score) and earn continuing medical education (CME) credit, please go to http://www.medscape.org/journal/eid. Credit cannot be obtained for tests completed on paper, although you may use the worksheet below to keep a record of your answers.

You must be a registered user on http://www.medscape.org. If you are not registered on http://www.medscape.org, please click on the "Register" link on the right hand side of the website.

Only one answer is correct for each question. Once you successfully answer all post-test questions, you will be able to view and/or print your certificate. For questions regarding this activity, contact the accredited provider, CME@medscape.net. For technical assistance, contact CME@medscape.net. American Medical Association's Physician's Recognition Award (AMA PRA) credits are accepted in the US as evidence of participation in CME activities. For further information on this award, please go to https://www.ama-assn.org. The AMA has determined that physicians not licensed in the US who participate in this CME activity are eligible for AMA PRA Category 1 Credits™. Through agreements that the AMA has made with agencies in some countries, AMA PRA credit may be acceptable as evidence of participation in CME activities. If you are not licensed in the US, please complete the questions online, print the AMA PRA CME credit certificate, and present it to your national medical association for review.

Article Title

Transmission of Hepatitis A Virus through Combined Liver–Small Intestine–Pancreas Transplantation

CME Questions

1. Which of the following statements regarding hepatitis A virus (HAV) and its transmission is most accurate?

A. HAV is frequently associated with a prolonged infectious carrier state
B. HAV prevalence in the United States has not changed since the introduction of the HAV vaccine
C. HAV may cause relapsing and fulminant hepatitis
D. Parenteral transmission of HAV through infected blood products is fairly common

2. Which of the following statements regarding the donor of the infected tissue in the current study is most accurate?

A. The donor had received 2 doses of the HAV vaccine
B. The donor also passed HAV infection to the recipient of his or her heart
C. The donor also passed HAV infection to the recipient of his or her kidney
D. Pretransplant testing for HAV on the donor's organs was probably not done

3. Which of the following statements regarding laboratory testing of patients with HAV infection in the current study is most accurate?

A. The 2 home health nurses had HAV RNA with genetically identical sequences
B. Only 1 of the 2 home health nurses tested positive for HAV RNA
C. The visceral organ recipient tested positive for HAV RNA in the stool but not serum after transplant
D. HAV RNA persisted in the visceral organ recipient in the serum longer than the stool

Looking for trusted information about vaccinating your child?

Visit www.cdc.gov/vaccines/parents. Learn about the vaccines your baby needs from a reliable source. The CDC's website explains the 14 diseases vaccines prevent, CDC's recommended schedule, possible side effects, how to comfort your baby during vaccine visits and more. Talk to your child's doctor, and visit our website to get the facts about vaccines.

U.S. Department of Health and Human Services
Centers for Disease Control and Prevention

Immunization. Power to Protect.

CDC PROVIDES INFORMATION ABOUT MRSA SKIN INFECTIONS.

Visit **www.cdc.gov/MRSA** or call **1-800-CDC-INFO** to order provider materials including:

- Clinician guidelines
- Evaluation & treatment recommendations
- Patient education materials
- Posters
- Fact sheets
- Flyers

Developed with support from the CDC Foundation through an educational grant from Pfizer Inc.

Emerging Infectious Diseases is a peer-reviewed journal established expressly to promote the recognition of new and reemerging infectious diseases around the world and improve the understanding of factors involved in disease emergence, prevention, and elimination.

The journal is intended for professionals in infectious diseases and related sciences. We welcome contributions from infectious disease specialists in academia, industry, clinical practice, and public health, as well as from specialists in economics, social sciences, and other disciplines. Manuscripts in all categories should explain the contents in public health terms. For information on manuscript categories and suitability of proposed articles, see below and visit http://wwwnc.cdc.gov/eid/pages/author-resource-center.htm.

Summary of Authors' Instructions

Author's Instructions. For a complete list of EID's manuscript guidelines, see the author resource page: http://wwwnc.cdc.gov/eid/page/author-resource-center.

Manuscript Submission. To submit a manuscript, access Manuscript Central from the Emerging Infectious Diseases web page (www.cdc.gov/eid). Include a cover letter indicating the proposed category of the article (e.g., Research, Dispatch), verifying the word and reference counts, and confirming that the final manuscript has been seen and approved by all authors. Complete provided Authors Checklist.

Manuscript Preparation. For word processing, use MS Word. Set the document to show continuous line numbers. List the following information in this order: title page, article summary line, keywords, abstract, text, acknowledgments, biographical sketch, references, tables, and figure legends. Appendix materials and figures should be in separate files.

Title Page. Give complete information about each author (i.e., full name, graduate degree(s), affiliation, and the name of the institution in which the work was done). Clearly identify the corresponding author and provide that author's mailing address (include phone number, fax number, and email address). Include separate word counts for abstract and text.

Keywords. Use terms as listed in the National Library of Medicine Medical Subject Headings index (www.ncbi.nlm.nih.gov/mesh).

Text. Double-space everything, including the title page, abstract, references, tables, and figure legends. Indent paragraphs; leave no extra space between paragraphs. After a period, leave only one space before beginning the next sentence. Use 12-point Times New Roman font and format with ragged right margins (left align). Italicize (rather than underline) scientific names when needed.

Biographical Sketch. Include a short biographical sketch of the first author—both authors if only two. Include affiliations and the author's primary research interests.

References. Follow Uniform Requirements (www.icmje.org/index.html). Do not use endnotes for references. Place reference numbers in parentheses, not superscripts. Number citations in order of appearance (including in text, figures, and tables). Cite personal communications, unpublished data, and manuscripts in preparation or submitted for publication in parentheses in text. Consult List of Journals Indexed in Index Medicus for accepted journal abbreviations; if a journal is not listed, spell out the journal title. List the first six authors followed by "et al." Do not cite references in the abstract.

Tables. Provide tables within the manuscript file, not as separate files. Use the MS Word table tool, no columns, tabs, spaces, or other programs. Footnote any use of boldface. Tables should be no wider than 17 cm. Condense or divide larger tables. Extensive tables may be made available online only.

Figures. Submit editable figures as separate files (e.g., Microsoft Excel, PowerPoint). Photographs should be submitted as high-resolution (600 dpi) .tif or .jpeg files. Do not embed figures in the manuscript file. Use Arial 10 pt. or 12 pt. font for lettering so that figures, symbols, lettering, and numbering can remain legible when reduced to print size. Place figure keys within the figure. Figure legends should be placed at the end of the manuscript file.

Videos. Submit as AVI, MOV, MPG, MPEG, or WMV. Videos should not exceed 5 minutes and should include an audio description and complete captioning. If audio is not available, provide a description of the action in the video as a separate Word file. Published or copyrighted material (e.g., music) is discouraged and must be accompanied by written release. If video is part of a manuscript, files must be uploaded with manuscript submission. When uploading, choose "Video" file. Include a brief video legend in the manuscript file.

Types of Articles

Perspectives. Articles should not exceed 3,500 words and 50 references. Use of subheadings in the main body of the text is recommended. Photographs and illustrations are encouraged. Provide a short abstract (150 words), 1-sentence summary, and biographical sketch. Articles should provide insightful analysis and commentary about new and reemerging infectious diseases and related issues. Perspectives may address factors known to influence the emergence of diseases, including microbial adaptation and change, human demographics and behavior, technology and industry, economic development and land use, international travel and commerce, and the breakdown of public health measures.

Synopses. Articles should not exceed 3,500 words in the main body of the text or include more than 50 references. Use of subheadings in the main body of the text is recommended. Photographs and illustrations are encouraged. Provide a short abstract (not to exceed 150 words), a 1-line summary of the conclusions, and a brief biographical sketch of first author or of both authors if only 2 authors. This section comprises case series papers and concise reviews of infectious diseases or closely related topics. Preference is given to reviews of new and emerging diseases; however, timely updates of other diseases or topics are also welcome. If detailed methods are included, a separate section on experimental procedures should immediately follow the body of the text.

Research. Articles should not exceed 3,500 words and 50 references. Use of subheadings in the main body of the text is recommended. Photographs and illustrations are encouraged. Provide a short abstract (150 words), 1-sentence summary, and biographical sketch. Report laboratory and epidemiologic results within a public health perspective. Explain the value of the research in public health terms and place the findings in a larger perspective (i.e., "Here is what we found, and here is what the findings mean").

Policy and Historical Reviews. Articles should not exceed 3,500 words and 50 references. Use of subheadings in the main body of the text is recommended. Photographs and illustrations are encouraged. Provide a short abstract (150 words), 1-sentence summary, and biographical sketch. Articles in this section include public health policy or historical reports that are based on research and analysis of emerging disease issues.

Dispatches. Articles should be no more than 1,200 words and need not be divided into sections. If subheadings are used, they should be general, e.g., "The Study" and "Conclusions." Provide a brief abstract (50 words); references (not to exceed 15); figures or illustrations (not to exceed 2); tables (not to exceed 2); and biographical sketch. Dispatches are updates on infectious disease trends and research that include descriptions of new methods for detecting, characterizing, or subtyping new or reemerging pathogens. Developments in antimicrobial drugs, vaccines, or infectious disease prevention or elimination programs are appropriate. Case reports are also welcome.

Another Dimension. Thoughtful essays, short stories, or poems on philosophical issues related to science, medical practice, and human health. Topics may include science and the human condition, the unanticipated side of epidemic investigations, or how people perceive and cope with infection and illness. This section is intended to evoke compassion for human suffering and to expand the science reader's literary scope. Manuscripts are selected for publication as much for their content (the experiences they describe) as for their literary merit. Include biographical sketch.

Research Letters Reporting Cases, Outbreaks, or Original Research. EID publishes letters that report cases, outbreaks, or original research as Research Letters. Authors should provide a short abstract (50-word maximum), references (not to exceed 10), and a short biographical sketch. These letters should not exceed 800 words in the main body of the text and may include either 1 figure or 1 table. Do not divide Research Letters into sections.

Letters Commenting on Articles. Letters commenting on articles should contain a maximum of 300 words and 5 references; they are more likely to be published if submitted within 4 weeks of the original article's publication.

Commentaries. Thoughtful discussions (500–1,000 words) of current topics. Commentaries may contain references (not to exceed 15) but no abstract, figures, or tables. Include biographical sketch.

Books, Other Media. Reviews (250–500 words) of new books or other media on emerging disease issues are welcome. Title, author(s), publisher, number of pages, and other pertinent details should be included.

Conference Summaries. Summaries of emerging infectious disease conference activities (500–1,000 words) are published online only. They should be submitted no later than 6 months after the conference and focus on content rather than process. Provide illustrations, references, and links to full reports of conference activities.

Online Reports. Reports on consensus group meetings, workshops, and other activities in which suggestions for diagnostic, treatment, or reporting methods related to infectious disease topics are formulated may be published online only. These should not exceed 3,500 words and should be authored by the group. We do not publish official guidelines or policy recommendations.

Photo Quiz. The photo quiz (1,200 words) highlights a person who made notable contributions to public health and medicine. Provide a photo of the subject, a brief clue to the person's identity, and five possible answers, followed by an essay describing the person's life and his or her significance to public health, science, and infectious disease.

Etymologia. Etymologia (100 words, 5 references). We welcome thoroughly researched derivations of emerging disease terms. Historical and other context could be included.

Announcements. We welcome brief announcements of timely events of interest to our readers. Announcements may be posted online only, depending on the event date. Email to eideditor@cdc.gov.

In This Issue

Perspective

Synopses

Research

Dispatches

ISSN 1080-6040

DEPARTMENT OF HEALTH & HUMAN SERVICES
Public Health Service
Centers for Disease Control and Prevention (CDC)
Mailstop D61, Atlanta, GA 30329-4027

Official Business
Penalty for Private Use $300
Return Service Requested

MEDIA MAIL
POSTAGE & FEES PAID
PHS/CDC
Permit No. G 284